

University of Windsor

Scholarship at UWindor

Electronic Theses and Dissertations

Theses, Dissertations, and Major Papers

2022

Understanding Freshwater Ecosystems and Human Health Implications in Recreational Water through Microbial Characterization, Source Tracking, and Sediment-Microbe Dynamics

Danielle Gleason
University of Windsor

Follow this and additional works at: <https://scholar.uwindsor.ca/etd>



Part of the [Environmental Sciences Commons](#), and the [Microbiology Commons](#)

Recommended Citation

Gleason, Danielle, "Understanding Freshwater Ecosystems and Human Health Implications in Recreational Water through Microbial Characterization, Source Tracking, and Sediment-Microbe Dynamics" (2022). *Electronic Theses and Dissertations*. 8975.
<https://scholar.uwindsor.ca/etd/8975>

This online database contains the full-text of PhD dissertations and Masters' theses of University of Windsor students from 1954 forward. These documents are made available for personal study and research purposes only, in accordance with the Canadian Copyright Act and the Creative Commons license—CC BY-NC-ND (Attribution, Non-Commercial, No Derivative Works). Under this license, works must always be attributed to the copyright holder (original author), cannot be used for any commercial purposes, and may not be altered. Any other use would require the permission of the copyright holder. Students may inquire about withdrawing their dissertation and/or thesis from this database. For additional inquiries, please contact the repository administrator via email (scholarship@uwindsor.ca) or by telephone at 519-253-3000ext. 3208.

UNDERSTANDING FRESHWATER ECOSYSTEMS AND HUMAN HEALTH
IMPLICATIONS IN RECREATIONAL WATER THROUGH MICROBIAL
CHARACTERIZATION, SOURCE TRACKING, AND SEDIMENT-MICROBE
DYNAMICS

by

Danielle Gleason

A Dissertation
Submitted to the Faculty of Graduate Studies
Through the Faculty of Science
And in support of the Great Lakes Institute for Environmental Research
In Partial Fulfillment of the Requirements for
The Degree of Doctor of Philosophy
At the University of Windsor

Windsor, Ontario, Canada

2022

© 2022 Danielle Gleason

UNDERSTANDING FRESHWATER ECOSYSTEMS AND HUMAN HEALTH
IMPLICATIONS IN RECREATIONAL WATER THROUGH MICROBIAL
CHARACTERIZATION, SOURCE TRACKING, AND SEDIMENT-MICROBE
DYNAMICS

by

Danielle Gleason

APPROVED BY:

D. Walsh, External Examiner
Concordia University

P. Vacratsis
Department of Chemistry and Biochemistry

C. Semeniuk
Great Lakes Institute for Environmental Research

S.R. Chaganti
Cooperative Institute for Great Lakes Research, University of Michigan

C.G. Weisener, Co-Advisor
Great Lakes Institute for Environmental Research

I.G. Droppo, Co-Advisor
Environment and Climate Change Canada

October 14, 2022

DECLARATION OF CO-AUTHORSHIP / PREVIOUS PUBLICATION

I. Co-Authorship

I hereby declare that this thesis incorporates material that is result of joint research, as follows:

This thesis incorporates the outcome of joint research undertaken in collaboration with S.R. Chaganti, I.G. Droppo and C.G. Weisener, under the supervision of both I.G. Droppo and C.G. Weisener. Details of these collaborations for each data chapter are covered below. In all cases, the key ideas, primary contributions, experimental designs, data analysis and interpretation, and manuscript construction were primarily performed by myself.

Chapter 2 of the thesis was co-authored with I.G. Droppo and C.G. Weisener, under the supervision of both I.G. Droppo and C.G. Weisener. The contribution of co-authors was primarily through the provision of grant funding and experimental design. Co-authors also provided feedback for the purpose of editing and refining the manuscript.

Chapter 3 of the thesis was co-authored with S.R. Chaganti, I.G. Droppo and C.G. Weisener, under the supervision of both I.G. Droppo and C.G. Weisener. The contribution of co-authors was primarily through the provision of grant funding, experimental design, and consultation on statistical analyses. Co-authors also provided feedback for the purpose of editing and refining the manuscript.

Chapter 4 of the thesis was co-authored with I.G. Droppo and C.G. Weisener, under the supervision of both I.G. Droppo and C.G. Weisener. The contribution of co-authors was primarily through the provision of grant funding, experimental design, and sample collection. Co-authors also provided feedback for the purpose of editing and refining the manuscript.

Chapter 5 of the thesis was co-authored with I.G. Droppo and C.G. Weisener, under the supervision of both I.G. Droppo and C.G. Weisener. The contribution of co-authors was primarily through the provision of grant funding and experimental design. Co-authors also provided feedback for the purpose of editing and refining the manuscript.

I am aware of the University of Windsor Senate Policy on Authorship and I certify that I have properly acknowledged the contribution of other researchers to my thesis, and have obtained written permission from each of the co-author(s) to include the above material(s) in my thesis.

I certify that, with the above qualification, this thesis, and the research to which it refers, is the product of my own work.

II. Previous Publication

This thesis includes 4 original papers that have been previously published/submitted for publication in peer reviewed journals, as follows:

Thesis Chapter	Publication title/full citation	Publication status
Chapter 2	VanMensel, D., Droppo, I.G., Weisener, C.G. (2022) Exploring the microbial signature in bed sediment from Lake St. Clair and Lake Erie beaches: A spatiotemporal perspective.	Unpublished
Chapter 3	VanMensel, D., Chaganti, S.R., Droppo, I.G., Weisener, C.G. (2020) Exploring bacterial pathogen community dynamics in freshwater beach sediments: A tale of two lakes. <i>Environ. Microbiol.</i> 22(2), 568-583. doi:10.1111/1462-2920.14860	Published
Chapter 4	VanMensel, D., Droppo, I.G., Weisener, C.G. (2022) Identifying chemolithotrophic and pathogenic-related gene expression within suspended sediment flocs in freshwater environments: A metatranscriptomic assessment. <i>Sci. Total Environ.</i> 807:150996. doi:10.1016/j.scitotenv.2021.150996	Published
Chapter 5	VanMensel, D., Chaganti, S.R., Droppo, I.G., Weisener, C.G. Microbe-sediment interactions in Great Lakes recreational waters: Implications for human health risk. <i>Environ. Microbiol.</i>	Submitted by 2023

I certify that I have obtained a written permission from the copyright owner(s) to include the above published material(s) in my thesis. I certify that the above material describes work completed during my registration as a graduate student at the University of Windsor.

III. General

I declare that, to the best of my knowledge, my thesis does not infringe upon anyone's copyright nor violate any proprietary rights and that any ideas, techniques, quotations, or any other material from the work of other people included in my thesis, published or otherwise, are fully acknowledged in accordance with the standard referencing practices. Furthermore, to the extent that I have included copyrighted material that surpasses the bounds of fair dealing within the meaning of the Canada Copyright Act, I certify that I have obtained a written permission from the copyright owner(s) to include such material(s) in my thesis.

I declare that this is a true copy of my thesis, including any final revisions, as approved by my thesis committee and the Graduate Studies office, and that this thesis has not been submitted for a higher degree to any other University or Institution.

ABSTRACT

Contamination of natural aquatic ecosystems is a serious global concern as populations increase and the environment is impacted by climate change. Nonpoint source (NPS) contamination of allochthonous materials, such as sediments, nutrients, and microorganisms, is commonly introduced to a body of water through runoff and wash-off which cumulates over a large area, and is subsequently transported to surface waters (e.g., rivers, streams, lakes) and shorelines. The principal form of microbial contamination of water resources is often from fecal pollution derived from humans, domesticated animals, or wildlife, and contains a variety of human pathogens. There are also numerous factors (with limited research) affecting pathogen survival, persistence, and growth in these environments, complicating research models and progress, and our overall understanding of the microbiology of natural waters. Thus, the potential for human health risk associated with recreational water use can be difficult to recognise and regulate without appropriate testing to identify and characterize the pathogenic profile in these environments. Traditional water quality assessments involve the use of an indicator organism (e.g., *E. coli*) as a proxy for fecal contamination in recreational waters. However, there are several limitations to these simplistic approaches which lead to unreliable water quality evaluations. These tests 1) are infrequent, time consuming, and nonrepresentative of *in situ* conditions; 2) target only one organism but omit other waterborne pathogens; 3) involve culture-based techniques or the use of environmental DNA, which cannot inform on microbial activity; 4) neglect to identify contamination origin or source; and perhaps the most significant shortcoming of these assessments is

that they 5) overlook the sediment compartment, assuming pathogenic microbes only have planktonic lifestyles.

The research presented through this dissertation aims to address the knowledge gap regarding the concern for human health implications involving microbial contamination associated with recreational water use. A spatiotemporal microbial biosignature was first established for freshwater bed sediment in Laurentian Great Lakes beaches. This baseline allowed for focused mRNA-based metatranscriptomic and rRNA-based targeted transcriptomic assessments of both bed and suspended sediment fractions of the nearshore swimming zone. Results indicated significant microbial activity (through diverse metabolic functions as well as pathogenic-related gene expression) associated with both sediment fractions, suggesting freshwater sediment acts as a reservoir and secondary source for microorganisms (including waterborne pathogens) through sediment dynamics (e.g., erosion, resuspension, transport, deposition). Microbial biomass and activity were typically upregulated at low-energy, fine-grained locations, such as Belle River and Kingsville, Ontario beaches. Microbial source tracking (MST) evaluations determined avian sources (i.e., gulls and geese) to be the largest NPS of fecal indicator bacteria (FIB) associated with the sediment compartment along these freshwater shorelines. MST targets provided superior results over general FIB targets and traditional water quality assessments by exposing contamination source details.

The results obtained from this research significantly improve our understanding of freshwater ecosystems and human health implications in recreational water through microbial characterization (i.e., expansive community profiling and gene expression studies), MST, and sediment-microbe relationships.

DEDICATION

*To my mom and dad for their love and support.
To my husband and daughters for the motivation and inspiration.*

ACKNOWLEDGEMENTS

First and foremost, I would like to acknowledge my supervisors, Drs. Ian Droppo and Chris Weisener, for the opportunity to participate in such interesting and important research while simultaneously obtaining this degree. Together they have provided me the physical and mental tools I needed to successfully survive the last few years. It wasn't always (or ever) easy, but they were my academic support system, and it was reassuring knowing that they would back me up (or pull me up) if, and when, I needed it. Looking back, it's obvious to me how much our relationship has evolved – starting out as supervisors and student, to now team members and friends. Over time, both Chris and Ian allowed me the freedom and flexibility to take my research into my own hands and let me grow into a more independent scientist while exploring my own passions and ideas. Their leadership has guided me down an exciting path of learning, growing, and finding my way as a young environmental researcher. And for that, I am truly grateful.

I wish to thank my committee members, Dr. Subba Rao Chaganti, Dr. Christina Semeniuk, and Dr. Otis Vacratsis for their support, encouragement, and guidance over the last few years. Dr. Chaganti has been an integral member throughout my graduate studies, and he deserves great recognition for his consultation and assistance along the way. Dr. Semeniuk has supported me in more ways than just academically, and she has been a true role model whom I greatly admire. Dr. Vacratsis helped bring me back to reality and really look at the big picture of what my research is about; he asked the right questions that challenged me to be better. Thank you all for the influence you've had on me.

Thank you to my friends and colleagues at GLIER. Specifically, I want to shout out to Mary Lou Scratch, Christine Weisener, Kendra Thompson-Kumar, Sharon Lackie, and Shelby Mackie. These ladies have not only shown me friendship, but represent strong, independent leaders in the workplace who deserve respect and a round of applause. I thank you for being amazing, powerful women and for your help in keeping my head up and staying proud. Thank you to the entire Weisener Lab, past and present, for the lab and field assistance, discussions about science (and not), and memories along the way. Specifically, I thank Thomas Reid and Nick Falk for their friendship, help, and good times over the years together.

Big thanks to my mom and dad for everything they've done (and continue to do) for me. They are the reason I have had all the opportunities in my life and have always been on my side, no matter what. Their belief in me has never ever faltered, even when I doubted myself most. I can't express in words what their love and support has meant to me. Thank you from the bottom of my heart. I also thank my amazing sister, MaryAnn,

for being my best friend. She opened her heart and home to me when I needed her most and I don't think I could have managed to get through this degree without her support. She helped me get through one of the toughest times of my life, and we managed to have a pretty good time with more laughs than I can count. Her presence in my life has meant the world to me and I will forever be grateful for her. And thank you to Callie for always bringing a smile to my face and reminding me not to take life too seriously.

A very special thank you goes to my stepsister, Jodie. She has been a rock to me and helped me through grad school in countless ways. She saved me a long commute by providing a comfortable place to lay my head that was close to the University, intently listened to me practice for presentations and always asked questions, encouraged me when I needed a little push, and was always a great reminder of how to be a strong, independent woman, and a wonderful all-around person. I will always be appreciative for everything she has done for me. Thank you.

And finally, I want to thank my amazing and supportive husband, Jeff. You've been by my side from the beginning of this degree, and I couldn't have gotten through it without you. Your love and support have never wavered, and you have shown me what it truly means to be a supportive and loyal partner. To my sweet girls, Lucy and Marla – you both have brightened my whole world and keep me on my toes! The two of you make me strive to be better every day and I always want to make you proud.

Thank you to my family and friends for the support and motivation. I love you all.

TABLE OF CONTENTS

DECLARATION OF CO-AUTHORSHIP / PREVIOUS PUBLICATION.....	iii
ABSTRACT	vi
DEDICATION	viii
ACKNOWLEDGEMENTS	ix
LIST OF TABLES	xv
LIST OF FIGURES.....	xvi
LIST OF APPENDICES	xx
LIST OF ABBREVIATIONS / SYMBOLS	xxiii
CHAPTER 1: INTRODUCTION	1
1.0 Background.....	2
1.1 Beach Stressors: Contaminant Sources and Physical Dynamics.....	5
1.1.1 <i>The NPS continuum of allochthonous material delivery to recreational waters</i>	5
1.1.2 <i>Microbial contamination</i>	6
1.2 The Microbe-Sediment Relationship	8
1.2.1 <i>Importance of the sediment compartments</i>	8
1.2.2 <i>Microbe-sediment dynamics</i>	12
1.3 Aquatic Microorganisms: Small Size, Large Impact.....	15
1.3.1 <i>Diversity in numbers, structure, and function</i>	15
1.3.2 <i>Measuring the microbial potential through water monitoring</i>	18
1.4 Implications of Waterborne Human Pathogens in Recreational Waters	22
1.5 Research Focus	24
1.5.1 <i>Research hypotheses</i>	25
Figures and Tables	28
References.....	33
CHAPTER 2: EXPLORING THE MICROBIAL SIGNATURE IN BED SEDIMENT FROM LAKE ST. CLAIR AND LAKE ERIE BEACHES: A SPATIOTEMPORAL PERSPECTIVE ..	49
2.1 Introduction.....	50
2.2 Methods	53
2.2.1 <i>Site selection</i>	53
2.2.2 <i>Site sampling details</i>	54
2.2.3 <i>Nucleic acid extractions from freshwater bed sediment</i>	55
2.2.4 <i>Library preparation, quality control, and sequencing</i>	56
2.2.5 <i>Bioinformatics analysis</i>	57

2.3	Results.....	59
2.3.1	<i>Site descriptions and sediment characteristics</i>	59
2.3.2	<i>Sequencing statistics</i>	62
2.3.3	<i>Alpha diversity of freshwater beach sediments</i>	62
2.3.4	<i>Beta diversity of freshwater beach sediments</i>	63
2.3.5	<i>Taxonomic characterization of benthic bacterial communities</i>	64
2.4	Discussion.....	66
2.5	Conclusion	72
	Figures and Tables	74
	References.....	84
CHAPTER 3: EXPLORING BACTERIAL PATHOGEN COMMUNITY DYNAMICS IN FRESHWATER BEACH SEDIMENTS: A TALE OF TWO LAKES		92
3.0	Prologue.....	93
3.1	Introduction.....	93
3.2	Experimental Procedures.....	95
3.2.1	<i>Site selection, characteristics and sediment sampling</i>	95
3.2.2	<i>Extractions, library preparation, quality control and sequencing</i>	96
3.2.3	<i>Bioinformatic analysis</i>	98
3.3	Results and Discussion	99
3.3.1	<i>Beach sediment characteristics</i>	99
3.3.2	<i>Sequencing statistics and functional assignments</i>	100
3.3.3	<i>Taxonomic assessment</i>	101
3.3.4	<i>Transcriptomics and the active microbes</i>	102
3.3.5	<i>Environmental implications</i>	111
3.4	Conclusions.....	112
	Figures and Tables	114
	References.....	125
CHAPTER 4: IDENTIFYING CHEMOLITHOTROPHIC AND PATHOGENIC-RELATED GENE EXPRESSION WITHIN SUSPENDED SEDIMENT FLOCS IN FRESHWATER ENVIRONMENTS: A METATRANSCRIPTOMIC ASSESSMENT		135
	Graphical Abstract	136
4.0	Prologue.....	137
4.1	Introduction.....	137
4.2	Materials and Methods	140
4.2.1	<i>Study sites</i>	140
4.2.2	<i>TSS collections</i>	140

4.2.3	<i>Physicochemical measurements of the water column</i>	141
4.2.4	<i>SEM analysis</i>	142
4.2.5	<i>Extractions, library preparation, quality control, and sequencing</i>	142
4.2.6	<i>Bioinformatics analyses</i>	143
4.3	Results and Discussion	144
4.3.1	<i>Water nutrient stoichiometry and TSS biophysicochemical characteristics</i>	144
4.3.2	<i>Sequencing statistics and functional diversity</i>	147
4.3.3	<i>Biogeochemical cycling reveals chemolithotrophic activity</i>	149
4.3.4	<i>Expression of bacterial pathogenic-related transcripts in freshwater SS</i>	151
4.3.5	<i>Bed sediment comparison</i>	156
4.4	Conclusions	157
	Figures and Tables	160
	References	169
CHAPTER 5: MICROBE-SEDIMENT INTERACTIONS IN GREAT LAKES RECREATIONAL WATERS: IMPLICATIONS FOR HUMAN HEALTH RISK		176
5.0	Prologue	177
5.1	Introduction	177
5.2	Materials and Methods	180
5.2.1	<i>Sampling sites and collections</i>	180
5.2.2	<i>RNA extractions and sample preparation</i>	181
5.2.3	<i>Selection of candidate genes, primers, and probes</i>	182
5.2.4	<i>Quantitative PCR</i>	183
5.2.5	<i>Testing for lower limit of detection</i>	185
5.2.6	<i>Expression analysis</i>	185
5.2.7	<i>Statistical analysis</i>	186
5.3	Results and Discussion	187
5.3.1	<i>Prevalence of FIB, MST transcripts from freshwater sediments</i>	187
5.3.2	<i>Quantification of FIB, MST transcripts and factors effecting expression</i>	189
5.3.3	<i>Evaluating best approach for assessing microbial contamination in water</i>	197
5.4	Conclusion	199
	Figures and Tables	202
	References	210
CHAPTER 6: CONCLUSIONS, LIMITATIONS, AND FUTURE RECOMMENDATIONS		217
6.1	Major Contributions to Environmental Science	218
6.2	Research Limitations	221

6.3	Future Recommendations	223
	References.....	226
	APPENDICES.....	230
	APPENDIX A: SUPPLEMENTAL INFORMATION FOR CHAPTER 2.....	231
	APPENDIX B: SUPPLEMENTAL INFORMATION FOR CHAPTER 3	240
	APPENDIX C: SUPPLEMENTAL INFORMATION FOR CHAPTER 4.....	243
	APPENDIX D: SUPPLEMENTAL INFORMATION FOR CHAPTER 5.....	263
	VITA AUCTORIS	285

LIST OF TABLES

CHAPTER 1: INTRODUCTION	2
Table 1.1: Frequency of reported <i>E. coli</i> CFUs sampled from lake water exceeding acceptable levels at six public beaches in WEC. Percentages correspond to the number of times testing yielded failed results divided by total sampling days throughout the swimming season (shown below percentages), reported by WECHU from 2016 to 2021. Beaches which reported unsafe <i>E. coli</i> levels for human recreational activity at least 50% of the time are highlighted. Data retrieved from WECHU public access webpage (www.wechu.org).	32
CHAPTER 2: EXPLORING THE MICROBIAL SIGNATURE IN BED SEDIMENT FROM LAKE ST. CLAIR AND LAKE ERIE BEACHES: A SPATIOTEMPORAL PERSPECTIVE ..	50
Table 2.1: Physical properties of WEC freshwater beaches. Grain size and moisture content are used in combination with geographical features (i.e., barriers that shelter the beach) to determine high or low energy of the location.	83
CHAPTER 3: EXPLORING BACTERIAL PATHOGEN COMMUNITY DYNAMICS IN FRESHWATER BEACH SEDIMENTS: A TALE OF TWO LAKES	93
Table 3.1: Physicochemical conditions of the water column at Sandpoint (SP), Belle River (BR), Kingsville (KV), and Holiday (HD) beaches in WEC, Ontario.	123
Table 3.2: Tabulated summary of physical properties characterizing each beach as high or low energy. Data includes grain size (D_{50}), moisture content, and TOC determined from LOI, as well as observational input on water movement restriction and designation of high or low energy for each beach.	124
CHAPTER 4: IDENTIFYING CHEMOLITHOTROPHIC AND PATHOGENIC-RELATED GENE EXPRESSION WITHIN SUSPENDED SEDIMENT FLOCS IN FRESHWATER ENVIRONMENTS: A METATRANSCRIPTOMIC ASSESSMENT	137
Table 4.1: Tabulated summary of expressed transcripts annotated to the KO database, Level 1 categories. Expression represented as normalized logCPM values (top) and raw read values (bottom), duplicates averaged. Pairwise comparisons between sampling sites (lake, tributary) of the same location and season provide statistically significant differential expression ($p < 0.05$), denoted with greater than ($>$) or less than ($<$) symbol and bolded and italicized, where applicable.	168
CHAPTER 5: MICROBE-SEDIMENT INTERACTIONS IN GREAT LAKES RECREATIONAL WATERS: IMPLICATIONS FOR HUMAN HEALTH RISKS	177
Table 5.1: Genes targeted for RT-qPCR assays used to determine microbial contamination in freshwater sediments, including target category (i.e., FIB, MST, waterborne pathogen/virulence factor), animal source for MSTs, and gene codes and descriptions. Details on targets with detections in our dataset (from OpenArray® RT-qPCR assays) include coefficient of determination (R^2) from standard curves and PCR efficiency percentage (both determined from conventional qPCR assays). GenBank accession numbers are included for targets used for developing synthetic genes for standard curves.	208
Table 5.2: Significance values (p) for one-way ANOVAs explaining the effect on transcript expression from independent factors. GOI presented here include FIBs <i>Enterococcus</i> and <i>E. coli</i> , and MSTs for <i>Bacteroides</i> , goose, and seagull, as well as the combination of all GOI detected in this work. GOI are represented for both bed and suspended sediment (SS) fractions. Values with bold text depict results with significant differences ($p < 0.05$).	209

LIST OF FIGURES

CHAPTER 1: INTRODUCTION	2
Figure 1.1: Illustration depicting common sources of pollution and microbial contamination to nearshore beach zones. Upstream inputs are transported to watersheds and tributaries via runoff and wash-off processes, move to receiving waters (i.e., lakes and oceans) with water flow, and potentially lead to negative impacts on water quality and safety status of beaches. .	29
Figure 1.2: The flow of pathogenic pollution from source to recreational waters can be viewed schematically to illustrate the mechanisms and relationships involved in pathogen transport, survival, and ultimately water quality and human and ecosystem health.....	30
Figure 1.3: The flow of pathogenic pollution from source to recreational waters can be viewed schematically to illustrate the mechanisms and relationships related to pathogen transport, survival, and ultimately water quality and human and ecosystem health. Topics discussed in this dissertation are detailed by chapter (left, yellow) and sampling sites explained (right, grey).....	31
CHAPTER 2: EXPLORING THE MICROBIAL SIGNATURE IN BED SEDIMENT FROM LAKE ST. CLAIR AND LAKE ERIE BEACHES: A SPATIOTEMPORAL PERSPECTIVE ..	50
Figure 2.1: Satellite image of Windsor-Essex, Ontario, Canada surrounded by the freshwater of Lake St. Clair, the Detroit River, and Lake Erie. Sediment plumes entering Lake St. Clair from the Thames River (top) and Lake Erie from the Maumee River (bottom) are clearly visible...	75
Figure 2.2: A) *WEC in southwestern Ontario, Canada. Features include Lake St. Clair connected to Lake Erie by the Detroit River. Sampling sites (beaches) where bed sediment collections occurred (yellow circles) include B) Belle River (BR) and C) Sandpoint (SP) on Lake St. Clair, and D) Holiday Conservation (HD), E) Kingsville (KV), F) Leamington (LE), and G) Point Pelee (PP) on Lake Erie.....	76
Figure 2.3: Sediment coring material and examples. A) Sediment core in the PVC collection tube, fresh from the lake, on top of extruding device. B) Core being pushed up through the tube using extruding device; dewar containing liquid nitrogen in back (right). C) Sediment surface of lakebed exposed through the top of the tube for sample collection. D) Display of collection cryotubes prepared for a sample site. E) Aseptically scooping top layer of core into cryotube directly prior to preservation in liquid nitrogen.....	77
Figure 2.4: Spatial perspective boxplots of Chao1 richness estimator (top) and the Shannon diversity index (bottom) for all six sampling beaches in WEC, combined over the sampling year for both DNA (left) and cDNA (right) datasets. Center line within each box represents the median value. Letters atop boxes indicate where significant differences are attributed based on Tukey's post-hoc tests.	78
Figure 2.5: Temporal perspective boxplots of the Chao1 richness estimator for all six sampling beaches in WEC, displayed by sample month for both DNA (top) and cDNA (bottom) datasets. Center line within each box represents the median value.....	79
Figure 2.6: Temporal perspective boxplots of the Shannon diversity index for all six sampling beaches in WEC, displayed by sample month for both DNA (top) and cDNA (bottom) datasets. Center line within each box represents the median value.....	80
Figure 2.7: NMDS ordination plot of microbial community composition in the bed sediment of freshwater beaches. DNA (left) and cDNA (right) datasets are displayed, illustrating beta	

diversity between the six beaches sampled throughout WEC. Sample dates are combined for the year. Ellipses represent 95% of samples included.	81
Figure 2.8: Bar charts representative of the bacterial taxonomic composition for both DNA (left) and cDNA (right) fractions of the individual beaches, combined over the sampling year. A) Composition of bacterial phyla with all undefined and unclassified ASVs (i.e., “NA”) at the phylum level removed. B) Composition of Proteobacterial classes; relative abundance values were determined from total bacterial population. C) Composition of Proteobacterial orders; relative abundance values were determined from total bacterial population. “Other” contains the combined taxa for which individual relative abundances were < 3% for all locations. “NA” is the combination of undefined or unclassified ASVs at the taxon level specified. Both DNA and cDNA data share a common legend for each taxonomic level.	82
CHAPTER 3: EXPLORING BACTERIAL PATHOGEN COMMUNITY DYNAMICS IN FRESHWATER BEACH SEDIMENTS: A TALE OF TWO LAKES.....	93
Figure 3.1: Map of WEC; features displayed include Lake St. Clair, the Detroit River, Lake Erie and all four beaches sampled for this research. Photos of sediment cores appear next to the representative location.	115
Figure 3.2: Micro-sensor profiles of the bed sediment beach zone for (a) Sandpoint, (b) Belle River, (c) Holiday, and (d) Kingsville. DO and redox measurements were obtained through the sediment-water interface of these zones. Double-dashed horizontal line represents the sediment-water interface, where above the line is in the water column and below is into the bed sediment.	116
Figure 3.3: Taxonomic survey of the bed sediment at the four freshwater beaches. (a) Top abundant bacterial taxa of Sandpoint (SP), Belle River (BR), Kingsville (KV), and Holiday (HD) beaches. Note that phyla are represented for all groups except the Proteobacteria, which is broken down into its subsequent classes (Alpha-, Beta-, Delta-, Epsilon-, and Gamma-Proteobacteria). (b) Heatmap illustrating the relative abundance of potential human bacterial pathogens (genus level) present at each sample location based on DNA isolation and 16S rRNA amplification. Note the small percentage values, and the majority are members of the Gammaproteobacteria.* <i>Includes cultured and uncultured spp. while others represent cultured taxa only</i>	117
Figure 3.4: Distribution of all well-characterized transcripts from the bed sediment into functional categories for the four freshwater beaches.	118
Figure 3.5: Functional annotations assigned to transcripts involved in nitrogen metabolism, sulfur metabolism, and methanogenesis pathways within the top layer of bed sediment in four freshwater beaches. This heatmap uses colour range and proportional size scaling to allow for discernible comparisons. Expression is represented as percent abundance relative to <i>rpoC</i> gene.	119
Figure 3.6: Expression of nitrogen metabolism genes involved in denitrification, dissimilatory and assimilatory nitrate reduction, and nitrogen fixation within the nearshore bed sediment of Kingsville (KV) and Belle River (BR) public beaches. Expression is represented as percent abundance relative to <i>rpoC</i> gene.	120
Figure 3.7: Expression of transcripts with pathogenic relevance from the bed sediment beach samples at Belle River (BR) and Kingsville (KV) beaches. Expression is represented as percent abundance relative to <i>rpoC</i> gene.	121
Figure 3.8: Proposed universal bacterial pathogen. Schematic of genes involved in nitric oxide detoxification (blue), CAMP resistance (purple), <i>Salmonella</i> infection (red), and pertussis	

(green). Expression of functional annotations encoding illustrated transcripts appear directly above stated gene. Yellow circles represent nitric oxide. <i>Salmonella</i> virulence factors are translocated out of the pathogen through a type III secretion system (T3SS). Translocation of FHA/FhaB protein is through a two-partner secretion (TPS) system, which requires the secretion protein FhaC. Note there are three different y-axis scales (0-40%; 0-6%; 0.0-0.6%), used to clearly illustrate expression levels and comparisons between KV and BR. Expression of transcripts are represented as percentage relative to the housekeeping gene, <i>rpoC</i>	122
CHAPTER 4: IDENTIFYING CHEMOLITHOTROPHIC AND PATHOGENIC-RELATED GENE EXPRESSION WITHIN SUSPENDED SEDIMENT FLOCS IN FRESHWATER ENVIRONMENTS: A METATRANSCRIPTOMIC ASSESSMENT	137
Figure 4.1: Map of WEC showing the two tributaries and beaches of interest for this paper. Insets illustrate a closer view of sampling areas, including sampling locations (BR-lake, BR-trib, KV-lake, KV-trib). Land use is distinguished by colour; grey = urban, orange = agriculture/undifferentiated rural, blue = water.....	161
Figure 4.2: SEM images capturing various instances of biological activity within the SS fraction of the tributaries examined. In BR-trib, a) crystals indicative of biomineralization and b) dividing/replicating cells, and in KV-trib, c) a green alga (<i>Scenedesmus</i>) and d) an auxospore cell.	162
Figure 4.3: PCA of normalized metatranscriptomic data, using Euclidean distances between logCPM expression values. Functional similarity is illustrated between samples (beta-diversity) at Level 4 (gene transcript) resolution for all 8 groups (BR/KV-lake/trib-Summer/Fall). Groupings of samples from the same location (BR, KV) and season are encompassed by dotted blue ellipses. S = summer; F = fall; trib = tributary.	163
Figure 4.4: Gene expression heatmap of Level 3 pathways involved in Energy Metabolism (Level 2), utilizing KEGG annotations and KO database. Photosynthetic pathways have been filtered out to focus on chemolithotrophic activity (methane metabolism [ko00680]; carbon fixation pathways in prokaryotes [ko00720]; nitrogen metabolism [ko00910]; and sulfur metabolism [ko00920]). Expression represented as normalized logCPM values. Pairwise comparisons between sampling sites (lake, tributary) of the same location and season provide statistically significant differential expression ($p < 0.05$), denoted with an asterisk * where applicable.	164
Figure 4.5: Expression of N metabolism transcripts involved in denitrification, DNRA, ANRA, nitrogen fixation and nitrification pathways detected in SS samples. Heatmap uses colour range and volume proportional size scaling to illustrate expression comparisons of all samples. Expression represented as normalized logCPM values. [Volume proportional to cell value – linear.].....	165
Figure 4.6: Gene expression heatmap of Level 3 transcripts involved in Infectious Diseases (Level 2), utilizing KEGG annotations and KO database. Viral and parasitic pathways are omitted to allow the focus on translated cDNAs showing similarities with genes involved in bacterial infectious diseases (legionellosis [ko05134]; <i>V. cholerae</i> pathogenic cycle [ko05111]; <i>V. cholerae</i> infection [ko05110]; epithelial cell signaling in <i>H. pylori</i> infection [ko05120]; <i>Salmonella</i> infection [ko05132]; tuberculosis [ko05152]; pathogenic <i>E. coli</i> infection [ko05130]; <i>S. aureus</i> infection [ko05150]; and bacterial invasion of epithelial cells [ko05100]). Expression represented as normalized logCPM values. Pairwise comparisons between sampling sites (lake, tributary) of the same location and season provide statistically significant differential expression ($p < 0.05$) denoted with an asterisk * where applicable.....	166

Figure 4.7: Gene expression of functional annotations assigned to translated transcripts showing similarities with proteins involved in bacterial pathways playing part in Infectious Diseases. Heatmap uses colour range and volume proportional size scaling to illustrate expression comparisons of all samples. Expression represented as normalized logCPM values. [Volume proportional to cell value – logarithmic.]	167
CHAPTER 5: MICROBE-SEDIMENT INTERACTIONS IN GREAT LAKES	
RECREATIONAL WATERS: IMPLICATIONS FOR HUMAN HEALTH RISKS	177
Figure 5.1: Map of WEC displaying all sampling sites. Bed sediment (yellow circles) was collected from Sandpoint (SP), Belle River (BR), Holiday Conservation (HD), Kingsville (KV), Leamington (LE), and Point Pelee (PP). Suspended sediment (orange diamonds) was collected from the nearshore zone in the lake from both BR (top right panel) and KV (bottom right panel) as well as the adjacent tributary (top – Belle River; bottom – Mill Creek).	203
Figure 5.2: Boxplots displaying the distribution of expressed transcripts (log copies/g) at each beach location (Belle River, BR; Sandpoint, SP; Holiday, HD; Kingsville, KV; Leamington, LE; Point Pelee, PP) for all collection dates of bed sediment. (A) Targets separated by panel; (B) targets combined showing all sample points.	204
Figure 5.3: Heatmaps of expressed transcripts (log copies/g) of prominent GOI quantified from sediment samples. Targets include two FIB (<i>Enterococcus</i> 23S, <i>E. coli</i> 23S) and three MST (general <i>Bacteroides</i> 16S, goose, seagull). (A) Bed sediment samples: six beach locations, each with five collection dates between June and September of 2017. (B) Suspended sediment samples: collected seasonally (spring, summer, and fall) from the lake and tributary in Belle River and Kingsville. Cells with no colour indicate no detection.	205
Figure 5.4: Time series visualization comparing <i>E. coli</i> 23S transcript copies/g of sediment (green bars, left y axis) and <i>E. coli</i> CFUs (red line, right y axis) reported by WECHU for each of the six public beaches studied for bed sediment. CFU data available every week from Week 24-36; transcript data available for Weeks 22, 28, 30, 35, and 37 – not to be confused with no detection of <i>E. coli</i> transcripts for other weeks. Note y-left axis (transcript data) is unique for each graph, while y-right axis (CFU data) is consistent for all graphs.....	206
Figure 5.5: Conceptual diagram depicting the importance and value of targeting different groups of biomolecules from environmental samples through molecular techniques (i.e., qPCR tracking methods). There are three tiers to this hierarchy (i.e., fecal indicator organisms, microbial source tracking, and pathogen identifiers), and each level displays the intended target and biological information revealed from analysing environmental RNA (left) compared to DNA (right). The amount of microbial information gained increases moving up the levels. .	207

LIST OF APPENDICES

APPENDIX A: SUPPLEMENTAL INFORMATION FOR CHAPTER 2.....	231
Figure A-1: NMDS ordination plot of bacterial community composition in the bed sediment of freshwater beaches in WEC. DNA (left) and cDNA (right) datasets are displayed, illustrating beta diversity between sampling seasons (spring, summer, fall). Ellipses represent 95% of samples included.....	231
Figure A-2: NMDS ordination plot of bacterial community composition in the bed sediment of freshwater beaches with environmental factors (grey) included using envfit. DNA (left) and cDNA (right) datasets are displayed, illustrating beta diversity between the six beaches sampled throughout WEC and the influence of select environmental parameters. Categorical factors of Lake and Season are shown with blue diamond symbols. Sample dates are combined for the year.....	232
Table A-1: Physicochemical parameters of the water column. Measurements were recorded at each sediment sample collection for the six WEC beaches studied. Blank cells indicate missing data due to faulty equipment or unreliable probe calibration. DO, dissolved oxygen; ORP, oxidation-reduction potential.....	233
Table A-2: RNA concentrations of individual samples selected for cDNA analyses. Included is basic sample metadata (i.e., collection date and location), the method used for measuring concentration (Bioanalyzer, Qubit, or visualization on agarose gel electrophoresis), and the volume added to the pool of samples for additional normalization prior to sequencing. Volume added was based on agarose gel band intensity; either 2 (dark band), 5 (faint band), or 10 μ L (no visible band).	234
Table A-3: ANOVA and subsequent Tukey's post-hoc results for Chao1 richness estimator and Shannon diversity index on freshwater bed sediment samples. Sample size (n) given directly below dataset name. ANOVA values F and p represent the ratio of two mean squares and the significance value, respectively. Cells corresponding to treatment effect on diversity represent the mean value for that group with standard deviation in brackets. Red text indicates significant effect ($p < 0.05$). Lower case letters indicate where the differences are attributed, based on Tukey's post-hoc test, within the given factor and dataset.....	237
Table A-4: Beta diversity statistics. Permutational multivariate analysis of variance (PERMANOVA) using distance matrices and subsequent pairwise comparisons on freshwater bed sediment samples. Sample size (n) given directly below dataset name. P value represents the significance value with alpha level of 0.05. Lower case letters indicate where the differences are attributed, based on pairwise PERMANOVA, within the given factor and dataset.	238
Table A-5: Summary of microbial community composition for individual beaches, combined over the sampling year for both DNA and cDNA data. Values represent average relative abundance (%) of bacterial population for each individual beach within the taxon category specified at the left. "Other" contains the combined taxa for which individual relative abundances were $< 3\%$ for all locations. "NA" is the combination of undefined or unclassified ASVs at the taxon level specified at the left.....	239
APPENDIX B: SUPPLEMENTAL INFORMATION FOR CHAPTER 3	240
Figure B-1: Line graph depicting the percentage of incidences that reported CFU values of indicator <i>E. coli</i> in the water at WEC public beaches exceeded acceptable levels over the past 7 years. Thick solid lines indicate locations of interest to this manuscript (Belle River (BR),	

Holiday (HD), Kingsville (KV), Sandpoint (SP)), and thin dashed lines represent the other beaches monitored. Data provided by WECHU. Note: up until 2017, acceptable <i>E. coli</i> levels were less than 100 CFUs/100 mL; 2018 it changed to 200 CFUs/100 mL.	240
Table B-1: Summary of sequencing results obtained from the Ion Torrent PGM™. Data determined from recovered DNA and bioinformatics processing.	241
Table B-2. Summary of sequencing statistics for all samples obtained from the Illumina HiSeq 4000 run. Data determined from recovered mRNA and bioinformatics processing. Rows highlighted grey indicate the representative average values for the specified beach. bps = basepairs.	242
APPENDIX C: SUPPLEMENTAL INFORMATION FOR CHAPTER 4	243
Figure C-1: Principal components analysis (PCA) of metatranscriptomic data, examining the functional diversity between samples (beta-diversity) at Level 1 resolution of a) all 8 groups, b) location (BR vs KV), c) season (summer vs fall), and d) site (lake vs tributary). Each plot has the same axes (PC1: 89%, PC2: 6%) and coordinates for samples, but sample labeling modified to view comparisons.	243
Figure C-2: Gene expression heatmap of Level 3 transcripts involved in Energy Metabolism (Level 2), utilizing KEGG annotations and KO database. Pathways involved with photosynthesis [ko00195, ko00196, ko00710], oxidative phosphorylation [ko00190], and chemolithotrophic pathways (methane metabolism [ko00680]; carbon fixation pathways in prokaryotes [ko00720]; nitrogen metabolism [ko00910]; and sulfur metabolism [ko00920]). Expression represented as normalized logCPM values. Pairwise comparisons between sampling sites (lake, tributary) of the same location and season provide statistically significant differential expression ($p < 0.05$), denoted with an asterisk * where applicable.	244
Figure C-3: Functional annotations assigned to dominant transcripts involved in chemolithotrophic Energy Metabolism (methane metabolism [ko00680]; carbon fixation pathways in prokaryotes [ko00720]; nitrogen metabolism [ko00910]; and sulfur metabolism [ko00920]). Heatmap uses colour range and volume proportional size scaling to illustrate expression comparisons of all samples. Expression represented as normalized logCPM values. To demonstrate dominant transcripts, filtering cut-off was set to 50 logCPM total (cumulative for all 8 averaged samples). [Volume proportional to cell value – linear].	245
Figure C-4: Illustrating logFC (fold change) of functional transcripts between sampling sites (lake, tributary) of the same location and season involved in bacterial Infectious Diseases. Transcripts are sorted to their respective pathway. Blue indicates greater expression in the lake; red indicates greater expression in the tributary; x axis explains the degree of expression (logFC). Pairwise comparisons with differential expression ($p < 0.05$) are denoted with an asterisk * where applicable.	246
Table C-1: Summary of seasonal nutrients and total suspended solids (TSS) measured from the water column at each study site. DIC, dissolved inorganic carbon; DOC, dissolved organic carbon; TN, total nitrogen; TP, total phosphorous; NA, not available.	247
Table C-2: Summary of sequencing statistics for all samples obtained from the Illumina HiSeq 4000 PE100 metatranscriptomics run. BR = Belle River; KV = Kingsville; trib = tributary; S = summer; F = fall; bp = basepair; RIN = RNA integrity number; QC = quality control.	248
Table C-3: Summary of raw data used for normalization and statistical tests. The count of sub-categories (in brackets) and genes with observed expression for each category annotated in the KEGG database through MG-RAST (Levels 1, 2 and select pathways of relevance for Level 3) is represented. All samples are the same. Categories/pathways of relevance to this study are	

highlighted. For Level 3 pathways, corresponding ko number is given in square brackets before pathway names.	250
Table C-4: Tabulated summary of gene expression profiles, including raw reads and normalized logCPM values for all replicates (16), for all relevant categories/pathways (Levels 1, 2 and 3) and transcripts (Level 4) with corresponding ko numbers.	252
Table C-5: Tabulated summary of expressed transcripts annotated to the KO database, Level 1 categories. Expression represented as normalized logCPM values (top) and raw read values (bottom), duplicates averaged. Pairwise comparisons between location (BR vs KV), season (summer vs fall), and site (lake vs tributary) provide statistically significant differential expression ($p < 0.05$), denoted with greater than (>) or less than (<) symbol and shaded, where applicable.	262
APPENDIX D: SUPPLEMENTAL INFORMATION FOR CHAPTER 5	263
Figure D-1: Standard curves for the seven GOI detected in this study, generated from complete synthetic genes in plasmid cloning vectors with known copy numbers. Equation of the linear regression line and coefficient of determination (R^2) are displayed within each panel.....	263
Figure D-2: Heatmaps of expressed transcripts (log copies/g) of all (7) GOI quantified from sediment samples. Targets include two FIB (<i>Enterococcus</i> 23S, <i>E. coli</i> 23S) and five MST (general <i>Bacteroides</i> 16S, dog, goose, seagull, human). (A) Bed sediment samples: six beach locations, each with five collection dates between June and September of 2017. (B) Suspended sediment samples: collected seasonally (spring, summer, fall) from the lake and tributary in Belle River and Kingsville. Cells with no colour indicate no detection.....	264
Table D-1: Sample collection details for bed and suspended sediment, including collection dates (2017), corresponding season, and number of samples processed for this research.	265
Table D-2: Unfiltered metadata, includes sampling details (e.g., sample ID, collection date, location, site, sample collection method (centrifuge = suspended sediment, core = bed sediment), weight of extracted sediment, and cDNA concentration) and qPCR results (chip ID, target ID, average Ct and standard deviation, raw transcript expression copy numbers, and final transcript expression copy numbers adjusted for dilutions and sediment weight).	266
Table D-3: Plasmid serial dilutions used for assays of known concentrations for generating standard curves. Values represent plasmid concentration (i.e., number of copies/ μ L).	281
Table D-4: Limit of detection (LOD) and quantification (LOQ) for each gene of interest (GOI) identified in the sediment samples. Copy number determined from serial dilutions and qPCR assays performed for generating standard curves. P1= Plasmid 1; P2 = Plasmid 2.	282
Table D-5: ANOVA and subsequent Tukey's post-hoc results. Sample size (n) given directly below target name (bed, suspended sediment). ANOVA values F and p represent the ratio of two mean squares and the significance value, respectively. Cells corresponding to treatment effect on GOI target represent the mean value (log copies/g) for that group with standard deviation in brackets. Red text indicates significant effect ($p < 0.05$). Lower case letters indicate where the differences are attributed, based on Tukey's post-hoc test. SS; suspended sediment.	283
Table D-6: Pearson's correlation (r) summary of FIB and MST targets detected in bed and suspended sediment samples.	284

LIST OF ABBREVIATIONS / SYMBOLS

ANOVA	Analysis of variance
ARB	Antibiotic-resistant bacteria
ARG	Antibiotic resistance gene
ASV	Amplicon sequence variant
CFU	Colony forming unit
D ₅₀	Median particle size
DO	Dissolved oxygen
DOC	Dissolved organic carbon
EPS	Extracellular polymeric substances
FIB	Fecal indicator bacteria
GL	(Laurentian) Great Lake
HAB	Harmful algal bloom
HGT	Horizontal gene transfer
HTS	High-throughput sequencing
MST	Microbial source tracking
NGS	Next generation sequencing
NMDS	Non-metric multidimensional scaling
NPS	Nonpoint source
PERMANOVA	Permutational multivariate analysis of variance
PGM	Personal Genome Machine
qPCR	Quantitative (real-time) polymerase chain reaction
RIN	RNA integrity number
SS	Suspended sediment
TSS	Total suspended solids

WEC(HU)	Windsor-Essex County (Health Unit)
WOPHC	Waterborne organisms of public health concern
WWTP	Wastewater treatment plant

§	Section
---	---------

Sampling sites:

BR	West Belle River Beach (Belle River)
HD	Holiday Conservation Beach (Amherstburg)
KV	Lakeside Beach (Kingsville)
LE	Seacliff Beach (Leamington)
PP	Northwest Beach (Point Pelee)
SP	Sandpoint Beach (Windsor)

CHAPTER 1: INTRODUCTION

CHAPTER 1: INTRODUCTION

1.0 Background

Aquatic environments – lotic or lentic, freshwater and marine – provide many essential benefits to humans including economic, health, recreation, and cultural value (Papadopoulou et al., 2018), yet their microbial associations can also present significant health risks to humans. In North America, legislation has played a key role in the protection and security of both inland and coastal fresh and marine water. Of significance, and importance to this research, is the Great Lakes Water Quality Agreement (GLWQA) between Canada and the United States of America, established in 1972. This statute, largely based on the 1909 Boundary Waters Treaty between the two countries and guided by the International Joint Commission (IJC), commits both nations to “restore and maintain the chemical, physical, and biological integrity of the waters of the Great Lakes Basin Ecosystem” (Canada-United States, 1972). The Laurentian Great Lakes (herein referred to as the Great Lakes, GLs) are one of the most attractive and important natural resources in the world, making up 21% of the world supply of surface fresh water (Waples et al., 2008). This North American system, which represents a large portion of the geographical divide between Canada and USA with nearly 17,000 km of freshwater coastline (IJC, 2022), is composed of five large interconnecting lakes (Superior, Michigan, Huron, Erie, and Ontario) that channel to the Atlantic Ocean via the St. Lawrence River. These waters have been a major source for transportation, trade, leisure, migration of waterfowl, fishing, and more, providing the foundation for the economies of both countries for centuries. In fact, the Great Lakes-St. Lawrence region generates about six trillion USD of gross domestic product per year and provides more than 52 million jobs in a diverse range of professions (IJC, 2022). Additionally, considering the great dependence of this watershed to agriculture and the fact that 40 million people rely on the GLs

for their drinking water source (IJC, 2022), the importance of this water system is immeasurable and protecting its precious supply of fresh water is of great importance.

Each of the GLs has their own unique characteristics (i.e., aquatic species, water volume, geologic underlay, recreational activities, etc.) as well as threats which need to be evaluated for water security purposes. Anthropogenic impacts, like invasive species (Sterner et al., 2017; Waples et al., 2008), biological/chemical contamination (Cornwell et al., 2015; Hull et al., 2015), heavy nutrient inputs (Baker et al., 2014; Chaffin et al., 2013; Cloutier et al., 2015; Ho and Michalak, 2017), and climate change (Huot et al., 2019; Natural Resources Defense Council, 2014), all have direct measurable influences on these systems, and effectively result in changes to ecosystem dynamics. For example, in the 1970s a significant reduction of eutrophication was observed in all five GLs following the control of phosphorous inputs from large wastewater treatment plants (WWTPs) and in household detergents – an implementation endorsed by the GLWQA (Dove and Chapra, 2015). Eutrophication can have detrimental effects on aquatic ecosystem health, subsequently leading to anoxic zones, reduced production, and harmful algal blooms (HABs) that can potentially result in negative health outcomes to humans and other animals that come into contact (Bullerjahn et al., 2016). Lake Erie, however, has experienced a resurgence of serious eutrophication over the past few decades, despite the continued controls over phosphorous loading from large point sources (Kerr et al., 2016). Now the focus is largely concentrated toward reducing both phosphorous and nitrogen inputs to the watershed despite the growing evidence that nitrogen reduction (or even elimination) does not aid in combating eutrophication (Schindler et al., 2016, 2008). Instead, research is pushing for stronger regulations to reduce nonpoint sources of phosphorous, largely due to increasing intensification of agriculture and high runoff (Kane et al., 2014; Michalak et al., 2013).

Despite the above stressors and their links to human health, the risks are still not fully understood in relation to the evolving microbiome. Certain types of microbes commonly associated with aquatic systems (i.e., waterborne) can cause a number of illnesses, collectively

recognised as *pathogens*. Not only can pathogens cause deleterious health effects and life-threatening disease for individuals, but they also result in negative economic burdens. In the United States, for example, a recent study estimated 90 million recreational water use-related illnesses (e.g., gastrointestinal; respiratory, ear, eye, and skin symptoms) nationwide, translating to an economic cost of \$2.2-3.7 billion per year (DeFlorio-Barker et al., 2018). Microbial contamination in bathing and recreational water is a critical issue worldwide and unfortunately, the problem has grown in severity over recent years as a result of climate change and an increasing global population (Levy et al., 2016).

Pathogenic pollution (e.g., fecal contamination) in bathing and recreational waters is a serious issue around the globe, including the GLs region. Typically, this type of pollution is assessed through traditional water quality tests of culturing and counting fecal indicator bacteria (FIB), such as enterococci or *Escherichia coli*, collected from the water column. Although this approach has been the standard for water safety monitoring for decades, it has several major limitations. 1) These conventional tests are time consuming since culturing typically requires 24-48 hrs for sufficient growth and enumeration. This means, by the time results are publicly available, they are inapt given changing weather conditions and rapid water quality variations due to the dynamic nature of aquatic environments (McPhedran et al., 2013; Shahraki et al., 2021). 2) Because these tests are simplistic and low resolution, they cannot inform on strain-level (i.e., pathogens of concern), activity of the microbial community (i.e., gene expression), or microbial source/origin (e.g., avian, sewage overflow, agricultural). And 3) perhaps of greatest importance is the oversight of traditional tests to include the role that microbe-sediment interactions play in mediating the risk of pathogens to humans as well as the influence they have on water quality in aquatic systems. This is problematic because microorganisms, including pathogens, are known to attach to and colonize grain particles of aquatic environments (Baker et al., 2021; Haller et al., 2009; Ishii et al., 2007). These limitations have been widely recognised over recent years (Sousa

et al., 2015) and research is now focused on these shortcomings to provide more reliable testing approaches and models for microbial contamination in natural waters.

Considering both natural and anthropogenic perspectives, the GLs are affected by a myriad of constant, occasional, and new influences that add pressure to their ecosystem dynamics, function, health, and fate. While some of these influences are known, many, such as the role of suspended and bed sediments with the microbial consortia and human health risks, remain unclear. Studying these important freshwater systems through multidisciplinary approaches and communicating the research and collaborating with the scientific community helps our overall understanding in our effort to protect them now and for future generations.

1.1 Beach Stressors: Contaminant Sources and Physical Dynamics

1.1.1 The NPS continuum of allochthonous material delivery to recreational waters

The close relationship between humans and recreational water underpins the importance to investigate and protect freshwater aquatic systems. Nearshore beach zones receive pollution and harmful substances from a variety of processes and sources, leading to degradation of water quality (Figure 1.1). From a management perspective, point sources of unrestricted effluent (e.g., untreated discharge from WWTPs (Mbanga et al., 2020) and oil spills (Beyer et al., 2016)), are easy to identify and often can be treated through various mitigation strategies. Nonpoint sources (NPSs) or diffuse chronic contaminations, however, are less tangible since they do not originate from a single source but cumulate over a large area and are therefore much more difficult to identify and regulate. For example, precipitation and snowmelt (stormwater) contribute to erosion and flooding in developed locations (e.g., cities), and consequently transport material from terrestrial landscapes to surface water such as rivers, streams, and lakes (Hooda et al., 2000; Montgomery, 2007). As a result, impervious surfaces (e.g., paved roads/parking lots, buildings)

impact infiltration of water, enhancing stormwater runoff from urban areas and is now identified as the largest NPS of pollutants entering waterbodies (Almakki et al., 2019; Arnone and Walling, 2007; Imteaz et al., 2013; Yuan et al., 2017).

The NPS transport continuum of allochthonous loads (i.e., sediments, nutrients, inorganic and organic contaminants, microorganisms) from headwater sources to recreational waters via creeks, rivers, agricultural drains, and urban/industrial runoff for example, can lead to the alteration of water quality with concomitant impacts on aquatic and human health. Furthermore, modifications of the contaminant itself can occur over this distance of NPS transport, such as physical (e.g., changes in particle size, flocculation; Droppo, 2001), chemical (e.g., chemical transformations leading to increased toxicity; Dempsey et al., 1993), and biological (e.g., introduction of new organisms, change in virulence; Trunk et al., 2018) deviations. In terms of microbial pollution, these changes can potentially result in a uniquely different structural and functional profile of the microbial population once delivered to recreational beaches – an aspect which should be considered when investigating NPS contamination of beach zones. It should be recognised, however, that the assessment of transport routes of contaminants to water systems is beyond the scope of this dissertation. For more information on contaminant sources (microbial pollution) and transportation to waterways, the reader is referred to two recent review articles on the topics and references therein; Devane et al., 2018 and Islam et al., 2021.

1.1.2 Microbial contamination

The principal form of microbial contamination of water resources is often related to forms of fecal pollution and can be attributed to humans (i.e., untreated sewage discharged into the environment), domesticated animals (e.g., agricultural runoff containing manure from fields or feedlots), or wildlife (e.g., waterfowl) (Craun et al., 2005; DiCarlo et al., 2020; Ksoll et al., 2007; Maguire et al., 2019). It is well-documented that animal feces contain opportunistic

pathogens and antibiotic resistance genes (ARGs) (Delahoy et al., 2018; Penakalapati et al., 2017; Zhao et al., 2020) – factors that pose significant and growing threats to public and aquatic health. In this light, regulations to control point sources of fecal discharge into the environment are a staple in the health and prosperity of the developed world, focusing on socio-economic principles such as safe water, sanitation, and hygiene (WASH). Globally, however, bathing and recreational waters (i.e., beaches) still pose a concerning level of human health risk related to aquatic biological hazards (DeFlorio-Barker et al., 2018). For example, several public beaches in southwestern Ontario, Canada frequently receive failing water quality assessments throughout the swimming season due to elevated levels of *E. coli* in the water column (Table 1.1). Although very little information is currently available on the full suite of waterborne pathogen presence and activity within aquatic nearshore zones, VanMensel and colleagues recently identified expression of pathogen-related genes in two freshwater beaches (VanMensel et al., 2020 – Chapter 3; VanMensel et al., 2022– Chapter 4). It is this potential of illness and concomitant economic losses that drives the research in this area to investigate NPS origins, especially when identification of FIB suggests alternative, unregulated sources.

Perhaps the largest NPS of FIB and pathogens to aquatic environments can be attributed to the reservoir within foreshore sands and submerged bed sediment (Badgley et al., 2011; Devane et al., 2020; Perkins et al., 2014). It has been demonstrated that FIB can not only survive or persist for extended periods within the sediment compartment but reports of “naturalized” FIB isolated from such locations suggest these microbes have adapted to these habitats and incorporated themselves into the indigenous community (Ishii et al., 2006a; Palmer et al., 2020). This situation further questions the reliability of FIB to serve as a proxy for fecal contamination in aquatic environments. These reports highlight sediment/sand as an important secondary habitat and NPS in beach water quality, especially during resuspension events (e.g., large energy waves, high swimmer density) of submerged particle-bound microbes. Yet this consideration is neglected when recreational water quality is assessed.

While fecal sources are the main source of pathogens, it is important to recognise that there are other sources of non-indigenous microorganisms that can be prevalent in the aquatic environment as well. Pathogens and other biologically harmful substances (i.e., antibiotic-resistant bacteria (ARBs) and ARGs) can also originate from NPSs such as urban runoff/wash-off (Almakki et al., 2019; Arnone and Walling, 2007), industrial sources (Mallin and Cahoon, 2003), or invasive species (Padilla and Williams, 2004). Furthermore, Baquero (et al., 2008) described how the release of industrial antibiotics to water environments has high potential for altering microbial ecosystems, pressuring water-indigenous microbes and exerting selective activities which can result in antibiotic resistance. From this perspective, traditional water quality assessments relying on the enumeration of FIB for beachgoer safety is not sufficient. As such, these microbial communities are poorly characterized, and therefore, their true potential of human health risk is undefined.

1.2 The Microbe-Sediment Relationship

It has long been recognised that bacteria prefer attachment to particles over a planktonic existence (Costerton et al., 1987), yet there still remains a lack of understanding on microbe-sediment relationships in aquatic systems and how these associations impact water quality and consequently human health risk.

1.2.1 Importance of the sediment compartments

Suspended and bed sediments are integral components of aquatic systems that can drive the physical, chemical, and biological dynamics both temporally and spatially within recreation waters. The bed sediment is often referred to as a reservoir of nutrients, contaminants, and

microbes which have a transient existence within a dynamic environment. The ‘building blocks’ of the bed sediment are the suspended sediment (SS) floc that rain down onto the bed, provided the shear stress at the sediment interface is low enough for deposition to occur. The physical (e.g., density), chemical (e.g., nutrient richness), and biological (e.g., microbial consortium) characteristics of the bed sediment profile are in a continual state of flux depending on the changing sources and inorganic and organic/biological makeup of the SS. Once deposited, pathogens (and accompanying microorganisms) have the opportunity to establish themselves and flourish as new members of the benthic community. However, this sediment and its various components can become mobile again if the critical erosion threshold is surpassed; the material can then be deposited in a new location with concomitant impacts. For a comprehensive discussion on sediment dynamics within rivers and lakes, the reader is referred to Droppo (2001) and Droppo et al. (2007).

1.2.1.1 Suspended flocs

Sediment is a broad term that encompasses a wide range of particle sizes and grain minerals within aquatic settings. Cohesive sediment describes fine-grain particles that tend to aggregate (or stick) together, like silt ($<63\ \mu\text{m}$) and clay ($<2\ \mu\text{m}$) and the colloidal fraction of clay minerals ($<0.1\ \mu\text{m}$) (Grabowski et al., 2011). Given the large surface area-to-volume ratio, clay particles are typically the most electrochemically active components of sediment and therefore are largely responsible for the cohesion of these sediments via van der Waals forces and electrostatic attraction (Righetti and Lucarelli, 2007).

Flocs are heterogenous, complex assemblages in aquatic environments composed of inorganic particles (i.e., cohesive sediments), an active biological component (e.g., bacteria), an inactive biological component (e.g., detritus), and water (held within and flowing through)

(Droppo, 2001). As such, flocs have often been referred to as ‘suspended biofilms’ (Droppo et al. 2005). These structures are ubiquitously found within the water column and are held together through the cohesion of sediment particles as well as from the extracellular polymeric substances (EPS) that are secreted by some of the microbial community members involved (Gerbersdorf and Wieprecht, 2015). They are physically, chemically, and biologically in a constant state of flux with their surrounding environment, as the aquatic medium is dynamic itself and continuously supplying additional building materials (e.g., inorganic particles, microorganisms), and nutrients, energy, and chemicals for microbial metabolism and growth (Lai et al., 2018). Consequently, flocs are known to influence the surrounding water quality through their continual interaction with the aquatic surroundings (Liss et al., 1996).

Flocculation is a complex cycle of microbial attachment to sediment particles, floc growth and microbial secretion of EPS, floc deposition and incorporation into the bed, followed by erosion and resuspension back into the water column when turbulence/shear stress surpasses the erosion threshold (Lai et al., 2018). Previous studies have identified that this process significantly alters sediment dynamics and hydrodynamic properties compared to the pure-mineral dynamics. In particular, colloid particles do not readily settle out of suspension because of their small size; however, flocculation increases the effective particle size, thus encouraging sedimentation of these minerals (Droppo, 2001; Grabowski et al., 2011). In terms of sediment-bound contaminants (e.g., pathogens), a laboratory wave flume study demonstrated the dynamic interaction of bacteria with sediment particles and highlighted the need to recognise eroded flocs as a transport vector of bacteria with regards to beach quality monitoring (Sousa et al., 2015). Flocculation supports the dispersal of such material and leads to the seeding of the bed with allochthonous substances, allowing introduced microbes an opportunity for establishment within the benthic community (Anderson et al., 2006; Sousa et al., 2015).

Considering the complicated mechanisms for floc formation/breakage and diverse composition (i.e., physical, chemical, and biological variations in general), Droppo (et al., 1997) appropriately defined a flocculated particle as an;

‘individual microecosystem (composed of a matrix of water, inorganic and organic particles) with autonomous and interactive physical, chemical and biological functions or behaviours operating within the floc matrix.’

1.2.1.2 Bed sediment and associated microbial biofilms

Bed sediment serves as substrates for microbial attachment and the formation of sessile biofilms. Biofilms are a functional component for the health and function of the microbiome in both marine and freshwater environments (Noe et al., 2020). They are surface-attached assemblages that represent a complex consortium of microorganisms and provide many benefits to the microbes involved, including access to nutrients and dissolved organic carbon (DOC) (Donlan, 2002) and protection from predation (Weitere et al., 2005). In addition, they serve as protection from other environmental perturbations (e.g., ultraviolet radiation, extreme temperature and pH fluctuations, antibiotics, etc.; Yin et al., 2019), and provide community living advantages such as quorum sensing (Jayatilake et al., 2017; Pasmore and Costerton, 2003) and strong potential for horizontal gene transfer (HGT; Abe et al., 2021). These heterogeneous assemblages are composed of a range of microorganisms such as autotrophic, heterotrophic and chemolithotrophic species which capitalize on both organic and inorganic material in the sediment and water column (Donlan, 2002). As such, they are dependent on external factors and considered to be in a constant state of flux.

The primary matrix component of biofilms, aside from microbial cells, is the EPS provided by the microorganisms themselves, which are mainly composed of polysaccharides, proteins and lipids that confer the anionic property important for surface attraction/attachment

and the resilient architecture of the three-dimensional matrix (Decho, 1990; Donlan, 2002; Flemming, 2011). In essence they are the sticky material that ‘glues’ inorganic (i.e., sediment) and organic (e.g., bacteria) particles together. This microbial mediation of cohesion and aggregation of particles in suspension or on the bed (biofilm integration) has often been referred to as biostabilization (Droppo, 2001; Droppo et al., 2007; Noffke and Paterson, 2008; Reid et al., 2016). Biostabilization is cyclic as microbial associations and functions vary given changing environmental conditions in the water column and at the sediment water interface (Gerbersdorf and Wieprecht, 2015).

Overall, the growth, metabolic activity, and survival of biofilm members outcompete their free-living companions by far, and since FIB *E. coli* and enterococci have both been described to form sand-associated biofilms (Phillips et al., 2011; Wang et al., 2011), research on aquatic biofilms is particularly important. In the context of human health risk from recreational water use, if FIBs can grow and thrive within biofilms, other waterborne organisms of human health concern (i.e., pathogens) can also be expected to be present and active here, warranting a thorough investigation of sediment-associated microbial communities in recreational waters.

1.2.2 Microbe-sediment dynamics

There has been considerable research on pure-mineral energy dynamics in marine and freshwater systems, yet the accuracy and reliability of predictive models is greatly reduced when the microbial layer, water quality, and the contribution from tributaries are included (Madani et al., 2020; Mooney et al., 2020). There are many physical, biochemical, and hydrometeorological factors that add to the complexity of microbe-sediment relationships, such as particle size (Wijesiri et al., 2016), water flow/current (Gao et al., 2015; Kashefipour et al., 2006), nutrient availability (Moncada et al., 2019), and decay rates vs. naturalization (Ishii et al., 2006a), among many others. This makes it extremely difficult to develop a reliable predictive model for

microbial contamination of natural waters and beach zones (Madani et al., 2020; Weiskerger and Phanikumar, 2020). Recently, however, Madani (et al., 2022, 2020) developed numerical models of Lake St. Clair to better simulate and understand hydrodynamics and water quality. The research on pure-mineral energy dynamics serves as the baseline and beginning to comprehend the complicated transport, storage, and fate of sediment-associated microorganisms in aquatic systems.

1.2.2.1 The impact of sediment dynamics on aquatic ecosystem health

Investigating pure-sediment dynamics in diverse settings has led to the development of localized models for specific tributaries or shorelines (Park and Latrubesse, 2014; Shrestha et al., 2013). Filling these knowledge gaps has provided an overall understanding of sediment energetics (i.e., erosion, deposition, transport, and resuspension) within nearshore beach zones (Hatono and Yoshimura, 2020). Anthropogenic (e.g., swimmers) and natural (e.g., extreme weather) events can influence sediment dynamics leading to an over or under supply of fine-grained materials which can alter the overall synergy of the entire ecosystem in many ways (Noe et al., 2020). For example, high concentrations of fine-grain particles and increased sedimentation rates can lead to steep vertical geochemical gradients (e.g., dissolved oxygen, REDOX) at the sediment-water interface (Chen et al., 2013). This can have negative biological impacts, such as restricted growth of important benthic algae (Yamada and Nakamura, 2002) and submerged aquatic vegetation (SAV), impacting juvenile fish populations that these SAV beds support (Jarvis and Moore, 2015). Conversely, high concentrations of SS can directly affect aquatic biota by decreasing light penetration and therefore suppressing primary production (Wood and Armitage, 1997), clogging fish gills (Kemp et al., 2011), and can even alter fish movement and predator-prey interactions (Kjelland et al., 2015). Further, high levels of SS diminish the

perception of water quality and value for recreational use and aesthetic purposes (Gibbs et al., 2002).

The role of SS has long been considered an important vector for various organic and inorganic materials. Several studies have reported on the sorption/desorption processes of bound nutrients (e.g., P and N) and contaminants (e.g., metals, organic matter, etc.) with sediment and how these relationships are important for understanding contaminant fate during transport and storage in sediment accumulation zones (Foster et al., 2000; Owens et al., 2019; Withers and Jarvie, 2008; Yunker et al., 2002). Strong correlations between pollutant affinity and suspended particles can affect reactivity, toxicity, and mobility of pollutants, which highlights the significance of particle-bound contaminants in the degradation of water quality (Dempsey et al., 1993). Recognising this key feature of sediment in aquatic environments is critical for researchers and policymakers to understand the source, distribution, and fate of water contaminants, especially those derived from NPSs. Unfortunately, most sediment dynamics studies and models to date do not consider the significant association between sediment particles and microbiology, yet there is much evidence that microbe-sediment relationships play a key role in the overall health and function of aquatic systems (Droppo et al., 2009; Haller et al., 2009; Huettel et al., 2014; Sassi et al., 2020). Therefore, it is important to investigate these relationships, study their dynamics, and identify the microbial content associated with both bed and suspended particles, especially considering the strong case for sediment as a vector for other types of contaminants in water.

1.2.2.2 Energy dynamics in the beach zone

The stability of suspended (floc) and bed sediment, and therefore, aquatic and human health risk, is related to the varying critical shear stresses imposed on suspended floc and bed substrates by the ambient water energies. Oscillating energy levels derived by such entities as

wind (i.e., wave height), current (i.e., longshore or river inputs), and anthropogenic disturbances (e.g., swimmer density) will clearly have an influence on the source, fate, and effect of microorganisms (pathogens). Higher energy affects episodic floc breakage and bed erosion events resulting in elevated levels of planktonic microbes/pathogens (Fabbri et al., 2017; Peterson et al., 2015). The “release” of sediment-associated microbes into the planktonic phase may result in; 1) a wider geographical distribution of health risk, and 2) a localized (i.e., recreational waters/beaches) increase in ingestible microbes with concomitant increasing health risk. As such, it has been demonstrated that beaches with naturally lower wave energy (e.g., from natural embayment or from construction of man-made piers) tend to have greater levels of FIB (Feng et al., 2016), as compared to high-energy locations which are much less favourable to harbour FIB due to limits in flocculation, microbial/floc settling and deposition (Abreu et al., 2016; Donahue et al., 2017; Yamahara et al., 2007).

1.3 Aquatic Microorganisms: Small Size, Large Impact

1.3.1 Diversity in numbers, structure, and function

Marine and freshwater environments host a vast array of diverse microorganisms that provide an extremely wide range of essential ecological functions to preserve and protect the surrounding ecosystem (Zinger et al., 2012). Although a great deal of uncertainty accompanies the prediction of earth’s biodiversity, it has been estimated that the bacterial population of the global ocean consists of 2×10^6 different taxa, while a ton of soil can contain 4×10^6 different taxa (Curtis et al., 2002). The uncertainty of these estimations can be attributed to the many different geochemical niches found throughout aquatic systems (e.g., biofilms – on bed sediments, suspended particles, other aquatic biota such as fish or vegetation; planktonic organisms in varying hydrological conditions; the influx of new microbial content via NPS; etc.).

Specialized metabolic activities of aquatic microorganisms include biodegradation of chemical hazards, such as heavy metals (Dixit et al., 2015), petroleum (Zaki et al., 2015), and plastics (Ganesh et al., 2020), of natural and anthropogenic environmental toxins (e.g., microcystin; Salter et al., 2021), and an incredible range of biogeochemical processes that are vital to closing the loop of organic and nutrient recycling and overall environmental sustainability (Falkowski et al., 2008). Further, these resilient microscopic communities have a remarkable ability to adapt to a changing environment (i.e., plasticity) and evolve new strategies for survival when required (Beier et al., 2015; Fasching et al., 2020), emphasizing the robustness and influence of these tiny organisms. Despite the positive influence microorganisms have on the global ecology and overall health, waterborne pathogens and their associated human diseases are a major public health concern around the world, with increasing risk due to climate change and a growing population (Levy et al., 2016).

1.3.1.1 Waterborne organisms of public health concern and fecal indicator organisms

Waterborne pathogens are ubiquitous in natural aquatic environments and can directly affect other water-associated organisms, including fish populations (Austin, 2011; Leung et al., 2019), aquatic plants (e.g., in aquaponics systems; Mori and Smith, 2019), and coral reefs (Rosenberg et al., 2007; Sweet et al., 2013), or indirectly such as the case of introducing plant pathogens to agricultural crops through the application of contaminated irrigation water (Hong and Moorman, 2005). Waterborne human pathogens, however, have received most of the scholarly attention as the potential for human health risk from exposure to contaminated water sources has been a major public health concern for over a century – since the profound discovery of a bacterium in drinking water (i.e., *Vibrio cholerae*) as the aetiologic agent of cholera (Koch, 1884; Snow, 1855).

According to Farrell (et al., 2021), waterborne organisms of public health concern (WOPHC) are microorganisms that are transmitted in water and have the potential to cause illness or disease to humans. There are numerous factors that contribute to disease development such as minimal infectious dose (MID), pathogenicity, host susceptibility, and environmental conditions (Ramírez-Castillo et al., 2015). Furthermore, survival and persistence of WOPHC in the environment depend on various factors such as temperature, UV light exposure, availability of nutrients, and predation or microbial competition (Korajkic et al., 2019). Each pathogen is unique in these features, thus complicating detection, identification, source tracking, and further investigation in aquatic systems.

The recognition that water contaminated with sewage spreads human diseases (like cholera) led to the implementation of testing for fecal pollution in water sources, including drinking and bathing waters (Holcomb and Stewart, 2020). Microorganisms present in feces are naturally derived from the gastrointestinal tract. Although the bacterial species composition of this community in a particular host (e.g., humans) can vary on a daily basis and between individuals, the composition at the genus level is generally considered stable (Cabral, 2010). Several studies have characterized the microbial community directly from the gut (Faith et al., 2010) or fecal material (Ervin et al., 2013; Lee et al., 2011), but detection, identification, and quantification in the environment is a bigger challenge, especially of pathogenic taxa which can be of low concentration and difficult to culture (Cabral, 2010). Therefore, the concept of using a microbial proxy to implicitly measure fecal pollution was introduced – *indicator organisms*.

E. coli is a highly versatile and diverse bacterium that holds a complex multifaceted niche in nature. It is primarily found in the gut of mammals, including humans, and is discharged into the environment in large quantities through fecal matter (Ahmed et al., 2016). It is also quite easy to work with and has a generation time 20 minutes under ideal conditions. For these reasons, *E. coli* has been branded as the gold-standard FIB used to measure environmental contamination and unsafe conditions for humans in recreational water. However, *E. coli* also naturally resides in

other habitats, such as the gut microbiomes of birds, reptiles, and fish, as well as in soil, water, sediment, plants, and food (Leimbach et al. 2013). Furthermore, there are hundreds of *E. coli* strains, yet only about 53% of the species' pan-genome is shared among all members (Park et al., 2019), which explains how there are both commensal and several pathogenic variations. To further add to the complexity of these organisms, many commensal strains contain virulence-associated genes and therefore hold the potential to turn from harmless to dangerous depending on various environmental factors, which are not necessarily predictable (Zhang et al., 2021). Additionally, pressure from the mammalian immune system can cause pathoadaptive mutations in commensal *E. coli*, and result in the evolution to pathogenicity (Proença et al., 2017).

The use of FIB such as the fecal coliform *E. coli* to predict fecal pollution has been used for over 150 years, and still proves valuable for simple and general water quality assessments (Holcomb and Stewart, 2020). However, there are many recognised limitations of the FIB approach as well, including the inconsistent relationships between FIB quantification, the presence of pathogens, and human health risks (Fewtrell and Kay, 2015; Korajkic et al., 2018).

1.3.2 Measuring the microbial potential through water monitoring

According to a 2013 US survey (Natural Resources Defense Council, 2014), the GLs had the most frequent cases of *E. coli* concentrations that exceeded acceptable levels in the country. Water quality assessments in North America are commonly performed at public beaches following a United States Environmental Protection Agency (USEPA) protocol. In this approach, water quality is determined by enumeration of *E. coli* colony forming units (CFUs) from defined volumes of collected water (USEPA, 2000). Similar approaches have been implemented around the world, with European recreational waters evaluated for CFUs of FIB (*E. coli* or enterococci) in the water column under the Bathing Water Directive (Farrell et al., 2021). *E. coli* is acknowledged as a FIB because they are found in the intestines and feces of humans and animals

(McQuaig et al., 2012; Whitman et al., 2014). Therefore, the assumption with this enumeration method is that, when high levels of *E. coli* are found in water, it generally indicates contamination from human or animal waste, which could potentially mean there are other harmful bacteria in the water as well (Roslev and Bukh, 2011).

Unfortunately, these water quality assessments have several limitations, and the results can be misleading when evaluating the status of a particular location. First, the sampling method is flawed; tests are only performed occasionally (i.e., low frequency), with low volume and small number of samples (Farrell et al., 2021). This is problematic as several studies have identified substantially high same-day variability of microbial concentrations in recreational water, both spatially and temporally (McPhedran et al., 2013; Shahraki et al., 2021; Wyer et al., 2018).

Second, water tests typically occur during low activity periods (i.e., calm conditions, no beachgoers), are time consuming, and disregard any physical factors that can have an impact on the water quality. In other words, these tests assume pathogens are planktonic organisms, while it is largely understood that bacteria prefer attachment to particles (Costerton et al., 1987). For instance, storm events accompanied by strong winds and waves are capable of resuspending bed sediment into the water column; past studies have shown that sediment dynamics (resuspension, erosion, transport, deposition) influence both the temporal and spatial variation in microbial communities within both the sediment and water compartments (Feng et al., 2013; Ge et al., 2012; Phillips et al., 2014; Wainright, 1990). It has been reported that benthic microbial communities can be up to 10,000 times denser than those in the water column (Probandt et al., 2018), with more than 99% of those microbes attached to sand grains in sandy sediments (Rusch et al., 2003). On the other hand, there is convincing evidence that fine-grained cohesive sediments, which have a tendency toward flocculation, also have strong associations with aquatic microorganisms (Shen et al., 2019), including pathogenic bacteria (Droppo et al., 2009). Furthermore, several studies have documented that sand reservoirs of FIB play a large role in

beach water samples exceeding regulatory limits (Alm et al., 2003; Beversdorf et al., 2007; Cloutier et al., 2015; Yamahara et al., 2009).

Lastly, these simple water quality assessments only target and enumerate one general organism (i.e., FIB) that does not relate to important human health aspects such as strain-level (i.e., pathogens of concern), activity of the microbial community (i.e., gene expression), or contamination source or origin (e.g., avian, sewage overflow, agricultural). Therefore, the status of the water may not be accurately represented by these traditional water quality assessments and calls for improved sampling, molecular techniques, and analyses approaches. Especially considering the growing body of literature demonstrating the lack of reliable relationships between detected FIB concentrations with notable WOPHC and human health risks in aquatic environments (Fewtrell and Kay, 2015; Korajkic et al., 2018), it is time for standard recreational water quality assessments to be revised.

1.3.2.1 Novel techniques

Improved molecular techniques are required to properly evaluate recreational water quality and human health safety more precisely and quickly than current culture-dependent enumeration methods, particularly when more than one target is desired (Wolk and Hayden, 2011). Presently, the approach of quantifying a single FIB (e.g., *E. coli*) within the water column does not inform the full biological potential for human health risks during recreational water use in the nearshore beach zone (as discussed above).

The paradigm shift that led to a new wave of studying microbiology without culturing bias was the application of PCR, a revolutionary technique that allows exponential amplification of specific DNA sequences (Mullis et al., 1986; Saiki et al., 1985). Quantitative real-time PCR (qPCR) has become a leading tool for detection and quantification of multiple specific molecular

targets on multiple samples simultaneously (e.g., microfluidic, nanofluidic plates; Friedrich et al., 2016; Morrison et al., 2006; Shahraki et al., 2019). This approach has been successfully utilized for source tracking pathogens (e.g., *Bacteroides*, *E. coli*) in various environments and media (e.g., wastewater, rivers, lakes) from various origin species (e.g., human, avian, bovine) (Edge et al., 2021; Li et al., 2021; Phelan et al., 2019).

Advancing molecular technology even further, new meta-omics techniques have gained popularity over the last few decades, provided by massive parallel sequencing (or next-generation sequencing, NGS) technology (e.g., Illumina and Ion Torrent platforms), and have facilitated a significant expansion of our knowledge regarding uncultured microbial communities in various environments (Handelsman, 2004). These innovative approaches have expanded environmental studies of uncultured microorganisms from simple taxonomic surveys (i.e., metagenomics) to include the functional potential of the community (i.e., metatranscriptomics), the active phenotype of the community (i.e., metaproteomics), and the physiology (or active metabolisms) of the community (i.e., metabolomics) (Aguar-Pulido et al., 2016; Handelsman, 2004).

The above-mentioned techniques offer several advantages over culture-based methods, including *in situ* investigations and the simultaneous sequencing of multiple targets (i.e., multiplexing) and samples (i.e., metabarcoding). Considering these techniques and tools are becoming more readily available (Morrison et al., 2006), more feasible, and have much higher sensitivity (Friedrich et al., 2016) than traditional water quality assessments, it is important they are applied more frequently (on both sediment and water compartments of aquatic environments) to provide greater depth of knowledge on the microbial structure, diversity, functional capacity, pathogen sources, and potential human health risks.

1.4 Implications of Waterborne Human Pathogens in Recreational Waters

The abundance and influence of pathogens in aquatic systems depends on several factors including the degree of contamination, the organism's ability to persist in the new environment, physical and biological reservoirs (e.g., sediments, aquatic vegetation), and potential for mobility. For instance, once introduced into a body of water, some pathogenic bacteria are able to not only survive for long periods of time (Baker et al., 2021), but have been shown to thrive in their new environment (Ishii et al., 2006a). These observations conflict with the notion of classical growth cycles and decay rates of microorganisms since variations will always exist when comparing dynamic systems (i.e., natural environment) to a controlled laboratory microcosm (Haller et al., 2009; Korajkic et al., 2019). Pathogens can take refuge in environmental reservoirs, like the green alga *Cladophora* (Byappanahalli et al., 2009; Ishii et al., 2006b) or harboured in sediment (Chandran et al., 2011), which improves survival in beach environments. This makes it especially difficult to identify or confirm recent fecal contamination, thus complicating the safety status determination of a beach for recreational water use.

Pathogenic contamination in bathing waters poses significant challenges to water managers, policymakers, and scientists alike as many critical stressors affect these locations (Figure 1.2). Human pathogens in recreational waters have several documented origins, including domesticated animals, wildlife, and humans themselves (Craun et al., 2005; Ksoll et al., 2007). Their departure from these sources and subsequent transport to new locations is an important vector to study and understand in relation to human health. The affinity of pathogenic microorganisms for, and their distribution within, sediment is still unclear. Identifying the presence of pathogens (bacterial, viral, protozoan, etc.) can be a large challenge on its own considering their microscopic size and possibly low abundance in the environment. Limited source tracking information pertaining to the pollution type is even more problematic, especially if it is NPS. Recent advances in sampling approaches, processing tools, and the ability to interpret

statistical trends in microbial consortia (bioinformatic databases; Ju and Zhang, 2015) have substantially narrowed the knowledge gap in this area.

Research on waterborne pathogens in recreational waters has gained scientific interest and appreciation in recent years, yet our understanding is still limited. There are many variables (that have been accounted for so far) that influence the potential for human disease or illness from recreational water use; for example, point and nonpoint sources (and degree) of contamination, the influx and availability of nutrients to support the microbial community, and environmental conditions such as wave energy, temperature, and geological characteristics (e.g., sediment grain size and mineralogy). The synthesis of this subject and, therefore, development of reliable predictive models is not straightforward. As such, current methods to determine accurate beach water quality are unreliable at best (Weiskerger and Phanikumar, 2020).

Considering aquatic microorganisms (and pathogens) have strong associations with (and reliance on) sediment particles for survival and function, it is imperative that both the suspended (i.e., flocs) and bed sediment compartments be thoroughly investigated at the molecular level. To properly assess nearshore environments for potential human health risk during recreational water use, a full microbial (and molecular) baseline of freshwater ecosystems is required, and inclusion of the sediment compartments is key. It is necessary to characterize the presence and activity of the microbial community associated with the sediment in freshwater ecosystems to improve our understanding of human health risk in recreational waters. This dissertation will address some fundamental unknowns in this subject with respect to bacterial pathogen distribution, community identification and functional activity associated with the sediment (bed and floc) in freshwater environments. As these fields of research continue to advance and more knowledge is gained, communication and collaborations will be increasingly important to safeguarding not only human health in recreational water, but natural aquatic environments as a whole.

1.5 Research Focus

The research incorporated into this dissertation addresses water security concerns regarding microbial community composition and functionality within freshwater systems, linking the presence, activity, and transport of pathogens with sediment-microbe dynamics (Figure 1.3). There are five main types of microbial pathogens: bacteria, viruses, protozoa, fungi, and the eggs and larvae of helminths (Parker et al., 2016). The research presented here focuses on bacterial microorganisms, converging on bacterial pathogens associated with suspended and bed sediment from freshwater beach samples.

The overall goal of this dissertation is to bridge the knowledge gap between sediment-microbe dynamics, aquatic pathogen activity, and water security of freshwater ecosystems. The main objectives are to, 1) characterize the microbial community of freshwater nearshore sediments through genomic techniques, 2) identify the key metabolic activities that drive these communities and specifically identify gene expression with regards to pathogenicity through transcriptomic approaches, 3) understand what role the sediment compartment plays concerning microbial structure and function (spatially and temporally), as well as how it behaves as a transport vector and/or reservoir to support microbial habitats, and 4) utilize novel genomic and molecular techniques to link the microbe-sediment relationship in freshwater systems to potential human health risks within recreational waters. This dissertation has four research-based chapters (two are published and one was recently submitted), all which build sequentially on one another towards fulfilling the objectives of this thesis. Here, pathogen potential within Laurentian Lake environments is addressed, with the findings of this research applicable throughout the GLs and other large freshwater systems in Canada and around the world.

1.5.1 Research hypotheses

Chapter 1 provides a comprehensive literature review on topics and concepts related to the research explored throughout this dissertation. This chapter provides the reader with background information on environmental stressors (microbial pathogens in particular) of beach zone areas, microbe-sediment relationships, the impactful role the sediment compartments (suspended and bed) play in water quality and overall ecosystem health, recreational water quality assessments (traditional approaches and novel techniques currently being explored), and the potential for human health risk in these environments. This chapter also highlights the knowledge gaps in the field and emphasizes how the research presented in subsequent chapters of this dissertation contributes to our overall understanding of human health risks in recreational waters and how it can be used to advance research and strategies for freshwater security.

Chapter 2 assessed the microbial community composition within the bed sediment of local freshwater beaches. The first hypothesis of this research is that the aquatic bacterial community composition within the bed sediment of local freshwater beaches varies spatially and temporally. It is expected that pathogenic taxa display greater abundance correlated to warmer temperatures and certain sediment characteristics (i.e., finer grain size provides a more suitable microbial habitat for biofilm formation and pathogen proliferation). To test this hypothesis, the microbial consortia of nearshore bed sediment at select beaches on Lake St. Clair and Lake Erie was characterized from spring through fall in 2017. In particular, the sediments were taxonomically evaluated and cross-referenced to the complementing physicochemical attributes of the sites. Altogether, this chapter provides a holistic perspective of the geochemical drivers and microbial structure of these nearshore zones over space and time.

Chapter 3 investigates the microbial functionality (i.e., gene expression) within the freshwater beach bed sediments. The second hypothesis of this research suggests that the bacterial community within the nearshore bed sediment of freshwater beaches shows greater metabolic and

pathogenic-related activity in correlation with finer grain size and low-energy dynamics in comparison to high-energy, larger particle beaches. To test this hypothesis, RNA was isolated from four local beaches and analysed through metatranscriptomics, focusing on chemolithotrophic metabolisms and pathogenic-related pathways. The work in Chapter 3 takes the taxonomic assessment of these bed sediments from Chapter 2 a step further by providing insight into the functionality of these communities. Although taxonomic approaches can identify the potential of a microbial community, we gain additional and critical knowledge of the microbial activity through transcriptomics. This work evaluates the functional annotations being expressed by the microbes present and provides key evidence of a wide range of activities, specifically concentrated on energy metabolism and pathogenicity. Through this chapter, we obtain a stronger level of understanding of these bed sediment communities and further evaluate their potential to affect the quality of the overlaying water column and, ultimately, the health risks these areas hold for humans and aquatic species.

Chapter 4 examines the microbial activity (i.e., gene expression) within the SS fraction of two local tributaries and their adjacent nearshore beach zones. The third hypothesis suggests that microbial content, including bacteria with pathogenic-related transcripts, is capable of relocation through aquatic systems via association with SS/flocs. To test this hypothesis, Chapter 4 evaluates sediment dynamics and microbe-sediment interactions of freshwater systems by investigating the expression of transcripts collected from total suspended solids (TSS) in freshwater tributaries as well as adjacent nearshore zones in the receiving lake. A comprehensive investigation into the SS fraction links our understanding of the microbial community function in the nearshore with the vector of transportation via moving sediment. This information is directly valuable for understanding how bacterial pathogens reach our swimming zones in the GLs through NPSs by considering sediment movement from adjacent tributaries, with a look into what these waters contain and where they come from (e.g., agricultural landscapes). This research chapter is also useful for investigating the perspective of bed sediment potential to act as a

bacterial source or sink (considering SS/flocs are the building materials of the bed), and what this might mean in terms of water quality during resuspension events and erosion/deposition.

Chapter 5 explores the potential for human health risk in greater detail at the local beaches, building off the combined data/results from the previous research chapters. The fourth hypothesis assesses if the sediment compartment (both bed and suspended) shows notable association with active FIB, microbial source tracking (MST) genes, and select pathogens, both spatially and temporally, within freshwater environments. To test this hypothesis, samples were selected for targeted transcriptomics through multiplex qPCR to quantify gene markers of specific waterborne bacterial pathogens (i.e., virulence factors), FIB, and MST genes. In general, this work supports and builds off the findings presented in the previous chapters; Chapter 5 aims to examine the spatiotemporal pathogenic gene expression associated with the bed sediment of the swimming zone of freshwater beaches throughout southwestern Ontario. It also aims to seasonally characterize the pathogenic gene expression connected with SS of local tributaries and their respective receiving beaches and examine the cyclic interplay between the bed and SS of freshwater systems. This assessment corroborates the previous research in this dissertation with high-specificity RNA sequencing to deduce the presence and activity of specific pathogenic strains as well as MST genes that will better describe human health risks with recreational water use and help guide management of these public locations.

Chapter 6 provides a summary of conclusions and major findings of the research presented throughout. This chapter is a concise synthesis of the previous chapters and provides insight into where future research should focus to continue advancing our understanding of human health risks in recreational waters, with the fundamental goal of identifying and characterizing the microbial and molecular content of these systems and treating and protecting these precious freshwater environments now and in the future.

Figures and Tables

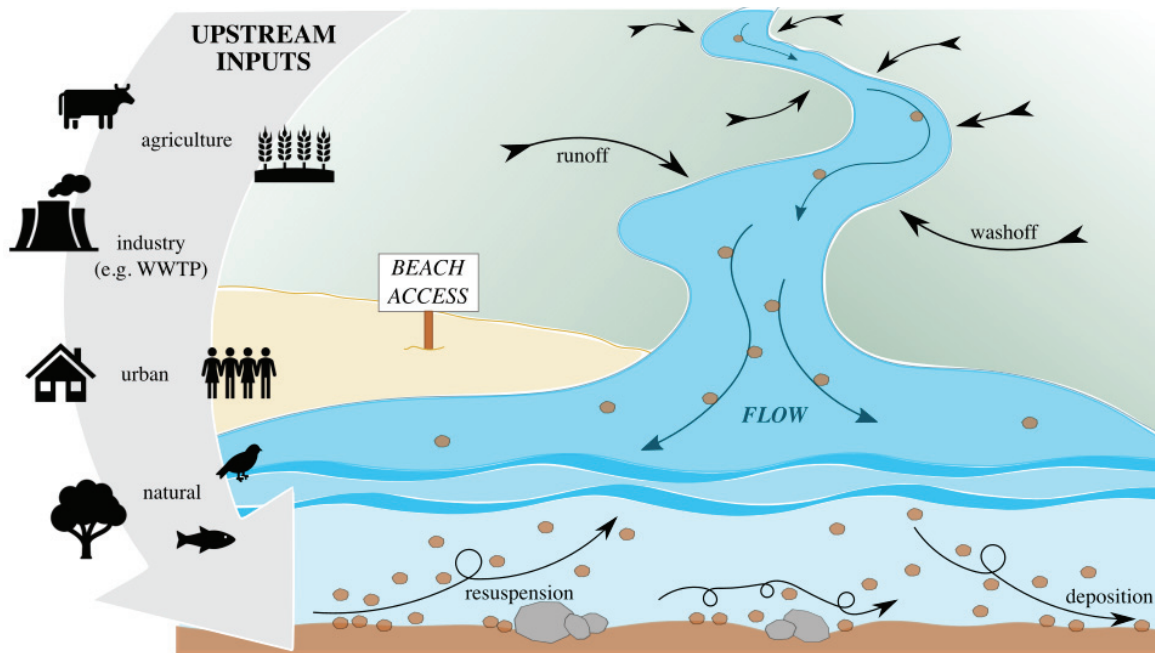


Figure 1.1: Illustration depicting common sources of pollution and microbial contamination to nearshore beach zones. Upstream inputs are transported to watersheds and tributaries via runoff and wash-off processes, move to receiving waters (i.e., lakes and oceans) with water flow, and potentially lead to negative impacts on water quality and safety status of beaches.

Modified from VanMensel et al. 2022.

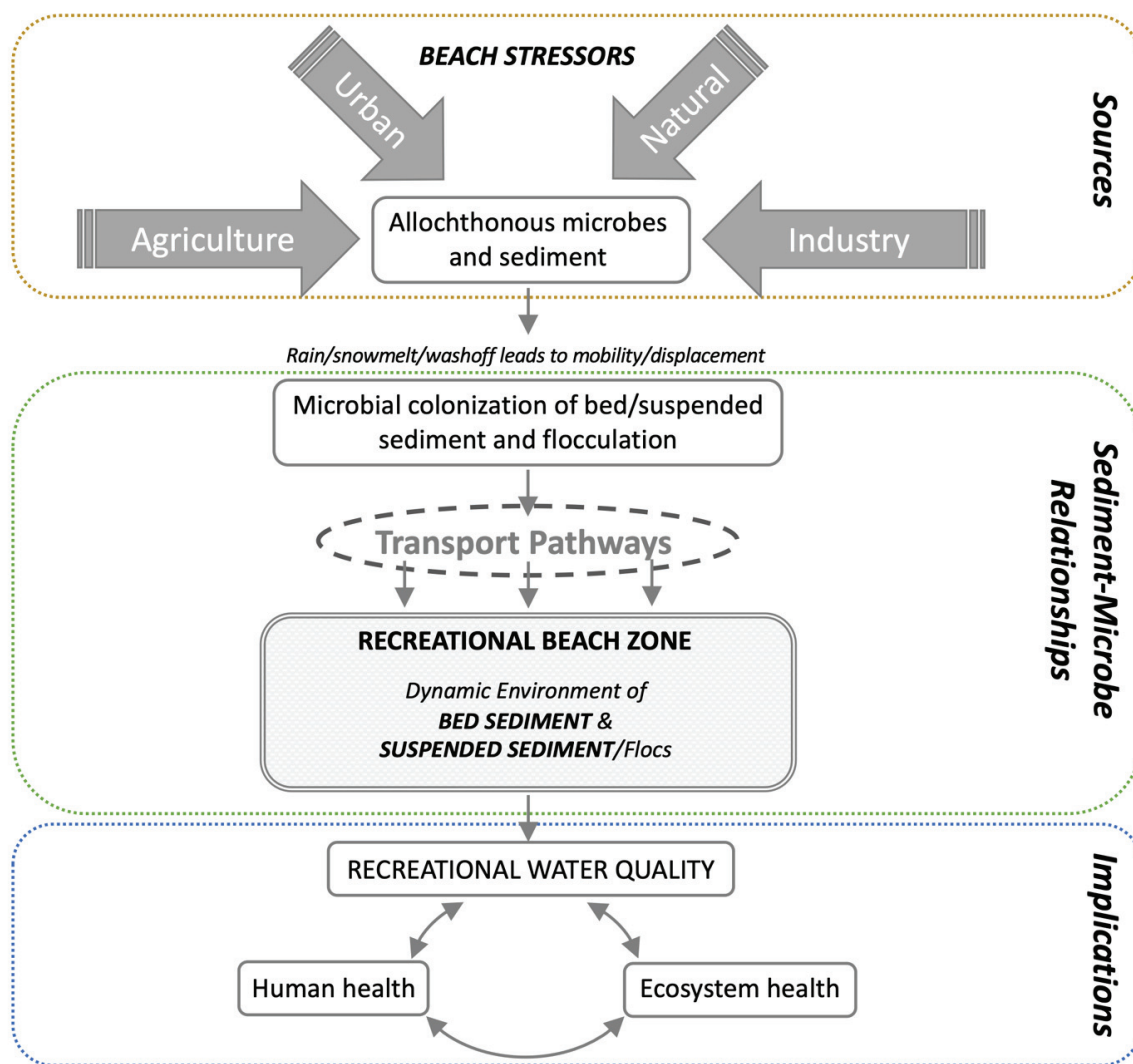


Figure 1.2: The flow of pathogenic pollution from source to recreational waters can be viewed schematically to illustrate the mechanisms and relationships involved in pathogen transport, survival, and ultimately water quality and human and ecosystem health.

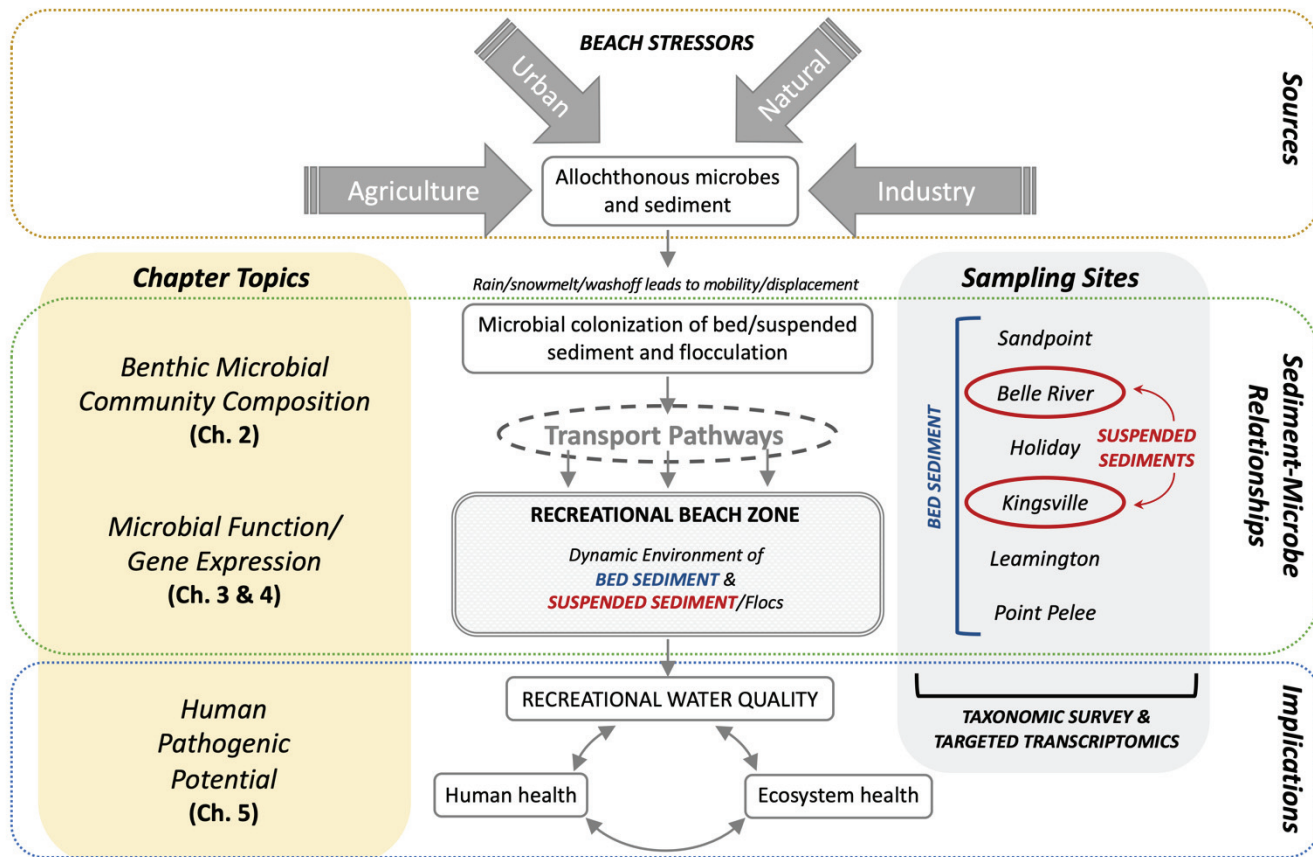


Figure 1.3: The flow of pathogenic pollution from source to recreational waters can be viewed schematically to illustrate the mechanisms and relationships related to pathogen transport, survival, and ultimately water quality and human and ecosystem health. Topics discussed in this dissertation are detailed by chapter (left, yellow) and sampling sites explained (right, grey).

Table 1.1: Frequency of reported *E. coli* CFUs sampled from lake water exceeding acceptable levels at six public beaches in WEC. Percentages correspond to the number of times testing yielded failed results divided by total sampling days throughout the swimming season (shown below percentages), reported by WECHU from 2016 to 2021. Beaches which reported unsafe *E. coli* levels for human recreational activity at least 50% of the time are highlighted. Data retrieved from WECHU public access webpage (www.wechu.org).

Public Beach	2016	2017	2018	2019	2020	2021
West Belle River Beach (Belle River, ON)	86% 12/14	57% 8/14	60% 9/15	27% 4/15	27% 4/15	56% 10/18
Sandpoint Beach (Windsor, ON)	36% 5/14	38% 5/13	41% 7/17	40% 6/15	n/a	39% 7/18
Holiday Conservation Beach (Amherstburg, ON)	64% 9/14	21% 3/14	14% 2/14	n/a	n/a	18% 3/17
Mettawas Beach (Kingsville, ON)	71% 10/14	56% 9/16	50% 7/14	63% 10/16	n/a	74% 14/19
Seacliff Beach (Leamington, ON)	21% 3/14	17% 2/12	36% 5/14	20% 3/15	n/a	24% 4/17
Point Pelee North West Beach (Point Pelee National Park, ON)	43% 6/14	23% 3/13	21% 3/14	7% 1/15	n/a	12% 2/17

n/a; data not available.

References

- Abe, K., Nomura, N., Suzuki, S., 2021. Biofilms: Hot spots of horizontal gene transfer (HGT) in aquatic environments, with a focus on a new HGT mechanism. *FEMS Microbiol. Ecol.* 96, 1–12. <https://doi.org/10.1093/FEMSEC/FIAA031>
- Abreu, R., Figueira, C., Romão, D., Brandão, J., Freitas, M.C., Andrade, C., Calado, G., Ferreira, C., Campos, A., Prada, S., 2016. Sediment characteristics and microbiological contamination of beach sand – A case–study in the archipelago of Madeira. *Sci. Total Environ.* 573, 627–638. <https://doi.org/10.1016/j.scitotenv.2016.08.160>
- Aguiar-Pulido, V., Huang, W., Suarez-Ulloa, V., Cickovski, T., Mathee, K., Narasimhan, G., 2016. Metagenomics, Metatranscriptomics, and Metabolomics Approaches for Microbiome Analysis. *Evol. Bioinforma.* 12, 5–16. <https://doi.org/10.4137/EBO.S36436>
- Ahmed, W., Hughes, B., Harwood, V.J., 2016. Current status of marker genes of bacteroides and related taxa for identifying sewage pollution in environmental waters. *Water (Switzerland)* 8. <https://doi.org/10.3390/w8060231>
- Alm, E.W., Burke, J., Spain, A., 2003. Fecal indicator bacteria are abundant in wet sand at freshwater beaches. *Water Res.* 37, 3978–3982. [https://doi.org/10.1016/S0043-1354\(03\)00301-4](https://doi.org/10.1016/S0043-1354(03)00301-4)
- Almakki, A., Jumas-Bilak, E., Marchandin, H., Licznar-Fajardo, P., 2019. Antibiotic resistance in urban runoff. *Sci. Total Environ.* 667, 64–76. <https://doi.org/10.1016/j.scitotenv.2019.02.183>
- Anderson, W.B., Slawson, R.M., Kouwen, N., 2006. Hydrologic Modeling of Pathogen Fate and Transport 40, 4746–4753. <https://doi.org/10.1021/es060426z>
- Arnone, R.D., Walling, J.P., 2007. Waterborne pathogens in urban watersheds. *J. Water Health* 5, 149–162. <https://doi.org/10.2166/wh.2006.001>
- Austin, B., 2011. Taxonomy of bacterial fish pathogens. *Vet. Res.* 42, 1–13. <https://doi.org/10.1186/1297-9716-42-20>
- Badgley, B.D., Thomas, F.I.M., Harwood, V.J., 2011. Quantifying environmental reservoirs of fecal indicator bacteria associated with sediment and submerged aquatic vegetation. *Environ. Microbiol.* 13, 932–942. <https://doi.org/10.1111/j.1462-2920.2010.02397.x>
- Baker, C.A., Almeida, G., Lee, J.A., Gibson, K.E., 2021. Pathogen and Surrogate Survival in Relation to Fecal Indicator Bacteria in Freshwater Mesocosms. *Appl. Environ. Microbiol.* 87, 1–14. <https://doi.org/10.1128/AEM.00558-21>
- Baker, D.B., Confesor, R., Ewing, D.E., Johnson, L.T., Kramer, J.W., Merryfield, B.J., 2014.

- Phosphorus loading to Lake Erie from the Maumee, Sandusky and Cuyahoga rivers: The importance of bioavailability. *J. Great Lakes Res.* 40, 502–517.
<https://doi.org/10.1016/j.jglr.2014.05.001>
- Baquero, F., Martínez, J.L., Cantón, R., 2008. Antibiotics and antibiotic resistance in water environments. *Curr. Opin. Biotechnol.* 19, 260-265.
<https://doi.org/10.1016/j.copbio.2008.05.006>
- Beier, S., Rivers, A.R., Moran, M.A., Obernosterer, I., 2015. Phenotypic plasticity in heterotrophic marine microbial communities in continuous cultures. *ISME J.* 9, 1141–1151.
<https://doi.org/10.1038/ismej.2014.206>
- Beversdorf, L.J., Bornstein-Forst, S.M., McLellan, S.L., 2007. The potential for beach sand to serve as a reservoir for *Escherichia coli* and the physical influences on cell die-off. *J. Appl. Microbiol.* 102, 1372–1381. <https://doi.org/10.1111/j.1365-2672.2006.03177.x>
- Beyer, J., Trannum, H.C., Bakke, T., Hodson, P. V., Collier, T.K., 2016. Environmental effects of the Deepwater Horizon oil spill: A review. *Mar. Pollut. Bull.* 110, 28–51.
<https://doi.org/10.1016/j.marpolbul.2016.06.027>
- Bullerjahn, G.S., McKay, R.M., Davis, T.W., Baker, D.B., Boyer, G.L., D'Anglada, L. V., Doucette, G.J., Ho, J.C., Irwin, E.G., Kling, C.L., Kudela, R.M., Kurmayer, R., Michalak, A.M., Ortiz, J.D., Otten, T.G., Paerl, H.W., Qin, B., Sohngen, B.L., Stumpf, R.P., Visser, P.M., Wilhelm, S.W., 2016. Global solutions to regional problems: Collecting global expertise to address the problem of harmful cyanobacterial blooms. A Lake Erie case study. *Harmful Algae* 54, 223–238. <https://doi.org/10.1016/j.hal.2016.01.003>
- Byappanahalli, M.N., Sawdey, R., Ishii, S., Shively, D.A., Ferguson, J.A., Whitman, R.L., Sadowsky, M.J., 2009. Seasonal stability of *Cladophora*-associated *Salmonella* in Lake Michigan watersheds. *Water Res.* 43, 806–814. <https://doi.org/10.1016/j.watres.2008.11.012>
- Cabral, J.P., 2010. Water microbiology. Bacterial pathogens and water. *Int. J. Environ. Res. Public Health* 7, 3657–3703. <https://doi.org/10.3390/ijerph7103657>
- Canada-United States, 1972. Great Lakes Water Quality Agreement, accessed May 25, 2022.
<http://www.ijc.org/en/who/mission/glwqa>
- Chaffin, J.D., Bridgeman, T.B., Bade, D.L., 2013. Nitrogen Constrains the Growth of Late Summer Cyanobacterial Blooms in Lake Erie. *Adv. Microbiol.* 03, 16–26.
<https://doi.org/10.4236/aim.2013.36A003>
- Chandran, A., Varghese, S., Kandeler, E., Thomas, A., Hatha, M., Mazumder, A., 2011. An assessment of potential public health risk associated with the extended survival of indicator and pathogenic bacteria in freshwater lake sediments. *Int. J. Hyg. Environ. Health* 214, 258–

264. <https://doi.org/10.1016/j.ijheh.2011.01.002>
- Chen, M., Walshe, G., Chi Fru, E., Ciborowski, J.J.H., Weisener, C.G., 2013. Microcosm assessment of the biogeochemical development of sulfur and oxygen in oil sands fluid fine tailings. *Appl. Geochemistry* 37, 1–11. <https://doi.org/10.1016/j.apgeochem.2013.06.007>
- Cloutier, D.D., Alm, E.W., McLellan, S.L., 2015. Influence of land use, nutrients, and geography on microbial communities and fecal indicator abundance at Lake Michigan beaches. *Appl. Environ. Microbiol.* 81, 4904–4913. <https://doi.org/10.1128/AEM.00233-15>
- Cornwell, E.R., Goyette, J.O., Sorichetti, R.J., Allan, D.J., Kashian, D.R., Sibley, P.K., Taylor, W.D., Trick, C.G., 2015. Biological and chemical contaminants as drivers of change in the Great Lakes-St. Lawrence river basin. *J. Great Lakes Res.* 41, 119–130. <https://doi.org/10.1016/j.jglr.2014.11.003>
- Costerton, J.W., Cheng, K.J., Geesey, G.G., Ladd, T.I., Nickel, J.C., Dasgupta, M., Marrie, T.J., 1987. Bacterial Biofilms in Nature and Disease. *Ann. Rev. Microbiol.* 41, 435–464. <https://doi.org/10.1146/annurev.mi.41.100187.002251>
- Craun, G.F., Calderon, R.L., Craun, M.F., 2005. Outbreaks associated with recreational water in the United States. *Int. J. Environ. Health Res.* 15, 243–262. <https://doi.org/10.1080/09603120500155716>
- Curtis, T.P., Sloan, W.T., Scannell, J.W., 2002. Estimating prokaryotic diversity and its limits. *Proc. Natl. Acad. Sci. U. S. A.* 99, 10494–10499. <https://doi.org/10.1073/pnas.142680199>
- Decho, A.W., 1990. Microbial exopolymer secretions in ocean environments – their role(s) in food webs and marine processes. *Oceanography and Marine Biology* 28, 73–153.
- DeFlorio-Barker, S., Wing, C., Jones, R.M., Dorevitch, S., 2018. Estimate of incidence and cost of recreational waterborne illness on United States surface waters. *Environ. Heal. A Glob. Access Sci. Source* 17, 1–10. <https://doi.org/10.1186/s12940-017-0347-9>
- Delahoy, M.J., Wodnik, B., McAliley, L., Penakalapati, G., Swarthout, J., Freeman, M.C., Levy, K., 2018. Pathogens transmitted in animal feces in low- and middle-income countries. *Int. J. Hyg. Environ. Health* 221, 661–676. <https://doi.org/10.1016/j.ijheh.2018.03.005>
- Dempsey, B.A., Tai, Y.L., Harrison, S.G., 1993. Mobilization and removal of contaminants associated with urban dust and dirt. *Water Sci. Technol.* 28, 225–230. <https://doi.org/10.2166/wst.1993.0424>
- Devane, M.L., Moriarty, E., Weaver, L., Cookson, A., Gilpin, B., 2020. Fecal indicator bacteria from environmental sources; strategies for identification to improve water quality monitoring. *Water Res.* 185, 116204. <https://doi.org/10.1016/j.watres.2020.116204>
- Devane, M.L., Weaver, L., Singh, S.K., Gilpin, B.J., 2018. Fecal source tracking methods to

- elucidate critical sources of pathogens and contaminant microbial transport through New Zealand agricultural watersheds – A review. *J. Environ. Manage.* 222, 293–303.
<https://doi.org/10.1016/j.jenvman.2018.05.033>
- DiCarlo, A.M., Weisener, C.G., Drouillard, K.G., 2020. Evidence for Microbial Community Effect on Sediment Equilibrium Phosphorus Concentration (EPC0). *Bull. Environ. Contam. Toxicol.* 105, 736–741. <https://doi.org/10.1007/s00128-020-03019-0>
- Dixit, R., Wasiullah, Malaviya, D., Pandiyan, K., Singh, U.B., Sahu, A., Shukla, R., Singh, B.P., Rai, J.P., Sharma, P.K., Lade, H., Paul, D., 2015. Bioremediation of heavy metals from soil and aquatic environment: An overview of principles and criteria of fundamental processes. *Sustain.* 7, 2189–2212. <https://doi.org/10.3390/su7022189>
- Donahue, A., Feng, Z., Kelly, E., Reniers, A., Solo-Gabriele, H.M., 2017. Significance of beach geomorphology on fecal indicator bacteria levels. *Mar. Pollut. Bull.* 121, 160–167.
<https://doi.org/10.1016/j.marpolbul.2017.05.024>
- Donlan, R.M., 2002. Biofilms: microbial life on surfaces. *Emerg. Infect. Dis.* 8, 881–90.
<https://doi.org/10.3201/eid0809.020063>
- Dove, A., Chapra, S.C., 2015. Long-term trends of nutrients and trophic response variables for the Great Lakes. *Limnol. Oceanogr.* 60, 696–721. <https://doi.org/10.1002/lno.10055>
- Droppo, I.G., 2001. Rethinking what constitutes suspended sediment. *Hydrol. Process.* 15, 1551–1564. <https://doi.org/10.1002/hyp.228>
- Droppo, I.G., Leppard, G., Flannigan, D., Liss, S., 1997. The Freshwater Floc - A functional relationship of water and organic and inorganic floc constituents affecting suspended sediment properties. *Water, Air Soil Pollut.* 99, 43–54.
- Droppo, I.G., Leppard, G.G., Liss, S.N., Milligan, T.G., 2005. Flocculation in natural and engineered environmental systems. (Eds. Ian G. Droppo, Gary G. Leppard, Steven N. Liss and Timothy G. Milligan). CRC Press, Boca Raton, FL, USA. 438 pp. ISBN 1-56670-615-7
- Droppo, I.G., Liss, S.N., Williams, D., Nelson, T., Jaskot, C., Trapp, B., 2009. Dynamic existence of waterborne pathogens within river sediment compartments. Implications for water quality regulatory affairs. *Environ. Sci. Technol.* 43, 1737–1743.
<https://doi.org/10.1021/es802321w>
- Droppo, I.G., Ross, N., Skafel, M., Liss, S.N., 2007. Biostabilization of cohesive sediment beds in a freshwater wave-dominated environment. *Limnol. Oceanogr.* 52, 577–589.
- Edge, T.A., Boyd, R.J., Shum, P., Thomas, J.L., 2021. Microbial source tracking to identify fecal sources contaminating the Toronto Harbour and Don River watershed in wet and dry weather. *J. Great Lakes Res.* 47, 366–377. <https://doi.org/10.1016/j.jglr.2020.09.002>

- Ervin, J.S., Russell, T.L., Layton, B.A., Yamahara, K.M., Wang, D., Sassoubre, L.M., Cao, Y., Keltz, C.A., Sivaganesan, M., Boehm, A.B., Holden, P.A., Weisberg, S.B., Shanks, O.C., 2013. Characterization of fecal concentrations in human and other animal sources by physical, culture-based, and quantitative real-time PCR methods. *Water Res.* 47, 6873–6882. <https://doi.org/10.1016/j.watres.2013.02.060>
- Fabbri, S., Li, J., Howlin, R.P., Rmaile, A., Gottenbos, B., De Jager, M., Starke, E.M., Aspiras, M., Ward, M.T., Cogan, N.G., Stoodley, P., 2017. Fluid-driven interfacial instabilities and turbulence in bacterial biofilms. *Environ. Microbiol.* 19, 4417–4431. <https://doi.org/10.1111/1462-2920.13883>
- Faith, J.J., Rey, F.E., O'Donnell, D., Karlsson, M., McNulty, N.P., Kallstrom, G., Goodman, A.L., Gordon, J.I., 2010. Creating and characterizing communities of human gut microbes in gnotobiotic mice. *ISME J.* 4, 1094–1098. <https://doi.org/10.1038/ismej.2010.110>
- Falkowski, P.G., Fenchel, T., Delong, E.F., 2008. The microbial engines that drive earth's biogeochemical cycles. *Science* (80-.). 320, 1034–1039. <https://doi.org/10.1126/science.1153213>
- Farrell, M.L., Joyce, A., Duane, S., Fitzhenry, K., Hooban, B., Burke, L.P., Morris, D., 2021. Evaluating the potential for exposure to organisms of public health concern in naturally occurring bathing waters in Europe: A scoping review. *Water Res.* 206. <https://doi.org/10.1016/j.watres.2021.117711>
- Fasching, C., Akotoye, C., Bižić, M., Fonvielle, J., Ionescu, D., Mathavarajah, S., Zoccarato, L., Walsh, D.A., Grossart, H.P., Xenopoulos, M.A., 2020. Linking stream microbial community functional genes to dissolved organic matter and inorganic nutrients. *Limnol. Oceanogr.* 65, S71–S87. <https://doi.org/10.1002/lno.11356>
- Feng, Z., Reniers, A., Haus, B.K., Solo-Gabriele, H.M., 2013. Modeling sediment-related enterococci loading, transport, and inactivation at an embayed nonpoint source beach. *Water Resour. Res.* 49, 693–712. <https://doi.org/10.1029/2012WR012432>
- Feng, Z., Reniers, A., Haus, B.K., Solo-Gabriele, H.M., Kelly, E.A., 2016. Wave energy level and geographic setting correlate with Florida beach water quality. *Mar. Pollut. Bull.* 104, 54–60. <https://doi.org/10.1016/j.marpolbul.2016.02.011>
- Fewtrell, L., Kay, D., 2015. Recreational Water and Infection: A Review of Recent Findings. *Curr. Environ. Heal. reports* 2, 85–94. <https://doi.org/10.1007/s40572-014-0036-6>
- Flemming, H.C., 2011. The perfect slime. *Colloids Surfaces B Biointerfaces* 86, 251–259. <https://doi.org/10.1016/j.colsurfb.2011.04.025>
- Foster, G.D., Roberts, E.C., Gruessner, B., Velinsky, D.J., 2000. Hydrogeochemistry and

- transport of organic contaminants in an urban watershed of Chesapeake Bay (USA). *Appl. Geochemistry* 15, 901–915. [https://doi.org/10.1016/S0883-2927\(99\)00107-9](https://doi.org/10.1016/S0883-2927(99)00107-9)
- Friedrich, S., Zec, H., Wang, T.-H., 2016. Analysis of single nucleic acid molecules in micro- and nano-fluidics. *Physiol. Behav.* 16, 790–811. <https://doi.org/10.1039/c5lc01294e>.
- Ganesh, K.A., Anjana, K., Hinduja, M., Sujitha, K., Dharani, G., 2020. Review on plastic wastes in marine environment – Biodegradation and biotechnological solutions. *Mar. Pollut. Bull.* 150, 110733. <https://doi.org/10.1016/j.marpolbul.2019.110733>
- Gao, G., Falconer, R.A., Lin, B., 2015. Modelling the fate and transport of faecal bacteria in estuarine and coastal waters. *Mar. Pollut. Bull.* 100, 162–168. <https://doi.org/10.1016/j.marpolbul.2015.09.011>
- Ge, Z., Whitman, R.L., Nevers, M.B., Phanikumar, M.S., Byappanahalli, M.N., 2012. Nearshore hydrodynamics as loading and forcing factors for *Escherichia coli* contamination at an embayed beach. *Limnol. Oceanogr.* 57, 362–381. <https://doi.org/10.4319/lo.2012.57.1.0362>
- Gerbersdorf, S.U., Wieprecht, S., 2015. Biostabilization of cohesive sediments: Revisiting the role of abiotic conditions, physiology and diversity of microbes, polymeric secretion, and biofilm architecture. *Geobiology* 13, 68–97. <https://doi.org/10.1111/gbi.12115>
- Gibbs, J.P., Halstead, J.M., Boyle, K.J., Huang, J.-C., 2002. An Hedonic Analysis of the Effects of Lake Water Clarity on New Hampshire Lakefront Properties. *Agric. Resour. Econ. Rev.* 31, 39–46. <https://doi.org/10.1017/s1068280500003464>
- Grabowski, R.C., Droppo, I.G., Wharton, G., 2011. Erodibility of cohesive sediment: The importance of sediment properties. *Earth-Science Rev.* 105, 101–120. <https://doi.org/10.1016/j.earscirev.2011.01.008>
- Haller, L., Amedegnato, E., Poté, J., Wildi, W., 2009. Influence of Freshwater Sediment Characteristics on Persistence of Fecal Indicator Bacteria. *Water. Air. Soil Pollut.* 203, 217–227. <https://doi.org/10.1007/s11270-009-0005-0>
- Handelsman, J., 2004. Metagenomics: Application of Genomics to Uncultured Microorganisms. *Microbiol. Mol. Biol. Rev.* 68, 669–685. <https://doi.org/10.1128/MBR.68.4.669-685.2004>
- Hatono, M., Yoshimura, K., 2020. Development of a global sediment dynamics model. *Prog. Earth Planet. Sci.* 7. <https://doi.org/10.1186/s40645-020-00368-6>
- Ho, J.C., Michalak, A.M., 2017. Phytoplankton blooms in Lake Erie impacted by both long-term and springtime phosphorus loading. *J. Great Lakes Res.* 43, 221–228. <https://doi.org/10.1016/j.jglr.2017.04.001>
- Holcomb, D.A., Stewart, J.R., 2020. Microbial Indicators of Fecal Pollution: Recent Progress and Challenges in Assessing Water Quality. *Curr. Environ. Heal. Reports* 7, 311–324.

- <https://doi.org/10.1007/s40572-020-00278-1>
- Hong, C.X., Moorman, G.W., 2005. Plant pathogens in irrigation water: Challenges and opportunities. *CRC. Crit. Rev. Plant Sci.* 24, 189–208.
- <https://doi.org/10.1080/07352680591005838>
- Hooda, P.S., Edwards, A.C., Anderson, H.A., Miller, A., 2000. A review of water quality concerns in livestock farming areas. *Sci. Total Environ.* 250, 143–167.
- [https://doi.org/10.1016/S0048-9697\(00\)00373-9](https://doi.org/10.1016/S0048-9697(00)00373-9)
- Huettel, M., Berg, P., Kostka, J.E., 2014. Benthic exchange and biogeochemical cycling in permeable sediments. *Ann. Rev. Mar. Sci.* 6, 8.1-8.29. <https://doi.org/10.1146/annurev-marine-051413-012706>
- Hull, R.N., Kleywegt, S., Schroeder, J., 2015. Risk-based screening of selected contaminants in the Great Lakes Basin. *J. Great Lakes Res.* 41, 238–245.
- <https://doi.org/10.1016/j.jglr.2014.11.013>
- Huot, Y., Brown, C.A., Potvin, G., Antoniadis, D., Baulch, H.M., Beisner, B.E., Bélanger, S., Brazeau, S., Cabana, H., Cardille, J.A., del Giorgio, P.A., Gregory-Eaves, I., Fortin, M.J., Lang, A.S., Laurion, I., Maranger, R., Prairie, Y.T., Rusak, J.A., Segura, P.A., Siron, R., Smol, J.P., Vinebrooke, R.D., Walsh, D.A., 2019. The NSERC Canadian Lake Pulse Network: A national assessment of lake health providing science for water management in a changing climate. *Sci. Total Environ.* 695, 133668.
- <https://doi.org/10.1016/j.scitotenv.2019.133668>
- Imteaz, M.A., Ahsan, A., Rahman, A., Mekanik, F., 2013. Modelling stormwater treatment systems using MUSIC: Accuracy. *Resour. Conserv. Recycl.* 71, 15–21.
- <https://doi.org/10.1016/j.resconrec.2012.11.007>
- International Joint Commission (IJC), 2022. Great Lakes Water Quality, accessed May 25, 2022. <https://ijc.org/en/what/glwq>
- Ishii, S., Hansen, D.L., Hicks, R.E., Sadowsky, M.J., 2007. Beach sand and sediments are temporal sinks and sources of *Escherichia coli* in lake superior. *Environ. Sci. Technol.* 41, 2203–2209. <https://doi.org/10.1021/es0623156>
- Ishii, S., Ksoll, W.B., Hicks, R.E., Sadowsky, M.J., 2006a. Presence and Growth of Naturalized *Escherichia coli* in Temperate Soils from Lake Superior Watersheds 72, 612–621.
- <https://doi.org/10.1128/AEM.72.1.612>
- Ishii, S., Yan, T., Shively, D.A., Byappanahalli, M.N., Whitman, R.L., Sadowsky, M.J., 2006b. *Cladophora* (Chlorophyta) spp. harbor human bacterial pathogens in nearshore water of Lake Michigan. *Appl. Environ. Microbiol.* 72, 4545–4553.

- <https://doi.org/10.1128/AEM.00131-06>
- Islam, M.M.M., Iqbal, M.S., D'Souza, N., Islam, M.A., 2021. A review on present and future microbial surface water quality worldwide. *Environ. Nanotechnology, Monit. Manag.* 16, 100523. <https://doi.org/10.1016/j.enmm.2021.100523>
- Jarvis, J.C., Moore, K.A., 2015. Effects of Seed Source, Sediment Type, and Burial Depth on Mixed-Annual and Perennial *Zostera marina* L. Seed Germination and Seedling Establishment. *Estuaries and Coasts* 38, 964–978. <https://doi.org/10.1007/s12237-014-9869-3>
- Jayathilake, P.G., Jana, S., Rushton, S., Swailes, D., Bridgens, B., Curtis, T., Chen, J., 2017. Extracellular polymeric substance production and aggregated bacteria colonization influence the competition of microbes in biofilms. *Front. Microbiol.* 8. <https://doi.org/10.3389/fmicb.2017.01865>
- Ju, F., Zhang, T., 2015. Experimental Design and Bioinformatics Analysis for the Application of Metagenomics in Environmental Sciences and Biotechnology. *Environ. Sci. Technol.* 49, 12628–12640. <https://doi.org/10.1021/acs.est.5b03719>
- Kane, D.D., Conroy, J.D., Peter Richards, R., Baker, D.B., Culver, D.A., 2014. Re-eutrophication of Lake Erie: Correlations between tributary nutrient loads and phytoplankton biomass. *J. Great Lakes Res.* 40, 496–501. <https://doi.org/10.1016/j.jglr.2014.04.004>
- Kashefipour, S.M., Lin, B., Falconer, R.A., 2006. Modelling the fate of faecal indicators in a coastal basin. *Water Res.* 40, 1413–1425. <https://doi.org/10.1016/j.watres.2005.12.046>
- Kemp, P., Sear, D., Collins, A., Naden, P., Jones, I., 2011. The impacts of fine sediment on riverine fish. *Hydrol. Process.* 25, 1800–1821. <https://doi.org/10.1002/hyp.7940>
- Kerr, J.M., Depinto, J. V., Mcgrath, D., Sowa, S.P., Swinton, S.M., 2016. Sustainable management of Great Lakes watersheds dominated by agricultural land use 42, 1252–1259.
- Kjelland, M.E., Woodley, C.M., Swannack, T.M., Smith, D.L., 2015. A review of the potential effects of suspended sediment on fishes: potential dredging-related physiological, behavioral, and transgenerational implications. *Environ. Syst. Decis.* 35, 334–350. <https://doi.org/10.1007/s10669-015-9557-2>
- Koch, R., 1884. On cholera bacteria. In: Carter KC; translator. *Essays of Robert Koch*. Connecticut: Greenwood Press; 1987. pg. 171-177.
- Korajkic, A., McMinn, B.R., Harwood, V.J., 2018. Relationships between microbial indicators and pathogens in recreational water settings. *Int. J. Environ. Res. Public Health* 15, 1–39. <https://doi.org/10.3390/ijerph15122842>
- Korajkic, A., Wanjugi, P., Brooks, L., Cao, Y., Harwood, V.J., 2019. Persistence and Decay of

- Fecal Microbiota in Aquatic Habitats. *Microbiol. Mol. Biol. Rev.* 83.
<https://doi.org/10.1128/membr.00005-19>
- Ksoll, W.B., Ishii, S., Sadowsky, M.J., Hicks, R.E., 2007. Presence and sources of fecal coliform bacteria in epilithic periphyton communities of Lake Superior. *Appl. Environ. Microbiol.* 73, 3771–3778. <https://doi.org/10.1128/AEM.02654-06>
- Lai, H., Fang, H., Huang, L., He, G., Reible, D., 2018. A review on sediment bioflocculation: Dynamics, influencing factors and modeling. *Sci. Total Environ.* 642, 1184–1200.
<https://doi.org/10.1016/j.scitotenv.2018.06.101>
- Lee, J.E., Lee, S., Sung, J., Ko, G., 2011. Analysis of human and animal fecal microbiota for microbial source tracking. *ISME J.* 5, 362–365. <https://doi.org/10.1038/ismej.2010.120>
- Leimbach, A., Hacker, J., Dobrindt, U., 2013. *E. coli* as an all-rounder: the thin line between commensalism and pathogenicity. *Current Topics in Microbiology and Immunology* 358:3–32. doi: 10.1007/82_2012_303.
- Leung, K.Y., Wang, Q., Yang, Z., Siame, B.A., 2019. *Edwardsiella piscicida*: A versatile emerging pathogen of fish. *Virulence* 10, 555–567.
<https://doi.org/10.1080/21505594.2019.1621648>
- Levy, K., Woster, A.P., Goldstein, R.S., Carlton, E.J., 2016. Untangling the Impacts of Climate Change on Waterborne Diseases: A Systematic Review of Relationships between Diarrheal Diseases and Temperature, Rainfall, Flooding, and Drought. *Environ. Sci. Technol.* 50, 4905–4922. <https://doi.org/10.1021/acs.est.5b06186>
- Li, E., Saleem, F., Edge, T.A., Schellhorn, H.E., 2021. Biological indicators for fecal pollution detection and source tracking: A review. *Processes* 9. <https://doi.org/10.3390/pr9112058>
- Liss, S.N., Droppo, I.G., Flannigan, D.T., Leppard, G.G., 1996. Floc architecture in wastewater and natural riverine systems. *Environ. Sci. Technol.* 30, 680–686.
<https://doi.org/10.1021/es950426r>
- Madani, M., Seth, R., Leon, L.F., Valipour, R., McCrimmon, C., 2020. Three dimensional modelling to assess contributions of major tributaries to fecal microbial pollution of lake St. Clair and Sandpoint Beach. *J. Great Lakes Res.* 46, 159–179.
<https://doi.org/10.1016/j.jglr.2019.12.005>
- Madani, M., Seth, R., Valipour, R., Leon, L.F., Hipsey, M.R., 2022. Modelling of nearshore microbial water quality at confluence of a local tributary in Lake St. Clair. *J. Great Lakes Res.* 48, 489–501. <https://doi.org/10.1016/j.jglr.2022.01.019>
- Maguire, T.J., Spencer, C., Grgicak-Mannion, A., Drouillard, K., Mayer, B., Mundle, S.O.C., 2019. Distinguishing point and non-point sources of dissolved nutrients, metals, and legacy

- contaminants in the Detroit River. *Sci. Total Environ.* 681, 1–8.
<https://doi.org/10.1016/j.scitotenv.2019.04.311>
- Mallin, M.A., Cahoon, L.B., 2003. Industrialized animal production - A major source of nutrient and microbial pollution to aquatic ecosystems. *Popul. Environ.* 24, 369–385.
<https://doi.org/10.1023/A:1023690824045>
- Mbanga, J., Abia, A.L.K., Amoako, D.G., Essack, S.Y., 2020. Quantitative microbial risk assessment for waterborne pathogens in a wastewater treatment plant and its receiving surface water body. *BMC Microbiol.* 20, 1–12. <https://doi.org/10.1186/s12866-020-02036-7>
- McPhedran, K., Seth, R., Bejankiwar, R., 2013. Occurrence and predictive correlations of *Escherichia coli* and *Enterococci* at Sandpoint beach (Lake St Clair), Windsor, Ontario and holiday beach (Lake Erie), Amherstburg, Ontario. *Water Qual. Res. J. Canada* 48, 99–110.
<https://doi.org/10.2166/wqrjc.2013.132>
- McQuaig, S., Griffith, J., Harwood, V.J., 2012. Association of Fecal Indicator Bacteria with Human Viruses and Microbial Source Tracking Markers at Coastal Beaches Impacted by 6423–6432. <https://doi.org/10.1128/AEM.00024-12>
- Michalak, A.M., Anderson, E.J., Beletsky, D., Boland, S., Bosch, N.S., Bridgeman, T.B., Chaffin, J.D., Cho, K., Confesor, R., Daloglu, I., DePinto, J. V., Evans, M.A., Fahnenstiel, G.L., He, L., Ho, J.C., Jenkins, L., Johengen, T.H., Kuo, K.C., LaPorte, E., Liu, X., McWilliams, M.R., Moore, M.R., Posselt, D.J., Richards, R.P., Scavia, D., Steiner, A.L., Verhamme, E., Wright, D.M., Zagorski, M.A., 2013. Record-setting algal bloom in Lake Erie caused by agricultural and meteorological trends consistent with expected future conditions. *Proc. Natl. Acad. Sci.* 110, 6448–6452. <https://doi.org/10.1073/pnas.1216006110>
- Moncada, C., Hassenrück, C., Gärdes, A., Conaco, C., 2019. Microbial community composition of sediments influenced by intensive mariculture activity. *FEMS Microbiol. Ecol.* 95, 1–12.
<https://doi.org/10.1093/femsec/fiz006>
- Montgomery, D.R., 2007. Soil erosion and agricultural sustainability. *Proc. Natl. Acad. Sci. U. S. A.* 104, 13268–13272. <https://doi.org/10.1073/pnas.0611508104>
- Mooney, R.J., Stanley, E.H., Rosenthal, W.C., Esselman, P.C., Kendall, A.D., McIntyre, P.B., 2020. Outsized nutrient contributions from small tributaries to a Great Lake. *Proc. Natl. Acad. Sci. U. S. A.* 117, 28175–28182. <https://doi.org/10.1073/pnas.2001376117>
- Mori, J., Smith, R., 2019. Transmission of waterborne fish and plant pathogens in aquaponics and their control with physical disinfection and filtration: A systematized review. *Aquaculture* 504, 380–395. <https://doi.org/10.1016/j.aquaculture.2019.02.009>
- Morrison, T., Hurley, J., Garcia, J., Yoder, K., Katz, A., Roberts, D., Cho, J., Kanigan, T., Ilyin,

- S.E., Horowitz, D., Dixon, J.M., Brenan, C.J.H., 2006. Nanoliter high throughput quantitative PCR. *Nucleic Acids Res.* 34, 1–9. <https://doi.org/10.1093/nar/gkl639>
- Mullis, K., Faloona, F., Scharf, S., Saiki, R., Horn, G., Erlich, H., 1986. Specific enzymatic amplification of DNA in vitro: the polymerase chain reaction. *Cold Spring Harb Symp Quant Biol* 51, 263–273. <https://doi.org/10.1101/sqb.1986.051.01.032>
- Natural Resources Defense Council, 2014. Testing the Waters 2014: A guide to water quality at vacation beaches.
- Noe, G.B., Cashman, M.J., Skalak, K., Gellis, A., Hopkins, K.G., Moyer, D., Webber, J., Benthem, A., Maloney, K., Brakebill, J., Sekellick, A., Langland, M., Zhang, Q., Shenk, G., Keisman, J., Hupp, C., 2020. Sediment dynamics and implications for management: State of the science from long-term research in the Chesapeake Bay watershed, USA. *Wiley Interdiscip. Rev. Water* 7, 1–28. <https://doi.org/10.1002/wat2.1454>
- Noffke, N., Paterson, D., 2008. Microbial interactions with physical sediment dynamics, and their significance for the interpretation of Earth’s biological history. *Geobiology* 6, 1–4. <https://doi.org/10.1111/j.1472-4669.2007.00132.x>
- Owens, P.N., Gateuille, D.J., Petticrew, E.L., Booth, B.P., French, T.D., 2019. Sediment-associated organopollutants, metals and nutrients in the Nechako River, British Columbia: a current study with a synthesis of historical data. *Can. Water Resour. J.* 44, 42–64. <https://doi.org/10.1080/07011784.2018.1531063>
- Padilla, D.K., Williams, S.L., 2004. Beyond ballast water: Aquarium and ornamental trades as sources of invasive species in aquatic ecosystems. *Front. Ecol. Environ.* 2, 131–138. [https://doi.org/10.1890/1540-9295\(2004\)002\[0131:BBWAAO\]2.0.CO;2](https://doi.org/10.1890/1540-9295(2004)002[0131:BBWAAO]2.0.CO;2)
- Palmer, J.A., Law, J.Y., Soupir, M.L., 2020. Spatial and temporal distribution of *E. coli* contamination on three inland lake and recreational beach systems in the upper Midwestern United States. *Sci. Total Environ.* 722, 137846. <https://doi.org/10.1016/j.scitotenv.2020.137846>
- Papadopoulou, L., Phillips, P., Twigger-Ross, C., Krisht, S., 2018. The value of bathing waters and the influence of bathing water quality: Literature review, Scottish Government.
- Park, E., Latrubesse, E.M., 2014. Modeling suspended sediment distribution patterns of the Amazon River using MODIS data. *Remote Sens. Environ.* 147, 232–242. <https://doi.org/10.1016/j.rse.2014.03.013>
- Park, S.C., Lee, K., Kim, Y.O., Won, S., Chun, J., 2019. Large-scale genomics reveals the genetic characteristics of seven species and importance of phylogenetic distance for estimating pan-genome size. *Front. Microbiol.* 10, 1–12. <https://doi.org/10.3389/fmicb.2019.00834>

- Pasmore, M., Costerton, J.W., 2003. Biofilms, bacterial signaling, and their ties to marine biology. *J. Ind. Microbiol. Biotechnol.* 30, 407–413. <https://doi.org/10.1007/s10295-003-0069-6>
- Penakalapati, G., Swarthout, J., Delahoy, M.J., McAliley, L., Wodnik, B., Levy, K., Freeman, M.C., 2017. Exposure to Animal Feces and Human Health: A Systematic Review and Proposed Research Priorities. *Environ. Sci. Technol.* 51, 11537–11552. <https://doi.org/10.1021/acs.est.7b02811>
- Perkins, T.L., Clements, K., Baas, J.H., Jago, C.F., Jones, D.L., Malham, S.K., McDonald, J.E., 2014. Sediment composition influences spatial variation in the abundance of human pathogen indicator bacteria within an estuarine environment. *PLoS One* 9. <https://doi.org/10.1371/journal.pone.0112951>
- Peterson, B.W., He, Y., Ren, Y., Zerdoum, A., Libera, M.R., Sharma, P.K., van Winkelhoff, A.J., Neut, D., Stoodley, P., van der Mei, H.C., Busscher, H.J., 2015. Viscoelasticity of biofilms and their recalcitrance to mechanical and chemical challenges. *FEMS Microbiol. Rev.* 39, 234–245. <https://doi.org/10.1093/femsre/fuu008>
- Phelan, S., Soni, D., Morales Medina, W.R., Fahrenfeld, N.L., 2019. Comparison of qPCR and amplicon sequencing based methods for fecal source tracking in a mixed land use estuarine watershed. *Environ. Sci. Water Res. Technol.* 5, 2108–2123. <https://doi.org/10.1039/c9ew00719a>
- Phillips, M.C., Feng, Z., Vogel, L.J., Reniers, A.J.H.M., Haus, B.K., Enns, A.A., Zhang, Y., Hernandez, D.B., Solo-Gabriele, H.M., 2014. Microbial release from seeded beach sediments during wave conditions. *Mar. Pollut. Bull.* 79, 114–122. <https://doi.org/10.1016/j.marpolbul.2013.12.029>
- Phillips, M.C., Solo-Gabriele, H.M., Reniers, A.J.H.M., Wang, J.D., Kiger, R.T., Abdel-Mottaleb, N., 2011. Pore water transport of enterococci out of beach sediments. *Mar. Pollut. Bull.* 62, 2293–2298. <https://doi.org/10.1016/j.marpolbul.2011.08.049>
- Probandt, D., Eickhorst, T., Ellrott, A., Amann, R., Knittel, K., 2018. Microbial life on a sand grain: From bulk sediment to single grains. *ISME J.* 12, 623–633. <https://doi.org/10.1038/ismej.2017.197>
- Proença, J.T., Barral, D.C., Gordo, I., 2017. Commensal-to-pathogen transition: One-single transposon insertion results in two pathoadaptive traits in *Escherichia coli*-macrophage interaction. *Sci. Rep.* 7, 1–12. <https://doi.org/10.1038/s41598-017-04081-1>
- Ramírez-Castillo, F.Y., Loera-Muro, A., Jacques, M., Garneau, P., Avelar-González, F.J., Harel, J., Guerrero-Barrera, A.L., 2015. Waterborne pathogens: Detection methods and challenges.

- Pathogens 4, 307–334. <https://doi.org/10.3390/pathogens4020307>
- Reid, T., VanMensel, D., Droppo, I.G., Weisener, C.G., 2016. The symbiotic relationship of sediment and biofilm dynamics at the sediment water interface of oil sands industrial tailings ponds. *Water Res.* 100, 337–347. <https://doi.org/10.1016/j.watres.2016.05.025>
- Righetti, M., Lucarelli, C., 2007. May the Shields theory be extended to cohesive and adhesive benthic sediments? *J. Geophys. Res. Ocean.* 112, 1–14. <https://doi.org/10.1029/2006JC003669>
- Rosenberg, E., Koren, O., Reshef, L., Efrony, R., Zilber-Rosenberg, I., 2007. The role of microorganisms in coral health, disease and evolution. *Nat. Rev. Microbiol.* 5, 355–362. <https://doi.org/10.1038/nrmicro1635>
- Roslev, P., Bukh, A.S., 2011. State of the art molecular markers for fecal pollution source tracking in water. *Appl. Microbiol. Biotechnol.* 89, 1341–1355. <https://doi.org/10.1007/s00253-010-3080-7>
- Rusch, A., Huettel, M., Reimers, C.E., Taghon, G.L., Fuller, C.M., 2003. Activity and distribution of bacterial populations in Middle Atlantic Bight shelf sands. *Fems Microbiol. Ecol.* 44, 89–100. [https://doi.org/10.1016/S0168-6496\(02\)00458-0](https://doi.org/10.1016/S0168-6496(02)00458-0)
- Saiki, R.K., Scharf, S., Faloona, F., Mullis, K.B., Horn, G.T., Erlich, H.A., Arnheim, N., 1985. Enzymatic Amplification of Beta-Globin Genomic Sequences and Restriction Site Analysis for Diagnosis of Sickle Cell Anemia. *Science* (80-.). 230, 1350–1354.
- Salter, C., VanMensel, D., Reid, T., Birbeck, J., Westrick, J., Mundle, S.O.C., Weisener, C.G., 2021. Investigating the microbial dynamics of microcystin-LR degradation in Lake Erie sand. *Chemosphere* 272, 129873. <https://doi.org/10.1016/j.chemosphere.2021.129873>
- Sassi, H.P., van Ogtrop, F., Morrison, C.M., Zhou, K., Duan, J.G., Gerba, C.P., 2020. Sediment re-suspension as a potential mechanism for viral and bacterial contaminants. *J. Environ. Sci. Heal. - Part A Toxic/Hazardous Subst. Environ. Eng.* 55, 1398–1405. <https://doi.org/10.1080/10934529.2020.1796118>
- Schindler, D.W., Carpenter, S.R., Chapra, S.C., Hecky, R.E., Orihel, D.M., 2016. Reducing phosphorus to curb lake eutrophication is a success. *Environ. Sci. Technol.* 50, 8923–8929. <https://doi.org/10.1021/acs.est.6b02204>
- Schindler, D.W., Hecky, R.E., Findlay, D.L., Stainton, M.P., Parker, B.R., Paterson, M.J., Beaty, K.G., Lyng, M., Kasian, S.E.M., 2008. Eutrophication of lakes cannot be controlled by reducing nitrogen input: Results of a 37-year whole-ecosystem experiment. *Proc. Natl. Acad. Sci. U. S. A.* 105, 11254–11258. <https://doi.org/10.1073/pnas.0805108105>

- Shahraki, A.H., Chaganti, S.R., Heath, D.D., 2021. Diel Dynamics of Freshwater Bacterial Communities at Beaches in Lake Erie and Lake St. Clair, Windsor, Ontario. *Microb. Ecol.* 81, 1–13. <https://doi.org/10.1007/s00248-020-01539-0>
- Shahraki, A.H., Heath, D., Chaganti, S.R., 2019. Recreational water monitoring: Nanofluidic qRT-PCR chip for assessing beach water safety. *Environ. DNA* 1, 305–315. <https://doi.org/10.1002/edn3.30>
- Shen, X., Toorman, E.A., Lee, B.J., Fettweis, M., 2019. An Approach to Modeling Biofilm Growth During the Flocculation of Suspended Cohesive Sediments. *J. Geophys. Res. Ocean.* <https://doi.org/10.1029/2018JC014493>
- Shrestha, B., Babel, M.S., Maskey, S., Van Griensven, A., Uhlenbrook, S., Green, A., Akkharath, I., 2013. Impact of climate change on sediment yield in the Mekong River basin: A case study of the Nam Ou basin, Lao PDR. *Hydrol. Earth Syst. Sci.* 17, 1–20. <https://doi.org/10.5194/hess-17-1-2013>
- Snow, J., 1855. On the mode of communication of cholera. John Churchill.
- Sousa, A.J., Droppo, I.G., Liss, S.N., Warren, L., Wolfaardt, G., 2015. Influence of wave action on the partitioning and transport of unattached and floc-associated bacteria in fresh water. *Can. J. Microbiol.* 61, 584–596.
- Sterner, R.W., Ostrom, P., Ostrom, N.E., Klump, J.V., Steinman, A.D., Dreelin, E.A., Zanden, M.J. Vander, Fisk, A.T., 2017. Grand challenges for research in the Laurentian Great Lakes. <https://doi.org/10.1002/lno.10585>
- Sweet, M.J., Bythell, J.C., Nugues, M.M., 2013. Algae as Reservoirs for Coral Pathogens. *PLoS One* 8. <https://doi.org/10.1371/journal.pone.0069717>
- Trunk, T., Khalil, H.S., Leo, J.C., 2018. Bacterial autoaggregation. *AIMS Microbiol.* 4, 140–164. <https://doi.org/10.3934/microbiol.2018.1.140>
- USEPA, U.S. Environmental Protection Agency, 2000. Improved enumeration methods for the recreational water quality indicators: enterococci and *Escherichia coli*. EPA/821/R-97/004. Office of Science and Technology, U.S. Environmental Protection Agency, Washington, D.C.
- VanMensel, D., Chaganti, S.R., Droppo, I.G., Weisener, C.G., 2020. Exploring bacterial pathogen community dynamics in freshwater beach sediments: A tale of two lakes. *Environ. Microbiol.* 22, 568–583. <https://doi.org/10.1111/1462-2920.14860>
- VanMensel, D., Droppo, I.G., Weisener, C.G., 2022. Identifying chemolithotrophic and pathogenic-related gene expression within suspended sediment flocs in freshwater environments: A metatranscriptomic assessment. *Sci. Total Environ.* 807, 150996.

- <https://doi.org/10.1016/j.scitotenv.2021.150996>
- Wainright, S., 1990. Sediment-to-water fluxes of particulate material and microbes by resuspension and their contribution to the planktonic food web. *Mar. Ecol. Prog. Ser.* 62, 271–281. <https://doi.org/10.3354/meps062271>
- Wang, A., Lin, B., Sleep, B.E., Liss, S.N., 2011. The Impact of Biofilm Growth on Transport of *Escherichia coli* O157:H7 in Sand. *Ground Water* 49, 20–31. <https://doi.org/10.1111/j.1745-6584.2010.00690.x>
- Waples, J.T., Eadie, B., Klump, J.V., Margaret, S., Cotner, J., McKinley, G., 2008. The Laurentian Great Lakes. *NORTH Am. Cont. MARGINS A Synth. Plan. Work.*
- Weiskerger, C.J., Phanikumar, M.S., 2020. Numerical modeling of microbial fate and transport in natural waters: Review and implications for normal and extreme storm events. *Water (Switzerland)* 12. <https://doi.org/10.3390/W12071876>
- Weitere, M., Bergfeld, T., Rice, S.A., Matz, G., Kjelleberg, S., 2005. Grazing resistance of *Pseudomonas aeruginosa* biofilms depends on type of protective mechanism, developmental stage and protozoan feeding mode. *Environ. Microbiol.* 7, 1593–1601. <https://doi.org/10.1111/j.1462-2920.2005.00851.x>
- Whitman, R.L., Harwood, V.J., Edge, T.A., Nevers, M.B., Byappanahalli, M., Vijayavel, K., Brandão, J., Sadowsky, M.J., Alm, E.W., Crowe, A., Ferguson, D., Ge, Z., Halliday, E., Kinzelman, J., Kleinheinz, G., Przybyla-Kelly, K., Staley, C., Staley, Z., Solo-Gabriele, H.M., 2014. Microbes in beach sands: Integrating environment, ecology and public health, *Reviews in Environmental Science and Biotechnology*. <https://doi.org/10.1007/s11157-014-9340-8>
- Wijesiri, B., Egodawatta, P., McGree, J., Goonetilleke, A., 2016. Understanding the uncertainty associated with particle-bound pollutant build-up and wash-off: A critical review. *Water Res.* 101, 582–596. <https://doi.org/10.1016/j.watres.2016.06.013>
- Withers, P.J.A., Jarvie, H.P., 2008. Delivery and cycling of phosphorus in rivers: A review. *Sci. Total Environ.* 400, 379–395. <https://doi.org/10.1016/j.scitotenv.2008.08.002>
- Wolk, D.M., Hayden, R.T., 2011. Quantitative molecular methods, *Molecular Microbiology*. American Society of Microbiology, pp. 83-105.
- Wood, P.J., Armitage, P.D., 1997. Biological effects of fine sediment in the lotic environment. *Environ. Manage.* 21, 203–217. <https://doi.org/10.1007/s002679900019>
- World Health Organisation (WHO), 2017. Cholera fact sheet.
- Wyer, M.D., Kay, D., Morgan, H., Naylor, S., Clark, S., Watkins, J., Davies, C.M., Francis, C., Osborn, H., Bennett, S., 2018. Within-day variability in microbial concentrations at a UK

- designated bathing water: Implications for regulatory monitoring and the application of predictive modelling based on historical compliance data. *Water Res.* X 1, 100006. <https://doi.org/10.1016/j.wroa.2018.10.003>
- Yamada, H., Nakamura, F., 2002. Effect of fine sediment deposition and channel works on periphyton biomass in the Makomanai River, northern Japan. *River Res. Appl.* 18, 481–493. <https://doi.org/10.1002/rra.688>
- Yamahara, K.M., Layton, B.A., Santoro, A.E., Boehm, A.B., 2007. Beach sands along the California coast are diffuse sources of fecal bacteria to coastal waters. *Environ. Sci. Technol.* 41, 4515–4521. <https://doi.org/10.1021/es062822n>
- Yamahara, K.M., Walters, S.P., Boehm, A.B., 2009. Growth of enterococci in unaltered, unseeded beach sands subjected to tidal wetting. *Appl. Environ. Microbiol.* 75, 1517–1524. <https://doi.org/10.1128/AEM.02278-08>
- Yin, W., Wang, Y., Liu, L., He, J., 2019. Biofilms: The microbial “protective clothing” in extreme environments. *Int. J. Mol. Sci.* 20. <https://doi.org/10.3390/ijms20143423>
- Yuan, Q., Guerra, H.B., Kim, Y., 2017. An investigation of the relationships between rainfall conditions and pollutant wash-off from the paved road. *Water (Switzerland)* 9. <https://doi.org/10.3390/w9040232>
- Yunker, M.B., Macdonald, R.W., Vingarzan, R., Mitchell, H., Goyette, D., Sylvestre, S., 2002. PAHs in the Fraser River basin: a critical appraisal of PAH ratios as indicators of PAH source and composition. *Org. Geochem.* 33, 489–515.
- Zaki, M.S., Authman, M.M.N., Abbas, H.H.H., 2015. Bioremediation of petroleum contaminants in aquatic environments (Review Article). *Life Sci. J.* 12, 109–121.
- Zhang, S., Chen, Shuling, Rehman, M.U., Yang, H., Yang, Z., Wang, M., Jia, R., Chen, Shun, Liu, M., Zhu, D., Zhao, X., Wu, Y., Yang, Q., Huan, J., Ou, X., Mao, S., Gao, Q., Sun, D., Tian, B., Cheng, A., 2021. Distribution and association of antimicrobial resistance and virulence traits in *Escherichia coli* isolates from healthy waterfowls in Hainan, China. *Ecotoxicol. Environ. Saf.* 220, 112317. <https://doi.org/10.1016/j.ecoenv.2021.112317>
- Zhao, H., Sun, R., Yu, P., Alvarez, P.J.J., 2020. High levels of antibiotic resistance genes and opportunistic pathogenic bacteria indicators in urban wild bird feces. *Environ. Pollut.* 266, 115200. <https://doi.org/10.1016/j.envpol.2020.115200>
- Zinger, L., Gobet, A., Pommier, T., 2012. Two decades of describing the unseen majority of aquatic microbial diversity. *Mol. Ecol.* 21, 1878–1896. <https://doi.org/10.1111/j.1365-294X.2011.05362.x>

CHAPTER 2: EXPLORING THE MICROBIAL SIGNATURE IN BED SEDIMENT
FROM LAKE ST. CLAIR AND LAKE ERIE BEACHES: A SPATIOTEMPORAL
PERSPECTIVE

CHAPTER 2: EXPLORING THE MICROBIAL SIGNATURE IN BED SEDIMENT FROM LAKE ST. CLAIR AND LAKE ERIE BEACHES: A SPATIOTEMPORAL PERSPECTIVE

2.1 Introduction

Characterizing the microbial composition associated with freshwater coastlines and beach zones is of vital importance for accurately understanding the potential for human health risk related to recreational water use. Identifying microbial organisms (e.g., bacteria) within aquatic environments in undisturbed locations/conditions provides baseline knowledge of the most important component of this biosphere – the primary producers and nutrient cyclers. As microorganisms are coupled to many biogeochemical cycles in the environment, microbial community diversity and composition studies can provide strong insights into the function, health, resilience, and natural processes of a particular location (Astudillo-García et al., 2019; Lear et al., 2009). Further, this microbial baseline can help highlight perturbations and stressors to the ecosystem as a function of anthropogenic-induced environmental pressures such as varying land use (e.g., agricultural activities; Trivedi et al., 2016), and contamination events (e.g., untreated sewage discharge; McClary-Gutierrez et al., 2021). Evaluating microbial community changes across space and time can provide early warnings of significant environmental changes which may be of concern for human and overall ecosystem health (Baho et al., 2012; Shade et al., 2012). In addition, identifying contamination events and sources within aquatic environments can potentially allow for prompt remediation responses and safe restoration to natural ecosystem function (Dickerson et al., 2007; Kinzelman and McLellan, 2009; Korajkic et al., 2011). Typically, characterization assessments have been conducted on planktonic microbes within freshwater and marine surface waters (Hahn, 2006; Pommier et al., 2007; Vega et al., 2021), but less research has investigated the microbial community associated with the bed sediment and how the benthic microbes influence coastal water quality. This is a concern as many previous studies

have found concentrations of FIB (e.g., enterococci, *E. coli*) in sediments to be significantly greater compared to the overlying water column (Badgley et al., 2010; Benjamin et al., 2013; Korajkic et al., 2009). In fact, a recent report revealed *E. coli* concentrations in riverbed sediment were 10-100 times higher compared to the water compartment (Fluke et al., 2019).

The GLs have long been threatened by poor water quality due to anthropogenic reasons, such as increasing urbanization and agricultural practices, which inadvertently affect human health and safety associated with water use (Dove and Chapra, 2015; Krantzberg, 2008; Sterner et al., 2017). These activities contribute to contaminated stormwater which collects in the watershed and progresses to the lakes, impacting water quality and overall ecosystem health along these freshwater shorelines (Figure 2.1). The principal form of microbial contamination is often related to fecal pollution, including untreated sewage discharge into the environment, agricultural runoff, or wildlife (Craun et al., 2005; DiCarlo et al., 2020; Ksoll et al., 2007; Maguire et al., 2019). High levels of FIB detected in the water is cause for concern regarding recreational water use as these organisms have traditionally been correlated with nearby fecal pollution and human illness (Thoe et al., 2018; Wade et al., 2006). If fecal matter is assumed to be in the nearshore water, it can be expected that other human pathogenic microbes may also be present. For health and safety precautions, Canadian public beaches are closed for use when FIB levels exceed the criterion set by government regulations. Using *E. coli* as the indicator organism, the guideline values for fresh recreational water are a geometric mean concentration (minimum five samples) of ≤ 200 CFUs/100 mL or a single-sample maximum concentration of ≤ 400 CFUs/100 mL (Government of Canada, 2022). However, the accurate pathogenic potential of GL beaches comes from the entire suite of viable pathogens present and is therefore misrepresented by the assumption of only free-floating FIB on sampling design. Sediment-water interactions play an important role in the distribution of microbiota (including pathogens) and the overall functional dynamics of the freshwater medium (including water quality) (Droppo et al., 2009; Fries et al., 2008; Gao et al.,

2011). The current knowledge of the diversity and function of microorganisms associated with the sediment compartment of freshwater environments is insufficient for sustainable management of freshwater resources.

The present study focuses on public freshwater beaches located on Lake St. Clair and Lake Erie prone to frequent summer closures due to high levels of *E. coli* in the water with potential risks to humans through regular beach activities (e.g., swimming, playing in the sand, etc.). The objectives of this work were to 1) investigate how the biodiversity of the benthic microbial community changes spatially and through seasonal variations (spring to fall), 2) characterize and contrast the bacterial profile of the nearshore bed sediment of six freshwater beaches, and 3) compare differences of bed sediment microbial communities between bulk DNA of the lakebed-associated microbial communities to the active microbial component (i.e., RNA). In the context of this dissertation, this chapter seeks to contrast the primary microbial consortia and functional potential of these six beach sediment environments and will provide a baseline comparison to complement previous microbial characterization of the overlying water and supplementary studies which build off this data. To address these objectives, environmental DNA and RNA were isolated from the nearshore sediment, the V5/V6 hypervariable region of the 16S rRNA gene was targeted through PCR, and the amplicons were sequenced with NGS technology using the Ion Torrent platform. Alpha and beta diversity metrics were explored, and community composition was analysed. Insights from this work will confirm whether specific microbiome differences exist in these sediment areas and whether they will impact ecosystem health and function in these freshwater systems. The information gathered from this chapter can be used to advance supplementary studies related to aquatic microbial communities and further our understanding of how the microbial component influences the health and function of natural freshwater ecosystems.

2.2 Methods

2.2.1 Site selection

Windsor-Essex County (WEC) is the southernmost region of Ontario, Canada which is dominated by agricultural landscapes with freshwater borders of Lake St. Clair, the Detroit River and Lake Erie (Figure 2.1). The large freshwater shoreline of WEC makes this area popular for recreational water use, yet agricultural runoff and drainage collection in the local watershed causes concern for human health and safety. This area is prone to beach closures due to the frequent detection of high levels of FIB and blue-green algae in the water column. Sampling sites for the research considered in this dissertation are located on Lakes St. Clair and Erie and were selected based on historical water quality data reported by the WEC Health Unit (WECHU; www.wechu.org) (Table 1.1). Although all sampling locations are situated in WEC, each beach demonstrates unique physical, chemical, and biological characteristics and will be discussed throughout this chapter and remainder of this dissertation.

Six public beaches in the region were selected for regular sampling of lakebed sediment in the nearshore (i.e., swimming zone); Holiday Beach in Amherstburg (HD), Lakeside Beach in Kingsville (KV), Seaside Beach in Leamington (LE), Point Pelee Northwest Beach (PP), Sandpoint Beach in Windsor (SP), and West Belle River Beach in Belle River (BR). Four of these beaches are located on the north shore of Lake Erie (HD, KV, LE, and PP), and the other two (SP and BR) are situated on the southern shoreline of Lake St. Clair (Figure 2.2A). Collectively, these samples are representative of a spatiotemporal perspective on the bed sediment of the WEC local public beaches.

2.2.2 *Site sampling details*

Surface lakebed sediment in the nearshore (i.e., swimming zone with approximately waist-deep water) was collected several times between April and November of 2017 at each beach. Specifically, clear PVC tubes (diameter = 67 mm) were gently pushed through the sediment layer, top plugged, then carefully pulled back up until the bottom could be plugged within the water column. Sediment cores were manually pushed up through the top of the tube using a metal rod on the bottom plug to expose the sediment surface layer (Figure 2.3). Sediment was scooped into sterile cyrotubes from the top 1-2 cm of the cored sediment (in duplicate or triplicate), and subsequently flash frozen in a dewar (Molecular Dimensions CX-100 Dry Shipper) filled with liquid nitrogen. Once back at the laboratory, samples were transferred to the freezer and stored at -80°C until nucleic acid extractions were performed. Long-term storage of microbial samples at -80°C is the preferred method to maintain nucleic acid (i.e., DNA and RNA) yield and integrity from lakebed sediments (Rissanen et al., 2010).

Physicochemical parameters of the overlaying lake water were measured at each sediment collection using the YSI 6600 V2 or Exo 2 sonde with calibrated sensors (Hoskin Scientific) to record temperature, pH, dissolved oxygen (DO), conductivity, oxidation-reduction potential (ORP), and turbidity (Table A-1). These measurements were taken from the nearshore proximal to sediment sample collection but prior to sediment coring to avoid subsequent bed disturbances and resuspension.

Physicochemical parameters of the bed sediment were evaluated to characterize the benthic microbial habitat (Table 2.1). Sediment granulometry was determined by sieving dried (~48 h at 50°C), bulk bed sediment from the upper layer within the nearshore swim zone. Eight sieves were utilized for grain size characterization, ranging from 63 to 2000 µm. Sediment moisture content was determined by mass before and after drying. Beaches were designated as

either sheltered (low energy) or not sheltered (high energy) based on observation of restricted water flow due to manmade structures (e.g., adjacent piers), degree of embayment, and observed wave heights over the duration of site visits over a two-year period (2016 and 2017).

2.2.3 *Nucleic acid extractions from freshwater bed sediment*

DNA extractions were performed using DNeasy PowerSoil Isolation kits or were co-eluted with RNA using RNeasy PowerSoil Total RNA and RNeasy PowerSoil DNA Elution kits (Qiagen). DNA isolation followed the manufacturer's protocol with final resuspension in 100 μ L RNase-free water and stored at -20°C until further processing.

RNA isolation followed the manufacturer's protocol with slight modifications as follows. Sample weight was increased from 2 g to 5 g and extractions began with sediment still in a semi-frozen state to minimize RNA degradation. DNase/RNase-free reagents, tubes, and pipet tips were kept chilled on ice when practical; exceptions include reagents that require room temperature and sample transfers. RNA precipitation was extended to > 12 h at 20°C to increase yield, and the final pellet was resuspended in 50 μ L RNase-free water to increase concentration. RNase Inhibitor (Invitrogen) was added to the resuspended pellet to minimize degradation. Potential DNA contamination was removed using the RapidOut DNA Removal kit (Thermo Fisher Scientific), following the manufacturer's recommendations. Aliquots of extracted RNA isolations were stored at -80°C until further processing.

RNA concentrations were determined in-house using either the Agilent 2100 Bioanalyzer (Agilent Technologies) or fluorometrically using the Qubit 2.0 Fluorometer and RNA Broad-Range Assay kit (Thermo Fisher Scientific) (Table A-2). Samples assessed using the Bioanalyzer were also tested for RNA quality assurance, many which were previously published (VanMensel et al., 2022, 2020). Typically, the RNA integrity number (RIN) was 6.0 or greater, an acceptable

quality value for sequencing and additional downstream analyses (Gallego Romero et al., 2014). However, there is no consensus on the threshold for sample inclusion with RIN values as low as 3.95 reported as acceptable, depending on the particular study and importance of RNA degradation (Weis et al., 2007).

Complementary DNA (cDNA) was synthesized from the purified total RNA extracts using a High-Capacity cDNA Reverse Transcription kit (Applied Biosystems), following the manufacturer's protocol. Where necessary, cDNA was diluted with ddH₂O to give more uniform final concentrations of all samples before proceeding with sequencing (Table A-2). cDNA samples were stored at -20°C until further processing.

2.2.4 Library preparation, quality control, and sequencing

Libraries were developed using a two-stage PCR approach; first to target the 16S rRNA gene, and second to barcode each sample for proper identification in downstream analyses. A set of primers (VanMensel et al., 2017) was used for PCR₁, targeting the V5/V6 hypervariable region within the 16S rRNA bacterial gene for each sample. Reactions were performed in 25 µL volumes containing 1 µL template DNA/cDNA, 2.5 µL 10× Taq buffer (GenScript), 0.5 U Taq DNA polymerase (GenScript), and final concentrations of 0.3 M dimethyl sulfoxide (DMSO), 1 mg/mL bovine serum albumin (BSA), 200 µM of each primer, 200 µM each dNTP (Thermo Scientific), and 2.5 mM total MgCl₂ (includes buffer). PCR₁ thermocycler conditions consisted of (i) initial denaturation at 95°C for 5 min, (ii) 25 cycles of 94°C for 15 sec, 60°C for 15 sec, and 72°C for 30 sec, followed by (iii) a final elongation at 72°C for 1 min. Amplicon products were purified following an approach using solid phase reversible immobilization (SPRI) beads previously described (Vo and Jedlicka, 2014). A second short-cycle amplification (PCR₂) was performed to tag each sample using a unique IonX barcode as the forward primer and a universal

reverse primer (UniB-P1) (VanMensel et al., 2017). Reactions were performed in 25 μ L volumes containing 12 μ L purified PCR₁ product and the same units of reagents as described for PCR₁ above. PCR₂ thermocycler conditions are the same as described for PCR₁ except 2 min at 94°C for initial denaturation, annealing temperature of 55°C and a total of 7 cycles. PCR₂ products were pooled accordingly with respect to gel electrophoresis band intensity for normalization purposes and by nucleic acid fraction (DNA or cDNA). Condensed samples were subjected to slow agarose gel electrophoresis using Tris-acetate EDTA (TAE) buffer and the desired products were obtained via band excision. Products were purified using a Gel Extraction kit (Qiagen), following the manufacturer's instructions, and subsequently analysed on the Bioanalyzer using a High Sensitivity DNA kit (Agilent Technologies) for concentration and purity. Finally, samples were diluted to ~50 pmol/L, pooled by nucleic acid fraction (DNA or cDNA) and sequenced on the Ion Torrent Personal Genome Machine (PGM™) using an Ion 530™ Chip kit with an Ion 530™ Kit-Chef (ThermoFisher Scientific) for each nucleic acid fraction. It should be noted that the chips used for sequencing these samples also included samples from other projects, which would affect sequencing depth and average read counts per sample.

2.2.5 *Bioinformatics analysis*

Raw sequencing data were processed into tables of bacterial counts with the Qiime2 (v.2019.10) bioinformatics pipeline. Qiime2 (Bolyen et al., 2019) is the successor platform to QIIME (Quantitative Insights into Microbial Taxonomy), an open-source bioinformatics pipeline for microbiome analysis of marker gene (e.g., 16S, 18S rRNA) amplicon sequencing. Raw, demultiplexed sequences from the Ion Torrent PGM™ were assigned into amplicon sequence variants (ASVs) with trimming set at 29 basepairs (bp) and truncating at 275 bp. Taxonomy was

assigned based on the SILVA (v.132.99) reference database trained 515F-926R specific to version 2019.10 of Qiime2.

Statistical analyses were performed in RStudio v.1.4.1103 (RStudio Team, 2021). Diversity metrics were evaluated in the vegan package (v. 2.5-7). Chao1 richness estimator was calculated on unfiltered sequences; Shannon-Weiner diversity index was determined with singletons removed because this approach is highly sensitive to the singleton count (Willis, 2019). One-way analysis of variance (ANOVA) was used to test significant differences between treatments using an alpha level of 0.05. Tukey's post-hoc analysis followed ANOVA, where appropriate, to distinguish where the differences were attributed. For beta diversity, raw feature (ASV) abundance data was filtered for low read counts (i.e., < 3000 reads/sample were removed) and ASVs with zero reads after filtering were subsequently removed. Distance matrices were calculated with the avgdist function in vegan using Bray-Curtis dissimilarity metric, rarified at 3000 samples to account for uneven sampling depth. Non-metric multidimensional scaling (NMDS) ordination was explored with the metaMDS function (ellipses representing 95% confidence). Permutational multivariate analysis of variance (PERMANOVA) and subsequent pairwise comparisons were performed to test for significance between groupings within NMDS ordinations. For taxonomic evaluations, filtered data (samples with > 3000 reads) was further filtered for Bacteria and normalized via total sums scaling (i.e., relative abundance in relation to the total bacterial population per sample). This approach removes technical bias related to different sequencing depth of each sample and allows for direct comparison of the data. All graphical representations were created with the ggplot2 package.

2.3 Results

2.3.1 Site descriptions and sediment characteristics

As discussed above, the energy which a beach is subjected to can play a large role in the resuspension and transport of sediments and therefore potential pathogens. As such, each sample location has been assessed for energy level (e.g., high or low) based on the following criteria: beaches with bed sediment of median particle size (D_{50}) < 500 μm and moisture content > 20% were designated as low energy; otherwise, the site was defined as high energy (Table 2.1). Although these criteria are somewhat arbitrary, in combination with field observations (e.g., geography, man-made structures), it does provide for a clear division in energy levels between sample sites.

West Belle River Beach (BR) This beach (42°17'51.1"N, 82°42'39.2"W) is located on the west side of the mouth of Belle River – a main tributary that flows through agricultural land upstream, then through the urbanized town of Belle River before it reaches Lake St. Clair (Figure 2.2B). This agriculturally stressed river collects manure and chemical fertilizer from the surrounding fields in its watershed (DiCarlo et al., 2020) and is reportedly a major source of microbial contamination to the lake, significantly impacting water quality (Madani et al., 2021). A marina adjacent to this beach, on the east side of the river mouth, is protected by 600 m of breakwater and is a barrier to longshore drift (Madani et al., 2022). In addition, a 150 m jetty was recently built that extends into the lake at the river mouth. With the marina and jetty, this beach is sheltered and hydrologically low energy with minimal water movement/displacement and the D_{50} of bed sediment in the nearshore swim zone was fine-grained (66 μm) with a moisture content of 22.16% (Table 2.1). Consequently, BR is one of the most problematic beaches in WEC based on historic beach closures because of high *E. coli* levels detected in the water (Table 1.1).

Windsor's Sandpoint Beach (SP) This beach (42°20'19.0"N, 82°55'08.4"W) is situated at the source of the Detroit River, approximately 1 km east of where Little River discharges into the Detroit River (Figure 2.2C). The Little River Pollution Control Plant (LRPCP) sits approximately 1 km upstream of the confluence of this tributary and the Detroit River, and with a capacity of 73,000 m³/day, produces effluent with some of the highest quality in the province (City of Windsor, 2022). There is no obvious barrier at this beach to restrict water flow or longshore drift from the east, yet due to bathymetry and the geographical layout of the shoreline, this site has some of the highest retention times (e.g., water age reaching ≥ 15 days at the peak of summer) of the entire lake at any given time (Bocaniov and Scavia, 2018). Sediment characteristics revealed grain size D_{50} of 517 μm and moisture content of 18.31% and was therefore described as a high-energy site (Table 2.1). Accordingly, SP beach typically does not exceed *E. coli* concentration regulations (Table 1.1).

Holiday Conservation Beach (HD) This beach (42°01'51.4"N, 83°02'36.0"W) is located on Lake Erie near the outlet of the Detroit River in a large conservation park in Amherstburg (Figure 2.2D). This rural setting is surrounded by wetlands, forest, and agricultural landscapes. There is no noticeable embayment at the beach nor any physical barrier (manmade or natural) that restricts water flow along the shore. In fact, hydrological dynamics often allow the water input from the Detroit River to reach the shoreline at this beach location, as can be seen by the extension of sediment plumes from arial perspectives (Figure 2.1). HD is not routinely impacted by beach closures (Table 1.1), although when it is, water *E. coli* levels can be extremely elevated (www.wechu.org). This may be due to a combination of varied water volume and flow velocity from the Detroit River, which affects lake hydrodynamics, and the concentration of TSS and the associated FIB in this suspended phase. Lakebed physicochemistry indicated surface sediment to

be the coarsest of all six beaches (D_{50} of 1,201 μm), with the lowest moisture content (10.44%), suggesting HD beach to be the highest in energy of all beaches studied (Table 2.1).

Kingsville's Lakeside Beach (KV) This beach ($42^{\circ}01'32.3''\text{N}$, $82^{\circ}44'26.8''\text{W}$) is situated on Lake Erie and has strong similarities to BR, including proximity to the mouth of an influencing tributary – Mill Creek (Figure 2.2E). Although Kingsville is not directly within the dense greenhouse region in WEC, Mill Creek is considered “greenhouse influenced” because it contains higher concentrations of nutrients and trace metals in comparison to other tributaries farther removed (Maguire et al., 2018). It is also impacted by the surrounding residential land use closer to the lake. KV beach is located on both sides of the mouth of Mill Creek, and a natural pier extending out into the lake restricts immediate flow from the tributary west but simultaneously directs and confines its discharge to the eastern embayed beach, thus impacting the water quality. In fact, likewise to BR, KV is also considered one of the most problematic beaches in WEC regarding frequent summer closures due to high levels of *E. coli* (Table 1.1). Bed sediment is fine-grained in the nearshore zone (D_{50} of 102 μm) and moisture content was comparatively high for the region (24.77%), characterizing this beach as low energy (Table 2.1).

Leamington's Seacliff Beach (LE) This beach ($42^{\circ}01'44.4''\text{N}$, $82^{\circ}36'20.2''\text{W}$) is the largest and longest stretching beach of the group, set within the concentrated greenhouse region on Lake Erie (Figure 2.2F). Although slightly embayed, LE beach is mostly open and exposed to the eastward water movement along the shoreline, especially in early winter as a result of strong wind-driven currents shown by hydrodynamic modelling (Niu et al., 2015). A jetty, ferry dock, and marina are all positioned immediately east of this beach, potentially restricting persistent longshore drift; however, LE is considered high energy based on hydrodynamics and physicochemical measurements ($D_{50} = 656 \mu\text{m}$, moisture = 17.21%) of the nearshore lakebed

(Table 2.1). Historical data on *E. coli* levels reflects this high-energy beach, with closures generally occurring < 25% of the swimming season (Table 1.1).

Point Pelee's Northwest Beach (PP) Unlike the other Lake Erie beaches in this study, this beach (41°58'02.6"N, 82°32'05.2"W) faces west in the western basin and within Point Pelee provincial park (Figure 2.2G). It has no physical barriers and as previous hydrodynamic modelling of Lake Erie has shown (Niu et al., 2015), experiences no restricted water movement from the incoming eastward lake current. Physicochemical characteristics indicated grain size (D_{50}) of 838 μm in the nearshore with moisture content of 14.70% (Table 2.1). For these reasons, PP beach is considered one of the highest energy beaches in WEC with infrequent summer closures based on *E. coli* levels (Table 1.1).

2.3.2 Sequencing statistics

Sequencing for each nucleic acid fraction was performed on separate chips for the Ion Torrent PGM™. After filtering raw sequence data, the DNA chip generated 298 samples and 88,628 ASVs (average 34,148 reads/sample), and the cDNA chip produced 188 samples and 54,286 ASVs (average 24,145 reads/sample).

2.3.3 Alpha diversity of freshwater beach sediments

Both DNA and cDNA datasets characterize the lakebed microbial community from Lake St. Clair (BR and SP) and Lake Erie (HD, KV, LE, and PP). For a spatial perspective of community diversity, the samples in each dataset were grouped by location with all collection dates combined (Figure 2.4). Chao1 richness average values for the six beaches ranged from 637

– 777 (DNA) and 503 – 780 (cDNA) while Shannon diversity average values for the six beaches ranged from 4.70 – 4.95 (DNA) and 5.04 – 5.47 (cDNA) (Table A-3). For DNA, ANOVA or Tukey’s test results revealed no significant differences observed between any of the beaches. However, cDNA showed HD, KV, and LE beaches (all Lake Erie beaches) to have the lowest Chao1 and Shannon diversity compared to the others.

From a temporal perspective, Chao1 richness and Shannon diversity for each individual beach generally increased over the course of the sampling period (April through November). For Chao1 richness, variability was high for the DNA dataset (both within collection date and over time for each beach) but was lower for the cDNA and showed a more obvious increasing trend over time (Figure 2.5). Shannon diversity showed a noticeable increasing trend for DNA, and although the cDNA dataset showed this increasing tendency, it showed less distinction over time (i.e., more gradual than DNA) and lower variability each month (Figure 2.6). ANOVA and Tukey’s post-hoc results confirm this trend (Table A-3); although both diversity metrics revealed that collection date is a significant factor for cDNA, the Shannon diversity of the DNA data showed extremely high significance ($p < 2^{-16}$) compared to the Chao1 richness of the DNA data ($p > 0.05$) with earlier sampling dates (i.e., April, June) typically lower in Shannon index than later sampling dates (i.e., August, September, November).

2.3.4 *Beta diversity of freshwater beach sediments*

NMDS ordination of the microbial community associated with bed sediment of the freshwater beaches illustrates the differences in (dis)similarity between the beaches for the DNA and cDNA datasets (Figure 2.7). For the DNA, ellipses (95% confidence level) are mostly overlapping for all six beaches, but there is greater separation by beach observed for the cDNA data. For both datasets, however, PERMANOVA revealed significant differences ($p = 0.001$) of

the microbial communities from the individual beaches both spatially and temporally (Table A-4).

Ordination was repeated with microbial points reassigned according to season (Figure A-1), which demonstrated clear distinction for the DNA data; fall samples show full separation from spring samples with the summer ellipse overlapping nearly all spring samples and a large portion of the fall samples. Correspondingly, the cDNA ordination plot shows a similar overlap between spring and summer samples, yet there is no fall representation for the cDNA fraction to confirm this observation with the viable microbiota.

Beta diversity was evaluated further by incorporating environmental factors to assess their influence on the microbial community (Figure A-2). Although it is difficult to interpret these results because the clustering of microbial plots is compact in the ordinations, there are a few conclusions that can be made. Specific water parameters showed similar direction of influence to each other for both the DNA and cDNA datasets; temperature, DO, and pH appeared to influence the microbiota in a similar fashion, and likewise for turbidity and ORP, while the influence of conductivity showed a distinct direction compared to the others. For DNA, since there is such a distinct separation of the fall samples, it appears that both conductivity and turbidity are considerably more dominant factors for the spring. For cDNA, the most discernible observation is that turbidity has the strongest influence specifically on KV beach.

2.3.5 Taxonomic characterization of benthic bacterial communities

Taxonomy was assigned against the SILVA database (v.132.99). In this version of SILVA, the conventional class Betaproteobacteria has been reclassified as the order Betaproteobacteriales under the class Gammaproteobacteria; this reclassification was kept for our taxonomic evaluation.

At the phylum level, undefined or unclassified taxa (i.e., “NA”) accounted for 49-53% of the DNA and only 4-19% of the cDNA for all locations investigated (Table A-5). After removing NA taxa, the community composition revealed Proteobacteria to be the dominant group for all locations in both DNA (37-50%) and cDNA (64-85%) data (Figure 2.8A). In the DNA, Bacteroidetes was the second most represented phylum (16-32%) with the highest percentage observed at KV (32%), followed by Acidobacteria (7-20%) with the highest proportion recorded at LE (16%) and PP (20%). All other phyla described < 9% of the DNA within the lakebed at each beach. For the cDNA data, aside from the highly dominant Proteobacteria, other notable phyla were the Cyanobacteria (1-24%) and Actinobacteria (3-16%). Specifically, the Cyanobacteria were most metabolically active at Lake St. Clair beaches (BR = 24%, SP = 19%), in comparison to Lake Erie sites which all presented only 1% relative abundance for this phylum. Actinobacteria was most highly represented at HD (11%), LE (12%), and PP (16%) – all Lake Erie beaches. All other phyla accounted for < 8% of the cDNA within the bed sediment at each location.

Examining the bacterial community composition at the class level within the prevalent Proteobacteria phylum, Gammaproteobacteria was the dominant group, making up 25-37% and 57-80% of the total bacterial composition for DNA and cDNA, respectively (Figure 2.8B). Alphaproteobacteria was also evident as a main group in the DNA data (5-10%) but did not appear to be a key group of the active community, accounting for < 3% of the cDNA at each beach. The Deltaproteobacteria were present at all beaches in each dataset but at very low percentages (< 3% for each condition), and the Magnetococcia (the only other Proteobacterial class identified) were negligible, detected < 0.00 %, if at all. The remainder proportion of taxa at this level (2-4%) were unclassified/undefined (i.e., NA).

At the taxonomic level of order within the Proteobacteria phylum, the most dominant group was the Betaproteobacteriales, explaining 16-27% (DNA) and 46-69% (cDNA) of the total bacterial consortia associated with bed sediment at the freshwater beaches (Figure 2.8C). The

Enterobacteriales were also represented at each beach for both DNA (5-7%) and cDNA (3-8%) datasets, while the Rhodobacterales only showed high enough presence (> 3% at KV) to be observed in the DNA as its own representation; all representations of this order in the cDNA dataset were < 3% and was therefore grouped with “Other”.

2.4 Discussion

As the macromolecular composition of bacterial cells is directly related to the metabolic activity and the synthesis potential and activity of microbial proteins can be measured with RNA levels (Blazewicz et al., 2013; Bremer and Dennis, 2008; Schaechter et al., 1958), cDNA sequencing data can theoretically be used as a proxy to evaluate potentially active microbes in a given environment. A recent study by Falk (et al., 2019) demonstrated the utility of evaluating messenger RNA (mRNA) from freshwater sediments contaminated with organic chemicals and metals to assess the ability of benthic microbes to cope with anthropogenic pressures. Combining RNA analyses with DNA assessments can complement taxonomic studies and primarily aid in the fundamental understanding of whole community structure and dynamics (De Vrieze et al., 2018). For example, simply sequencing the DNA of microorganisms from nearshore beach zones as a public safety measure and tool for evaluating water quality can be misleading regarding expressed or active members (Rytönen et al., 2021). In this present study, we quantify both cDNA and bulk environmental DNA (eDNA) from the lakebed of freshwater public beaches to assess the differences in biodiversity, relative abundance of major active and total benthic microbes, and overall community structure.

In support of this view, alpha diversity of the microbial community within the freshwater lakebed samples was represented by the Chao1 richness estimator and Shannon-Weiner index (Figure 2.4). For the Chao1 richness, each beach showed higher average and median values in the

DNA dataset compared to cDNA, except for PP which exhibited high variability in the cDNA and could be the reason why this relationship appears different (Table A-3). As expected, these results suggest that some of the taxa units accounted for in the DNA dataset do not represent active members of the community (i.e., dead or dormant cells, or free DNA fragments) and can falsely represent a more microbially rich environment than in actuality. On the other hand, the Shannon diversity metric was greater in the cDNA representation compared to DNA for each beach. This indicates a higher biodiversity (i.e., evenness since richness was observed to be reduced) exemplified by the active community compared to total eDNA which embodies all states of microbial genetic material (e.g., alive and active; dormant/inactive; dead; free DNA fragments in the environment). This suggests some species represented by the eDNA fraction are not transcriptionally active in these sediments, as corroborated by the Chao1 results, which may be because they are dormant (i.e., spores) or fragmented and free genetic material (i.e., detritus) residing at the sediment surface as bioavailable carbon (Liu et al., 2020). Statistically, there was no spatial variation in microbial diversity for the DNA dataset for either Chao1 richness or Shannon diversity metrics (Table A-3), suggesting physical (e.g., grain size) variations did not influence the total eDNA richness or composition within the bed sediment. However, there was a significant difference identified spatially in the cDNA data, with HD, KV, and LE beaches (Lake Erie) recording the lowest Chao1 richness and Shannon diversity compared to the others. This suggests dissimilarities of biodiversity between the beaches at the active bacterial component level. In fact, ANOVA demonstrated this difference between the two lakes overall, with Lake St. Clair having a significantly higher Shannon value than Lake Erie within the cDNA data ($p < 0.05$; Table A-3). This indicates greater biodiversity in the active bacterial community of Lake St. Clair sediments (as represented by the Shannon index) and may reflect differences in hydrological dynamics (Gao et al., 2015), nutrient availability (Moncada et al., 2019), and/or the various input tributaries and their associated microbial components within each of these lakes (Madani et al., 2022, 2020). Chao1 richness, however, did not show a significant difference ($p > 0.05$) between

the lakes for DNA or cDNA datasets, suggesting the difference of active microbial diversity can be attributed to an increase in evenness among the bacterial community.

From a temporal perspective, both cDNA and bulk eDNA datasets demonstrated general increase in biodiversity from spring through fall for both Chao1 richness (Figure 2.5) and Shannon diversity (Figure 2.6). This correlates with increasing temperatures and swimmer density during the spring and summer months, which corroborate previous studies demonstrating greater biomass and microbial heterotrophic activity when seasonal temperatures were higher (Unimke et al., 2017; Wilhelm et al., 2014). Unexpectedly, all November DNA samples also follow this increasing trend in biodiversity (i.e., Shannon metric), even though temperatures and beach activities are dramatically reduced at this point of the year. Based on this diversity measure alone, this may reflect the recalcitrant structure of the DNA molecule itself, demonstrating a strong delay of microbial assembly turnover due to its environmental persistence, especially within sediments, leading to a greater proportion of nonviable microbes (or free eDNA) during the colder, less productive months (Haller et al., 2009; Pawlowski et al., 2022; Zimmer-faust et al., 2017). Microbial richness (i.e., Chao1), however, showed a decrease for November samples in the DNA dataset, demonstrating the die-off or degradation of biomass as temperatures decrease and environmental conditions decline for supporting microbial life. Therefore, the increasing trend of Shannon diversity metric for November samples in the DNA dataset is likely due to an increase in microbial evenness, suggesting the community is more evenly distributed by its existing members. Unfortunately, we do not have the corresponding November cDNA samples to compare and assess this assumption. Seasonal variations and patterns of microbial diversity and activity, however, are common in freshwater sediments and water ecosystems (Fang et al., 2022; Oest et al., 2018; Yi et al., 2021), and there is evidence that coastal benthic habitats are especially impacted by changing environmental conditions (e.g., seasonal temperature fluctuations; climate change), although research on this topic regarding microbes (and pathogens) in sediment is lacking in current literature (Hicks et al., 2018).

Beta diversity was illustrated through NMDS ordination plots (Figure 2.7), and while the microbial communities from the beaches overlapped considerably for both datasets, there was greater separation in the cDNA data. This is likely a reflection of the higher biodiversity and dynamic functional properties within the active community, correlating with alpha diversity results. Comparison of the two NMDS plots demonstrates that the functioning community is not accurately represented by the basic eDNA assembly. Although it is possible (and likely) that all the ASVs detected in cDNA were also represented in the bulk eDNA, it is the composition of the cDNA fraction that better explains microbial functionality within a sample and therefore, more accurately represents the microbial community (De Vrieze et al., 2018). This information is important with regards to human health risks within recreational waters.

Considering the influence of physicochemical parameters of the water column described through NMDS (Figure A-2), turbidity appears to be the one environmental variable that demonstrated a distinguishable impact on the microbial communities at the sediment-water interface. Turbidity is strongly associated with spring DNA samples compared to fall. This correlates with springtime snowmelt, greater volumes of precipitation, and higher levels of erosion associated with runoff (Wu et al., 2017). In terms of cDNA, turbidity shows the strongest influence at KV, which has been described as a low-energy beach with fine-grained sediment particles influenced by a structural barrier (§2.3.1). It should be noted that turbidity is an important indicator for the proportion of SS and its impact on light attenuation (Carpenter and Carpenter, 1983). Accordingly, the benthic primary producers will be more reliant on other forms of energy when light is limited. In the case of KV, the microbiome may rely more on chemolithotrophic activity in contrast to photosynthesis as the DOC associated with SS falls to the bed surface and provides increased food for these metabolic processes (Learman et al., 2016; Orcutt et al., 2011). Surface sediment communities would therefore be expected to shift their functional properties in response to the different environmental conditions and be reflected in the cDNA analysis. In fact, past studies have reported on the chemolithotrophic capabilities of

taxonomically recognised phototrophs under limited light conditions (de Wit and van Gernerden, 1987), supporting the importance for gene expression assessments to inform on actual functionality *in situ*.

Taxonomic assessment of the microbial communities revealed prominent differences between the two datasets (Figure 2.8). The largest distinction was the disparity in relative abundance of unclassified/undefined ASVs (i.e., “NA”) at the phylum level (Table A-5), indicating about half of the bulk eDNA in the bed sediment of these beaches is composed of unknown or uncharacterized microorganisms compared to only 4-19% for the cDNA fraction. This suggests that the active bacterial community primarily consists of microbes that have been previously characterized, and that the bulk eDNA may reflect damaged or degraded genetic material (e.g., dead cells, detritus) which has been integrated into the bed sediment following deposition (Eisenhofer and Weyrich, 2019). After removal of NA taxa, the most dominant phylum was the Proteobacteria in both datasets. Within the Bacteria domain, this group is the largest and phenotypically most diverse with a vast array of morphologies and physiologies, including diverse chemolithotrophic metabolisms (Kerstens et al., 2006). The Proteobacteria, comprising several known human pathogens (e.g., *E. coli* under the Enterobacteriales order of Gammaproteobacteria), are abundant throughout the environment, consisting of members largely recognised for their nutrient cycling and diverse degradation capabilities (Rizzatti et al., 2017). The notably higher relative abundances in the cDNA dataset for the dominant Proteobacteria (phylum), Gammaproteobacteria (class), and Betaproteobacteriales (order), suggests that the community represented by bulk eDNA underestimates the bacterial activity within the bed sediment environment. However, this may be an acceptable approach to gauge which higher taxa group(s) to investigate further with enhanced resolution (Tiwari et al., 2021). It is noteworthy that out of 48 unique orders within the Proteobacteria (includes all classes) that resulted in any detection from any of the freshwater bed sediment samples, only three (Betaproteobacteriales, Enterobacteriales, and Rhodobacterales) revealed > 3% of the total bacterial community in at

least one beach. This underpins the high importance of these groups to freshwater ecosystem function.

The Cyanobacteria were the second most active phylum in Lake St. Clair sediments but did not show appreciable abundance in any Lake Erie beaches. This indicates a dependence on phototrophic metabolism and perhaps a sedimentary reservoir of these microbes, which, under ideal conditions, may resuspend and progress into problematic HABs along the shoreline (Nwosu et al., 2021; Zhang et al., 2021). Although the western basin of Lake Erie is very shallow (mean depth 7.4 m; max. depth 19 m) with fine sediment particles (LaMP Lake Erie, 2011), Lake St. Clair is more shallow (mean depth 3.9 m; max. depth 6.4 m) and therefore has a greater potential for resuspension under similar wind conditions (Bocaniov et al., 2019). This information supports Lake St. Clair bed sediment as a sink with potential to behave as a secondary source of Cyanobacteria with resuspension events. In turn, the release of Cyanobacteria from the lakebed into the water column may contribute to larger, more intense HABs in Lake St. Clair than otherwise without this reservoir. In that case, Lake Erie HAB development, size, and intensity can be attributed to other factors, such as high water input from contaminated (e.g., Detroit River; Maguire et al., 2019) and agriculturally stressed (e.g., Maumee River; Michalak et al., 2013) tributaries.

The research presented here provides a broad microbial baseline of freshwater beach sediments and includes both bulk eDNA and cDNA analysis of the 16S rRNA gene. This approach allowed for an important evaluation of the utility of simple DNA studies (e.g., culture-based approaches) compared to gene expression studies designed for recreational water quality assessments related to potential human health risks. Our results suggest that combining RNA (i.e., cDNA) analysis with DNA assessments can complement taxonomic studies and aid in our overall understanding of freshwater ecosystems.

2.5 Conclusion

Traditional approaches to evaluate microbial water quality from shorelines and beaches is inadequate to inform on accurate human health risks with recreational water activities. Foremost, the sediment compartment is largely neglected in these assessments, yet past research has recognised that sediment-water interactions play a critical role in FIB survival, growth, distribution, and persistence in aquatic environments. We collected nearshore surface sediment from Canadian beaches on Lakes St. Clair and Erie from April through November (2017) and analysed both bulk eDNA and cDNA fractions by targeting and sequencing the 16S rRNA gene with NGS technology. According to the Chao1 richness and Shannon alpha diversity metrics, cDNA data showed greater evenness diversity than bulk eDNA at each beach examined. Benthic biodiversity demonstrated no spatial differences from the eDNA, but a significant difference ($p < 0.05$) between lakes in the active community (cDNA), with Lake St. Clair more diverse than Lake Erie. This may be a reflection of the high proportion (19-24%) of Cyanobacteria identified in Lake St. Clair beaches compared to the negligible detection (~1%) of this phylum in Lake Erie sites. Temporally, the general trend observed was an increase in diversity at each location from spring to fall, correlating with increasing temperature and purportedly more suitable environmental conditions for microbial survival and growth. Beta diversity revealed high overlap of all beaches from the eDNA but a very distinct separation of the spring and fall samples. This was largely driven by higher turbidity in springtime because of seasonal hydrodynamic variations due to snowmelt, high volumes (and frequency) of precipitation (i.e., storms; resuspension events), and subsequent runoff. On the other hand, cDNA demonstrated more dissimilarity between sites, indicating more diverse functioning communities associated with the bed sediment, and turbidity was most influential to the active microbial community at KV beach compared to the others.

Bacterial taxonomic assignments demonstrated all locations were dominant in Proteobacteria, with the active representation displaying much stronger prominence of this phylum than eDNA. Within this group, the Gammaproteobacteria was the largest class and the Betabacteriales was the largest order, for both eDNA and cDNA. Although microbial composition shows subtle differences spatially, the largest differences were between the bulk eDNA and cDNA datasets. Our results suggest that the community represented by bulk eDNA underestimates the bacterial activity within the bed sediment, which supports the use of cDNA analysis as a complement to bulk eDNA studies. Additionally, we recommend that the sediment compartment be assessed in combination with the overlying water when recreational water quality is evaluated as sediment resuspension of benthic microorganisms may have a stronger impact on water quality than previously recognised.

The results of this work establish a valuable microbial baseline of freshwater sediment environments in the GL system. Moreover, the work presented here provides the basis for exploring these habitats further to gain a higher understanding of freshwater microbiomes and how they influence water quality and ecosystem health as well as their potential for affecting human health relating to recreational water use. High-resolution gene expression studies, such as metatranscriptomics, were applied and described in subsequent chapters of this dissertation to examine the functioning sediment communities in more depth. Specifically, Chapter 3 investigates bacterial chemolithotrophic metabolism and pathogenic-related gene expression from bed sediment beach samples at four of the WEC beaches (BR, SP, HD, and KV). Chapter 4 examines the same functional aspects of the microbiome from the SS fraction from tributary source and nearshore beach zones of the low-energy locations (BR and KV) to evaluate SS as a microbial transport vector. Both chapters utilize metatranscriptomics for a deep resolution of sediment-associated microbial activity. Such research will help define microbial profiles of freshwater sediment environments and further our understanding of how these systems function with the goal of improving human health risks related to recreational water use.

Figures and Tables



Figure 2.1: Satellite image of Windsor-Essex, Ontario, Canada surrounded by the freshwater of Lake St. Clair, the Detroit River, and Lake Erie. Sediment plumes entering Lake St. Clair from the Thames River (top) and Lake Erie from the Maumee River (bottom) are clearly visible.

Photo credit: Landsat 9 NASA (image captured on October 31, 2021)



Figure 2.2: A) *WEC in southwestern Ontario, Canada. Features include Lake St. Clair connected to Lake Erie by the Detroit River. Sampling sites (beaches) where bed sediment collections occurred (yellow circles) include B) Belle River (BR) and C) Sandpoint (SP) on Lake St. Clair, and D) Holiday Conservation (HD), E) Kingsville (KV), F) Leamington (LE), and G) Point Pelee (PP) on Lake Erie

*Source: Ministry of Natural Resources and Forestry, Make a Topographic Map
[www.liaapplications.lrc.gov.on.ca]

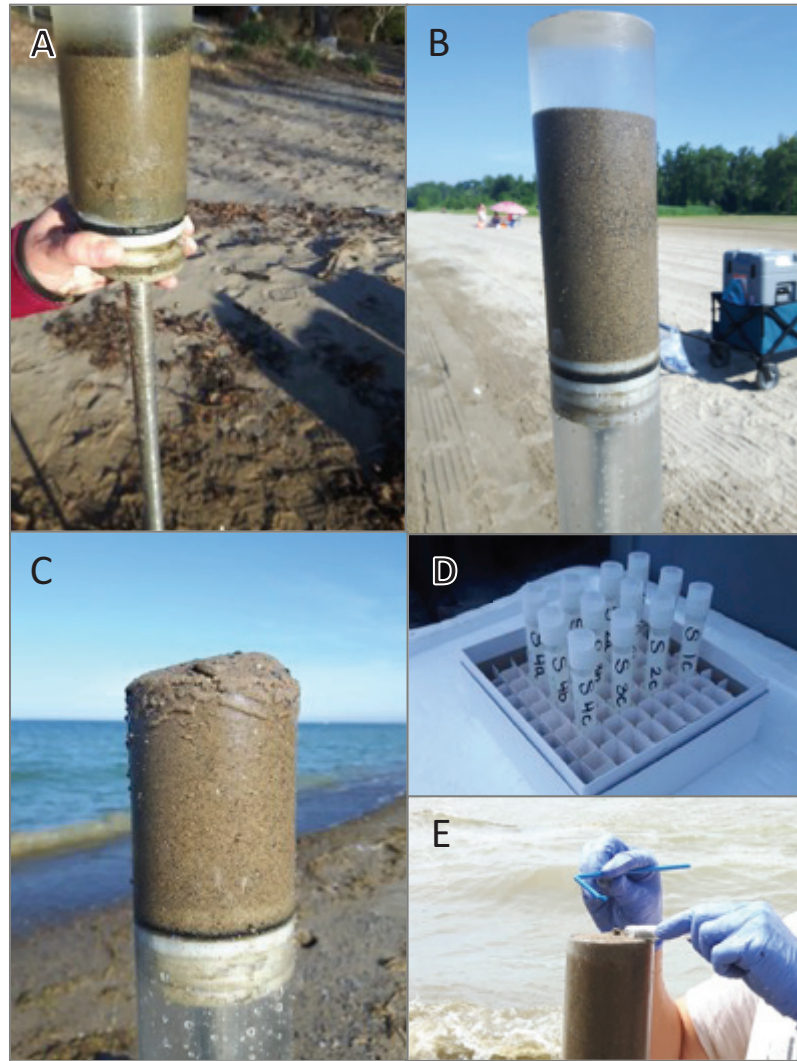


Figure 2.3: Sediment coring material and examples. A) Sediment core in the PVC collection tube, fresh from the lake, on top of extruding device. B) Core being pushed up through the tube using extruding device; dewar containing liquid nitrogen in back (right). C) Sediment surface of lakebed exposed through the top of the tube for sample collection. D) Display of collection cryotubes prepared for a sample site. E) Aseptically scooping top layer of core into cryotube directly prior to preservation in liquid nitrogen.

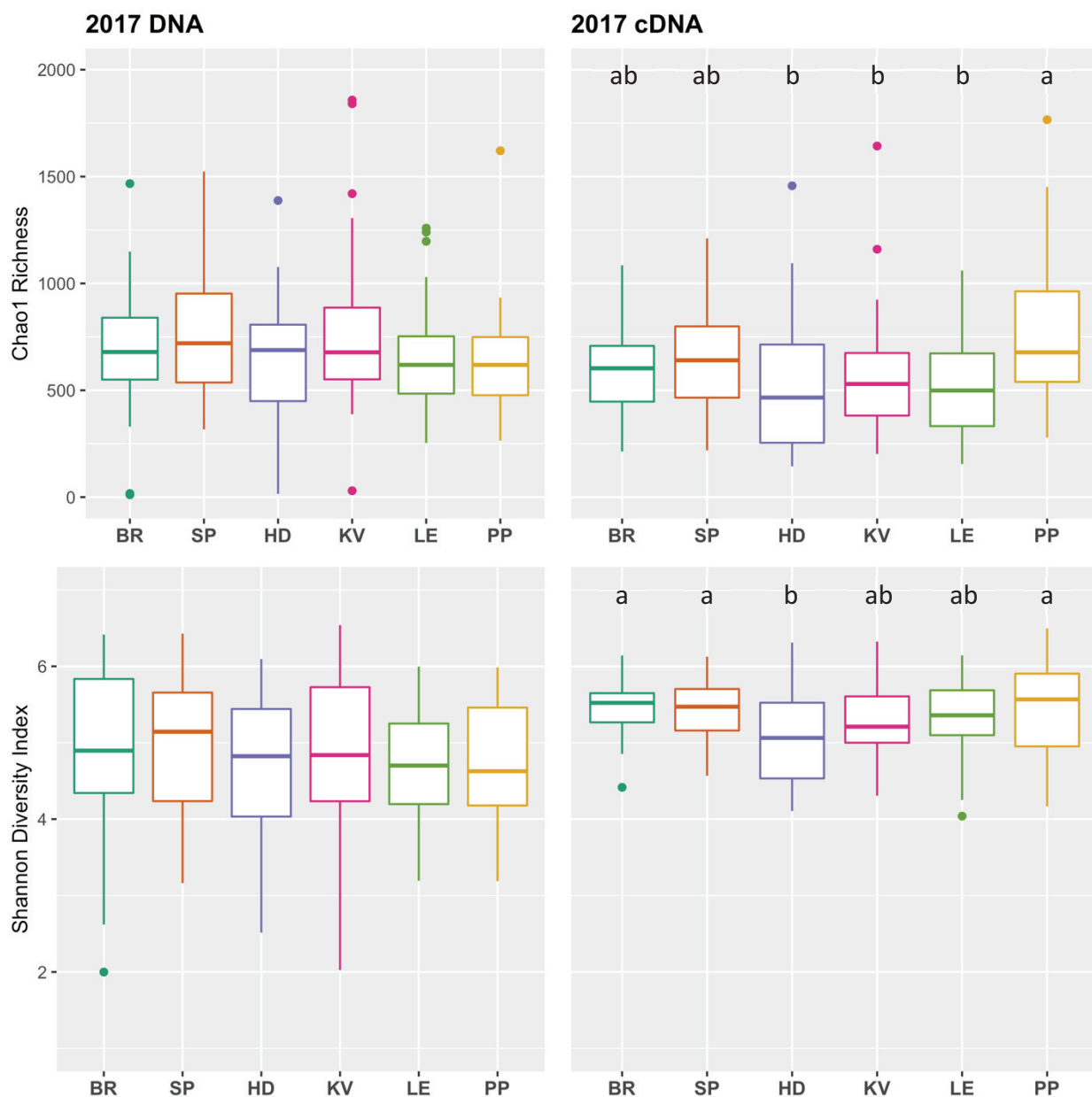


Figure 2.4: Spatial perspective boxplots of Chao1 richness estimator (top) and the Shannon diversity index (bottom) for all six sampling beaches in WEC, combined over the sampling year for both DNA (left) and cDNA (right) datasets. Center line within each box represents the median value. Letters atop boxes indicate where significant differences are attributed based on Tukey's post-hoc tests.

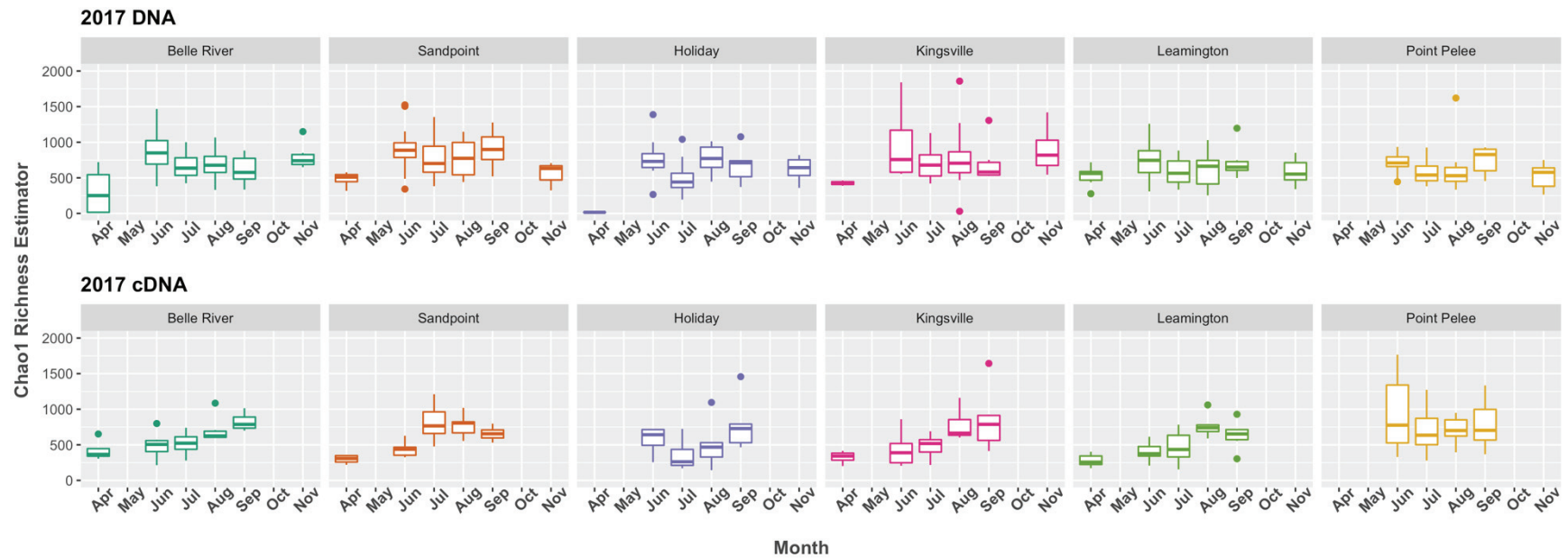


Figure 2.5: Temporal perspective boxplots of the Chao1 richness estimator for all six sampling beaches in WEC, displayed by sample month for both DNA (top) and cDNA (bottom) datasets. Center line within each box represents the median value.

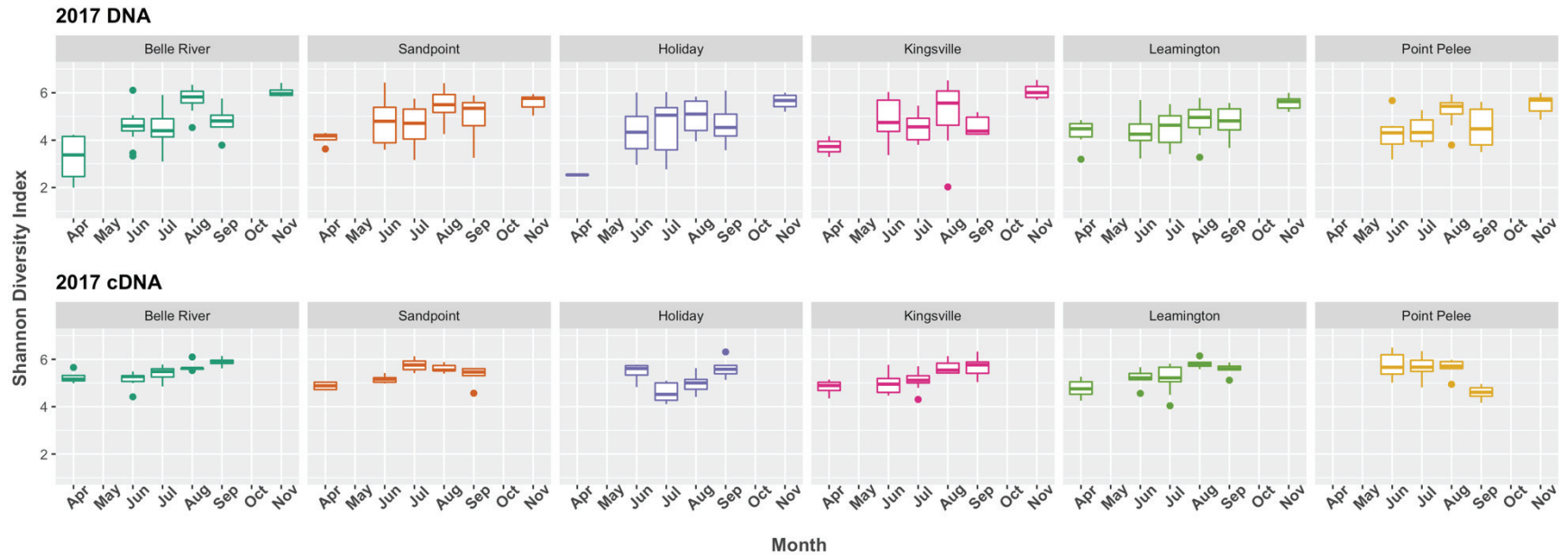


Figure 2.6: Temporal perspective boxplots of the Shannon diversity index for all six sampling beaches in WEC, displayed by sample month for both DNA (top) and cDNA (bottom) datasets. Center line within each box represents the median value.

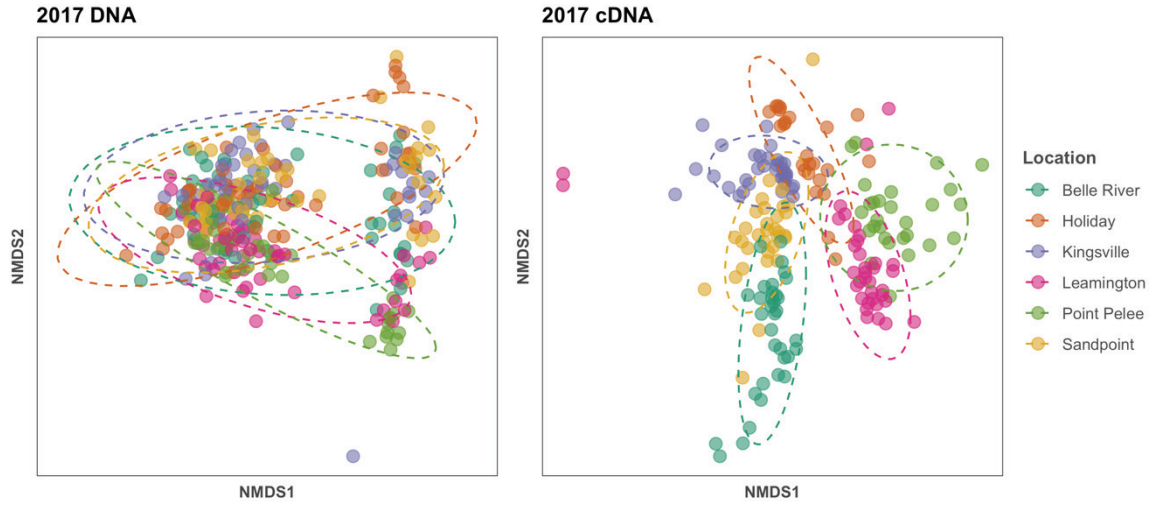


Figure 2.7: NMDS ordination plot of microbial community composition in the bed sediment of freshwater beaches. DNA (left) and cDNA (right) datasets are displayed, illustrating beta diversity between the six beaches sampled throughout WEC. Sample dates are combined for the year. Ellipses represent 95% of samples included.

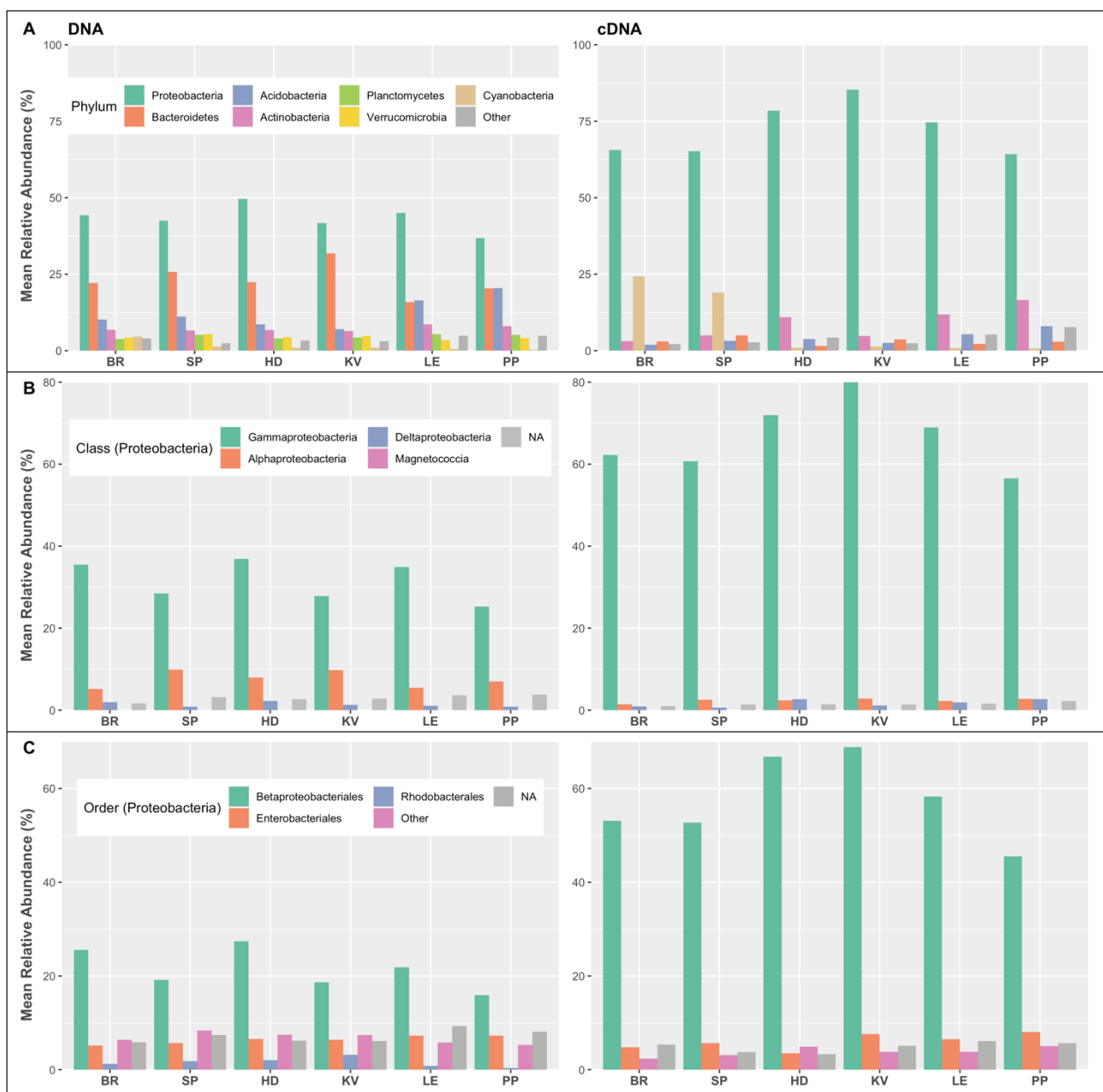


Figure 2.8: Bar charts representative of the bacterial taxonomic composition for both DNA (left) and cDNA (right) fractions of the individual beaches, combined over the sampling year. A) Composition of bacterial phyla with all undefined and unclassified ASVs (i.e., “NA”) at the phylum level removed. B) Composition of Proteobacterial classes; relative abundance values were determined from total bacterial population. C) Composition of Proteobacterial orders; relative abundance values were determined from total bacterial population. “Other” contains the combined taxa for which individual relative abundances were < 3% for all locations. “NA” is the combination of undefined or unclassified ASVs at the taxon level specified. Both DNA and cDNA data share a common legend for each taxonomic level.

Table 2.1: Physical properties of WEC freshwater beaches. Grain size and moisture content are used in combination with geographical features (i.e., barriers that shelter the beach) to determine high or low energy of the location.

		Grain size, D ₅₀ (µm)	Moisture (%)	Sheltered?	High/low energy*
Lake St. Clair	Belle River (BR)	66	22.16	Yes	Low
	Sandpoint (SP)	517	18.31	No	High
Lake Erie	Holiday (HD)	1,201	10.44	No	High
	Kingsville (KV)	102	24.77	Yes	Low
	Leamington (LE)	656	17.21	No	High
	Point Pelee (PP)	838	14.70	No	High

* Assignment based on D₅₀ (low < 500 µm < high) and moisture content (low > 20% > high)

References

- Astudillo-García, C., Hermans, S.M., Stevenson, B., Buckley, H.L., Lear, G., 2019. Microbial assemblages and bioindicators as proxies for ecosystem health status: potential and limitations. *Appl. Microbiol. Biotechnol.* 103, 6407–6421. <https://doi.org/10.1007/s00253-019-09963-0>
- Badgley, B.D., Thomas, F.I.M., Harwood, V.J., 2010. The effects of submerged aquatic vegetation on the persistence of environmental populations of *Enterococcus* spp. *Environ. Microbiol.* 12, 1271–1281. <https://doi.org/10.1111/j.1462-2920.2010.02169.x>
- Baho, D.L., Peter, H., Tranvik, L.J., 2012. Resistance and resilience of microbial communities - Temporal and spatial insurance against perturbations. *Environ. Microbiol.* 14, 2283–2292. <https://doi.org/10.1111/j.1462-2920.2012.02754.x>
- Benjamin, L., Atwill, E.R., Jay-Russell, M., Cooley, M., Carychao, D., Gorski, L., Mandrell, R.E., 2013. Occurrence of generic *Escherichia coli*, *E. coli* O157 and *Salmonella* spp. in water and sediment from leafy green produce farms and streams on the Central California coast. *Int. J. Food Microbiol.* 165, 65–76. <https://doi.org/10.1016/j.ijfoodmicro.2013.04.003>
- Blazewicz, S.J., Barnard, R.L., Daly, R.A., Firestone, M.K., 2013. Evaluating rRNA as an indicator of microbial activity in environmental communities: limitations and uses. *ISME J.* 7, 2061–2068. <https://doi.org/10.1038/ismej.2013.102>
- Bocaniov, S.A., Scavia, D., 2018. Nutrient Loss Rates in Relation to Transport Time Scales in a Large Shallow Lake (Lake St. Clair, USA—Canada): Insights From a Three-Dimensional Model. *Water Resour. Res.* 54, 3825–3840. <https://doi.org/10.1029/2017WR021876>
- Bocaniov, S.A., Van Cappellen, P., Scavia, D., 2019. On the Role of a Large Shallow Lake (Lake St. Clair, USA-Canada) in Modulating Phosphorus Loads to Lake Erie. *Water Resour. Res.* 55, 10548–10564. <https://doi.org/10.1029/2019WR025019>
- Bojko, O., Kabala, C., 2014. Loss-on-ignition as an estimate of total organic carbon in the mountain soils. *Polish J. Soil Sci.* XLVII, 71–79.
- Bolyen, E., Rideout, J.R., Dillon, M.R., Bokulich, N.A., Abnet, C.C., Al-Ghalith, G.A., Alexander, H., et al., 2019. Reproducible, interactive, scalable and extensible microbiome data science using QIIME 2. *Nat. Biotechnol.* 37, 852–857. <https://doi.org/10.1038/s41587-019-0209-9>
- Bremer, H., Dennis, P.P., 2008. Modulation of Chemical Composition and Other Parameters of the Cell at Different Exponential Growth Rates. *EcoSal Plus* 3. <https://doi.org/10.1128/ecosal.5.2.3>

- Carpenter, D.J., Carpenter, S.M., 1983. Modeling inland water quality using Landsat data. *Remote Sens. Environ.* 13, 345–352. [https://doi.org/10.1016/0034-4257\(83\)90035-4](https://doi.org/10.1016/0034-4257(83)90035-4)
- City of Windsor, 2022. Little River Pollution Control Plant. Retrieved on August 22, 2022, from: <https://www.citywindsor.ca/residents/environment/Pollution-Control/Laboratory/Pages/Little-River-Pollution-Control-Plant.aspx>
- Craun, G.F., Calderon, R.L., Craun, M.F., 2005. Outbreaks associated with recreational water in the United States. *Int. J. Environ. Health Res.* 15, 243–262. <https://doi.org/10.1080/09603120500155716>
- De Vrieze, J., Pinto, A.J., Sloan, W.T., Zeeshan Ijaz, U., 2018. The active microbial community more accurately reflects the anaerobic digestion process: 16S rRNA (gene) sequencing as a predictive tool. *Microbiome* 6, 63.
- de Wit, R., van Gernerden, H., 1987. Chemolithotrophic growth of the phototrophic sulfur bacterium *Thiocapsa roseopersicina*. *FEMS Microbiol. Lett.* 45, 117–126. [https://doi.org/10.1016/0378-1097\(87\)90033-4](https://doi.org/10.1016/0378-1097(87)90033-4)
- DiCarlo, A.M., Weisener, C.G., Drouillard, K.G., 2020. Evidence for Microbial Community Effect on Sediment Equilibrium Phosphorus Concentration (EPC0). *Bull. Environ. Contam. Toxicol.* 105, 736–741. <https://doi.org/10.1007/s00128-020-03019-0>
- Dickerson, J.W., Hagedorn, C., Hassall, A., 2007. Detection and remediation of human-origin pollution at two public beaches in Virginia using multiple source tracking methods. *Water Res.* 41, 3758–3770. <https://doi.org/10.1016/j.watres.2007.02.055>
- Dove, A., Chapra, S.C., 2015. Long-term trends of nutrients and trophic response variables for the Great Lakes. *Limnol. Oceanogr.* 60, 696–721. <https://doi.org/10.1002/lno.10055>
- Droppo, I.G., Liss, S.N., Williams, D., Nelson, T., Jaskot, C., Trapp, B., 2009. Dynamic existence of waterborne pathogens within river sediment compartments. Implications for water quality regulatory affairs. *Environ. Sci. Technol.* 43, 1737–1743. <https://doi.org/10.1021/es802321w>
- Eisenhofer, R., Weyrich, L.S., 2019. Assessing alignment-based taxonomic classification of ancient microbial DNA. *PeerJ* 2019, 1–24. <https://doi.org/10.7717/peerj.6594>
- Falk, N., Reid, T., Skoyles, A., Grgicak-Mannion, A., Drouillard, K., Weisener, C.G., 2019. Microbial metatranscriptomic investigations across contaminant gradients of the Detroit River. *Sci. Total Environ.* 690, 121–131. <https://doi.org/10.1016/j.scitotenv.2019.06.451>
- Fang, G., Yu, H., Sheng, H., Chen, C., Tang, Y., Liang, Z., 2022. Seasonal variations and co-occurrence networks of bacterial communities in the water and sediment of artificial habitat in Laoshan Bay, China. *PeerJ* 9, 1–25. <https://doi.org/10.7717/peerj.12705>

- Fluke, J., González-Pinzón, R., Thomson, B., 2019. Riverbed Sediments Control the Spatiotemporal Variability of *E. coli* in a Highly Managed, Arid River. *Front. Water* 1. <https://doi.org/10.3389/frwa.2019.00004>
- Fries, J.S., Characklis, G.W., Noble, R.T., 2008. Sediment-water exchange of *Vibrio* sp. and fecal indicator bacteria: Implications for persistence and transport in the Neuse River Estuary, North Carolina, USA. *Water Res.* 42, 941–950. <https://doi.org/10.1016/j.watres.2007.09.006>
- Gallego Romero, I., Pai, A.A., Tung, J., Gilad, Y., 2014. RNA-seq: Impact of RNA degradation on transcript quantification. *BMC Biol.* 12, 1–13. <https://doi.org/10.1186/1741-7007-12-42>
- Gao, G., Falconer, R.A., Lin, B., 2015. Modelling the fate and transport of faecal bacteria in estuarine and coastal waters. *Mar. Pollut. Bull.* 100, 162–168. <https://doi.org/10.1016/j.marpolbul.2015.09.011>
- Gao, G., Falconer, R.A., Lin, B., 2011. Numerical modelling of sediment-bacteria interaction processes in surface waters. *Water Res.* 45, 1951–1960. <https://doi.org/10.1016/j.watres.2010.12.030>
- Government of Canada, 2022. Guidelines for Canadian Recreational Water Quality – Third Edition. Retrieved on August 24, 2022, from: <https://www.canada.ca/en/health-canada/services/publications/healthy-living/guidelines-canadian-recreational-water-quality-third-edition/guidelines-canadian-recreational-water-quality-third-edition-page-9.html>
- Hahn, M.W., 2006. The microbial diversity of inland waters. *Curr. Opin. Biotechnol.* 17, 256–261. <https://doi.org/10.1016/j.copbio.2006.05.006>
- Haller, L., Amedegnato, E., Poté, J., Wildi, W., 2009. Influence of Freshwater Sediment Characteristics on Persistence of Fecal Indicator Bacteria. *Water. Air. Soil Pollut.* 203, 217–227. <https://doi.org/10.1007/s11270-009-0005-0>
- Hicks, N., Liu, X., Gregory, R., Kenny, J., Lucaci, A., Lenzi, L., Paterson, D.M., Duncan, K.R., 2018. Temperature driven changes in benthic bacterial diversity influences biogeochemical cycling in coastal sediments. *Front. Microbiol.* 9. <https://doi.org/10.3389/fmicb.2018.01730>
- Kerstens, K., De Vos, P., Gillis, M., Swings, J., Vandamme, P., Stakebrandt, E., 2006. Introduction to the Proteobacteria, Prokaryotes Vol. 5. https://doi.org/10.1007/0-387-30745-1_1 noi
- Kinzelman, J.L., McLellan, S.L., 2009. Success of science-based best management practices in reducing swimming bans-a case study from Racine, Wisconsin, USA. *Aquat. Ecosyst. Heal. Manag.* 12, 187–196. <https://doi.org/10.1080/14634980902907466>
- Korajkic, A., Badgley, B.D., Brownell, M.J., Harwood, V.J., 2009. Application of microbial source tracking methods in a Gulf of Mexico field setting. *J. Appl. Microbiol.* 107, 1518–

1527. <https://doi.org/10.1111/j.1365-2672.2009.04351.x>
- Korajkic, A., Brownell, M.J., Harwood, V.J., 2011. Investigation of human sewage pollution and pathogen analysis at Florida Gulf coast Beaches. *J. Appl. Microbiol.* 110, 174–183. <https://doi.org/10.1111/j.1365-2672.2010.04869.x>
- Krantzberg, G., 2008. The Great Lakes, a 35th year anniversary: Time to look forward. *Electron. Green J.* <https://doi.org/10.5070/g312610732>
- Ksoll, W.B., Ishii, S., Sadowsky, M.J., Hicks, R.E., 2007. Presence and sources of fecal coliform bacteria in epilithic periphyton communities of Lake Superior. *Appl. Environ. Microbiol.* 73, 3771–3778. <https://doi.org/10.1128/AEM.02654-06>
- LaMP Lake Erie, 2011. Lake Erie binational nutrient management strategy: Protecting Lake Erie by managing phosphorus. *Prepared by the Lake Erie LaMP Work Group Nutrient Management Task Group.*
- Lear, G., Boothroyd, I.K.G., Turner, S.J., Roberts, K., Lewis, G.D., 2009. A comparison of bacteria and benthic invertebrates as indicators of ecological health in streams. *Freshw. Biol.* 54, 1532–1543. <https://doi.org/10.1111/j.1365-2427.2009.02190.x>
- Learman, D.R., Henson, M.W., Thrash, J.C., Temperton, B., Brannock, P.M., Santos, S.R., Mahon, A.R., Halanych, K.M., 2016. Biogeochemical and microbial variation across 5500 km of Antarctic surface sediment implicates organic matter as a driver of benthic community structure. *Front. Microbiol.* 7, 1–11. <https://doi.org/10.3389/fmicb.2016.00284>
- Liu, S., Zheng, N., Zhao, S., Wang, J., 2020. Exploring the diversity of active ureolytic bacteria in the rumen by comparison of CDNA and GDNA. *Animals* 10, 1–11. <https://doi.org/10.3390/ani10112162>
- Madani, M., Seth, R., Leon, L.F., Valipour, R., McCrimmon, C., 2021. Microbial modelling of Lake St. Clair: Impact of local tributaries on the shoreline water quality. *Ecol. Modell.* 458, 109709. <https://doi.org/10.1016/j.ecolmodel.2021.109709>
- Madani, M., Seth, R., Leon, L.F., Valipour, R., McCrimmon, C., 2020. Three dimensional modelling to assess contributions of major tributaries to fecal microbial pollution of lake St. Clair and Sandpoint Beach. *J. Great Lakes Res.* 46, 159–179. <https://doi.org/10.1016/j.jglr.2019.12.005>
- Madani, M., Seth, R., Valipour, R., Leon, L.F., Hipsey, M.R., 2022. Modelling of nearshore microbial water quality at confluence of a local tributary in Lake St. Clair. *J. Great Lakes Res.* 48, 489–501. <https://doi.org/10.1016/j.jglr.2022.01.019>
- Maguire, T.J., Spencer, C., Grgicak-Mannion, A., Drouillard, K., Mayer, B., Mundle, S.O.C., 2019. Distinguishing point and non-point sources of dissolved nutrients, metals, and legacy

- contaminants in the Detroit River. *Sci. Total Environ.* 681, 1–8.
<https://doi.org/10.1016/j.scitotenv.2019.04.311>
- Maguire, T.J., Wellen, C., Stammler, K.L., Mundle, S.O.C., 2018. Increased nutrient concentrations in Lake Erie tributaries influenced by greenhouse agriculture. *Sci. Total Environ.* 633, 433–440. <https://doi.org/10.1016/j.scitotenv.2018.04.374>
- McClary-Gutierrez, J.S., Driscoll, Z., Nenn, C., Newton, R.J., 2021. Human Fecal Contamination Corresponds to Changes in the Freshwater Bacterial Communities of a Large River Basin. *Microbiol. Spectr.* 9. <https://doi.org/10.1128/spectrum.01200-21>
- Michalak, A.M., Anderson, E.J., Beletsky, D., Boland, S., Bosch, N.S., Bridgeman, T.B., Chaffin, J.D., et al., 2013. Record-setting algal bloom in Lake Erie caused by agricultural and meteorological trends consistent with expected future conditions. *Proc. Natl. Acad. Sci.* 110, 6448–6452. <https://doi.org/10.1073/pnas.1216006110>
- Moncada, C., Hassenrück, C., Gärdes, A., Conaco, C., 2019. Microbial community composition of sediments influenced by intensive mariculture activity. *FEMS Microbiol. Ecol.* 95, 1–12. <https://doi.org/10.1093/femsec/fiz006>
- Niu, Q., Xia, M., Rutherford, E.S., Mason, D.M., Anderson, E.J., Schwab, D.J., 2015. Investigation of interbasin exchange and interannual variability in Lake Erie using an unstructured-grid hydrodynamic model. *J. Geophys. Res. Ocean.* 120, 2212–2232. <https://doi.org/10.1002/2014JC010457>.Received
- Nwosu, E.C., Roeser, P., Yang, S., Ganzert, L., Dellwig, O., Pinkerneil, S., Brauer, A., Dittmann, E., Wagner, D., Liebner, S., 2021. From water into sediment—tracing freshwater cyanobacteria via dna analyses. *Microorganisms* 9. <https://doi.org/10.3390/microorganisms9081778>
- Oest, A., Alsaffar, A., Fenner, M., Azzopardi, D., Tiquia-Arashiro, S.M., 2018. Patterns of change in metabolic capabilities of sediment microbial communities in river and lake ecosystems. *Int. J. Microbiol.* 2018, 5–7. <https://doi.org/10.1155/2018/6234931>
- Orcutt, B.N., Sylvan, J.B., Knab, N.J., Edwards, K.J., 2011. Microbial Ecology of the Dark Ocean above, at, and below the Seafloor. *Microbiol. Mol. Biol. Rev.* 75, 361–422. <https://doi.org/10.1128/mnbr.00039-10>
- Pawlowski, J., Bruce, K., Panksep, K., Aguirre, F.I., Amalfitano, S., Apothéloz-Perret-Gentil, L., Baussant, T., et al., 2022. Environmental DNA metabarcoding for benthic monitoring: A review of sediment sampling and DNA extraction methods. *Sci. Total Environ.* 818. <https://doi.org/10.1016/j.scitotenv.2021.151783>
- Pommier, T., Canback, B., Riemann, L., Bostrom, K.H., Simu, K., Lundberg, P., Tunlid, A.,

- Hagstrom, A., 2007. Global patterns of diversity and community structure in marine bacterioplankton. *Mol. Ecol.* 16, 867–880. <https://doi.org/10.1111/j.1365-294X.2006.03189.x>
- Rissanen, A.J., Kurhela, E., Aho, T., Oittinen, T., Tirola, M., 2010. Storage of environmental samples for guaranteeing nucleic acid yields for molecular microbiological studies. *Appl. Microbiol. Biotechnol.* 88, 977–984. <https://doi.org/10.1007/s00253-010-2838-2>
- Rizzatti, G., Lopetuso, L.R., Gibiino, G., Binda, C., Gasbarrini, A., 2017. Proteobacteria: A common factor in human diseases. *Biomed Res. Int.* 2017. <https://doi.org/10.1155/2017/9351507>
- Rytkönen, A., Tiwari, A., Hokajärvi, A.M., Uusheimo, S., Vepsäläinen, A., Tulonen, T., Pitkänen, T., 2021. The Use of Ribosomal RNA as a Microbial Source Tracking Target Highlights the Assay Host-Specificity Requirement in Water Quality Assessments. *Front. Microbiol.* 12, 1–16. <https://doi.org/10.3389/fmicb.2021.673306>
- Schaechter, M., Maaloe, O., Kjeldgaard, N., 1958. Dependency on medium and temperature of cell size and chemical composition during balanced growth of *Salmonella typhimurium*. *J. gen. Microbiol.* 19, 592–606.
- Shade, A., Read, J.S., Youngblut, N.D., Fierer, N., Knight, R., Kratz, T.K., Lottig, N.R., Roden, E.E., Stanley, E.H., Stombaugh, J., Whitaker, R.J., Wu, C.H., McMahon, K.D., 2012. Lake microbial communities are resilient after a whole-ecosystem disturbance. *ISME J.* 6, 2153–2167. <https://doi.org/10.1038/ismej.2012.56>
- Sterner, R.W., Ostrom, P., Ostrom, N.E., Klump, J.V., Steinman, A.D., Dreelin, E.A., Zanden, M.J. Vander, Fisk, A.T., 2017. Grand challenges for research in the Laurentian Great Lakes. <https://doi.org/10.1002/lno.10585>
- Thoe, W., Lee, O.H.K., Leung, K.F., Lee, T., Ashbolt, N.J., Yang, R.R., Chui, S.H.K., 2018. Twenty five years of beach monitoring in Hong Kong: A re-examination of the beach water quality classification scheme from a comparative and global perspective. *Mar. Pollut. Bull.* 131, 793–803. <https://doi.org/10.1016/j.marpolbul.2018.05.002>
- Tiwari, A., Oliver, D.M., Bivins, A., Sherchan, S.P., Pitkänen, T., 2021. Bathing water quality monitoring practices in europe and the United States. *Int. J. Environ. Res. Public Health* 18. <https://doi.org/10.3390/ijerph18115513>
- Trivedi, P., Delgado-Baquerizo, M., Anderson, I.C., Singh, B.K., 2016. Response of soil properties and microbial communities to agriculture: Implications for primary productivity and soil health indicators. *Front. Plant Sci.* 7, 1–13. <https://doi.org/10.3389/fpls.2016.00990>
- Unimke, A.A., Bassey, I.U., Mmuogbulam, A.O., Nseabasi-maina, N., 2017. Seasonal

- Implications on the Microbiological and Physicochemical Characteristics of Sediments.
- VanMensel, D., Chaganti, S.R., Boudens, R., Reid, T., Ciborowski, J., Weisener, C., 2017. Investigating the Microbial Degradation Potential in Oil Sands Fluid Fine Tailings Using Gamma Irradiation : A Metagenomic Perspective. *Microb. Ecol.* 74, 362–372. <https://doi.org/10.1007/s00248-017-0953-7>
- VanMensel, D., Chaganti, S.R., Droppo, I.G., Weisener, C.G., 2020. Exploring bacterial pathogen community dynamics in freshwater beach sediments: A tale of two lakes. *Environ. Microbiol.* 22, 568–583. <https://doi.org/10.1111/1462-2920.14860>
- VanMensel, D., Droppo, I.G., Weisener, C.G., 2022. Identifying chemolithotrophic and pathogenic-related gene expression within suspended sediment flocs in freshwater environments: A metatranscriptomic assessment. *Sci. Total Environ.* 807, 150996. <https://doi.org/10.1016/j.scitotenv.2021.150996>
- Vega, L., Jaimes, J., Morales, D., Martínez, D., Cruz-Saavedra, L., Muñoz, M., Ramírez, J.D., 2021. Microbial Communities' Characterization in Urban Recreational Surface Waters Using Next Generation Sequencing. *Microb. Ecol.* 81, 847–863. <https://doi.org/10.1007/s00248-020-01649-9>
- Vo, A.T.E., Jedlicka, J.A., 2014. Protocols for metagenomic DNA extraction and Illumina amplicon library preparation for faecal and swab samples. *Mol. Ecol. Resour.* 14, 1183–1197. <https://doi.org/10.1111/1755-0998.12269>
- Wade, T.J., Calderon, R.L., Sams, E., Beach, M., Brenner, K.P., Williams, A.H., Dufour, A.P., 2006. Rapidly measured indicators of recreational water quality are predictive of swimming-associated gastrointestinal illness. *Environ. Health Perspect.* 114, 24–28. <https://doi.org/10.1289/ehp.8273>
- Weis, S., Llenos, I.C., Dulay, J.R., Elashoff, M., Martínez-Murillo, F., Miller, C.L., 2007. Quality control for microarray analysis of human brain samples: The impact of postmortem factors, RNA characteristics, and histopathology. *J. Neurosci. Methods* 165, 198–209. <https://doi.org/10.1016/j.jneumeth.2007.06.001>
- Wilhelm, S.W., Lecleir, G.R., Bullerjahn, G.S., Mckay, R.M., Saxton, M.A., Twiss, M.R., Bourbonniere, R.A., 2014. Seasonal changes in microbial community structure and activity imply winter production is linked to summer hypoxia in a large lake. *FEMS Microbiol. Ecol.* 87, 475–485. <https://doi.org/10.1111/1574-6941.12238>
- Willis, A.D., 2019. Rarefaction, alpha diversity, and statistics. *Front. Microbiol.* 10. <https://doi.org/10.3389/fmicb.2019.02407>
- Wu, Y., Ouyang, W., Hao, Z., Yang, B., Wang, L., 2017. Snowmelt water drives higher soil

- erosion than rainfall water in a mid-high latitude upland watershed. *J. Hydrol.* 556.
<https://doi.org/10.1016/j.jhydrol.2017.11.037>
- Yi, Y., Lin, C., Wang, W., Song, J., 2021. Habitat and seasonal variations in bacterial community structure and diversity in sediments of a Shallow lake. *Ecol. Indic.* 120, 106959.
<https://doi.org/10.1016/j.ecolind.2020.106959>
- Zhang, H., Huo, S., Yeager, K.M., Wu, F., 2021. Sedimentary DNA record of eukaryotic algal and cyanobacterial communities in a shallow Lake driven by human activities and climate change. *Sci. Total Environ.* 753, 141985. <https://doi.org/10.1016/j.scitotenv.2020.141985>
- Zimmer-faust, A.G., Thulsiraj, V., Marambio-jones, C., Cao, Y., Grif, J.F., Holden, P.A., Jay, J.A., 2017. Effect of freshwater sediment characteristics on the persistence of fecal indicator bacteria and genetic markers within a Southern California watershed 119, 1–11.
<https://doi.org/10.1016/j.watres.2017.04.028>

CHAPTER 3: EXPLORING BACTERIAL PATHOGEN COMMUNITY DYNAMICS IN FRESHWATER BEACH SEDIMENTS: A TALE OF TWO LAKES

Published: VanMensel D, Chaganti SR, Droppo IG, Weisener CG (2020) Exploring bacterial pathogen community dynamics in freshwater beach sediments: A tale of two lakes. *Environmental Microbiology* 22:568-583, doi:10.1111/1462-2920.14860

CHAPTER 3: EXPLORING BACTERIAL PATHOGEN COMMUNITY DYNAMICS IN FRESHWATER BEACH SEDIMENTS: A TALE OF TWO LAKES

3.0 Prologue

The knowledge gained from Chapter 2 directed the focus and research of subsequent chapters in this dissertation by identifying rudimentary differences between the chosen beaches. The microbial baseline established from the previous chapter, together with accompanying physical and geochemical characteristics identified, allowed the traditionally problematic beaches to be differentiated from the others. This distinction provided reason to narrow the scope of ensuing research which is technologically and fiscally expensive as well as labour intensive. Specifically, metatranscriptomic analysis was employed on bed sediment samples from four of the beaches explored here (Chapter 3) as well as on SS samples from the two most problematic beaches (Chapter 4). These subsequent chapters provide high resolution insights into the active microbial community associated with the sediment compartment of freshwater shorelines, deeply advancing our current understanding of these environments and the potential risks they present on human health during recreational water activities.

3.1 Introduction

Pathogen contamination of water resources is a major concern throughout the world. At public beaches, routinely quantifying indicator bacteria (e.g., *E. coli*) within the water column is common for the assessment of public health risk. However, these simple assessments disregard physical (e.g., energy) and geochemical (e.g., nutrients, redox) factors as well as contributions from the sediment. According to a 2013 U.S. survey (Natural Resources Defense Council, 2014),

waters in the GLs had the most frequent cases of high beach action value (BAV) *E. coli* that exceeded acceptable levels. These water quality assessments are often performed during the recreational season (e.g., May-September in the GLs region) and focus on the water compartment only. This approach lacks context with respect to physical factors (e.g., disturbance of nearshore sediments) that require consideration. For instance, storm events can result in the resuspension of bed sediment in the water column within nearshore environments. Past studies have shown that sediment dynamics (i.e., resuspension, erosion, transport, deposition) influence both the temporal and spatial variation in microbial communities in sediment and water compartments (Droppo et al., 2011; Phillips et al., 2014; Reid et al., 2016). In comparison to the water column, benthic sediment microbial communities have been reported to harbor considerably higher concentrations of bacteria (Droppo et al., 2009; Probandt et al., 2018), with more than 99% of those microbes attached to mineral grains (Rusch et al., 2003). Several studies have documented that sand reservoirs of FIB contribute to beach water samples exceeding regulatory limits (Alm et al., 2003; Beversdorf et al., 2007; Cloutier et al., 2015; Yamahara et al., 2009), although with limited understanding of the sediment bacterial community (i.e., total structure and functional potential). In many cases, the status of the water may not be accurately represented by traditional water quality assessments (e.g., indicator bacterial counts) that resource managers routinely use in water quality monitoring programs.

In the past 15 years our ability to track community and compositional changes within the microbiome of environmental ecosystems has improved and benefitted with the introduction of high-throughput sequencing (HTS) (Mohiuddin et al., 2017; Ramirez et al., 2018; Shahraki et al., 2019). These advancements have enabled the detection of species *in situ* without the limitation of isolating and culturing single organisms, which do not represent larger community dynamics (Handelsman, 2004; Stewart, 2012; Su et al., 2012). Nevertheless, taxonomic surveys alone can be misleading because they cannot represent the activity (i.e., metabolic status) of the community. The advancement of transcriptomic technology, however, provides higher resolution to observe

functional gene expression (Falk et al., 2018; Reid et al., 2018; Weisener et al., 2017). Thus, the insight we gain from mRNA can complement taxonomic surveys since it allows us to investigate the functioning community (Crovadore et al., 2017; Goltsman et al., 2015; Zhang et al., 2017), improving our understanding of a microbial system.

Previous studies regarding pathogens in recreational waters have not linked geochemical parameters and physical characteristics/dynamics in conjunction with functional genomics for enhanced insight into the microbial community. To investigate these physicochemical/microbial relationships, we sampled four public freshwater beaches (two from Lake St. Clair and two from Lake Erie within southern Ontario) and focused on the active microbial community at the sediment-water interface in the nearshore zone. Using functional genomic techniques, we 1) identified the microbial community profile and gene expression within these beach sediments, 2) characterized the pathogenic potential within the nearshore beaches, and 3) linked pathogenic gene expression to the local sediment and water characteristics.

3.2 Experimental Procedures

3.2.1 Site selection, characteristics and sediment sampling

WEC (Figure 3.1) is strongly recognized for its vast and successful agricultural land use, including livestock farms as well as high crop yields through conventional farming and greenhouse productions. Windsor-Essex County Health Unit (WECHU) subjects public beaches to weekly water quality testing each year from June through September, reporting on indicator *E. coli* CFUs as well as the status of the beach (i.e., open, caution, closed) based on these findings (www.wechu.org).

Sampling was conducted within 24 hours; Lake Erie locations (HD and KV) on July 7, 2016, and Lake St. Clair locations (SP and BR) on July 8, 2016. These sampling dates were

during peak summer temperatures and consequently, high recreational water usage. Additionally, this sampling week reflects some of the highest *E. coli* counts of the 2016 season in WEC public beaches according to WECHU data. Bed sediment samples were collected through a gravity coring technique previously described (§2.2.2).

Total organic carbon (TOC) was assessed by loss-on-ignition (LOI) (Bojko and Kabala, 2014) on bulk bed sediment from the upper layer. Sediment granulometry, moisture content, and designation as either sheltered (low-energy) or not sheltered (high-energy) were previously described (§2.2.2) and reported (Table 2.1).

In situ electrochemical measurements across the sediment-water interface were obtained from micro-electrode sensors (Unisense) controlled using the autonomous Unisense MiniProfiler MP4 shallow water field profiling unit. It was pre-programmed for precise, controlled deployment of sensors across a desired distance to obtain depth profiles of DO and electrochemical potential (redox). Water column parameters (depth, temperature, conductivity (SPC), total dissolved solids (TDS), salinity, DO, pH, ORP, turbidity, chlorophyll a (Chl a), and phycocyanin (BGA-PC)) were measured using the EXO2 sonde with calibrated sensors (Hoskin Scientific) in the nearshore proximal to sediment sample collection but prior to sediment coring to avoid subsequent bed disturbances and resuspension.

3.2.2 *Extractions, library preparation, quality control and sequencing*

Sediment DNA extractions were performed using PowerSoil Total DNA Isolation kits (MoBio) following the manufacturers instructions. DNA libraries were developed using a two-stage PCR approach and amplicon product purification was accomplished with SPRI beads (details in §2.2.4). Samples were diluted to ~50 pmol/L, pooled and sequenced on the Ion Torrent PGM™ using an Ion 318v2™ Chip kit with an Ion PGM™ Hi-Q View Chef 400 kit (ThermoFisher Scientific).

Sediment RNA extractions were performed using PowerSoil Total RNA Isolation kits (MoBio) following the manufacturers protocol with slight modifications previously described (§2.2.3). The final pellet was resuspended in 60 μL RNase-free water to increase concentration. Aliquots of extracted RNA isolations were kept at $-80\text{ }^{\circ}\text{C}$ until further processing. Quality and quantity of extracted RNA samples were assessed in-house using the Agilent 2100 Bioanalyzer (Agilent Technologies) to confirm sufficient values for sequencing. Samples with RIN > 8.0 and concentrations $> 100\text{ ng}/\mu\text{L}$ were acceptable and sent to the Genome Quebec Innovation Center at McGill University in Quebec, Canada for metatranscriptomic analysis. There, total RNA was quantified using a NanoDrop Spectrophotometer ND-1000 (NanoDrop Technologies, Inc.) and RIN was assessed using a 2100 Bioanalyzer. rRNA were depleted using Ribo-Zero rRNA Removal kit specific for yeast then for bacteria (Epicentre/Illumina). Residual RNA was cleaned up using RiboMinus[™] Concentration Module columns (Invitrogen) and eluted directly in the Elute/Frag/Prime buffer of the Illumina TruSeq RNA Sample Preparation Kit v2. The remaining protocol was performed as per the manufacturer's recommendations, except that cDNA was sheared on a Covaris instrument. Libraries were quantified using the Quant-iT[™] PicoGreen[®] dsDNA Assay Kit (Life Technologies) and the Kapa Illumina GA with Revised Primers-SYBR Fast Universal kit (Kapa Biosystems). Average size fragment was determined using a LabChip GX (PerkinElmer) instrument. The libraries were normalized and pooled and then denatured in 0.05N NaOH and neutralized using HT1 buffer. ExAMP was added to the mix following the manufacturer's instructions. The pool was loaded at 200 pM on an Illumina cBot and the flowcell was run on a HiSeq 4000 for 2x100 cycles (paired-end mode). A phiX library was used as a control and mixed with libraries at 1% level. The Illumina control software was HCS HD 3.4.0.38, the real-time analysis program was RTA v. 2.7.7. Program bcl2fastq2 v2.18 was then used to demultiplex samples and generate fastq reads. Samples were sequenced in duplicate to validate sample accuracy.

Raw sequence data sets for both 16S rRNA and metatranscriptomic data have been deposited in the Sequence Read Archive (<http://www.ncbi.nlm.nih.gov/sra>) under PRJNA482773.

3.2.3 *Bioinformatic analysis*

Taxonomic analysis of the bacterial community was performed on DNA data using MacQIIME. Submitted sequences were assigned into operational taxonomic units (OTUs) using open-reference OTU picking at 97% similarity, and taxonomy was assigned based on the SILVA database (Pruesse et al., 2007; Yilmaz et al., 2014). Cumulative-sum scaling (CSS) normalization was applied to account for uneven sample reads and allow for acceptable comparisons (Paulson et al., 2013).

The open-source pipeline MetaTrans (Martinez et al., 2016) was used to analyze the functionality of the active microbial communities from our mRNA samples. From the Illumina platform, we obtained paired-end reads in fastq format (Phred +33) separated into individual files for each single-end read. Raw reads were filtered using the Kraken pipeline (Davis et al., 2013; Wood and Salzberg, 2014) and reads with length less than 30 nt were removed. mRNA was sorted from rRNA/tRNA using SortMeRNA (Kopylova et al., 2012). To recover a functional profile for each sample, mRNA reads were mapped against the M5nr database (Wilke et al., 2015), and differentially expressed functions were determined through the DESeq2 package (Love et al., 2014). All functional annotations were assigned using the KO (Kyoto Encyclopedia of Genes and Genomes (KEGG) Orthology) database, and those that were assigned to recognized functional groups were normalized within each sample to housekeeping gene *rpoC* (DNA-directed RNA polymerase beta' subunit; Colston et al., 2014; Nieto et al., 2009). Transcripts that were not recognized or encoded for poorly characterized functions were excluded from further analysis. The entire transcriptome was obtained through this approach, which allowed for a full overview of the microbial activity within these bed sediments. However, we did ultimately

narrow our results to focus on those involved, either directly or indirectly, with infectious diseases and pathogenicity. Pathogenic gene selection was determined through the KEGG database, targeting functional annotations under *Infectious Diseases*. Functional assignments were interpreted and plotted within Aabel 3 graphical software to present visualizations of the represented data.

3.3 Results and Discussion

3.3.1 Beach sediment characteristics

WEC is located between Lake St. Clair and Lake Erie (Figure 3.1) and is part of the greater Lake Erie watershed. Four public beaches in WEC were selected for this study based on geochemical and physical characteristics as well as historical water quality data provided by the WECHU and results obtained from Chapter 2; HD and KV are both located on Lake Erie, and SP and BR are both located on Lake St. Clair. Physicochemical analyses of these beaches (e.g., TOC, particle size, energy conditions) were undertaken to demonstrate the variations and similarities between sites within the two lakes. This qualitative and quantitative information assisted with the explanation of analytical bacterial trends, pathogen presence, and the degree of microbial activity.

Tables 3.1 and 3.2 provide the different geochemical parameters evaluated. Both SP and HD beaches represented high-energy locations, while BR and KV beaches were influenced by restricted water flow due to adjacent artificial piers and represented low-energy sites as exhibited by coastal embayment and lower wave energy (Table 3.2). Grain size distribution of bulk bed sediment revealed that BR and KV consisted of finer grains (D_{50} of 66 and 102 μm , respectively) in the nearshore zone compared to SP and HD (D_{50} of 517 and 1201 μm , respectively); a further suggestion of their lower energy. The close packing of these fine grains at BR and KV results in a

decrease in relative porosity and an increase in hydrostatic pressures, which can result in steep vertical geochemical gradients (Chen et al., 2013).

The concentration of DO and measured Eh across the sediment-water interface (Figure 3.2) associated with SP and HD bed sediments was diffuse. In contrast, BR and KV quickly became anoxic as a function of depth and were characterized by sharp DO gradients and measured Eh values across the sediment-water interface. This is partially related to the smaller grain size at BR and KV reducing convection and the rate of diffusion of DO to depth within the sediments (Neira et al., 2015). DO was completely consumed within the top 2 cm of the sediment-water interface at BR (Figure 3.2b) and within the top 1 cm at KV (Figure 3.2d) with a net decrease in concentration of ~260 and 175 $\mu\text{mol/L}$, respectively.

Geographically, the beaches represent diverse locations; both BR and KV are proximal to adjacent urban tributaries (the Belle River connects with Lake St. Clair at West Belle River beach and Mill Creek reaches Lake Erie at Lakeside beach in Kingsville) while SP and HD are near the inlet and outlet of the Detroit River, respectively. Watersheds traversing through urban and agriculture landscapes are well documented as important sources of chemical (i.e., fertilizer and nutrient loadings) and biological (i.e., FIB) contaminants, and subsequently influence their downstream deposition zones (Droppo et al., 2011; Kerr et al., 2016). Additionally, compared with other beaches in WEC that are regularly monitored for water quality by WECHU, BR and KV have historically demonstrated high frequencies of indicator *E. coli* counts exceeding acceptable levels (i.e., 100 CFUs/100 mL up until 2017; 200 CFUs/100 mL thereafter) in the water column (Figure B-1).

3.3.2 Sequencing statistics and functional assignments

For taxonomic analysis derived from recovered DNA, each location consisted of four replicate samples, which were averaged to represent their respective beach. Sequencing from the

Ion Torrent produced 295,630 written sequences for the 16 samples, summarized in Table B-1. Sequence count per sample yielded 4462/64,640/18,476 reads representing minimum/maximum/mean, respectively. This dataset clustered into 13,134 bacterial OTUs at 97% sequence similarity.

Regarding the metatranscriptomic profiles derived from isolated mRNA, sequencing statistics for all samples obtained from the Illumina HiSeq 4000 run are summarized in Table B-2. Duplicates for each sample site are averaged. Altogether, the metatranscriptomics run resulted in 24-28 million reads for each beach. The sum of different identified functional annotations assigned through the KEGG database for each sample site all exceeded 550,000 reads. To allow normalized comparisons between sites, expression levels are represented as a percentage relative to *rpoC* (DNA-directed RNA polymerase beta' subunit) from each sample.

3.3.3 *Taxonomic assessment*

Taxonomic surveys of the bed sediment at the four beaches showed Proteobacteria as the most abundant phylum in all locations, representing at least 30% of the community (Figure 3.3a). Other top phyla include Bacteroidetes, Acidobacteria, Actinobacteria, Chloroflexi, Nitrospirae, and Firmicutes, all which have been extensively reported to inhabit sedimentary environments (Cheng et al., 2017; Solo-Gabriele et al., 2016; Xie et al., 2016). The relative abundance of major phyla and Proteobacteria classes appear to differ between the beach locations with no obvious trend relating to one lake system over the other. The exception pertains to BR and KV beaches, which showed a closer similarity to each other rather than to their same-lake beach counterpart. Perhaps this is not surprising, however, since both BR and KV are similar physically and geochemically and represent beaches influenced by low-energy dynamics, as previously described (Tables 3.1 and 3.2).

Genus level investigation of the beach sediments identified some genera that comprise well-characterized native pathogenic organisms, including *Escherichia-Shigella*, *Legionella*, and *Pseudomonas* (Figure 3.3b). These organisms have also been observed in previous studies as described by Whitman and colleagues (2014), which provides a detailed review of microbes in beach sands with a focus on human pathogens. Although it should be noted that 1) these organisms illustrate very low relative abundance ($< 0.1\%$), and 2) this data was determined solely on DNA extractions of the entire biomass and therefore cannot be considered a representation of the living microbial community. Regardless, it is still valuable information since it demonstrates that these types of organisms are capable of transport within these environments and may potentially be transmitted to people via recreational activities. Possible vectors for transport may be through 1) surface wash-off of sediment via rain and snow melt, 2) riverbed sediment erosion (representing contemporary storage of pathogens mobilized with sufficient shear/flow), or 3) possibly sourced directly from animals frequenting the beaches (i.e., gulls or dogs) (Alm et al., 2018; Cloutier and McLellan, 2017; Droppo et al., 2011, 2009; Edge and Hill, 2005). Therefore, since there is evidence that these organisms can be isolated from the bed sediment in freshwater beaches, it is important to further investigate these communities and determine their level of functionality to evaluate their pathogenic potential through transcriptomic approaches.

3.3.4 *Transcriptomics and the active microbes*

3.3.4.1 Metatranscriptomics reveals overall gene expression

Metatranscriptomic analysis of our dataset provided an extensive amount of functional annotations encoding genes from all functional categories recognized by the KO system (Figure 3.4). Of all the characterized expressed transcripts (3 million combined) that document these beaches, we observe similar proportions between the four sites. However, two major functional

categories appeared to be responsible for subtle variations between the two lake systems. When compared, Lake Erie sites illustrated higher proportion of *posttranslational modification, protein turnover, chaperones*, while Lake St. Clair showed higher percentage of *energy production and conversion*. Major variations such as water movement patterns and retention time at these beaches are the potential influencing factors for these differences in gene expression between lake samples. For instance, hydrological models (Anderson and Schwab, 2011; Niu and Xia, 2017) show considerably longer water retention times for the southern shoreline of Lake St. Clair (water age of 30 days, i.e., SP and BR) compared to northern Lake Erie shorelines in the Western Basin (i.e., HD and KV). This inherently may account for the increased energy production and conversion in Lake St. Clair samples since the sediment microbial community would presumably have longer time to utilize nutrients before being redistributed by long-shore drift. Regardless, these two categories combine to explain 28-33% of the entire characterized transcriptome for each site, suggesting that the microbial communities are growing and are metabolically active.

The dynamic nearshore hydrology associated with SP and HD illustrated the largest differences in both aforementioned functional categories; *posttranslational modification, protein turnover, chaperones* (9% at SP vs. 18% at HD), and *energy production and conversion* (23% at SP vs. 15% at HD). These variances may reflect ecosystem adaptations to environmental differences such as the overlying water conditions (Table 3.1), variability in organic material (Table 3.2) or nutrient availability (Leimena et al., 2013). Benthic microorganisms may move through diverse environments throughout their life cycle within the lower water column and at the sediment-water interface, including those found in freshwater ecosystems, and nutrient availability is not always constant. These bacteria respond to nutrient variations via chemotaxis and specialized motility functions to direct motion toward areas of higher nutrient density. In contrast, beneath the sediment-water interface microbial functional relationships may be constrained to niche environments thus occupying a heterogeneous distribution. In this context, these microbial pockets may be controlled in part by nutrient availability, restricted to mineral

attachment, available carbon, and suitable electron donors. These functions are also associated with biofilm formation as well as pathogens in search of hosts, referred to as quorum sensing (Miller and Bassler, 2001). Taken altogether, pathogens that assimilate and respond to nutrient variation have been reported to subsequently modify their expression of virulence factors (Rohmer et al., 2011; Somerville and Proctor, 2009). Therefore, since metabolism influences bacterial pathogen colonization, it is important to analyze metabolic pathways and microbial nutrient cycling within the sediment environment.

3.3.4.2 Influence of biogeochemical elemental cycling (C, S, N) in beach sands

Expression of functional assignments involved in nitrogen and sulfur cycling, and methanogenesis pathways for all four beaches were investigated (Figure 3.5). In general, all beaches shared similar functional expression with respect to transcripts related to methanogenesis and S cycling (whether high or low expression), regardless of historical contamination profiles (i.e., *E. coli* CFUs) and geochemical and energy properties. Most of the highly expressed transcripts were annotated to N metabolism, where defined differences are demonstrated between the beaches belonging to Lake St. Clair and those on Lake Erie. From the S metabolism and methanogenesis perspective, however, there was not obvious variation in expression among the beaches and the majority of expressed transcripts demonstrated low levels of expression. In fact, since we sampled from the surface of the bed sediment where oxygen can still diffuse (to a certain extent), we did not expect to identify high activity of these metabolisms typically associated with lower redox zones. This suggests that biological N cycling plays a key role in energy metabolism at the sediment-water interface and hence, microbial differences between the lake systems concerning the bed sediment of the nearshore beach environments. As expression levels at beaches belonging to the same lake appear to follow similar trends based on both a metabolic and taxonomic perspective, a more in-depth comparison was made between two

beaches, one from each lake. Based on their similar physical, geochemical, and taxonomic properties (Tables 3.1 and 3.2, Figure 3.3), BR and KV were selected for further comparison of microbial functional differences. Interestingly, the phylum Nitrospirae was observed for the range of beach environments. This is significant since this phylum often contains one class of ubiquitous organism *Nitrospira*, responsible for nitrite oxidation within the nitrogen cycling. Overall though, when we compare gene function attributes, the weighted distributions of genes in these subsurface environments tend to be influenced by denitrification mechanisms. Within this context we highlight below the trends observed.

Comparison of BR and KV beaches in this study showed significantly ($p < 0.05$) different expression levels of transcripts encoding annotations belonging to N cycling (Figure 3.6). Expression of *nar/napB* and *norB* in KV showed 50% up-regulation, and 30% up-regulation for *nosZ*, all significantly differentially expressed compared to BR ($p < 0.05$). Denitrifying genes with high expression levels such as these at KV are comparable to sediment sampled at a discharge zone of a local wastewater treatment plant (Weisener et al., 2017). Because there is such high expression for denitrification suggests that excessive amounts of bioavailable nitrate are present at KV beach for microbial utilization. This nitrate could potentially be sourced from either fecal contamination (i.e., wildlife excrement) or high levels of fertilizer runoff from agricultural or residential landscapes that deposits in these low-energy shorelines (Melton et al., 2014; Weisener et al., 2017). On the other hand, BR showed higher expression of transcripts encoding for assimilatory nitrate reduction to ammonia, ANRA (*nirA*; 15% at BR vs. 4% at KV) and N fixation (*nifDH*; 33% at BR vs. 3% at KV), both pathways leading to production of ammonia. Biological N fixation is an essential function of microorganisms because fixed inorganic N compounds are required for biosynthesis of organic compounds and cellular survival (Wang et al., 2016). If bioavailable N species (such as nitrate) are not at sufficient concentrations, microbes will fix atmospheric N to acquire this essential nutrient (Salk et al., 2018). In this case, a large number of characterized nitrogen-fixing bacteria in soils belong to the Alphaproteobacteria

(Tsoy et al., 2016), which are represented at all four beaches with relative abundance of 4-7% (Figure 3.3a). We identified much higher expression of *nifDH* at BR compared to KV, suggesting that BR contained low bioavailable N, resulting in the microbial community to rely on N fixation to supply a sufficient amount of bioavailable N for essential cellular processes. This, in turn, highlights the contrasting chemical characteristics of these two locations with respect to nutrient content.

Key differences in N metabolism exist between the two beaches/lake environments. The microbial community associated with Lake Erie shorelines appears influenced by respiratory and detoxification strategies, while Lake St. Clair shorelines have developed metabolisms that are energy focused (e.g., biosynthesis and primary production). In some context this is understandable since there exists long hydraulic residence times along the Lake St. Clair southern shore thus creating a stable physical environment in which primary producers can flourish (Michalak et al., 2013). It is worth noting that KV demonstrated the highest Chl concentrations (53.45 µg/L) of all sites, while BR reported much less in comparison (4.77 µg/L; Table 3.1). However, these values reflect planktonic communities and may not represent biofilm established on/within the sediment surface. In fact, taxonomic results showed the relative abundance of Cyanobacteria at BR (0.68%) was six times greater than at KV (0.11%). Furthermore, a sharp spike in DO was recorded at BR immediately below the sediment-water interface (Figure 3.2b), adding more evidence of phototrophic biofilm activity on the bed sediment.

3.3.4.3 Significance of bacterial survival and the influence of nitric oxide

Expression of bacterial transcripts encoding N metabolism demonstrated specialized mechanisms employed by the bacteria for metabolizing/detoxifying nitric oxide (Figure 3.7). Nitric oxide (NO) is a toxic, intermediate molecule of the N cycle and organisms employ diverse systems to defend against (and/or utilize) its harmful effects (Poole, 2005). Bacteria, including

pathogens, have evolved unique mechanisms for NO detoxification in order to survive and succeed in their environment (Gardner et al., 2002; Gilberthorpe and Poole, 2008; Spiro, 2012). Enterobacteria, for example, possess several NO-detoxifying mechanisms, the most prominent being the flavohemoglobin Hmp and the flavorubredoxin NorV (Gilberthorpe and Poole, 2008; Poole, 2005). Also, cytochrome *c* nitrite reductases (NrfA) are present in the periplasm of Gram-negative bacteria, which reduce nitrite directly to ammonia, bypassing production of NO altogether (Mohan et al., 2004). Genomic analysis of many pathogenic enteric bacteria reveals the presence of *nrf* genes as it plays an important role in NO management in oxygen-limited environments (Poock et al., 2002). In our dataset (Figure 3.7), expression of *norV* at BR (41.74%) is strongly upregulated compared to KV (11.38%), while *nrfA* shows greater expression at KV (15.73%) than BR (2.72%). Regarding *hmp*, expression at either beach is low (<0.15%), yet is expressed, nonetheless.

The transcriptional regulator NsrR has gained attention in recent years because of its suggested key role in controlling the complete periplasmic bacterial stress response to NO (Bodenmiller and Spiro, 2006; Filenko et al., 2007). Tucker and colleagues (2010) demonstrated that NO directly affects the Fe-S cluster of NsrR, which is responsible for controlling the transcription of NO-detoxifying genes (i.e., *hmp* and *nrfA*). Furthermore, it has been shown that these aforementioned enzymes constitute a cooperative network in pathogenic bacteria to detoxify NO (Figure 3.8; Bodenmiller and Spiro, 2006; Gilberthorpe and Poole, 2008; Rodionov et al., 2005; Tucker et al., 2010). Our results show transcription of several NO-reducing genes in both BR and KV yet no expression of *nsrR*. This suggests that NO is present in these beaches, but also that the bacteria are actively metabolizing it for their survival, which may include those with pathogenic capabilities.

Examining N metabolism and genes involved in N cycling, especially NO detoxification, aid in discerning how bacterial pathogens are able to adapt to hazardous environments and ultimately survive (Gardner et al., 2002; Gilberthorpe and Poole, 2008; Spiro, 2012). Expression

of transcripts encoding pathogenicity and infectious diseases, however, portray the diverse risk associated with recreational water usage in freshwater systems.

3.3.4.4 Expression of genes encoding pathogenicity

3.3.4.4.1 Signatures of *Salmonella* infection

In our study, the direct link to pathogenic potential comes from the expression of virulence factors detected in the beach sediments (Figures 3.7 and 3.8). Here, we detected expression of the transcript encoding the secreted effector protein *pipB2* at BR (39.83%) as well as KV (2.51%). Additionally, the *Salmonella* virulence factor *sspH2* also demonstrated expression at both beaches, with 3.35% at BR and 2.28% at KV.

These pathogen-related genetic factors have been reported to play active roles involved in modifying the host cytoskeleton (SspH2; Bakowski et al., 2008; Haraga et al., 2008; Miao et al., 2003), and pathogen replication (PipB2; Henry et al., 2006; Szeto et al., 2009). Reports on these genes, however, are typically associated with medical microbiology, not environmental systems; *Salmonella* pathogens are not commonly believed to survive in beach environments, much less the source of these organisms is not well understood (Pandey et al., 2014). Biological contaminants are typically introduced into aquatic ecosystems by surface and subsurface runoff, wastewater and agricultural discharge, or avian/animal excrement (Field and Samadpour, 2007; Ksoll et al., 2007). Additionally, more recent environmental studies have provided evidence for bacterial pathogen survival in natural environments. For example, in the GLs it has been reported that aquatic vegetation (i.e., green alga *Cladophora*) can serve as an environmental reservoir for bacterial pathogens such as *Salmonella* thus improving their chances of survival in beach environments (Byappanahalli et al., 2009; Ishii et al., 2006). Based on this, it is possible that beachgoers may be exposed to these enteric pathogens during recreational activities.

Our data, combined with the expression data of the NO-detoxification transcripts, suggest that pathogenic organisms were present and active in these beach bed sediments at the time of sampling. However, contrary to the taxonomic analysis (Figure 3.3b), the transcriptomic data specifically revealed expression of genes involved with *Salmonella* pathogenicity. A plausible explanation for this could be HGT in these environments and may be the underlying mechanism for gene acquisition by other organisms (Heß et al., 2018; Madsen et al., 2012; Molin and Tolker-Nielsen, 2003). This consideration helps support the proposal that taxonomic surveys alone perhaps do not capture the underlying pathogenic potential of a system; this is especially important when considering human health risks at public beaches for recreation water use.

3.3.4.4.2 Expression of genes involved in pertussis

Pertussis (aka whooping cough) is a highly contagious respiratory disease that affects humans (de Gouw et al., 2011). Although *Bordetella pertussis*, the aetiological agent of the disease, is not a known waterborne pathogen and has not been reported in environmental samples, expression of transcripts encoding for genes involved in the disease were identified in our samples (Figures 3.7 and 3.8). Other *Bordetella spp.* have been detected in environmental samples (e.g., sediment, water) and there is recent belief that this genus is of environmental origin (Soumana et al., 2017).

Consistently, the highest expression of transcripts in this list (Figure 3.7) belonged to BR. The ATP-binding cassette, *hlyB/cyaB*, showed highest expression at BR with 17.96%, and 2.55% at KV. These are homologous transporter proteins that are required for secretion of virulence factors (Zaitseva et al., 2005). One virulence factor of pertussis is filamentous hemagglutinin, FhaB/FHA (Melvin et al., 2015), which plays an important role in the adhesion of virulent organisms to the respiratory tract of the host (Locht et al., 1993). Translocation of this protein across the outer membrane of *B. pertussis* requires the secretion protein FhaC (Mazar and Cotter,

2006; Melvin et al., 2015; Noël et al., 2012). Expression of *fhaB* and *fhaC* were detected in both beach sediments, with BR showing higher expression (6.04% and 3.41%) compared to KV (3.44% and 0.48%), respectively.

Fimbriae also function as critically important mediators of adherence for many Gram-negative bacterial pathogens (Remaut et al., 2008) and are recognized as a primary mechanism of virulence (Connell et al., 1996). Although there was no expression of transcripts encoding fimbrial proteins in our dataset, there was expression of the outer membrane usher protein (FimD)/periplasmic chaperone (FimC) in both BR (0.14%) and KV (0.09%), demonstrating functional gene expression related to pertussis. Again, this contradicts our taxonomy data since *Bordetella* was not represented (Figure 3.3b) yet perhaps can be explained by HGT in these subsurface environments.

3.3.4.4.3 Expression of other (pathogenic) transcripts

In both locations, we report expression of two different genes with cationic antimicrobial peptide (CAMP) resistance functionality, an important characteristic of pathogenic organisms to colonize their host (Joo et al., 2016; Peschel et al., 1999, 2001). DltB and MprF are both membrane proteins specific to Gram-positive bacteria, and catalyze similar reactions (Li et al., 2007). The phosphatidylglycerol lysyltransferase, *mprF*, showed 0.60% expression in BR beach bed sediment and 0.05% expression at KV. Expression of membrane protein transcript *dltB* was also more highly expressed at BR (1.82%) than KV (0.75%). This data is important to consider because ARB are a serious threat to human health and treating bacterial infections is becoming increasingly more challenging due to ARG. Additionally, the evolution and spread of ARB and ARG is not well understood, especially when considering the natural environment (Leonard et al., 2015).

3.3.5 *Environmental implications*

Water quality assessments of public beaches have traditionally focused on simplistic evaluations concentrated on taxonomic surveys within the water column only, and neglect to incorporate the interconnection of the physical and geochemical characteristics to these microbial evaluations (Heaney et al., 2012, 2009). However, the water and sediment compartments are perpetually linked as they influence each other in their dynamic setting, and it has been argued that sediment may have stronger association with microbial life than the planktonic counterpart (Droppo et al., 2011; Probandt et al., 2018). Our observations of expressed transcripts associated with non-waterborne pathogens present in beach environments is evidence of the possible transport of these pathogens from the terrestrial to the aquatic system by attachment to sediment particles.

In our present study, we investigated the microbial community structure and function of bed sediment at freshwater beaches and, together with the physicochemical analysis of the sediment and surrounding water characteristics, we can evaluate location properties as an improved means for determining the safety of public beaches for recreational use. As other studies have reported, freshwater beach sands can be considered a reservoir of bacterial pathogens (Mohiuddin et al., 2017; Sousa et al., 2015), and smaller particle sizes of these sediments are associated with persistence of FIB (Zimmer-faust et al., 2017). Both BR and KV beaches are representative of low-energy environments with tightly packed small sediment particles restricting diffusion of DO with depth (Figure 3.2). These physical features are indicative of higher potential for increased microbial persistence and activity, including bacterial pathogens, as we have shown in this work. As such, these types of locations may potentially have a higher risk related to aquatic and human health.

Through HGT, microorganisms can acquire specialized functions for a multitude of activities, including pathogenicity (Molin and Tolker-Nielsen, 2003). Moreover, HGT potential is

increased in densely populated locations, such as biofilms and sedimentary environments (Madsen et al., 2012). This supports the fact that taxonomic surveys alone cannot determine the true pathogenic potential of a system and are an out-dated means for public beach evaluations. Our research validates this as gene expression data of our beach sediments revealed pathogenic potential typical of particular organisms (e.g., *Salmonella* and *Bordetella*; Figures 3.7 and 3.8), yet our taxonomy assessment did not identify the aetiological taxa (Figure 3.3). For these reasons, we introduce a proposed universal bacterial pathogen model (Figure 3.8), which considers the combined and synergistic processes used by microbes that may acquire these functions by HGT in these densely populated and physically dynamic subsurface systems.

3.4 Conclusions

Energy metabolism and nutrient cycling are functional processes that can be analyzed *in situ* to better characterize the active microbial community in environmental samples. Insight into these functions helps us understand the overall biogeochemistry of a system and can lead to underlying mechanisms of additional microbial lifestyles, such as pathogen survival and persistence. Although our transcriptomic sediment observations here share characteristics similar to those most observed in clinical trials and research, we were able to demonstrate clear evidence of bacterial pathogenic potential in the selected freshwater beach sediments through gene expression data. This information significantly contributes to our current understanding of human health risks regarding recreational water use and provides valuable insight into the true potential biohazards that should be considered by management and policymakers when evaluating the status of public beaches.

While this study did not investigate the level of gene expression required to induce infection or lead to toxicity effects, it is the first to provide transcriptomic evidence of bacterial pathogenic gene expression within the bed sediment of freshwater beach environments. This

information allowed us to evaluate location characteristics in relation to the microbiota and can lead to predictive inference at other freshwater beaches to evaluate their likelihood of posing human health risks. Often this type of information is typically overlooked since most research investigates taxonomic surveys or is focused within the water compartment only. Furthermore, we illustrated evidence of pathogens other than *E. coli*, highlighting the fact that these ecosystems can harbour more human health concerns than what is currently being portrayed through traditional water quality assessments. We also considered HGT as a viable avenue for pathogenic gene acquisition in these densely microbial-populated environments, further supporting the idea that simplistic taxonomic surveys of the water column are outdated and unreliable for determining the bacterial health risks of public beaches. Finally, we propose a multifaceted assessment of beach systems that includes sediment characteristics and biogeochemical evaluations in addition to pathogenic gene expression of the nearshore subsurface environment. With this approach, we can build a comprehensive database of biogeochemical properties of these systems to help guide predictive assessments at problematic beaches.

Acknowledgements

The authors would like to thank Shelby Mackie in the Environmental Genomics Facility (EGF) and Courtney Spencer at the Great Lakes Institute for Environmental Research (GLIER), University of Windsor. We acknowledge the Genome Quebec Innovation Center at McGill University in Quebec, Canada for metatranscriptomic analysis. We express thanks for funding support for this project from NSERC Strategic Partnerships Program entitled “Great Lakes Water Security: Microbial community characterization, source tracking, and remediation through metagenomics” REF341061127. Finally, we thank our anonymous reviewers for their constructive feedback, which helped us revise this manuscript.

Figures and Tables

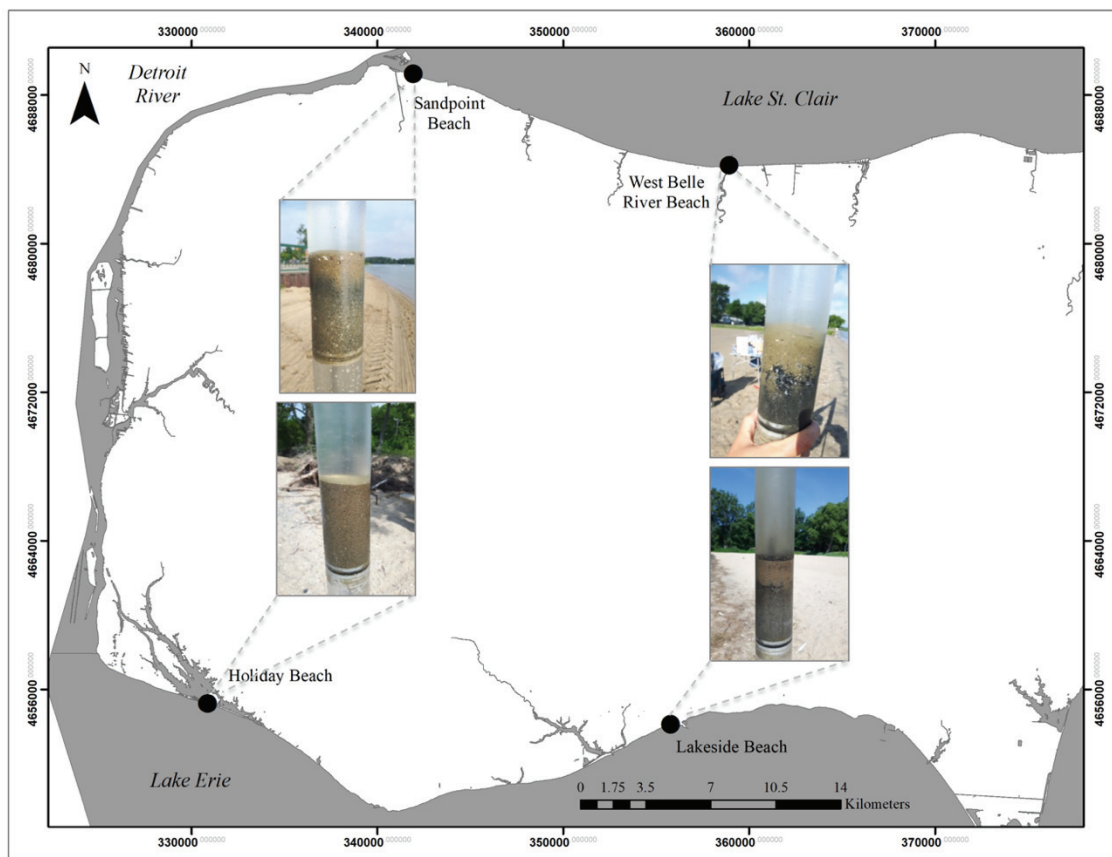


Figure 3.1: Map of WEC; features displayed include Lake St. Clair, the Detroit River, Lake Erie and all four beaches sampled for this research. Photos of sediment cores appear next to the representative location.

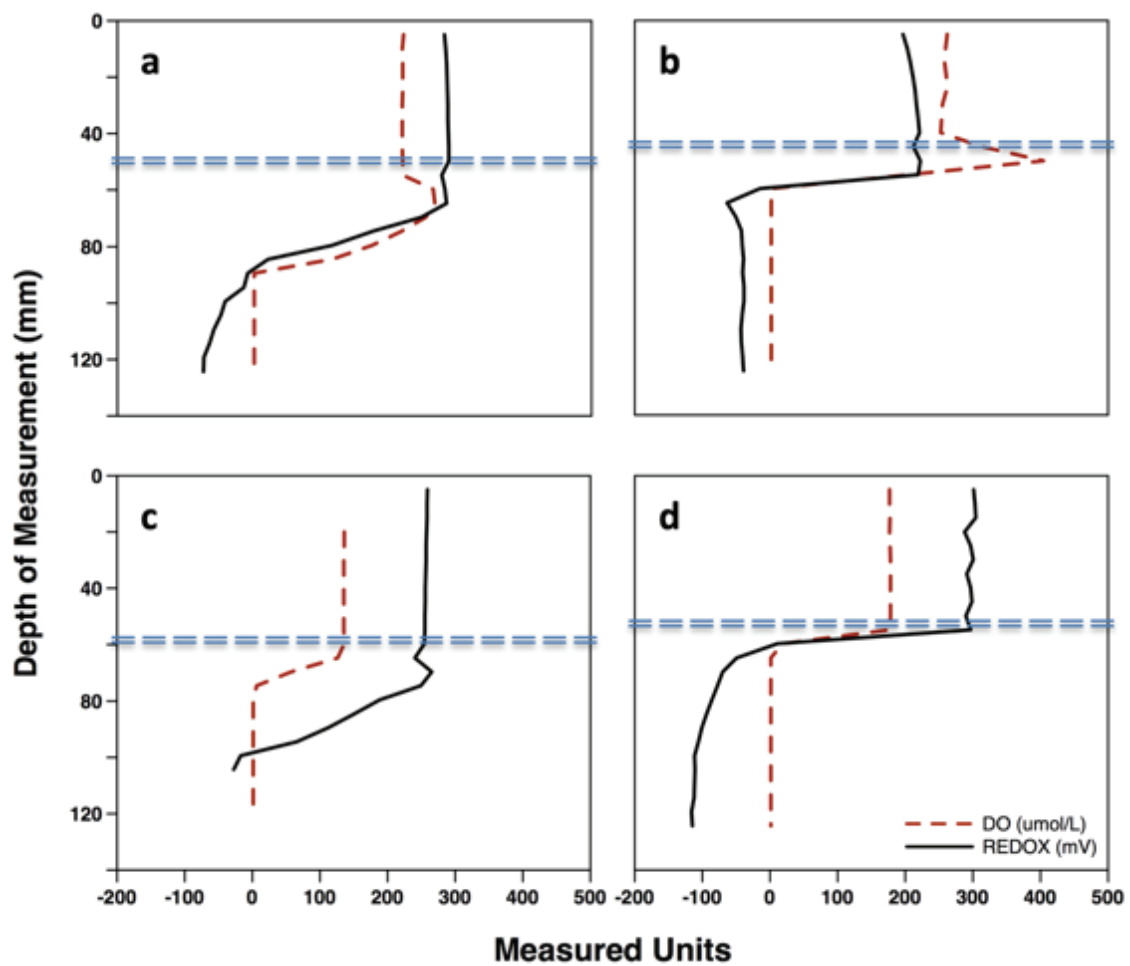


Figure 3.2: Micro-sensor profiles of the bed sediment beach zone for (a) Sandpoint, (b) Belle River, (c) Holiday, and (d) Kingsville. DO and redox measurements were obtained through the sediment-water interface of these zones. Double-dashed horizontal line represents the sediment-water interface, where above the line is in the water column and below is into the bed sediment.

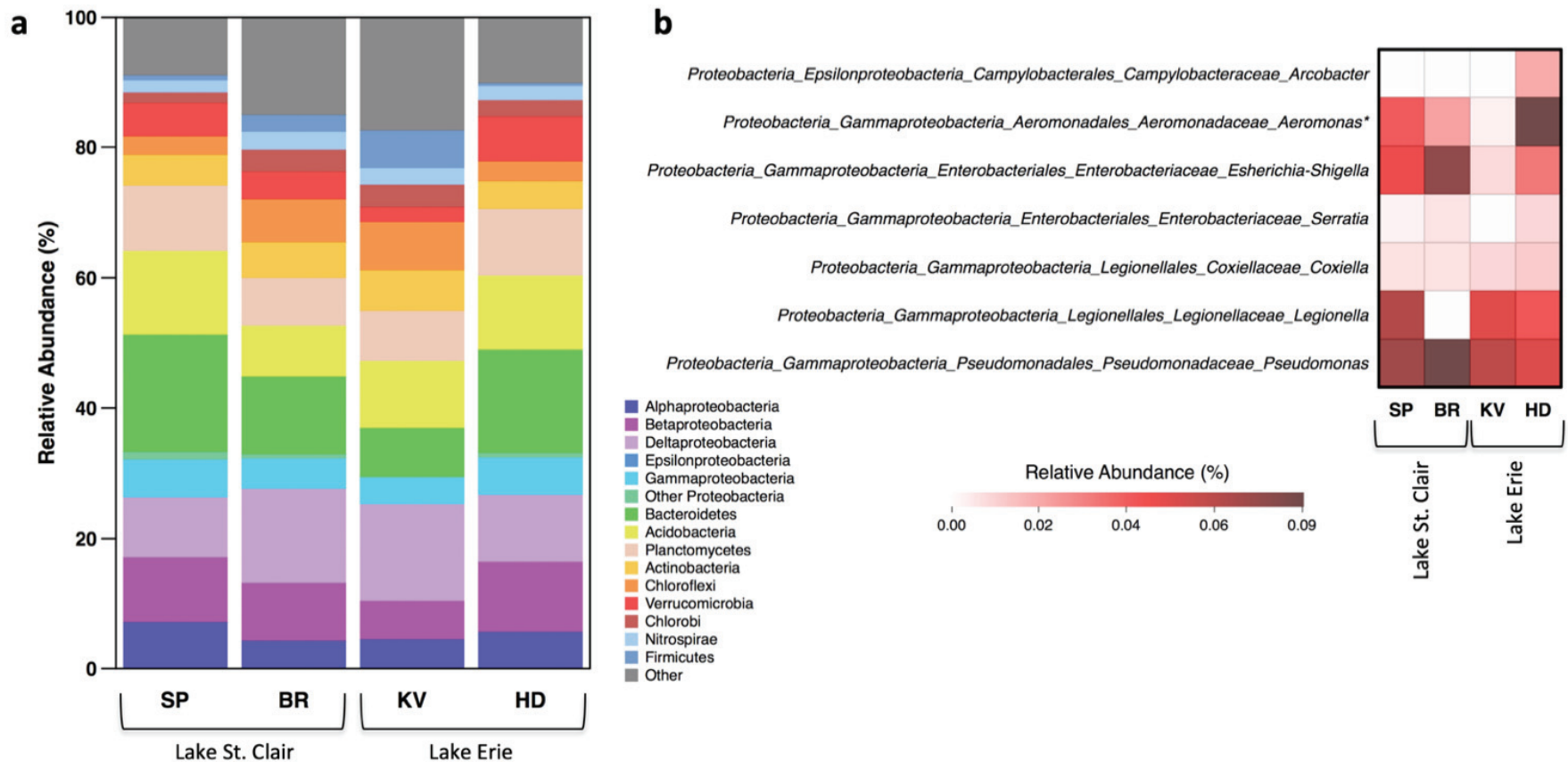


Figure 3.3: Taxonomic survey of the bed sediment at the four freshwater beaches. (a) Top abundant bacterial taxa of Sandpoint (SP), Belle River (BR), Kingsville (KV), and Holiday (HD) beaches. Note that phyla are represented for all groups except the Proteobacteria, which is broken down into its subsequent classes (Alpha-, Beta-, Delta-, Epsilon-, and Gamma-Proteobacteria). (b) Heatmap illustrating the relative abundance of potential human bacterial pathogens (genus level) present at each sample location based on DNA isolation and 16S rRNA amplification. Note the small percentage values, and the majority are members of the Gammaproteobacteria. * Includes cultured and uncultured spp. while others represent cultured taxa only

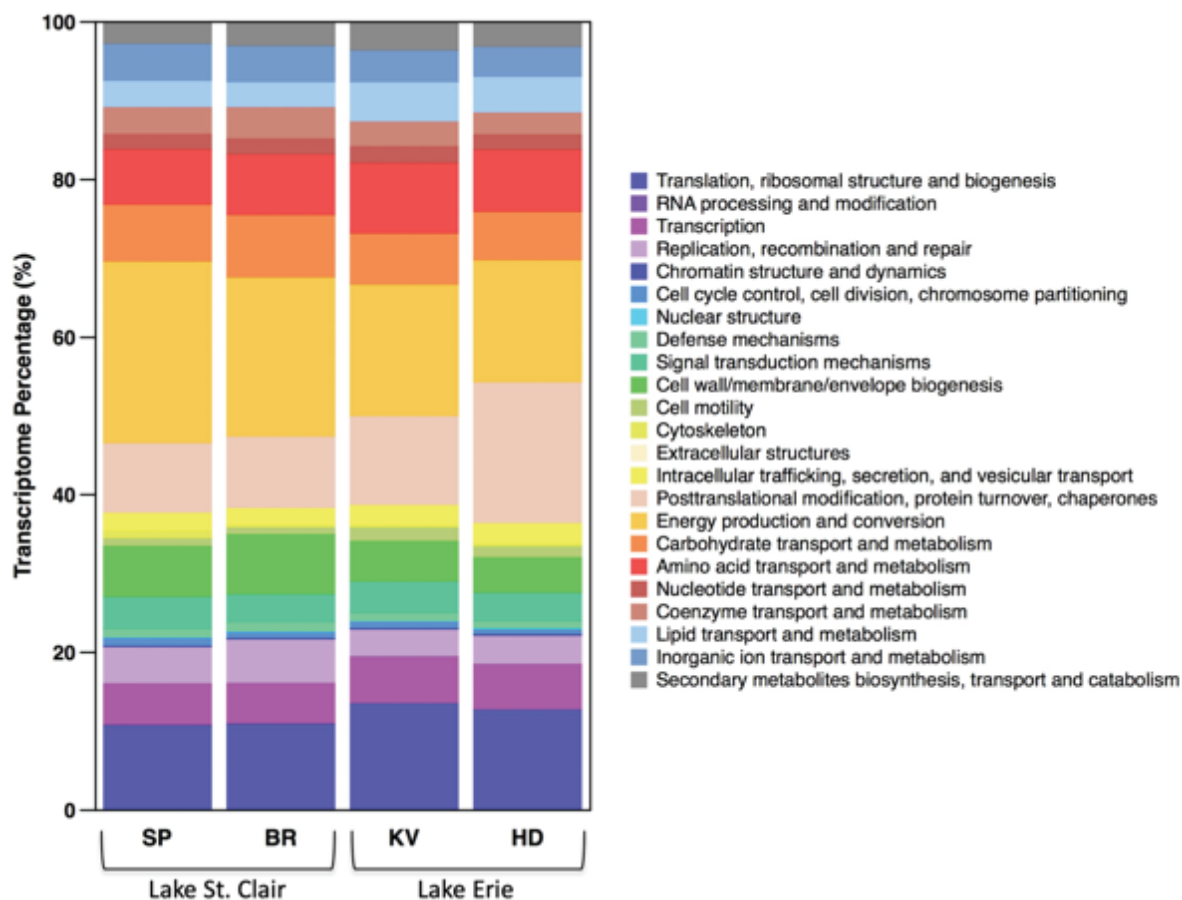


Figure 3.4: Distribution of all well-characterized transcripts from the bed sediment into functional categories for the four freshwater beaches.

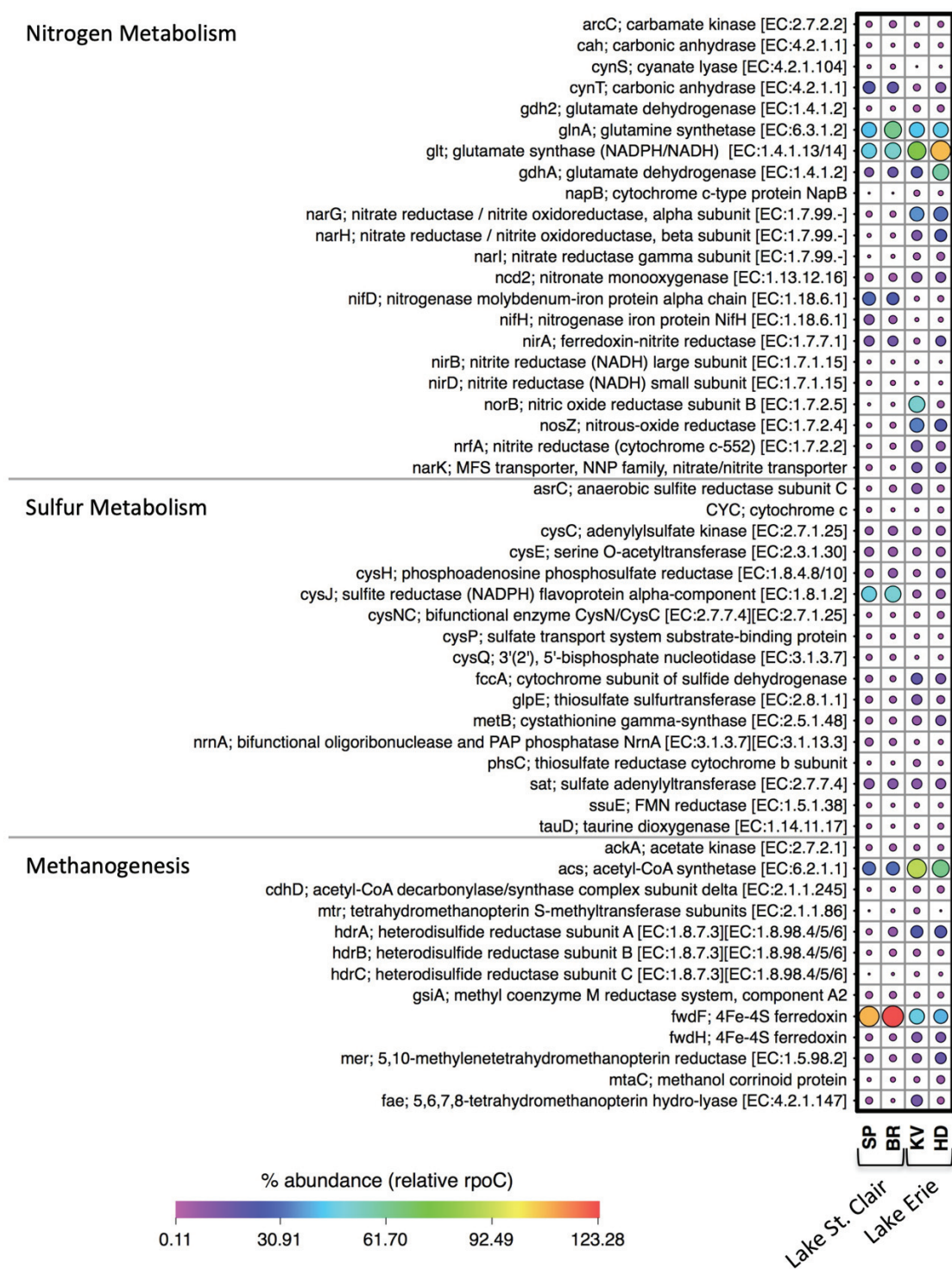


Figure 3.5: Functional annotations assigned to transcripts involved in nitrogen metabolism, sulfur metabolism, and methanogenesis pathways within the top layer of bed sediment in four freshwater beaches. This heatmap uses colour range and proportional size scaling to allow for discernible comparisons. Expression is represented as percent abundance relative to *rpoC* gene.

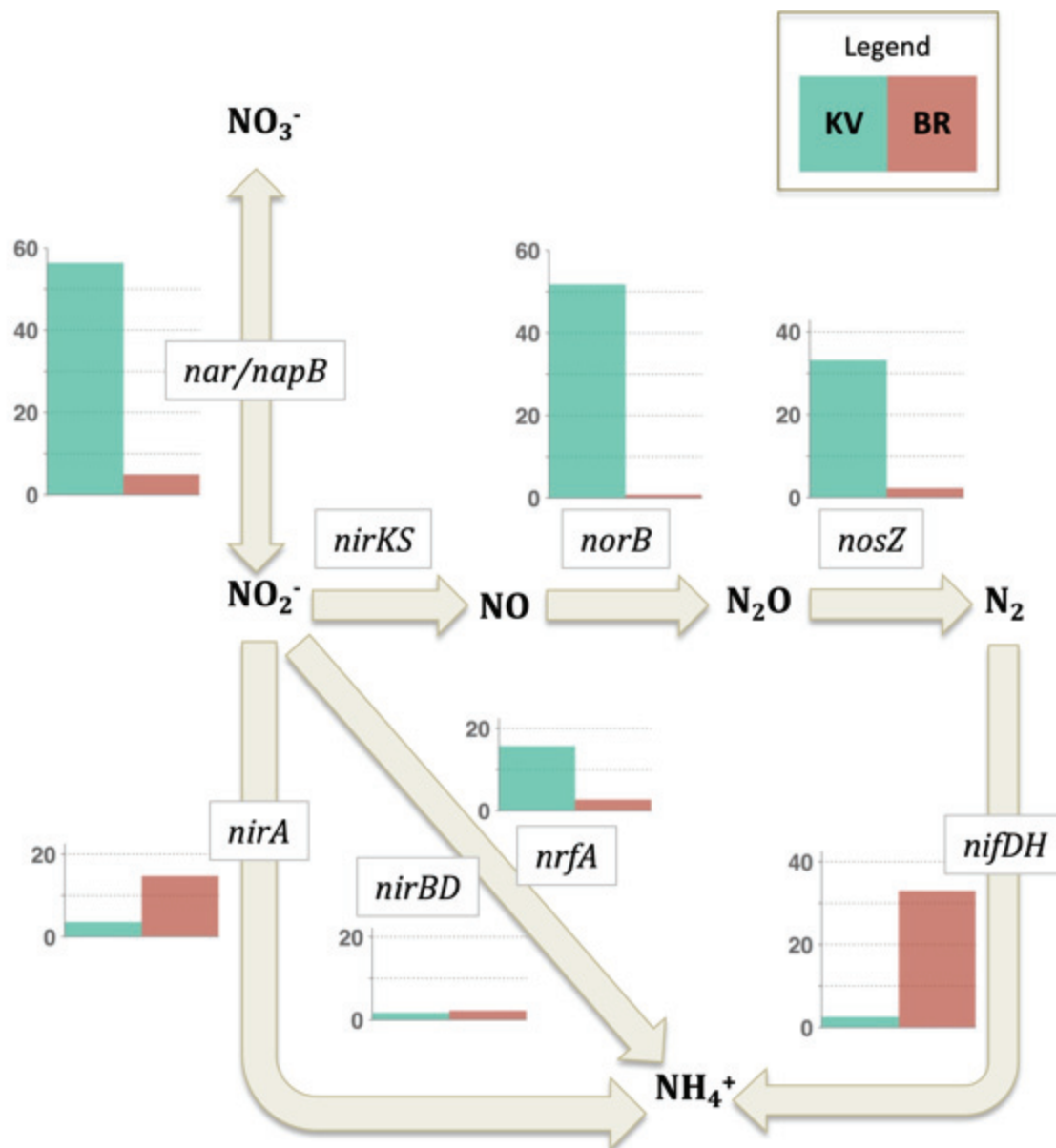


Figure 3.6: Expression of nitrogen metabolism genes involved in denitrification, dissimilatory and assimilatory nitrate reduction, and nitrogen fixation within the nearshore bed sediment of Kingsville (KV) and Belle River (BR) public beaches. Expression is represented as percent abundance relative to *rpoC* gene.

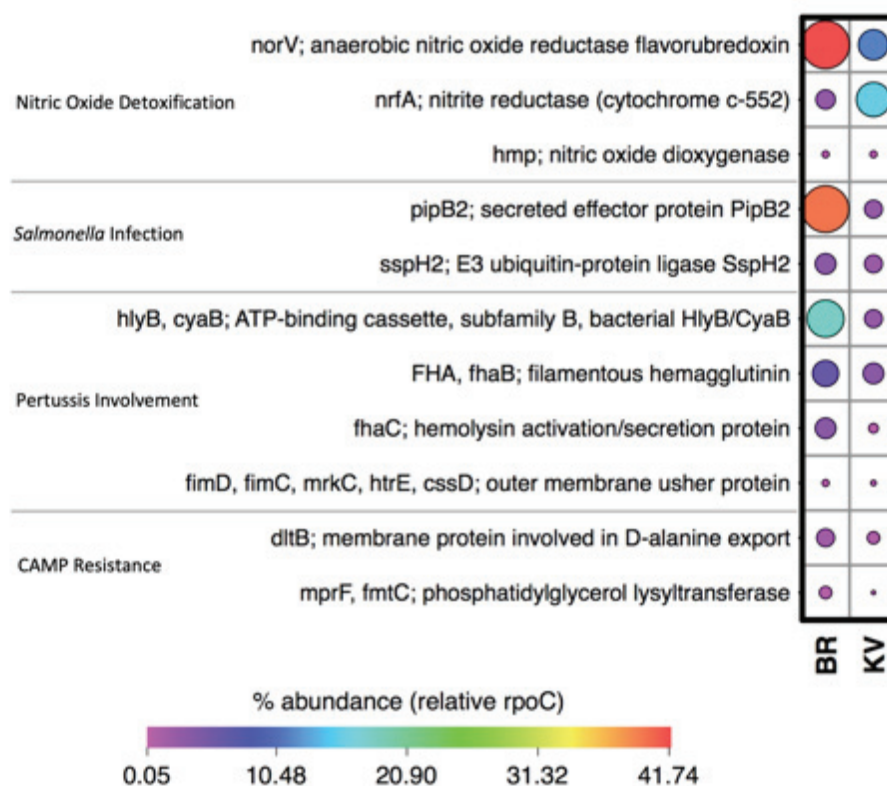


Figure 3.7: Expression of transcripts with pathogenic relevance from the bed sediment beach samples at Belle River (BR) and Kingsville (KV) beaches. Expression is represented as percent abundance relative to *rpoC* gene.

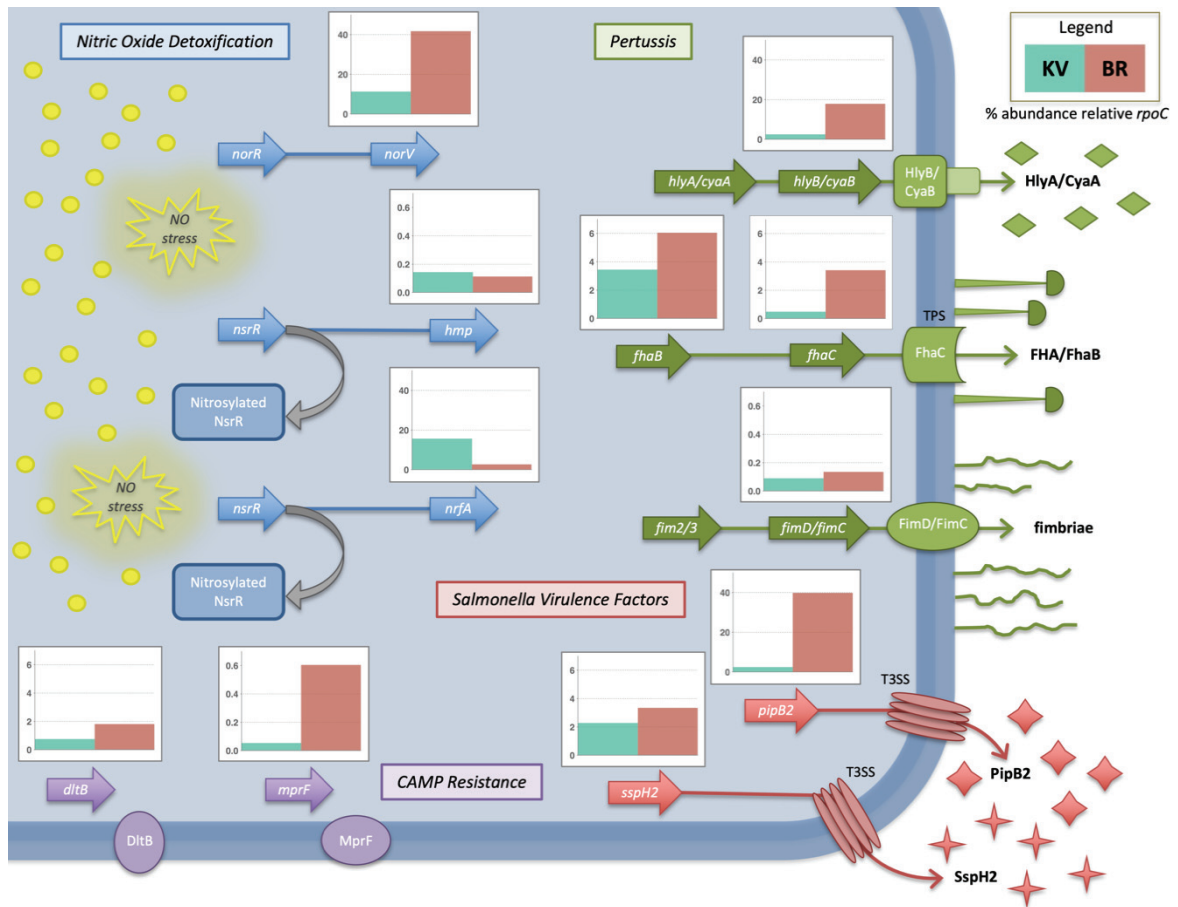


Figure 3.8: Proposed universal bacterial pathogen. Schematic of genes involved in nitric oxide detoxification (blue), CAMP resistance (purple), *Salmonella* infection (red), and pertussis (green). Expression of functional annotations encoding illustrated transcripts appear directly above stated gene. Yellow circles represent nitric oxide. *Salmonella* virulence factors are translocated out of the pathogen through a type III secretion system (T3SS). Translocation of FHA/FhaB protein is through a two-partner secretion (TPS) system, which requires the secretion protein FhaC. Note there are three different y-axis scales (0-40%; 0-6%; 0.0-0.6%), used to clearly illustrate expression levels and comparisons between KV and BR. Expression of transcripts are represented as percentage relative to the housekeeping gene, *rpoC*.

Table 3.1: Physicochemical conditions of the water column at Sandpoint (SP), Belle River (BR), Kingsville (KV), and Holiday (HD) beaches in WEC, Ontario.

Beach	Depth (m)	Temperature (°C)	SPC ($\mu\text{S cm}^{-1}$)	TDS (mg L^{-1})	Salinity (psu)	ODO (mg L^{-1})	pH	ORP (mV)	Turbidity (NTU)	Chl a ($\mu\text{g L}^{-1}$)	BGA-PC ($\mu\text{g L}^{-1}$)
SP	0.58	26.1	237.1	154	0.11	7.97	8.40	103.4	4.77	0.79	0.42
BR	0.44	23.7	229.5	149	0.11	9.03	8.44	110.1	31.24	4.77	1.21
KV	0.13	25.6	490.0	319	0.23	11.55	8.60	119.0	55.82	53.45	3.89
HD	0.59	25.8	250.8	163	0.12	7.17	8.04	114.7	34.99	6.08	1.11

Table 3.2: Tabulated summary of physical properties characterizing each beach as high or low energy. Data includes grain size (D_{50}), moisture content, and TOC determined from LOI, as well as observational input on water movement restriction and designation of high or low energy for each beach.

Beach	Grain size, D_{50} (μm) *	Moisture (%) *	TOC (% LOI)	Sheltered? *	High/Low Energy *
SP	517	18.31	0.83	No	High
BR	66	22.16	0.85	Yes	Low
KV	102	24.77	0.48	Yes	Low
HD	1201	10.44	0.37	No	High

** Note: these data are repeated from Chapter 2, where they are described in more detail.*

References

- Alm, E.W., Burke, J., Spain, A., 2003. Fecal indicator bacteria are abundant in wet sand at freshwater beaches. *Water Res.* 37, 3978–3982. [https://doi.org/10.1016/S0043-1354\(03\)00301-4](https://doi.org/10.1016/S0043-1354(03)00301-4)
- Alm, E.W., Daniels-Witt, Q.R., Learman, D.R., Ryu, H., Jordan, D.W., Gehring, T.M., Santo Domingo, J., 2018. Potential for gulls to transport bacteria from human waste sites to beaches. *Sci. Total Environ.* 615, 123–130. <https://doi.org/10.1016/j.scitotenv.2017.09.232>
- Anderson, E.J., Schwab, D.J., 2011. Relationships between wind-driven and hydraulic flow in Lake St. Clair and the St. Clair River Delta. *J. Great Lakes Res.* 37, 147–158. <https://doi.org/10.1016/j.jglr.2010.11.007>
- Bakowski, M.A., Braun, V., Brumell, J.H., 2008. Salmonella-containing vacuoles: Directing traffic and nesting to grow. *Traffic* 9, 2022–2031. <https://doi.org/10.1111/j.1600-0854.2008.00827.x>
- Beversdorf, L.J., Bornstein-Forst, S.M., McLellan, S.L., 2007. The potential for beach sand to serve as a reservoir for *Escherichia coli* and the physical influences on cell die-off. *J. Appl. Microbiol.* 102, 1372–1381. <https://doi.org/10.1111/j.1365-2672.2006.03177.x>
- Bodenmiller, D.M., Spiro, S., 2006. The *yjeB* (*nsrR*) Gene of *Escherichia coli* Encodes a Nitric Oxide-Sensitive Transcriptional Regulator The *yjeB* (*nsrR*) Gene of *Escherichia coli* Encodes a Nitric Oxide-Sensitive Transcriptional Regulator. *J. Bacteriol.* 188, 874–881. <https://doi.org/10.1128/JB.188.3.874>
- Bojko, O., Kabala, C., 2014. Loss-on-ignition as an estimate of total organic carbon in the mountain soils. *Polish J. Soil Sci.* XLVII, 71–79.
- Byappanahalli, M.N., Sawdey, R., Ishii, S., Shively, D.A., Ferguson, J.A., Whitman, R.L., Sadowsky, M.J., 2009. Seasonal stability of *Cladophora*-associated *Salmonella* in Lake Michigan watersheds. *Water Res.* 43, 806–814. <https://doi.org/10.1016/j.watres.2008.11.012>
- Chen, M., Walshe, G., Chi Fru, E., Ciborowski, J.J.H., Weisener, C.G., 2013. Microcosm assessment of the biogeochemical development of sulfur and oxygen in oil sands fluid fine tailings. *Appl. Geochemistry* 37, 1–11. <https://doi.org/10.1016/j.apgeochem.2013.06.007>
- Cheng, J., Lam, K.N., Engel, K., Hall, M., Neufeld, J.D., Charles, T.C., 2017. Functional metagenomics: Tools and applications - Chapter 1: Metagenomic Cosmid Libraries Suitable for Functional Screening in Proteobacteria. *Funct. Metagenomics Tools Appl.* 1–11. <https://doi.org/10.1007/978-3-319-61510-3>
- Cloutier, D.D., Alm, E.W., McLellan, S.L., 2015. Influence of land use, nutrients, and geography

- on microbial communities and fecal indicator abundance at Lake Michigan beaches. Appl. Environ. Microbiol. 81, 4904–4913. <https://doi.org/10.1128/AEM.00233-15>
- Cloutier, D.D., McLellan, S.L., 2017. Distribution and differential survival of traditional and alternative indicators of fecal pollution at freshwater beaches. Appl. Environ. Microbiol. 83, 1–16. <https://doi.org/10.1128/AEM.02881-16>
- Colston, S.M., Fullmer, M.S., Beka, L., Lamy, B., Peter Gogarten, J., Graf, J., 2014. Bioinformatic genome comparisons for taxonomic and phylogenetic assignments using aeromonas as a test case. MBio 5, 1–13. <https://doi.org/10.1128/mBio.02136-14>
- Connell, H., Agace, W., Klemm, P., Schembri, M., Märrild, S., Svanborg, C., 1996. Type 1 fimbrial expression enhances *Escherichia coli* virulence for the urinary tract. Proc. Natl. Acad. Sci. United States Am. 93, 9827–9832. <https://doi.org/10.1073/pnas.93.18.9827>
- Crovadore, J., Soljan, V., Calmin, G., Chablais, R., Cochard, B., Lefort, F., 2017. Metatranscriptomic and metagenomic description of the bacterial nitrogen metabolism in waste water wet oxidation effluents. Heliyon 3, e00427. <https://doi.org/10.1016/j.heliyon.2017.e00427>
- Davis, M.P.A., van Dongen, S., Abreu-Goodger, C., Bartonicek, N., Enright, A.J., 2013. Kraken: A set of tools for quality control and analysis of high-throughput sequence data. Methods 63, 41–49. <https://doi.org/10.1016/j.ymeth.2013.06.027>
- de Gouw, D., Diavatopoulos, D.A., Bootsma, H.J., Hermans, P.W.M., Mooi, F.R., 2011. Pertussis: A matter of immune modulation. FEMS Microbiol. Rev. 35, 441–474. <https://doi.org/10.1111/j.1574-6976.2010.00257.x>
- Droppo, I.G., Krishnappan, B.G., Liss, S.N., Marvin, C., Biberhofer, J., 2011. Modelling sediment-microbial dynamics in the South Nation River, Ontario, Canada: Towards the prediction of aquatic and human health risk. Water Res. 45, 3797–3809. <https://doi.org/10.1016/j.watres.2011.04.032>
- Droppo, I.G., Liss, S.N., Williams, D., Nelson, T., Jaskot, C., Trapp, B., 2009. Dynamic existence of waterborne pathogens within river sediment compartments. Implications for water quality regulatory affairs. Environ. Sci. Technol. 43, 1737–1743. <https://doi.org/10.1021/es802321w>
- Edge, T.A., Hill, S., 2005. Occurrence of antibiotic resistance in *Escherichia coli* from surface waters and fecal pollution sources near Hamilton, Ontario. Can. J. Microbiol. 51, 501–505. <https://doi.org/10.1139/w05-028>
- Falk, N., Chaganti, S.R., Weisener, C.G., 2018. Evaluating the microbial community and gene regulation involved in crystallization kinetics of ZnS formation in reduced environments.

- Geochim. Cosmochim. Acta 220, 201–216. <https://doi.org/10.1016/j.gca.2017.09.039>
- Field, K.G., Samadpour, M., 2007. Fecal source tracking, the indicator paradigm, and managing water quality 41, 3517–3538. <https://doi.org/10.1016/j.watres.2007.06.056>
- Filenko, N., Spiro, S., Browning, D.F., Squire, D., Overton, T.W., Cole, J., Constantinidou, C., 2007. The NsrR regulon of *Escherichia coli* K-12 includes genes encoding the hybrid cluster protein and the periplasmic, respiratory nitrite reductase. *J. Bacteriol.* 189, 4410–4417. <https://doi.org/10.1128/JB.00080-07>
- Gardner, A.M., Helmick, R.A., Gardner, P.R., 2002. Flavorubredoxin, an Inducible Catalyst for Nitric Oxide Reduction and Detoxification in *Escherichia coli* * 277, 8172–8177. <https://doi.org/10.1074/jbc.M110471200>
- Gilberthorpe, N.J., Poole, R.K., 2008. Nitric oxide homeostasis in *Salmonella typhimurium*: Roles of respiratory nitrate reductase and flavohemoglobin. *J. Biol. Chem.* 283, 11146–11154. <https://doi.org/10.1074/jbc.M708019200>
- Goltsman, D.S.A., Comolli, L.R., Thomas, B.C., Banfield, J.F., 2015. Community transcriptomics reveals unexpected high microbial diversity in acidophilic biofilm communities. *ISME J.* 9, 1014–1023. <https://doi.org/10.1038/ismej.2014.200>
- Handelsman, J., 2004. Metagenomics: Application of Genomics to Uncultured Microorganisms. *Microbiol. Mol. Biol. Rev.* 68, 669–685. <https://doi.org/10.1128/MBR.68.4.669-685.2004>
- Haraga, A., Ohlson, M.B., Miller, S.I., 2008. *Salmonellae* interplay with host cells. *Nat. Rev. Microbiol.* 6, 53–66. <https://doi.org/10.1038/nrmicro1788>
- Heaney, C.D., Sams, E., Dufour, A.P., Brenner, K.P., Haugland, R.A., Chern, E., Wing, S., Marshall, S., Love, D.C., Serre, M., Noble, R., Wade, T.J., 2012. Fecal indicators in sand, sand contact, and risk of enteric illness among beachgoers. *Epidemiology* 23, 95–106. <https://doi.org/10.1097/EDE.0b013e31823b504c.Fecal>
- Heaney, C.D., Sams, E., Wing, S., Marshall, S., Brenner, K., Dufour, A.P., Wade, T.J., 2009. Contact with beach sand among beachgoers and risk of illness. *Am. J. Epidemiol.* 170, 164–172. <https://doi.org/10.1093/aje/kwp152>
- Henry, T., Couillault, C., Rockenfeller, P., Boucrot, E., Dumont, A., Schroeder, N., Knodler, L.A., Lecine, P., Steele-mortimer, O., Borg, J., Gorvel, J., 2006. The *Salmonella* effector protein PipB2 is a linker for kinesin-1 103, 13497–13502.
- Heß, S., Berendonk, T.U., Kneis, D., 2018. Antibiotic resistant bacteria and resistance genes in the bottom sediment of a small stream and the potential impact of remobilization. *FEMS Microbiol. Ecol.* 1–11. <https://doi.org/10.1093/femsec/fiy128>
- Ishii, S., Yan, T., Shively, D.A., Byappanahalli, M.N., Whitman, R.L., Sadowsky, M.J., 2006.

- Cladophora (Chlorophyta) spp. harbor human bacterial pathogens in nearshore water of Lake Michigan. *Appl. Environ. Microbiol.* 72, 4545–4553.
<https://doi.org/10.1128/AEM.00131-06>
- Joo, H., Fu, C., Otto, M., Otto, M., 2016. Bacterial strategies of resistance to antimicrobial peptides.
- Kerr, J.M., Depinto, J. V, Mcgrath, D., Sowa, S.P., Swinton, S.M., 2016. Sustainable management of Great Lakes watersheds dominated by agricultural land use 42, 1252–1259.
- Kopylova, E., Noé, L., Touzet, H., 2012. SortMeRNA: Fast and accurate filtering of ribosomal RNAs in metatranscriptomic data. *Bioinformatics* 28, 3211–3217.
<https://doi.org/10.1093/bioinformatics/bts611>
- Ksoll, W.B., Ishii, S., Sadowsky, M.J., Hicks, R.E., 2007. Presence and sources of fecal coliform bacteria in epilithic periphyton communities of Lake Superior. *Appl. Environ. Microbiol.* 73, 3771–3778. <https://doi.org/10.1128/AEM.02654-06>
- Leimena, M.M., Ramiro-Garcia, J., Davids, M., van den Bogert, B., Smidt, H., Smid, E.J., Boekhorst, J., Zoetendal, E.G., Schaap, P.J., Kleerebezem, M., 2013. A comprehensive metatranscriptome analysis pipeline and its validation using human small intestine microbiota datasets. *BMC Genomics* 14, 530.
- Leonard, A.F.C., Zhang, L., Balfour, A.J., Garside, R., Gaze, W.H., 2015. Human recreational exposure to antibiotic resistant bacteria in coastal bathing waters. *Environ. Int.* 82, 92–100.
<https://doi.org/10.1016/j.envint.2015.02.013>
- Li, M., Lai, Y., Villaruz, A.E., Cha, D.J., Sturdevant, D.E., Otto, M., 2007. Gram-positive three-component antimicrobial peptide-sensing system. *Proc. Natl. Acad. Sci.* 104, 9469–9474.
<https://doi.org/10.1073/pnas.0702159104>
- Locht, C., Bertin, P., Menozzi, F.D., Renauld, G., 1993. The filamentous haemagglutinin, a multifaceted adhesion produced by virulent Bordetella spp. *Mol. Microbiol.* 9, 653–660.
- Love, M.I., Huber, W., Anders, S., 2014. Moderated estimation of fold change and dispersion for RNA-seq data with DESeq2. *Genome Biol.* 15, 1–21. <https://doi.org/10.1186/s13059-014-0550-8>
- Madsen, J.S., Burmølle, M., Hansen, L.H., Sørensen, S.J., 2012. The interconnection between biofilm formation and horizontal gene transfer. *FEMS Immunol. Med. Microbiol.* 65, 183–195. <https://doi.org/10.1111/j.1574-695X.2012.00960.x>
- Martinez, X., Pozuelo, M., Pascal, V., Campos, D., Gut, I., Gut, M., Azpiroz, F., Guarner, F., Manichanh, C., 2016. MetaTrans: an open-source pipeline for metatranscriptomics. *Sci. Rep.* 6, 26447. <https://doi.org/10.1038/srep26447>

- Mazar, J., Cotter, P.A., 2006. Topology and maturation of filamentous haemagglutinin suggest a new model for two-partner secretion. *Mol. Microbiol.* 62, 641–654.
<https://doi.org/10.1111/j.1365-2958.2006.05392.x>
- Melton, E.D., Stief, P., Behrens, S., Kappler, A., Schmidt, C., 2014. High spatial resolution of distribution and interconnections between Fe- and N-redox processes in profundal lake sediments. *Environ. Microbiol.* 16, 3287–3303. <https://doi.org/10.1111/1462-2920.12566>
- Melvin, J.A., Scheller, E. V., Noël, C.R., Cotter, P.A., 2015. New insight into filamentous hemagglutinin secretion reveals a role for full-length FhaB in *Bordetella* virulence. *MBio* 6, 12–15. <https://doi.org/10.1128/mBio.01189-15>
- Miao, E.A., Brittnacher, M., Haraga, A., Jeng, R.L., Welch, M.D., Miller, S.I., 2003. Salmonella effectors translocated across the vacuolar membrane interact with the actin cytoskeleton. *Mol. Microbiol.* 48, 401–415. <https://doi.org/10.1046/j.1365-2958.2003.t01-1-03456.x>
- Michalak, A.M., Anderson, E.J., Beletsky, D., Boland, S., Bosch, N.S., Bridgeman, T.B., Chaffin, J.D., Cho, K., Confesor, R., Daloglu, I., DePinto, J. V., Evans, M.A., Fahnenstiel, G.L., He, L., Ho, J.C., Jenkins, L., Johengen, T.H., Kuo, K.C., LaPorte, E., Liu, X., McWilliams, M.R., Moore, M.R., Posselt, D.J., Richards, R.P., Scavia, D., Steiner, A.L., Verhamme, E., Wright, D.M., Zagorski, M.A., 2013. Record-setting algal bloom in Lake Erie caused by agricultural and meteorological trends consistent with expected future conditions. *Proc. Natl. Acad. Sci.* 110, 6448–6452. <https://doi.org/10.1073/pnas.1216006110>
- Miller, M.B., Bassler, B.L., 2001. Quorum sensing in bacteria. *Annu. Rev. Microbiol.* 55, 165–99. <https://doi.org/10.1146/annurev.micro.55.1.165>
- Mohan, S.B., Schmid, M., Jetten, M., Cole, J., 2004. Detection and widespread distribution of the *nrfA* gene encoding nitrite reduction to ammonia, a short circuit in the biological nitrogen cycle that competes with denitrification 49, 433–443.
<https://doi.org/10.1016/j.femsec.2004.04.012>
- Mohiuddin, M.M., Salama, Y., Schellhorn, H.E., Golding, G.B., 2017. Shotgun metagenomic sequencing reveals freshwater beach sands as reservoir of bacterial pathogens. *Water Res.* 115, 360–369. <https://doi.org/10.1016/j.watres.2017.02.057>
- Molin, S., Tolker-Nielsen, T., 2003. Gene transfer occurs with enhanced efficiency in biofilms and induces enhanced stabilisation of the biofilm structure. *Curr. Opin. Biotechnol.* 14, 255–261. [https://doi.org/10.1016/S0958-1669\(03\)00036-3](https://doi.org/10.1016/S0958-1669(03)00036-3)
- Natural Resources Defense Council, 2014. Testing the Waters 2014: A guide to water quality at vacation beaches.
- Neira, J., Ortiz, M., Morales, L., Acevedo, E., 2015. Oxygen diffusion in soils: Understanding the

- factors and processes needed for modeling. *Chil. J. Agric. Res.* 75, 35–44.
<https://doi.org/10.4067/s0718-58392015000300005>
- Nieto, P.A., Covarrubias, P.C., Jedlicki, E., Holmes, D.S., Quatrini, R., 2009. Selection and evaluation of reference genes for improved interrogation of microbial transcriptomes: Case study with the extremophile *Acidithiobacillus ferrooxidans*. *BMC Mol. Biol.* 10.
<https://doi.org/10.1186/1471-2199-10-63>
- Niu, Q., Xia, M., 2017. The role of wave-current interaction in Lake Erie's seasonal and episodic dynamics. *J. Geophys. Res. Ocean.* 122, 7291–7311. <https://doi.org/10.1002/2017JC013288>
- Noël, C.R., Mazar, J., Melvin, J.A., Sexton, J.A., Cotter, P.A., 2012. The prodomain of the *Bordetella* two-partner secretion pathway protein FhaB remains intracellular yet affects the conformation of the mature C-terminal domain. *Mol. Microbiol.* 86, 988–1006.
<https://doi.org/10.1111/mmi.12036>
- Pandey, P.K., Kass, P.H., Soupir, M.L., Biswas, S., Singh, V.P., 2014. Contamination of water resources by pathogenic bacteria. *AMB Express* 4, 1–16. <https://doi.org/10.1186/s13568-014-0051-x>
- Paulson, J.N., Colin Stine, O., Bravo, H.C., Pop, M., 2013. Differential abundance analysis for microbial marker-gene surveys. *Nat. Methods* 10, 1200–1202.
<https://doi.org/10.1038/nmeth.2658>
- Peschel, A., Otto, M., Jack, R.W., Kalbacher, H., Jung, G., Götz, F., 1999. Inactivation of the *dlt* operon in *Staphylococcus aureus* confers sensitivity to defensins, protegrins, and other antimicrobial peptides. *J. Biol. Chem.* 274, 8405–8410.
<https://doi.org/10.1074/JBC.274.13.8405>
- Peschel, B.A., Jack, R.W., Otto, M., Collins, L.V., Staubitz, P., Nicholson, G., Kalbacher, H., Nieuwenhuizen, W.F., Jung, G., Tarkowski, A., Kessel, K.P.M. Van, Strijp, J.A.G. Van, 2001. *Staphylococcus aureus* Resistance to Human Defensins and Evasion of Neutrophil Killing via the Novel Virulence Factor MprF Is Based on Modification of Membrane Lipids with L -Lysine 193, 1067–1076.
- Phillips, M.C., Feng, Z., Vogel, L.J., Reniers, A.J.H.M., Haus, B.K., Enns, A.A., Zhang, Y., Hernandez, D.B., Solo-Gabriele, H.M., 2014. Microbial release from seeded beach sediments during wave conditions. *Mar. Pollut. Bull.* 79, 114–122.
<https://doi.org/10.1016/j.marpolbul.2013.12.029>
- Poock, S.R., Leach, E.R., Moir, J.W.B., Cole, J.A., Richardson, D.J., 2002. Respiratory Detoxification of Nitric Oxide by the Cytochrome *c* Nitrite Reductase of *Escherichia coli*. *J. Biol. Chem.* 277, 23664–23669. <https://doi.org/10.1074/jbc.M200731200>

- Poole, R.K., 2005. Nitric oxide and nitrosative stress tolerance in bacteria. *Biochem. Soc. Trans.* 33, 176–180. <https://doi.org/10.1042/BST0330176>
- Probandt, D., Eickhorst, T., Ellrott, A., Amann, R., Knittel, K., 2018. Microbial life on a sand grain: From bulk sediment to single grains. *ISME J.* 12, 623–633. <https://doi.org/10.1038/ismej.2017.197>
- Pruesse, E., Quast, C., Knittel, K., Fuchs, B.M., Ludwig, W., Peplies, J., Glöckner, F.O., 2007. SILVA: A comprehensive online resource for quality checked and aligned ribosomal RNA sequence data compatible with ARB. *Nucleic Acids Res.* 35, 7188–7196. <https://doi.org/10.1093/nar/gkm864>
- Ramirez, K.S., Knight, C.G., De Hollander, M., Brearley, F.Q., Constantinides, B., Cotton, A., Creer, S., Crowther, T.W., Davison, J., Delgado-Baquerizo, M., Dorrepaal, E., Elliott, D.R., Fox, G., Griffiths, R.I., Hale, C., Hartman, K., Houlden, A., Jones, D.L., Krab, E.J., Maestre, F.T., McGuire, K.L., Monteux, S., Orr, C.H., Van Der Putten, W.H., Roberts, I.S., Robinson, D.A., Rocca, J.D., Rowntree, J., Schlaeppli, K., Shepherd, M., Singh, B.K., Straathof, A.L., Bhatnagar, J.M., Thion, C., Van Der Heijden, M.G.A., De Vries, F.T., 2018. Detecting macroecological patterns in bacterial communities across independent studies of global soils. *Nat. Microbiol.* 3, 189–196. <https://doi.org/10.1038/s41564-017-0062-x>
- Reid, T., Chaganti, S.R., Droppo, I.G., Weisener, C.G., 2018. Novel insights into freshwater hydrocarbon-rich sediments using metatranscriptomics: Opening the black box. *Water Res.* 136, 1–11. <https://doi.org/10.1016/j.watres.2018.02.039>
- Reid, T., VanMensel, D., Droppo, I.G., Weisener, C.G., 2016. The symbiotic relationship of sediment and biofilm dynamics at the sediment water interface of oil sands industrial tailings ponds. *Water Res.* 100, 337–347. <https://doi.org/10.1016/j.watres.2016.05.025>
- Remaut, H., Tang, C., Henderson, N.S., Pinkner, J.S., Wang, T., Hultgren, S.J., Thanassi, D.G., Waksman, G., Li, H., 2008. Fiber Formation across the Bacterial Outer Membrane by the Chaperone/Usher Pathway. *Cell* 133, 640–652. <https://doi.org/10.1016/j.cell.2008.03.033>
- Rodionov, D.A., Dubchak, I.L., Arkin, A.P., Alm, E.J., Gelfand, M.S., 2005. Dissimilatory metabolism of nitrogen oxides in bacteria: Comparative reconstruction of transcriptional networks. *PLoS Comput. Biol.* 1, 0415–0431. <https://doi.org/10.1371/journal.pcbi.0010055>
- Rohmer, L., Hocquet, D., Miller, S.I., 2011. Are pathogenic bacteria just looking for food? Metabolism and microbial pathogenesis. *Trends Microbiol.* 19, 341–348. <https://doi.org/10.1016/j.tim.2011.04.003>

- Rusch, A., Huettel, M., Reimers, C.E., Taghon, G.L., Fuller, C.M., 2003. Activity and distribution of bacterial populations in Middle Atlantic Bight shelf sands. *Fems Microbiol. Ecol.* 44, 89–100. [https://doi.org/Pii S0168-6496\(02\)00458-0](https://doi.org/Pii%20S0168-6496(02)00458-0) Doi 10.1016/S0168-6496(02)00458-0
- Salk, K.R., Bullerjahn, G.S., McKay, R.M.L., Chaffin, J.D., Ostrom, N.E., 2018. Nitrogen cycling in Sandusky Bay, Lake Erie: Oscillations between strong and weak export and implications for harmful algal blooms. *Biogeosciences* 15, 2891–2907. <https://doi.org/10.5194/bg-15-2891-2018>
- Shahraki, A.H., Chaganti, S.R., Heath, D., 2019. Assessing high-throughput environmental DNA extraction methods for meta-barcode characterization of aquatic microbial communities. *J. Water Health* 17, 37–49. <https://doi.org/10.2166/wh.2018.108>
- Solo-Gabriele, H.M., Harwood, V.J., Kay, D., Fujioka, R.S., Sadowsky, M.J., Whitman, R.L., Wither, A., Caniça, M., Da Fonseca, R.C., Duarte, A., Edge, T.A., Gargaté, M.J., Gunde-Cimerman, N., Hagen, F., Mclellan, S.L., Da Silva, A.N., Babič, M.N., Prada, S., Rodrigues, R., Romão, D., Sabino, R., Samson, R.A., Segal, E., Staley, C., Taylor, H.D., Veríssimo, C., Viegas, C., Barroso, H., Brandão, J.C., 2016. Beach sand and the potential for infectious disease transmission: Observations and recommendations. *J. Mar. Biol. Assoc. United Kingdom* 96, 101–120. <https://doi.org/10.1017/S0025315415000843>
- Somerville, G.A., Proctor, R.A., 2009. At the Crossroads of Bacterial Metabolism and Virulence Factor Synthesis in *Staphylococci*. *Microbiol. Mol. Biol. Rev.* 73, 233–248. <https://doi.org/10.1128/MMBR.00005-09>
- Soumana, I.H., Linz, B., Harvill, E.T., 2017. Environmental origin of the genus *Bordetella*. *Front. Microbiol.* 8, 1–10. <https://doi.org/10.3389/fmicb.2017.00028>
- Sousa, A.J., Droppo, I.G., Liss, S.N., Warren, L., Wolfaardt, G., 2015. Influence of wave action on the partitioning and transport of unattached and floc-associated bacteria in fresh water. *Can. J. Microbiol.* 61, 584–596.
- Spiro, S., 2012. Nitrous oxide production and consumption: regulation of gene expression by gas-sensitive transcription factors. *Philos. Trans. R. Soc. B* 367, 1213–1225. <https://doi.org/10.1098/rstb.2011.0309>
- Stewart, E.J., 2012. Growing unculturable bacteria. *J. Bacteriol.* 194, 4151–4160. <https://doi.org/10.1128/JB.00345-12>
- Su, C., Lei, L., Duan, Y., Zhang, K.Q., Yang, J., 2012. Culture-independent methods for studying environmental microorganisms: Methods, application, and perspective. *Appl. Microbiol. Biotechnol.* 93, 993–1003. <https://doi.org/10.1007/s00253-011-3800-7>

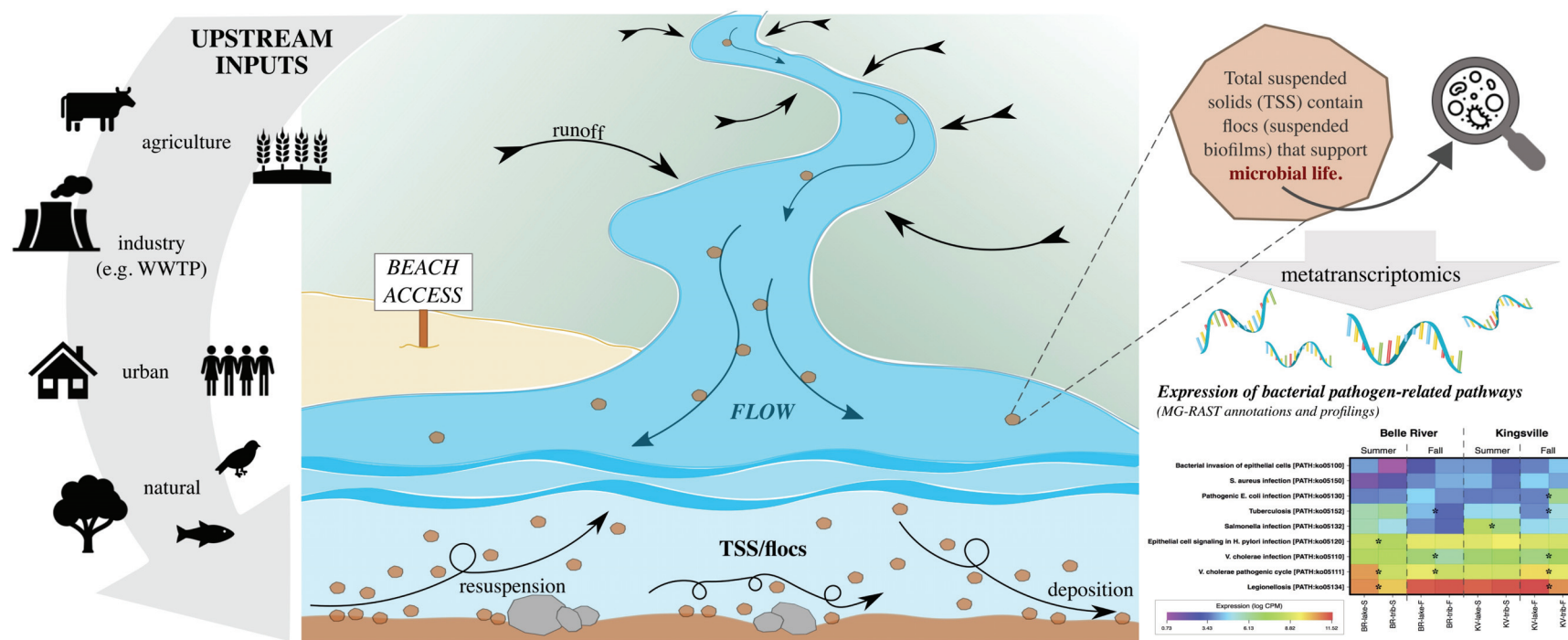
- Szeto, J., Namolovan, A., Osborne, S.E., Coombes, B.K., Brumell, J.H., 2009. Salmonella-containing vacuoles display centrifugal movement associated with cell-to-cell transfer in epithelial cells. *Infect. Immun.* 77, 996–1007. <https://doi.org/10.1128/IAI.01275-08>
- Tsoy, O. V., Ravcheev, D.A., Čuklina, J., Gelfand, M.S., 2016. Nitrogen fixation and molecular oxygen: Comparative genomic reconstruction of transcription regulation in Alphaproteobacteria. *Front. Microbiol.* 7, 1–14. <https://doi.org/10.3389/fmicb.2016.01343>
- Tucker, N.P., Le Brun, N.E., Dixon, R., Hutchings, M.I., 2010. There's NO stopping NsrR, a global regulator of the bacterial NO stress response. *Trends Microbiol.* 18, 149–156. <https://doi.org/10.1016/j.tim.2009.12.009>
- Wang, J., Yan, D., Dixon, R., Wang, Y., 2016. Deciphering the Principles of Bacterial Nitrogen Dietary Preferences : a. *Am. Soc. Microbiol.* 7, 1–9. <https://doi.org/10.1128/mBio.00792-16>.Editor
- Weisener, C., Lee, J., Chaganti, S.R., Reid, T., Falk, N., Drouillard, K., 2017. Investigating sources and sinks of N₂O expression from freshwater microbial communities in urban watershed sediments. *Chemosphere* 188, 697–705. <https://doi.org/10.1016/j.chemosphere.2017.09.036>
- Whitman, R.L., Harwood, V.J., Edge, T.A., Nevers, M.B., Byappanahalli, M., Vijayavel, K., Brandão, J., Sadowsky, M.J., Alm, E.W., Crowe, A., Ferguson, D., Ge, Z., Halliday, E., Kinzelman, J., Kleinheinz, G., Przybyla-Kelly, K., Staley, C., Staley, Z., Solo-Gabriele, H.M., 2014. Microbes in beach sands: Integrating environment, ecology and public health, *Reviews in Environmental Science and Biotechnology*. <https://doi.org/10.1007/s11157-014-9340-8>
- Wilke, A., Bischof, J., Harrison, T., Bretin, T., D'Souza, M., Gerlach, W., Matthews, H., Paczian, T., Wilkening, J., Glass, E.M., Desai, N., Meyer, F., 2015. A RESTful API for Accessing Microbial Community Data for MG-RAST. *PLoS Comput. Biol.* 11, 1–8. <https://doi.org/10.1371/journal.pcbi.1004008>
- Wood, D.E., Salzberg, S.L., 2014. Kraken: Ultrafast metagenomic sequence classification using exact alignments. *Genome Biol.* 15. <https://doi.org/10.1186/gb-2014-15-3-r46>
- Xie, Y., Wang, J., Wu, Y., Ren, C., Song, C., Yang, J., Yu, H., Giesy, J.P., Zhang, X., 2016. Using in situ bacterial communities to monitor contaminants in river sediments. *Environ. Pollut.* 212, 348–357. <https://doi.org/10.1016/j.envpol.2016.01.031>
- Yamahara, K.M., Walters, S.P., Boehm, A.B., 2009. Growth of enterococci in unaltered, unseeded beach sands subjected to tidal wetting. *Appl. Environ. Microbiol.* 75, 1517–1524. <https://doi.org/10.1128/AEM.02278-08>

- Yilmaz, P., Parfrey, L.W., Yarza, P., Gerken, J., Pruesse, E., Quast, C., Schweer, T., Peplies, J., Ludwig, W., Glöckner, F.O., 2014. The SILVA and “all-species Living Tree Project (LTP)” taxonomic frameworks. *Nucleic Acids Res.* 42, 643–648.
<https://doi.org/10.1093/nar/gkt1209>
- Zaitseva, J., Jenewein, S., Jumpertz, T., Holland, I.B., Schmitt, L., 2005. H662 is the linchpin of ATP hydrolysis in the nucleotide-binding domain of the ABC transporter HlyB. *EMBO J.* 24, 1901–1910. <https://doi.org/10.1038/sj.emboj.7600657>
- Zhang, X., Liu, X., Liang, Y., Xiao, Y., Ma, L., Guo, X., Miao, B., Liu, H., Peng, D., Huang, W., Yin, H., 2017. Comparative genomics unravels the functional roles of co-occurring acidophilic bacteria in bioleaching heaps. *Front. Microbiol.* 8, 1–15.
<https://doi.org/10.3389/fmicb.2017.00790>
- Zimmer-faust, A.G., Thulsiraj, V., Marambio-jones, C., Cao, Y., Grif, J.F., Holden, P.A., Jay, J.A., 2017. Effect of freshwater sediment characteristics on the persistence of fecal indicator bacteria and genetic markers within a Southern California watershed 119, 1–11.
<https://doi.org/10.1016/j.watres.2017.04.028>

CHAPTER 4: IDENTIFYING CHEMOLITHOTROPHIC AND PATHOGENIC-
RELATED GENE EXPRESSION WITHIN SUSPENDED SEDIMENT FLOCS IN
FRESHWATER ENVIRONMENTS: A METATRANSCRIPTOMIC ASSESSMENT

Published: VanMensel D, Droppo IG, Weisener CG (2022) Identifying chemolithotrophic and pathogenic-related gene expression within suspended sediment flocs in freshwater environments: A metatranscriptomic assessment. *Science and the Total Environment* 807:150996, doi.org/10.1016/j.scitotenv.2021.150996

Graphical Abstract



CHAPTER 4: IDENTIFYING CHEMOLITHOTROPHIC AND PATHOGENIC-RELATED GENE EXPRESSION WITHIN SUSPENDED SEDIMENT FLOCS IN FRESHWATER ENVIRONMENTS: A METATRANSCRIPTOMIC ASSESSMENT

4.0 Prologue

While Chapter 2 provided a microbial baseline of freshwater bed sediment with which to use as a guide for subsequent focused research, Chapter 3 expanded our knowledge of the functionality of these bed environments at the transcriptomic level with gene expression data. The research presented in the following chapter, however, encompasses the same metatranscriptomic approach but extends to the suspended sediment fraction. Insights gathered here provide necessary information pertaining to the microbiome associated with suspended sediment (and its role as a microbial/pathogen transport vector) in freshwater systems. This work improves our understanding of potential health risks related to recreational water use.

4.1 Introduction

The introduction and proliferation of pathogenic organisms in aquatic environments is a serious global issue that consequently leads to unsafe drinking water, illness and disease, poor ecosystem quality, and economic losses (DeFlorio-Barker et al., 2018; Levy et al., 2016). Health and safety related to recreational water use can be monitored through water quality assessments, which typically involve simple culture-based identification tests of FIB (Rodrigues and Cunha, 2017). While these tests are widely used, they are merely a snapshot of past conditions since culturing methods take 24-48 hours for enumeration results. Further, these assessments are void within hours to minutes because aquatic systems are dynamic entities that are constantly shifting

and changing to the active environment (Shahraki et al., 2019). For example, a study by McPhedran and colleagues (2013) highlighted the extreme variability in *E. coli* and *Enterococci* concentrations in the water column at public beaches on a day-to-day basis with no observable trend, although both FIB correlated with each other. These outdated water quality tests lead to unreliable determinations of beach status for recreational use. Finally, they do not provide important information such as strain-level (i.e., pathogens of concern), gene expression (i.e., activity of microbial population), or possible source of contamination. There are a variety of point and nonpoint sources for microbial pollution in aquatic ecosystems (e.g., sanitary sewer overflow, waterfowl, agricultural livestock/urban runoff). Identifying the source, origin (e.g., human vs. livestock) and biophysical factors (e.g., river flows, waves, combined sewer overflows) that determine pathogen concentration and distribution are critical for managing beaches and determining human health risks to exposure (Byappanahalli et al., 2015).

Although bacteria in aquatic systems prefer attachment to particles compared to a planktonic lifestyle (Costerton et al., 1987), there continues to remain a lack of information regarding sediment-microbial interactions. Standard tests for FIB in aquatic systems assume these organisms are planktonic in nature (Federigi et al., 2019). More recently, however, there has been increased interest regarding the association of microorganisms with sediments (both bed and suspended) and the roll this plays for source, fate and effect of pathogens in fluvial and lacustrine systems (Alm et al., 2003; Mohiuddin et al., 2017; VanMensel et al., 2020). A recent study by Reid et al. (2020) showed the transport of active microbial communities was associated with the TSS fraction of a riverine system in the Athabasca region of northern Alberta, Canada. The attachment of microbes to sediment is related to their affiliation with nutrients, DOC and protection from predation through colonization of particle surfaces (Gerba and McLeod, 1976). Microbial physiological production of EPS secretion and electrochemical attractions are the main processes promoting particle flocculation (Droppo et al., 1997) and results in a viable community within multi-particle structures that have been described as suspended biofilms (Liss, 2002). The

process of increasing particle size via flocculation (i.e., creating flocs) has a strong influence over the transport and fate of the sediment and associated microbes (Droppo et al., 2009) and has been shown to promote floc deposition to the sediment bed surface (Wotton, 2007).

This study applies metatranscriptomics to investigate the active microbial community associated with SS transporting potential bacterial pathogens to lacustrine beaches where they may pose human health risks. It is hypothesized that the gene expression data of SS in the littoral zone of a freshwater lake compares with that of the contributing respective tributary to illustrate this vector of pathogenic transportation. Two distinct locations in WEC (Ontario, Canada) were assessed to test this hypothesis, and samples were collected seasonally to add a temporal perspective. Furthermore, it is hypothesized that beach proximity and geographical factors influencing SS deposition within the sediment bed catchment may influence the established microbial community (i.e., biofilm) (Byappanahalli et al., 2015; VanMensel et al., 2020). This research aims to 1) provide initial insight to the active microbial community that is associated with SS in freshwater lotic systems, 2) explore the correlation of SS in tributaries to the SS in the lake nearshore beach zone, and 3) compare the SS fraction with data of the nearshore bed sediment to determine if pathogenicity potential at beaches may be partially explained by deposition of SS in these locations. We investigate SS as a transport vector of viable microbial contamination originating within its watersheds and eventual fate to the bed sediment in the nearshore zone. To our knowledge, this work is the first to investigate SS as a nonpoint source of bacterial contamination and the bed sediment as a pathogen reservoir in aquatic microbial communities based on gene expression surveys and has significant potential to help address the large, growing problem of microbial contamination impacting freshwater security.

4.2 Materials and Methods

4.2.1 *Study sites*

WEC is in Ontario, Canada between Lake St. Clair and Lake Erie (Figure 4.1) and is part of the GLs watershed. This area is largely recognized for its broad and successful agricultural land use (i.e., conventional farming, greenhouses, livestock). Additionally, the vast proximity to freshwater renders this area popular to recreational water use. Two distinct locations in WEC were selected for this study –BR and KV. Both locations are lakeshore towns with public beach access and notable tributaries that reach each lake proximal to these public beaches (Belle River in BR; Mill Creek in KV). Both BR and KV beaches involved in this study have previously been described as sheltered and low energy (i.e., restricted water flow), accompanied by steep REDOX gradients and expression of pathogenic gene transcripts observed in the bed sediment of the nearshore (VanMensel et al., 2020 - Chapter 2). These details suggest there is little incoming sediment transport via waves or currents that could advocate lacustrine origin. Therefore, we assume the sediment load (both bed and suspended) in these locations is mostly of riverine origin. While both tributaries are agriculturally stressed, the fields surrounding Belle River are reportedly fertilized with a combination of manure and chemicals, which eventually runoff into the river (DiCarlo et al., 2020), while Mill Creek is considered ‘greenhouse influenced’, containing higher concentrations of nutrients and trace metals than tributaries not influenced by greenhouses in the area (Maguire et al., 2018).

4.2.2 *TSS collections*

Our sampling sites included the tributaries (Belle River and Mill Creek) as well as each lake (St. Clair, Erie) within the swimming zone of the public beaches (i.e., nearshore) in BR and

KV (Figure 4.1). To distinguish our sampling sites, we designate ‘trib’ and ‘lake’ for the tributary and nearshore in the lake, respectively. Samples were collected on the same day from each location (BR and KV) and each site (tributary and lake) in both the summer (July 11) and fall (November 28) of 2017, allowing for spatial and temporal analyses.

SS was collected by a portable continuous flow centrifuge (Alfa-Laval), with a flow rate of 4 L min^{-1} and filtration efficiencies greater than 90% recovery. Water was pumped from each site at approximately mid-depth (1-2 m above bed surface) in the water column using a 5C-MD March submersible pump. Filtered sediment was transferred from the centrifuge collection bowl to sterile cryotubes on site and immediately flash frozen in liquid nitrogen to minimize RNA degradation. Samples were kept at -80°F until nucleic acid extractions were performed (Rissanen et al., 2010).

4.2.3 Physicochemical measurements of the water column

Water samples were collected and sent to the Canada Center for Inland Waters (Environment and Climate Change Canada, Burlington, ON) for additional analyses. TSS concentration (mg L^{-1}) and recovery ($\% \text{ recovery} = \text{outflow TSS} / \text{inflow TSS}$) were determined through vacuum filtration of a $0.45 \text{ }\mu\text{m}$ membrane filter. The CILAS 930 particle size analyzer (CILAS, Orleans, France) was used to define the size distribution of SS (D_{50}) from 0.2 to $500 \text{ }\mu\text{m}$ diameter. Seasonal samples were also analyzed for nutrient concentrations in the water column; total nitrogen (TN) was determined by alkaline digestion and automated flow injection analyzer colorimetric hydrazine method (B0270W), total phosphorous (TP) was measured by automated continuous flow analyzer colorimetric ascorbic acid method (B0271W), and both dissolved organic and inorganic carbon (DOC, DIC) were analyzed through automated UV digestion and infrared detection (B0255W) (Environment and Climate Change Canada).

4.2.4 SEM analysis

SS collections were analyzed by Scanning Electron Microscopy (SEM) to investigate particle distribution and evidence of biological activity (e.g., cellular reproduction, REDOX). Specifically, the Environmental SEM (FEI Quanta200F, Eindhoven, Netherlands) was used at the Great Lakes Institutes for Environmental Research (GLIER), University of Windsor (Windsor, Ontario, Canada). Analysis was performed at low vacuum with a theoretical spot size of 3.9 nm. Both secondary electron (SE) and backscattered electron (BSE) detectors were used.

4.2.5 Extractions, library preparation, quality control, and sequencing

Sediment RNA extractions were performed using RNeasy PowerSoil Total RNA kits (Qiagen), following the manufacturer's instructions with slight modifications previously described (§2.2.3). Sample weight for SS here was between 1-2 g and the final pellets resuspended in 50 μL RNase-free water. Immediately following resuspension of the pellet, RNase inhibitor (Invitrogen) was added to minimize degradation and potential DNA contamination was removed using the RapidOut DNA Removal kit (Thermo Scientific), following the manufacturer's instructions. Aliquots of extracted RNA isolations were kept at -80°C until quality testing and further processing.

Extracted RNA was assessed in-house using the Agilent 2100 Bioanalyzer (Agilent Technologies) to confirm sufficient quality and quantity for sequencing. Samples with RIN > 6.5 and concentrations $> 100 \text{ ng } \mu\text{L}^{-1}$ were acceptable for sequencing. Samples with RIN values < 6.5 were subject to at least one clean-up step using the RNeasy MinElute Cleanup kit (Qiagen), following the manufacturer's instructions. Once RIN was deemed acceptable and concentration

remained $> 100 \text{ ng } \mu\text{L}^{-1}$, samples were sent to the Genome Quebec Innovation Center at McGill University for metatranscriptomic analysis. Additional quality control (QC) checks were performed at Genome Quebec prior to sequencing. Bacteria and yeast rRNA depletion was performed before sequencing, enhancing mRNA quantity in each sample for improved functional assignments (refer to §3.2.2 for details). Samples were sequenced on the Illumina HiSeq 4000 PE100 sequencer in duplicate to validate sample accuracy. Raw sequence files have been deposited in the NCBI Sequence Read Archive (SRA) under accession PRJNA726406.

4.2.6 *Bioinformatics analyses*

Metatranscriptomic sequencing data obtained from Genome Quebec were processed through the MG-RAST (Metagenomics Rapid Annotations using Subsystems Technology) pipeline (Meyer et al., 2008), a public online resource for phylogenetic and functional analysis of high-throughput sequencing data. Raw paired-end sequence files were submitted, and the pipeline performed pairing, quality filtering, and annotation of functional transcripts (mRNA) to the KO (KEGG orthology) database. The KO approach to annotation involves four levels of functional descriptions, with Level 1 being the most general categories and Level 4 including annotations at the transcript/functional level (i.e., highest resolution). We selected ‘representative hit’ for annotation assignment because it makes counts additive and therefore allows the comparison of different profiles (Wilke et al. 2013). Downstream analysis of this preprocessed data continued with cut-off values set for maximum e-value (10^{-5}), minimum percent identity (60%), minimum alignment length (15), and minimum abundance (1). The dataset was filtered for lowly expressed transcripts; to pass filtering, transcripts required at least 2 counts per million (CPM) (Chen et al., 2020) in at least one sample (1 of 16). This cut-off threshold filtered out approximately 20% of annotated genes (Bourgon et al., 2010). Further processing (normalization, differential analyses)

was accomplished using the START app, a web-based RNA-seq analysis and visualization resource (Nelson et al., 2017). Filtered, raw expression values were normalized to logCPM values and differential analysis tests were performed using the Bioconductor package edgeR. This approach performs pairwise comparisons between two or more groups using the quantile-adjusted conditional maximum likelihood (qCML) method. Differential expression is determined using an exact test that is based on the qCML method and has strong parallels with Fisher's exact test but is adapted for over-dispersed data (Robinson et al., 2010). Before examining the expression of functional transcripts, additional filtering was performed. After normalization, remaining lowly expressed transcripts that did not exhibit at least 2 logCPM in at least one sample (1 of 16) were additionally removed. From a biological perspective, transcripts that are not expressed at a meaningful quantity in any sample are not biologically important. Downstream analyses mainly focused on pairwise comparisons between sampling sites (lake vs. tributary) of the same location and season, although all statistical pairwise comparisons were performed. START and Aabel 3 graphical software were used for visualizations and illustrations of gene expression correlations. Duplicate samples were averaged for illustrative purposes, where appropriate.

4.3 Results and Discussion

4.3.1 *Water nutrient stoichiometry and TSS biophysicochemical characteristics*

Grain size distribution reveals cohesive sediments in suspension, with D_{50} (μm) of 21.86 (BR-lake), 23.19 (BR-trib), 33.06 (KV-lake), and 21.33 (KV-trib). It is well-documented that cohesive SS is typically transported in flocculated form, which is a heterogeneous assembly of active and non-viable biological components, inorganic particles, and water (Droppo, 2001 and references therein). Smaller particle size equates to greater surface area to volume ratio, which is advantageous for microbial colonization given the concentration of DOC and nutrients on the

particle (Bradford et al., 2013). Furthermore, SS associated with flocculation in aquatic systems are the physical building blocks of bed sediment when they settle out of suspension (Droppo, 2009; Droppo et al., 2009; Wu et al., 2009). Previous studies have reported the association of pathogenic bacteria with beach sediment and nearshore flocs/SS (Sousa et al., 2015), and supports that SS is a major vector of pathogens to the bed sediment.

Physicochemical measurements were used to characterize the SS collection of each sampling site (Table C-1). In most cases, nutrients analyzed (TN, TP, DOC, DIC) showed consistent concentrations throughout the sampling seasons (spring to fall), suggesting nutrient and biogeochemical cycling are relatively constant over the long term. In the spring, BR showed lower lake concentrations of TN at $1220 \mu\text{g L}^{-1}$ vs. the tributary at $2740 \mu\text{g L}^{-1}$. TP concentrations were $64.2 \mu\text{g L}^{-1}$ and $152 \mu\text{g L}^{-1}$ for the lake and tributary, respectively. A similar relationship was observed in the fall, showing $1080 \mu\text{g L}^{-1}$ and $5150 \mu\text{g L}^{-1}$ for TN and $41.1 \mu\text{g L}^{-1}$ and $157 \mu\text{g L}^{-1}$ for TP from both the lake and tributary, respectively. TP concentrations in BR lake and tributary are consistent based on spring and fall events. In contrast, fall TN concentrations experienced a 2-fold increase in the tributary, but remained similar in the lake. By comparison, the KV sampling location showed a similar trend between spring and fall patterns. In the spring, TN concentrations from lake and tributary were measured at $2540 \mu\text{g L}^{-1}$ and $5350 \mu\text{g L}^{-1}$ and TP concentrations were $310 \mu\text{g L}^{-1}$ and $472 \mu\text{g L}^{-1}$, respectively. In the fall, concentrations of TP are comparable at $213 \mu\text{g L}^{-1}$ in the lake and $568 \mu\text{g L}^{-1}$ in the tributary. The strongest deviation to this was observed for TN concentrations in the fall showing a 2-fold increase (from 5350 to $11,100 \mu\text{g L}^{-1}$) in the tributary. Remarkably, the debate of contributing factors to excess nutrient impacts on aquatic environments have often been segregated to P only paradigms at the expense of considering combined P and N impacts (Paerl et al., 2011; Schindler et al., 2016; Tong et al., 2018). Excessive nutrients can lead to eutrophic conditions, excess algal mats and possibly links to increased pathogen presence and activity (VanMensel et al., 2020). N and P loadings are often strongly correlated to external nutrient inputs rather than internal and material weathering sources

(Tong et al., 2020, 2018). Nutrient loading can be influenced by a range of conditions including hydrological, wastewater treatment facilities, agriculture population density, and other land use patterns (Kellerman et al., 2014; Müller et al., 1998). Observed N:P mass ratios in BR lake and tributary measured at 19 and 18 in the spring, increasing to 26 and 33 in the fall, respectively. In contrast, N:P mass ratios in KV lake and tributary were 8 and 11 in the spring, and 12 and 20 in the fall, respectively. The overall observed differences reflect a possible imbalance between TN and TP, and this can have significant impacts on aquatic food webs often leading to preferential enrichment of nitrogen fixing microorganisms, favouring planktonic species which may preferentially scavenge P (e.g., *Microcystis spp.*) and impact rates of energy transfer through food webs (Tong et al., 2020, 2018). In this case, TN:TP mass ratios are higher in BR compared to KV locations suggesting significant TN enrichment relative to TP. We can observe the impacts of TN enrichment on the microbial community function associated with the TSS sampled from these sites, which will be discussed in subsequent sections of this chapter.

Suspended solids were examined under SEM to document morphology and composition (Figure 4.2). Collections from the tributaries showed consistent fine-grain minerals along with high proportion of attached bacteria and other organic substrates (e.g., diatoms, microbial cells, algal filaments). In BR tributary samples, we observed truncated rod-shaped cells proximal to amorphous iron oxides (Figure 4.2a) (Elliott et al., 2014; Faivre and Godec, 2015; Konhauser, 1997). Observed microbial cells (Figure 4.2b) were quite abundant for all the flocs collected. KV tributary samples, on the other hand, showed more evidence of algae, with a green alga (*Scenedesmus*) present in one of our samples (Figure 4.2c) as well as a rare image of a spherical auxospore cell (Figure 4.2d), both in the presence of diverse diatoms. *Scenedesmus* is one of the most common freshwater algae genera, and has been known to proliferate in N-rich environments (Ishaq et al., 2016; Msanne et al., 2020). The detection of the auxospore strongly corroborates biological activity, as it is recognized as a specialized zygote cell known only to diatoms that is

characteristic of reproduction and the restitution of large cell size (Kaczmarska and Ehrman, 2021, 2015).

4.3.2 *Sequencing statistics and functional diversity*

The metatranscriptomics dataset obtained from the Illumina HiSeq consisted of 16 paired-end sequence files, with over 18.8 million reads per sample. Sequencing statistics from the Illumina run are summarized in Appendix C (Table C-2). Relevant raw data used for normalization/statistical tests and a summary of gene expression profiles (i.e., transcripts, number, category, raw reads, normalized logCPM values) are also found in Appendix C (Tables C-3 and C-4, respectively).

Principle components analysis (PCA) of the metatranscriptomic dataset illustrates strong clustering (i.e., similarity) of replicate samples, suggesting all eight groups are acceptable representations of their respective microbial functionality (Figure 4.3). We can further cluster these groups to show the similarity between both lake and tributary of the same location and season (dotted blue ellipses). An exception to this was KV-Fall samples, which showed less similarity between lake and tributary based on distance of separation. This may be attributed to low water flow from Mill Creek into Lake Erie during late fall, in combination with a strong eastward current on the shoreline of the lake, directing the tributary outflow away from the sampling site for the lake. Recent hydrodynamic modeling of Lake Erie (Niu et al., 2015) showed dominant northeastward water movement in the nearshore of the western basin as a result of strong wind-driven currents in early winter as opposed to spring and summer. However, the other groupings (BR-Summer, BR-Fall, KV-Summer) all display high inter-group similarity, suggesting these tributaries have important influences on the microbial functional diversity in the nearshore of the receiving zone (Madani et al., 2020). This is a vital facet to unveil regarding recreational water use as it can help us better understand the degree of influence that adjacent

tributaries can have on water quality of nearshore swim zones, and the environmental conditions (i.e., climate) that are associated.

We classified the metatranscriptomic data at Level 1 functional categories and applied pairwise statistical testing between lake and tributary samples from each location and season to determine differential expression ($p < 0.05$; Table 4.1). There are six Level 1 functional categories; of particular interest to our study on human health risks associated with recreational water use is *Human Diseases*. This functional category shows differential expression between lake and tributary in three situations (BR-Summer, KV-Summer, KV-Fall), where it is upregulated in the tributary compared to the lake. At the same time, *Metabolism* is also differentially expressed for the same three situations, suggesting these categories are linked in terms of gene expression regulation. Microbial metabolic processes are the life-sustaining biochemical reactions that determine the growth and survival of an ecosystem. It defines the ability of the other functional categories to perform because it is responsible for providing the building blocks and energy required for all cellular activities (Chubukov et al., 2014). In other words, the microbial metabolism of an aquatic system is, in part, responsible for the health of that system. For this reason, we examine the functionality of both *Metabolism* and *Human Diseases* in subsequent sections to understand human health risks associated with recreational water use.

We further used Level 1 data to analyze overall comparisons statistically and separately between locations (BR vs. KV), seasons (summer vs. fall), and sites (lake vs. tributary) (Figure C-1, Table C-5). Results reveal location and temporal components exhibit differential expression ($p < 0.05$) in some of these categories, but lake and tributary samples did not significantly differ from each other overall. Regarding location, BR and KV are quite different from each other, with four categories differentially expressed. BR exhibits upregulation of *Cellular Processes* and *Human Diseases*, while *Genetic Information Processing (GIP)* and *Organismal Systems* are upregulated in KV. Since the *Organismal Systems* category is heavily focused on high-level characteristics of complex organisms, it does not pertain to our study here on bacteria. However,

the differences highlighted between BR and KV can likely be explained from the variation of land use in the surrounding areas, mainly agricultural practices, which influence local tributaries as a result of farmland runoff (DiCarlo et al., 2020; Maguire et al., 2018). Each tributary receives its own unique blend of soil, nutrients, contaminants, microorganisms, etc. from the surrounding landscapes, and each environment will support particular active microbial communities.

With seasonal comparisons, both *Human Diseases* and *Metabolism* are upregulated in the summer. This suggests warmer temperatures better support bacterial metabolism and activity related to human disease (i.e., bacterial waterborne enteric diseases) (Levy et al., 2016). Irrespective, at this level of resolution, it is difficult to interpret what these differences represent at the functional level. Taken altogether, however, our results show that encoded amino acids (AAs) of cDNAs showing similarities with genes involved in *Human Diseases* to be most dominantly expressed in BR (both lake and tributary) during the summer season, which consequently is peak timing for recreational water use.

4.3.3 *Biogeochemical cycling reveals chemolithotrophic activity*

Photosynthetic processes [ko00195, ko00196, ko00710] show high expression in our samples (12.70 – 17.06, 9.90 – 14.89, 8.06 – 12.15 logCPM, respectively) and were, as expected, always higher in the summer compared to fall (Figure C-2). This dominance of photosynthetic processes demonstrates primary production utilizing solar energy within our SS samples, in both lakes and tributaries. The purpose of investigating the expression of transcripts involved in energy metabolism, however, was to examine the dominant chemolithotrophic activity of the microbes in these systems. Chemolithotrophs are important bacterial groups that contribute immensely to global biogeochemical cycling, which are the processes of recycling essential nutrients (e.g., nitrogen, carbon, sulfur) for cellular life in nature (Dworkin, 2012; Rundell et al., 2014). These pathways are important for ecosystem persistence and studying their transcriptomes can help

identify environmental conditions and perturbations (Falk et al., 2019). Therefore, our focus here is on the transcriptomic expression of chemolithotrophic pathways (Figure 4.4): methane metabolism [ko00680] (10.61 – 12.11 logCPM), carbon fixation pathways in prokaryotes [ko00720] (10.30 – 13.27 logCPM), nitrogen (N) metabolism [ko00910] (11.36 – 13.80 logCPM), and sulfur (S) metabolism [ko00920] (10.72 – 11.41 logCPM). Although these four pathways appear to be similar in their level of expression and distribution in all samples, there are a few that show differential expression ($p < 0.05$) in their comparative counterparts. BR lake and tributary differ from each other in diverse ways from summer to fall. In the summer, carbon fixation in BR-lake is upregulated while N metabolism in BR-trib is upregulated. In the fall, S metabolism is upregulated in BR-lake while methane metabolism is upregulated in BR-trib. This is suggesting that both BR lake and tributary rely on different metabolic pathways depending on the season, which may correlate with nutrient availability, precipitation, and run-off patterns (Nelson, 2009). In KV, on the other hand, there is upregulation of carbon cycling in the lake compared to the tributary, especially in the fall when both methane metabolism and carbon fixation are significantly more expressed ($p < 0.05$). Carbon fixation is an important characteristic of some autotrophic microorganisms to recycle oxidized or inorganic carbon into organic biomolecules for energy purposes (Kelly, 1981). Clearly there is strong evidence of both photosynthetic and chemosynthetic microbial activity in all samples, demonstrating a healthy level of primary production within the SS fraction of these freshwater systems. This further supports the SEM observations (Figure 4.2) that demonstrate microbial activity associated with the TSS.

Previous research has highlighted an association between N metabolism and the survivability of bacterial pathogens (Amon et al., 2010; VanMensel et al., 2020). Therefore, we created a holistic schematic of N cycling pathways overlayed with expression data for individual genes responsible for specific reactions (Figure 4.5). In this perspective, we observe the dominant trends of N metabolism occurring with confidence as we identify clusters of genes to support the

trend as opposed to just one or two transcripts being expressed. In the SS, denitrification is the most highly expressed pathway for all samples, with KV-Summer displaying the highest level of expression for the transcripts involved. These results corroborate the research from our previous work on the bed sediment for these same beaches (VanMensel et al., 2020), where KV displayed dominant denitrification expression compared to BR. However, BR displayed a stronger expression of ammonification in the bed sediment compared to KV, which contradicts our SS results here. Interestingly, we also identified expression of transcripts involved in several other N transformation pathways in the SS, including dissimilatory and assimilatory nitrate reduction to ammonia (DNRA, ANRA), N fixation, and nitrification. This suggests that the SS is complex and vast enough to support both aerobic and anaerobic microsites and is perhaps more microbially complex than previously understood (Xia et al., 2018). Expression data of the most dominant transcripts for the chemolithotrophic metabolisms of carbon, N, and S can be found in (Figure C-3).

4.3.4 *Expression of bacterial pathogenic-related transcripts in freshwater SS*

Examining energy metabolism helps explain the functionality of a microbial community in a system, and ultimately how bacteria are able to survive and adapt to their environment (VanMensel et al., 2020). The overall observed metabolic expression strongly suggests that quality conditions exist for diverse microbial establishment, including pathogens. This is especially prevalent during temperature extremes (e.g., summer months). During our study the detection of relevant gene signatures identified for *Infectious Diseases* (Level 2) ranged from 10.95 – 12.57 logCPM in SS (Table C-4). Our results identify nine bacterial infectious disease pathways (Level 3) exhibiting gene expression within all samples (Figure 4.6). From a broad view, BR-lake shows higher overall expression than BR-trib in both summer and fall. This either suggests that BR-trib is not the only contribution of bacterial contaminants to the adjacent beach,

or that bacterial pathogens are able to establish and proliferate better here. In fact, recent studies modeling nutrient loss rates and water transport in Lake St. Clair demonstrated this WEC shoreline is dominated by nutrient-rich, productive waters from the Thames and Sydenham Rivers, and is also accompanied by longer residence times and higher biomass (Bocaniov and Scavia, 2018; Madani et al., 2020). Specifically, transcripts showing similarities with genes involved in the pathways legionellosis [ko05134], *Vibrio cholerae* pathogenic cycle [ko05111] and infection [ko05110], epithelial cell signaling in *Helicobacter pylori* infection [ko05120], and tuberculosis [ko05152] are all upregulated ($p < 0.05$) compared to the tributary in either the summer or fall or both. None of the nine bacterial pathogenic-related pathways exhibit upregulation in the tributary compared to the lake. We suspect this is due to differences in the source of contamination as well as the nearshore/beach embayment providing a low energy, high nutrient environment, which promotes the establishment and growth of bacteria (VanMensel et al., 2020).

KV data follows suite in the summer with the lake showing overall greater expression of bacterial pathogenic-related pathways compared to the tributary, although only one pathway, *Salmonella* infection [ko05132], is differentially expressed ($p < 0.05$). This particular pathway, however, may or may not be accurately represented as it is based on the expression of a single transcript that is also known to function in other pathways (Mohan et al., 2004). Without validation through phylogenetic analyses, these results should be taken with caution, especially since only one transcript is representative of an entire pathway. Similar to BR, KV beach has been described as sheltered and low-energy (Chapter 2) allowing bacteria to establish biofilms on the bed sediment and suspended floc communities (Droppo et al., 2009). In the fall, however, KV-trib demonstrates higher expression of bacterial pathogenic-related pathways compared to KV-lake. For the other three pairwise comparisons (Figure 4.6), differentially expressed ($p < 0.05$) pathways all display higher expression in the lake sample compared to the tributary. However, as described above (§4.3.2, Figure 4.3, Table 4.1), KV-Fall shows less similarity

between the lake and tributary samples. This location is constrained by impacts from longshore eastward currents in the western basin of Lake Erie during late fall, where receiving waters from Mill Creek flow away from the lake sampling site. In this context, the microbial functional characterizations show less correlation to each other than the other pairwise comparisons. For KV-Fall, cDNAs inferred AA sequences showing similarities with proteins involved in legionellosis and *V. cholerae* pathogenic cycle pathways both display upregulation in the lake, while *V. cholerae* infection, tuberculosis and pathogenic *E. coli* infection pathways show higher expression in the tributary compared to the lake.

Overall, legionellosis showed the highest expression for bacterial infectious disease pathways (Figure 4.6), yet it is the expression of a single transcript (*sdhA*; 10.03 – 11.76 logCPM) responsible for this representation (Figure 4.7). It should be noted, again, that expression of just a single transcript within a pathway should be cautiously considered, especially if that transcript has been documented to function in multiple pathways. SdhA, for example, also has a role in several metabolism pathways, such as the citrate cycle (TCA), and without additional validation approaches, it cannot be confirmed that this functional feature is correctly annotated to this pathogenic pathway. However, we present our results as an attempt to draw attention to these kinds of studies and as a call for further research into the active microbial community associated with sediment in aquatic systems. *Legionella spp.* are waterborne pathogens that are responsible for legionellosis, such as Legionnaires' disease, of which many cases are sporadic and unexplained events (van Heijnsbergen et al., 2014). For survival and successful replication in the host cell, these pathogens require a specialized *Legionella*-containing vacuole (LCV). The transcript *sdhA* encodes for a subunit of the succinate dehydrogenase flavoprotein [EC:1.3.99.1], and has been reported an essential substrate to maintain LCV integrity; without SdhA, the LCV is disrupted and there is rapid host cell death and degradation of the bacteria (Creasey and Isberg, 2012). *Legionella* has been well-documented in freshwater systems, including both the water and sediment compartments (Li et al., 2016; Mohiuddin et al., 2019). This study, however, is the first

to report expression of transcripts directly related to the viability of these pathogens from the suspended fraction of the sediment compartment in freshwater tributaries and littoral regions. Conversely, a recent study (also conducted in WEC) by Shahraki et al. (2019) reported no detection of select *L. pneumophila* virulence genes in beach sand or nearshore lake water. However, our research identified the functional active genes within the bacterial community by isolating mRNA extracted from the TSS in the water column, while the study by Shahraki and colleagues focused on the DNA fraction of the planktonic community. These differences may suggest that *L. pneumophila* are not free-living bacteria in freshwater. Growing research on these pathogens in the natural environment are building on the concern for human health implications, especially considering climate change (Walker, 2018).

The representation of *V. cholerae* in our TSS samples is highlighted by several expressed transcripts involved in both the pathogenic cycle and infection of these waterborne pathogens (Figure 4.7). Based on the expression of 14 transcripts related to these pathways, it is difficult to determine whether they are more expressed in the tributaries or the lakes since similarities exist. For example, BR-Summer, BR-Fall, and KV-Summer, show that some transcripts (1-2) are upregulated in the tributary while one (*rpoS*) was consistently upregulated in the lake (Figure C-4). KV-Fall, on the other hand, showed differential expression ($p < 0.05$) of more transcripts, with five upregulated in the lake compared to only two upregulated in the tributary. Again, KV-Fall samples may not provide reliable pairwise comparisons if the lake hydrology and current flow from Mill Creek tends to move eastward away from the lake sampling site. Regardless, several *V. cholerae* pathogenic-related transcripts are being expressed in all SS samples, emphasizing a potential vector of concern for recreational water use. *V. cholerae* has previously been reported in natural freshwater systems. In fact, freshwater systems are considered to be an environmental reservoir for the pathogenic bacteria (Islam et al., 2020; Shapiro et al., 1999). Several environmental reservoirs of *V. cholerae* have been identified in aquatic systems, including some freshwater fish species, and it is believed that these fish may play a role in the global distribution

of the pathogen (Halpern and Izhaki, 2017). Further, a study by Vital et al. (2007) showed that a toxigenic strain of *V. cholerae* (O1) was able to grow extensively in different kinds of freshwater. Additionally, a recent study by Daboul et al. (2020) described the detection of *V. cholerae* isolates from the Maumee River (which discharges into Lake Erie) and the shore of Lake Erie, supporting our findings of the expression of these related transcripts.

Other bacterial infectious disease pathways that showed notable expression of related transcripts in our samples included epithelial cell signaling in *H. pylori* infection [ko05120], *Salmonella* infection [ko05132], tuberculosis [ko05152], pathogenic *E. coli* infection [ko05130], *Staphylococcus aureus* infection [ko05150], and bacterial invasion of epithelial cells [ko05100]. Although detected, some degree of caution is warranted in the interpretation of these latter cases as the expression of only 1-2 transcripts may not be indicative of an abundant source, especially if these transcripts have been reported to function in other pathways. For example, only one transcript (NCL) involved in *E. coli* infection showed expression in our samples, which is a cell surface receptor of the infected eukaryotic host cell (Sinclair and O'Brien, 2002). Therefore, this information may not explicitly indicate there is active pathogenic *E. coli* in these samples. This is interesting, however, since *E. coli* detection in water is considered the gold standard approach for determining water quality in recreational areas, yet we did not identify enough expression of related transcripts to confirm these pathogens are active or pose potential health risks in our samples. Nonetheless, RNA-seq analysis showed expression of six transcripts encoding AA sequences similar to proteins involved in *H. pylori* infection, five involved in tuberculosis, and three involved in *S. aureus* infection. This information suggests that these infectious diseases may warrant further research within freshwater systems, especially since we know the aetiological agents responsible can survive and be transmitted through contaminated aqueous environments (Boehnke, 2017; Oliver, 2010; Pandey et al., 2014).

4.3.5 Bed sediment comparison

SS in natural aquatic systems are the physical building blocks of the bed sediment (Droppo, 2009), and therefore it is important to understand how both bed and TSS fractions contribute to pathogenic contamination and possible resuspension when considering these areas for recreational water use. VanMensel et al. (2020) and Chapter 3 showed the prevalence of expression of pathogenic-related activity recovered from the bed sediment at the same BR and KV public beaches observed in the current study. These results, along with our SS findings shown here, can be correlated. It is interesting the similarities and consistency considering samples were collected on different days for the summer collection of bed and suspended sediments, as well as seasonally for TSS. This is especially true for the observed metabolic activity related to N cycling which was consistent from season to season if not year to year.

Of particular interest for human health risks in these waters is the expression of transcripts with pathogenic relevance. Surprisingly, there is no obvious overlap of pathogenic-related transcript observances between the bed and SS. In the bed sediment, reported pathogenic-related transcripts encoded for *Salmonella* effector proteins (*pipB2*, *sppH2*), as well as four genes involved in pertussis (*hlyB/cyaB*, *fhaB*, *fhaC*, *fimD*). Other related transcripts were involved in nitric oxide detoxification and CAMP resistance. None of these transcripts showed expression in our SS samples (Figure 4.7). In fact, although we did observe expression of one transcript in the SS involved in *Salmonella* infection (*nrfA*), caution is advised as it is only one transcript that also functions in other pathways (i.e., DNRA) (Mohan et al., 2004). Furthermore, there was no indication of active pertussis in our SS samples.

It is important to consider several details for this comparison. First, although the RNA-seq approach was the same for each study, the samples were sequenced on different Illumina platforms, and the raw sequences were processed and statistically analyzed separately. This means direct comparisons should be approached with caution. Second, the sample collections

occurred on different days. The functional differences we see between the SS and bed may be a reflection of the dynamic nature of these aquatic systems (McPhedran et al., 2013; Shahraki et al., 2019), which further supports the need for more reliable assessment methods. And finally, hydrodynamic processes have been shown to influence grain size distribution and geochemical material composition (e.g., elements, nutrients) throughout the water column, contributing to variation with depth (Bouchez et al., 2011; Chalov et al., 2020; Lupker et al., 2011). Therefore, it is possible that hydrological processes may result in different transcriptomic signatures depending on the depth of sampling. Although, we believe the degree of variation with respect to depth is likely minimal when considering mixing effects from the flow of the tributaries and current in the lakes, especially since our study sites were all shallow. Future studies could address this knowledge gap on the variation of environmental transcriptomes with depth in aquatic systems.

4.4 Conclusions

Exposure to contaminated water is a global topic of concern and can result in serious economic and health implications. This study uses novel metatranscriptomic approaches to investigate the relevance of SS microbial populations on water quality in the littoral zone of freshwater lakes, and how it can ultimately affect human health with regards to recreational water use in these areas. Analyzing both suspended and bed sediment fractions allow for a much more comprehensive understanding of the water conditions and allows policymakers to make better informed decisions regarding beach status for recreational use. To our knowledge, this study is the first to investigate the expression of microbial transcripts associated with SS in freshwater systems within the context of pathogenic activity and the relation to human health risks.

Results show both adjacent tributary and beach SS have similar microbial functional signatures and are strongly correlated by site and season, suggesting these tributaries are

effectively influencing nearshore water quality in the lakes. Chemolithotrophic activity illustrated these correlations, and showed denitrification as the dominant N cycling pathway occurring in SS.

Overall, the expression of pathogenic-related transcripts was significantly greater ($p < 0.05$) in SS sampled from the lakes than from the adjacent tributaries. Likewise, expression was greater ($p < 0.05$) during the summer compared to fall.

Expression of transcripts showing similarities with nine bacterial infectious disease pathways were identified in the SS samples. The most highly expressed pathways belonged to legionellosis (i.e., *sdhA*, which is integral to the survival of the pathogen-containing vacuole), and several transcripts involved in *V. cholerae* pathogenic cycle and infection.

Pathogenic-related transcript expression data of SS did not strongly complement previously reported expression data of bed sediment from the same beaches. Although, pathogenic-related transcripts were identified in both sediment fractions, suggesting the sediment compartment has an important relationship with pathogen activity and should be considered when evaluating beach water for recreational use.

Our results support the perspective that SS in natural aquatic systems behaves as a strong transport vector for microbial contamination and pathogen transport to littoral zones and beaches of lakes, making this facet an important area for further research as it pertains to human health with regards to recreational water use. These findings highlight deficiencies in our understanding of pathogen potential in environmental systems, requiring further systematic studies on the role of microbial community expression of emerging pathogen biomarkers in natural aquatic environments.

Acknowledgements

The authors would like to thank Environment and Climate Change Canada for access to centrifuge equipment and field sampling support, as well as Christine Jaskot for analytical assistance. We also extend thanks to Nicolas Falk and Thomas Reid for their help with fieldwork as well. Special thanks to Courtney Spencer for map generation and Sharon Lackie (University of Windsor) with assistance and expertise on the SEM, and to Genome Quebec (McMaster University) for RNA-seq using their Illumina platform. Funding support for this project came from NSERC Strategic Partnerships Program entitled ‘Great Lakes Water Security: Microbial community characterization, source tracking, and remediation through meta-genomics’ REF341061127. We also extend thanks to the three reviewers for their constructive feedback, which helped us revise the manuscript.

Figures and Tables

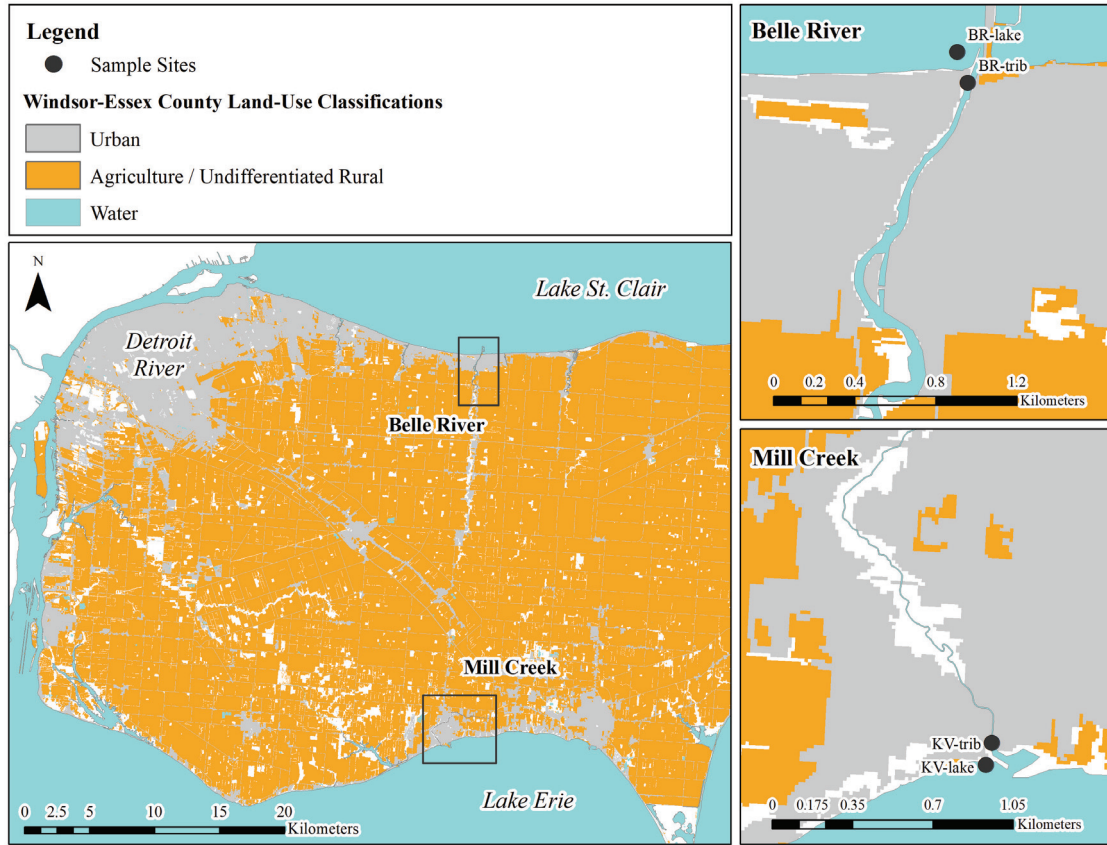


Figure 4.1: Map of WEC showing the two tributaries and beaches of interest for this paper. Insets illustrate a closer view of sampling areas, including sampling locations (BR-lake, BR-trib, KV-lake, KV-trib). Land use is distinguished by colour; grey = urban, orange = agriculture/undifferentiated rural, blue = water.

Data source: Southern Ontario Land Resource Information System (SOLRIS) 3.0 (geohub.lio.gov.on.ca).

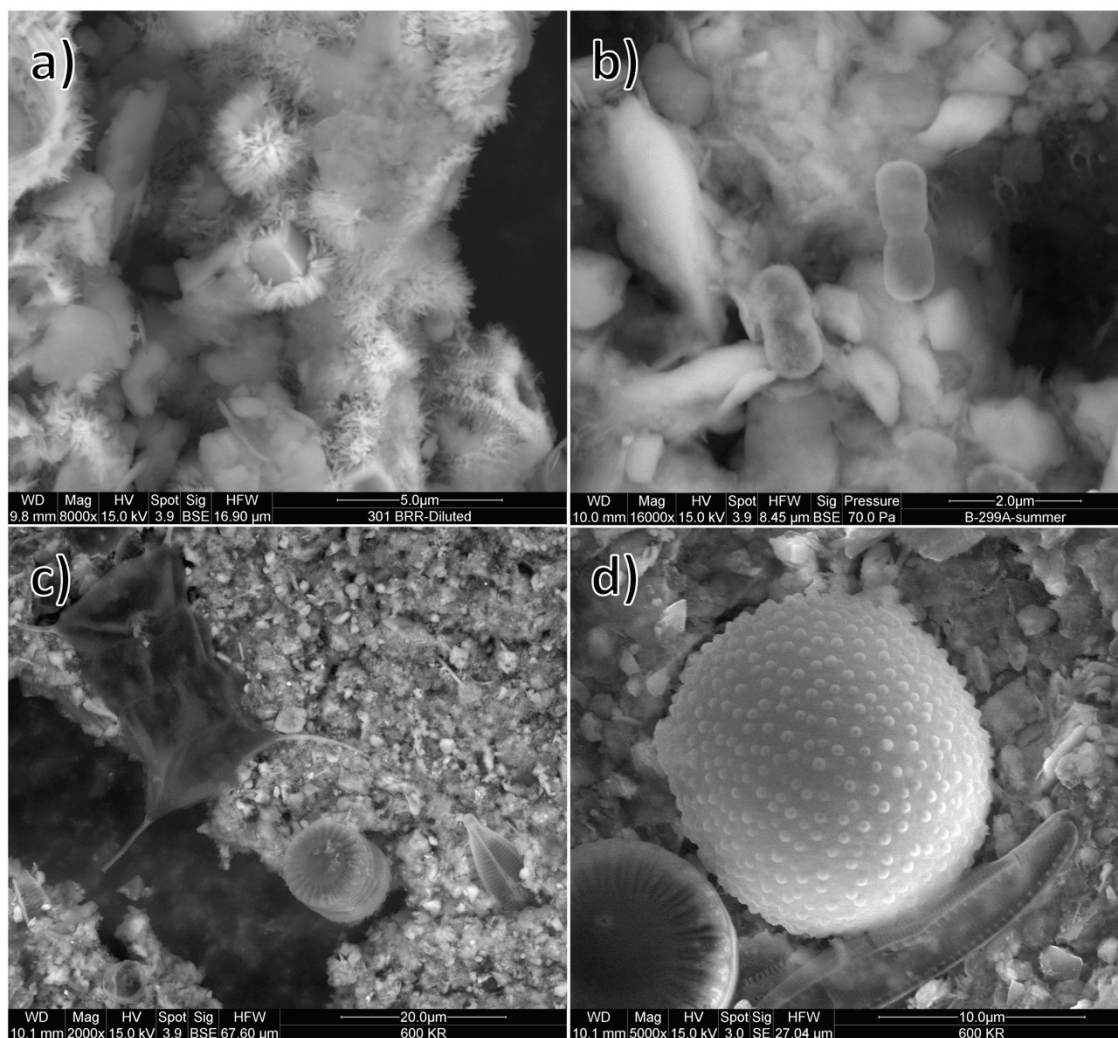


Figure 4.2: SEM images capturing various instances of biological activity within the SS fraction of the tributaries examined. In BR-trib, a) crystals indicative of biomineralization and b) dividing/replicating cells, and in KV-trib, c) a green alga (*Scenedesmus*) and d) an auxospore cell.

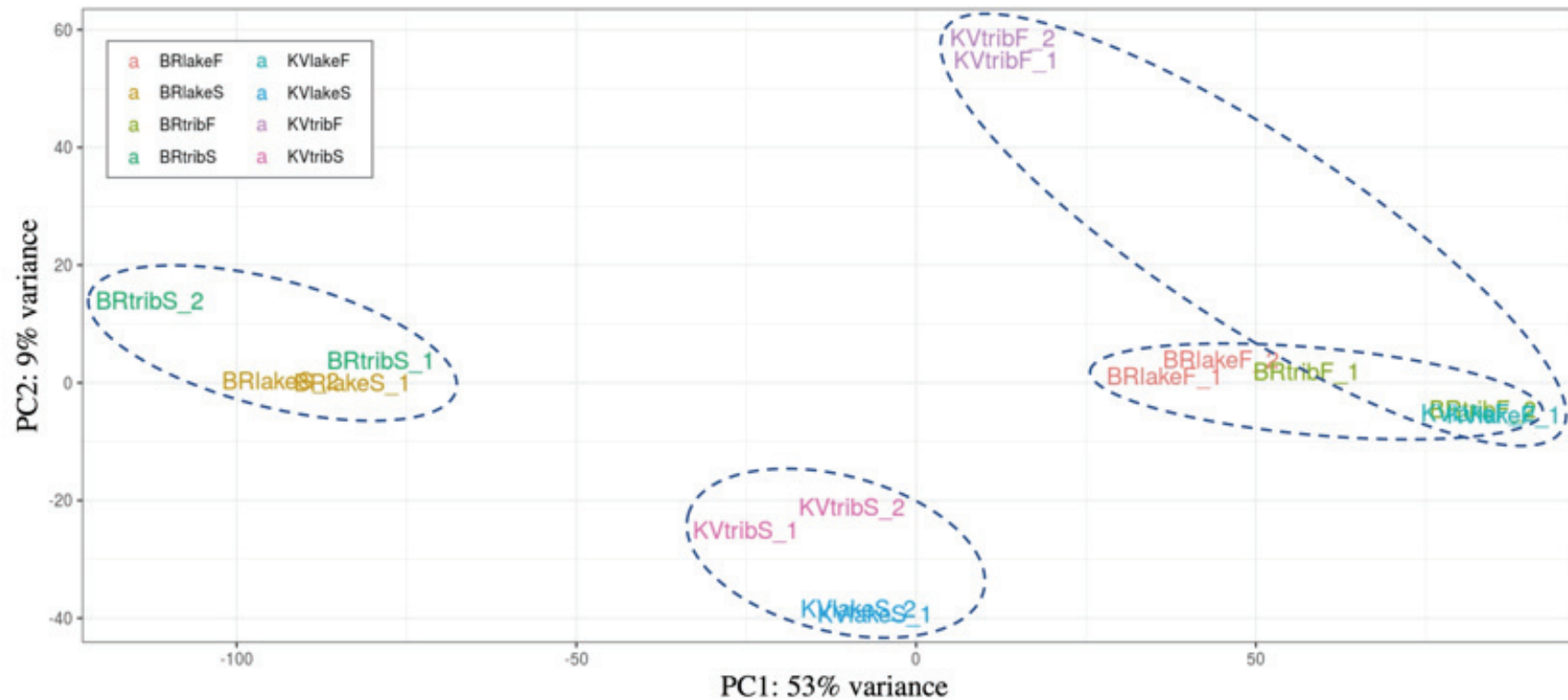


Figure 4.3: PCA of normalized metatranscriptomic data, using Euclidean distances between logCPM expression values. Functional similarity is illustrated between samples (beta-diversity) at Level 4 (gene transcript) resolution for all 8 groups (BR/KV-lake/trib-Summer/Fall). Groupings of samples from the same location (BR, KV) and season are encompassed by dotted blue ellipses. S = summer; F = fall; trib = tributary.

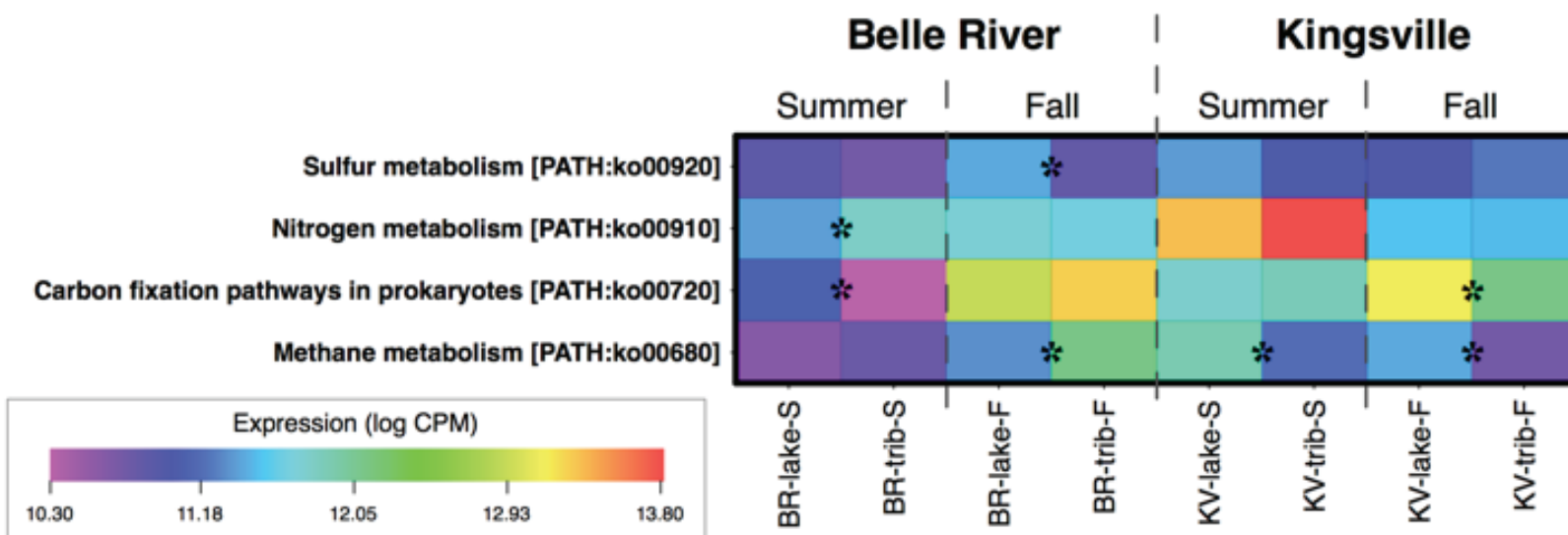


Figure 4.4: Gene expression heatmap of Level 3 pathways involved in Energy Metabolism (Level 2), utilizing KEGG annotations and KO database. Photosynthetic pathways have been filtered out to focus on chemolithotrophic activity (methane metabolism [ko00680]; carbon fixation pathways in prokaryotes [ko00720]; nitrogen metabolism [ko00910]; and sulfur metabolism [ko00920]). Expression represented as normalized logCPM values. Pairwise comparisons between sampling sites (lake, tributary) of the same location and season provide statistically significant differential expression ($p < 0.05$), denoted with an asterisk * where applicable.

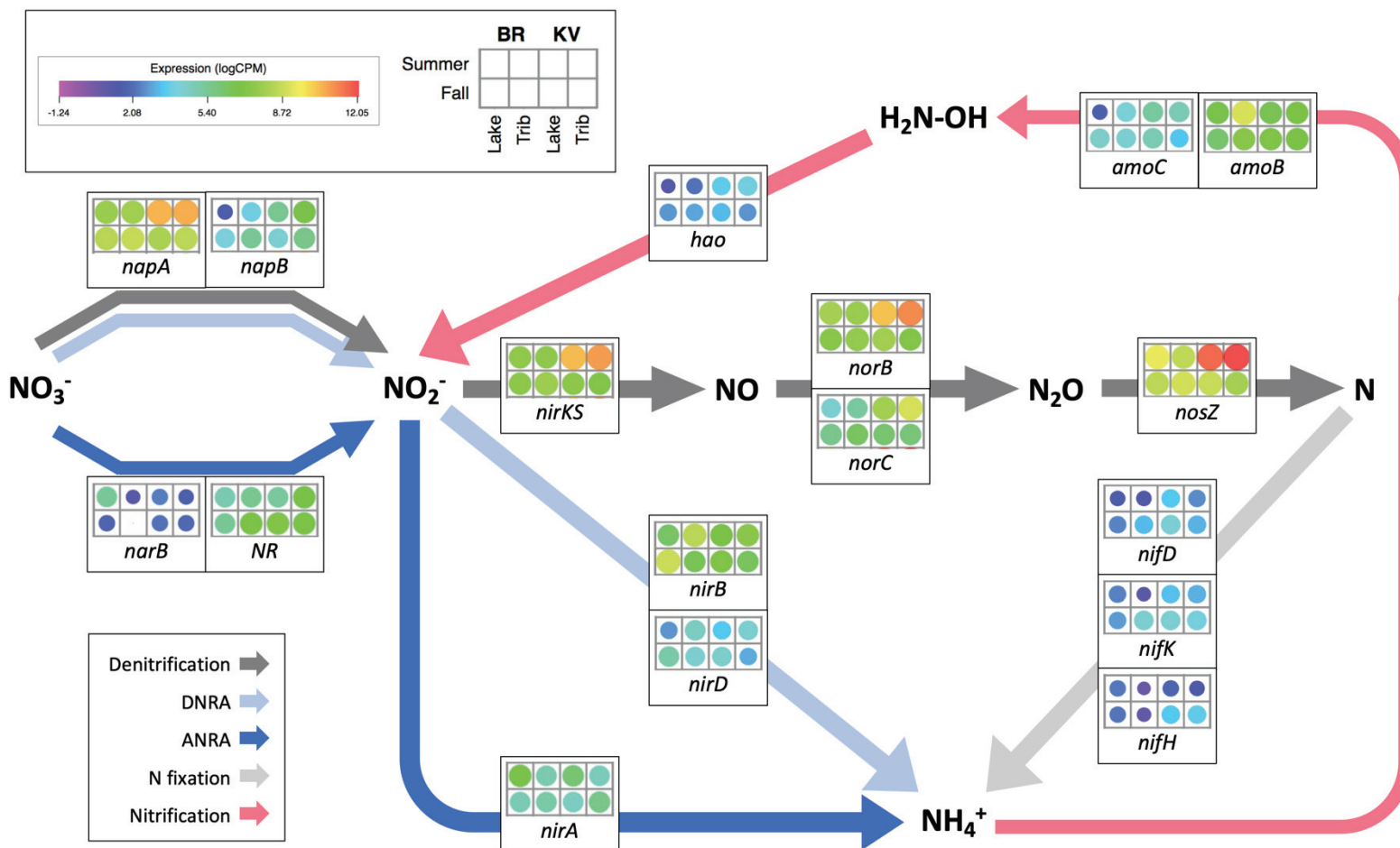


Figure 4.5: Expression of N metabolism transcripts involved in denitrification, DNRA, ANRA, nitrogen fixation and nitrification pathways detected in SS samples. Heatmap uses colour range and volume proportional size scaling to illustrate expression comparisons of all samples. Expression represented as normalized logCPM values. [Volume proportional to cell value – linear.]

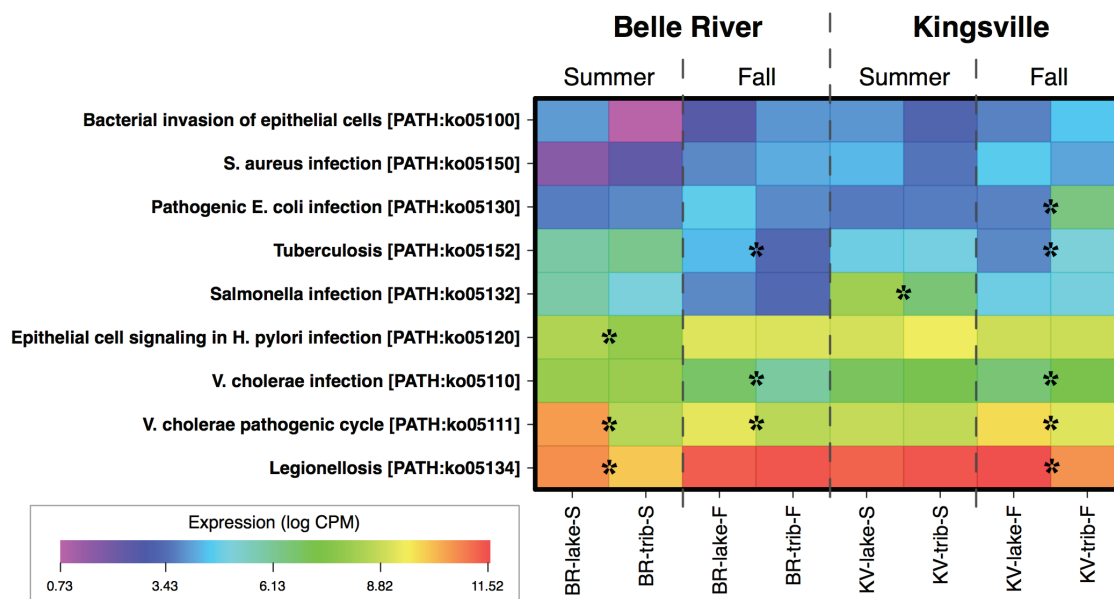


Figure 4.6: Gene expression heatmap of Level 3 transcripts involved in Infectious Diseases (Level 2), utilizing KEGG annotations and KO database. Viral and parasitic pathways are omitted to allow the focus on translated cDNAs showing similarities with genes involved in bacterial infectious diseases (legionellosis [ko05134]; *V. cholerae* pathogenic cycle [ko05111]; *V. cholerae* infection [ko05110]; epithelial cell signaling in *H. pylori* infection [ko05120]; *Salmonella* infection [ko05132]; tuberculosis [ko05152]; pathogenic *E. coli* infection [ko05130]; *S. aureus* infection [ko05150]; and bacterial invasion of epithelial cells [ko05100]). Expression represented as normalized logCPM values. Pairwise comparisons between sampling sites (lake, tributary) of the same location and season provide statistically significant differential expression ($p < 0.05$) denoted with an asterisk * where applicable.

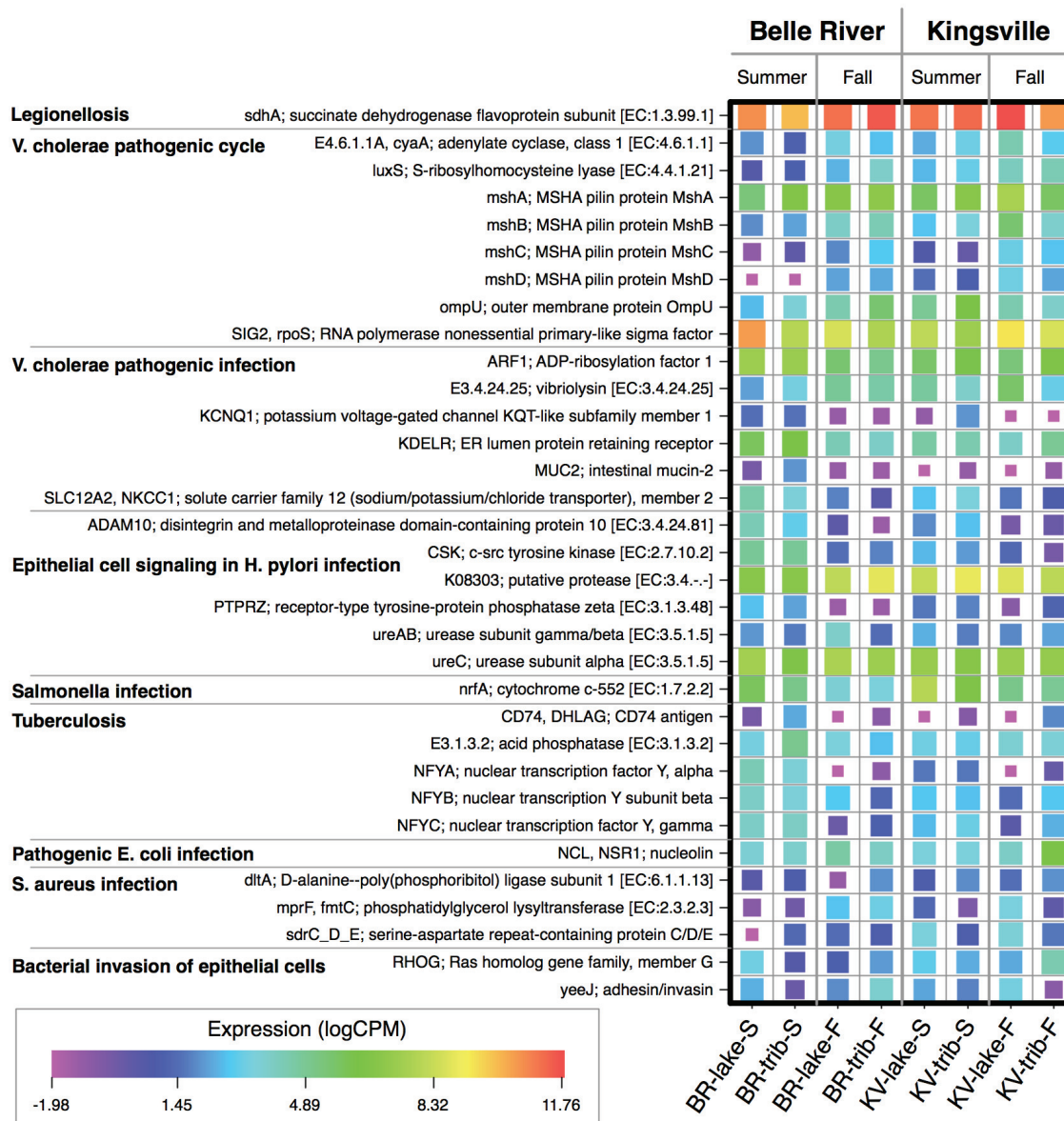


Figure 4.7: Gene expression of functional annotations assigned to translated transcripts showing similarities with proteins involved in bacterial pathways playing part in Infectious Diseases. Heatmap uses colour range and volume proportional size scaling to illustrate expression comparisons of all samples. Expression represented as normalized logCPM values. [Volume proportional to cell value – logarithmic.]

Table 4.1: Tabulated summary of expressed transcripts annotated to the KO database, Level 1 categories. Expression represented as normalized logCPM values (top) and raw read values (bottom), duplicates averaged. Pairwise comparisons between sampling sites (lake, tributary) of the same location and season provide statistically significant differential expression ($p < 0.05$), denoted with greater than (>) or less than (<) symbol and bolded and italicized, where applicable.

Expression	Belle River (BR)				Kingsville (KV)			
	Summer		Fall		Summer		Fall	
	Lake	Trib	Lake	Trib	Lake	Trib	Lake	Trib
Cellular Processes	16.45 (138,724)	16.45 (98,420)	16.14 (152,274)	16.21 (195,897)	<i>15.76</i> (100,213) < <i>16.00</i> (110,912)		16.21 (252,918)	16.18 (144,540)
Environmental Information Processing	16.38 (131,088)	16.25 (85,501)	<i>16.53</i> (200,080) < <i>16.86</i> (306,928)		<i>16.49</i> (167,267) < <i>16.67</i> (176,248)		<i>16.77</i> (373,232) > <i>16.41</i> (170,259)	
Genetic Information Processing	<i>18.19</i> (460,769) > <i>17.98</i> (285,528)		<i>18.38</i> (721,198) > <i>18.23</i> (793,209)		<i>18.18</i> (534,231) < <i>18.28</i> (540,760)		<i>18.51</i> (1,245,628) < <i>18.64</i> (797,406)	
Human Diseases	<i>15.73</i> (83,731) < <i>16.45</i> (98,128)		14.36 (44,151)	14.17 (47,810)	<i>14.47</i> (41,180) < <i>14.81</i> (48,697)		<i>13.85</i> (49,240) < <i>14.87</i> (58,288)	
Metabolism	<i>18.82</i> (710,252) < <i>18.92</i> (543,926)		18.77 (943,285)	18.82 (1,191,874)	<i>18.90</i> (883,153) > <i>18.77</i> (760,230)		<i>18.65</i> (1,369,174) > <i>18.53</i> (738,643)	
Organismal Systems	14.12 (27,303)	13.90 (17,082)	14.23 (40,628)	14.14 (46,452)	14.32 (36,826)	14.30 (34,194)	14.47 (75,767)	14.31 (39,696)

References

- Alm, E.W., Burke, J., Spain, A., 2003. Fecal indicator bacteria are abundant in wet sand at freshwater beaches. *Water Res.* 37, 3978–3982. [https://doi.org/10.1016/S0043-1354\(03\)00301-4](https://doi.org/10.1016/S0043-1354(03)00301-4)
- Amon, J., Titgemeyer, F., Burkovski, A., 2010. Common patterns - unique features: nitrogen metabolism and regulation in Gram-positive bacteria. *FEMS Microbiol. Rev.* 34, 588–605. <https://doi.org/10.1111/j.1574-6976.2010.00216.x>
- Bocaniov, S.A., Scavia, D., 2018. Nutrient Loss Rates in Relation to Transport Time Scales in a Large Shallow Lake (Lake St. Clair, USA—Canada): Insights From a Three-Dimensional Model. *Water Resour. Res.* 54, 3825–3840. <https://doi.org/10.1029/2017WR021876>
- Boehnke, K.F., 2017. Risk of Infection from Exposure to Waterborne *Helicobacter pylori*? PhD dissertation, University of Michigan, Michigan, USA.
- Bouchez, J., Gaillardet, J., France-Lanord, C., Maurice, L., Dutra-Maia, P., 2011. Grain size control of river suspended sediment geochemistry: Clues from Amazon River depth profiles. *Geochemistry, Geophys. Geosystems* 12, 1–24. <https://doi.org/10.1029/2010GC003380>
- Bourgon, R., Gentleman, R., Huber, W., 2010. Independent filtering increases detection power for high-throughput experiments. *Proc. Natl. Acad. Sci. U. S. A.* 107, 9546–9551. <https://doi.org/10.1073/pnas.0914005107>
- Bradford, S.A., Morales, V.L., Zhang, W., Harvey, R.W., Packman, A.I., Mohanram, A., Welty, C., 2013. Transport and fate of microbial pathogens in agricultural settings. *Crit. Rev. Environ. Sci. Technol.* 43, 775–893. <https://doi.org/10.1080/10643389.2012.710449>
- Byappanahalli, M.N., Nevers, M.B., Whitman, R.L., Ge, Z., Shively, D., Spoljaric, A., Przybyla-Kelly, K., 2015. Wildlife, urban inputs, and landscape configuration are responsible for degraded swimming water quality at an embayed beach. *J. Great Lakes Res.* 41, 156–163. <https://doi.org/10.1016/j.jglr.2014.11.027>
- Chalov, S., Moreido, V., Sharapova, E., Efimova, L., Efimov, V., Lychagin, M., Kasimov, N., 2020. Hydrodynamic controls of particulate metals partitioning along the lower selenga river-main tributary of the Lake Baikal. *Water (Switzerland)* 12. <https://doi.org/10.3390/W12051345>
- Chen, Y., McCarthy, D., Ritchie, M., Robinson, M., Smyth, G., Hall, E., 2020. edgeR: differential analysis of sequence read count data User's Guide. *R Packag.* 1–121.
- Chubukov, V., Gerosa, L., Kochanowski, K., Sauer, U., 2014. Coordination of microbial

- metabolism. *Nat. Rev. Microbiol.* 12, 327–340. <https://doi.org/10.1038/nrmicro3238>
- Costerton, J.W., Cheng, K.J., Geesey, G.G., Ladd, T.I., Nickel, J.C., Dasgupta, M., Marrie, T.J., 1987. Bacterial Biofilms in Nature and Disease. *Ann. Rev. Microbiol.* 41, 435–464. <https://doi.org/10.1146/annurev.mi.41.100187.002251>
- Creasey, E.A., Isberg, R.R., 2012. The protein SdhA maintains the integrity of the *Legionella*-containing vacuole. *Proc. Natl. Acad. Sci. U. S. A.* 109, 3481–3486. <https://doi.org/10.1073/pnas.1121286109>
- Daboul, J., Weghorst, L., DeAngelis, C., Plecha, S.C., Saul-McBeth, J., Matson, J.S., 2020. Characterization of *Vibrio cholerae* isolates from freshwater sources in northwest Ohio. *PLoS One* 15, 1–12. <https://doi.org/10.1371/journal.pone.0238438>
- DeFlorio-Barker, S., Wing, C., Jones, R.M., Dorevitch, S., 2018. Estimate of incidence and cost of recreational waterborne illness on United States surface waters. *Environ. Heal. A Glob. Access Sci. Source* 17, 1–10. <https://doi.org/10.1186/s12940-017-0347-9>
- DiCarlo, A.M., Weisener, C.G., Drouillard, K.G., 2020. Evidence for Microbial Community Effect on Sediment Equilibrium Phosphorus Concentration (EPC0). *Bull. Environ. Contam. Toxicol.* 105, 736–741. <https://doi.org/10.1007/s00128-020-03019-0>
- Droppo, I.G., 2009. Biofilm structure and bed stability of five contrasting freshwater sediments. *Mar. Freshw. Res.* 60, 690–699.
- Droppo, I.G., 2001. Rethinking what constitutes suspended sediment. *Hydrol. Process.* 15, 1551–1564. <https://doi.org/10.1002/hyp.228>
- Droppo, I.G., Leppard, G., Flannigan, D., Liss, S., 1997. The Freshwater Floc - A functional relationship of water and organic and inorganic floc constituents affecting suspended sediment properties. *Water, Air Soil Pollut.* 99, 43–54.
- Droppo, I.G., Liss, S.N., Williams, D., Nelson, T., Jaskot, C., Trapp, B., 2009. Dynamic existence of waterborne pathogens within river sediment compartments. Implications for water quality regulatory affairs. *Environ. Sci. Technol.* 43, 1737–1743. <https://doi.org/10.1021/es802321w>
- Dworkin, M., 2012. Sergei Winogradsky: A founder of modern microbiology and the first microbial ecologist. *FEMS Microbiol. Rev.* 36, 364–379. <https://doi.org/10.1111/j.1574-6976.2011.00299.x>
- Elliott, A.V.C., Plach, J.M., Droppo, I.G., Warren, L.A., 2014. Collaborative microbial Fe-redox cycling by pelagic floc bacteria across wide ranging oxygenated aquatic systems. *Chem. Geol.* 366, 90–102.
- Faivre, D., Godec, T.U., 2015. From bacteria to mollusks: The principles underlying the

- biomineralization of iron oxide materials. *Angew. Chemie - Int. Ed.* 54, 4728–4747.
<https://doi.org/10.1002/anie.201408900>
- Falk, N., Reid, T., Skoyles, A., Grgicak-Mannion, A., Drouillard, K., Weisener, C.G., 2019. Microbial metatranscriptomic investigations across contaminant gradients of the Detroit River. *Sci. Total Environ.* 690, 121–131. <https://doi.org/10.1016/j.scitotenv.2019.06.451>
- Federigi, I., Verani, M., Donzelli, G., Cioni, L., Carducci, A., 2019. The application of quantitative microbial risk assessment to natural recreational waters: A review. *Mar. Pollut. Bull.* 144, 334–350. <https://doi.org/10.1016/j.marpolbul.2019.04.073>
- Gerba, C.P., McLeod, J.S., 1976. Effects of sediments on the survival of *Escherichia coli* in marine waters. *Appl. Environ. Microbiol.* 32, 114–120.
<https://doi.org/10.1128/aem.32.1.114-120.1976>
- Halpern, M., Izhaki, I., 2017. Fish as hosts of *Vibrio cholerae*. *Front. Microbiol.* 8, 1–7.
<https://doi.org/10.3389/fmicb.2017.00282>
- Ishaq, A.G., Matias-Peralta, H.M., Basri, H., 2016. Bioactive Compounds from Green Microalga *Scenedesmus* and its Potential Applications: A Brief Review. *Pertanika J. Trop. Agric. Sci.* 39, 1–16.
- Islam, M. Sirajul, Zaman, M.H., Islam, M. Shafiqul, Ahmed, N., Clemens, J.D., 2020. Environmental reservoirs of *Vibrio cholerae*. *Vaccine* 38, A52–A62.
<https://doi.org/10.1016/j.vaccine.2019.06.033>
- Kaczmarek, I., Ehrman, J.M., 2021. Enlarge or die! An auxospore perspective on diatom diversification. *Org. Divers. Evol.* <https://doi.org/10.1007/s13127-020-00476-7>
- Kaczmarek, I., Ehrman, J.M., 2015. Auxosporulation in *Paralia* *Guyana* *macgillivrayi* (bacillariophyta) and possible new insights into the habit of the earliest diatoms. *PLoS One* 10, 1–27. <https://doi.org/10.1371/journal.pone.0141150>
- Kellerman, A.M., Dittmar, T., Kothawala, D.N., Tranvik, L.J., 2014. Chemodiversity of dissolved organic matter in lakes driven by climate and hydrology. *Nat. Commun.* 5, 1–8.
<https://doi.org/10.1038/ncomms4804>
- Kelly, D.P., 1981. Introduction to the Chemolithotrophic Bacteria. *The Prokaryotes* 997–1004.
https://doi.org/10.1007/978-3-662-13187-9_79
- Konhauser, K.O., 1997. Bacterial iron biomineralisation in nature. *FEMS Microbiol. Rev.* 20, 315–326. [https://doi.org/10.1016/S0168-6445\(97\)00014-4](https://doi.org/10.1016/S0168-6445(97)00014-4)
- Levy, K., Woster, A.P., Goldstein, R.S., Carlton, E.J., 2016. Untangling the Impacts of Climate Change on Waterborne Diseases: A Systematic Review of Relationships between Diarrheal Diseases and Temperature, Rainfall, Flooding, and Drought. *Environ. Sci. Technol.* 50,

- 4905–4922. <https://doi.org/10.1021/acs.est.5b06186>
- Li, X., Harwood, V.J., Nayak, B., Weidhaas, J., 2016. Ultrafiltration and Microarray Detect Microbial Source Tracking Marker and Pathogen Genes in Riverine and Marine Systems. *Appl. Environ. Microbiol.* 82, 1625–1635. <https://doi.org/10.1128/aem.02583-15>
- Liss, S.N., Microbial flocs suspended biofilms. In: *The Encyclopaedia of Environmental Microbiology*, Vol. 4, G. Bitton, Ed., Wiley-Interscience, New York, 2002, pp. 2000-2012. ISBN: 978-0-471-35450-5
- Lupker, M., France-Lanord, C., Lavé, J., Bouchez, J., Galy, V., Métivier, F., Gaillardet, J., Lartiges, B., Mugnier, J.L., 2011. A Rouse-based method to integrate the chemical composition of river sediments: Application to the Ganga basin. *J. Geophys. Res. Earth Surf.* 116, 1–24. <https://doi.org/10.1029/2010JF001947>
- Madani, M., Seth, R., Leon, L.F., Valipour, R., McCrimmon, C., 2020. Three dimensional modelling to assess contributions of major tributaries to fecal microbial pollution of lake St. Clair and Sandpoint Beach. *J. Great Lakes Res.* 46, 159–179. <https://doi.org/10.1016/j.jglr.2019.12.005>
- Maguire, T.J., Wellen, C., Stammler, K.L., Mundle, S.O.C., 2018. Increased nutrient concentrations in Lake Erie tributaries influenced by greenhouse agriculture. *Sci. Total Environ.* 633, 433–440. <https://doi.org/10.1016/j.scitotenv.2018.04.374>
- McPhedran, K., Seth, R., Bejankiwar, R., 2013. Occurrence and predictive correlations of *Escherichia coli* and *Enterococci* at Sandpoint beach (Lake St Clair), Windsor, Ontario and holiday beach (Lake Erie), Amherstburg, Ontario. *Water Qual. Res. J. Canada* 48, 99–110. <https://doi.org/10.2166/wqrjc.2013.132>
- Meyer, F., Paarmann, D., D’Souza, M., Olson, R., Glass, E.M., Kubal, M., Paczian, T., Rodriguez, A., Stevens, R., Wilke, A., Wilkening, J., Edwards, R.A., 2008. The metagenomics RAST server - A public resource for the automatic phylogenetic and functional analysis of metagenomes. *BMC Bioinformatics* 9, 1–8. <https://doi.org/10.1186/1471-2105-9-386>
- Mohan, S.B., Schmid, M., Jetten, M., Cole, J., 2004. Detection and widespread distribution of the *nrfA* gene encoding nitrite reduction to ammonia, a short circuit in the biological nitrogen cycle that competes with denitrification 49, 433–443. <https://doi.org/10.1016/j.femsec.2004.04.012>
- Mohiuddin, M.M., Botts, S.R., Paschos, A., Schellhorn, H.E., 2019. Temporal and spatial changes in bacterial diversity in mixed use watersheds of the Great Lakes region. *J. Great Lakes Res.* 45, 109–118. <https://doi.org/10.1016/j.jglr.2018.10.007>

- Mohiuddin, M.M., Salama, Y., Schellhorn, H.E., Golding, G.B., 2017. Shotgun metagenomic sequencing reveals freshwater beach sands as reservoir of bacterial pathogens. *Water Res.* 115, 360–369. <https://doi.org/10.1016/j.watres.2017.02.057>
- Msanne, J., Polle, J., Starkenburg, S., 2020. An assessment of heterotrophy and mixotrophy in *Scenedesmus* and its utilization in wastewater treatment. *Algal Res.* 48, 101911. <https://doi.org/10.1016/j.algal.2020.101911>
- Müller, B., Lotter, A.F., Sturm, M., Ammann, A., 1998. Influence of catchment quality and altitude on the water and sediment composition of 68 small lakes in Central Europe. *Aquat. Sci.* 60, 316–337. <https://doi.org/10.1007/s000270050044>
- Nelson, C.E., 2009. Phenology of high-elevation pelagic bacteria: The roles of meteorologic variability, catchment inputs and thermal stratification in structuring communities. *ISME J.* 3, 13–30. <https://doi.org/10.1038/ismej.2008.81>
- Nelson, J.W., Sklenar, J., Barnes, A.P., Minnier, J., 2017. The START App: A web-based RNAseq analysis and visualization resource. *Bioinformatics* 33, 447–449. <https://doi.org/10.1093/bioinformatics/btw624>
- Niu, Q., Xia, M., Rutherford, E.S., Mason, D.M., Anderson, E.J., Schwab, D.J., 2015. Investigation of interbasin exchange and interannual variability in Lake Erie using an unstructured-grid hydrodynamic model. *J. Geophys. Res. Ocean.* 120, 2212–2232. <https://doi.org/10.1002/2014JC010457>. Received
- Oliver, J.D., 2010. Recent findings on the viable but nonculturable state in pathogenic bacteria. *FEMS Microbiol. Rev.* 34, 415–425. <https://doi.org/10.1111/j.1574-6976.2009.00200.x>
- Paerl, H.W., Xu, H., McCarthy, M.J., Zhu, G., Qin, B., Li, Y., Gardner, W.S., 2011. Controlling harmful cyanobacterial blooms in a hyper-eutrophic lake (Lake Taihu, China): The need for a dual nutrient (N & P) management strategy. *Water Res.* 45, 1973–1983. <https://doi.org/10.1016/j.watres.2010.09.018>
- Pandey, P.K., Kass, P.H., Soupir, M.L., Biswas, S., Singh, V.P., 2014. Contamination of water resources by pathogenic bacteria. *AMB Express* 4, 1–16. <https://doi.org/10.1186/s13568-014-0051-x>
- Reid, T., Droppo, I.G., Weisener, C.G., 2020. Tracking functional bacterial biomarkers in response to a gradient of contaminant exposure within a river continuum. *Water Res.* 168, 115167. <https://doi.org/10.1016/j.watres.2019.115167>
- Rissanen, A.J., Kurhela, E., Aho, T., Oittinen, T., Tirola, M., 2010. Storage of environmental samples for guaranteeing nucleic acid yields for molecular microbiological studies. *Appl. Microbiol. Biotechnol.* 88, 977–984. <https://doi.org/10.1007/s00253-010-2838-2>

- Robinson, M.D., McCarthy, D.J., Smyth, G.K., 2010. edgeR: A Bioconductor package for differential expression analysis of digital gene expression data. *Bioinformatics* 26, 139–140. <https://doi.org/10.1093/bioinformatics/btp616>
- Rodrigues, C., Cunha, M.Â., 2017. Assessment of the microbiological quality of recreational waters: indicators and methods. *Euro-Mediterranean J. Environ. Integr.* 2. <https://doi.org/10.1007/s41207-017-0035-8>
- Rundell, E.A., Banta, L.M., Ward, D. V., Watts, C.D., Birren, B., Esteban, D.J., 2014. 16S rRNA Gene Survey of Microbial Communities in Winogradsky Columns. *PLoS One* 9. <https://doi.org/10.1371/journal.pone.0104134>
- Schindler, D.W., Carpenter, S.R., Chapra, S.C., Hecky, R.E., Orihel, D.M., 2016. Reducing phosphorus to curb lake eutrophication is a success. *Environ. Sci. Technol.* 50, 8923–8929. <https://doi.org/10.1021/acs.est.6b02204>
- Shahraki, A.H., Chaganti, S.R., Heath, D., 2019. Assessing high-throughput environmental DNA extraction methods for meta-barcode characterization of aquatic microbial communities. *J. Water Health* 17, 37–49. <https://doi.org/10.2166/wh.2018.108>
- Shapiro, R.L., Otieno, M.R., Adcock, P.M., Phillips-Howard, P.A., Hawley, W.A., Kumar, L., Waiyaki, P., Nahlen, B.L., Slutsker, L., Mintz, E., Hutwagner, L., Ouma, C., Onyango, M., Alaii, J., Yongo, W., Okullo, J., Okech, R., Oluoch, N., Oginga, T., Akuku, J.A., Wanga, R., Ochieng, J.B., Odhiambo, S.A., Orure, J., Molge, H., Ondieki, T.N., Agwanda, M.O., Shoute, E., Ochola, G., Otieno, J., Obel, J., 1999. Transmission of epidemic *Vibrio cholerae* O1 in rural western Kenya associated with drinking water from Lake Victoria: An environmental reservoir for cholera? *Am. J. Trop. Med. Hyg.* 60, 271–276. <https://doi.org/10.4269/ajtmh.1999.60.271>
- Sinclair, J.F., O'Brien, A.D., 2002. Cell surface-localized nucleolin is a eukaryotic receptor for the adhesin intimin- γ of enterohemorrhagic *Escherichia coli* O157:H7. *J. Biol. Chem.* 277, 2876–2885. <https://doi.org/10.1074/jbc.M110230200>
- Sousa, A.J., Droppo, I.G., Liss, S.N., Warren, L., Wolfaardt, G., 2015. Influence of wave action on the partitioning and transport of unattached and floc-associated bacteria in fresh water. *Can. J. Microbiol.* 61, 584–596.
- Tong, Y., Qiao, Z., Wang, X., Liu, X., Chen, G., Zhang, W., Dong, X., Yan, Z., Han, W., Wang, R., Wang, M., Lin, Y., 2018. Human activities altered water N:P ratios in the populated regions of China. *Chemosphere* 210, 1070–1081. <https://doi.org/10.1016/j.chemosphere.2018.07.108>
- Tong, Y., Wang, M., Peñuelas, J., Liu, X., Paerl, H.W., Elser, J.J., Sardans, J., Couture, R.M.,

- Larssen, T., Hu, H., Dong, X., He, W., Zhang, W., Wang, X., Zhang, Y., Liu, Y., Zeng, S., Kong, X., Janssen, A.B.G., Lin, Y., 2020. Improvement in municipal wastewater treatment alters lake nitrogen to phosphorus ratios in populated regions. *Proc. Natl. Acad. Sci. U. S. A.* 117, 1–7. <https://doi.org/10.1073/pnas.1920759117>
- van Heijnsbergen, E., de Roda Husman, A.M., Lodder, W.J., Bouwknecht, M., Docters van Leeuwen, A.E., Bruin, J.P., Euser, S.M., den Boer, J.W., Schalk, J.A.C., 2014. Viable *Legionella pneumophila* bacteria in natural soil and rainwater puddles. *J. Appl. Microbiol.* 117, 882–890. <https://doi.org/10.1111/jam.12559>
- VanMensel, D., Chaganti, S.R., Droppo, I.G., Weisener, C.G., 2020. Exploring bacterial pathogen community dynamics in freshwater beach sediments: A tale of two lakes. *Environ. Microbiol.* 22, 568–583. <https://doi.org/10.1111/1462-2920.14860>
- Vital, M., Füsclin, H.P., Hammes, F., Egli, T., 2007. Growth of *Vibrio cholerae* O1 Ogawa Eltor in freshwater. *Microbiology* 153, 1993–2001. <https://doi.org/10.1099/mic.0.2006/005173-0>
- Walker, J.T., 2018. The influence of climate change on waterborne disease and *Legionella*: a review. *Perspect. Public Health* 138, 282–286. <https://doi.org/10.1177/1757913918791198>
- Wotton, R.S., 2007. Do benthic biologists pay enough attention to aggregates formed in the water column of streams and rivers? *J. North Am. Benthol. Soc.* 26, 1–11. [https://doi.org/10.1899/0887-3593\(2007\)26\[1:DBBPEA\]2.0.CO;2](https://doi.org/10.1899/0887-3593(2007)26[1:DBBPEA]2.0.CO;2)
- Wu, J., Rees, P., Storrer, S., Alderisio, K., Dorner, S., 2009. Fate and transport modeling of potential pathogens: The contribution from sediments. *J. Am. Water Resour. Assoc.* 45, 35–44. <https://doi.org/10.1111/j.1752-1688.2008.00287.x>
- Xia, X., Zhang, S., Li, S., Zhang, Liwei, Wang, G., Zhang, Ling, Wang, J., Li, Z., 2018. The cycle of nitrogen in river systems: Sources, transformation, and flux. *Environ. Sci. Process. Impacts* 20, 863–891. <https://doi.org/10.1039/c8em00042e>

CHAPTER 5: MICROBE-SEDIMENT INTERACTIONS IN GREAT LAKES
RECREATIONAL WATERS: IMPLICATIONS FOR HUMAN HEALTH RISK

CHAPTER 5: MICROBE-SEDIMENT INTERACTIONS IN GREAT LAKES RECREATIONAL WATERS: IMPLICATIONS FOR HUMAN HEALTH RISKS

5.0 Prologue

The research presented in Chapters 2, 3, and 4 provide valuable and detailed insights into the microbial communities associated with freshwater sediment, with a focus on metabolic activities and pathogenic-related gene expression. While Chapter 3 focused on the bed sediment and Chapter 4 focused on the suspended sediment, the research described in this Chapter 5 combines the two perspectives in a proof-of-concept novel approach to studying these types of natural systems with targeted nanofluidic multiplex qPCR. Emphasis is on the active microbes (i.e., RNA) targeting FIB, MST, and bacterial pathogens/virulence genes to demonstrate an improved approach for recreational water quality assessments that is faster than traditional methods with the prospect for greater optimization (i.e., multiple specific gene sequences can be simultaneously targeted to suit individual research objectives).

5.1 Introduction

Local, regional, and global pathogen contamination of water resources is in a continual state of flux, depending largely on anthropogenic activities. For example, land-use dynamics, such as expansion and/or contraction of urban (Ting et al., 2021), industrial (Bouchali et al., 2022), agricultural (Susi and Laine, 2021), and forestry (Wang et al., 2021) areas, increases/decreases in land, water, and atmospheric pollution, and climate change (Brandão et al., 2022) all contribute to (and influence the level of) microbial pollution in aquatic ecosystems.

Waterborne diseases have increased in prevalence around the world, which is directly linked to the proliferation of microbial pathogens within our environment (Levy et al., 2016).

One of the most socioeconomic and ecosystem/human health aspects of pathogen and microbial consortium changes is related to recreational water use. Typically, human health implications have been monitored through culturing techniques, targeting generic taxonomic groups such as FIB (e.g., *E. coli*, enterococci) from the water column (Rodrigues and Cunha, 2017). Although these approaches are not costly and have been followed for decades, they are time consuming and do not provide vital information such as source of contamination (e.g., human vs. avian) or if the organism is even pathogenic (i.e., strain-level resolution). Furthermore, these tests are infrequent (i.e., once a week during the swimming season) with small number of samples (Farrell et al., 2021), which is concerning because previous studies reported very high same-day variability of microbial concentrations in bathing waters, both spatially and temporally (McPhedran et al., 2013; Shahraki et al., 2021; Wyer et al., 2018). Besides, the microbial community associated with benthic sediments has been reported to harbour considerably higher bacterial concentrations than the overlying water (Droppo et al., 2009; Probandt et al., 2018), yet the sediment compartment is neglected in these traditional assessments due to challenges extracting sediment-associated nucleic acids (especially unstable RNA; Wood et al., 2019) and the lack of clear and consistent methodology (e.g., sampling, preservation, and extraction protocols) throughout the literature (Pawlowski et al., 2022).

Quantitative real-time PCR (qPCR) is an evolving tool for simultaneous detection and quantification of multiple specific molecular targets on multiple samples (e.g., microfluidic, nanofluidic plates) (Friedrich et al., 2016; Morrison et al., 2006; Shahraki et al., 2019b). In the context of environmental studies, qPCR has become a leading method for MST of pathogenic contamination (e.g., *Bacteroides*, *E. coli*) in multiple environments and media (e.g., ground water, wastewater, rivers, lakes, and oceans) from multiple species (e.g., human, avian, bovine) (Edge et al., 2021; Li et al., 2021; Phelan et al., 2019). In fact, human health investigations related to

human-water interactions of various sources, such as wastewater (e.g., Jäger et al., 2018; Tiwari et al., 2022), stormwater (e.g., Staley et al., 2018), groundwater (e.g., Mattioli et al., 2021; Soumastre et al., 2022), drinking water sources (e.g., Åström et al., 2015), and recreational water use (e.g., Rytönen et al., 2021; Sinigalliano et al., 2021), are often processed using PCR tracking methods. Typically, these studies target DNA molecules and in the case of assessing recreational water, focus on the water compartment only. However, it is becoming increasingly acknowledged that the sediment fractions (both bed and suspended) play an important role in the survival, growth, distribution, and persistence of microbes (including pathogens) in aquatic systems (Droppo et al., 2009; Fries et al., 2008; Gao et al., 2011). Additionally, although it poses greater challenges both logistically and mechanistically, utilizing the RNA component for analyses (rather than DNA) can better describe functioning processes (e.g., metabolism and virulence pathways via mRNA) *in situ* and provide a more accurate representation of the active microbial community (i.e., viable microbes via rRNA) (Deutscher, 2006; Rytönen et al., 2021). Overcoming major challenges recognised in the literature, this research aims to demonstrate a streamlined process for 1) successful RNA isolation from freshwater sediments (bed and suspended) which includes sample collection protocols and appropriate preservation of nucleic acids, and 2) quantification of targeted genes from isolated RNA through the recently developed novel utility of nanofluidic multiplex reverse transcriptase qPCR (RT-qPCR) for effectively evaluating the active microbial community associated with aquatic sediments.

This study is the first to utilize environmental RNA (rRNA and mRNA) isolated from both bed and SS as molecular targets to assess the active microbial community in relation to water quality in freshwater beaches using a nanofluidic TaqMan® OpenArray® RT-qPCR chip. Our objectives were to 1) examine the spatiotemporal gene expression of FIB, MST genes, and waterborne bacterial pathogenic virulence factors associated with benthic sediment of the swimming zone at freshwater beaches; 2) seasonally characterize the gene expression of FIB, MST genes, and bacterial virulence factors associated with SS of local tributaries and their

respective receiving beaches; and 3) test the OpenArray® RT-qPCR chip on the sediment compartment to evaluate if this reservoir/medium contains evidence of active (i.e., expression of mRNA virulence factors and/or rRNA of pathogenic strains) common waterborne bacterial pathogens at freshwater beaches. The information gained from this work will expand our understanding of human health risk potential from recreational waters with high-specificity RNA sequencing to deduce the presence and comparatively quantify gene expression of FIB, MST genes, and specific pathogenic strains associated with freshwater sediments. The utility of MST genes provides both enhanced resolution and spatial context to describe human health risks within recreational waters and will help guide the management of these public locations. Moreover, as we successfully targeted multiple genes from multiple samples simultaneously, the methods validated in this study on sediments could be adopted for regular microbial monitoring of recreational water quality.

5.2 Materials and Methods

5.2.1 Sampling sites and collections

WEC is the southernmost region of Ontario, Canada with vast agricultural landscapes surrounded by freshwater from Lake St. Clair, the Detroit River and Lake Erie (Figure 5.1). The surrounding fresh water of the GLs renders this area popular for recreational water use, yet agricultural influence from drainage contributions in the local watershed causes concern for human health and safety. Frequent beach closures often result in this area due to high levels of FIB and blue-green algae detected in the water column. Six public beaches in WEC were selected for this study based on historical water quality data reported by the WECHU (www.wechu.org) and built off locations previously selected for metatranscriptomic investigation of bacterial gene

expression associated with the bed (VanMensel et al., 2020 – Chapter 3) and SS (VanMensel et al., 2022 – Chapter 4).

Sampling sites are located throughout WEC (Figure 5.1). Surface bed sediment samples were collected from the nearshore (i.e., swimming) zone of local public beaches; four located on the north shore of Lake Erie –HD, KV, LE and PP – and two situated on the southern shoreline of Lake St. Clair – SP and BR. All bed sediment samples were collected via sediment coring, as previously described (Chapter 2) and denote several time points representing a spatiotemporal study throughout the 2017 swimming season (June through September) of the WEC local public beaches (Table D-1). TSS were collected seasonally (spring, summer, and fall) in 2017 from the nearshore zone of KV and BR beaches as well as from their adjacent tributaries (Mill Creek and Belle River, respectively; Table D-1). These samples were acquired using a water pump and a continuous flow centrifuge as previously described (VanMensel et al., 2022 – Chapter 4). Overall, 172 bed sediment samples and 32 SS samples were selected for targeted transcriptomics, totaling 204 samples processed on the OpenArray® qPCR chips.

5.2.2 RNA extractions and sample preparation

Total RNA from sediment was extracted using the RNeasy PowerSoil Total RNA kits (Qiagen), following the manufacturer's instructions including slight modifications as previously described (VanMensel et al., 2020), with sample weight 2 or 5 g and final pellet resuspended in 50 or 60 μ L RNase-free water for suspended and bed sediment samples, respectively. Note that sample weight was different for suspended and bed sediment due to differing concentrations of isolated RNA; specifically, SS was fine-grained, cohesive sediment (i.e., $D_{50} < 35 \mu\text{m}$; VanMensel et al., 2022 - Chapter 4) and consequently held greater concentrations of biomass compared to bed sediment samples. RNase inhibitor (Invitrogen) was added to the resuspended pellet to minimize degradation. Potential DNA contamination was removed using the RapidOut

DNA Removal kit (Thermo Fisher Scientific), following the manufacturer's recommendations. Total RNA concentrations were determined using either the Agilent 2100 Bioanalyzer (Agilent Technologies) or fluorometrically using the Qubit 2.0 Fluorometer and RNA Broad-Range Assay kit (Thermo Fisher Scientific) (Table D-2). Select samples were tested for RNA quality assurance using the Bioanalyzer, previously published (VanMensel et al., 2022, 2020). Typically, RIN was 6.0 or greater. We used a two-step RT-qPCR approach in which the reverse transcription of the RNA template was performed first, followed by the amplification of the cDNA in a separate reaction. cDNA was synthesized from the purified total RNA extracts using a High-Capacity cDNA Reverse Transcription kit (Applied Biosystems), following the manufacturer's protocol. Where necessary, cDNA was diluted with ddH₂O to give more uniform final concentrations of all samples before qPCR (Table D-2). cDNA samples were stored at -20 °C until used in qPCR assays.

5.2.3 *Selection of candidate genes, primers, and probes*

There were 28 genes of interest (GOI) used for this study including targets for *Enterococcus*, *E. coli*, *Bacteroides*, goose, seagull, cow, pig, dog, human, and several bacterial waterborne pathogenic virulence factors. The development and design of this nanofluid OpenArray® chip was for the purpose of monitoring recreational water safety regarding microbial contamination (Shahraki et al., 2019b). Details on the 28 candidate genes included on these chips can be found in Table 5.1. Gene targets are designated as either FIB (3), MST (8), or pathogen identifiers (17). Primers and probe sequences are previously published, and primer/probe validation was performed by Shahraki and colleagues (2019b).

5.2.4 *Quantitative PCR*

5.2.4.1 Multiplex RT-qPCR assays using nanofluidic technology

TaqMan® OpenArray® chips from Applied Biosystems (Burlington, ON, Canada) were used to assess environmental RNA isolated from sediment on a QuantStudio 12K Flex Real-Time PCR System, following the manufacturer's protocol. Each chip contained 48 subarrays of 56 through-holes, resulting in a total of 2,688 through-holes per chip. Therefore, we were able to run 48 samples in duplicate for 28 GOI on each chip, which resulted in five chips for 204 samples. cDNA (2.5 µL) was combined with an equal amount of TaqMan® OpenArray® Real-Time Master Mix (Applied Biosystems) and manually loaded onto custom designed OpenArray® chips (Shahraki et al., 2019b) that were preloaded with the primer and probe sequences for each GOI by the manufacturer. Chips were run on a QuantStudio 12K Flex Real-Time PCR system (Applied Biosystems) using default settings for the OpenArray® technology.

5.2.4.2 Generation of standard curves for quantifying transcripts

Additional TaqMan® qPCR assays were performed for GOI that showed usable results from the OpenArray® assays, using known concentrations, to create standard curves for the purpose of determining absolute concentrations in our samples (Figure D-1). Specifically, there were seven targets – FIB_ Ecoli_23S, FIB_Enterococcus_23S, MST_genBac, MST_dog, MST_goose, MST_seagull, MST_human_mito – that required standard curves. These individual assays were necessary for quantification purposes as the OpenArray® chips did not include standards in attempt to maximize the number of samples analyzed. Complete target gene fragments were synthesized and cloned into plasmid vectors and used for this purpose (Integrated DNA Technologies). Primers and probes for these assays are the same as those previously

described (Shahraki et al., 2019). Six 10-fold dilutions were implemented for each plasmid with known copy numbers (Table D-3). Reactions were performed in 10 μ L volumes containing TaqMan® Fast Advanced Master Mix (Applied Biosystems) (5 μ L), ddH₂O (3.5 μ L), the respective target assay (0.5 μ L), and plasmid (1 μ L). Cyclor conditions started at 50 °C for 2 min, then 95 °C for 10 min, followed by 40 cycles of 95 °C for 15 s (denaturation) and 60 °C for 1 min (annealing/extension). Assays were performed in duplicate with Ct variation between technical replicates less than one cycle. Standard curves were based on five of the serial dilutions (dilutions 1-5) with the most dilute series (dilution 6) omitted due to high Ct variation in duplicates. PCR efficiency for each GOI was calculated from the slope of the standard curve (Bustin et al., 2009).

5.2.4.3 Testing for natural inhibitors

To test the presence of PCR inhibitors, additional RT-qPCR assays were run on all samples with the inclusion of TaqMan® Exogenous Internal Positive Control (IPC; Thermo Fisher Scientific), following the manufacturer's instructions. A negative or no-template control (NTC) and a no-amplification control (NAC) were also run for each assay. All reactions were run in duplicate in 96-well reaction plates on the QuantStudio 12K Flex Real-Time PCR System (Applied Biosystems). Reactions were performed in 25 μ L volumes following the manufacturer's protocol, with 2.5 μ L cDNA or blocker (NAC) or extra ddH₂O (NTC). Cycling conditions were the same for all IPC reactions: 60 °C for 30 s, 95 °C for 10 s, 40 cycles of 95 °C for 15 s (denaturation) and 60 °C for 1 min (annealing/extension), and finally 60 °C for 30 s.

5.2.5 *Testing for lower limit of detection*

Supplementary standard PCR tests were performed on three pathogen virulence genes (*gltA*, *lip*, *regA*) to determine if they were truly absent in our samples or if concentrations were below detection limits for the OpenArray® RT-qPCR assays. These targets were detected in environmental samples (i.e., lake water) previously reported (Shahraki et al. 2019b) and therefore seemed the most likely (out of all virulence targets) to be present in our samples as well. The three GOI were tested on 13 sediment samples (selected from problematic/contaminated locations BR and KV, based on results reported from VanMensel et al., 2020 – Chapter 3), and involved two separate rounds of amplification in an intense effort to increase the concentration of target if present: the first round consisted of 20 PCR cycles, followed by a second round of 40 additional PCR cycles. First round reactions were performed in 25 µL volumes containing 1X buffer, 2 mM MgSO₄, 0.2 mM dNTPs, 0.2 µM primers (same as above; Shahraki et al., 2019b), 0.1 µL Taq polymerase, and 1 µL of template cDNA. After the first round, each sample was carried into the second round and tested twice with the same master mix as the first round but using either 1 or 10 µL of the first-round amplification product in separate assays. Water (ddH₂O) volume was adjusted for differing volumes of template to total 25 µL for the reactions. Cycling conditions were the same for each primer set: initial denaturation for 1 min at 95 °C, followed by 20/40 cycles of 95 °C (30 sec), 60 °C (30 sec), 72 °C (30 sec), and a final extension of 5 min at 72 °C. Results (presence/absence) were visualized on agarose gels and inspected for bands of appropriate length.

5.2.6 *Expression analysis*

Results obtained from the OpenArray® RT-qPCR assays were filtered for usable data. Samples exhibiting ‘undetermined’ Ct values or values outside the range of the corresponding

standard curve were removed before further processing, with the exception of determining the prevalence of target detections in which case only samples with Ct values below the limit of detection were removed. Samples which had only one duplicate with valid results were also removed. Mean Ct values for each duplicate were carried forward for sample processing. Absolute quantification (log copy number per gram of sediment) was calculated for each sample using the equation of the line-of-best-fit from the appropriate standard curve, considering all dilution factors and weight of starting sediment material.

5.2.7 *Statistical analysis*

Statistical analyses were performed in RStudio v1.4.1103 (RStudio Team, 2021). Filtered data (i.e., samples which had Ct values interpolated on the standard curves) was separated by bed or SS for statistical tests and log copies per gram of sediment (log copies/g) was used for statistical processing. One-way ANOVA was performed on all target genes to determine if independent factors (e.g., season, collection date, lake, location, chip ID) had any significant effect on the expression of transcripts. A significant transcriptional response was established using a 0.05 alpha level. Tukey's HSD (honestly significant difference) test followed ANOVA, where appropriate, to distinguish where the differences were attributed. Heatmaps and graphs were generated using the ggplot2 package in RStudio for visualization of gene expression levels at the different sampling locations (or sites) over time. Boxplot and heatmap figures include all data resulting from samples with Ct values above the limit of detections (i.e., unfiltered) to avoid misleading visualizations. Specifically, samples with Ct values which were lower than the Ct values of the most concentrated known standard were included to avoid the perception of undetected targets.

5.3 Results and Discussion

5.3.1 Prevalence of FIB, MST transcripts from freshwater sediments

Out of the 28 target GOI included on the OpenArray® chips, seven (25%) were detected in the sediment samples and consisted of either FIB or MST; none of the 17 pathogen identifiers were detected in any of the samples. Standard curves generated for each of these showed very high R^2 values (> 0.997) (Figure D-1). The limit of detection (LOD) was determined to be 2 and 3 copies for the genes located on Plasmid1 and Plasmid2, respectively, while the limit of quantification (LOQ) varied between 25 and 2580 copies for the genes tested (Table D-4). It should be noted that there were no internal PCR inhibitors identified for any sample.

There were 165/172 (95.9%) bed and 28/32 (87.5%) SS samples that returned usable data. Of these samples with detections, *Enterococcus* and *E. coli* FIB targets showed high prevalence in the bed (86.1% and 80.6%) compared to SS (57.1% and 39.3%), respectively. As the primer sets used for these targets result in highly conserved amplicons (i.e., 23S rRNA) providing expression evident at low resolution, it is not surprising to find this association. Regardless, it is important to realize that FIB have been reported to survive and thrive in warm and cold marine and freshwater sediments for extended periods of time (Droppo et al., 2011; Korajkic et al., 2019). Survival is significantly improved for microorganisms associated with sediment habitats as compared to free-floating planktonic microbes (Baker et al., 2021) given the sediment compartment represents a place for colonization, protection from predators, and a source of food (i.e., DOC) (Droppo et al., 2009). These results support that bed sediments represent contemporary long-term storage of FIB (derived from the settling of the SS), which when resuspended back into the water column may have significant human health implications (Baker et al., 2021; Droppo et al., 2011). In beach shoreline settings, resuspension risk can be exasperated by both hydrological and human impacts (e.g., swimmers, storm events, currents and/or waves). Thus, detection and identification of FIB in the water column does not necessarily

represent a recent source but could be derived from long-term contributions of a host of microbes within the sediments of the ecosystem. Although our results do not reveal new information in this regard, the utility of the OpenArray® RT-qPCR approach presents an optimized, faster method to reach informative conclusions about microbial contamination and activity in environmental samples than traditional culture-based methods or those focused solely on DNA.

The five MST targets detected (general *Bacteroides*, dog, goose, seagull, human) help identify common sources of fecal contamination at the beaches. The general *Bacteroides* marker (MST_genBac) was identified in 99.4% of bed and 100% of SS samples. This bacterial group has been used as an alternative fecal pollution signature because of its high abundance (~25% of anaerobes) in the feces of warm-blooded animals and has host-specific distributions (Ahmed et al., 2016; Okabe et al., 2007; Wexler, 2007). Of these distributions, we also detected dog- and goose-specific *Bacteroides* in the bed (12.1 and 83.0%) and SS (3.6 and 96.4%), respectively. These results suggest MST_genBac is strongly characterised by goose-specific *Bacteroides* in both the bed and suspended sediment fractions, and dog-specific *Bacteroides* represents a major portion of the remaining targets identified. MST_seagull (i.e., *Catellibacillus marimammalium*) was also identified in a high proportion of these samples, especially within the bed (71.5%) compared to SS (21.4%), possibly suggesting longer term residence times in bed sediments. It has been widely acknowledged that both geese and gulls are important sources of fecal contamination to aquatic ecosystems, especially in the GLs (Nevers et al., 2018; Staley et al., 2018). Furthermore, a recent study recommends the use of rRNA-based approaches for MST assays targeting bird fecal contamination (Rytönen et al., 2021), supporting our study and substantiating the results.

Notably, none of the waterborne pathogen virulence factors were detected in any of the samples from the OpenArray® RT-qPCR assays. This suggests that the targets included in our examination were either not present, present but not active in the microbial community, or their transcript levels were below our LOD. Unfortunately, standard curves were only generated for the

seven GOI which showed detections for our samples, which fell into categories of FIB or MST. Therefore, to determine if these pathogen target levels were present but simply below the LOD, we selected three of the virulence factors (*gltA*, *lip*, *regA*) and performed additional conventional PCR assays with an increased number of cycles (i.e., 60 total cycles) using samples with presumably the greatest likelihood of contamination (based on VanMensel et al., 2020 – Chapter 3). These tests indicated no visible bands at the expected amplicon size on agarose gels, suggesting no detectable RNA for virulence factors surveyed from the samples selected. These results are taken as representative for the entire dataset.

5.3.2 *Quantification of FIB, MST transcripts and factors effecting expression*

A chip effect was tested as a quality control measure and was observed because samples were not distributed randomly between the five chips (Table 5.2). Specifically, all SS samples were loaded on chip CXR25 (Table D-5). This effect was substantial ($p \lll 0.05$) for the combination of all genes, and was especially attributed to FIB_Ecoli, MST_genBac, and MST_goose. However, considering these targets also showed significant differences ($p \lll 0.05$) in the comparison of bed vs. SS gene expression (Table D-5), it is not surprising we observe a chip effect as well.

5.3.2.1 Bed sediment as a reservoir for pathogens

Bed sediment samples from the six public beaches were collected five times during the swimming season (June through September) in 2017 (Table D-1), allowing for a spatiotemporal analysis of all targeted transcripts identified (Figure D-2A). One-way ANOVAs revealed independent factors contributing a significant ($p < 0.05$) effect on the level of RNA of each GOI

(Table 5.2, Table D-5). The human mitochondria target (MT-ND2) was omitted as its own representative for these statistical analyses because it only had one observance detected at LE beach on Sep-13 (2.22 log copies/g). Mitochondrial DNA has been widely used as a source tracking target to assess recreational waters for host-specific fecal contamination with high sensitivity and specificity (Malla and Haramoto, 2020; Tanvir Pasha et al., 2020). The detection of this target at LE strongly suggests possible human fecal contamination in this area on that date.

From a spatial perspective, location showed the most substantial effect on the level of RNA, with all targets in the bed sediment having significant variation between the beaches ($p < 0.05$; Table 5.2). A post-hoc Tukey's test revealed BR and KV consistently had the largest contribution of expressed RNA levels (Table D-5, Figure 5.2), corroborating previous research which reported these beaches consisted of much finer grain particles in the bed sediment with steep redox gradients (VanMensel et al., 2020 – Chapter 3). Both locations were described as low energy due to coastal embayment and therefore, restricted water movement. These conditions provide an adequate environment for biofilm establishment and microbial fortification. Extensive research in freshwater environments has shown that FIB and other potential pathogens can persist and potentially grow in secondary habitats, including beach sand and sediment (Alm et al., 2006; Ishii et al., 2007; Ksoll et al., 2007; Mathai et al., 2019). Comparing the two lakes, it appears that Lake St. Clair harbours a significantly greater ($p < 0.05$) level of RNA expression from the genes we targeted (Table 5.2), specifically those representing *E. coli*, general *Bacteroides*, and gulls. Although we know that waterfowl are large non-point source contributors of fecal pollution to recreational nearshore zones of aquatic environments (Edge and Hill, 2007; Staley et al., 2018), our results for bed sediment suggest contamination from gulls is significantly ($p < 0.05$) more prominent at Lake St. Clair shorelines compared to Lake Erie, suggesting different geographic preferences for these birds in WEC.

Temporal bed sediment sample collection (i.e., collection date and season) also showed some variations in the level of RNA with time ($p < 0.05$), but with no obvious pattern (Table 5.2,

Table D-5). Statistically this could be due to the lower number of collection dates (five) and a reflection that these environments represent heterogeneous sediment matrices with unpredictable potential for variation due to numerous environmental pressures, as seen through previous studies with high frequencies of FIB variability (McPhedran et al., 2013; Shahraki et al., 2019a).

5.3.2.1.1 FIB quantification

Two of the three GOI included on the chip representing FIB targets – *Enterococcus* 23S and *E. coli* 23S – were detected at all six beaches for nearly every sample collection; the exceptions were at PP with *Enterococcus* undetected Aug-31 and *E. coli* undetected Jul-26 (Figure 5.3A). Overall, both targets were detected with the highest levels at BR and KV; *Enterococcus* ranged from 3.17 – 4.24 (mean = 3.77) and 3.60 – 4.19 (mean = 3.94) log copies/g, and *E. coli* ranged from 3.10 – 4.17 (mean = 3.64) and 3.13 – 3.32 (mean = 3.23) log copies/g, respectively. Both targets were also frequently detected at SP, HD, LE, and PP but with much lower average levels; *Enterococcus* was revealed at 2.43, 2.85, 2.71, and 2.62 log copies/g, and *E. coli* results were 2.44, 1.93, 2.68, and 2.03 log copies/g, respectively.

Taxonomic presence and abundance of indicator organisms (i.e., FIB) has been the criterion for characterizing recreational waters for many years (Rodrigues and Cunha, 2017), however, this approach has many limitations, including the concept of microbial decay rate. There are many studies that have explored the decay rate of various allochthonous microbes in aquatic systems, most focusing on FIB and other organisms of human health concern (Boehm et al., 2018; Tiwari et al., 2019). Unfortunately, results are typically determined under controlled conditions (i.e., benchtop mesocosm experiments) and therefore, have limited transferability into the natural environment, which is dynamic and complex (Madani et al., 2020). Generalizations are difficult to determine due to the inconsistent effects of environmental factors, which can be abiotic (e.g., turbulence, temperature, pH, exposure to UV light) and biotic (e.g., duration within

the aquatic environment, grazing by protozoa, presence of plasmids) (Barcina et al., 1997; Korajkic et al., 2019). It is also becoming increasingly acknowledged that the sediment compartment plays a large influential role on the survival of FIB in aquatic ecosystems (Haller et al., 2009; Perkins et al., 2016), yet the impact this factor has on survival rates is also debatable, depending on the bed or suspended fraction and available carbon. Furthermore, this can be exasperated by the survival strategy of some microbes which enter a dormant or viable but non-culturable (VBNC) state due to adverse environmental conditions (X. H. Zhang et al., 2021). Therefore, the consideration of decay rates for FIB in recreational water is increasingly convoluted and irrelevant.

Culturing FIB from water samples, however, is commonplace for safety assessments of recreational water (Rodrigues and Cunha, 2017), including the public beaches in WEC. Using the publicly available *E. coli* CFU data (www.wechu.org), we qualitatively compared our *E. coli* expression data for the beaches studied over the 2017 swimming season and observed no discernible trend between the two approaches for the six beaches (Figure 5.4). In other words, the weeks which showed high CFU levels did not necessarily correlate with high expression of transcripts, on a relative scale. In fact, the variability of CFU data tracked on a weekly basis was substantial. This is likely not surprising as other studies have also shown high variability of FIB levels at freshwater beaches on a daily basis (McPhedran et al., 2013). These comparisons further highlight the inaccuracies of relying on DNA and culture-based methods for waterborne pathogen assessments in recreational waters.

Targeting RNA in RT-qPCR assays of environmental samples has many advantages over DNA and simple taxonomic surveys and can offer more reliable results (Rytönen et al., 2021). While DNA evaluations can provide taxonomic information of organisms present and therefore describes the potential of a microbial community, RNA analysis informs on the functioning microbes thus providing insights on how these communities are interacting with and influencing their environment *in situ*. The existence of mRNA transcripts is transient; once expressed, their

lifetime is limited as they await to be translated into proteins (Pawlowski et al., 2022). If there is no immediate need for translation, the molecule decays or is degraded via RNase activity, and the cell ceases further transcription as an effort to save unnecessary expenditure of energy (Ohyama et al., 2014). Although rRNA is generally considered a stable class of RNA as its degradation is more dependent on physiological conditions compared to mRNA (Abelson et al., 1974; Deutscher, 2006), it is still much less stable than DNA and has been reported to be unstable in resting cells compared to growing cells (Abelson et al., 1974). As such, environmental RNA is a suitable indicator for the assessment of active environmental microbes *in situ*. In this study we isolated and analysed viable mRNA and rRNA, which represent the active microbial community better than traditional water quality assessment methods (i.e., culture-dependant). Samples were collected from the bed sediment within the nearshore swimming/wading zone where the likelihood of resuspension via hydrological (i.e., waves) or anthropological (i.e., physical disturbance of bed) activity is the greatest. Therefore, this approach better characterizes the potential health risks for beachgoers at any given time point, especially considering bed sediment constitutes an important reservoir of pathogens in the environment (Droppo et al., 2009; Vogel et al., 2016).

5.3.2.1.2 MST marker quantification

MST_human and MST_dog targets were detected infrequently and with low quantification (Figure D-2), and therefore, were removed for visualization purposes to allow focus on targets which were consistently detected. Three MST targets – general *Bacteroides*, goose, and seagull – were consistently detected at all six beaches with only a handful of samples showing no detection (Figure 5.3A). MST_genBac was detected at all beaches on all sampling occasions and had the highest rRNA levels out of all GOI for all beaches, with averages of 4.89 (BR), 4.02 (SP), 3.46 (HD), 5.40 (KV), 3.98 (LE), and 3.39 (PP) log copies/g. Like FIB

transcripts, BR and KV showed the highest expression of MST_genBac of all locations, ranging from 4.58 – 5.19 and 5.18 – 5.68 log copies/g, respectively. It must be noted that MST_genBac was detected at KV on all sampling occasions with high concentration; however, as the Ct values for Jun-01, Jul-13, and Jul-26 fell outside of our standard curve, these samples were filtered from our dataset. For this instance only, we extrapolated the concentration values from the standard curve to show that this target was highly present at KV beach on all sampling occasions; otherwise, MST_genBac appears as though it was not detected at KV on Jun-01, Jul-13, or Jul-26 – which is not the case. This compromises the accuracy of these concentration values but allows us to retain valuable data to this research. As this GOI targets the highly conserved 16S rRNA gene (Shahraki et al., 2019b), its detection represents a broad range of *Bacteroides spp.* with host-specific targets falling under its umbrella. Microbes belonging to the *Bacteroides* genus are abundant in the gut and feces of many warm-blooded animals and have become a common target in MST of environmental samples (Ahmed et al., 2016; Gómez-Doñate et al., 2016). Therefore, we expected expression levels for this target to be among the highest for our environmental dataset, especially at the more contaminated locations (i.e., BR and KV) as previously reported (VanMensel et al., 2020 – Chapter 3; VanMensel et al., 2022 – Chapter 4).

The other two avian MST targets (goose and seagull) in our study were detected at all beaches with average expression levels of 2.90 and 3.14 (BR), 1.86 and 1.62 (SP), 1.97 and 1.49 (HD), 3.80 and 2.03 (KV), 2.21 and 2.43 (LE), and 1.89 and 1.81 (PP) log copies/g, respectively. Expression of MST_goose was significantly greater ($p < 0.05$) at KV (ranging from 3.54 – 4.31 log copies/g) than all other locations, while expression of MST_seagull was significantly greater ($p < 0.05$) at BR (ranging from 2.67 – 3.75 log copies/g) than all other locations (Table D-5). These results corroborate ANOVA results for lake effect on the dataset, suggesting geese are the more dominant source of legacy fecal pollution at Lake Erie shorelines, and seagull excrement is more problematic at Lake St. Clair shorelines.

Waterfowl are among the most important non-point sources of fecal pollution to aquatic ecosystems, and at times, reported to contribute more *E. coli* to the sand and water at freshwater beaches than municipal wastewater (Edge and Hill, 2007). Geese and gulls have long been viewed as culprits in recreational beach and water contamination. Droppings from geese have been reported to contain 1.53×10^4 fecal coliforms per gram of feces and gull droppings had 3.68×10^8 coliforms per gram (Alderisio and DeLuca, 1999). Although the conventional belief is that *E. coli* from avian sources (i.e., waterfowl) is not as pathogenic to humans compared to human sources (i.e., wastewater contamination), from a recreational water use perspective, there is growing evidence that environmental contamination of bird-sourced *E. coli* could pose greater human health risks than originally thought (Nesporova et al., 2021; Russo et al., 2021; S. Zhang et al., 2021). Genomic sequencing of avian-sourced *E. coli* has identified multiple antibiotic resistance and virulence-associated genes, suggesting waterfowl may represent an emerging potential threat of pathogenic and resistant *E. coli* strains with resulting public health concerns. Because these birds (e.g., geese, gulls) frequent nearshore water and foreshore sand at beaches and considering gulls can produce up to 62 fecal droppings per day (Gould and Fletcher, 1978), the sediment can serve as a significant reservoir of pathogens and an important secondary source of contamination into adjacent waters (Edge and Hill, 2007; Vogel et al., 2016). Our results support that these birds are significantly contributing to poor water quality at freshwater beaches, especially at BR and KV. Further, with Canada goose populations in North America rapidly increasing over the last several decades (Conover, 2011), the situation is expected to continue to escalate.

5.3.2.2 Suspended sediment as a transportation vector for active microbes

Suspended sediment samples from BR and KV were collected in the spring, summer, and fall of 2017 to produce a seasonal assessment of the expression of GOI transcripts associated with

this sediment fraction (Figure D-2B). Unlike bed sediment, a location (i.e., lake) dependence did not appear to have a substantial effect on the level of RNA related to SS (Table D-5).

Furthermore, we did not identify any significant differences ($p > 0.05$) between the RNA expression levels from the lake or tributary, suggesting the suspended fraction is homogeneously mixed within the nearshore zones of these locations.

MST_genBac was the most highly expressed GOI at each beach for all seasons. Average expression values of this GOI were 4.86, 4.77, and 5.14 log copies/g in BR and 6.19, 5.13, and 4.69 log copies/g in KV for the spring, summer, and fall, respectively. MST_goose was also detected at each beach for all seasons, with average expression values of 3.42, 3.19, and 3.91 log copies/g in BR and 4.76, 3.46, and 3.60 log copies/g in KV for the spring, summer, and fall, respectively. MST_seagull was not as prevalent in the SS samples, detected in KV for all seasons (mean values for spring = 3.29, summer = 4.40, and fall = 2.05 log copies/g), but only detected in BR for the fall (1.88 log copies/g). Correlating with bed sediment results, findings for SS suggest waterfowl is a major contributor to freshwater pollution (Edge and Hill, 2007; Staley et al., 2018).

Targets for FIB were present within the SS at both locations throughout the seasons (Figure 5.3B). Although expression was not as prevalent as *Bacteroides* MST targets, FIB_Enterococcus was detected in the dataset with average seasonal values ranging from 1.78 – 4.89 log copies/g, and FIB_Ecoli ranging from 2.97 – 5.09 log copies/g. With the concern that deposited sediment in aquatic systems may represent a reservoir of pathogenic microbes (Baker et al., 2021; Korajkic et al., 2019; VanMensel et al., 2020), our results that FIB transcripts were isolated from SS reveals added concern for the role that sediment plays regarding human health and safety in recreational waters, such as mobility.

In contrast to the bed sediment, all targets (except MST_genBac) showed significant differences ($p < 0.05$) regarding a temporal (i.e., seasonal) effect associated with SS (Table 5.2). Specifically, spring and summer samples were always greater in expression levels compared to the fall (Table D-5). We expected to observe variation in expression corresponding to typical

seasonal weather patterns, such as greater rainfall and runoff during spring (which can collect and transport fecal droppings from upstream down to the lake and adjacent beaches), followed by a drier summer with less water movement (Lu et al., 2021). Although MST_genBac did not show temporal significant differences ($p > 0.05$) associated with SS, this target revealed the highest expression levels for any target throughout the seasons (mean values for spring = 5.75, summer = 5.04, and fall = 4.92 log copies/g), suggesting a continual concern of fecal contamination regardless of seasonal variations. As mentioned above, there was not a significant variation between SS from the tributaries compared to the lake, suggesting these adjacent watershed channels are important sources of suspended solids to the beaches, continually sourcing the nearshore zone with new sediment and microbiota and influencing the quality of water (Madani et al., 2022). These results may therefore suggest that SS represents a ubiquitous phase for microbial/pathogen dynamics within recreational waters by; 1) representing the building blocks of bed sediment and an accelerated settling mechanism of microbes to the bed with subsequent and transient biofilm development, and/or 2) the transport mechanism via turbulence of recently eroded bed sediments and/or recently received SS/microbes via various means (e.g., river flow, ground water upwelling, direct surface wash-off).

5.3.3 *Evaluating best approach for assessing microbial contamination in water*

Pearson's correlation test demonstrated a low to moderate linear correlation between FIB and the combination of our host-specific MST targets in the nearshore freshwater bed sediment (Table D-6). The correlation coefficient (r) between *E. coli* & MST (combined host-specific) and *Enterococcus* & MST (combined host-specific) was measured around 0.5 for both, suggesting a mild positive correlation. When both FIB were individually paired with MST_genBac, however, there was no correlation observed. SS showed similar results but demonstrated a high linear correlation ($r = 0.87$) between *Enterococcus* & MST_genBac with no correlation ($r = 0.12$)

between *Enterococcus* & MST (combined host-specific). There is a large contrast between sample sizes for bed (172) and SS (32), which may explain these dissimilarities. Alternatively, these results may suggest different relationships between the microbial community members within these sediment matrices, which may reflect highly diverse physicochemical environments and living conditions regarding, for example, nutrient/DOC concentrations/availability, presence of inhibitors, microbial concentration and competition, etc.

Traditional water quality assessments of culturing planktonic FIB provide minimal information regarding human health risk in recreational waters. Current literature on the topic is clear that infrequent culturing or DNA-based assessments of general FIB taxa in the water column does not support a path toward improving microbial contamination to shorelines. This is because traditional approaches cannot inform on true pathogenicity potential or contamination source/origin. To advance our understanding of these systems and the inherent potential for human health risk, sampling, processing, and analysis methods must be improved to address these shortcomings. The present study offers a suitable and novel approach through RT-qPCR with multiple gene targets (including FIB, MST, and pathogen identifiers), which provides additional necessary information to increase our understanding of freshwater shorelines and the safety of human recreational water use (Figure 5.5). We demonstrated that utilizing environmental RNA provides higher quality results on the active microbial community *in situ*. The inclusion of FIB targets (i.e., 23S rRNA sequences) reveals the presence of microbes that may be of pathogenic concern for humans, while MST targets provided information on contamination source, which is important for next steps involving pollution mitigation. Incorporating targets precisely for specific pathogen virulence factors increases the microbial information gained from such molecular evaluations. Although we did not detect the presence of any mRNA pathogen identifiers (i.e., virulence factors) in our samples, the inclusion of these GIOs and level of analysis is perhaps the decisive approach to characterizing the pathogenic community of environmental systems. Targeting mRNA sequences that correspond to active virulence provides

an additional and essential layer of microbial detail by describing the specific pathogens present and active.

5.4 Conclusion

This research is the first to isolate and quantify transcripts (i.e., environmental RNA) from freshwater lakebed and SS for the purpose of evaluating potential human health risk in recreational waters. Through a quantitative assessment of targeted transcriptomics using a custom designed nanofluidic RT-qPCR chip, FIB (i.e., *Enterococcus* and *E. coli*) and MST (general *Bacteroides*, goose, seagull) were detected in both bed and SS samples from freshwater environments.

BR and KV beaches consistently had the largest contribution of expressed GOI in the bed sediment compared to other locations, supporting previous research stating low energy beaches with fine sediment particles provide suitable habitats for microbial populations, including pathogens. As a result, fine-grained bed sediment may represent important contemporary long-term storage of FIB. Specifically, BR and KV showed significantly greater expression ($p < 0.05$) of *Enterococcus*, *E. coli*, general *Bacteroides*, and goose MST within the bed sediment compared to other locations. There was a seasonal influence on the expression of transcripts associated with SS (with spring and summer revealing greater expression levels compared to the fall) but no significant variation between tributary and lake, suggesting this fraction represents a ubiquitous phase for microbial/pathogen dynamics within these aquatic ecosystems. Further, our results suggest both geese and gulls are significant contributors to legacy fecal pollution resulting in poor water quality at freshwater beaches, especially those with fine grain particles and restricted water movement. With growing research on *E. coli* genomic sequencing and identification of multiple antibiotic resistant and virulence-associated genes from waterfowl sources, the high prevalence and magnitude of goose and gull MSTs in the freshwater sediment indicates wildlife

contamination of recreational waters (i.e., geese, gulls) and deserves a re-evaluation with regards to human health risks, especially around the GLs.

A difference in RNA expression levels was observed between sediment fractions – bed vs. suspended – with *E. coli*, general *Bacteroides*, and goose MST showing significantly greater ($p \lll 0.05$) expression levels in SS compared to the bed. This is surprising due to the significant difference in habitat substrates (planktonic vs. benthic) and therefore life-sustaining nutrients and energy. Nutrients and DOC are plentiful in the bed sediments and pore waters, whereas for the SS the supply of life's needs is less plentiful. However, considering the suspended fraction may contain a large collection of allochthonous material (e.g., bacteria, cohesive sediment, nutrients) from a wide geographical region (i.e., the watershed collection basin for these lakes), it can be expected that this matrix may harbour and support a sizable active microbial community. Further, we cannot neglect the role of SS in the microbial dynamics of recreational waters, given it is a principal delivery mechanism of nutrients and DOC to the bed for sustaining a thriving benthic community. It is also largely responsible for the seeding of the benthic microbial community and possibly its temporal evolution given the SS may contain new organisms/pathogens transported from external locations.

Regardless of the expression features here, the importance of this work is the detection of transcripts with pathogenic relevance from the sediment compartment in freshwater environments. Irrespective of if the bed or suspended fraction revealed greater expression of transcripts, the ultimate outcome is that sediments in aquatic systems are associated with harmful bacteria actively expressing the transcripts targeted. This has major implications on our current understanding of how water quality is assessed as well as the transportation and survival of microbes in aquatic ecosystems. Remarkably, the suspended fraction exhibited a stronger level of RNA targets detected compared to the bed sediment as there was a very significant difference between the quantity of cumulated RNA for bed and SS ($p \lll 0.05$). This emphasizes that microbial association with suspended solids is likely an important and viable transportation

option for pathogens in freshwater systems. Furthermore, transient events (e.g., storms) may result in erosion and consequently the introduction of long-term stored microorganisms/pathogens and new sediments with increased delivery via rivers and overland flows. This study has served to expand our understanding of MST and pathogen risk potential using novel high-specificity RNA sequencing to deduce the presence and quantify the activity of specific pathogenic strains. This will allow scientists, water managers, and policymakers to better ascertain human health risks within recreational waters and guide management strategies for these public locations.

Acknowledgements

The authors thank Shelby Mackie in the Environmental Genomics Facility (EGF) at the Great Lakes Institute for Environmental Research (GLIER), University of Windsor for consultations on troubleshooting, running the IPC assays, and all her help with the QuantStudio 12K Flex Real-Time PCR System. We thank Environment and Climate Change Canada (ECCC) for access to centrifuge equipment and acknowledge ECCC, Nick Falk, and Thomas Reid for sample collection assistance. This work was supported by the NSERC Strategic Partnerships Program entitled ‘Great Lakes Water Security: Microbial community characterization, source tracking, and remediation through meta-genomics’ REF341061127. The authors declare no conflict of interest.

Figures and Tables

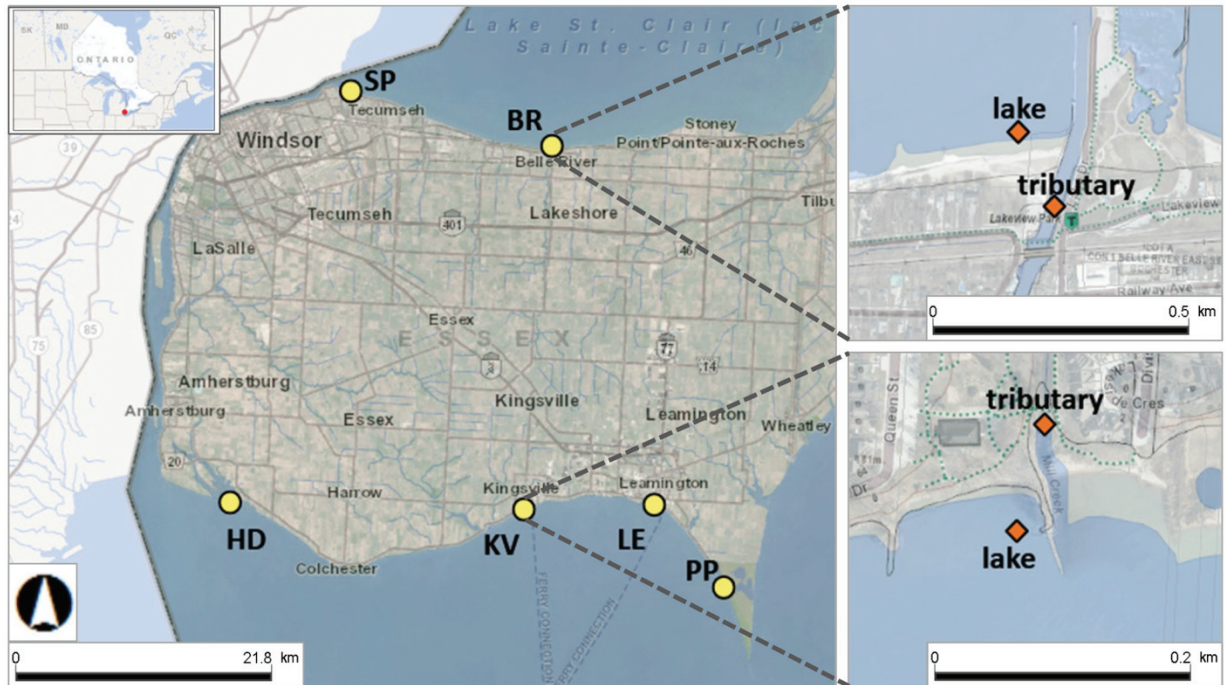


Figure 5.1: Map of WEC displaying all sampling sites. Bed sediment (yellow circles) was collected from Sandpoint (SP), Belle River (BR), Holiday Conservation (HD), Kingsville (KV), Leamington (LE), and Point Pelee (PP). Suspended sediment (orange diamonds) was collected from the nearshore zone in the lake from both BR (top right panel) and KV (bottom right panel) as well as the adjacent tributary (top – Belle River; bottom – Mill Creek).

Source: Ontario Ministry of Natural Resources and Forestry, *Make a Topographic Map*

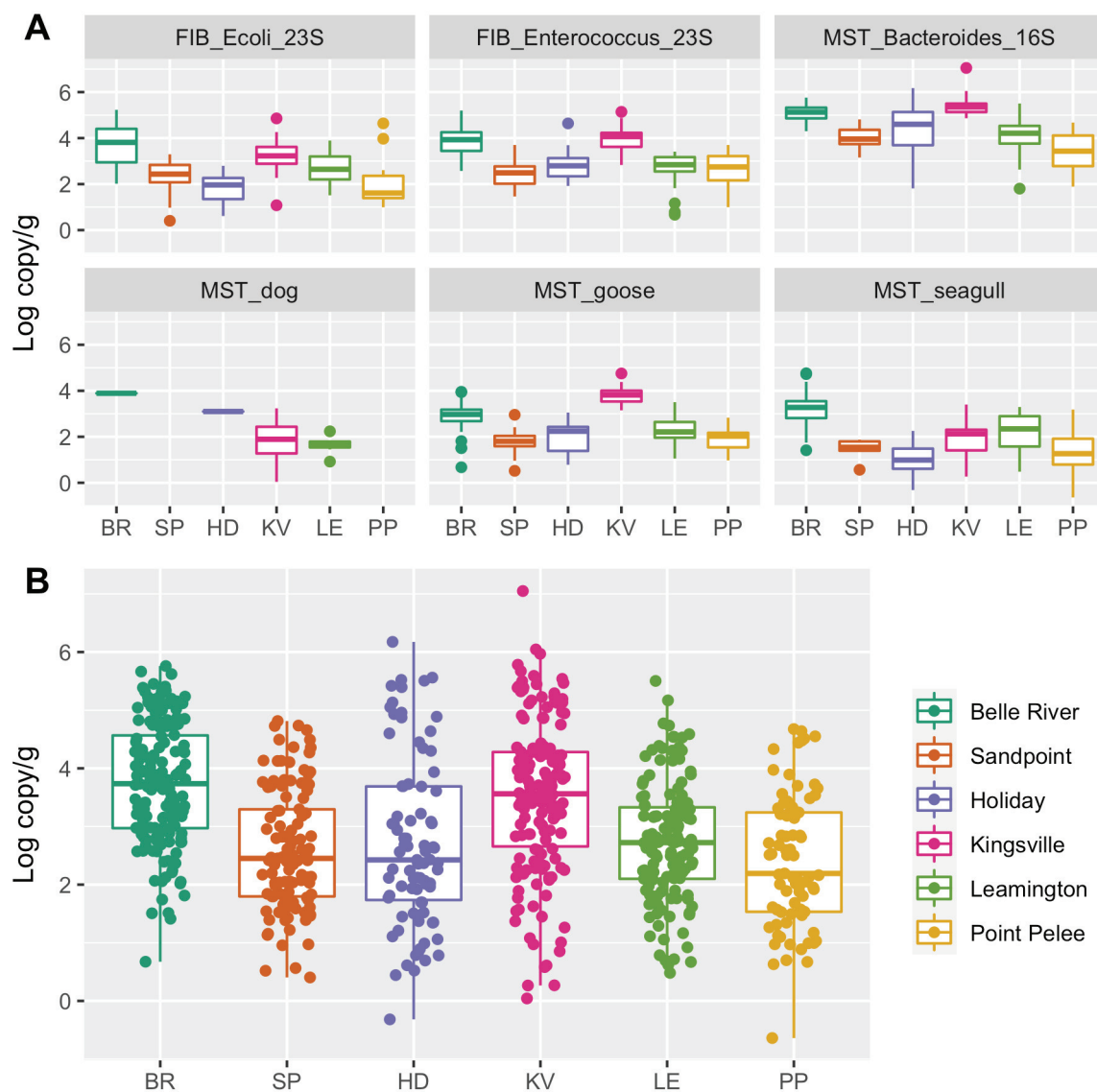


Figure 5.2: Boxplots displaying the distribution of expressed transcripts (log copies/g) at each beach location (Belle River, BR; Sandpoint, SP; Holiday, HD; Kingsville, KV; Leamington, LE; Point Pelee, PP) for all collection dates of bed sediment. (A) Targets separated by panel; (B) targets combined showing all sample points.

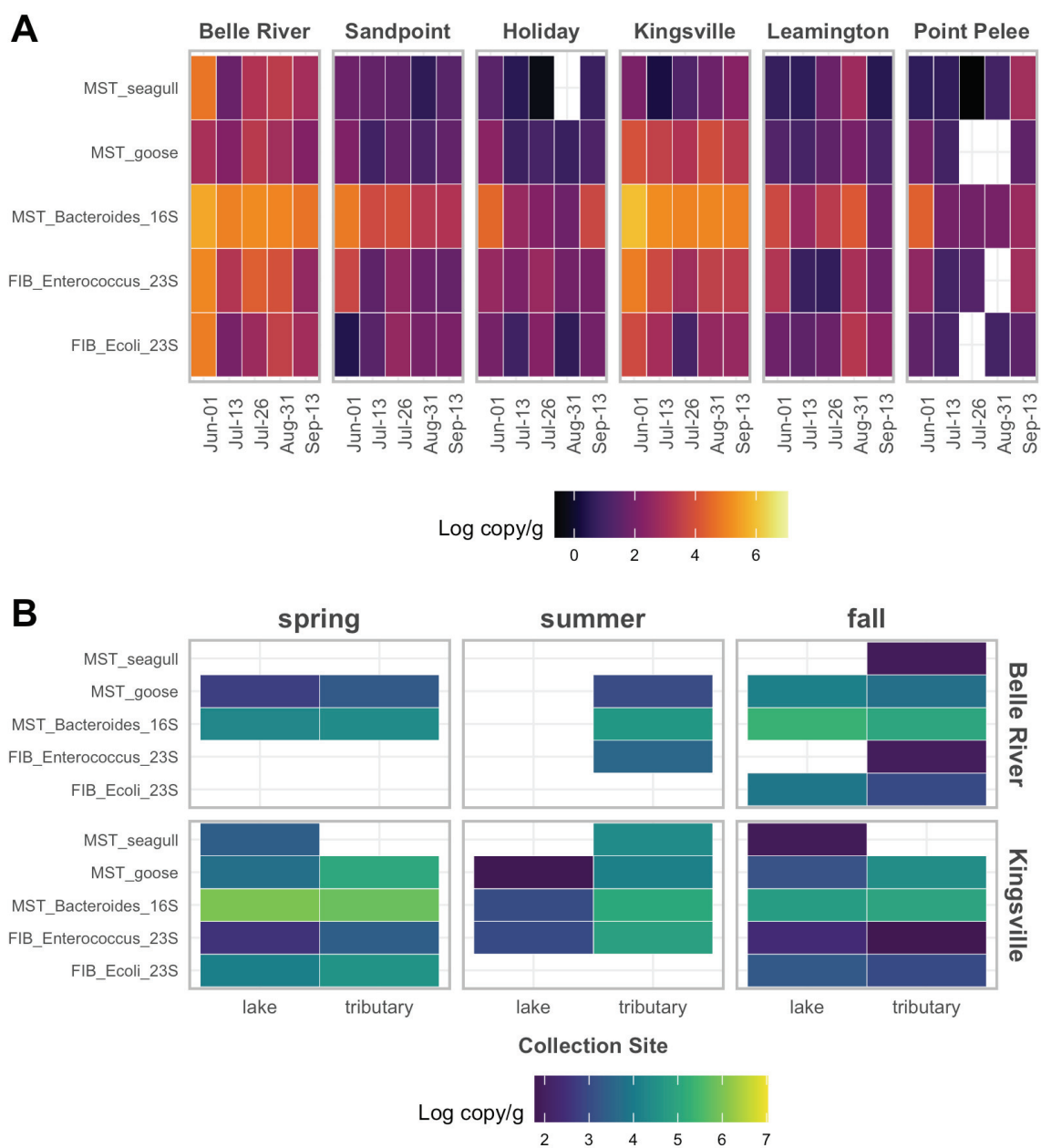


Figure 5.3: Heatmaps of expressed transcripts (log copies/g) of prominent GOI quantified from sediment samples. Targets include two FIB (*Enterococcus* 23S, *E. coli* 23S) and three MST (general *Bacteroides* 16S, goose, seagull). (A) Bed sediment samples: six beach locations, each with five collection dates between June and September of 2017. (B) Suspended sediment samples: collected seasonally (spring, summer, and fall) from the lake and tributary in Belle River and Kingsville. Cells with no colour indicate no detection.

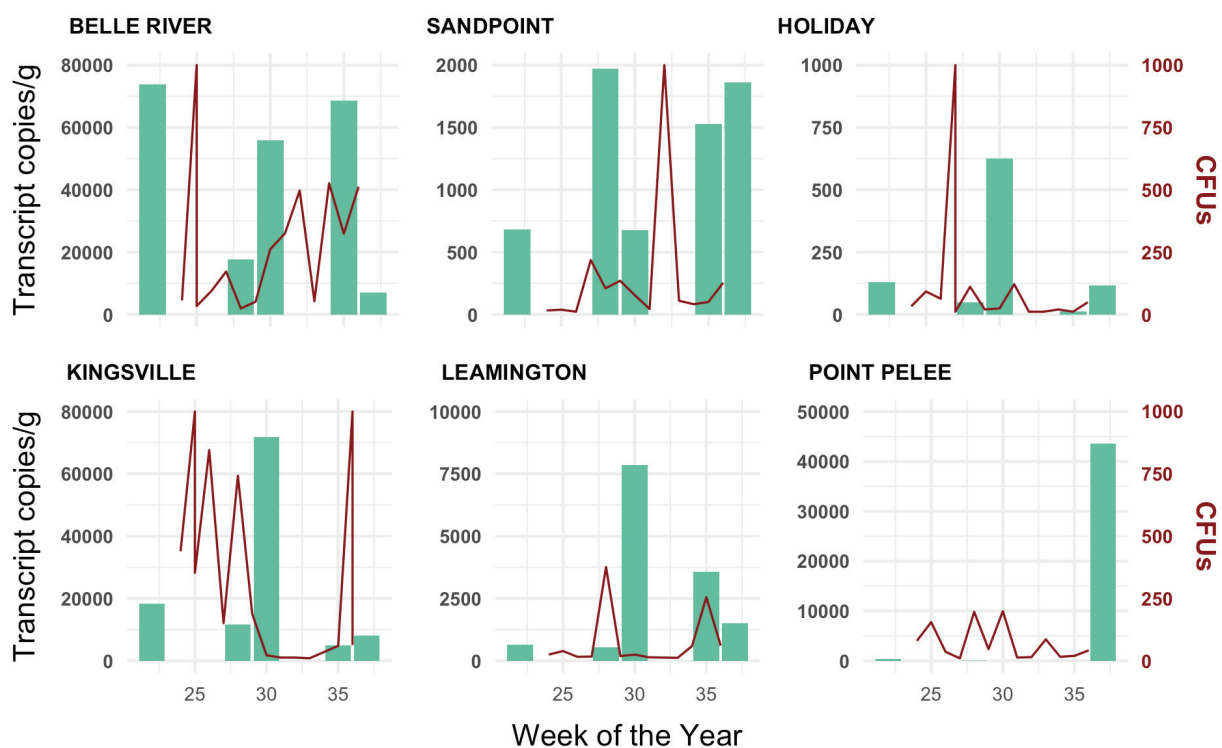


Figure 5.4: Time series visualization comparing *E. coli* 23S transcript copies/g of sediment (green bars, left y axis) and *E. coli* CFUs (red line, right y axis) reported by WECHU for each of the six public beaches studied for bed sediment. CFU data available every week from Week 24-36; transcript data available for Weeks 22, 28, 30, 35, and 37 – not to be confused with no detection of *E. coli* transcripts for other weeks. Note y-left axis (transcript data) is unique for each graph, while y-right axis (CFU data) is consistent for all graphs.

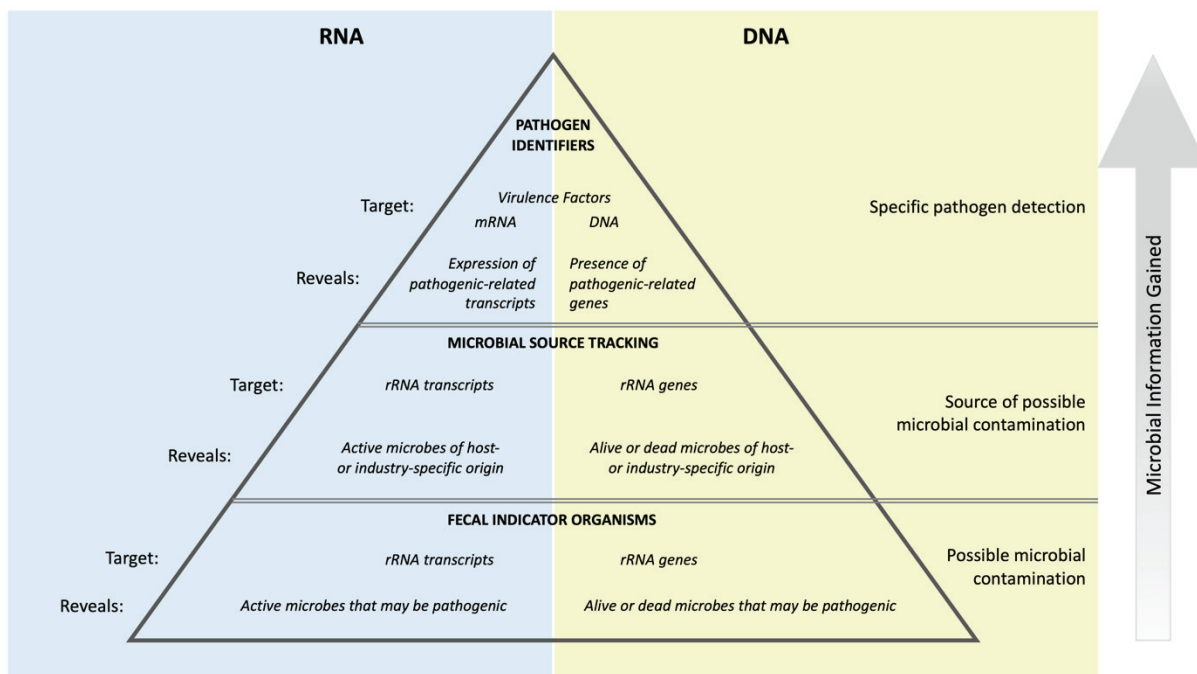


Figure 5.5: Conceptual diagram depicting the importance and value of targeting different groups of biomolecules from environmental samples through molecular techniques (i.e., qPCR tracking methods). There are three tiers to this hierarchy (i.e., fecal indicator organisms, microbial source tracking, and pathogen identifiers), and each level displays the intended target and biological information revealed from analysing environmental RNA (left) compared to DNA (right). The amount of microbial information gained increases moving up the levels.

Table 5.1: Genes targeted for RT-qPCR assays used to determine microbial contamination in freshwater sediments, including target category (i.e., FIB, MST, waterborne pathogen/virulence factor), animal source for MSTs, and gene codes and descriptions. Details on targets with detections in our dataset (from OpenArray® RT-qPCR assays) include coefficient of determination (R^2) from standard curves and PCR efficiency percentage (both determined from conventional qPCR assays). GenBank accession numbers are included for targets used for developing synthetic genes for standard curves.

Species/Target		Gene	Detected?	R^2	PCR Eff.	Accession
Fecal indicator bacteria (FIB)						
<i>Enterococcus</i> spp.		23S rRNA	Y	0.9976	91.98	NR121924.1
<i>Escherichia coli</i>		<i>uidA</i> ; beta-glucuronidase enzyme	N			
<i>Escherichia coli</i>		23S rRNA	Y	0.9995	90.14	DQ682619.1
Microbial source tracking (MST)						
<i>Methanobrevibacter smithii</i>	Human	<i>nifH</i> ; nitrogenase iron protein	N			
Human C40 mitochondria	Human	MT-ND2; mitochondrially encoded NADH dehydrogenase 2	Y	0.9991	93.63	AY714044.1
<i>Bacteroides-Prevotella</i>	General	16S rRNA	Y	0.9991	91.66	CP075195.1
<i>Bacteroides</i> spp.	Dog	16S rRNA	Y	0.9984	91.95	AY695700.1
<i>Catellibacterium marimammalium</i>	Seagull	16S rRNA	Y	0.9972	91.54	AJ854484.1
<i>Bacteroides</i> spp.	Goose	16S rRNA	Y	0.9995	94.39	GU222217.1
<i>Bacteroides</i> spp.	Cow	16S rRNA	N			
<i>Bacteroides</i> spp.	Pig	16S rRNA	N			
Pathogen identifier/virulence factors						
<i>Salmonella typhimurium</i>		<i>invA</i> ; type III secretion system export apparatus protein	N			
<i>Campylobacter coli</i>		<i>gylA</i> ; serine hydroxymethyltransferase	N			
<i>Escherichia coli</i> O157:H7		<i>stx2</i> ; Shiga toxin 2	N			
<i>Escherichia coli</i> O157:H7		<i>manC</i> ; mannose-1-phosphate guanylyltransferase	N			
<i>Klebsiella pneumoniae</i>		<i>phoE</i> ; outer membrane porin protein E	N			
<i>Legionella pneumophila</i>		<i>mipA</i> ; macrophage infectivity potentiator	N			
<i>Escherichia coli</i> O111		<i>manC</i> ; mannose-1-phosphate guanylyltransferase	N			
<i>Escherichia coli</i> O26		<i>manC</i> ; mannose-1-phosphate guanylyltransferase	N			
<i>Pseudomonas aeruginosa</i>		<i>regA</i> ; exotoxin A regulatory protein	N			
<i>Vibrio cholerae</i>		<i>ctxA</i> ; cholera toxin gene	N			
<i>Acinetobacter baumannii</i>		<i>gltA</i> ; citrate synthase	N			
<i>Shigella</i> spp.		<i>ipaH</i> ; invasion plasmid antigen H gene	N			
<i>Campylobacter jejuni</i>		<i>hipO</i> ; hippuricase gene	N			
<i>Staphylococcus aureus</i>		<i>gyrA</i> ; DNA gyrase subunit A	N			
<i>Listeria monocytogenes</i>		<i>hly</i> ; listeriolysin O precursor	N			
<i>Mycobacterium avium</i>		<i>rpoB</i> ; RNA polymerase beta-subunit	N			
<i>Aeromonas hydrophila</i>		<i>lip</i> ; extracellular lipase	N			

Table 5.2: Significance values (p) for one-way ANOVAs explaining the effect on transcript expression from independent factors. GOI presented here include FIBs *Enterococcus* and *E. coli*, and MSTs for *Bacteroides*, goose, and seagull, as well as the combination of all GOI detected in this work. GOI are represented for both bed and suspended sediment (SS) fractions. Values with bold text depict results with significant differences ($p < 0.05$).

	GOI	Season	Collection Date ^b	Lake	Location ^c	Site ^d	Others ^e	
Bed	<i>FIB Enterococcus</i>	0.663	0.195	0.801	<2e-16 ***	--	Bed vs. SS	0.516
	<i>FIB E. coli</i>	0.0604	0.0219 *	0.00391 **	2.19e-12 ***	--		1.2e-04 ***
	<i>MST Bacteroides</i>	0.00214 **	0.0369 *	8.98e-04 ***	2.55e-09 ***	--		8.39e-12 ***
	<i>MST goose</i>	0.47	0.382	0.112	<2e-16 ***	--		2.39e-10 ***
	<i>MST seagull</i>	0.594	0.0313 *	1.47e-05 ***	3.22e-11 ***	--		0.188
	ALL ^a	0.898	0.00991 **	4.59e-04 ***	<2e-16 ***	--		<2e-16 ***
SS	<i>FIB Enterococcus</i>	0.00178 **	--	0.712	--	0.631	Chip ID	0.973
	<i>FIB E. coli</i>	7.65e-04 ***	--	0.319	--	0.343		4.62e-04 ***
	<i>MST Bacteroides</i>	0.0882	--	0.138	--	0.98		5.28e-10 ***
	<i>MST goose</i>	0.0318 *	--	0.257	--	0.0779		2.38e-08 ***
	<i>MST seagull</i>	0.00296 **	--	0.359	--	0.645		0.101
	ALL ^a	2.31e-04 ***	--	0.436	--	0.14		<2e-16 ***

Significance values: * $0.05 > p > 0.01$; ** $0.01 > p > 0.001$; *** $p < 0.001$

^a Includes all GOI detected in this work (FIBs *Enterococcus* and *E. coli*, and MSTs for *Bacteroides*, dog, goose, seagull, and human)

^b Collection Date values for SS data not recorded as they exactly correspond to Season results

^c Location values for SS data not recorded as they exactly correspond to Lake results

^d Site values for bed sediment data not applicable as only one sampling site existed (i.e., nearshore beach)

^e Others refers to additional ANOVA tests which include the combination of bed and SS samples (i.e., Bed vs. SS, Chip ID)

References

- Ahmed, W., Hughes, B., Harwood, V.J., 2016. Current status of marker genes of bacteroides and related taxa for identifying sewage pollution in environmental waters. *Water (Switzerland)* 8. <https://doi.org/10.3390/w8060231>
- Alderisio, K.A., DeLuca, N., 1999. Seasonal enumeration of fecal coliform bacteria from the feces of ring-billed gulls (*Larus delawarensis*) and Canada geese (*Branta canadensis*). *Appl. Environ. Microbiol.* 65, 5628–5630. <https://doi.org/10.1128/aem.65.12.5628-5630.1999>
- Alm, E.W., Burke, J., Hagan, E., 2006. Persistence and potential growth of the fecal indicator bacteria, *Escherichia coli*, in shoreline sand at Lake Huron. *J. Great Lakes Res.* 32, 401–405. [https://doi.org/10.3394/0380-1330\(2006\)32\[401:PAPGOT\]2.0.CO;2](https://doi.org/10.3394/0380-1330(2006)32[401:PAPGOT]2.0.CO;2)
- Åström, J., Pettersson, T.J.R., Reischer, G.H., Norberg, T., Hermansson, M., 2015. Incorporating expert judgments in utility evaluation of bacteroidales qpcr assays for microbial source tracking in a drinking water source. *Environ. Sci. Technol.* 49, 1311–1318. <https://doi.org/10.1021/es504579j>
- Baker, C.A., Almeida, G., Lee, J.A., Gibson, K.E., 2021. Pathogen and surrogate survival in relation to fecal indicator bacteria in freshwater mesocosms. *Appl. Environ. Microbiol.* 87, 1–14. <https://doi.org/10.1128/AEM.00558-21>
- Barcina, I., Lebaron, P., Vives-Rego, J., 1997. Survival of allochthonous bacteria in aquatic systems: a biological approach. *FEMS Microbiol. Ecol.* 23, 1–9.
- Boehm, A.B., Graham, K.E., Jennings, W.C., 2018. Can we swim yet? Systematic review, meta-analysis, and risk assessment of aging sewage in surface waters. *Environ. Sci. Technol.* 52, 9634–9645. <https://doi.org/10.1021/acs.est.8b01948>
- Bouchali, R., Mandon, C., Marti, R., Michalon, J., Aigle, A., Marjolet, L., Vareilles, S., Kouyi, G.L., Polomé, P., Toussaint, J.Y., Cournoyer, B., 2022. Bacterial assemblages of urban microbiomes mobilized by runoff waters match land use typologies and harbor core species involved in pollutant degradation and opportunistic human infections. *Sci. Total Environ.* 815, 152662. <https://doi.org/10.1016/j.scitotenv.2021.152662>
- Brandão, J., Weiskerger, C., Valério, E., Pitkänen, T., Meriläinen, P., Avolio, L., Heaney, C.D., Sadowsky, M.J., 2022. Climate change impacts on microbiota in beach sand and water: Looking ahead. *Int. J. Environ. Res. Public Health* 19.
- Bustin, S.A., Benes, V., Garson, J.A., Hellemans, J., Huggett, J., Kubista, M., Mueller, R., Nolan, T., Pfaffl, M.W., Shipley, G.L., Vandesompele, J., Wittwer, C.T., 2009. The MIQE

- guidelines: Minimum information for publication of quantitative real-time PCR experiments. *Clin. Chem.* 55, 611–622. <https://doi.org/10.1373/clinchem.2008.112797>
- Conover, M.R., 2011. Population growth and movements of Canada geese in New Haven County, Connecticut, during a 25-year period. *Waterbirds* 34, 412–421. <https://doi.org/10.1675/063.034.0403>
- Droppo, I.G., Krishnappan, B.G., Liss, S.N., Marvin, C., Biberhofer, J., 2011. Modelling sediment-microbial dynamics in the South Nation River, Ontario, Canada: Towards the prediction of aquatic and human health risk. *Water Res.* 45, 3797–3809. <https://doi.org/10.1016/j.watres.2011.04.032>
- Droppo, I.G., Liss, S.N., Williams, D., Nelson, T., Jaskot, C., Trapp, B., 2009. Dynamic existence of waterborne pathogens within river sediment compartments. Implications for water quality regulatory affairs. *Environ. Sci. Technol.* 43, 1737–1743. <https://doi.org/10.1021/es802321w>
- Edge, T.A., Boyd, R.J., Shum, P., Thomas, J.L., 2021. Microbial source tracking to identify fecal sources contaminating the Toronto Harbour and Don River watershed in wet and dry weather. *J. Great Lakes Res.* 47, 366–377. <https://doi.org/10.1016/j.jglr.2020.09.002>
- Edge, T.A., Hill, S., 2007. Multiple lines of evidence to identify the sources of fecal pollution at a freshwater beach in Hamilton Harbour, Lake Ontario. *Water Res.* 41, 3585–3594. <https://doi.org/10.1016/j.watres.2007.05.012>
- Friedrich, S., Zec, H., Wang, T.-H., 2016. Analysis of single nucleic acid molecules in micro- and nano-fluidics. *Physiol. Behav.* 16, 790–811. <https://doi.org/10.1039/c5lc01294e>
- Gómez-Doñate, M., Casanovas-Massana, A., Muniesa, M., Blanch, A.R., 2016. Development of new host-specific *Bacteroides* qPCRs for the identification of fecal contamination sources in water. *Microbiologyopen* 5, 83–94. <https://doi.org/10.1002/mbo3.313>
- Gould, D.J., Fletcher, M.R., 1978. Gull droppings and their effects on water quality. *Water Res.* 12, 665–672. [https://doi.org/10.1016/0043-1354\(78\)90176-8](https://doi.org/10.1016/0043-1354(78)90176-8)
- Haller, L., Amedegnato, E., Poté, J., Wildi, W., 2009. Influence of freshwater sediment characteristics on persistence of fecal indicator bacteria. *Water. Air. Soil Pollut.* 203, 217–227. <https://doi.org/10.1007/s11270-009-0005-0>
- Ishii, S., Hansen, D.L., Hicks, R.E., Sadowsky, M.J., 2007. Beach sand and sediments are temporal sinks and sources of *Escherichia coli* in lake superior. *Environ. Sci. Technol.* 41, 2203–2209. <https://doi.org/10.1021/es0623156>
- Jäger, T., Alexander, J., Kirchen, S., Dötsch, A., Wieland, A., Hiller, C., Schwartz, T., 2018. Live-dead discrimination analysis, qPCR assessment for opportunistic pathogens, and

- population analysis at ozone wastewater treatment plants. *Environ. Pollut.* 232, 571–579.
<https://doi.org/10.1016/j.envpol.2017.09.089>
- Korajkic, A., Wanjugi, P., Brooks, L., Cao, Y., Harwood, V.J., 2019. Persistence and decay of fecal microbiota in aquatic habitats. *Microbiol. Mol. Biol. Rev.* 83.
<https://doi.org/10.1128/membr.00005-19>
- Ksoll, W.B., Ishii, S., Sadowsky, M.J., Hicks, R.E., 2007. Presence and sources of fecal coliform bacteria in epilithic periphyton communities of Lake Superior. *Appl. Environ. Microbiol.* 73, 3771–3778. <https://doi.org/10.1128/AEM.02654-06>
- Levy, K., Woster, A.P., Goldstein, R.S., Carlton, E.J., 2016. Untangling the impacts of climate change on waterborne diseases: A systematic review of relationships between diarrheal diseases and temperature, rainfall, flooding, and drought. *Environ. Sci. Technol.* 50, 4905–4922. <https://doi.org/10.1021/acs.est.5b06186>
- Li, E., Saleem, F., Edge, T.A., Schellhorn, H.E., 2021. Biological indicators for fecal pollution detection and source tracking: A review. *Processes* 9. <https://doi.org/10.3390/pr9112058>
- Lu, Z., Liu, Z., Zhang, C., Wei, Q., Zhang, S., Li, M., 2021. Spatial and seasonal variations of sediment bacterial communities in a river-bay system in South China. *Appl. Microbiol. Biotechnol.* 105, 1979–1989. <https://doi.org/10.1007/s00253-021-11142-z>
- Madani, M., Seth, R., Leon, L.F., Valipour, R., McCrimmon, C., 2020. Three dimensional modelling to assess contributions of major tributaries to fecal microbial pollution of lake St. Clair and Sandpoint Beach. *J. Great Lakes Res.* 46, 159–179.
<https://doi.org/10.1016/j.jglr.2019.12.005>
- Madani, M., Seth, R., Valipour, R., Leon, L.F., Hipsey, M.R., 2022. Modelling of nearshore microbial water quality at confluence of a local tributary in Lake St. Clair. *J. Great Lakes Res.* 48, 489–501. <https://doi.org/10.1016/j.jglr.2022.01.019>
- Malla, B., Haramoto, E., 2020. Host-specific mitochondrial DNA markers for tracking the sources of fecal pollution. *Curr. Opin. Environ. Sci. Heal.* 16, 34–46.
<https://doi.org/10.1016/j.coesh.2020.02.006>
- Mathai, P.P., Dunn, H.M., Magnone, P., Zhang, Q., Ishii, S., Chun, C.L., Sadowsky, M.J., 2019. Association between submerged aquatic vegetation and elevated levels of *Escherichia coli* and potential bacterial pathogens in freshwater lakes. *Sci. Total Environ.* 657, 319–324.
<https://doi.org/10.1016/j.scitotenv.2018.11.484>
- Mattioli, M.C., Benedict, K.M., Murphy, J., Kahler, A., Kline, K.E., Longenberger, A., Mitchell, P.K., Watkins, S., Berger, P., Shanks, O.C., Barrett, C.E., Barclay, L., Hall, A.J., Hill, V., Weltman, A., 2021. Identifying septic pollution exposure routes during a waterborne

- norovirus outbreak - A new application for human-associated microbial source tracking qPCR. *J. Microbiol. Methods* 180, 106091. <https://doi.org/10.1016/j.mimet.2020.106091>
- McPhedran, K., Seth, R., Bejankiwar, R., 2013. Occurrence and predictive correlations of *Escherichia coli* and *Enterococci* at Sandpoint beach (Lake St Clair), Windsor, Ontario and holiday beach (Lake Erie), Amherstburg, Ontario. *Water Qual. Res. J. Canada* 48, 99–110. <https://doi.org/10.2166/wqrjc.2013.132>
- Morrison, T., Hurley, J., Garcia, J., Yoder, K., Katz, A., Roberts, D., Cho, J., Kanigan, T., Ilyin, S.E., Horowitz, D., Dixon, J.M., Brennan, C.J.H., 2006. Nanoliter high throughput quantitative PCR. *Nucleic Acids Res.* 34, 1–9. <https://doi.org/10.1093/nar/gkl639>
- Nesporova, K., Wyrsh, E., Valcek, A., Bitar, I., Chaw, K., Harris, P., Hrabak, J., Literak, I., Djordjevic, S., Dolejska, M., 2021. *Escherichia coli* Sequence Type 457 is an emerging extended-spectrum-beta-lactam-resistant lineage with reservoirs in wildlife and food-producing animals 65, 1–18.
- Nevers, M.B., Byappanahalli, M.N., Shively, D., Buszka, P.M., Jackson, P.R., Phanikumar, M.S., 2018. Identifying and eliminating sources of recreational water quality degradation along an urban coast. *J. Environ. Qual.* 47, 1042–1050. <https://doi.org/10.2134/jeq2017.11.0461>
- Ohyama, H., Sakai, T., Agari, Y., Fukui, K., Nakagawa, N., Shinkai, A., Masui, R., Kuramitsu, S., 2014. The role of ribonucleases in regulating global mRNA levels in the model organism *Thermus thermophilus* HB8. *BMC Genomics* 15, 1–14. <https://doi.org/10.1186/1471-2164-15-386>
- Okabe, S., Okayama, N., Savichtcheva, O., Ito, T., 2007. Quantification of host-specific *Bacteroides-Prevotella* 16S rRNA genetic markers for assessment of fecal pollution in freshwater. *Appl. Microbiol. Biotechnol.* 74, 890–901. <https://doi.org/10.1007/s00253-006-0714-x>
- Ontario Ministry of Northern Development, Mines, Natural Resources and Forestry, 2022. Make a Topographic Map. Retrieved April 1, 2022, from https://www.lnoapplications.lrc.gov.on.ca/MakeATopographicMap/index.html?viewer=Make_A_Topographic_Map.MATM
- Pawlowski, J., Bruce, K., Panksep, K., Aguirre, F.I., Amalfitano, S., Apothéloz-Perret-Gentil, L., Baussant, T., Bouchez, A., Carugati, L., Cermakova, K., Cordier, T., Corinaldesi, C., Costa, F.O., Danovaro, R., Dell’Anno, A., Duarte, S., Eisendle, U., Ferrari, B.J.D., Frontalini, F., Frühe, L., Haegerbaeumer, A., Kisand, V., Krolicka, A., Lanzén, A., Leese, F., Lejzerowicz, F., Lyautey, E., Maček, I., Sagova-Marečková, M., Pearman, J.K., Pochon, X., Stoeck, T., Vivien, R., Weigand, A., Fazi, S., 2022. Environmental DNA metabarcoding for benthic

- monitoring: A review of sediment sampling and DNA extraction methods. *Sci. Total Environ.* 818. <https://doi.org/10.1016/j.scitotenv.2021.151783>
- Perkins, T.L., Perrow, K., Rajko-Nenow, P., Jago, C.F., Jones, D.L., Malham, S.K., McDonald, J.E., 2016. Decay rates of faecal indicator bacteria from sewage and ovine faeces in brackish and freshwater microcosms with contrasting suspended particulate matter concentrations. *Sci. Total Environ.* 572, 1645–1652. <https://doi.org/10.1016/j.scitotenv.2016.03.076>
- Phelan, S., Soni, D., Morales Medina, W.R., Fahrenfeld, N.L., 2019. Comparison of qPCR and amplicon sequencing based methods for fecal source tracking in a mixed land use estuarine watershed. *Environ. Sci. Water Res. Technol.* 5, 2108–2123. <https://doi.org/10.1039/c9ew00719a>
- Probandt, D., Eickhorst, T., Ellrott, A., Amann, R., Knittel, K., 2018. Microbial life on a sand grain: From bulk sediment to single grains. *ISME J.* 12, 623–633. <https://doi.org/10.1038/ismej.2017.197>
- Rodrigues, C., Cunha, M.Â., 2017. Assessment of the microbiological quality of recreational waters: indicators and methods. *Euro-Mediterranean J. Environ. Integr.* 2. <https://doi.org/10.1007/s41207-017-0035-8>
- RStudio Team, 2021. RStudio: Integrated Development Environment for R. RStudio, PBC, Boston, MA, URL <http://www.rstudio.com/>
- Russo, T.P., Pace, A., Varriale, L., Borrelli, L., Gargiulo, A., Pompameo, M., Fioretti, A., Dipineto, L., 2021. Prevalence and antimicrobial resistance of enteropathogenic bacteria in yellow-legged gulls (*Larus michahellis*) in southern Italy. *Animals* 11, 1–9. <https://doi.org/10.3390/ani11020275>
- Rytkönen, A., Tiwari, A., Hokajärvi, A.M., Uusheimo, S., Vepsäläinen, A., Tulonen, T., Pitkänen, T., 2021. The use of ribosomal RNA as a microbial source tracking target highlights the assay host-specificity requirement in water quality assessments. *Front. Microbiol.* 12, 1–16. <https://doi.org/10.3389/fmicb.2021.673306>
- Shahraki, A.H., Chaganti, S.R., Heath, D., 2019a. Assessing high-throughput environmental DNA extraction methods for meta-barcode characterization of aquatic microbial communities. *J. Water Health* 17, 37–49. <https://doi.org/10.2166/wh.2018.108>
- Shahraki, A.H., Heath, D., Chaganti, S.R., 2019b. Recreational water monitoring: Nanofluidic qRT-PCR chip for assessing beach water safety. *Environ. DNA* 1, 305–315. <https://doi.org/10.1002/edn3.30>
- Sinigalliano, C., Kim, K., Gidley, M., Yuknavage, K., Knee, K., Palacios, D., Bautista, C.,

- Bonacolta, A., Lee, H.W., Maurin, L., 2021. Microbial source tracking of fecal indicating bacteria in coral reef waters, recreational waters, and groundwater of Saipan by real-time quantitative PCR. *Front. Microbiol.* 11, 1–20. <https://doi.org/10.3389/fmicb.2020.596650>
- Soumastre, M., Piccini, J., Rodríguez-Gallego, L., González, L., Rodríguez-Graña, L., Calliari, D., Piccini, C., 2022. Spatial and temporal dynamics and potential pathogenicity of fecal coliforms in coastal shallow groundwater wells. *Environ. Monit. Assess.* 194. <https://doi.org/10.1007/s10661-021-09672-0>
- Staley, Z.R., Boyd, R.J., Shum, P., Edge, T.A., 2018. Microbial source tracking using quantitative and digital PCR to identify sources of fecal contamination in stormwater, river water, and beach water in a Great Lakes area of concern. *Appl. Environ. Microbiol.* 84. <https://doi.org/10.1128/AEM.01634-18>
- Susi, H., Laine, A.L., 2021. Agricultural land use disrupts biodiversity mediation of virus infections in wild plant populations. *New Phytol.* 230, 2447–2458. <https://doi.org/10.1111/nph.17156>
- Tanvir Pasha, A.B.M., Hinojosa, J., Phan, D., Lopez, A., Kapoor, V., 2020. Detection of human fecal pollution in environmental waters using human mitochondrial DNA and correlation with general and human-associated fecal genetic markers. *J. Water Health* 18, 8–18. <https://doi.org/10.2166/wh.2019.197>
- Ting, A.S.Y., Zoqratt, M.Z.H.M., Tan, H.S., Hermawan, A.A., Talei, A., Khu, S.T., 2021. Bacterial and eukaryotic microbial communities in urban water systems profiled via Illumina MiSeq platform. *3 Biotech* 11, 1–15. <https://doi.org/10.1007/s13205-020-02617-3>
- Tiwari, A., Kauppinen, A., Pitkänen, T., 2019. Decay of *Enterococcus faecalis*, *Vibrio cholerae* and MS2 coliphage in a laboratory mesocosm under brackish beach conditions. *Front. Public Heal.* 7, 1–12. <https://doi.org/10.3389/fpubh.2019.00269>
- Tiwari, A., Lipponen, A., Hokajärvi, A.-M., Luomala, O., Sarekoski, A., Rytönen, A., Österlund, P., Al-Hello, H., Juutinen, A., Miettinen, I.T., Savolainen-Kopra, C., Pitkänen, T., 2022. Detection and quantification of SARS-CoV-2 RNA in wastewater influent in relation to reported COVID-19 incidence in Finland. *Water Res.* 215, 118220. <https://doi.org/10.1016/j.watres.2022.118220>
- VanMensel, D., Chaganti, S.R., Droppo, I.G., Weisener, C.G., 2020. Exploring bacterial pathogen community dynamics in freshwater beach sediments: A tale of two lakes. *Environ. Microbiol.* 22, 568–583. <https://doi.org/10.1111/1462-2920.14860>
- VanMensel, D., Droppo, I.G., Weisener, C.G., 2021. Identifying chemolithotrophic and pathogenic-related gene expression within suspended sediment flocs in freshwater

- environments: A metatranscriptomic assessment. *Sci. Total Environ.* 807, 150996.
<https://doi.org/10.1016/j.scitotenv.2021.150996>
- Vogel, L.J., Carroll, D.M.O., Edge, T.A., Robinson, C.E., 2016. Release of *Escherichia coli* from foreshore sand and pore water during intensified wave conditions at a recreational beach.
<https://doi.org/10.1021/acs.est.6b00707>
- Wang, C., Hu, R., Strong, P.J., Zhuang, W., Huang, W., Luo, Z., Yan, Q., He, Z., Shu, L., 2021. Prevalence of antibiotic resistance genes and bacterial pathogens along the soil–mangrove root continuum. *J. Hazard. Mater.* 408, 124985.
<https://doi.org/10.1016/j.jhazmat.2020.124985>
- Wexler, H.M., 2007. *Bacteroides*: the Good, the Bad, and the Nitty-Gritty. *Clin. Microbiol. Rev.* 20, 593–621. <https://doi.org/10.1128/CMR.00008-07>
- Wood, S.A., Pochon, X., Ming, W., von Ammon, U., Woods, C., Carter, M., Smith, M., Inglis, G., Zaiko, A., 2019. Considerations for incorporating real-time PCR assays into routine marine biosecurity surveillance programmes: A case study targeting the Mediterranean fanworm (*Sabella spallanzanii*) and club tunicate (*Styela clava*). *Genome* 62, 137–146.
<https://doi.org/10.1139/gen-2018-0021>
- Wyer, M.D., Kay, D., Morgan, H., Naylor, S., Clark, S., Watkins, J., Davies, C.M., Francis, C., Osborn, H., Bennett, S., 2018. Within-day variability in microbial concentrations at a UK designated bathing water: Implications for regulatory monitoring and the application of predictive modelling based on historical compliance data. *Water Res.* X 1, 100006.
<https://doi.org/10.1016/j.wroa.2018.10.003>
- Zhang, S., Chen, Shuling, Rehman, M.U., Yang, H., Yang, Z., Wang, M., Jia, R., Chen, Shun, Liu, M., Zhu, D., Zhao, X., Wu, Y., Yang, Q., Huan, J., Ou, X., Mao, S., Gao, Q., Sun, D., Tian, B., Cheng, A., 2021. Distribution and association of antimicrobial resistance and virulence traits in *Escherichia coli* isolates from healthy waterfowls in Hainan, China. *Ecotoxicol. Environ. Saf.* 220, 112317. <https://doi.org/10.1016/j.ecoenv.2021.112317>
- Zhang, X.H., Ahmad, W., Zhu, X.Y., Chen, J., Austin, B., 2021. Viable but nonculturable bacteria and their resuscitation: implications for cultivating uncultured marine microorganisms. *Mar. Life Sci. Technol.* 3, 189–203. <https://doi.org/10.1007/s42995-020-00041-3>

CHAPTER 6: CONCLUSIONS, LIMITATIONS, AND FUTURE RECOMMENDATIONS

CHAPTER 6: CONCLUSIONS, LIMITATIONS, AND FUTURE RECOMMENDATIONS

6.1 Major Contributions to Environmental Science

Pathogenic contamination of aquatic ecosystems is a concern around the globe as anthropogenic activities (e.g., increasing agricultural practices; increasing population; release of wastewater) and climate change (e.g., increasing temperatures and precipitation events) lead to amplified concentration and shifts in activity of harmful microorganisms in the environment (Brandão et al., 2022; Levy et al., 2016; Susi and Laine, 2021; Trivedi et al., 2016). Microbial contamination can result in detrimental outcomes to overall ecosystem health, but also poses great risk to human health and safety given our reliance on important water resources, such as drinking water (Åström et al., 2015), groundwater (Mattioli et al., 2021; Soumastre et al., 2022), and recreational water (Rytönen et al., 2021; Sinigalliano et al., 2021). Therefore, integration of a multidisciplinary themed research approach is imperative. This dissertation expands our understanding of the potential human health risks related to recreational water using high-resolution microbial assessments, such as expansive community profiling and gene expression studies through meta-omics approaches. The research draws increased focus to the importance of sediment-microbial interactions, with subsequent physical and biological dynamics that drive the erosion, transport, and fate of microbes/pathogens within the water column and impact on their survival, growth, and persistence.

The establishment of an aquatic microbial baseline signature is an important criterion to accurately assess how the natural microbiota governs ecosystem health, function, and fate (Astudillo-García et al., 2019; Lear et al., 2009). Such baselines provide a meaningful research approach for identifying causal environmental changes or perturbations, such as the introduction of contaminants (biological or otherwise), or physicochemical fluctuations (e.g., temperature, DO, turbidity). An established baseline allows for method development providing quicker

detection and improving remediation efforts. The definition of *microbial baseline*, however, is difficult to decipher because natural ecosystems, like marine or freshwater shorelines, are ever-changing and adapting to their dynamic surroundings. Nothing in nature is static, especially at the microscopic level. It is also challenging to determine comparison reference locations for the same reasons. Therefore, as important as this information is, its determination may be considered subjective depending on the environmental characteristics used to define the reference or baseline. Chapter 2 of this dissertation focused on sequencing and analyses of the 16S rRNA gene (specifically the V5/V6 hypervariable region) of both DNA and RNA isolated from a series of bed sediment samples from GL freshwater beaches to establish the sediment microbial biosignature. The purpose of this work was to not only characterize the microbial signature of these habitats, but also to help guide the research through metatranscriptomics to observe the relevant gene expression within the suspended and bed sediment compartments with relation to human health aspects in recreational waters. This chapter revealed little to no variation in biodiversity (i.e., Shannon-Weiner index) on a spatial scale around WEC but showed a steady increase of biodiversity from spring into fall at all beaches, corroborating previous work on this topic (Fang et al., 2022; Hicks et al., 2018; Oest et al., 2018; Yi et al., 2021). Taxonomic assessment revealed Proteobacteria to be the most dominant bacterial phylum in these freshwater sediments, with Gammaproteobacteria (class) and Betabacteriales (order) having the greatest representations within this phylum. The main conclusion of Chapter 2 was that, although both DNA and cDNA (i.e., RNA) datasets demonstrated general similarities in biodiversity and community composition across all beaches examined, the DNA component underestimated microbial activity within the bed sediment. Not only does this highlight bed sediment as a habitat for microbial activity but supports the importance of analysing the RNA fraction of environmental samples as a complement to DNA or culture-based methods for microbial water quality assessments, especially when it pertains to potential human health risks. As mentioned, further investigation of this active community through using metatranscriptomics was applied

(Chapters 3 and 4) to examine sediment microbial nuances that may contribute to water quality variations.

Transcriptomic approaches to characterize microbial structure and function of freshwater bed (Chapter 3) and suspended (Chapter 4) sediment provide an opportunity to simultaneously assess basic microbial physiology and metabolic processes as well as the expression of genes with pathogenic relevance in these environments. Both Chapters 3 and 4 describe novel research in exploring the functioning bacteria of freshwater sediments and demonstrating the utility of high-throughput sequencing and omics approaches on natural media largely unexplored in such great depth. We used metatranscriptomics to characterize the chemolithotrophic activity of the sedimentary bacterial communities and highlighted which pathogenic-related genes demonstrated expression in these environments. The most important implication from Chapters 3 and 4 was the detection of genes which have been identified in bacterial pathogenic-related activity. Chapter 3 revealed expression of genes with known involvement in *Salmonella* infection and pertussis as well as antimicrobial (i.e., CAMP) resistance from within freshwater bed sediment. Chapter 4 showed that SS was associated with expression of genes involved in several bacterial infectious disease pathways, most notably *V. cholerae*. These studies revealed the involvement of the sediment compartment to harbour potentially pathogenic microbes, aiding in our understanding of sediment-microbe relationships and overall freshwater ecosystem functionality. These chapters are among the first studies to successfully employ transcriptomic approaches on aquatic sediment *in situ*, especially the suspended fraction (Chapter 4).

The introduction of allochthonous microbes (including pathogens) to natural waters and shorelines can be attributed to both point and nonpoint sources (NPSs). Although point sources of contamination, such as untreated discharge from WWTPs (Mbanga et al., 2020), are easier to identify, mitigate, and manage, NPSs are often less tangible since they are a cumulation of contributions (e.g., feces of waterfowl; agricultural runoff) collected over the entire watershed (Almakki et al., 2019; Hooda et al., 2000; Montgomery, 2007; Yuan et al., 2017). As such, NPSs

are less understood than point sources, are more complex, diverse, and require greater intervention for improvement and reclamation strategies. Thus, research on NPS microbial contamination to aquatic shorelines is of great importance yet is currently lacking in the literature, especially regarding sediment-associated microbial contaminants. Chapter 5 of this dissertation addresses this knowledge gap with a multiplex qPCR approach using nanofluidic technology focused on RNA isolated from both bed and suspended freshwater sediment samples. Gene targets included FIB (*Enterococcus*, *E. coli*), MST genes (from human, canine, cattle, and avian sources), and several virulence factors of waterborne bacterial pathogens. Although virulence factors did not reveal detection from our mRNA targets, the results from this chapter provide spatiotemporal data on rRNA-based FIB and MST genes from the sediment of GL shorelines. This data is valuable in advancing our understanding of freshwater sediment-microbe associations with regards to potential human health risks in recreational waters. More notably, it demonstrates a proof-of-concept novel approach to studying these types of natural systems with targeted nanofluidic multiplex qPCR that is faster than traditional methods with the prospect for greater optimization (i.e., multiple specific gene sequences can be simultaneously targeted to suit individual research objectives).

6.2 Research Limitations

While the research presented throughout this dissertation provides new knowledge regarding sediment-microbe relationships and the active microbial component associated with the sediment compartment (bed and suspended) of freshwater ecosystems, there are drawbacks that must be acknowledged when considering the results reported. Primarily, it is important to recognise that the use of 16S rRNA as a marker gene in microbial ecology, while widely used and accepted, has limitations. Most notably is that microbial genomes have varying 16S rRNA gene copy numbers (GCNs) and sequence variation between closely related taxa or even within a

genome between copy numbers. Of bacterial genomes, Proteobacteria (Gammaproteobacteria in particular) have been reported to contain some of the highest 16S rRNA GCNs (5.8 ± 2.8) and are therefore disproportionately represented within the community (Větrovský and Baldrian, 2013). While this information likely affects the community profiles determined in Chapters 2 and 3, a recent paper recommends against correcting for the variation in GCNs in microbiome surveys due to the poor performance of existing tools that claim to estimate and adjust for GCN (Louca et al., 2018). Furthermore, considering that the microbial profiles determined in Chapter 2 were explicitly compared between the DNA and RNA (cDNA) datasets of the same samples, the proportion of community members should theoretically remain constant because GCNs would be the same for DNA and RNA from the same organism. Regardless, this inadequacy concerning the use of 16S rRNA as a marker gene in microbial ecology studies must be considered when interpreting community structure of environmental microbiomes. In such cases, supplemental assessments, like metagenomics, can offer supportive data on microbial composition.

Another major limitation to consider from the research discussed in this dissertation is the use of mRNA to study the activity of waterborne pathogens within freshwater sediment *in situ* (Chapter 5). For example, virulence factors might not be expected to be expressed if the pathogen is not actively infecting a host, yet the microorganism may still be metabolically active and hold the potential for infection if the opportunity arose. In fact, this may explain why we did not detect any virulence factors from the sediment samples using the nanofluidic qPCR approach in our study, suggesting that our results cannot be interpreted as there being no active pathogens in our samples, but simply no active infection with respect to the pathogens targeted. Regardless of this limitation, our results still provide valuable information regarding the pathogenicity (or lack of) targeted waterborne pathogens associated with freshwater sediment. Moreover, the novelty of the method employed in this chapter demonstrated an optimized and quick approach for targeted transcriptomics of *in situ* environmental samples that should be explored further.

6.3 Future Recommendations

The research presented throughout this dissertation encompasses a large range of microbial information, specifically considering the metatranscriptomic investigations in Chapters 3 and 4. Metatranscriptomics is the application of advanced high-throughput sequencing which provides the whole gene expression profile of entire complex microbial communities. It allows researchers to examine the full extent of microbial activities at a single time point *in situ* (Moran, 2009). The amount of genetic information gained from this approach is enormous (i.e., a typical metatranscriptome dataset contains many millions of RNA-seq reads; Bashardes et al., 2016) and can be overwhelming if there is not a specific objective to address and focus the bioinformatics. With this in mind, the data obtained from the metatranscriptomics in both Chapters 3 and 4 were focused on bacterial metabolic activities and genes with pathogenic relevance. However, this only scratched the surface of the dataset. There are many other microbial functional categories that could (and should) be explored within these datasets to gain a more comprehensive understanding of the functioning microbiome, including cell signaling and communication (e.g., quorum sensing), defense mechanisms, and cell motility (e.g., bacterial chemotaxis). Furthermore, the pathogenicity potential of the viral community should also be explored as emerging and re-emerging viral diseases from waterborne human pathogenic viruses are also a serious threat to human health (Louten, 2016; Rodríguez-Lázaro et al., 2012; Zhang et al., 2022).

Another relevant and interesting area of research that needs to be explored with relation to human health risks from recreational waters is the study of microplastics in aquatic systems. The toxic effect of microplastics on living organisms is presenting as a serious and growing environmental issue around the world. However, microplastic contamination in aquatic environments also provides new microbial niches for attachment of bacteria (Yang et al., 2020). Similar to SS, it has been recognized as a potential vector for microbial/pathogen transport (Viršek et al., 2017); unlike SS, however, it provides a very different attachment surface and

therefore involves different mechanisms for microbial association. Research pertaining to this subject is still new and developing (Ayush et al., 2022; Bhagwat et al., 2021).

Concerning the treatment of waterborne bacterial pathogens and a possible solution for safe recreational water, phage therapy is an exciting, rediscovered field that may present as a viable and beneficial route to eliminate harmful environmental bacteria. Phage therapy is the use of bacteriophages for the treatment of pathogenic bacterial infections. The advantage and versatility of this approach has long been recognised, yet it is now being considered for many various uses, including human health, agriculture, and protection of fragile ecosystems. Previous studies have demonstrated its utility against vibriosis (Wang et al., 2017) and cottonmouth disease (Prasad et al., 2011) in fish, and has been stated that it may soon play an important role in the safeguarding of aquatic environments (Doss et al., 2017).

Environmental microbiology and microbial ecology have been progressive and evolving fields of science since their inception in the late nineteenth century. Both Martinus Beijerinck and Sergei Winogradsky are credited with first identifying and describing environmental microorganisms and the essential biogeochemical processes they regulate throughout the natural environment. At the time, their scientific contributions and achievements were overshadowed by those of their contemporaries, Louis Pasteur and Robert Koch, because their work did not concern human disease. However, modern-day research strongly employs a multidisciplinary approach, and as such, these two, once removed fields of microbiology are now merging to investigate human health implications regarding waterborne pathogens and recreational water use. The blending of these disciplines is a driving force that has led to water quality regulations and safety assessments and can be attributed to improving our quality and standard of life. Furthermore, Winogradsky's legacy to modern microbiology is arguably his recognition that microbes must be studied *in situ* or as close as possible to their natural habitat if we truly want to understand their role in catalyzing chemical changes in complex natural ecosystems (Dworkin, 2012).

The principles established by Beijerinck and Winogradsky remain at the forefront of environmental microbial studies and can be seen throughout the research described in this dissertation. Insights gathered from this research thesis emphasize the relevance of freshwater sediment-microbe relationships and their influence on water quality and human health risks. The results presented, advance our understanding of environmental science as a whole and add important insights to the complex natural world surrounding us and the central function of the biological element we cannot see – the *environmental microbiome*.

References

- Almakki, A., Jumas-Bilak, E., Marchandin, H., Licznar-Fajardo, P., 2019. Antibiotic resistance in urban runoff. *Sci. Total Environ.* 667, 64–76.
<https://doi.org/10.1016/j.scitotenv.2019.02.183>
- Åström, J., Pettersson, T.J.R., Reischer, G.H., Norberg, T., Hermansson, M., 2015. Incorporating expert judgments in utility evaluation of bacteroidales qpcr assays for microbial source tracking in a drinking water source. *Environ. Sci. Technol.* 49, 1311–1318.
<https://doi.org/10.1021/es504579j>
- Astudillo-García, C., Hermans, S.M., Stevenson, B., Buckley, H.L., Lear, G., 2019. Microbial assemblages and bioindicators as proxies for ecosystem health status: potential and limitations. *Appl. Microbiol. Biotechnol.* 103, 6407–6421. <https://doi.org/10.1007/s00253-019-09963-0>
- Ayush, P.T., Ko, J.H., Oh, H.S., 2022. Characteristics of Initial Attachment and Biofilm Formation of *Pseudomonas aeruginosa* on Microplastic Surfaces. *Appl. Sci.* 12.
<https://doi.org/10.3390/app12105245>
- Bashiardes, S., Zilberman-Schapira, G., Elinav, E., 2016. Use of metatranscriptomics in microbiome research. *Bioinform. Biol. Insights* 10, 19–25.
<https://doi.org/10.4137/BBI.S34610>
- Bhagwat, G., O'Connor, W., Grainge, I., Palanisami, T., 2021. Understanding the Fundamental Basis for Biofilm Formation on Plastic Surfaces: Role of Conditioning Films. *Front. Microbiol.* 12, 1–10. <https://doi.org/10.3389/fmicb.2021.687118>
- Brandão, J., Weiskerger, C., Valério, E., Pitkänen, T., Meriläinen, P., Avolio, L., Heaney, C.D., Sadowsky, M.J., 2022. Climate Change Impacts on Microbiota in Beach Sand and Water: Looking Ahead. *Int. J. Environ. Res. Public Health* 19.
- Doss, J., Culbertson, K., Hahn, D., Camacho, J., Barekzi, N., 2017. A review of phage therapy against bacterial pathogens of aquatic and terrestrial organisms. *Viruses* 9.
<https://doi.org/10.3390/v9030050>
- Dworkin, M., 2012. Sergei Winogradsky: A founder of modern microbiology and the first microbial ecologist. *FEMS Microbiol. Rev.* 36, 364–379. <https://doi.org/10.1111/j.1574-6976.2011.00299.x>
- Fang, G., Yu, H., Sheng, H., Chen, C., Tang, Y., Liang, Z., 2022. Seasonal variations and co-occurrence networks of bacterial communities in the water and sediment of artificial habitat in Laoshan Bay, China. *PeerJ* 9, 1–25. <https://doi.org/10.7717/peerj.12705>

- Hicks, N., Liu, X., Gregory, R., Kenny, J., Lucaci, A., Lenzi, L., Paterson, D.M., Duncan, K.R., 2018. Temperature driven changes in benthic bacterial diversity influences biogeochemical cycling in coastal sediments. *Front. Microbiol.* 9. <https://doi.org/10.3389/fmicb.2018.01730>
- Hooda, P.S., Edwards, A.C., Anderson, H.A., Miller, A., 2000. A review of water quality concerns in livestock farming areas. *Sci. Total Environ.* 250, 143–167. [https://doi.org/10.1016/S0048-9697\(00\)00373-9](https://doi.org/10.1016/S0048-9697(00)00373-9)
- Lear, G., Boothroyd, I.K.G., Turner, S.J., Roberts, K., Lewis, G.D., 2009. A comparison of bacteria and benthic invertebrates as indicators of ecological health in streams. *Freshw. Biol.* 54, 1532–1543. <https://doi.org/10.1111/j.1365-2427.2009.02190.x>
- Levy, K., Woster, A.P., Goldstein, R.S., Carlton, E.J., 2016. Untangling the Impacts of Climate Change on Waterborne Diseases: A Systematic Review of Relationships between Diarrheal Diseases and Temperature, Rainfall, Flooding, and Drought. *Environ. Sci. Technol.* 50, 4905–4922. <https://doi.org/10.1021/acs.est.5b06186>
- Louca, S., Doebeli, M., Parfrey, L.W., 2018. Correcting for 16S rRNA gene copy numbers in microbiome surveys remains an unsolved problem. *Microbiome* 6, 1–12. <https://doi.org/10.1186/s40168-018-0420-9>
- Louten, J., 2016. Emerging and Reemerging Viral Diseases, in: *Essential Human Virology*. pp. 291–310.
- Mattioli, M.C., Benedict, K.M., Murphy, J., Kahler, A., Kline, K.E., Longenberger, A., Mitchell, P.K., Watkins, S., Berger, P., Shanks, O.C., Barrett, C.E., Barclay, L., Hall, A.J., Hill, V., Weltman, A., 2021. Identifying septic pollution exposure routes during a waterborne norovirus outbreak - A new application for human-associated microbial source tracking qPCR. *J. Microbiol. Methods* 180, 106091. <https://doi.org/10.1016/j.mimet.2020.106091>
- Mbanga, J., Abia, A.L.K., Amoako, D.G., Essack, S.Y., 2020. Quantitative microbial risk assessment for waterborne pathogens in a wastewater treatment plant and its receiving surface water body. *BMC Microbiol.* 20, 1–12. <https://doi.org/10.1186/s12866-020-02036-7>
- Montgomery, D.R., 2007. Soil erosion and agricultural sustainability. *Proc. Natl. Acad. Sci. U. S. A.* 104, 13268–13272. <https://doi.org/10.1073/pnas.0611508104>
- Moran, M.A., 2009. Metatranscriptomics: Eavesdropping on Complex Microbial Communities. *Microbe* 4, 329–335.
- Oest, A., Alsaffar, A., Fenner, M., Azzopardi, D., Tiquia-Arashiro, S.M., 2018. Patterns of change in metabolic capabilities of sediment microbial communities in river and lake ecosystems. *Int. J. Microbiol.* 2018, 5–7. <https://doi.org/10.1155/2018/6234931>
- Prasad, Y., Arpana, Kumar, D., Sharma, A.K., 2011. Lytic bacteriophages specific to

- Flavobacterium columnare rescue catfish, *Clarias batrachus* (Linn.) from columnaris disease. *J. Environ. Biol.* 32, 161–168.
- Rodríguez-Lázaro, D., Cook, N., Ruggeri, F.M., Sellwood, J., Nasser, A., Nascimento, M.S.J., D’Agostino, M., Santos, R., Saiz, J.C., Rzezutka, A., Bosch, A., Gironés, R., Carducci, A., Muscillo, M., Kovač, K., Diez-Valcarce, M., Vantarakis, A., von Bonsdorff, C.H., de Roda Husman, A.M., Hernández, M., van der Poel, W.H.M., 2012. Virus hazards from food, water and other contaminated environments. *FEMS Microbiol. Rev.* 36, 786–814. <https://doi.org/10.1111/j.1574-6976.2011.00306.x>
- Rytönen, A., Tiwari, A., Hokajärvi, A.M., Uusheimo, S., Vepsäläinen, A., Tulonen, T., Pitkänen, T., 2021. The Use of Ribosomal RNA as a Microbial Source Tracking Target Highlights the Assay Host-Specificity Requirement in Water Quality Assessments. *Front. Microbiol.* 12, 1–16. <https://doi.org/10.3389/fmicb.2021.673306>
- Sinigalliano, C., Kim, K., Gidley, M., Yuknavage, K., Knee, K., Palacios, D., Bautista, C., Bonacolta, A., Lee, H.W., Maurin, L., 2021. Microbial Source Tracking of Fecal Indicating Bacteria in Coral Reef Waters, Recreational Waters, and Groundwater of Saipan by Real-Time Quantitative PCR. *Front. Microbiol.* 11, 1–20. <https://doi.org/10.3389/fmicb.2020.596650>
- Soumastre, M., Piccini, J., Rodríguez-Gallego, L., González, L., Rodríguez-Graña, L., Calliari, D., Piccini, C., 2022. Spatial and temporal dynamics and potential pathogenicity of fecal coliforms in coastal shallow groundwater wells. *Environ. Monit. Assess.* 194. <https://doi.org/10.1007/s10661-021-09672-0>
- Susi, H., Laine, A.L., 2021. Agricultural land use disrupts biodiversity mediation of virus infections in wild plant populations. *New Phytol.* 230, 2447–2458. <https://doi.org/10.1111/nph.17156>
- Trivedi, P., Delgado-Baquerizo, M., Anderson, I.C., Singh, B.K., 2016. Response of soil properties and microbial communities to agriculture: Implications for primary productivity and soil health indicators. *Front. Plant Sci.* 7, 1–13. <https://doi.org/10.3389/fpls.2016.00990>
- Větrovský, T., Baldrian, P., 2013. The Variability of the 16S rRNA Gene in Bacterial Genomes and Its Consequences for Bacterial Community Analyses. *PLoS One* 8, 1–10. <https://doi.org/10.1371/journal.pone.0057923>
- Viršek, M.K., Lovšin, M.N., Koren, Š., Kržan, A., Peterlin, M., 2017. Microplastics as a vector for the transport of the bacterial fish pathogen species *Aeromonas salmonicida*. *Mar. Pollut. Bull.* 125, 301–309. <https://doi.org/10.1016/j.marpolbul.2017.08.024>
- Wang, Y., Barton, M., Elliott, L., Li, X., Abraham, S., O’Dea, M., Munro, J., 2017.

- Bacteriophage therapy for the control of *Vibrio harveyi* in greenlip abalone (*Haliotis laevigata*). *Aquaculture* 473, 251–258. <https://doi.org/10.1016/j.aquaculture.2017.01.003>
- Yang, Y., Liu, W., Zhang, Z., Grossart, H.P., Gadd, G.M., 2020. Microplastics provide new microbial niches in aquatic environments. *Appl. Microbiol. Biotechnol.* 104, 6501–6511. <https://doi.org/10.1007/s00253-020-10704-x>
- Yi, Y., Lin, C., Wang, W., Song, J., 2021. Habitat and seasonal variations in bacterial community structure and diversity in sediments of a Shallow lake. *Ecol. Indic.* 120, 106959. <https://doi.org/10.1016/j.ecolind.2020.106959>
- Yuan, Q., Guerra, H.B., Kim, Y., 2017. An investigation of the relationships between rainfall conditions and pollutant wash-off from the paved road. *Water (Switzerland)* 9. <https://doi.org/10.3390/w9040232>
- Zhang, M., Altan-Bonnet, N., Shen, Y., Shuai, D., 2022. Waterborne Human Pathogenic Viruses in Complex Microbial Communities: Environmental Implication on Virus Infectivity, Persistence, and Disinfection. *Environ. Sci. Technol.* 56, 5381–5389. <https://doi.org/10.1021/acs.est.2c00233>

APPENDICES

APPENDIX A: SUPPLEMENTAL INFORMATION FOR CHAPTER 2

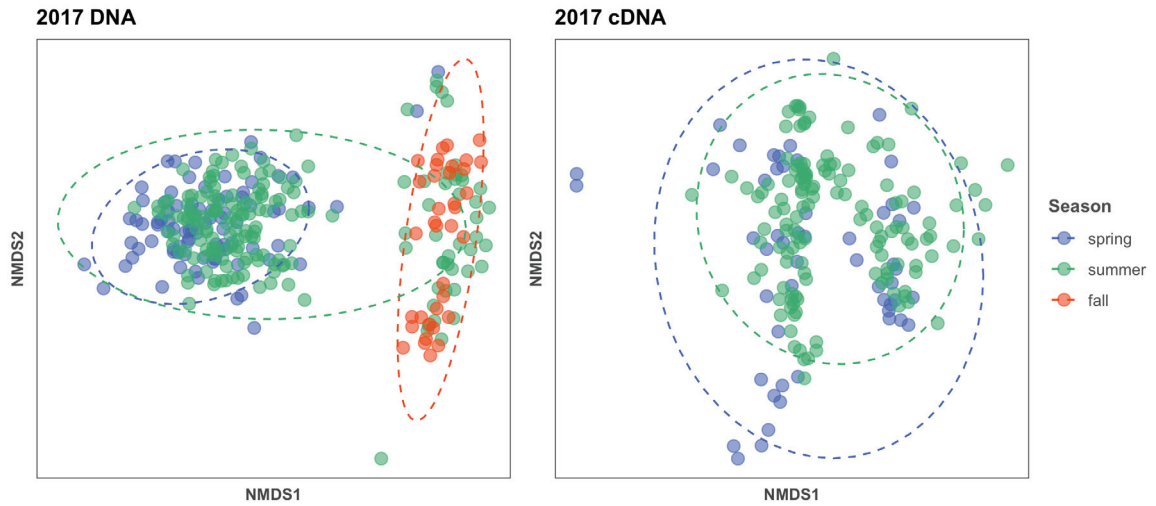


Figure A-1: NMDS ordination plot of bacterial community composition in the bed sediment of freshwater beaches in WEC. DNA (left) and cDNA (right) datasets are displayed, illustrating beta diversity between sampling seasons (spring, summer, fall). Ellipses represent 95% of samples included.

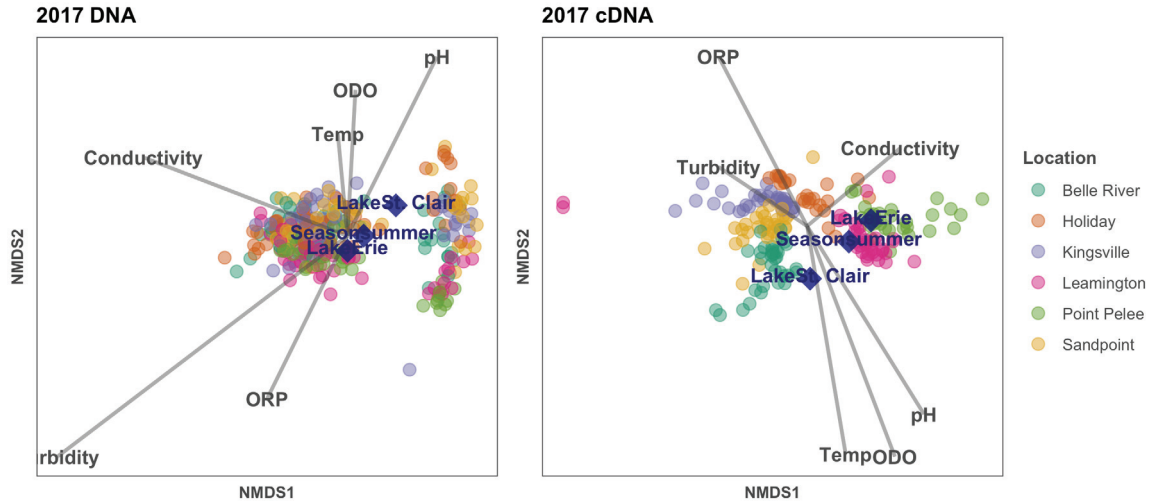


Figure A-2: NMDS ordination plot of bacterial community composition in the bed sediment of freshwater beaches with environmental factors (grey) included using envfit. DNA (left) and cDNA (right) datasets are displayed, illustrating beta diversity between the six beaches sampled throughout WEC and the influence of select environmental parameters. Categorical factors of Lake and Season are shown with blue diamond symbols. Sample dates are combined for the year.

Table A-1: Physicochemical parameters of the water column. Measurements were recorded at each sediment sample collection for the six WEC beaches studied. Blank cells indicate missing data due to faulty equipment or unreliable probe calibration. DO, dissolved oxygen; ORP, oxidation-reduction potential.

Beach	Date (MM/DD)	Temperature (°C)	pH	DO (% sat.)	Conductivity ($\mu\text{S cm}^{-1}$)	ORP (mV)	Turbidity (NTU)
Belle River	04/12	12.37	8.97		309	128	
	06/01	21.88	7.17		355.8	141	10.49
	06/13	25.02	7.61		298.8	89	
	07/13						11.4
	07/26	24.5	8.85	123.6	256.1	163.8	13.6
	08/10						
	08/31	21.28	8.12	116.9		-111.5	39.6
	09/13	20.93	8.26	107.2		-119.5	6.6
	11/08	11.07	7.6	96		-80.2	264.9
Holiday	04/12	11.18	7.56		315	213	
	06/01	17.47	7.07		261.8	172	21.4
	06/13	23.47	7.29		247.6	142	
	07/13						77.4
	07/26	22.9	8.38	96.2	217.2	199.5	44
	08/10						
	08/31	22.91	7.51	112.8		-76.1	48.8
	09/13	18.59	8	102.9		-104.2	34.7
	11/08	7.84	8.2	86.5		-112.9	15.1
Kingsville	04/12	12.08	7.86		886.5	201	
	06/01	18.26	7.13		667.4	178	17.6
	06/13	22.69	7.28		874.9	141	
	07/13						31
	07/26	21.4	8.19	95.9	559	180.7	21.7
	08/10						
	08/31	21.34	7.63	114.5		-83.1	12.5
	09/13	19.46	7.84	108.4		-94.7	57.3
	11/08	7.55	7.26	91.8		-60.6	234.5
Leamington	04/12	9.43	8.9		281.6	139	
	06/01	18.53	7.18		302.2	146	24.3
	06/13	23.95	7.54		287.8	104	
	07/13						36.3
	07/26	22.5	8.35	96.6	233.5	184.3	4.5
	08/10						
	08/31	22.65	7.85	121.5		-96.2	8.7
	09/13	20.06	8.05	105.3		-107.3	8.6
	11/08	9.61	7.48	97.4		-72.9	15.7
Point Pelee	06/01	20.05	7.22		298.7	138	25.9
	06/13	22.42	7.92		265.2	90	
	07/13						21
	07/26	23.4	8.4	96.7	231.8	196.7	2.3
	08/10						
	08/31	23	7.98	119.3		-103.6	7.6
	09/13	19.96	8.19	108.7		-115.6	17.6
	11/08	10.66	7.52	101.7		-75.7	16.7
Sandpoint	04/12	12.25	8.95		326.7	118	
	06/01	19.31	7.07		248.7	143	8.17
	06/13	23.95	7.75		270	83	
	07/13						2.82
	07/26	23.6	8.95	116.8	222.1	165.4	3.2
	08/10						
	08/31	21.45	7.93	109.7		-100.2	61.4
	09/13	20.02	8.31	106.1		-122.2	4.6
	11/08	8.35	7.79	90.5		-90.3	78.6

Table A-2: RNA concentrations of individual samples selected for cDNA analyses. Included is basic sample metadata (i.e., collection date and location), the method used for measuring concentration (Bioanalyzer, Qubit, or visualization on agarose gel electrophoresis), and the volume added to the pool of samples for additional normalization prior to sequencing. Volume added was based on agarose gel band intensity; either 2 (dark band), 5 (faint band), or 10 μ L (no visible band).

Sample ID	Collection Date	Location	Concentration (ng/ μ L)	Method	Volume Added (μ L)
WE_2017-04-12_BR_cDNA_1a	2017-04-12	Belle River	#N/A	Gel	2
WE_2017-04-12_BR_cDNA_1b	2017-04-12	Belle River	#N/A	Gel	2
WE_2017-04-12_BR_cDNA_2a	2017-04-12	Belle River	#N/A	Gel	2
WE_2017-04-12_BR_cDNA_2b	2017-04-12	Belle River	#N/A	Gel	2
WE_2017-06-01_BR_cDNA_1a	2017-06-01	Belle River	348	Qubit	5
WE_2017-06-01_BR_cDNA_1b	2017-06-01	Belle River	263	Qubit	2
WE_2017-06-01_BR_cDNA_2a	2017-06-01	Belle River	374	Qubit	2
WE_2017-06-01_BR_cDNA_2b	2017-06-01	Belle River	188	Qubit	2
WE_2017-06-01_BR_cDNA_4a	2017-06-01	Belle River	107	Qubit	5
WE_2017-06-01_BR_cDNA_4b	2017-06-01	Belle River	90.1	Qubit	5
WE_2017-07-13_BR_cDNA_1a	2017-07-13	Belle River	116	Qubit	2
WE_2017-07-13_BR_cDNA_1b	2017-07-13	Belle River	127	Qubit	2
WE_2017-07-13_BR_cDNA_2a	2017-07-13	Belle River	183	Qubit	2
WE_2017-07-13_BR_cDNA_2b	2017-07-13	Belle River	65.6	Qubit	2
WE_2017-07-13_BR_cDNA_4a	2017-07-13	Belle River	67.8	Qubit	2
WE_2017-07-13_BR_cDNA_4b	2017-07-13	Belle River	89.2	Qubit	2
WE_2017-07-26_BR_cDNA_1a	2017-07-26	Belle River	222	Qubit	2
WE_2017-07-26_BR_cDNA_1b	2017-07-26	Belle River	204	Qubit	10
WE_2017-07-26_BR_cDNA_2a	2017-07-26	Belle River	137	Qubit	5
WE_2017-07-26_BR_cDNA_2b	2017-07-26	Belle River	240	Qubit	2
WE_2017-07-26_BR_cDNA_3a	2017-07-26	Belle River	79.5	Qubit	2
WE_2017-07-26_BR_cDNA_3b	2017-07-26	Belle River	85.4	Qubit	2
WE_2017-08-31_BR_cDNA_1a	2017-08-31	Belle River	122	Qubit	2
WE_2017-08-31_BR_cDNA_1b	2017-08-31	Belle River	113	Qubit	2
WE_2017-08-31_BR_cDNA_2a	2017-08-31	Belle River	128	Qubit	2
WE_2017-08-31_BR_cDNA_2b	2017-08-31	Belle River	142	Qubit	2
WE_2017-08-31_BR_cDNA_3a	2017-08-31	Belle River	36.4	Qubit	5
WE_2017-08-31_BR_cDNA_3b	2017-08-31	Belle River	126	Qubit	2
WE_2017-09-13_BR_cDNA_2a	2017-09-13	Belle River	101	Qubit	2
WE_2017-09-13_BR_cDNA_2b	2017-09-13	Belle River	238	Qubit	2
WE_2017-09-13_BR_cDNA_3a	2017-09-13	Belle River	116	Qubit	2
WE_2017-06-01_HD_cDNA_3a	2017-06-01	Holiday	#N/A	Gel	2
WE_2017-06-01_HD_cDNA_3b	2017-06-01	Holiday	#N/A	Gel	2
WE_2017-06-01_HD_cDNA_2a	2017-06-01	Holiday	46.8	Qubit	5
WE_2017-06-01_HD_cDNA_2b	2017-06-01	Holiday	56.7	Qubit	5
WE_2017-07-13_HD_cDNA_1a	2017-07-13	Holiday	0	Qubit	2
WE_2017-07-13_HD_cDNA_2a	2017-07-13	Holiday	11.6	Qubit	2
WE_2017-07-13_HD_cDNA_2b	2017-07-13	Holiday	13.1	Qubit	2
WE_2017-07-13_HD_cDNA_4a	2017-07-13	Holiday	17	Qubit	2
WE_2017-07-13_HD_cDNA_4b	2017-07-13	Holiday	33.4	Qubit	5
WE_2017-07-26_HD_cDNA_1a	2017-07-26	Holiday	44.2	Qubit	2
WE_2017-07-26_HD_cDNA_1b	2017-07-26	Holiday	0	Qubit	2
WE_2017-07-26_HD_cDNA_2b	2017-07-26	Holiday	45.2	Qubit	2
WE_2017-07-26_HD_cDNA_3a	2017-07-26	Holiday	58	Qubit	2
WE_2017-07-26_HD_cDNA_3b	2017-07-26	Holiday	60.3	Qubit	2
WE_2017-08-31_HD_cDNA_1a	2017-08-31	Holiday	0	Qubit	2
WE_2017-08-31_HD_cDNA_1b	2017-08-31	Holiday	9	Qubit	2
WE_2017-08-31_HD_cDNA_2a	2017-08-31	Holiday	7.4	Qubit	5
WE_2017-08-31_HD_cDNA_2b	2017-08-31	Holiday	12.2	Qubit	2
WE_2017-08-31_HD_cDNA_3b	2017-08-31	Holiday	11	Qubit	10
WE_2017-09-13_HD_cDNA_1b	2017-09-13	Holiday	19.5	Qubit	2
WE_2017-09-13_HD_cDNA_2a	2017-09-13	Holiday	10.8	Qubit	5
WE_2017-09-13_HD_cDNA_2b	2017-09-13	Holiday	29.4	Qubit	5
WE_2017-09-13_HD_cDNA_3a	2017-09-13	Holiday	57.5	Qubit	5
WE_2017-09-13_HD_cDNA_3b	2017-09-13	Holiday	60.8	Qubit	2
WE_2017-04-12_KV_cDNA_1a	2017-04-12	Kingsville	#N/A	Gel	2
WE_2017-04-12_KV_cDNA_1b	2017-04-12	Kingsville	#N/A	Gel	2

WE_2017-04-12_KV_cDNA_2a	2017-04-12	Kingsville	#N/A	Gel	2
WE_2017-04-12_KV_cDNA_2b	2017-04-12	Kingsville	#N/A	Gel	5
WE_2017-06-01_KV_cDNA_1a	2017-06-01	Kingsville	69.3	Qubit	2
WE_2017-06-01_KV_cDNA_1b	2017-06-01	Kingsville	46.8	Qubit	2
WE_2017-06-01_KV_cDNA_4a	2017-06-01	Kingsville	#N/A	Gel	5
WE_2017-06-01_KV_cDNA_4b	2017-06-01	Kingsville	10.7	Qubit	2
WE_2017-06-01_KV_cDNA_2a	2017-06-01	Kingsville	510	Qubit	5
WE_2017-06-01_KV_cDNA_2b	2017-06-01	Kingsville	449	Qubit	5
WE_2017-07-13_KV_cDNA_1a	2017-07-13	Kingsville	74.5	Qubit	2
WE_2017-07-13_KV_cDNA_1b	2017-07-13	Kingsville	89.6	Qubit	2
WE_2017-07-13_KV_cDNA_2a	2017-07-13	Kingsville	81.2	Qubit	2
WE_2017-07-13_KV_cDNA_2b	2017-07-13	Kingsville	97.6	Qubit	2
WE_2017-07-13_KV_cDNA_4a	2017-07-13	Kingsville	84.8	Qubit	10
WE_2017-07-13_KV_cDNA_4b	2017-07-13	Kingsville	86.8	Qubit	2
WE_2017-07-26_KV_cDNA_1a	2017-07-26	Kingsville	117	Qubit	10
WE_2017-07-26_KV_cDNA_1b	2017-07-26	Kingsville	114	Qubit	2
WE_2017-07-26_KV_cDNA_2a	2017-07-26	Kingsville	88.9	Qubit	2
WE_2017-07-26_KV_cDNA_2b	2017-07-26	Kingsville	56.7	Qubit	2
WE_2017-07-26_KV_cDNA_3a	2017-07-26	Kingsville	24.6	Qubit	2
WE_2017-07-26_KV_cDNA_3b	2017-07-26	Kingsville	17.2	Qubit	2
WE_2017-08-31_KV_cDNA_1a	2017-08-31	Kingsville	239	Qubit	2
WE_2017-08-31_KV_cDNA_1b	2017-08-31	Kingsville	249	Qubit	5
WE_2017-08-31_KV_cDNA_2a	2017-08-31	Kingsville	191	Qubit	10
WE_2017-08-31_KV_cDNA_2b	2017-08-31	Kingsville	115	Qubit	2
WE_2017-08-31_KV_cDNA_3a	2017-08-31	Kingsville	70.7	Qubit	2
WE_2017-08-31_KV_cDNA_3b	2017-08-31	Kingsville	118	Qubit	2
WE_2017-09-13_KV_cDNA_1a	2017-09-13	Kingsville	255	Qubit	2
WE_2017-09-13_KV_cDNA_2a	2017-09-13	Kingsville	103	Qubit	10
WE_2017-09-13_KV_cDNA_2b	2017-09-13	Kingsville	133	Qubit	10
WE_2017-04-12_LE_cDNA_1a	2017-04-12	Leamington	#N/A	Gel	2
WE_2017-04-12_LE_cDNA_1b	2017-04-12	Leamington	#N/A	Gel	2
WE_2017-04-12_LE_cDNA_2a	2017-04-12	Leamington	#N/A	Gel	2
WE_2017-04-12_LE_cDNA_2b	2017-04-12	Leamington	#N/A	Gel	2
WE_2017-04-12_LE_cDNA_4a	2017-04-12	Leamington	#N/A	Gel	2
WE_2017-04-12_LE_cDNA_4b	2017-04-12	Leamington	#N/A	Gel	2
WE_2017-06-01_LE_cDNA_1a	2017-06-01	Leamington	72	Bioanalyzer	2
WE_2017-06-01_LE_cDNA_1b	2017-06-01	Leamington	35.5	Qubit	2
WE_2017-06-01_LE_cDNA_4a	2017-06-01	Leamington	13	Qubit	2
WE_2017-06-01_LE_cDNA_4b	2017-06-01	Leamington	#N/A	Gel	2
WE_2017-06-01_LE_cDNA_2a	2017-06-01	Leamington	37.8	Qubit	5
WE_2017-06-01_LE_cDNA_2b	2017-06-01	Leamington	0	Qubit	5
WE_2017-07-13_LE_cDNA_1a	2017-07-13	Leamington	0	Qubit	2
WE_2017-07-13_LE_cDNA_1b	2017-07-13	Leamington	0	Qubit	10
WE_2017-07-13_LE_cDNA_2a	2017-07-13	Leamington	10.7	Qubit	2
WE_2017-07-13_LE_cDNA_2b	2017-07-13	Leamington	0	Qubit	2
WE_2017-07-13_LE_cDNA_4a	2017-07-13	Leamington	12.3	Qubit	2
WE_2017-07-13_LE_cDNA_4b	2017-07-13	Leamington	14.6	Qubit	2
WE_2017-07-26_LE_cDNA_1a	2017-07-26	Leamington	19.7	Qubit	2
WE_2017-07-26_LE_cDNA_1b	2017-07-26	Leamington	30.7	Qubit	5
WE_2017-07-26_LE_cDNA_2a	2017-07-26	Leamington	5.3	Qubit	2
WE_2017-07-26_LE_cDNA_2b	2017-07-26	Leamington	34.4	Qubit	2
WE_2017-07-26_LE_cDNA_3a	2017-07-26	Leamington	50.1	Qubit	2
WE_2017-07-26_LE_cDNA_3b	2017-07-26	Leamington	61.8	Qubit	5
WE_2017-08-31_LE_cDNA_1a	2017-08-31	Leamington	51.5	Qubit	5
WE_2017-08-31_LE_cDNA_1b	2017-08-31	Leamington	78.8	Qubit	5
WE_2017-08-31_LE_cDNA_2a	2017-08-31	Leamington	45.2	Qubit	5
WE_2017-08-31_LE_cDNA_2b	2017-08-31	Leamington	68.8	Qubit	2
WE_2017-08-31_LE_cDNA_3a	2017-08-31	Leamington	22.5	Qubit	5
WE_2017-08-31_LE_cDNA_3b	2017-08-31	Leamington	24.9	Qubit	2
WE_2017-09-13_LE_cDNA_1a	2017-09-13	Leamington	7.7	Qubit	2
WE_2017-09-13_LE_cDNA_1b	2017-09-13	Leamington	25.7	Qubit	2
WE_2017-09-13_LE_cDNA_2a	2017-09-13	Leamington	52.7	Qubit	2
WE_2017-09-13_LE_cDNA_3a	2017-09-13	Leamington	50.3	Qubit	5
WE_2017-09-13_LE_cDNA_3b	2017-09-13	Leamington	31.1	Qubit	10
WE_2017-06-01_PP_cDNA_1a	2017-06-01	Point Pelee	90	Bioanalyzer	5
WE_2017-06-01_PP_cDNA_1b	2017-06-01	Point Pelee	46.9	Qubit	5
WE_2017-06-01_PP_cDNA_2a	2017-06-01	Point Pelee	72.3	Qubit	5

WE_2017-06-01_PP_cDNA_2b	2017-06-01	Point Pelee	17.7	Qubit	2
WE_2017-06-01_PP_cDNA_4a	2017-06-01	Point Pelee	28.2	Qubit	2
WE_2017-06-01_PP_cDNA_4b	2017-06-01	Point Pelee	26.2	Qubit	2
WE_2017-07-13_PP_cDNA_1a	2017-07-13	Point Pelee	0	Qubit	2
WE_2017-07-13_PP_cDNA_1b	2017-07-13	Point Pelee	0	Qubit	2
WE_2017-07-13_PP_cDNA_2a	2017-07-13	Point Pelee	0	Qubit	2
WE_2017-07-13_PP_cDNA_2b	2017-07-13	Point Pelee	5.8	Qubit	2
WE_2017-07-13_PP_cDNA_4a	2017-07-13	Point Pelee	12	Qubit	2
WE_2017-07-13_PP_cDNA_4b	2017-07-13	Point Pelee	6.5	Qubit	2
WE_2017-07-26_PP_cDNA_1b	2017-07-26	Point Pelee	0	Qubit	5
WE_2017-07-26_PP_cDNA_2a	2017-07-26	Point Pelee	9.5	Qubit	2
WE_2017-07-26_PP_cDNA_2b	2017-07-26	Point Pelee	6.2	Qubit	2
WE_2017-07-26_PP_cDNA_3a	2017-07-26	Point Pelee	8.3	Qubit	5
WE_2017-08-31_PP_cDNA_1b	2017-08-31	Point Pelee	0	Qubit	2
WE_2017-08-31_PP_cDNA_1c	2017-08-31	Point Pelee	#N/A	Gel	2
WE_2017-08-31_PP_cDNA_2a	2017-08-31	Point Pelee	#N/A	Gel	10
WE_2017-08-31_PP_cDNA_2b	2017-08-31	Point Pelee	16.1	Qubit	5
WE_2017-08-31_PP_cDNA_3a	2017-08-31	Point Pelee	0	Qubit	2
WE_2017-08-31_PP_cDNA_3b	2017-08-31	Point Pelee	0	Qubit	2
WE_2017-09-13_PP_cDNA_1a	2017-09-13	Point Pelee	#N/A	Gel	5
WE_2017-09-13_PP_cDNA_2a	2017-09-13	Point Pelee	#N/A	Gel	10
WE_2017-09-13_PP_cDNA_2b	2017-09-13	Point Pelee	6.6	Qubit	10
WE_2017-04-12_SP_cDNA_1a	2017-04-12	Sandpoint	#N/A	Gel	2
WE_2017-04-12_SP_cDNA_1b	2017-04-12	Sandpoint	#N/A	Gel	2
WE_2017-04-12_SP_cDNA_2a	2017-04-12	Sandpoint	#N/A	Gel	2
WE_2017-04-12_SP_cDNA_2b	2017-04-12	Sandpoint	#N/A	Gel	2
WE_2017-06-01_SP_cDNA_1a	2017-06-01	Sandpoint	114	Qubit	2
WE_2017-06-01_SP_cDNA_1b	2017-06-01	Sandpoint	41.4	Qubit	5
WE_2017-06-01_SP_cDNA_2a	2017-06-01	Sandpoint	60.7	Qubit	5
WE_2017-06-01_SP_cDNA_2b	2017-06-01	Sandpoint	80.8	Qubit	5
WE_2017-06-01_SP_cDNA_4a	2017-06-01	Sandpoint	101	Qubit	2
WE_2017-06-01_SP_cDNA_4b	2017-06-01	Sandpoint	37.1	Qubit	2
WE_2017-07-13_SP_cDNA_1a	2017-07-13	Sandpoint	164	Qubit	2
WE_2017-07-13_SP_cDNA_1b	2017-07-13	Sandpoint	183	Qubit	2
WE_2017-07-13_SP_cDNA_2a	2017-07-13	Sandpoint	110	Qubit	2
WE_2017-07-13_SP_cDNA_2b	2017-07-13	Sandpoint	94.7	Qubit	2
WE_2017-07-13_SP_cDNA_4a	2017-07-13	Sandpoint	145	Qubit	5
WE_2017-07-26_SP_cDNA_1a	2017-07-26	Sandpoint	104	Qubit	2
WE_2017-07-26_SP_cDNA_1b	2017-07-26	Sandpoint	117	Qubit	2
WE_2017-07-26_SP_cDNA_2a	2017-07-26	Sandpoint	131	Qubit	5
WE_2017-07-26_SP_cDNA_2b	2017-07-26	Sandpoint	314	Qubit	10
WE_2017-07-26_SP_cDNA_3a	2017-07-26	Sandpoint	75.3	Qubit	2
WE_2017-07-26_SP_cDNA_3b	2017-07-26	Sandpoint	70	Qubit	2
WE_2017-08-31_SP_cDNA_1a	2017-08-31	Sandpoint	119	Qubit	5
WE_2017-08-31_SP_cDNA_2a	2017-08-31	Sandpoint	135	Qubit	2
WE_2017-08-31_SP_cDNA_2b	2017-08-31	Sandpoint	139	Qubit	2
WE_2017-08-31_SP_cDNA_3a	2017-08-31	Sandpoint	83.1	Qubit	2
WE_2017-09-13_SP_cDNA_1a	2017-09-13	Sandpoint	186	Qubit	10
WE_2017-09-13_SP_cDNA_1b	2017-09-13	Sandpoint	132	Qubit	10
WE_2017-09-13_SP_cDNA_3a	2017-09-13	Sandpoint	106	Qubit	2
WE_2017-09-13_SP_cDNA_3b	2017-09-13	Sandpoint	145	Qubit	2

Table A-3: ANOVA and subsequent Tukey's post-hoc results for Chao1 richness estimator and Shannon diversity index on freshwater bed sediment samples. Sample size (n) given directly below dataset name. ANOVA values F and p represent the ratio of two mean squares and the significance value, respectively. Cells corresponding to treatment effect on diversity represent the mean value for that group with standard deviation in brackets. Red text indicates significant effect ($p < 0.05$). Lower case letters indicate where the differences are attributed, based on Tukey's post-hoc test, within the given factor and dataset.

Factor	Treatment	Chao1 Richness Estimator		Shannon Diversity Metric	
		DNA n = 298	cDNA n = 188	DNA n = 298	cDNA n = 188
Season	ANOVA (F, p)	1.381, 0.253	15.59, 1.12e-04 ***	35.37, 1.71e-14 ***	10.71, 1.27e-03 **
	spring	738 (340)	468 (294) b	4.38 (0.899) c	5.14 (0.460) b
	summer	681 (262)	647 (271) a	4.85 (0.846) b	5.41 (0.510) a
	fall	664 (237)	--	5.74 (0.381) a	--
Lake	ANOVA (F, p)	3.116, 0.0785	0.451, 0.503	2.058, 0.152	5.354, 0.0218 *
	St. Clair	736 (286)	617 (227)	4.92 (0.945)	5.45 (0.381) a
	Erie	675 (282)	587 (316)	4.76 (0.891)	5.27 (0.558) b
Location	ANOVA (F, p)	2.823, 0.0166 *	4.012, 1.77e-03 **	0.928, 0.463	3.04, 0.0116 *
	Belle River	695 (271) a	590 (205) ab	4.89 (1.02)	5.47 (0.372) a
	Sandpoint	777 (297) a	645 (249) ab	4.95 (0.876)	5.43 (0.396) a
	Holiday	641 (278) a	509 (314) b	4.70 (1.03)	5.04 (0.587) b
	Kingsville	776 (355) a	572 (294) b	4.94 (0.981)	5.25 (0.491) ab
	Leamington	642 (229) a	503 (229) b	4.70 (0.753)	5.30 (0.508) ab
	Point Pelee	637 (232) a	780 (370) a	4.72 (0.785)	5.46 (0.623) a
Collection Date	ANOVA (F, p)	0.471, 0.493	39.31, 2.47e-09 ***	80.24, <2e-16 ***	23.11, 3.15e-06 ***
	2017-04-12	399 (240)	325 (110) d	3.76 (0.855) c	4.91 (0.347) c
	2017-06-01	784 (319)	544 (333) bcd	4.58 (0.894) b	5.27 (0.468) abc
	2017-06-13	864 (292)	--	4.50 (0.804) b	--
	2017-07-13	625 (200)	483 (282) cd	4.46 (0.752) bc	5.13 (0.565) bc
	2017-07-26	639 (251)	635 (207) abc	4.57 (0.759) b	5.48 (0.444) a
	2017-08-10	635 (225)	--	5.64 (0.376) a	--
	2017-08-31	792 (345)	710 (223) ab	4.83 (0.966) b	5.58 (0.381) a
	2017-09-13	725 (248)	756 (286) a	4.71 (0.744) b	5.45 (0.533) ab
	2017-11-08	664 (237)	--	5.74 (0.381) a	--

Significance values: * = $0.05 > p > 0.01$; ** = $0.01 > p > 0.001$; *** = $p < 0.001$

Table A-4: Beta diversity statistics. Permutational multivariate analysis of variance (PERMANOVA) using distance matrices and subsequent pairwise comparisons on freshwater bed sediment samples. Sample size (n) given directly below dataset name. P value represents the significance value with alpha level of 0.05. Lower case letters indicate where the differences are attributed, based on pairwise PERMANOVA, within the given factor and dataset.

Factor	Treatment	DNA n = 298	cDNA n = 188
Season	P value	0.001 ***	0.001 ***
	spring	b	a
	summer	c	b
	fall	a	--
Lake	P value	0.001 ***	0.001 ***
	St. Clair	b	b
	Erie	a	a
Location	P value	0.001 ***	0.001 ***
	Belle River	a	a
	Sandpoint	f	e
	Holiday	b	b
	Kingsville	c	c
	Leamington	d	d
	Point Pelee	e	de
Collection Date	P value	0.001 ***	0.001 ***
	2017-04-12	ab	a
	2017-06-01	a	b
	2017-06-13	abc	--
	2017-07-13	cd	c
	2017-07-26	bcd	d
	2017-08-10	cd	--
	2017-08-31	bcd	e
	2017-09-13	abcd	f
	2017-11-08	d	--

Significance values: * = 0.05 > p > 0.01; ** = 0.01 > p > 0.001; *** = p < 0.001

Table A-5: Summary of microbial community composition for individual beaches, combined over the sampling year for both DNA and cDNA data. Values represent average relative abundance (%) of bacterial population for each individual beach within the taxon category specified at the left. “Other” contains the combined taxa for which individual relative abundances were < 3% for all locations. “NA” is the combination of undefined or unclassified ASVs at the taxon level specified at the left.

Taxa			Belle River		Sandpoint		Holiday		Kingsville		Leamington		Point Pelee	
			DNA	cDNA	DNA	cDNA	DNA	cDNA	DNA	cDNA	DNA	cDNA	DNA	cDNA
PHYLUM	Includes NA	<i>Acidobacteria</i>	4.93	1.82	5.68	2.95	4.28	3.57	3.60	2.43	7.58	4.96	9.88	6.31
		<i>Actinobacteria</i>	3.17	2.96	3.26	4.72	3.13	10.34	2.93	4.54	3.23	10.94	3.24	13.40
		<i>Bacteroidetes</i>	12.05	2.79	13.46	4.47	12.41	1.45	15.82	3.51	8.33	2.03	10.07	2.30
		<i>Cyanobacteria</i>	~	22.99	~	18.02	~	0.86	~	1.26	~	0.79	~	0.40
		<i>Proteobacteria</i>	21.86	61.78	22.08	61.07	24.89	74.71	20.43	81.77	21.30	69.70	17.99	52.13
		Other	9.14	2.00	6.88	2.57	6.29	4.00	7.05	2.31	6.52	4.85	6.98	6.32
		NA	48.84	5.67	48.65	6.20	49.01	5.06	50.17	4.18	53.04	6.73	51.84	19.15
	NA removed	<i>Acidobacteria</i>	10.14	1.94	11.11	3.17	8.62	3.80	6.99	2.54	16.38	5.33	20.46	7.98
		<i>Actinobacteria</i>	6.08	3.14	6.61	4.97	6.75	10.96	6.42	4.73	8.62	11.78	8.03	16.48
		<i>Bacteroidetes</i>	22.11	2.97	25.71	4.93	22.32	1.54	31.82	3.68	15.86	2.18	20.39	2.91
		<i>Cyanobacteria</i>	4.60	24.23	1.32	18.99	0.99	0.93	0.93	1.33	0.58	0.84	0.21	0.71
		<i>Planctomycetes</i>	3.80	~	5.12	~	4.00	~	4.30	~	5.33	~	5.11	~
		<i>Proteobacteria</i>	44.26	65.60	42.44	65.19	49.67	78.49	41.73	85.30	45.02	74.65	36.85	64.21
		<i>Verrucomicrobia</i>	4.27	~	5.32	~	4.34	~	4.72	~	3.35	~	4.12	~
		Other	4.02	2.13	2.37	2.75	3.26	4.29	3.09	2.41	4.85	5.22	4.84	7.71
Proteobacteria CLASS ^a	Includes NA	<i>Alphaproteobacteria</i>	5.18	1.45	9.92	2.53	7.63	2.42	9.79	2.81	5.44	2.24	6.97	2.73
		<i>Deltaproteobacteria</i>	1.94	0.95	0.88	0.63	2.20	2.65	1.32	1.18	1.10	1.89	0.88	2.68
		<i>Gammaproteobacteria</i>	35.48	62.24	28.49	60.70	36.85	71.95	27.78	79.97	34.89	68.96	25.26	56.55
		<i>Magnetococcia</i>	0.00	0.00	0.00	0.00	0.00	0.00	0.00	0.00	0.00	0.00	0.00	0.00
		NA	1.65	0.96	3.15	1.33	2.69	1.47	2.83	1.35	3.59	1.56	3.74	2.25
Proteobacteria ORDER ^a	Includes NA	<i>Betaproteobacteriales</i>	25.54	53.14	19.17	52.70	27.42	66.78	18.65	68.81	21.87	58.28	15.90	45.50
		<i>Enterobacteriales</i>	5.15	4.77	5.69	5.68	6.55	3.47	6.35	7.61	7.25	6.48	7.28	8.00
		<i>Rhodobacterales</i>	1.29	~	1.80	~	2.04	~	3.17	~	0.80	~	0.33	~
		Other	6.40	2.37	8.38	3.08	7.46	4.92	7.42	3.80	5.78	3.81	5.26	5.05
		NA	5.89	5.32	7.40	3.72	6.20	3.32	6.13	5.08	9.32	6.10	8.08	5.66

^a Values in this taxonomic category are calculated relative to total bacterial population; sum of values for each beach equals total *Proteobacteria* relative abundance determined (with NA removed).

~ Indicates this taxon is included in “Other” (i.e., contains < 3% for each beach within the specified taxon category).

APPENDIX B: SUPPLEMENTAL INFORMATION FOR CHAPTER 3

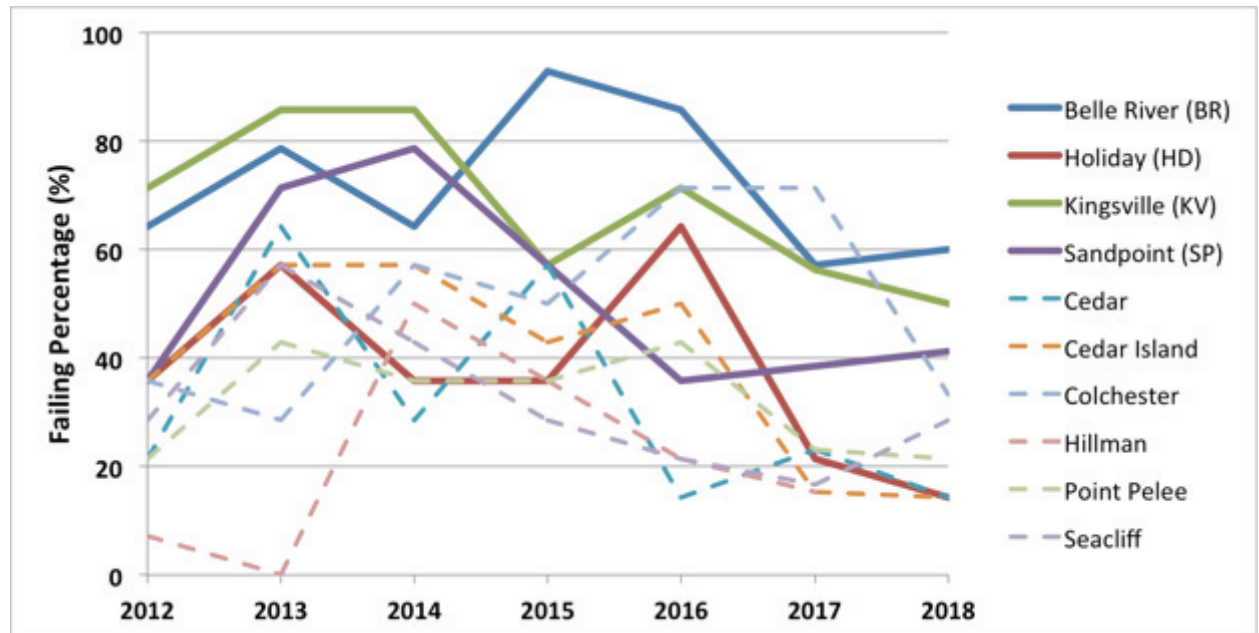


Figure B-1: Line graph depicting the percentage of incidences that reported CFU values of indicator *E. coli* in the water at WEC public beaches exceeded acceptable levels over the past 7 years. Thick solid lines indicate locations of interest to this manuscript (Belle River (BR), Holiday (HD), Kingsville (KV), Sandpoint (SP)), and thin dashed lines represent the other beaches monitored. Data provided by WECHU. Note: up until 2017, acceptable *E. coli* levels were less than 100 CFUs/100 mL; 2018 it changed to 200 CFUs/100 mL.

Table B-1: Summary of sequencing results obtained from the Ion Torrent PGM™. Data determined from recovered DNA and bioinformatics processing.

Sample	# of reads	Avg reads
Sandpoint-a	11818	18,261.25
Sandpoint-b	28934	
Sandpoint-c	4462	
Sandpoint-d	27831	
BelleRiver-a	15657	12,930
BelleRiver-b	18972	
BelleRiver-c	7386	
BelleRiver-d	9705	
Kingsville-a	19644	11,329.5
Kingsville-b	5079	
Kingsville-c	8174	
Kingsville-d	12421	
Holiday-a	25089	31,386.75
Holiday-b	64640	
Holiday-c	11653	
Holiday-d	24165	

Table B-2. Summary of sequencing statistics for all samples obtained from the Illumina HiSeq 4000 run. Data determined from recovered mRNA and bioinformatics processing. Rows highlighted grey indicate the representative average values for the specified beach. bps = basepairs

Sample	# of bps	# of reads	Sum of functional annotations
Sandpoint-a	5,320,888,200	26,604,441	
Sandpoint-b	6,131,861,200	30,659,306	
<i>Sandpoint avg</i>	<i>5,726,374,700</i>	<i>28,631,874</i>	<i>671,472</i>
BelleRiver-a	4,756,143,800	23,780,719	
BelleRiver-b	4,852,982,400	24,264,912	
<i>BelleRiver avg</i>	<i>4,804,563,100</i>	<i>24,022,816</i>	<i>790,941</i>
Kingsville-a	4,870,637,800	24,353,189	
Kingsville-b	4,926,629,200	24,633,146	
<i>Kingsville avg</i>	<i>4,898,633,500</i>	<i>24,493,168</i>	<i>578,129</i>
Holiday-a	4,909,666,000	24,548,330	
Holiday-b	5,245,205,000	26,226,025	
<i>Holiday avg</i>	<i>5,077,435,500</i>	<i>25,387,178</i>	<i>628,042</i>

APPENDIX C: SUPPLEMENTAL INFORMATION FOR CHAPTER 4

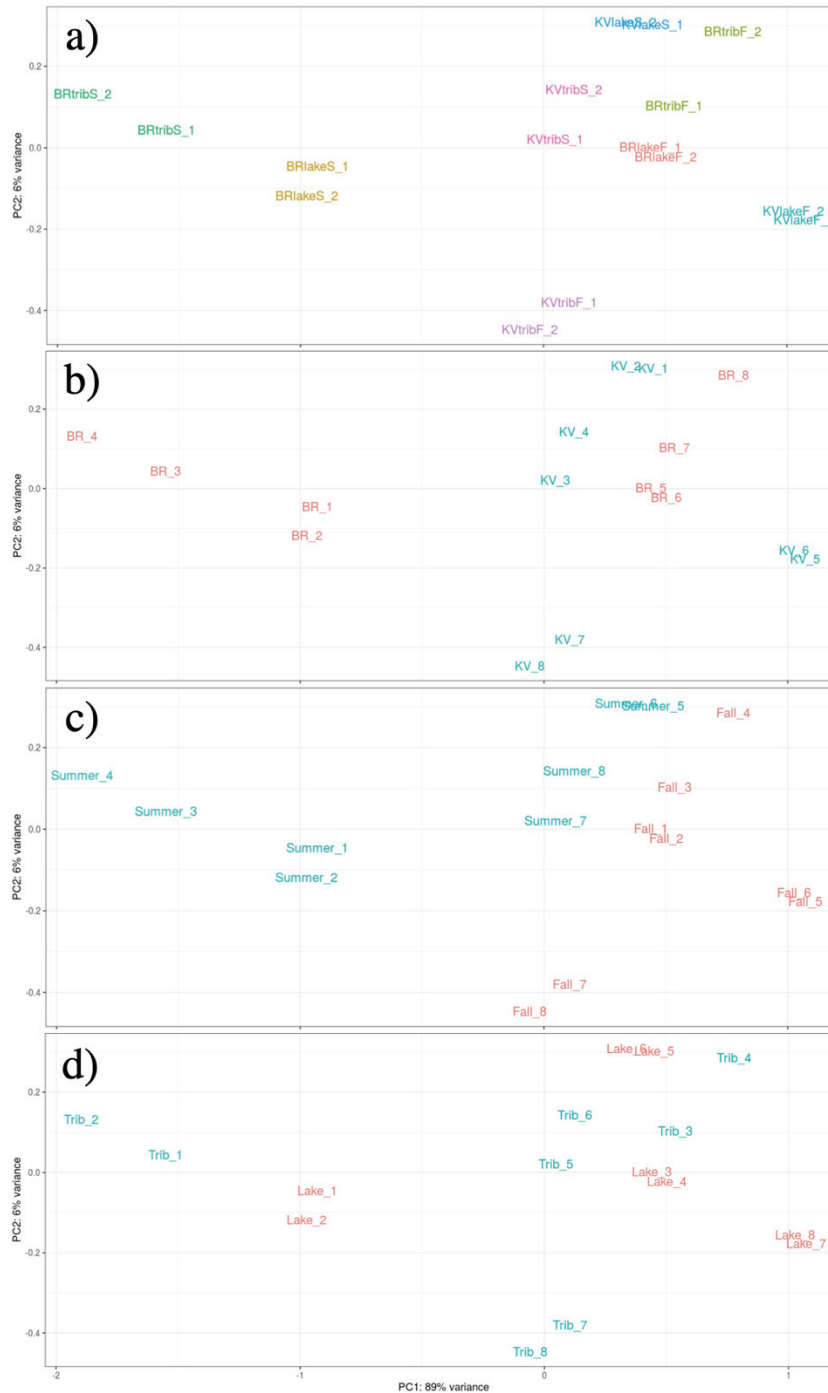


Figure C-1: Principal components analysis (PCA) of metatranscriptomic data, examining the functional diversity between samples (beta-diversity) at Level 1 resolution of a) all 8 groups, b) location (BR vs KV), c) season (summer vs fall), and d) site (lake vs tributary). Each plot has the same axes (PC1: 89%, PC2: 6%) and coordinates for samples, but sample labeling modified to view comparisons.

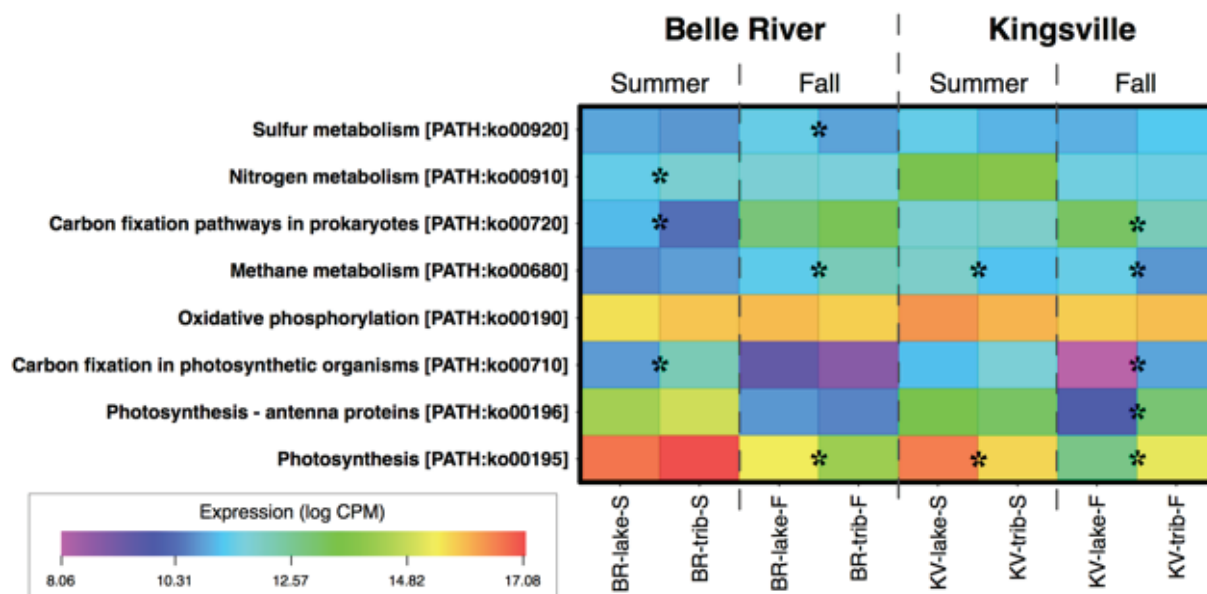


Figure C-2: Gene expression heatmap of Level 3 transcripts involved in Energy Metabolism (Level 2), utilizing KEGG annotations and KO database. Pathways involved with photosynthesis [ko00195, ko00196, ko00710], oxidative phosphorylation [ko00190], and chemolithotrophic pathways (methane metabolism [ko00680]; carbon fixation pathways in prokaryotes [ko00720]; nitrogen metabolism [ko00910]; and sulfur metabolism [ko00920]). Expression represented as normalized logCPM values. Pairwise comparisons between sampling sites (lake, tributary) of the same location and season provide statistically significant differential expression ($p < 0.05$), denoted with an asterisk * where applicable.

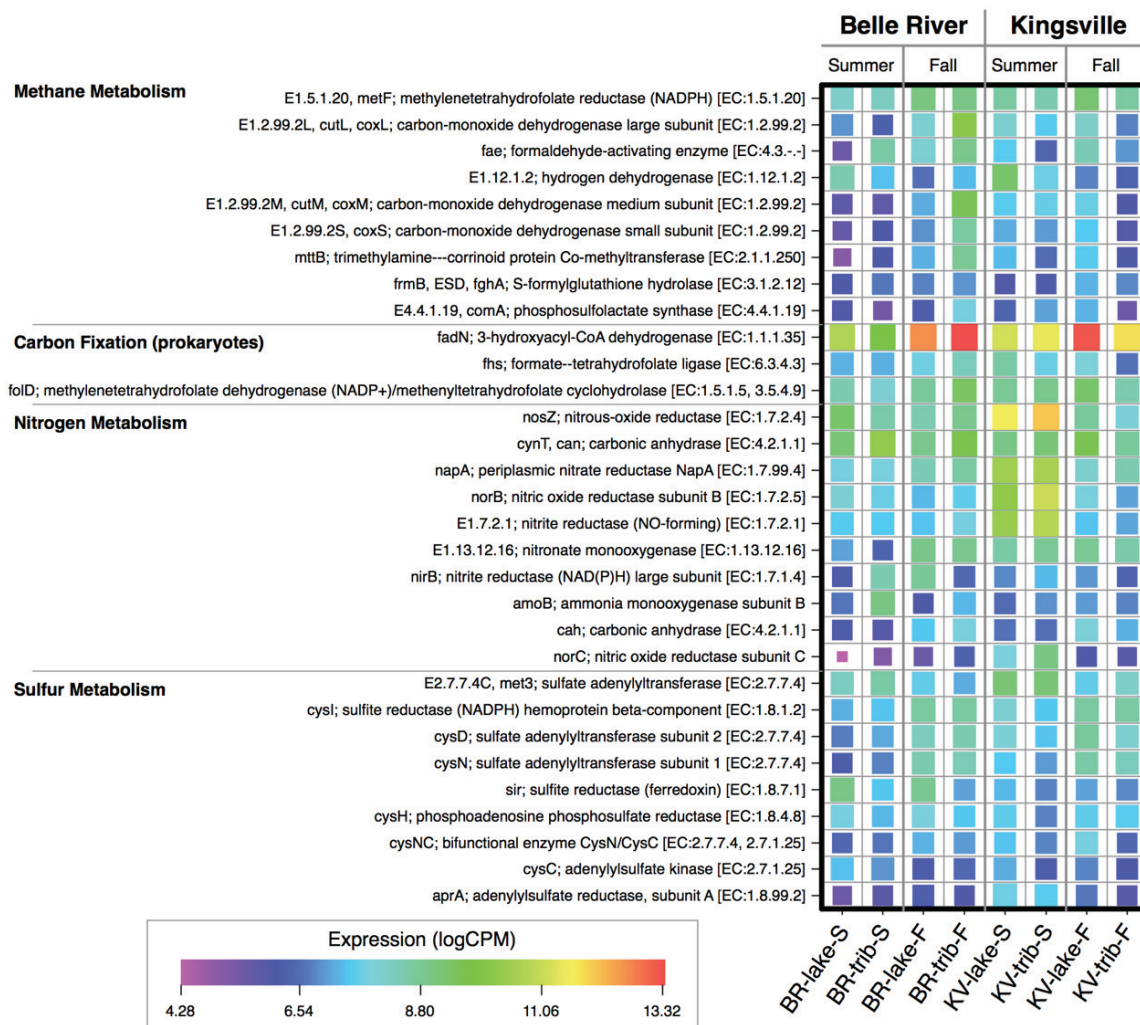


Figure C-3: Functional annotations assigned to dominant transcripts involved in chemolithotrophic Energy Metabolism (methane metabolism [ko00680]; carbon fixation pathways in prokaryotes [ko00720]; nitrogen metabolism [ko00910]; and sulfur metabolism [ko00920]). Heatmap uses colour range and volume proportional size scaling to illustrate expression comparisons of all samples. Expression represented as normalized logCPM values. To demonstrate dominant transcripts, filtering cut-off was set to 50 logCPM total (cumulative for all 8 averaged samples). [Volume proportional to cell value – linear].

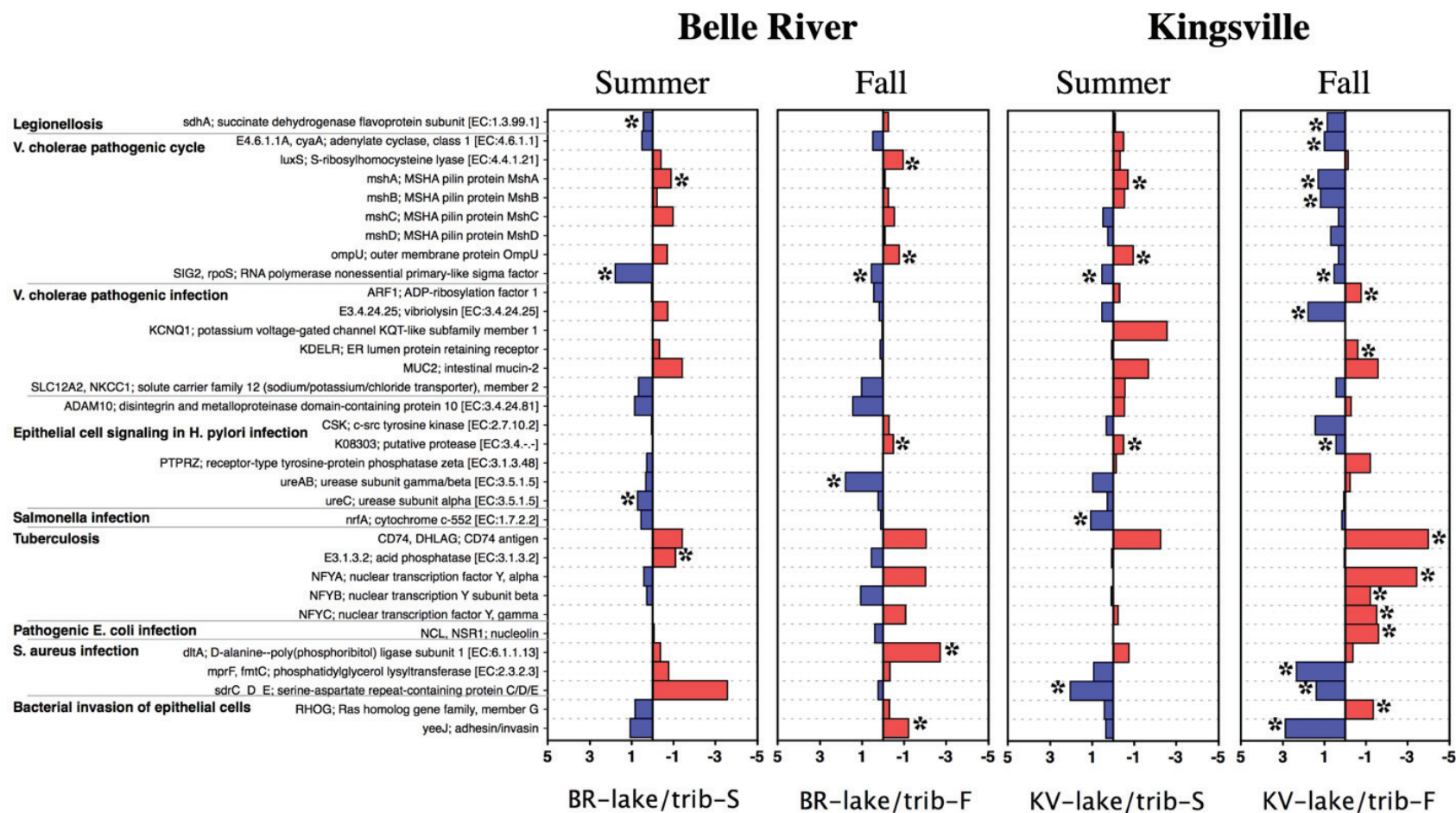


Figure C-4: Illustrating logFC (fold change) of functional transcripts between sampling sites (lake, tributary) of the same location and season involved in bacterial Infectious Diseases. Transcripts are sorted to their respective pathway. Blue indicates greater expression in the lake; red indicates greater expression in the tributary; x axis explains the degree of expression (logFC). Pairwise comparisons with differential expression ($p < 0.05$) are denoted with an asterisk * where applicable.

Table C-1: Summary of seasonal nutrients and total suspended solids (TSS) measured from the water column at each study site. DIC, dissolved inorganic carbon; DOC, dissolved organic carbon; TN, total nitrogen; TP, total phosphorous; NA, not available.

Season	Analysis		Belle River		Kingsville	
			Lake	Trib	Lake	Trib
SPRING	Nutrients ($\mu\text{g L}^{-1}$)	DIC	22,400	40,600	32,800	57,900
		DOC	5600	9400	5000	4800
		TN	1220	2740	2540	5350
		TP	64.2	152	310	472
	Mass ratio	TN:TP	19	18	8	11
	TSS	(mg L^{-1})	NA	NA	NA	NA
FALL	Nutrients ($\mu\text{g L}^{-1}$)	DIC	15,900	36,100	29,000	54,400
		DOC	5300	11,200	6800	4400
		TN	1080	5150	2600	11,100
		TP	41.1	157	213	568
	Mass ratio	TN:TP	26	33	12	20
	TSS	(mg L^{-1})	29.80	37.51	152.49	2.58

Table C-2: Summary of sequencing statistics for all samples obtained from the Illumina HiSeq 4000 PE100 metatranscriptomics run. BR = Belle River; KV = Kingsville; trib = tributary; S = summer; F = fall; bp = basepair; RIN = RNA integrity number; QC = quality control.

Sample	Illumina			Sequences that Passed QC (MG-RAST)			Sequences Post-Alignment	DRISEE %
	# bp	Reads	RIN					
BR-trib-S-1	4,455,413,200	22,277,066	6.6	6,802,611	%	TOTAL	972,201 identified protein features	2.709
				3,030,465	44.55	unknown protein		
				2,635,177	38.74	annotated protein	13,806 identified rRNA features	
				1,136,969	16.71	rRNA		
BR-trib-S-2	4,293,433,200	21,467,166	3.5	6,787,341	%	TOTAL	776,566 identified protein features	2.922
				2,943,490	43.23	unknown protein		
				2,300,809	33.90	annotated protein	14,758 identified rRNA features	
				1,552,042	22.87	rRNA		
BR-lake-S-1	4,209,918,000	21,049,590	6.5	6,920,467	%	TOTAL	1,169,114 identified protein features	4.308
				3,199,199	46.23	unknown protein		
				2,820,231	40.75	annotated protein	18,763 identified rRNA features	
				901,037	13.02	rRNA		
BR-lake-S-2	5,165,185,000	25,825,925	6.0	8,363,920	%	TOTAL	1,423,612 identified protein features	3.273
				3,675,143	43.94	unknown protein		
				3,419,448	40.88	annotated protein	17,455 identified rRNA features	
				1,269,329	15.18	rRNA		
BR-trib-F-1	4,579,984,200	22,899,921	7.2	9,377,559	%	TOTAL	2,377,799 identified protein features	3.341
				3,991,175	42.56	unknown protein		
				4,576,108	48.80	annotated protein	17,360 identified rRNA features	
				810,276	8.64	rRNA		
BR-trib-F-2	4,144,446,800	20,722,234	N/A	8,421,070	%	TOTAL	2,424,862 identified protein features	4.533
				3,294,945	39.13	unknown protein		
				4,832,530	57.39	annotated protein	11,142 identified rRNA features	
				293,595	3.49	rRNA		
BR-lake-F-1	3,769,649,400	18,848,247	7.3	6,569,697	%	TOTAL	1,694,309 identified protein features	1.976
				2,983,015	45.41	unknown protein		
				3,287,509	50.04	annotated protein	11,396 identified rRNA features	
				299,173	4.55	rRNA		
BR-lake-F-2	4,188,905,200	20,944,526	7.4	7,799,070	%	TOTAL	2,119,610 identified protein features	2.204
				3,463,239	44.41	unknown protein		
				4,055,108	51.99	annotated protein	12,834 identified rRNA features	
				280,723	3.60	rRNA		

KV-trib-S-1	3,940,870,200	19,704,351	6.4	6,592,782	%	TOTAL	1,379,402 identified protein features	2.264
				2,850,692	43.24	unknown protein		
				2,814,715	42.69	annotated protein	19,721 identified rRNA features	
				927,375	14.07	rRNA		
KV-trib-S-2	4,294,242,800	21,471,214	6.0	7,150,780	%	TOTAL	1,514,437 identified protein features	3.100
				3,230,328	45.17	unknown protein		
				3,241,252	45.33	annotated protein	18,466 identified rRNA features	
				679,200	9.50	rRNA		
KV-lake-S-1	3,931,840,000	19,659,200	6.7	6,640,172	%	TOTAL	1,480,388 identified protein features	3.196
				3,195,891	48.13	unknown protein		
				2,941,176	44.29	annotated protein	14,541 identified rRNA features	
				503,105	7.58	rRNA		
KV-lake-S-2	4,874,460,400	24,372,302	6.6	8,224,247	%	TOTAL	1,785,332 identified protein features	2.591
				3,947,001	47.99	unknown protein		
				3,665,505	44.57	annotated protein	16,230 identified rRNA features	
				611,741	7.44	rRNA		
KV-trib-F-1	4,003,853,200	20,019,266	6.3	7,708,199	%	TOTAL	1,599,289 identified protein features	2.272
				3,495,393	45.35	unknown protein		
				3,417,450	44.34	annotated protein	18,532 identified rRNA features	
				795,356	10.32	rRNA		
KV-trib-F-2	3,938,249,000	19,691,245	6.9	7,334,897	%	TOTAL	1,477,910 identified protein features	2.860
				3,445,322	46.97	unknown protein		
				3,137,435	42.77	annotated protein	16,776 identified rRNA features	
				752,140	10.25	rRNA		
KV-lake-F-1	4,291,099,200	21,455,046	8.0	9,421,118	%	TOTAL	2,875,224 identified protein features	6.404
				3,889,700	41.29	unknown protein		
				5,177,820	54.96	annotated protein	15,757 identified rRNA features	
				353,598	3.75	rRNA		
KV-lake-F-2	5,270,911,800	26,354,559	8.0	10,864,049	%	TOTAL	3,257,176 identified protein features	5.772
				4,521,632	41.62	unknown protein		
				5,952,703	54.79	annotated protein	14,847 identified rRNA features	
				389,714	3.59	rRNA		

Table C-3: Summary of raw data used for normalization and statistical tests. The count of sub-categories (in brackets) and genes with observed expression for each category annotated in the KEGG database through MG-RAST (Levels 1, 2 and select pathways of relevance for Level 3) is represented. All samples are the same. Categories/pathways of relevance to this study are highlighted. For Level 3 pathways, corresponding ko number is given in square brackets before pathway names.

Level 1	Level 2	Level 3
Cellular Processes (4) 689 genes	Cell communication (4) 164 genes	<i>None relevant to this study.</i>
	Cell growth & death (7) 171 genes	
	Cell motility (3) 93 genes	
	Transport & catabolism (5) 261 genes	
Environmental Information Processing (3) 839 genes	Membrane transport (3) 362 genes	<i>None relevant to this study.</i>
	Signal transduction (18) 444 genes	
	Signaling molecules & interaction (3) 33 genes	
Genetic Information Processing (4) 851 genes	Folding, sorting & degradation (7) 299 genes	<i>None relevant to this study.</i>
	Replication and repair (6) 124 genes	
	Transcription (3) 162 genes	
	Translation (5) 266 genes	
Human Diseases (7) 252 genes	Cancers (9) 43 genes	From Infectious diseases: [05100] Bacterial invasion of epithelial cells: 3 genes [05110] Vibrio cholerae infection: 6 genes [05111] Vibrio cholerae pathogenic cycle: 11 genes [05120] Epithelial cell signaling in H. pylori infection: 6 genes [05130] Pathogenic Escherichia coli infection: 1 gene [05132] Salmonella infection: 1 gene [05134] Legionellosis: 1 gene [05150] Staphylococcus aureus infection: 8 genes [05152] Tuberculosis: 5 genes
	Cardiovascular diseases (2) 11 genes	
	Endocrine & metabolic diseases (3) 12 genes	
	Immune diseases (4) 8 genes	
	Infectious diseases (22) 69 genes	
	Neurodegenerative diseases (5) 103 genes	
	Substance dependence (3) 6 genes	
Metabolism (11) 2053 genes	Amino acid metabolism (13) 464 genes	From Energy metabolism: [00190] Oxidative phosphorylation: 85 genes [00195] Photosynthesis: 54 genes [00196] Photosynthesis – antenna proteins: 37 genes [00680] Methane metabolism: 77 genes [00710] Carbon fixation in photosynthetic organisms: 4 genes [00720] Carbon fixation pathways in prokaryotes: 9 genes [00910] Nitrogen metabolism: 47 genes [00920] Sulfur metabolism: 15 genes
	Biosynthesis of other secondary metabolites (8) 28 genes	
	Carbohydrate metabolism (15) 391 genes	
	Energy metabolism (8) 328 genes	
	Glycan biosynthesis & metabolism (14) 117 genes	
	Lipid metabolism (14) 184 genes	
	Metabolism of cofactors & vitamins (12) 228 genes	
	Metabolism of other amino acids (5) 41 genes	
	Metabolism of terpenoids & polyketides (11) 76 genes	

	Nucleotide metabolism (2) 102 genes	
	Xenobiotics biodegradation & metabolism (18) 94 genes	
Organismal Systems (9) 149 genes	Circulatory system (2) 7 genes	None relevant to this study.
	Development (3) 34 genes	
	Digestive system (7) 38 genes	
	Endocrine system (4) 17 genes	
	Environmental adaptation (4) 16 genes	
	Excretory system (3) 9 genes	
	Immune system (9) 15 genes	
	Nervous system (3) 3 genes	
	Sensory system (4) 10 genes	

Note: Some of the genes indicated in this table were subsequently filtered out due to low expression and were deemed not biologically important for further investigations. The data represented in this table is what was used for normalization/statistical tests performed in the START app.

Table C-4: Tabulated summary of gene expression profiles, including raw reads and normalized logCPM values for all replicates (16), for all relevant categories/pathways (Levels 1, 2 and 3) and transcripts (Level 4) with corresponding ko numbers.

			BELLE RIVER								KINGSVILLE							
			Summer				Fall				Summer				Fall			
			Lake		Tributary		Lake		Tributary		Lake		Tributary		Lake		Tributary	
			BR-lake-S_1	BR-lake-S_2	BR-trib-S_1	BR-trib-S_2	BR-lake-F_1	BR-lake-F_2	BR-trib-F_1	BR-trib-F_2	KV-lake-S_1	KV-lake-S_2	KV-trib-S_1	KV-trib-S_2	KV-lake-F_1	KV-lake-F_2	KV-trib-F_1	KV-trib-F_2
TOTAL raw reads			1369502	1734234	1202975	1054193	1852646	2350584	2543799	2620544	1582209	1943531	1567908	1774173	3157233	3574684	2038064	1859601
Level 1																		
Cellular Processes		raw reads	117880	159569	99236	97605	133290	171257	185282	206512	88019	112407	111156	110667	239727	266110	151403	137677
		logCPM	16.399682	16.5081437	16.3538806	16.5511207	16.1297288	16.1502233	16.1531774	16.2677649	15.7256858	15.7864262	16.0791932	15.9182195	16.2272099	16.1953455	16.1699054	16.1818454
Environmental Information Processing		raw reads	114928	147249	91619	79383	175464	224695	284344	329513	146775	187759	170455	182040	355059	391404	182240	158278
		logCPM	16.3630934	16.3922214	16.2386642	16.2529966	16.5263341	16.5420272	16.7710904	16.941873	16.4634026	16.5265739	16.6959965	16.6362477	16.7938747	16.7519797	16.4373504	16.3830179
Genetic Information Processing		raw reads	400038	521500	318898	252157	631277	811120	821112	765306	486201	582261	506630	574889	1165596	1325660	822314	772499
		logCPM	18.1624971	18.2166279	18.0380372	17.9204137	18.3734295	18.3939718	18.3010299	18.1575727	18.1913464	18.1593552	18.2675359	18.2952732	18.5088097	18.5119579	18.611197	18.6700869
Human Diseases		raw reads	73351	94111	96542	99713	39867	48435	51935	43686	35391	46970	47691	49703	45569	52911	58012	58564
		logCPM	15.7152541	15.7464012	16.3141739	16.5819472	14.3884389	14.3281947	14.3182464	14.0267991	14.4112632	14.5275147	14.8584032	14.7634064	13.8319662	13.8649816	14.7859427	14.9486503
Metabolism		raw reads	638336	782168	576637	511215	837057	1049513	1152734	1231014	792613	973693	697727	822734	1278482	1459865	781697	695589
		logCPM	18.8366756	18.8014387	18.892605	18.9400209	18.7804819	18.7657044	18.7904383	18.8433108	18.8964097	18.9011557	18.7292657	18.8124155	18.6421736	18.6510819	18.5381172	18.5187891
Organismal Systems		raw reads	24969	29637	20043	14120	35691	45564	48392	44513	33210	40441	34249	34140	72800	78734	42398	36994
		logCPM	14.1605884	14.0794514	14.0461324	13.7619278	14.2288061	14.2400403	14.2163091	14.0538544	14.3194995	14.3115962	14.3807528	14.2215424	14.5078385	14.4383928	14.3335922	14.2859341
Level 1	Level 2																	
Human Diseases:	Cancers	raw reads	31304	39867	55839	62934	13484	16747	18565	16744	10680	14471	18644	19590	15953	18276	16403	17538
		logCPM	14.1843583	14.213027	15.2020335	15.4403951	12.9341302	12.9061722	12.9463307	12.8502631	12.7772568	12.904116	13.433472	13.3595211	12.5912937	12.4630026	13.1619258	13.4244368
	Cardiovascular diseases	raw reads	432	422	179	221	157	137	171	134	190	231	287	211	188	182	111	88
		logCPM	8.00659802	7.65302855	6.9198586	7.28909187	6.51377523	5.97838898	6.18889126	5.89115877	6.96737921	6.93794403	7.41408081	6.82600211	6.18933363	5.81959893	5.96055002	5.79229301
	Endocrine and metabolic diseases	raw reads	245	440	117	183	44	34	43	47	62	103	42	66	68	59	68	59
		logCPM	7.18944006	7.71321429	6.30805413	7.01737757	4.6888902	3.98539146	4.21223926	4.39108885	5.35777742	5.77641996	6.97785734	6.60528622	4.04483354	4.36760354	5.25732839	5.21876415
	Immune diseases	raw reads	8581	10284	15873	15065	2448	2593	3066	2078	2313	3144	4644	4302	2055	2314	3003	3331
		logCPM	12.3172813	12.2582892	13.3873598	13.377824	10.4727691	10.2152253	10.3484106	9.84023803	10.5703719	10.7017974	11.4283007	11.1726075	9.63507944	9.48196248	10.7126216	11.0281226
	Infectious diseases	raw reads	6527	9746	3809	2801	8159	11095	10784	12578	6680	8593	7631	8075	15696	18157	7367	6883
		logCPM	11.9225782	12.1807739	11.3283779	10.950747	12.2093766	12.3122036	12.1626714	12.4375379	12.1002965	12.152218	12.1447526	12.0809877	12.5678639	12.4535785	12.0071645	12.0751138
	Neurodegenerative Diseases	raw reads	25973	32925	20441	18183	15438	17631	19103	11889	15237	20176	16032	17102	11426	13644	30770	30413
		logCPM	13.915028	13.9370194	13.752243	13.6491661	13.1293616	12.9803814	12.9875433	12.3562666	13.2899083	13.383578	13.2157204	13.1635738	12.10981	12.041341	14.0694718	14.2186266
	Substance dependence	raw reads	289	427	284	326	137	198	203	216	229	252	241	242	209	272	290	252
		logCPM	7.42734396	7.67000021	7.58470332	7.84915953	6.31777427	6.50791449	6.4355794	6.57760161	7.23622656	7.06322482	7.16247493	7.02335067	6.34159721	6.39710987	7.34239169	7.305814
Metabolism:	Amino acid metabolism	raw reads	127085	160027	105185	81977	243796	321215	335653	374271	175703	219903	180271	201144	398738	455321	210604	184612
		logCPM	16.2057182	16.2180608	16.1156129	15.8217727	17.1104398	17.1676915	17.1226	17.3325826	16.8173628	16.8297019	16.7068262	16.7195289	17.2347779	17.1018018	16.84439	16.8203467
	Biosynthesis of Other Secondary Metabolites	raw reads	4695	5700	3978	2973	7294	9978	13522	15723	6553	7758	5316	6201	16691	19838	8967	7737
		logCPM	11.4473203	11.4069819	11.3910028	11.0367137	12.0477037	12.1591246	12.4890713	12.7594986	12.0726056	12.0047496	11.623257	11.700052	12.6565337	12.5813137	12.2906967	12.2438412
	Carbohydrate metabolism	raw reads	109269	142067	101985	97714	156054	202404	246821	282377	148859	186729	145194	170384	291510	334461	169311	146420
		logCPM	15.9878094	16.0463175	16.071041	16.0751178	16.4668122	16.5013915	16.6790955	16.9261227	16.578171	16.5937812	16.3946415	16.4800906	16.7828831	16.6567567	16.5295336	16.4859639
	Energy metabolism	raw reads	289538	341465	283010	264256	236290	270250	269812	236144	319017	383983	227063	282613	248200	277069	228504	209822
		logCPM	17.3936744	17.3114806	17.5435337	17.5104135	17.065324	16.9184473	16.8075846	16.6681675	17.6778559	17.6338757	17.0397508	17.210127	16.5508414	16.3851648	16.9620763	17.005016
	Glycan biosynthesis and metabolism	raw reads	6935	8075	4792	2763	14277	18231	24422	28308	10299	12129	10289	12067	30878	35606	14176	12502
		logCPM	12.0100485	11.9094424	11.6595642	10.9310431	13.0165719	13.0286593	13.3419155	13.6078083	12.7248513	12.6494212	12.5758904	12.6604925	13.5440414	13.4251409	12.9514229	12.936125
	Lipid metabolism	raw reads	16015	20029	12765	9636	29917	39055	44230	48402	24840	30149	23007	26352	54481	63746	26542	23845
		logCPM	13.2174539	13.2199415	13.0729868	12.7331075	14.0838214	14.1277494	14.1987436	14.3816529	13.9949804	13.9630366	13.7368271	13.7873071	14.363177	14.2653406	13.8562278	13.8676305
	Metabolism of cofactors and vitamins	raw reads	43205	53070	33029	29749	65630	79241	85460	95179	47960	60014	44769	54018	87401	102531	48484	43559
		logCPM	14.6492041	14.6257236	14.4445004	14.3594059	15.2171998	15.1484788	15.1489582	15.3572211	14.944136	14.956214	14.6972413	14.8228216	15.045067	14.950987	14.7254483	14.7369034
	Metabolism of other amino acids	raw reads	6998	8945	5682	4560	12863	16443	19803	23493	8272	10060	10027	11325	20487	22862	11130	9718
		logCPM	12.0230945	12.0570523	11.9053173	11.6537671	12.8661111	12.879744	13.0394615	13.3388355	12.806685	12.3796027	12.5386792	12.5689403	12.9521615	12.7859908	12.6024387	12.5727109
	Metabolism of terpenoids and polyketides	raw reads	8759	10730	6670	5244	21085	27884	31492	34399	13539	16238	12575	14909	35430	40110	15638	13819
		logCPM	12.3469002	12.3195346	12.136591	11.8553861	13.5790817	13.6416879	13.7087116	13.8889599	13.1194552	13.0730201	12.865335	12.9655981	13.7424046	13.5969787	13.0930241	13.0806148
	Nucleotide metabolism	raw reads	23493	28963	17939	11307	44629	57999	71013	79641	32565	40108	34402	38512	83899	96759	43093	39055
		logCPM	13.7702488	13.7520503	13.5638805	12.9638095	14.6608303	14.6982635	14.8817941	15.1000908	14.3856321	14.3748017	14.3172378	14.3346945	14.9860713	14.8673952	14.5533948	14.5794414
	Xenobiotics biodegradation and metabolism	raw reads	2344	3097	1602	1036	5222	6813	10506	13077	5006	6622	4814	5209	10767	11562	5248	4500
logCPM		10.4452999	10.5270052	10.0790369	9.5161459	11.5656304	11.6087015	12.1249946	12.4936644	11.6841347	11.7763472	11.4801642	11.4485786	12.024111	11.8024811	11.5178911	11.4620465	

[illegible]

Metabolism:	Energy metabolism:	Oxidative phosphorylation [PATH:ko0019] raw reads	75618	89521	73894	57890	115389	139582	145473	141215	122194	147723	100223	118639	172989	190251	117705	105373
		logCPM	15.5956394	15.4682126	15.9165272	15.6917921	15.9880708	15.8715099	15.7913311	15.6397786	16.3075549	16.3268102	15.918282	16.0734997	15.7686808	15.7265262	15.8946958	15.8793956
		Photosynthesis [PATH:ko00195] raw reads	167560	192423	163056	152813	87277	87514	70824	34413	148061	174312	72688	100597	20158	23858	69647	67911
		logCPM	16.7435116	16.5721916	17.0583625	17.0921691	15.5852403	15.1979863	14.7528965	13.6029326	16.5845724	16.5655869	15.4548596	15.8355096	12.6674737	12.7312133	15.1376573	15.2456108
		Photosynthesis - antenna proteins [PATH raw reads	31115	39889	30763	39326	3145	3705	5034	3179	16291	19350	11880	18679	2907	3423	15484	13717
		logCPM	14.3145303	14.3019873	14.6522743	15.1339646	10.790966	10.6362339	10.9386052	10.1669073	13.4005573	13.3943501	12.8417182	13.4064383	9.87405154	9.93038849	12.9684092	12.937967
		Methane metabolism [PATH:ko00680] raw reads	2426	3032	2447	1666	4465	6000	10544	13146	5703	7043	3521	4127	8285	9580	3253	2933
		logCPM	10.6337799	10.5845554	11.0003254	10.573167	11.2965062	11.3316366	12.0051548	12.2146495	11.8863367	11.9363368	11.0873566	11.228303	11.3847739	11.4149164	10.7176421	10.7126192
		Carbon fixation in photosynthetic organisms raw reads	2635	3460	4791	5594	1335	1453	1417	1018	3353	3923	3990	8041	841	917	3558	3289
		logCPM	10.7529853	10.7750273	11.9695524	12.3204935	9.55502034	9.28614456	9.11020651	8.52473448	11.1201346	11.0921769	11.2677407	12.1905117	8.08563751	8.03112575	10.8469155	10.877868
		Carbon fixation pathways in prokaryotes raw reads	3437	4109	1846	1124	12829	18833	23939	28904	5015	6599	6130	6449	28065	31451	8514	7686
		logCPM	11.1362837	11.0230103	10.5937709	10.0055343	12.8190898	12.9817701	13.1880466	13.3512536	11.7008784	11.8424003	11.8871882	11.8722312	13.1448777	13.1298333	12.1055766	12.1023428
		Nitrogen metabolism [PATH:ko00910] raw reads	3990	5233	4028	4147	6915	6981	7924	9275	14509	20273	25538	22302	8757	10438	5657	4849
		logCPM	11.3515005	11.3718242	11.7193062	11.8887057	11.9275248	11.5500882	11.5930622	11.7114763	13.2334343	13.4615746	13.9458027	13.6621888	11.4647016	11.5386534	11.5158178	11.4378449
		Sulfur metabolism [PATH:ko00920] raw reads	2757	3798	2185	1696	4935	6182	4657	4994	3891	4760	3093	3779	6198	7151	4686	4064
		logCPM	10.8182725	10.909477	10.8369656	10.5989106	11.4408826	11.3747437	10.8263157	10.8184166	11.3348008	11.3711522	10.900401	11.1012279	10.9661201	10.9930804	11.244163	11.183083
Level 1	Level 2	Level 3	Function; KO #															
Human Diseases:	Infectious diseases:	Bacterial invasion of ELMO1, CED12; engi raw reads	0	5	0	0	0	0	0	0	1	3	0	0	0	0	0	0
		logCPM	-1.9838792	1.52057602	-1.9838792	-1.9838792	-1.9838792	-1.9838792	-1.9838792	-1.9838792	-0.1963278	0.81064636	-1.9838792	-1.9838792	-1.9838792	-1.9838792	-1.9838792	-1.9838792
		RHOG; Ras homolog raw reads	13	19	9	0	1	13	12	8	10	19	7	12	10	18	37	43
		logCPM	3.14585395	3.34972566	2.98863243	-1.9838792	-0.4004938	2.4531594	2.35814129	1.95496007	2.68983809	3.28693031	2.07601203	2.75102273	2.0319802	2.65463673	4.13740417	4.51596648
		yeel; adhesin/Invasi raw reads	7	11	4	0	5	12	33	28	9	8	4	8	26	29	2	0
		logCPM	2.28766401	2.58701728	1.87503279	-1.9838792	1.47340145	2.34322178	3.7715784	3.69350468	2.54410199	2.08949034	1.3321171	2.1928983	3.35453905	3.32055338	0.25148238	-1.9838792
		Vibrio cholerae infe ARF1; ADP-ribosylat raw reads	230	340	199	158	69	154	78	69	96	92	158	103	105	130	152	218
		logCPM	7.25149292	7.47701003	7.41077784	7.21739611	5.13271267	5.95719941	4.99709632	4.97782498	5.90132492	5.53260492	6.48730521	5.80388223	5.34126427	5.45629421	6.16011274	6.84503198
		E3.4.24.25; vibriolys raw reads	5	11	12	10	57	64	38	55	38	54	13	20	132	154	22	13
		logCPM	1.83181137	2.58701728	3.39213608	3.27136738	4.8592652	4.69864466	4.59801031	4.39863803	4.57357399	4.79569358	3.533234	4.21803343	5.66957145	5.69941772	3.40144403	2.82646805
		KCNQ1, KV7.1; pota: raw reads	3	6	2	4	1	0	1	0	1	0	12	4	0	0	0	0
		logCPM	1.16158213	1.76226593	0.97118806	2.00501526	-0.4004938	-1.9838792	-0.6016506	-1.9838792	-0.1963278	-1.9838792	2.8171193	1.27054096	-1.9838792	-1.9838792	-1.9838792	-1.9838792
		KDEL; ER lumen pr raw reads	76	129	73	111	41	41	25	49	37	46	43	34	42	41	52	61
		logCPM	5.65877243	6.08219102	5.96767259	6.7090686	4.38882252	4.06405436	3.37956119	4.48872683	4.53551376	4.54046278	4.6206208	4.21803343	4.03276861	3.80939952	4.62239987	5.01572736
		MUC2; intestinal m raw reads	3	0	6	3	1	0	1	0	0	0	1	0	0	0	0	1
		logCPM	1.16158213	-1.9838792	2.42646463	1.6199526	-0.4004938	-1.9838792	-0.6016506	-1.9838792	-1.9838792	-1.9838792	-0.2880002	-1.9838792	-1.9838792	-1.9838792	-1.9838792	-0.3602955
		SLC12A2, NKCC1; so raw reads	27	50	12	13	12	4	1	5	8	16	27	15	8	7	5	2
		logCPM	4.17877534	4.72330053	3.39213608	3.64113559	2.65770547	0.8952933	-0.6016506	1.33225589	2.38197264	3.04599239	3.95800264	3.06207423	1.73217724	1.38033073	1.37676844	0.38427175
		Vibrio cholerae path acfC; accessory colo raw reads	1	1	5	1	1	0	0	3	2	0	0	2	3	3	1	1
		logCPM	-0.1293948	-0.3657627	2.17693615	0.25470197	-0.4004938	-1.9838792	-1.9838792	0.68876245	0.57795259	-1.9838792	-1.9838792	0.41431378	0.489403	0.33360006	-0.4706899	-0.3602955
		CQSA; CAI-1 autoind raw reads	2	0	1	2	1	0	0	1	1	4	4	3	1	2	1	1
		logCPM	0.65592009	-1.9838792	0.14617526	1.09313374	-0.4004938	-1.9838792	-1.9838792	-0.5025879	-0.1963278	1.17273908	1.3321171	0.90503689	-0.651781	-0.1134539	-0.4706899	-0.3602955
		E4.6.1.1A, cyaA; ade raw reads	5	8	4	1	15	31	15	14	13	20	51	18	61	16	14	14
		logCPM	1.83181137	2.15017092	1.87503279	0.25470197	2.96802726	3.66771559	2.66577135	2.72142386	1.9900725	2.85964217	2.92861006	3.46615251	4.30893878	4.37403003	2.95489849	2.92970585
		hapR; TetR/AcrR far raw reads	1	1	1	1	0	0	3	0	2	6	4	5	2	5	1	0
		logCPM	-0.1293948	-0.3657627	0.14617526	0.25470197	-1.9838792	-1.9838792	0.55717022	-1.9838792	0.57795259	1.70273954	1.3321171	1.56191157	0.02882223	0.94988391	-0.4706899	-1.9838792
		luxS; S-ribosylhomoi raw reads	2	2	2	12	12	12	30	37	15	7	22	10	40	55	53	29
		logCPM	0.65592009	0.37774327	0.97118806	1.09313374	2.65770547	2.34322178	3.63674301	4.08872948	3.25583459	1.9090361	3.66787073	2.49878354	3.96349302	4.22656999	4.64960119	3.95535811
		mshA; MSHA pilin p raw reads	75	64	156	72	212	288	248	332	76	125	194	218	560	535	112	106
		logCPM	5.63975986	5.0764208	7.06014613	6.08646479	6.74507916	6.85760389	6.65804041	7.23514194	5.5658949	5.97274561	6.78268272	6.88211789	7.74897332	7.49101904	5.72136051	5.80811634
		mshB; MSHA pilin p raw reads	5	7	5	5	36	30	41	50	11	12	24	16	110	146	25	31
		logCPM	1.83181137	1.9692166	2.17693615	2.30865488	4.20361156	3.62136621	4.07951592	4.51754824	2.82219374	2.64560041	3.79100826	3.15245162	5.40796947	5.62284028	3.58172062	4.05005574
		mshC; MSHA pilin p raw reads	1	0	1	1	4	14	15	17	3	2	1	2	28	21	15	11
		logCPM	-0.1293948	-1.9838792	0.14617526	0.25470197	1.18394267	2.5553094	2.66577135	2.99173952	1.07908068	0.32607838	-0.2880002	0.41431378	3.45890505	2.86873079	2.86492159	2.59477853
		mshD; MSHA pilin p raw reads	0	0	0	0	8	12	9	14	5	4	2	5	31	22	8	11
		logCPM	-1.9838792	-1.9838792	-1.9838792	-1.9838792	2.1013567	2.34322178	1.96662339	2.72142386	1.74528447	1.17273908	0.47016089	1.56191157	3.60253295	2.93357349	2.00118652	2.59477853
		ompU; outer memb raw reads	8	13	18	10	43	52	89	128	46	57	126	145	49	67	37	23
		logCPM	2.47094142	2.81865637	3.96547178	3.27136738	4.45672528	4.40232199	5.1860153	5.86395563	4.84654208	4.84676305	6.16183648	6.29539849	4.25197416	4.50780585	4.13740417	3.62705958
		SIG2, rpoS; RNA pol raw reads	1660	3679	292	273	675	1043	528	485	460	548	267	332	1763	1975	844	741
		logCPM	10.100907	10.9108578	7.96329496	8.00533973	8.41356827	8.71192394	7.74632171	7.78117954	8.15701561	8.10050361	7.24255982	7.48791088	9.40234966	9.37378191	8.62909665	8.60793645

Epithelial cell signal	ADAM10; disintegrin-like metalloprotease 10	raw reads	35	29	8	10	1	4	0	1	6	7	14	9	2	1	2	1	
		logCPM	4.54856037	3.94738932	2.82443996	3.27136738	-0.4004938	0.8952933	-1.9838792	-0.5025879	1.9900725	1.9090361	3.03209952	2.35393264	0.02882223	-0.7646631	0.25148238	-0.3602955	
	CSK; c-src tyrosine kinase	raw reads	38	58	32	28	6	5	11	5	8	13	8	7	4	9	1	1	
		logCPM	4.66597392	4.93551961	4.78529589	4.73230453	1.71437644	1.17746032	2.23906296	1.33225589	2.38197264	2.75658713	2.25780365	2.01160415	0.83789255	1.71142602	-0.4706899	-0.3602955	
	K08303; putative protein	raw reads	161	224	177	90	591	646	992	1147	489	580	802	877	1003	1252	533	519	
		logCPM	6.73794521	6.8760338	7.24202516	6.40731901	8.22199092	8.02132528	8.65532918	9.02203101	8.24514044	8.1823073	8.99715098	8.88804129	8.58904714	8.71648126	7.96652659	8.09459725	
	PTPRZ; receptor-type protein tyrosine phosphatase	raw reads	7	16	3	1	0	3	0	4	1	6	4	8	4	3	5	3	
		logCPM	2.28766401	3.10849071	1.49276432	2.9588519	-1.9838792	-0.6113059	-1.9838792	-0.5025879	1.9900725	1.17273908	1.3321171	2.1928983	-1.9838792	0.33360006	1.37676844	0.87294422	
	ureAB; urease subunit	raw reads	4	11	5	2	27	37	6	5	3	28	6	5	10	9	9	9	
		logCPM	1.53527255	2.58701728	2.17693615	1.09313374	3.79515733	3.91831115	1.42758015	1.33225589	1.07908068	3.83429622	1.86796502	1.56191157	2.0319802	1.71142602	2.16095287	2.3186267	
ureC; urease subunit	raw reads	261	353	112	85	466	458	346	416	246	280	177	221	367	493	313	267		
	logCPM	7.43362454	7.53106808	6.58317214	6.3251096	7.87949037	7.52571484	7.13744903	7.56005331	7.25515122	7.13302587	6.65069356	6.90179415	7.14021791	7.37324051	7.19957825	7.13696124		
Pathogenic Escherichia coli	NCL, NSR1; nucleoside diphosphate kinase	raw reads	15	29	18	13	39	67	46	28	24	16	19	21	38	45	138	167	
	logCPM	3.34680007	3.94738932	3.96547178	3.64113559	4.31756529	4.76410482	4.24317907	3.69350468	3.91951656	3.04599239	3.46089055	3.53496941	3.89072242	3.94138631	6.02122701	6.46152048		
Salmonella enterica	nfra; cytochrome c	raw reads	83	120	45	31	33	62	30	22	385	524	165	148	75	110	58	54	
	logCPM	5.78527534	5.97825804	5.27332289	4.87781742	4.07987931	3.18464411	3.63674301	3.35324943	7.9004891	8.03595539	6.5496742	6.32484863	4.85943167	5.21679574	4.77840851	4.84133825		
Pertussis toxin	cytA; anthrax edema factor	raw reads	3	10	1	2	5	8	4	14	10	4	4	6	10	8	5	5	
		logCPM	1.16158213	2.45557115	0.14617526	1.09313374	1.47340145	1.79375724	0.90886725	2.72142386	2.68983809	1.17273908	1.3321171	1.80420871	2.0319802	1.55535581	1.37676844	1.52796518	
	NLRP3, PYPAF1; NALP3	raw reads	0	0	0	0	0	0	0	0	0	0	0	0	0	0	5	4	
	logCPM	-1.9838792	-1.9838792	-1.9838792	-1.9838792	-1.9838792	-1.9838792	-1.9838792	-1.9838792	-1.9838792	-1.9838792	-1.9838792	-1.9838792	-1.9838792	-1.9838792	-1.9838792	1.37676844	1.23731429	
Legionella pneumophila	sdhA; succinate dehydrogenase	raw reads	2657	3027	1520	890	4233	6299	6526	7890	3514	4538	4338	4637	9053	10316	3125	2834	
	logCPM	10.7793973	10.6294736	10.3421449	9.70925973	11.06139	11.3055816	11.3723488	11.8035912	11.0893131	11.1491436	11.2624162	11.2899599	11.7622791	11.7582965	10.5169654	10.5425402		
Staphylococcus aureus	D-alanine--pol	raw reads	3	1	3	1	1	0	5	15	2	4	7	6	8	6	6	9	
		logCPM	1.16158213	-0.3657627	1.49276432	0.25470197	-0.4004938	-1.9838792	1.19141174	2.81726804	0.57795259	1.17273908	2.07601203	1.80420871	1.73217724	1.1811018	1.61620269	2.3186267	
	dlb; membrane protein	raw reads	0	0	0	0	4	0	2	1	1	1	4	2	2	0	3	2	
	logCPM	-1.9838792	-1.9838792	-1.9838792	-1.9838792	1.18394267	-1.9838792	0.09111073	-0.5025879	-0.1963278	-0.4088852	1.3321171	0.41431378	0.02882223	-1.9838792	0.73052249	0.38427175		
dlc; D-alanine--poly	raw reads	0	0	0	0	0	0	0	3	1	2	1	1	2	1	0	1	6	
	logCPM	-1.9838792	-1.9838792	-1.9838792	-1.9838792	-1.9838792	-1.9838792	-1.9838792	0.68876245	-0.1963278	-0.4088852	-0.2880002	0.41431378	-0.651781	-1.9838792	-0.4706899	1.76976494		
dltd; D-alanine trans	raw reads	0	0	0	0	0	1	1	0	0	0	0	1	0	2	0	9	6	
	logCPM	-1.9838792	-1.9838792	-1.9838792	-1.9838792	-1.9838792	-0.6113059	-0.6016506	-1.9838792	-1.9838792	-1.9838792	-0.2880002	-1.9838792	0.02882223	-1.9838792	2.16095287	1.76976494		
eta; exfoliative toxin	raw reads	0	0	0	0	0	4	9	0	0	0	0	0	0	0	0	0	0	
	logCPM	-1.9838792	-1.9838792	-1.9838792	-1.9838792	-1.9838792	0.8952933	0.90886725	2.11439445	-1.9838792	-1.9838792	-1.9838792	-1.9838792	-1.9838792	-1.9838792	-1.9838792	-1.9838792	-1.9838792	
mprf; fmsC; phosphatase	raw reads	0	2	3	0	11	18	22	21	3	5	3	0	21	41	3	1	1	
	logCPM	-1.9838792	0.37774327	1.49276432	-1.9838792	2.53741948	2.90402425	3.19990749	3.28783373	1.07908068	1.46194184	0.96457705	-1.9838792	3.05488175	3.80939952	0.73052249	-0.3602955	0.38427175	
sasG; surface protein	raw reads	3	1	2	0	4	0	4	2	4	1	5	1	5	7	0	4	4	
	logCPM	1.16158213	-0.3657627	0.97118806	-1.9838792	1.18394267	-1.9838792	0.90886725	0.21271859	1.45030041	-0.4088852	1.62477754	-0.3305089	1.11851494	1.38033073	-1.9838792	1.23731429	0.38427175	
sdrC_D_E; serine-ase	raw reads	0	0	3	2	4	7	2	7	9	41	3	3	25	44	4	8	9	
	logCPM	-1.9838792	-1.9838792	1.49276432	1.09313374	1.18394267	1.6160622	0.09111073	1.77569181	2.54410199	4.3763629	0.96457705	0.90503689	3.29938112	3.9095043	1.08953214	2.15781193	0.38427175	
Tuberculosis [PATH]	CD74, DHLG; CD74	raw reads	0	4	5	6	0	0	2	0	0	2	0	0	0	9	5	5	
		logCPM	-1.9838792	1.23008399	2.17693615	2.55936689	-1.9838792	-1.9838792	-1.9838792	0.21271859	-1.9838792	-1.9838792	0.47016089	-1.9838792	-1.9838792	-1.9838792	2.16095287	1.52796518	0.38427175
	E3.1.3.2; acid phosphatase	raw reads	13	22	43	26	22	27	17	12	14	20	11	21	37	33	29	20	19
	logCPM	3.14585395	3.55634286	5.2081371	4.62644445	3.50566028	3.47265232	2.83956576	2.50821904	3.15902366	3.35906127	2.69628552	5.53496941	3.85291269	3.50253456	3.79163761	3.42984691	0.38427175	
NFYA; nuclear transcription factor	raw reads	20	51	9	20	0	0	2	0	2	0	6	4	5	5	0	8	0	
	logCPM	3.7528473	4.75159892	2.98863243	4.2523559	-1.9838792	-1.9838792	0.09111073	-1.9838792	1.9900725	1.17273908	1.62477754	1.56191157	-1.9838792	-1.9838792	2.00118652	-1.9838792	0.38427175	
NFYB; nuclear transcription factor	raw reads	17	37	10	16	12	19	8	3	14	10	12	10	7	7	7	25	0	
	logCPM	3.52314858	4.29374082	3.13603304	3.93520421	2.65770547	2.9794599	1.80831595	0.68876245	3.15902366	2.39417631	2.8171193	2.49878354	1.35327725	1.38033073	1.82149832	3.7449903	0.38427175	
NFYC; nuclear transcription factor	raw reads	17	37	14	21	2	1	8	2	6	19	15	17	4	2	12	9	0	
	logCPM	3.52314858	4.29374082	3.60955706	4.2183364	0.33615622	-0.6113059	1.80831595	0.21271859	1.9900725	3.28693031	3.12865962	3.23749956	0.83798255	-0.1134539	2.55545593	2.3186267	0.38427175	

Metabolism:	Energy metabolism:Methane metabolism:cdhA; acetyl-CoA de	2	0	5	2	1	4	9	6	42	59	4	7	27	9	2	3
	logCPM	0.65592009	-1.9838792	2.17693615	1.09313374	-0.4004938	0.8952933	1.96662339	1.57094436	4.71650436	4.89608636	1.3321171	2.01160415	3.40766559	1.71142602	0.25148238	0.87294422
cdhB; acetyl-CoA de	raw reads	0	0	0	0	0	1	0	0	7	14	4	2	4	4	0	1
	logCPM	-1.9838792	-1.9838792	-1.9838792	-1.9838792	-1.9838792	-0.6113059	-1.9838792	-1.9838792	2.19928904	2.85964217	1.3321171	0.41431378	0.83798255	0.67440244	-1.9838792	-0.3602955
cdhC; acetyl-CoA de	raw reads	1	2	4	5	4	8	7	3	60	30	7	9	20	25	1	2
	logCPM	-0.1293948	0.37774327	1.87503279	2.30865488	1.18394267	1.79375724	1.63047158	0.68876245	5.22690974	3.93212622	2.07601203	2.35393264	2.98668521	3.11225797	-0.4706899	0.38427175
cdhD; acetyl-CoA de	raw reads	5	7	3	6	10	7	15	22	37	42	28	24	50	70	14	18
	logCPM	1.83181137	1.9692166	1.49276432	2.55936689	2.40618475	1.6160622	2.66577135	3.35324943	4.53551376	4.41071014	4.00963165	3.72367592	4.2807376	4.57031243	2.76895761	3.28159936
cdhE; acetyl-CoA de	raw reads	7	2	7	9	7	18	17	14	49	79	37	41	39	50	26	12
	logCPM	2.28766401	0.37774327	2.63913196	3.12355526	1.92080303	2.90402425	2.83956576	2.72142386	4.93691362	5.31411972	4.40621162	4.4847727	3.9275665	4.09101339	3.63713205	2.71526932
CODH-ACSA; carbon	raw reads	4	5	13	11	13	26	12	26	32	39	43	36	31	39	7	14
	logCPM	1.53527255	1.52057602	3.5049385	3.40543285	2.76872977	3.41946761	2.35814129	3.58875639	4.32851563	4.3051134	4.6206208	4.2994064	3.60253295	3.73858322	1.82149832	2.92970585
E1.12.1.2; hydrogen	raw reads	538	693	179	183	214	197	368	376	969	1331	389	363	297	295	173	151
	logCPM	8.47609427	8.50328746	7.25820846	7.42898035	6.75859392	6.31118275	7.22622788	7.41440804	9.23120706	9.37998444	7.78473468	7.61652366	6.83551003	6.6338436	6.34619422	6.31665939
E1.12.7.2; ferredoxin	raw reads	1	4	6	3	2	5	4	6	14	17	5	11	2	3	7	5
	logCPM	-0.1293948	1.23008399	2.42646463	1.6199526	0.33615622	1.17746032	0.90886725	1.57094436	3.1590236	3.13085522	1.62477754	2.63040878	0.02882223	0.33360006	1.82149832	1.52796518
E1.12.7.2G; ferredoxin	raw reads	3	5	7	8	3	4	0	0	7	4	0	6	1	2	0	0
	logCPM	1.16158213	1.52057602	2.63913196	2.9588519	0.82144776	0.8952933	-1.9838792	-1.9838792	2.19928904	1.17273908	-1.9838792	1.80420871	-0.651781	-0.1134539	-1.9838792	-1.9838792
E1.12.7.2S; ferredoxin	raw reads	0	5	2	1	14	13	21	23	4	12	13	9	17	36	20	10
	logCPM	-1.9838792	1.52057602	0.97118806	0.25470197	2.87181722	2.4531594	3.13468214	3.41582722	1.45030041	2.64560041	2.92861006	2.35393264	2.76031722	3.6253812	3.26738806	2.46329996
E1.14.13.8; dimethyl	raw reads	19	23	24	13	20	30	69	107	51	53	25	61	32	60	18	15
	logCPM	3.68026996	3.61912462	4.37466055	3.64113559	3.37136432	3.62136621	4.82170744	5.60665116	4.99416209	4.74274977	3.84884761	4.08666224	3.64739802	4.35047642	3.1195875	3.02604684
E1.2.99.2C; cooS; ca	raw reads	26	19	19	17	30	27	58	34	60	93	61	80	103	172	38	36
	logCPM	4.12510191	3.34972566	4.04224495	4.02126387	3.94453072	3.47265232	4.57360789	3.9686291	5.22690974	5.54811705	5.12071188	5.44118557	5.31369397	5.8581612	4.17533283	4.26272312
E1.2.99.2L; cutL, cox	raw reads	226	185	131	54	479	694	2061	3161	429	524	307	340	741	807	225	207
	logCPM	7.2262242	6.60071477	6.80868839	5.67321529	7.91914404	8.12462968	9.70979238	10.4840996	8.05645173	8.03595539	7.44364489	7.52221458	8.15260582	8.08336531	6.72431073	6.77050319
E1.2.99.2M; cutM, c	raw reads	94	88	106	30	256	395	1309	2159	320	347	283	457	547	585	144	115
	logCPM	5.96405065	5.53290131	6.50395297	4.83092515	7.01657419	7.31253554	9.05516317	9.93419997	7.63401258	7.44203291	7.32638596	7.94836595	7.71512762	7.61974348	6.08239355	5.9251764
E1.2.99.2S; coxS; ca	raw reads	80	84	129	43	233	295	750	1108	226	299	181	293	470	505	141	109
	logCPM	5.73241199	5.46616222	6.78654309	5.34641984	6.88103837	6.8921754	8.2521715	8.97214819	7.13302694	7.2275794	6.68285367	7.30789872	7.49653178	7.40788397	6.05213442	5.84820104
E1.2.99.5A; fwdA, fr	raw reads	7	4	40	30	62	66	139	150	47	41	19	27	120	107	54	36
	logCPM	2.28766401	1.23008399	5.10457623	4.83092515	4.97955779	4.7426131	5.8256145	6.09185554	4.87729922	4.3763629	3.46089055	3.89053014	5.53278432	5.17717796	4.67629912	4.26272312
E1.2.99.5B; fwdB, fr	raw reads	2	2	17	8	18	32	77	73	29	13	14	11	35	38	33	22
	logCPM	0.65592009	0.37774327	3.88438235	2.9588519	3.22327193	3.71262214	4.97862895	5.05849074	4.18837332	2.75658713	3.03209952	2.63040878	3.77418403	3.70182739	3.97485538	3.56427043
E1.2.99.5C; fwdC, fr	raw reads	6	1	15	5	13	25	33	30	23	17	10	7	23	19	14	9
	logCPM	2.07766793	-0.3657627	3.70709935	2.30865488	2.76872977	3.36424697	3.7715784	3.79115972	3.8591636	3.13085522	2.56439841	2.01160415	3.18230479	2.7295875	2.76895761	2.3186267
E1.2.99.5D; fwdD, fr	raw reads	2	0	1	0	1	2	0	0	4	7	1	0	0	0	0	0
	logCPM	0.65592009	-1.9838792	0.14617526	-1.9838792	-0.4004938	0.07915428	-1.9838792	-1.9838792	1.45030041	1.9090361	-0.2880002	-1.9838792	-1.9838792	-1.9838792	-1.9838792	-1.9838792
E1.2.99.5E; fwdE, fr	raw reads	0	1	0	1	3	8	4	1	6	4	2	6	2	1	1	3
	logCPM	-1.9838792	-0.3657627	-1.9838792	0.25470197	0.82144776	1.79375724	0.90886725	-0.5025879	1.9900725	1.17273908	0.47016089	1.80420871	0.02882223	-0.7646631	-0.4706899	0.87294422
E1.2.99.5F; fwdF, fr	raw reads	1	5	1	1	2	1	0	1	2	5	3	1	1	7	0	1
	logCPM	-0.1293948	1.52057602	0.14617526	0.25470197	0.33615622	-0.6113059	-1.9838792	-0.5025879	0.57795259	1.46194184	0.96457705	-0.3350859	-0.651781	1.38033073	-1.9838792	-0.3602955
E1.2.99.5G; fwdG, fr	raw reads	0	0	0	1	1	0	0	0	1	0	0	4	0	0	2	1
	logCPM	-1.9838792	-1.9838792	-1.9838792	0.25470197	-0.4004938	-1.9838792	-1.9838792	-1.9838792	-0.1963278	-1.9838792	-1.9838792	1.27054096	-1.9838792	-1.9838792	0.25148238	-0.3602955
E1.5.1.20; metF; me	raw reads	393	565	381	317	1004	1312	1154	1166	646	786	577	690	1570	1725	794	779
	logCPM	8.02339527	8.20891066	8.34677617	8.22072458	9.88601759	9.04277415	8.87343338	9.04572197	8.64654796	8.6204546	8.35299684	8.54226943	9.235148	9.17860529	8.54105067	8.68004064
E1.5.8.2; trimethylar	raw reads	1	2	1	1	5	13	23	5	7	1	1	1	5	7	6	1
	logCPM	-0.1293948	0.37774327	0.14617526	0.25470197	1.47340145	1.17746032	2.46813602	3.41582722	1.74528447	1.9090361	-0.2880002	-0.3350859	1.11851494	1.38033073	1.61620269	-0.3602955
E2.1.1.86A; mtrA; te	raw reads	4	3	6	0	0	10	4	7	23	32	21	9	15	29	3	4
	logCPM	1.53527255	0.86596405	2.42646463	-1.9838792	-1.9838792	2.09449154	0.90886725	1.77569181	3.8591636	4.02374151	3.60212239	2.35393264	2.5869046	3.32055338	0.73052249	1.23731429
E2.1.1.86B; mtrB; te	raw reads	0	0	0	0	0	1	0	10	3	2	3	2	4	0	0	0
	logCPM	-1.9838792	-1.9838792	-1.9838792	-1.9838792	-1.9838792	-0.6113059	-0.6016506	-1.9838792	2.68983809	0.81064636	0.47016089	0.90503689	0.02882223	0.67440244	-1.9838792	-1.9838792
E2.3.1.101, ftr; form	raw reads	4	6	25	14	47	53	116	102	21	47	13	15	61	97	37	29
	logCPM	1.53527255	1.76226593	4.4328508	3.7459612	4.5836351	4.42947728	5.56592898	5.53797639	3.73031069	4.57115617	2.92861006	3.06207423	4.56423102	5.03666267	4.13740417	3.95535811
E2.7.1.29, DAK1, DA	raw reads	41	28	26	19	48	33	88	90	71	69	32	41	88	118	64	58
	logCPM	4.77454678	3.89760736	4.48878469	4.17936219	4.61369182	3.75617299	5.16982733	5.35845043	5.46825362	5.12019146	4.19944348	4.4847727	5.08818734	5.31741401	4.91918104	4.94355405

E3.1.3.71, comB; 2- raw reads	97	88	26	11	34	41	90	101	63	53	33	38	102	102	43	62
logCPM	6.00919392	5.53290131	4.48878469	3.40543285	4.12231334	4.06405436	5.20202364	5.52384025	5.29683523	4.74274977	4.24323589	4.37643368	5.29970869	5.10863037	4.35132086	5.03900448
E4.4.1.19, comA; ph raw reads	111	106	86	26	129	198	447	622	201	204	251	229	375	484	106	78
logCPM	6.20298256	5.80005181	6.20323154	4.62644445	6.03057199	6.31846435	7.50636638	8.13974413	5.97427177	6.67713592	7.15356096	6.95298882	7.17127328	7.34670082	5.64231729	5.36793297
echA; ech hydrogen raw reads	4	3	1	0	1	3	1	3	12	14	2	1	1	1	1	2
logCPM	1.53527255	0.86596405	0.14617526	-1.9838792	-0.4004938	0.54418196	-0.6016506	0.68876245	2.94342066	2.85964217	0.47016089	-0.3350859	-0.651781	-0.7646631	-0.4706899	0.38427175
echB; ech hydrogen raw reads	2	0	0	1	0	0	0	0	14	10	1	1	1	0	0	0
logCPM	0.65592009	-1.9838792	-1.9838792	0.25470197	-1.9838792	-1.9838792	-1.9838792	-1.9838792	3.15902366	2.39417631	-0.2880002	-0.3350859	-0.651781	-1.9838792	-1.9838792	-1.9838792
echC; ech hydrogen raw reads	2	1	0	0	0	0	0	1	16	18	1	2	0	6	0	1
logCPM	0.65592009	-0.3657627	-1.9838792	-1.9838792	-1.9838792	-1.9838792	-1.9838792	-0.5025879	3.34655561	3.21100232	-0.2880002	0.41431378	-1.9838792	1.1811018	-1.9838792	-0.3602955
echE; ech hydrogen raw reads	5	1	1	0	1	0	1	2	21	18	3	7	11	5	2	0
logCPM	1.83181137	-0.3657627	0.14617526	-1.9838792	-0.4004938	-1.9838792	-0.6016506	0.21271859	3.73031069	3.21100232	0.96457705	2.01160415	2.16135334	0.94988391	0.25148238	-1.9838792
ehbQ; energy-conve raw reads	0	0	2	0	1	1	0	2	6	0	1	0	0	0	0	0
logCPM	-1.9838792	-1.9838792	0.97118806	-1.9838792	-0.4004938	-0.6113059	-1.9838792	0.21271859	1.9900725	-1.9838792	-0.2880002	-1.9838792	-1.9838792	-1.9838792	-1.9838792	-1.9838792
fae; formaldehyde- raw reads	79	74	530	329	487	675	1137	1060	304	361	126	170	809	1065	270	237
logCPM	5.71435148	5.28441266	8.82266254	8.27428473	7.9430154	8.08461831	8.85203404	8.90828746	7.56010864	7.49901474	6.16183648	6.52419728	8.27916425	8.48325237	6.98677012	6.96533654
fdhA; glutathione-in raw reads	29	49	51	26	213	314	184	166	22	26	13	28	174	191	93	75
logCPM	4.28047929	4.69443594	5.45278522	4.62644445	6.75185237	6.9820392	6.22866171	6.23756079	3.79617521	3.72934659	2.92861006	3.942119	6.06639015	6.00869967	5.45457604	5.31170268
frhA; coenzyme F42 raw reads	2	5	4	3	4	4	5	8	35	35	21	33	20	19	20	16
logCPM	0.65592009	1.52057602	1.87503279	1.6199526	1.18394267	0.8952933	1.19141174	1.95496007	4.45624181	4.15110124	4.24323589	3.39388787	3.05488175	2.80083599	3.1195875	3.11635508
frhB; coenzyme F42 raw reads	176	215	126	99	54	49	110	106	75	82	53	76	67	86	104	110
logCPM	6.8661687	6.8170017	6.75267442	6.54443184	4.78196061	4.31764773	5.48972761	5.59317524	5.54688873	5.36755554	4.91947644	5.36762675	4.69820159	4.86443514	5.61497698	5.86131887
frhD; coenzyme F42 raw reads	0	0	0	2	0	2	1	2	5	17	2	11	3	6	0	8
logCPM	-1.9838792	-1.9838792	-1.9838792	1.09313374	-1.9838792	0.07915428	-0.6016506	0.21271859	1.74528447	3.13085522	0.47016089	2.63040878	0.489403	1.1811018	-1.9838792	2.15781193
frhG; coenzyme F42 raw reads	0	0	5	0	2	2	2	0	9	9	8	4	7	6	3	1
logCPM	-1.9838792	-1.9838792	2.17693615	-1.9838792	0.33615622	0.07915428	0.09111073	-1.9838792	2.54410199	2.24986183	2.25780365	1.27054096	1.55513064	1.1811018	0.73052249	-0.3602955
frmB, ESD, fghA; S- raw reads	93	145	112	108	205	282	257	303	97	133	119	136	402	440	242	213
logCPM	5.94868343	6.25027871	6.58317214	6.66963706	6.69675491	6.82729715	6.70934217	7.10350817	5.91621235	6.0618944	6.07967394	6.20325951	7.27140821	7.20942135	6.82915044	6.81163174
gfa; S-(hydroxymeth raw reads	0	4	2	0	15	17	35	41	12	3	7	7	25	27	9	13
logCPM	-1.9838792	1.23008399	0.97118806	-1.9838792	2.96802726	2.82442553	3.85494043	4.23473532	2.94342066	0.81064636	2.07601203	2.01160415	3.29938112	3.22016161	2.16095287	2.82646805
hdrA; heterodisulfid raw reads	41	83	49	47	72	107	69	221	101	349	190	163	213	160	42	56
logCPM	4.77454678	5.44898361	5.39540959	5.47398078	5.19367998	5.43445616	5.29451364	4.97782498	7.10080933	7.45031226	6.75269523	6.43698208	5.97254205	6.16539527	4.31779891	4.89335122
hdrB; heterodisulfid raw reads	101	249	10	21	47	43	46	19	73	99	45	38	83	61	22	17
logCPM	6.06726828	7.02836902	3.13603304	4.32183364	4.5836351	4.13175255	4.24317907	3.14736951	5.50810833	5.63784235	4.68555007	4.37643368	5.00444091	4.37403003	3.40144403	3.20134179
hdrC; heterodisulfid raw reads	10	14	3	6	23	18	18	11	33	51	18	20	33	32	5	7
logCPM	2.77965176	2.92187418	1.49276432	2.55936689	3.5683938	2.90402425	2.91919439	2.3885045	4.37235954	4.68778878	3.38472705	3.46615251	3.69090985	3.45914575	1.37676844	1.9767961
hdrD; heterodisulfid raw reads	0	0	1	0	1	0	4	0	5	8	1	3	4	9	0	0
logCPM	-1.9838792	-1.9838792	0.14617526	-1.9838792	-0.4004938	-1.9838792	0.90886725	-1.9838792	1.74528447	2.08949034	-0.2880002	0.90503689	0.83798255	1.71142602	-1.9838792	-1.9838792
hdrE; heterodisulfid raw reads	0	0	2	0	0	0	1	1	4	5	0	0	0	0	1	0
logCPM	-1.9838792	-1.9838792	0.97118806	-1.9838792	-1.9838792	-1.9838792	-0.6016506	-0.5025879	1.45030041	1.46194184	-1.9838792	-1.9838792	-1.9838792	-1.9838792	-0.4706899	-1.9838792
K00400; methyl coe raw reads	1	3	0	2	2	1	1	1	4	3	2	3	5	7	0	0
logCPM	-0.1293948	0.86596405	-1.9838792	1.09313374	0.33615622	-0.6113059	-0.6016506	-0.5025879	1.45030041	0.81064636	0.47016089	0.90503689	1.11851494	1.38033073	-1.9838792	-1.9838792
K13039, comE; sulfo raw reads	0	3	0	0	0	3	0	2	0	0	0	0	1	3	6	0
logCPM	-1.9838792	0.86596405	-1.9838792	-1.9838792	-1.9838792	0.54418196	-1.9838792	0.21271859	-1.9838792	-1.9838792	-1.9838792	-1.9838792	-0.651781	0.33360006	1.61620269	-1.9838792
mch; methenyltetra raw reads	5	5	17	19	26	40	50	68	14	41	18	22	44	80	34	22
logCPM	1.83181137	1.52057602	3.88438235	4.17936219	3.7417197	4.02897549	4.36193173	4.95693356	3.15902366	4.3763629	3.38472705	3.60065265	4.09886956	4.76103723	4.01724112	3.56427043
mcrA; methyl-coenz raw reads	21	21	20	14	30	35	49	33	140	173	35	49	142	162	7	12
logCPM	3.82194772	3.49070424	4.11513823	3.7459612	3.94453072	3.83951862	4.33314733	3.92626616	6.4437263	6.43997732	4.32702388	4.73926854	5.77441974	5.77213452	1.82149832	2.71526932
mcrB; methyl-coenz raw reads	10	24	23	20	41	67	42	40	196	226	67	35	135	154	21	21
logCPM	2.77965176	3.67928786	4.31402423	4.2523559	4.38882252	4.76410482	4.11376761	4.19959564	6.92795549	6.82454255	5.25512466	4.25929356	5.70183368	5.69941772	3.33597255	3.49862373
mcrC; methyl-coenz raw reads	0	0	1	4	2	4	1	4	52	48	5	13	11	12	5	0
logCPM	-1.9838792	-1.9838792	0.14617526	2.00501526	0.33615622	0.8952933	-0.6016506	1.04609328	5.02195638	4.60121013	1.62477754	2.86232634	2.16135334	2.09834829	1.37676844	-1.9838792
mcrD; methyl-coenz raw reads	2	1	0	1	5	6	6	2	37	32	3	4	14	12	2	0
logCPM	0.65592009	-0.3657627	-1.9838792	0.25470197	1.47340145	1.4133652	1.42758015	0.21271859	4.53551376	4.02374151	0.96457705	1.27054096	2.49169856	2.09834829	0.25148238	-1.9838792
mcrG; methyl-coenz raw reads	12	4	13	3	17	10	23	10	75	126	15	25	56	67	4	6
logCPM	3.03380657	1.23008399	3.5049385	1.6199526	3.14310524	2.09449154	3.26231107	2.25794977	5.54688873	5.98419516	3.12865962	3.78146488	4.44222445	4.50780585	1.08953214	1.76976494

	mer; coenzyme F42	raw reads	10	11	15	6	23	29	40	35	64	78	23	17	73	72	11	14
		logCPM	2.77965176	2.58701728	3.70709935	2.55936689	3.5683938	3.5734782	4.04443124	4.00978351	5.31941033	5.29585872	3.73075286	3.23749956	4.82078172	4.61052791	2.4355544	2.92970585
	mtaA; [methyl-CoII	raw reads	0	0	0	0	0	0	0	1	0	4	0	0	0	1	1	0
		logCPM	-1.9838792	-1.9838792	-1.9838792	-1.9838792	-1.9838792	-1.9838792	-1.9838792	-0.5025879	-1.9838792	1.17273908	-1.9838792	-1.9838792	-1.9838792	-0.7646631	-0.4706899	-1.9838792
	mtaB; methanol--5	raw reads	0	3	3	1	6	9	15	17	59	66	10	22	22	32	5	4
		logCPM	-1.9838792	0.86596405	1.49276432	0.25470197	1.71437644	1.95194637	2.66577135	2.99173952	5.20282725	5.05653771	2.56439841	3.60065265	3.11999961	3.45914575	1.37676844	1.23731429
	mtaC; methanol cor	raw reads	1	0	0	0	1	4	13	3	18	23	2	5	13	8	3	3
		logCPM	-0.1293948	-1.9838792	-1.9838792	-1.9838792	-0.4004938	0.8952933	2.46813602	0.68876245	3.51249118	3.55605125	0.47016089	1.56191157	2.389763	1.55535581	0.73052249	0.87294422
	mtD; methylenetetra	raw reads	3	8	6	4	3	3	9	6	31	34	22	17	36	32	5	2
		logCPM	1.16158213	2.15017092	2.42646463	2.00501526	0.82144776	0.54418196	1.96662339	1.57094436	4.28329741	4.10988473	3.66787073	3.23749956	3.81408533	3.45914575	1.37676844	0.38427175
	mtdB; methylene-te	raw reads	8	10	35	23	43	77	122	141	33	40	26	19	86	98	58	47
		logCPM	2.47094142	2.45557115	4.91344475	4.45149143	4.45672528	4.96305795	5.63830662	6.00292948	4.37235954	4.34117795	3.90445722	3.39388787	5.0552698	5.05134628	4.77840851	4.64293323
	mtrC; tetrahydrome	raw reads	0	5	2	2	2	1	2	1	8	13	6	5	10	17	2	1
		logCPM	-1.9838792	1.52057602	0.97118806	1.09313374	0.33615622	-0.6113059	0.09111073	-0.5025879	2.38197284	2.75658713	1.86796502	1.56191157	2.0319802	2.57557772	0.25148238	-0.3602955
	mtrD; tetrahydrome	raw reads	2	2	0	0	4	3	2	1	10	19	3	6	17	9	3	2
		logCPM	0.65592009	0.37774327	-1.9838792	-1.9838792	1.18394267	0.54418196	0.09111073	-0.5025879	2.68983809	3.28693031	0.96457705	1.80420871	2.76031722	1.71142602	0.73052249	0.38427175
	mtrE; tetrahydrome	raw reads	2	6	3	3	9	9	6	27	29	13	6	9	13	14	0	4
		logCPM	0.65592009	1.76226593	1.49276432	1.6199526	0.82144776	1.95194637	1.96662339	1.57094436	4.08676093	3.8840403	1.86796502	2.35393264	2.389763	2.30852155	-1.9838792	1.23731429
	mtrG; tetrahydrome	raw reads	0	0	1	0	0	0	1	2	1	2	0	2	3	0	2	0
		logCPM	-1.9838792	-1.9838792	0.14617526	-1.9838792	-1.9838792	-1.9838792	-0.6016506	-0.5025879	0.57795259	1.46194184	-1.9838792	-0.3350859	0.489403	-0.1134539	-1.9838792	-1.9838792
	mtrH; tetrahydrome	raw reads	5	0	0	4	7	8	5	2	37	49	2	11	16	37	6	4
		logCPM	1.83181137	-1.9838792	-1.9838792	2.00501526	1.92080303	1.79375724	1.19141174	0.21271859	4.53551376	4.63065077	0.47016089	2.63040878	2.67621488	3.66411058	1.61620269	1.23731429
	mttB; trimethylamir	raw reads	44	69	89	62	270	395	1006	1046	277	297	145	177	483	511	147	133
		logCPM	4.87551755	5.18416174	6.25253336	5.87160153	7.09324372	7.31253554	8.67553487	8.88911621	7.42611166	7.21791324	6.36379799	6.58225517	7.53583995	7.42489866	6.11203104	6.13415623
	mttC; trimethylamir	raw reads	0	0	0	2	5	6	3	1	13	7	2	3	9	14	1	2
		logCPM	-1.9838792	-1.9838792	-1.9838792	1.09313374	1.47340145	1.4133652	0.55717022	-0.5025879	3.055246	1.9090361	0.47016089	0.90503689	1.88985241	2.30852155	-0.4706899	0.38427175
	mvhA, vhuA, vhcA; F	raw reads	2	8	0	2	4	5	8	12	42	33	7	11	21	23	1	2
		logCPM	0.65592009	2.15017092	-1.9838792	1.09313374	1.18394267	1.17746032	1.80831595	2.50821904	4.71650436	4.06745597	2.07601203	2.63040878	3.05488175	2.99562672	-0.4706899	0.38427175
	mvhD, vhuD, vhcD; F	raw reads	1	2	2	0	2	1	3	1	5	12	3	0	1	8	0	1
		logCPM	-0.1293948	0.37774327	0.97118806	-1.9838792	0.33615622	-0.6113059	0.55717022	-0.5025879	1.74528447	2.64560041	0.96457705	-1.9838792	-0.651781	1.55535581	-1.9838792	-0.3602955
	mvhG, vhuG, vhcG; I	raw reads	4	2	1	1	2	1	1	11	14	11	3	6	1	3	0	0
		logCPM	1.53527255	0.37774327	0.14617526	0.25470197	0.33615622	1.17746032	1.19141174	-0.5025879	3.15902366	2.52535852	1.3321171	-0.3350859	0.489403	1.1811018	-1.9838792	-1.9838792
	nhaA; Na+:H+ antipt	raw reads	50	40	22	11	143	179	307	437	129	120	80	123	383	508	111	80
		logCPM	5.05845037	4.40482016	4.25072713	3.40543285	6.17866974	6.17340852	6.96524469	7.63101019	6.32602778	5.91409388	5.50941081	6.05883424	7.20167422	7.4164164	5.70848373	5.40423803
	nhaB; Na+:H+ antipt	raw reads	7	5	2	4	22	16	6	9	12	7	14	15	60	60	8	3
		logCPM	2.28766401	1.52057602	0.97118806	2.00501526	3.50566028	2.74017729	1.42758015	2.11439445	2.94342066	1.9090361	3.03209952	3.06207423	4.5406412	4.35047642	2.00118652	0.87294422
	nhaC; Na+:H+ antipt	raw reads	8	12	19	15	13	36	23	31	26	32	16	30	29	47	17	14
		logCPM	2.47094142	2.70748084	4.04224495	3.84368344	2.76872977	3.87945272	3.26231107	3.83761531	4.03313849	4.02374151	3.21916035	4.0400719	3.5083869	4.00311148	3.0395917	2.92970585
	qhpA; quinohemopri	raw reads	9	12	14	2	10	20	29	29	46	44	16	30	15	15	10	19
		logCPM	2.63353818	2.70748084	3.60955706	1.09313374	2.40618475	3.0511464	3.58884417	3.74315831	4.84654208	4.47704467	3.21916035	4.0400719	2.5869046	2.40314043	2.30477723	3.35762649
	vhoA; F420-nonredu	raw reads	0	0	0	0	0	0	0	0	0	2	0	0	0	1	0	0
		logCPM	-1.9838792	-1.9838792	-1.9838792	-1.9838792	-1.9838792	-1.9838792	-1.9838792	-1.9838792	2.54410199	0.32607838	-1.9838792	-1.9838792	-1.9838792	-0.7646631	-1.9838792	-1.9838792
Carbon fixation path	fadN; 3-hydroxyacyl-	raw reads	2634	3117	1244	761	11573	17076	21675	26293	3564	4787	4890	5154	25663	28606	7513	6802
		logCPM	10.7668563	10.6717365	10.0531224	9.4834247	12.5122923	12.744266	13.1040138	13.5401014	11.1096939	11.2262004	11.4352039	11.4424461	13.2654331	13.2296632	11.7823529	11.8055168
	fhs; formate--tetrah	raw reads	253	261	221	125	398	569	735	757	607	791	372	361	666	687	204	179
		logCPM	7.38877883	7.09614462	7.5618424	6.88004652	7.65219345	7.83840973	8.22304957	8.42289221	8.55676879	8.62959713	7.72034273	7.60856325	7.99879879	7.85134161	6.58330993	6.56135449
	folD; methylenetetra	raw reads	505	682	360	226	780	1068	1420	1692	711	857	819	864	1588	1964	762	680
		logCPM	8.38483842	8.48022005	8.26504743	7.73305671	8.6220109	8.74607607	9.1725354	9.58266919	8.78478015	8.74514371	8.85795933	8.86650734	9.2515875	9.36572727	8.48174378	8.48408151
	K14469; acrylyl-CoA	raw reads	12	12	4	5	7	8	4	0	22	26	5	7	5	6	0	0
		logCPM	3.03380657	2.70748084	1.87503279	2.30865488	1.92080303	1.79375724	0.90886725	-1.9838792	3.79617521	3.72934659	1.62477754	2.01160415	1.11851494	1.1811018	-1.9838792	-1.9838792
	K14471, smtA; succi	raw reads	0	0	1	1	7	4	1	3	17	31	3	1	3	26	0	0
		logCPM	-1.9838792	-1.9838792	0.14617526	0.25470197	1.92080303	0.8952933	-0.6016506	0.68876245	3.43190778	3.97866097	0.96457705	-0.3350859	0.489403	3.16721836	-1.9838792	-1.9838792
	mcr; malonyl-CoA re	raw reads	7	9	0	1	4	4	2	2	7	21	1	2	0	3	0	0
		logCPM	2.28766401	2.31093716	-1.9838792	0.25470197	1.18394267	0.8952933	0.09111073	0.21271859	2.19928904	3.42775694	-0.2880002	0.41431378	-1.9838792	0.33360006	-1.9838792	-1.9838792
	mct; mesaconyl-CoA	raw reads	9	10	8	1	10	11	6	14	22	24	10	10	19	34	2	4
		logCPM	2.63353818	2.45557115	2.82443996	0.25470197	2.40618475	2.22421037	1.42758015	2.72142386	3.79617521	3.61615917	2.56439841	2.49878354	2.91510436	3.54465647	0.25148238	1.23731429

meH; mesaconyl-C4	raw reads	16	18	8	4	48	84	87	140	52	46	29	46	108	110	33	19
	logCPM	3.43766715	3.27370937	2.82443996	2.00501526	4.61369182	5.08761406	5.15345566	5.99270177	5.02195638	4.54046278	4.05947669	4.64901093	5.38165633	5.21679574	3.9748548	3.35762649
smtB; succinyl-CoA	raw reads	1	0	0	0	2	9	3	13	16	1	4	13	15	0	2	2
	logCPM	-0.1293948	-1.9838792	-1.9838792	-1.9838792	0.33615622	1.95194637	1.96662339	0.68876245	3.055246	3.04599239	-0.2880002	1.27054096	2.389763	2.40314043	-1.9838792	0.38427175
amoB; ammonia m	raw reads	136	196	568	570	152	149	465	280	139	182	205	222	343	360	283	173
	logCPM	6.49511916	6.68383223	8.92250722	9.06666609	6.26642776	5.90977837	7.56324461	6.98983505	6.4334145	6.51293598	6.86207222	6.90829371	7.04282732	6.92046228	7.05448066	6.51230087
amoC; ammonia m	raw reads	8	3	15	26	31	68	52	36	55	77	51	48	120	52	20	20
	logCPM	2.47094142	0.86596405	3.70709935	4.62644445	3.99107207	4.78528107	4.41783288	4.04979643	5.10226394	5.27736362	4.86445388	4.70980564	5.53278432	4.14677354	3.26738806	3.42984691
cah; carbonic anhydr	raw reads	106	132	77	58	320	444	462	628	132	218	162	174	627	714	329	270
	logCPM	6.13672067	6.11523553	6.04433179	5.77581576	7.3379388	7.48098932	7.55391927	8.15358176	6.35909132	6.772666	6.52327409	6.55765874	7.91183074	7.90689586	7.27138251	7.15305211
cynT, can; carbonic	raw reads	882	1058	1263	1480	890	1148	1674	1882	746	1043	992	1060	1847	2306	899	756
	logCPM	9.18886722	9.11335302	10.0749853	10.442806	8.81222769	8.85022786	9.40984809	9.73615823	8.85406742	9.02836417	9.13429891	9.1613239	9.46947654	9.59724286	8.72011841	8.6368306
E1.13.12.16; nitrona	raw reads	215	237	146	53	939	1200	1013	1145	583	764	774	804	1139	1307	823	658
	logCPM	7.15436271	6.95725179	6.96475565	5.6463831	8.88950517	8.91410538	8.68553257	9.01951444	8.49860802	8.57952461	8.77647515	8.76272985	8.77238019	8.77846935	8.59276959	8.43666841
E1.7.1.1; nitrate red	raw reads	47	54	43	51	87	95	249	298	61	72	170	215	335	390	256	206
	logCPM	4.96988149	4.83330871	5.20817311	5.59117352	5.46497921	5.26390374	6.66383153	7.07954721	5.25059682	5.181155	6.59262841	6.86216955	7.00884589	7.03570786	6.91011178	6.76353297
E1.7.2.1; nitrite red	raw reads	280	341	210	182	425	320	456	609	1979	2846	3513	3090	411	513	284	262
	logCPM	7.5348584	7.48124102	7.48828646	7.42108678	7.74677267	7.00929244	7.53508578	8.10929938	10.2611003	10.4761181	10.9581246	10.7044479	7.30329942	7.43052592	7.05955988	7.10973776
E1.7.99.1, hcp; hydr	raw reads	23	19	24	29	12	2	21	16	44	76	123	120	42	41	37	35
	logCPM	3.95094792	3.34972566	4.37466055	4.78245737	2.65770547	0.07915428	3.13468214	2.90713963	4.78298785	5.25862832	6.1271953	6.02334711	4.03276861	3.80939952	4.13740417	4.2226239
E1.7.99.4C; nitrate r	raw reads	17	24	12	8	277	251	212	298	74	81	97	112	236	262	92	101
	logCPM	3.52314858	3.67928786	3.39213608	2.9588519	7.13010279	6.65968597	6.43237771	7.07954721	5.52762883	5.3499626	5.78599158	5.9242119	6.50465917	6.46315797	5.43906959	5.73872958
E4.2.1.1; carbonic ar	raw reads	106	204	88	128	15	22	36	17	23	33	62	36	29	36	28	32
	logCPM	6.13672067	6.7414086	6.23628859	6.91418966	2.96802726	3.18464411	3.89488206	2.99173952	3.8591636	4.06745597	5.14400176	4.2994064	3.5083869	3.6253812	3.74195185	4.0951712
hao; hydroxylamine	raw reads	2	6	7	3	14	14	23	12	17	26	22	31	19	33	15	10
	logCPM	0.65592009	1.76226593	2.63913196	1.6199526	2.87181722	2.5553094	3.26231107	2.50821904	3.43190778	3.72934659	3.66787073	4.08666224	2.91510436	3.50253456	2.86492159	2.46329996
napA; periplasmic n	raw reads	323	427	299	220	776	688	827	1033	2127	2990	2965	2542	683	844	753	679
	logCPM	7.74070388	7.80529418	7.99743787	7.69428422	8.6145982	8.11211398	8.39305686	8.87108329	10.3651281	10.5473156	10.713487	10.4228522	8.0351267	8.14798069	8.46461484	8.48195984
napB; cytochrome c	raw reads	3	7	13	19	28	45	85	103	64	86	175	188	53	53	101	91
	logCPM	1.16158213	1.9692166	3.5049385	4.17936219	3.84668612	4.19641589	5.1201442	5.55197536	5.31941033	5.43585733	6.63434061	6.66901574	4.36373934	4.17386573	5.57296977	5.58906313
napC; cytochrome c	raw reads	33	29	35	25	85	65	55	81	278	321	494	382	54	81	47	39
	logCPM	4.46461572	3.94738932	4.91344475	4.57045144	5.43162092	4.72079638	4.49782184	5.2074348	7.43130293	7.32984042	8.12912397	7.69003431	4.39037828	4.77879307	4.47812343	4.37673803
napD; periplasmic n	raw reads	4	4	2	1	7	18	5	24	16	28	30	24	6	7	10	6
	logCPM	1.53527255	1.23008399	0.97118806	0.25470197	1.92080303	2.90402425	1.19141174	0.21271859	3.34655561	3.83429622	4.10765695	3.72367592	1.35327725	1.38033073	2.30477723	1.76976494
napE; periplasmic n	raw reads	0	0	0	0	2	2	6	7	2	0	1	0	5	0	4	5
	logCPM	-1.9838792	-1.9838792	-1.9838792	-1.9838792	0.33615622	0.07915428	1.42758015	1.77569181	0.57795259	-1.9838792	-0.2880002	-1.9838792	1.11851494	-1.9838792	1.08953214	1.52796518
napF; ferredoxin-tyr	raw reads	0	0	0	0	6	5	7	25	4	0	8	11	7	2	6	0
	logCPM	-1.9838792	-1.9838792	-1.9838792	-1.9838792	1.71437644	1.17746032	1.63047158	3.53338491	1.45030041	-1.9838792	2.25780365	2.63040878	1.55513064	-0.1134539	1.61620269	-1.9838792
napG; ferredoxin-tyr	raw reads	34	40	33	26	67	58	94	135	186	256	335	301	103	108	165	129
	logCPM	4.50719851	4.40482016	4.82928915	4.62644445	5.0905877	4.5580779	5.2643377	5.94044647	6.85256549	7.00398644	7.56939221	7.34670037	5.31369397	5.19050513	6.27810555	6.09026206
napH; ferredoxin-tyr	raw reads	22	30	21	23	45	30	50	57	171	240	184	195	34	55	66	58
	logCPM	3.88788918	3.99551063	4.18452498	4.45149143	4.52157522	3.62136621	4.36193173	4.70462517	6.73153601	6.91106646	6.70651186	6.72162853	3.73314769	4.22656999	4.96320983	4.94355405
narB; ferredoxin-nit	raw reads	59	76	4	1	4	13	0	1	5	14	4	7	13	10	6	8
	logCPM	5.29556666	5.32264052	1.87503279	0.25470197	1.18394267	2.4531594	-1.9838792	-0.5025879	1.74528447	2.85964217	1.3321171	2.01160415	2.389763	1.85224869	1.61620269	2.15781193
narV; nitrate reduct	raw reads	1	3	1	0	0	0	2	0	1	7	3	5	0	0	0	0
	logCPM	-0.1293948	0.86596405	0.14617526	-1.9838792	-1.9838792	-1.9838792	0.09111073	-1.9838792	-0.1963278	1.9090361	0.96457705	1.56191157	-1.9838792	-1.9838792	-1.9838792	-1.9838792
narW; nitrate reduct	raw reads	1	4	0	0	0	0	0	0	4	1	12	8	0	0	0	0
	logCPM	-0.1293948	1.23008399	-1.9838792	-1.9838792	-1.9838792	-1.9838792	-1.9838792	-1.9838792	1.45030041	-0.4088852	2.8171193	2.1928983	-1.9838792	-1.9838792	-1.9838792	-1.9838792
narY; nitrate reduct	raw reads	2	0	0	3	1	0	1	0	3	7	9	13	2	1	1	1
	logCPM	0.65592009	-1.9838792	-1.9838792	1.6199526	-0.4004938	-1.9838792	-0.6016506	-1.9838792	1.07908068	1.9090361	2.41923026	2.86232634	0.02882223	-0.7646631	-0.4706899	-0.3602955
narZ; nitrate reduct	raw reads	4	7	1	1	0	0	2	1	18	28	43	43	2	6	2	3
	logCPM	1.53527255	1.9692166	0.14617526	0.25470197	-1.9838792	-1.9838792	0.09111073	-0.5025879	3.51249118	3.83429622	4.6206208	4.55272759	0.02882223	1.1811018	0.25148238	0.87294422
NIAD; nitrate reduct	raw reads	4	1	5	2	0	0	2	0	1	5	5	1	0	1	1	0
	logCPM	1.53527255	-0.3657627	2.17693615	1.09313374	-1.9838792	-1.9838792	0.09111073	-1.9838792	-0.1963278	1.46194184	1.62477754	-0.3350859	-1.9838792	-0.7646631	-0.4706899	-1.9838792
nifB; nitrogen fixati	raw reads	0	6	1	0	2	14	8	16	4	6	2	2	9	11	16	1
	logCPM	-1.9838792	1.76226593	0.14617526	-1.9838792	0.33615622	2.5553094	1.80831595	2.90713963	1.45030041	1.70273954	0.47016089	0.41431378	1.88985241	1.98053969	2.95489849	-0.3602955

	nifD; nitrogenase m raw reads	5	4	2	3	14	9	18	25	18	19	5	20	57	46	18	16
	logCPM	1.83181137	1.23008399	0.97118806	1.6199526	2.87181722	1.95194637	2.91919439	3.53338491	3.51249118	3.28693031	1.62477754	3.46615251	4.46746517	3.97257898	3.1195875	3.11635508
	nifH; nitrogenase irc raw reads	7	8	2	1	10	9	6	2	5	7	1	15	24	36	22	26
	logCPM	2.28766401	2.15017092	0.97118806	0.25470197	2.40618475	1.95194637	1.42758015	0.21271859	1.74528447	1.9090361	-0.2880002	3.06207423	3.24203024	3.6253812	3.40144403	3.80052719
	nifHD2, nifI2; nitroge raw reads	0	0	0	0	0	1	0	0	2	0	0	1	0	1	5	5
	logCPM	-1.9838792	-1.9838792	-1.9838792	-1.9838792	-1.9838792	-0.6113059	-1.9838792	0.21271859	-1.9838792	-1.9838792	-0.2880002	-1.9838792	-0.651781	0.94988391	0.73052249	1.52796518
	nifK; nitrogenase m raw reads	5	14	2	2	13	16	50	43	16	18	16	13	55	50	53	18
	logCPM	1.83181137	2.92187418	0.97118806	1.09313374	2.76872977	2.74017729	4.36193173	4.30254674	3.34655561	3.21100232	3.21916035	2.86232634	4.41653426	4.09101339	4.64960119	3.28159936
	nifN; nitrogenase m raw reads	3	2	2	0	6	14	17	23	8	15	2	9	43	42	28	35
	logCPM	1.16158213	0.37774327	0.97118806	-1.9838792	1.71437644	2.5553094	2.83956576	3.41582722	2.38197264	2.955824	0.47016089	2.35393264	4.06619763	3.8435454	3.74195185	4.2226239
	nifT; nitrogen fixatio raw reads	0	0	0	0	0	2	2	0	0	4	3	0	4	2	6	3
	logCPM	-1.9838792	-1.9838792	-1.9838792	-1.9838792	-1.9838792	0.07915428	0.09111073	-1.9838792	-1.9838792	1.17273908	0.96457705	-1.9838792	0.83798255	-0.1134539	1.61620269	0.87294422
	nifV; homocitrate sy raw reads	3	2	0	0	2	10	19	13	7	18	5	14	22	11	16	6
	logCPM	1.16158213	0.37774327	-1.9838792	-1.9838792	0.33615622	2.09449154	2.99465692	2.61875636	2.19928904	3.21100232	1.62477754	2.96565453	3.11999961	1.98053969	2.95489849	1.76976494
	nifW; nitrogenase-s raw reads	0	0	0	0	2	4	6	3	0	3	3	0	1	1	5	0
	logCPM	-1.9838792	-1.9838792	-1.9838792	-1.9838792	0.33615622	0.8952933	1.42758015	0.68876245	-1.9838792	0.81064636	0.96457705	-1.9838792	-0.651781	-0.7646631	1.37676844	-1.9838792
	nirA; ferredoxin-nitr raw reads	139	210	49	24	53	71	69	82	126	61	30	69	61	71	92	94
	logCPM	6.52651012	6.78313138	5.39540959	4.51219722	4.75524368	4.84700636	4.82170744	5.22501642	5.93094772	5.98419516	4.10765695	5.2291196	4.56423102	4.59056029	5.43906959	5.6356155
	nirB; nitrite reducta raw reads	110	135	325	467	1084	818	197	208	170	235	354	320	354	331	168	157
	logCPM	6.18997142	6.14754008	8.11761792	8.77927154	9.09656999	8.36159675	6.32683059	6.56198472	6.72309462	6.88075729	7.18196737	7.43487573	7.08828215	6.79956036	6.30401684	6.37270052
	nirD; nitrite reducta raw reads	7	15	19	37	82	63	46	44	15	23	36	34	60	53	9	27
	logCPM	2.28766401	3.01819777	4.04224495	5.13106145	5.38009113	4.67614751	4.24317907	4.33529348	3.25583459	3.55605125	4.36716099	4.21803343	4.5406412	4.17386573	2.16095287	3.85400518
	norB; nitric oxide re raw reads	376	484	234	220	388	305	383	508	1791	2617	4339	3475	540	753	275	258
	logCPM	7.959662	7.98587312	7.64419731	7.69428422	7.6155284	6.94016901	7.28377111	7.84794822	10.1171253	10.3551188	11.2627487	10.8738299	7.69656869	7.98354294	7.01319005	7.08758296
	norC; nitric oxide re raw reads	26	41	48	32	108	96	161	201	358	498	967	841	162	208	125	110
	logCPM	4.12510191	4.44002406	5.36584276	4.9232334	5.77531671	5.27891775	6.03671126	6.51273112	7.79570536	7.96260687	9.09749146	8.8276032	5.96369975	6.13124752	5.87907074	5.86131887
	norC; nitric-oxide re raw reads	11	15	5	4	45	37	33	35	89	132	233	228	59	83	15	17
	logCPM	2.91231864	3.01819777	2.17693615	2.00501526	4.52157522	3.91831115	3.7715784	4.00978351	5.79257572	6.05104744	7.04640144	6.94668795	4.51665924	4.8136623	2.86492159	3.20134179
	norD; nitric-oxide re raw reads	3	4	1	2	10	8	10	19	20	44	42	43	9	18	8	8
	logCPM	1.16158213	1.23008399	0.14617526	1.09313374	2.40618475	1.79375724	2.10926461	3.14736951	3.66129476	4.10988473	4.58702643	4.55272759	1.88985241	2.65463673	2.00118652	2.15781193
	norF; nitric-oxide re raw reads	57	57	43	33	88	106	102	123	267	452	575	620	159	178	58	41
	logCPM	5.24613942	4.91063771	5.20817311	4.96726322	5.48137349	5.42098919	5.38142972	5.80672468	7.37314485	7.82293269	8.34799136	8.38805174	5.93684296	5.90741792	4.77840851	4.44803115
	nosZ; nitrous-oxide raw reads	895	1278	414	402	813	749	972	1231	4814	6524	8508	6886	1008	1335	506	479
	logCPM	9.20996717	9.38578787	8.46652664	8.56317871	8.68175455	8.23456378	8.62596398	9.1239485	11.5433898	11.6727949	12.2341334	11.8603868	8.59621648	8.80903253	7.89160625	7.97899979
	nrfB; cytochrome c-1 raw reads	0	1	0	0	1	0	0	1	5	3	2	2	0	0	0	0
	logCPM	-1.9838792	-0.3657627	-1.9838792	-1.9838792	-0.4004938	-1.9838792	-1.9838792	-0.5025879	1.74528447	0.81064636	0.47016089	0.41431378	-1.9838792	-1.9838792	-1.9838792	-1.9838792
	nrfC; protein NrfC; K raw reads	20	30	8	8	6	4	15	19	50	74	44	43	15	6	4	3
	logCPM	3.7528473	3.99551063	2.82443996	2.9588519	1.71437644	0.8952933	2.66577135	3.14736951	4.9658218	5.22041164	4.65345068	4.55272759	2.5869046	1.1811018	1.08953214	0.87294422
	nrfD; formate-deper raw reads	2	1	1	1	0	2	2	1	5	8	4	2	2	3	2	3
	logCPM	0.65592009	-0.3657627	0.14617526	0.25470197	-1.9838792	0.07915428	0.09111073	-0.5025879	1.74528447	2.08949034	1.3321171	0.41431378	0.02882223	0.33360006	0.25148238	0.87294422
	nrfD; protein NrfD; K raw reads	9	24	5	2	5	6	9	10	36	56	25	34	2	13	0	0
	logCPM	2.63353818	3.67928786	2.17693615	1.09313374	1.47340145	1.4133652	1.96662339	2.25794977	4.49642219	4.82145428	3.84884761	4.21803343	0.02882223	2.20725882	-1.9838792	-1.9838792
Sulfur metabolism	aprA; adenyllysulfat raw reads	60	95	66	59	146	185	172	131	357	394	340	325	266	294	116	117
	logCPM	5.31965943	5.64274473	5.82286014	5.80036498	6.2085195	6.22081029	6.13170379	5.89723521	7.79167444	7.62504265	7.59073762	7.45721112	6.67684548	6.62895729	5.77174818	5.94994846
	aprB; adenyllysulfat raw reads	17	41	24	15	41	34	33	37	83	116	83	81	54	77	21	28
	logCPM	3.52314858	4.44002406	4.37466055	3.84368344	4.38882252	3.79844759	3.7715784	4.08872948	5.63951045	5.86539284	5.5622327	5.45900383	4.39037828	4.70641964	3.33597255	3.9055715
	cysC; adenyllysulfat raw reads	232	330	175	105	137	182	192	209	218	300	127	135	289	324	133	144
	logCPM	7.26396323	7.43400335	7.22565825	6.62909744	6.11705098	6.19730408	6.28985959	6.56888566	7.08112766	7.23238831	6.17320113	6.19264893	6.79620499	6.76879369	5.96819608	6.24840207
	cysD; sulfate adenyl raw reads	164	196	203	121	551	863	722	916	417	465	298	308	1058	1272	562	515
	logCPM	6.76451783	6.68383223	7.4394469	6.83322783	8.12097378	8.43879865	8.19732614	8.69776203	8.01556089	7.8637956	7.40078184	7.3798163	8.66601593	8.73933174	8.04288595	8.08344551
	cysH; phosphoadenc raw reads	360	406	192	159	455	589	354	447	315	359	197	190	483	578	445	314
	logCPM	7.89699135	7.73262218	7.35919387	7.2264829	7.8450644	7.8881946	7.17036781	7.66361057	7.61132165	7.49101098	6.80477125	6.68424476	7.53583995	7.6023988	7.70648472	7.37049812
	cysI; sulfite reducta raw reads	208	298	224	155	749	1033	839	995	380	565	281	344	1041	1168	839	727
	logCPM	7.10669574	7.28707612	7.58126891	7.1897872	8.56354081	8.69803345	8.41382482	8.81704121	7.88165015	8.1445386	7.31617021	7.53906533	8.64266103	8.61634933	8.62052995	8.58043628

cysN; sulfate adenylyl raw reads	117	129	177	80	638	920	719	883	285	345	212	246	929	1162	733	564
logCPM	6.2786775	6.08219102	7.24202516	6.23793105	8.33229923	8.53100683	8.19132425	8.6448607	7.46712807	7.43370576	6.91040904	7.05609608	8.47855148	8.60892392	8.42580634	8.21445141
cysNC; bifunctional raw reads	127	159	175	68	304	376	289	301	279	325	186	216	586	652	169	170
logCPM	6.39662751	6.38283065	7.22565825	6.00431832	7.26405687	7.24153148	6.87825732	7.09397149	7.4364756	7.34767894	6.72207116	6.86884969	7.81437193	7.77598825	6.31255154	6.48713409
E1.8.2.1; sulfite dehydratase raw reads	26	26	30	14	95	140	255	300	48	55	127	171	279	284	158	144
logCPM	4.12510191	3.79257339	4.69306799	3.7459612	5.59119579	5.82028281	6.69809839	7.0891794	4.90741432	4.79569358	6.17320113	6.53263568	6.74551824	6.57916182	6.21577229	6.24840207
E1.8.3.1, SUOX; sulfite oxidase raw reads	42	59	47	56	69	64	39	33	93	96	54	55	33	78	62	48
logCPM	4.80899489	4.95997963	5.33565728	5.72542742	5.13271267	4.69864466	4.00847202	3.92626616	5.85571806	5.59367712	4.94622029	4.90442794	3.69090985	4.72485621	4.87376615	4.67300271
E2.7.7.4C, met3; sulfite oxidase raw reads	448	594	407	442	391	471	431	257	907	1185	807	1302	526	562	598	518
logCPM	8.21219258	8.28106255	8.4419424	8.69994231	7.62662608	7.56603967	7.45385389	6.86643337	9.13585443	9.21242837	8.83667624	9.45787068	7.65871888	7.56195287	8.13237804	8.09181739
E3.1.3.7, cysQ, MET; raw reads	19	50	25	23	14	21	17	12	26	37	30	13	10	8	25	14
logCPM	3.68026996	4.72330053	4.4328508	4.45149143	2.87181722	3.11943883	2.83956576	2.50821904	4.03313849	4.23016151	4.10765695	2.86232634	2.0319802	1.55535581	3.58172062	2.92970585
PAPS; 3'-phosphoadenylyl raw reads	174	226	171	123	223	211	109	64	88	100	94	63	66	75	265	228
logCPM	6.84971651	6.88883036	7.19235666	6.85682709	6.81789088	6.40992533	5.47662668	4.87020448	5.77634868	5.65226867	5.74087854	5.09880087	4.67671938	4.66882427	6.95985733	6.90959851
slr; sulfite reductase raw reads	660	1064	186	195	1012	973	353	280	272	279	151	254	352	386	219	240
logCPM	8.77076478	9.12150783	7.31346183	7.52048057	8.99746192	8.61175906	7.16629381	6.98983505	7.39987131	7.12787348	6.42211765	7.10217994	7.08012345	7.02086339	6.68541111	6.9834474

All values represented in this table are after preprocessing through MG-RAST and the first filtering for lowly expressed transcripts, which removed transcripts that did not have at least 2 CPM in at least 1/16 samples. In other words, the values represented in this table are the values that were used for normalization/statistical tests in START (raw reads; top number) or the corresponding normalized logCPM values (bottom number).

Note that some of the transcripts indicated in this table were subsequently filtered out due to remaining low expression and were deemed not biologically important for further investigations (see §4.2.6).

Categories/pathways/transcripts of relevance for this manuscript are highlighted.

CPM = counts per million.

Table C-5: Tabulated summary of expressed transcripts annotated to the KO database, Level 1 categories. Expression represented as normalized logCPM values (top) and raw read values (bottom), duplicates averaged. Pairwise comparisons between location (BR vs KV), season (summer vs fall), and site (lake vs tributary) provide statistically significant differential expression ($p < 0.05$), denoted with greater than (>) or less than (<) symbol and shaded, where applicable.

Expression (logCPM)	Location		Season		Site	
	BR	KV	Summer	Fall	Lake	Tributary
Cellular Processes	16.31 (146,329)	> 16.04 (152,146)	16.17 (112,067)	16.18 (186,407)	16.14 (161,032)	16.21 (137,442)
Environmental Information Processing	16.50 (180,899)	16.59 (221,751)	16.45 (140,026)	16.64 (262,625)	16.54 (217,917)	16.54 (184,734)
Genetic Information Processing	18.20 (565,176)	< 18.40 (779,506)	18.16 (455,322)	< 18.44 (889,360)	18.31 (740,457)	18.28 (604,226)
Human Diseases	15.18 (68,455)	> 14.50 (49,351)	15.36 (67,934)	> 14.31 (49,872)	14.60 (54,576)	15.07 (63,231)
Metabolism	18.83 (847,334)	18.71 (937,800)	18.85 (724,390)	> 18.69 (1,060,744)	18.78 (976,466)	18.76 (808,668)
Organismal Systems	14.10 (32,866)	< 14.35 (46,621)	14.16 (28,851)	14.29 (50,636)	14.29 (45,131)	14.16 (34,356)

APPENDIX D: SUPPLEMENTAL INFORMATION FOR CHAPTER 5

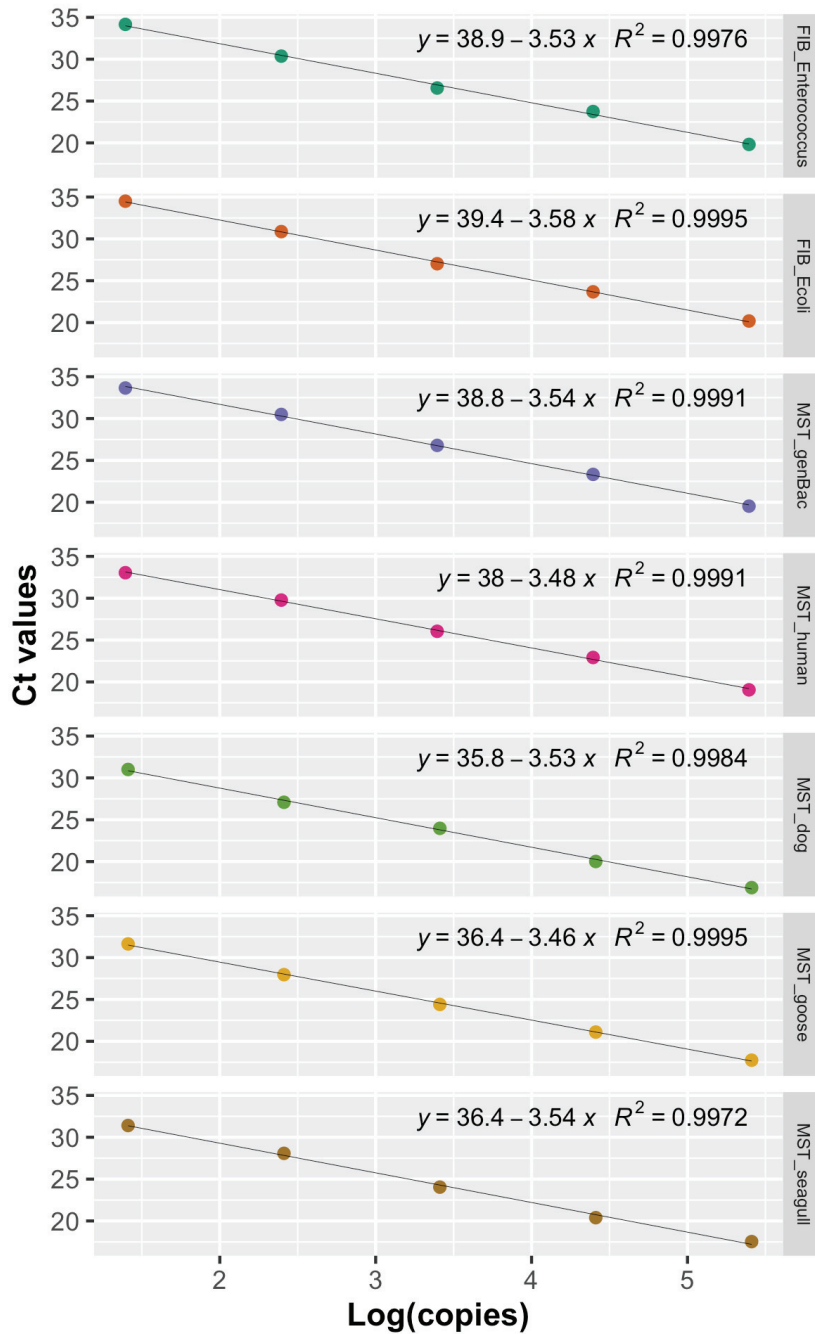


Figure D-1: Standard curves for the seven GOI detected in this study, generated from complete synthetic genes in plasmid cloning vectors with known copy numbers. Equation of the linear regression line and coefficient of determination (R^2) are displayed within each panel.

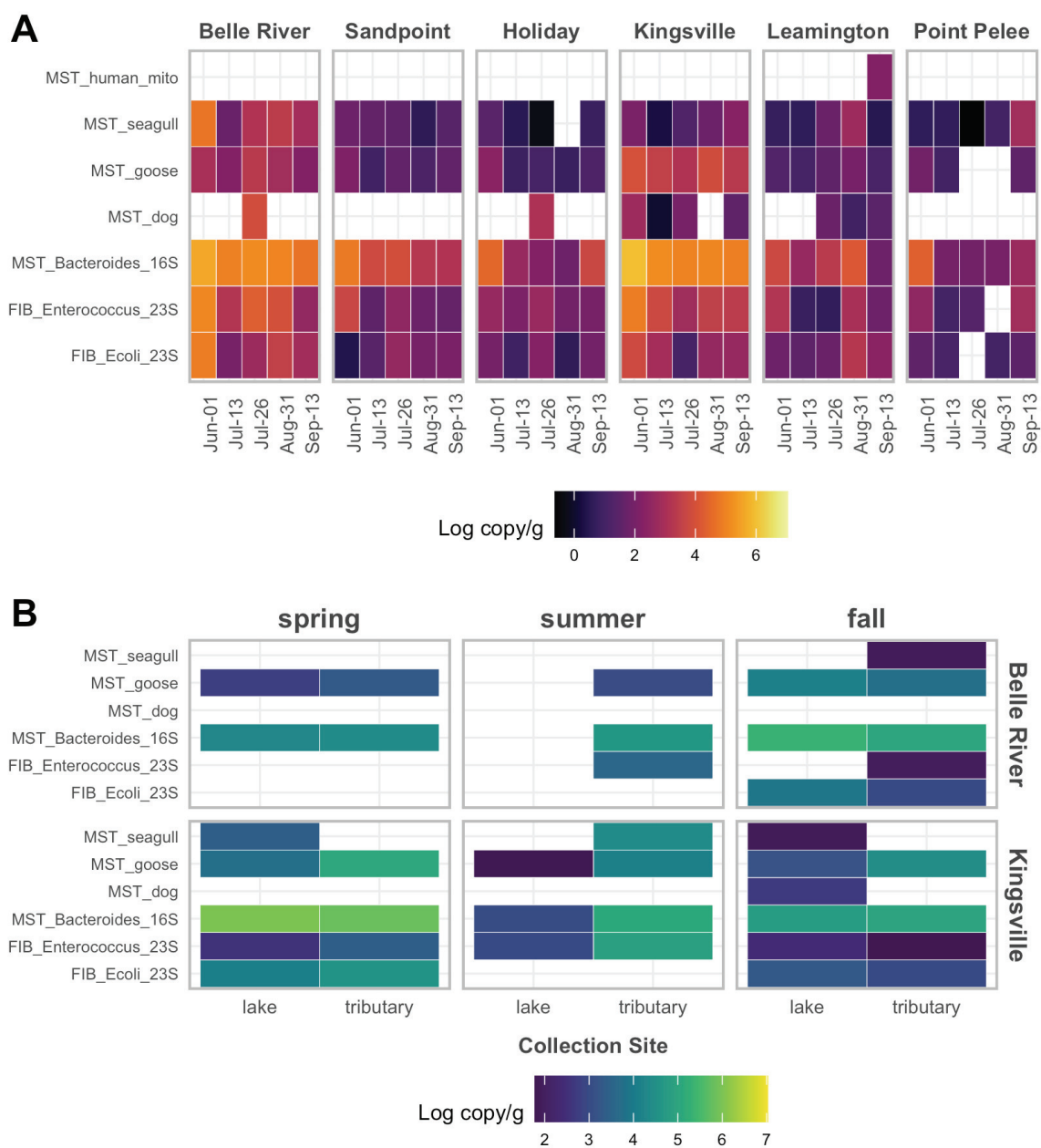


Figure D-2: Heatmaps of expressed transcripts (log copies/g) of all (7) GOI quantified from sediment samples. Targets include two FIB (*Enterococcus* 23S, *E. coli* 23S) and five MST (general *Bacteroides* 16S, dog, goose, seagull, human). (A) Bed sediment samples: six beach locations, each with five collection dates between June and September of 2017. (B) Suspended sediment samples: collected seasonally (spring, summer, fall) from the lake and tributary in Belle River and Kingsville. Cells with no colour indicate no detection.

Table D-1: Sample collection details for bed and suspended sediment, including collection dates (2017), corresponding season, and number of samples processed for this research.

BED SEDIMENT			SUSPENDED SEDIMENT		
Collection Date	Season	No. Samples	Collection Date	Season	No. Samples
June 1	Spring	30	April 19	Spring	14
July 13	Summer	35	July 11	Summer	10
July 26	Summer	35	November 28	Fall	8
August 31	Summer	36			
September 13	Summer	36			
TOTAL		172	TOTAL		32

Table D-2: Unfiltered metadata, includes sampling details (e.g., sample ID, collection date, location, site, sample collection method (centrifuge = suspended sediment, core = bed sediment), weight of extracted sediment, and cDNA concentration) and qPCR results (chip ID, target ID, average Ct and standard deviation, raw transcript expression copy numbers, and final transcript expression copy numbers adjusted for dilutions and sediment weight).

Sample ID	Chip ID	Target ID	Ct mean	Ct sd	Target log copy	Target copies	Collection Date	Location	Site	Sampling Method	cDNA Starting Concentration (ng/ul)	Concentration Method	Starting Concentration Range	cDNA Final Concentration (ng/ul)	Final Concentration Range	Starting Weight (g)	Dilution Factor 1	Dilution Factor 2	Final Target Copies/g	Final Target Log copies/g
SS_spring_BR_beach_cDNA_2	CXR25	MST_Bacteroides_16S	26.278	0.711	3.530259366	3390.465785	2017-04-19	Belle River	lake	centrifuge	1736	Qubit	very high	12.05555556	low	2	1	144	244113.5365	5.38759186
SS_spring_BR_river_cDNA_1	CXR25	MST_Bacteroides_16S	26.294	0.694	3.525738826	3355.357705	2017-04-19	Belle River	tributary	centrifuge	1390	Bioanalyzer	very high	9.652777778	low	2	1	144	241585.7547	5.38307132
SS_spring_BR_beach_cDNA_1	CXR25	MST_Bacteroides_16S	28.645	0.373	2.861501949	726.9456624	2017-04-19	Belle River	lake	centrifuge	1007	Bioanalyzer	high	18.64814815	low	2	1	54	19627.53288	4.29286571
SS_spring_BR_river_cDNA_3a	CXR25	MST_Bacteroides_16S	29.793	0.995	2.53715319	344.4714156	2017-04-19	Belle River	tributary	centrifuge	1572	Bioanalyzer	very high	10.91666667	low	2	1	144	24801.94192	4.39448569
SS_spring_BR_beach_cDNA_2	CXR25	MST_goose	30.446	1.68	1.714491917	51.81934472	2017-04-19	Belle River	lake	centrifuge	1736	Qubit	very high	12.05555556	low	2	1	144	3730.99282	3.57182441
SS_spring_BR_river_cDNA_1	CXR25	MST_goose	31.474	0.7	1.417725173	26.16526715	2017-04-19	Belle River	tributary	centrifuge	1390	Bioanalyzer	very high	9.652777778	low	2	1	144	1883.899234	3.27505767
SS_spring_BR_beach_cDNA_1	CXR25	MST_goose	31.721	2.127	1.346420323	22.20344297	2017-04-19	Belle River	lake	centrifuge	1007	Bioanalyzer	high	18.64814815	low	2	1	54	599.4929601	2.77778409
SS_sum_BR_river_cDNA_1	CXR25	FIB_Enterococcus_23S	30.399	0.731	2.411341491	257.8347746	2017-07-11	Belle River	tributary	centrifuge	898	Bioanalyzer	high	16.62962963	low	2	1	54	6961.538915	3.84270526
SS_sum_BR_river_cDNA_2	CXR25	FIB_Enterococcus_23S	31.383	0.946	2.132619533	135.7124007	2017-07-11	Belle River	tributary	centrifuge	872	Bioanalyzer	high	16.14814815	low	2	1	54	3664.23482	3.5639833
SS_sum_BR_river_cDNA_1	CXR25	MST_Bacteroides_16S	26.578	0.869	3.445499237	2789.325757	2017-07-11	Belle River	tributary	centrifuge	898	Bioanalyzer	high	16.62962963	low	2	1	54	75311.79544	4.876863
SS_sum_BR_river_cDNA_2	CXR25	MST_Bacteroides_16S	27.337	0.707	3.231056111	1702.378443	2017-07-11	Belle River	tributary	centrifuge	872	Bioanalyzer	high	16.14814815	low	2	1	54	45964.21796	4.66241988
SS_sum_BR_river_cDNA_1	CXR25	MST_goose	29.684	0.749	1.934468822	85.99413298	2017-07-11	Belle River	tributary	centrifuge	898	Bioanalyzer	high	16.62962963	low	2	1	54	2321.841591	3.36583259
SS_sum_BR_river_cDNA_2	CXR25	MST_goose	30.905	0.016	1.581986143	38.19320845	2017-07-11	Belle River	tributary	centrifuge	872	Bioanalyzer	high	16.14814815	low	2	1	54	1031.216628	3.01334991
SS_fall_BR_river_cDNA_1b	CXR25	FIB_Ecoli_23S	29.4	2.218	2.79498772	623.7171998	2017-11-28	Belle River	tributary	centrifuge	398	Bioanalyzer	medium	132.6666667	high	2	1	3	935.5757998	2.97107898
SS_fall_BR_beach_cDNA_1b	CXR25	FIB_Ecoli_23S	30.322	0.734	2.53767582	344.8862026	2017-11-28	Belle River	lake	centrifuge	850	Bioanalyzer	high	15.74074074	low	2	1	54	9311.927471	3.96903959
SS_fall_BR_beach_cDNA_1a	CXR25	FIB_Ecoli_23S	30.603	0.412	2.459254298	287.9083747	2017-11-28	Belle River	lake	centrifuge	794	Bioanalyzer	high	14.7037037	low	2	1	54	7773.526117	3.89061806
SS_fall_BR_river_cDNA_1b	CXR25	FIB_Enterococcus_23S	32.689	0.398	1.76268978	57.9014954	2017-11-28	Belle River	tributary	centrifuge	398	Bioanalyzer	medium	132.6666667	high	2	1	3	86.85224309	1.93878104
SS_fall_BR_river_cDNA_1b	CXR25	MST_Bacteroides_16S	22.322	0.704	4.647962932	44459.33184	2017-11-28	Belle River	tributary	centrifuge	398	Bioanalyzer	medium	132.6666667	high	2	1	3	66688.99776	4.82405419
SS_fall_BR_beach_cDNA_1b	CXR25	MST_Bacteroides_16S	24.65	0.703	3.990224332	9777.421365	2017-11-28	Belle River	lake	centrifuge	850	Bioanalyzer	high	15.74074074	low	2	1	54	263990.3768	5.4215881
SS_fall_BR_beach_cDNA_1a	CXR25	MST_Bacteroides_16S	24.993	0.913	3.893315251	7821.953884	2017-11-28	Belle River	lake	centrifuge	794	Bioanalyzer	high	14.7037037	low	2	1	54	211192.7549	5.32467902
SS_fall_BR_river_cDNA_1a	CXR25	MST_Bacteroides_16S	26.13	0.597	3.572074363	3733.140737	2017-11-28	Belle River	tributary	centrifuge	843	Bioanalyzer	high	15.61111111	low	2	1	54	100794.7999	5.00343813
SS_fall_BR_river_cDNA_1b	CXR25	MST_goose	24.694	0.282	3.375	2371.373706	2017-11-28	Belle River	tributary	centrifuge	398	Bioanalyzer	medium	132.6666667	high	2	1	3	3557.060558	3.55109126
SS_fall_BR_beach_cDNA_1b	CXR25	MST_goose	26.802	0.064	2.766454965	584.0566396	2017-11-28	Belle River	lake	centrifuge	850	Bioanalyzer	high	15.74074074	low	2	1	54	15769.52927	4.19781873
SS_fall_BR_beach_cDNA_1a	CXR25	MST_goose	27.073	0.081	2.688221709	487.7774388	2017-11-28	Belle River	lake	centrifuge	794	Bioanalyzer	high	14.7037037	low	2	1	54	13169.99085	4.11958547
SS_fall_BR_river_cDNA_1a	CXR25	MST_goose	28.343	0.736	2.321593533	209.6976355	2017-11-28	Belle River	tributary	centrifuge	843	Bioanalyzer	high	15.61111111	low	2	1	54	5661.836158	3.75295713
SS_fall_BR_river_cDNA_1b	CXR25	MST_seagull	30.326	0.479	1.707737037	51.01959851	2017-11-28	Belle River	tributary	centrifuge	398	Bioanalyzer	medium	132.6666667	high	2	1	3	76.52939777	1.8838283
SS_spring_KV_creek_cDNA_2	CXR25	FIB_Ecoli_23S	26.323	0.361	3.653717348	4505.233944	2017-04-19	Kingsville	tributary	centrifuge	936	Qubit	high	17.33333333	low	2	1	54	121641.3165	5.08508111
SS_spring_KV_creek_cDNA_3b	CXR25	FIB_Ecoli_23S	26.803	0.021	3.519758875	3309.473247	2017-04-19	Kingsville	tributary	centrifuge	722	Bioanalyzer	high	13.7037037	low	2	1	54	89355.77768	4.95112264
SS_spring_KV_creek_cDNA_3a	CXR25	FIB_Ecoli_23S	27.516	0.936	3.320774727	2093.026498	2017-04-19	Kingsville	tributary	centrifuge	572	Bioanalyzer	high	10.59259259	low	2	1	54	56511.71543	4.75213849
SS_spring_KV_creek_cDNA_1	CXR25	FIB_Ecoli_23S	29.683	1.947	2.716008038	520.0056202	2017-04-19	Kingsville	tributary	centrifuge	1232	Bioanalyzer	very high	8.555555556	low	2	1	144	37440.40466	4.57334053
SS_spring_KV_pier_cDNA_1	CXR25	FIB_Ecoli_23S	29.865	0.155	2.66521545	462.6104617	2017-04-19	Kingsville	lake	centrifuge	776	Bioanalyzer	high	14.7037037	low	2	1	54	12490.48247	4.09657921
SS_spring_KV_creek_cDNA_3b	CXR25	FIB_Enterococcus_23S	29.54	0.484	2.654656696	451.4988995	2017-04-19	Kingsville	tributary	centrifuge	722	Bioanalyzer	high	13.7037037	low	2	1	54	12190.47029	4.08602046
SS_spring_KV_creek_cDNA_2	CXR25	FIB_Enterococcus_23S	30.894	0.024	2.27113075	186.6941674	2017-04-19	Kingsville	tributary	centrifuge	936	Qubit	high	17.33333333	low	2	1	54	5040.742519	3.70249451
SS_spring_KV_pier_cDNA_1	CXR25	FIB_Enterococcus_23S	31.073	1.764	2.22042828	166.1224319	2017-04-19	Kingsville	lake	centrifuge	776	Bioanalyzer	high	14.7037037	low	2	1	54	4485.30566	3.65179204
SS_spring_KV_pier_cDNA_3a	CXR25	FIB_Enterococcus_23S	31.955	1.483	1.970598232	93.45407269	2017-04-19	Kingsville	lake	centrifuge	1171	Bioanalyzer	very high	8.131944444	low	2	1	144	6728.693234	3.82793073
SS_spring_KV_creek_cDNA_3a	CXR25	FIB_Enterococcus_23S	32.053	1.847	1.942839338	87.66744459	2017-04-19	Kingsville	tributary	centrifuge	572	Bioanalyzer	high	10.59259259	low	2	1	54	2367.026404	3.3742031
SS_spring_KV_pier_cDNA_2	CXR25	FIB_Enterococcus_23S	35.002	0.019	1.107523227	12.80923599	2017-04-19	Kingsville	lake	centrifuge	888	Qubit	high	16.44444444	low	2	1	54	345.8493717	2.53888699
SS_spring_KV_pier_cDNA_1	CXR25	MST_Bacteroides_16S	20.8	0.816	5.077979319	119668.3543	2017-04-19	Kingsville	lake	centrifuge	776	Bioanalyzer	high	14.7037037	low	2	1	54	3231045.566	6.50934308
SS_spring_KV_pier_cDNA_2	CXR25	MST_Bacteroides_16S	21.586	0.638	4.855907781	71764.18895	2017-04-19	Kingsville	lake	centrifuge	888	Qubit	high	16.44444444	low	2	1	54	1937633.102	6.28727155
SS_spring_KV_pier_cDNA_3b	CXR25	MST_Bacteroides_16S	21.84	1.326	4.784144205	60833.69629	2017-04-19	Kingsville	lake	centrifuge	1278	Bioanalyzer	very high	8.875	low	2	1	144	4380026.133	6.6414767
SS_spring_KV_creek_cDNA_3b	CXR25	MST_Bacteroides_16S	22.385	0.458	4.630163305	42673.99525	2017-04-19	Kingsville	tributary	centrifuge	722	Bioanalyzer	high	13.7037037	low	2	1	54	1152197.872	6.06152707
SS_spring_KV_creek_cDNA_1	CXR25	MST_Bacteroides_16S	22.88	0.364	4.490390902	30924.95611	2017-04-19	Kingsville	tributary	centrifuge	1232	Bioanalyzer	very high	8.555555556	low	2	1	144	2226596.814	6.34764159
SS_spring_KV_creek_cDNA_2	CXR25	MST_Bacteroides_16S	23.083	0.444	4.432954738	27099.09192	2017-04-19	Kingsville	tributary	centrifuge	936	Qubit	high	17.33333333	low	2	1	54	731675.4819	5.8643185
SS_spring_KV_creek_cDNA_3a	CXR25	MST_Bacteroides_16S	23.235	0.675	4.390009606	24547.63212	2017-04-19	Kingsville	tributary	centrifuge	572	Bioanalyzer	high	10.59259259	low	2	1	54	662786.0672	5.82137327
SS_spring_KV_pier_cDNA_3a	CXR25	MST_Bacteroides_16S	24.089	0.642	4.148725773	14083.9921	2017-04-19	Kingsville	lake	centrifuge	1171	Bioanalyzer	very high	8.131944444	low	2	1	144	1014047.431	6.00605827
SS_spring_KV_creek_cDNA_1	CXR25	MST_goose	22.79	0.057	3.92465358	8407.242601	2017-04-19	Kingsville	tributary	centrifuge	1232	Bioanalyzer	very high	8.555555556	low	2	1	144	605321.4673	5.78198608
SS_spring_KV_creek_cDNA_2	CXR25	MST_goose	22.821	0.085	3.915704388	8235.773383	2017-04-19	Kingsville	tributary	centrifuge	936	Qubit	high	17.33333333	low	2	1	54	22265.8813	5.34706815
SS_spring_KV_creek_cDNA_3b	CXR25	MST_goose	23.134	0.076	3.82534642	6688.77243	2017-04-19	Kingsville	tributary	centrifuge	722	Bioanalyzer	high	13.7037037	low	2	1	54	180596.8556	5.25671018
SS_spring_KV_creek_cDNA_3a	CXR25	MST_goose	23.766	0.02	3.642898383	4394.387831	2017-04-19	Kingsville	tributary	centrifuge	572	Bioanalyzer	high	10.59259259	low	2	1	54	118648.4714	5.07426215

SS_spring_KV_pier_cDNA_2	CXR25	MST_goose	26.081	0.422	2.974595843	943.1827362	2017-04-19	Kingsville	lake	centrifuge	888	Qubit	high	16.44444444	low	2	1	54	25465.93388	4.40595961
SS_spring_KV_pier_cDNA_1	CXR25	MST_goose	26.382	0.245	2.887702079	772.150716	2017-04-19	Kingsville	lake	centrifuge	776	Bioanalyzer	high	14.37037037	low	2	1	54	20848.06933	4.31906584
SS_spring_KV_pier_cDNA_3b	CXR25	MST_goose	28.357	0.754	2.317551963	207.7552288	2017-04-19	Kingsville	lake	centrifuge	1278	Bioanalyzer	very high	8.875	low	2	1	144	14958.37648	4.17488446
SS_spring_KV_pier_cDNA_3a	CXR25	MST_goose	29.796	0.846	1.902136259	79.82450951	2017-04-19	Kingsville	lake	centrifuge	1171	Bioanalyzer	very high	8.131944444	low	2	1	144	5747.364685	3.75946876
SS_spring_KV_pier_cDNA_1	CXR25	MST_seagull	30.125	0.524	1.764473424	58.13978537	2017-04-19	Kingsville	lake	centrifuge	776	Bioanalyzer	high	14.37037037	low	2	1	54	1569.774205	3.19583719
SS_spring_KV_pier_cDNA_3b	CXR25	MST_seagull	30.99	0.35	1.520309369	33.13670859	2017-04-19	Kingsville	lake	centrifuge	1278	Bioanalyzer	very high	8.875	low	2	1	144	2385.843019	3.37764187
SS_sum_KV_creek_cDNA_1	CXR25	FIB_Enterococcus_23S	28.205	0.771	3.032800816	1078.451989	2017-07-11	Kingsville	lake	centrifuge	1674	Bioanalyzer	very high	11.625	low	2	1	144	77648.54321	4.89013331
SS_sum_KV_pier_cDNA_1	CXR25	FIB_Enterococcus_23S	29.643	0.443	2.625481532	422.1643263	2017-07-11	Kingsville	lake	centrifuge	1092	Qubit	high	20.22222222	medium	2	1	54	11398.43681	4.0568453
SS_sum_KV_pier_cDNA_3b	CXR25	FIB_Enterococcus_23S	29.908	0.012	2.550419216	355.156049	2017-07-11	Kingsville	lake	centrifuge	240	Bioanalyzer	medium	80	medium	2	1	3	532.7340735	2.72651048
SS_sum_KV_pier_cDNA_2	CXR25	FIB_Enterococcus_23S	33.44	2.005	1.54996601	35.47856205	2017-07-11	Kingsville	lake	centrifuge	944	Qubit	high	17.48148148	low	2	1	54	957.9211754	2.98132977
SS_sum_KV_creek_cDNA_1	CXR25	MST_Bacteroides_16S	20.475	0.491	5.169802791	147843.6893	2017-07-11	Kingsville	lake	centrifuge	1674	Bioanalyzer	very high	11.625	low	2	1	144	10644745.63	7.02713529
SS_sum_KV_pier_cDNA_1	CXR25	MST_Bacteroides_16S	22.227	0.616	4.674803639	47293.73777	2017-07-11	Kingsville	lake	centrifuge	1092	Qubit	high	20.22222222	medium	2	1	54	1276930.92	6.1061674
SS_sum_KV_pier_cDNA_2	CXR25	MST_Bacteroides_16S	23.567	1.048	4.296208397	19779.1852	2017-07-11	Kingsville	lake	centrifuge	944	Qubit	high	17.48148148	low	2	1	54	534038.0003	5.72757216
SS_sum_KV_pier_cDNA_3b	CXR25	MST_Bacteroides_16S	26.081	1.067	3.585918517	3854.060406	2017-07-11	Kingsville	lake	centrifuge	240	Bioanalyzer	medium	80	medium	2	1	3	5781.09061	3.76200978
SS_sum_KV_creek_cDNA_2	CXR25	MST_Bacteroides_16S	27.263	0.76	3.25196361	1786.337888	2017-07-11	Kingsville	lake	centrifuge	1331	Bioanalyzer	very high	9.243055556	low	2	1	144	128616.3279	5.10929611
SS_sum_KV_pier_cDNA_3a	CXR25	MST_Bacteroides_16S	28.072	0.681	3.023393796	1055.343393	2017-07-11	Kingsville	lake	centrifuge	184	Bioanalyzer	low	88.32	medium	2	1	2.08333	1099.316034	3.04112256
SS_sum_KV_creek_cDNA_1	CXR25	MST_goose	25.593	0.445	3.115473441	1304.588185	2017-07-11	Kingsville	lake	centrifuge	1674	Bioanalyzer	very high	11.625	low	2	1	144	93930.34934	4.97280594
SS_sum_KV_pier_cDNA_1	CXR25	MST_goose	26.311	0.037	2.908198614	809.4660047	2017-07-11	Kingsville	lake	centrifuge	1092	Qubit	high	20.22222222	medium	2	1	54	21855.58213	4.33956238
SS_sum_KV_creek_cDNA_2	CXR25	MST_goose	28.432	0.381	2.295900693	197.6517632	2017-07-11	Kingsville	lake	centrifuge	1331	Bioanalyzer	very high	9.243055556	low	2	1	144	14230.92695	4.15323319
SS_sum_KV_pier_cDNA_2	CXR25	MST_goose	29.089	0.445	2.106235566	127.713135	2017-07-11	Kingsville	lake	centrifuge	944	Qubit	high	17.48148148	low	2	1	54	3448.254646	3.53759933
SS_sum_KV_pier_cDNA_3b	CXR25	MST_goose	30.217	2.629	1.780600462	60.339327	2017-07-11	Kingsville	lake	centrifuge	240	Bioanalyzer	medium	80	medium	2	1	3	90.50899049	1.95669172
SS_sum_KV_pier_cDNA_3a	CXR25	MST_goose	30.255	1.447	1.769630485	58.83428568	2017-07-11	Kingsville	lake	centrifuge	184	Bioanalyzer	low	88.32	medium	2	1	2.08333	61.28571425	1.78735925
SS_sum_KV_creek_cDNA_1	CXR25	MST_seagull	27.38	0.391	2.539306179	346.183521	2017-07-11	Kingsville	lake	centrifuge	1674	Bioanalyzer	very high	11.625	low	2	1	144	24925.20135	4.39663868
SS_fall_KV_pier_cDNA_1a	CXR25	FIB_Ecoli_23S	27.297	0.698	3.38189328	2409.313309	2017-11-28	Kingsville	lake	centrifuge	492	Bioanalyzer	medium	164	high	2	1	3	3613.969964	3.55798454
SS_fall_KV_pier_cDNA_1b	CXR25	FIB_Ecoli_23S	28.396	0.305	3.075184193	1189.006402	2017-11-28	Kingsville	lake	centrifuge	500	Bioanalyzer	medium	166.6666667	high	2	1	3	1783.509603	3.25127545
SS_fall_KV_creek_cDNA_1b	CXR25	FIB_Ecoli_23S	29.401	0.055	2.79470864	623.3165243	2017-11-28	Kingsville	lake	centrifuge	366	Bioanalyzer	medium	122	high	2	1	3	934.9747865	2.9707999
SS_fall_KV_pier_cDNA_1a	CXR25	FIB_Enterococcus_23S	30.618	1.117	2.34930886	223.5161253	2017-11-28	Kingsville	lake	centrifuge	492	Bioanalyzer	medium	164	high	2	1	3	335.2741879	2.52540012
SS_fall_KV_pier_cDNA_1b	CXR25	FIB_Enterococcus_23S	31.026	0.303	2.233741219	171.2936325	2017-11-28	Kingsville	lake	centrifuge	500	Bioanalyzer	medium	166.6666667	high	2	1	3	256.9404487	2.40983248
SS_fall_KV_creek_cDNA_1b	CXR25	FIB_Enterococcus_23S	33.259	2.771	1.601234988	39.92408647	2017-11-28	Kingsville	lake	centrifuge	366	Bioanalyzer	medium	122	high	2	1	3	59.8861297	1.77732625
SS_fall_KV_pier_cDNA_1a	CXR25	MST_Bacteroides_16S	21.371	1.111	4.91665254	82537.7337	2017-11-28	Kingsville	lake	centrifuge	492	Bioanalyzer	medium	164	high	2	1	3	123806.6006	5.09274738
SS_fall_KV_pier_cDNA_1b	CXR25	MST_Bacteroides_16S	22.423	1.234	4.619427022	41631.97571	2017-11-28	Kingsville	lake	centrifuge	500	Bioanalyzer	medium	166.6666667	high	2	1	3	62447.96357	4.79551828
SS_fall_KV_creek_cDNA_1b	CXR25	MST_Bacteroides_16S	25.519	0.005	3.744702492	5555.235724	2017-11-28	Kingsville	lake	centrifuge	366	Bioanalyzer	medium	122	high	2	1	3	8332.853585	3.92079375
SS_fall_KV_creek_cDNA_1a	CXR25	MST_Bacteroides_16S	26.247	0.62	3.539017913	3459.536465	2017-11-28	Kingsville	lake	centrifuge	712	Bioanalyzer	high	13.18518519	low	2	1	54	93407.48456	4.97038168
SS_fall_KV_pier_cDNA_1a	CXR25	MST_dog	26.984	0.489	2.508283538	322.3172416	2017-11-28	Kingsville	lake	centrifuge	492	Bioanalyzer	medium	164	high	2	1	3	483.4758624	2.6843748
SS_fall_KV_pier_cDNA_1a	CXR25	MST_goose	24.989	0.525	2.889838337	1949.11892	2017-11-28	Kingsville	lake	centrifuge	492	Bioanalyzer	medium	164	high	2	1	3	2923.67838	3.46592996
SS_fall_KV_creek_cDNA_1b	CXR25	MST_goose	25.563	0.161	3.124133949	1330.864833	2017-11-28	Kingsville	lake	centrifuge	366	Bioanalyzer	medium	122	high	2	1	3	1996.297249	3.30022521
SS_fall_KV_creek_cDNA_1a	CXR25	MST_goose	25.941	0.163	3.015011547	1035.16969	2017-11-28	Kingsville	lake	centrifuge	712	Bioanalyzer	high	13.18518519	low	2	1	54	27949.58163	4.44637531
SS_fall_KV_pier_cDNA_1b	CXR25	MST_goose	26.019	0.315	2.992494226	982.8658063	2017-11-28	Kingsville	lake	centrifuge	500	Bioanalyzer	medium	166.6666667	high	2	1	3	1474.298709	3.16858549
SS_fall_KV_pier_cDNA_1a	CXR25	MST_seagull	29.068	0.732	2.062833432	115.5668916	2017-11-28	Kingsville	lake	centrifuge	492	Bioanalyzer	medium	164	high	2	1	3	173.3503374	2.23892469
SS_fall_KV_pier_cDNA_1b	CXR25	MST_seagull	30.379	0.926	1.692776696	49.29202905	2017-11-28	Kingsville	lake	centrifuge	500	Bioanalyzer	medium	166.6666667	high	2	1	3	73.93804357	1.86886796
WE_2017-06-01_BR_cDNA_2a	CXR27	FIB_Ecoli_23S	27.643	0.886	3.285331547	1928.996978	2017-06-01	Belle River	beach	core	374	Qubit	medium	124.6666667	high	5	1.2	3	1388.877824	3.14266404
WE_2017-06-01_BR_cDNA_2b	CXR27	FIB_Ecoli_23S	29.228	0.907	2.842989507	696.6096824	2017-06-01	Belle River	beach	core	188	Qubit	low	90.24	medium	5	1.2	2.08333	348.3048412	2.54195951
WE_2017-06-01_BR_cDNA_1a	CXR27	FIB_Ecoli_23S	29.689	1.809	2.714333557	518.0045287	2017-06-01	Belle River	beach	core	348	Qubit	medium	116	high	5	1.2	3	372.9632606	2.57166605
WE_2017-06-01_BR_cDNA_1b	CXR27	FIB_Ecoli_23S	30.33	1.228	2.535443179	343.1177452	2017-06-01	Belle River	beach	core	263	Qubit	medium	87.66666667	medium	5	1.2	3	247.0447765	2.39277568
WE_2017-06-01_BR_cDNA_1a	CXR27	FIB_Enterococcus_23S	28.467	0.492	2.958588262	909.0510273	2017-06-01	Belle River	beach	core	348	Qubit	medium	116	high	5	1.2	3	654.5167397	2.81592076
WE_2017-06-01_BR_cDNA_2a	CXR27	FIB_Enterococcus_23S	28.504	1.73	2.948107863	887.3763771	2017-06-01	Belle River	beach	core	374	Qubit	medium	124.6666667	high	5	1.2	3	638.9109915	2.80544036
WE_2017-06-01_BR_cDNA_2b	CXR27	FIB_Enterococcus_23S	28.747	1.327	2.879277136	757.3160059	2017-06-01	Belle River	beach	core	188	Qubit	low	90.24	medium	5	1.2	2.08333	378.6580029	2.57824714
WE_2017-06-01_BR_cDNA_1b	CXR27	FIB_Enterococcus_23S	29.295	1.047	2.724053932	529.7292227	2017-06-01	Belle River	beach	core	263	Qubit	medium	87.66666667	medium	5	1.2	3	381.4054003	2.58138643
WE_2017-06-01_BR_cDNA_1a	CXR27	MST_Bacteroides_16S	21.256	1.124	4.949143923	88949.58428	2017-06-01	Belle River	beach	core	348	Qubit	medium	116	high	5	1.2	3	64043.70068	4.80647642
WE_2017-06-01_BR_cDNA_2a	CXR27	MST_Bacteroides_16S	21.591	1.106	4.854495112	71531.13434	2017-06-01	Belle River	beach	core	374	Qubit	medium	124.6666667	high	5	1.2	3	51502.41673	4.71182761
WE_2017-06-01_BR_cDNA_2b	CXR27	MST_Bacteroides_16S	21.742	0.852	4.811832514	64838.43354	2017-06-01	Belle River	beach	core	188	Qubit	low	90.24	medium	5	1.2	2.08333	32419.21677	4.51080252
WE_2017-06-01_BR_cDNA_1b	CXR27	MST_Bacteroides_16S	23.05	0.827	4.442278352	27687.15629	2017-06-01	Belle River	beach	core	263	Qubit	medium	87.66666667	medium	5	1.2	3	19934.75253	4.29961085
WE_2017-06-01_BR_cDNA_2b	CXR27	MST_goose	29.062	0.863	2.114030023	130.0259463	2017-06-01	Belle River	beach	core	188	Qubit	low	90.24	medium	5	1.2	2.08333	65.01297314	1.81300003
WE_2017-06-01_BR_cDNA_2a	CXR27	MST_goose	30.653	1.172	1.654734411	45.15797004	2017-06-01	Belle River	beach	core	374	Qubit	medium	124.6666667	high	5	1.2	3	32.51373843	1.51206691
WE_2017-06-01_BR_cDNA_1a	CXR27	MST_goose	30.67	0.129	1.64982679	44.65054763	2017-06-01	Belle River	beach	core	348	Qubit	medium	116	high	5	1.2	3	32.1483943	1.50715929

WE_2017-06-01_BR_cDNA_1b	CXR27	MST_goose	33.555	0.785	0.816974596	6.561068861	2017-06-01	Belle River	beach	core	263	Qubit	medium	87.66666667	medium	5	1.2	3	4.72396958	0.67430709
WE_2017-06-01_BR_cDNA_1a	CXR27	MST_seagull	27.336	0.723	2.551726085	356.2263858	2017-06-01	Belle River	beach	core	348	Qubit	medium	116	high	5	1.2	3	256.4829978	2.40905858
WE_2017-06-01_BR_cDNA_2a	CXR27	MST_seagull	28.551	1.056	2.208767324	161.7213375	2017-06-01	Belle River	beach	core	374	Qubit	medium	124.66666667	high	5	1.2	3	116.439363	2.06609982
WE_2017-06-01_BR_cDNA_1b	CXR27	MST_seagull	28.61	1.531	2.19211336	155.6371824	2017-06-01	Belle River	beach	core	263	Qubit	medium	87.66666667	medium	5	1.2	3	112.0587713	2.04944586
WE_2017-06-01_BR_cDNA_2b	CXR27	MST_seagull	30.302	0.699	1.714511531	51.82168508	2017-06-01	Belle River	beach	core	188	Qubit	low	90.24	medium	5	1.2	2.08333	25.91084254	1.41348154
WE_2017-07-26_BR_cDNA_3a	CXR27	FIB_Ecoli_23S	20.183	0.53	5.36726948	232953.6287	2017-07-26	Belle River	beach	core	79.5	Qubit	very low	79.5	medium	5	1.2	1	55908.87089	4.74748072
WE_2017-07-26_BR_cDNA_2a	CXR27	FIB_Ecoli_23S	21.956	0.538	4.872460371	74552.184	2017-07-26	Belle River	beach	core	137	Qubit	low	65.76	medium	5	1.2	2.08333	37276.092	4.57143038
WE_2017-07-26_BR_cDNA_1a	CXR27	FIB_Ecoli_23S	22.977	0.769	4.587519536	38682.94548	2017-07-26	Belle River	beach	core	222	Qubit	medium	74	medium	5	1.2	3	27851.72074	4.44485203
WE_2017-07-26_BR_cDNA_1b	CXR27	FIB_Ecoli_23S	23.195	0.566	4.526680063	33626.37582	2017-07-26	Belle River	beach	core	204	Qubit	low	97.92	medium	5	1.2	2.08333	16813.18791	4.22565007
WE_2017-07-26_BR_cDNA_2b	CXR27	FIB_Ecoli_23S	24.145	0.672	4.261553918	18262.23463	2017-07-26	Belle River	beach	core	240	Qubit	medium	80	medium	5	1.2	3	13148.80894	4.11888642
WE_2017-07-26_BR_cDNA_3b	CXR27	FIB_Ecoli_23S	27.42	3.039	3.347566421	2226.211496	2017-07-26	Belle River	beach	core	85.4	Qubit	very low	85.4	medium	5	1.2	1	534.290759	2.72777766
WE_2017-07-26_BR_cDNA_3a	CXR27	FIB_Enterococcus_23S	21.582	0.216	4.908792205	81057.31334	2017-07-26	Belle River	beach	core	79.5	Qubit	very low	79.5	medium	5	1.2	1	19453.7552	4.28900345
WE_2017-07-26_BR_cDNA_3b	CXR27	FIB_Enterococcus_23S	22.453	0.281	4.662077952	45928.04417	2017-07-26	Belle River	beach	core	85.4	Qubit	very low	85.4	medium	5	1.2	1	11022.7306	4.04228919
WE_2017-07-26_BR_cDNA_1b	CXR27	FIB_Enterococcus_23S	22.462	0.432	4.659528665	45659.23863	2017-07-26	Belle River	beach	core	204	Qubit	low	97.92	medium	5	1.2	2.08333	22829.61931	4.35849867
WE_2017-07-26_BR_cDNA_1a	CXR27	FIB_Enterococcus_23S	23.147	0.599	4.46549966	29207.85474	2017-07-26	Belle River	beach	core	222	Qubit	medium	74	medium	5	1.2	3	21029.65541	4.32283216
WE_2017-07-26_BR_cDNA_2a	CXR27	FIB_Enterococcus_23S	23.178	0.57	4.456718785	28623.23956	2017-07-26	Belle River	beach	core	137	Qubit	low	65.76	medium	5	1.2	2.08333	14311.61978	4.15568879
WE_2017-07-26_BR_cDNA_2b	CXR27	FIB_Enterococcus_23S	23.267	0.228	4.431509177	27009.04183	2017-07-26	Belle River	beach	core	240	Qubit	medium	80	medium	5	1.2	3	19446.51012	4.28884167
WE_2017-07-26_BR_cDNA_3b	CXR27	MST_Bacteroides_16S	18.727	0.596	5.663671809	460969.094	2017-07-26	Belle River	beach	core	85.4	Qubit	very low	85.4	medium	5	1.2	1	110632.5826	5.04388305
WE_2017-07-26_BR_cDNA_2a	CXR27	MST_Bacteroides_16S	18.863	1.334	5.625247217	421936.6176	2017-07-26	Belle River	beach	core	137	Qubit	low	65.76	medium	5	1.2	2.08333	210968.3088	5.32421722
WE_2017-07-26_BR_cDNA_3a	CXR27	MST_Bacteroides_16S	18.877	0.189	5.621291744	418111.1453	2017-07-26	Belle River	beach	core	79.5	Qubit	very low	79.5	medium	5	1.2	1	100346.6749	5.00150299
WE_2017-07-26_BR_cDNA_1b	CXR27	MST_Bacteroides_16S	19.209	0.306	5.527490535	336891.8735	2017-07-26	Belle River	beach	core	204	Qubit	low	97.92	medium	5	1.2	2.08333	168445.9368	5.22646054
WE_2017-07-26_BR_cDNA_1a	CXR27	MST_Bacteroides_16S	19.741	0.277	5.377182573	238332.1185	2017-07-26	Belle River	beach	core	222	Qubit	medium	74	medium	5	1.2	3	171599.1253	5.23451507
WE_2017-07-26_BR_cDNA_2b	CXR27	MST_Bacteroides_16S	20.029	0.676	5.29581285	197611.7889	2017-07-26	Belle River	beach	core	240	Qubit	medium	80	medium	5	1.2	3	142280.488	5.15314535
WE_2017-07-26_BR_cDNA_1b	CXR27	MST_dog	21.034	2.46	4.193310866	15606.69224	2017-07-26	Belle River	beach	core	204	Qubit	low	97.92	medium	5	1.2	2.08333	7803.34612	3.89228087
WE_2017-07-26_BR_cDNA_3a	CXR27	MST_goose	21.448	0.509	4.312066975	20514.78523	2017-07-26	Belle River	beach	core	79.5	Qubit	very low	79.5	medium	5	1.2	1	4923.548454	3.69227822
WE_2017-07-26_BR_cDNA_1b	CXR27	MST_goose	21.693	0.142	4.241339492	17431.68992	2017-07-26	Belle River	beach	core	204	Qubit	low	97.92	medium	5	1.2	2.08333	8715.84959	3.9403095
WE_2017-07-26_BR_cDNA_2a	CXR27	MST_goose	21.923	0.234	4.174942263	14960.36754	2017-07-26	Belle River	beach	core	137	Qubit	low	65.76	medium	5	1.2	2.08333	7480.183771	3.87391227
WE_2017-07-26_BR_cDNA_1a	CXR27	MST_goose	22.681	0.022	3.956120092	9038.993881	2017-07-26	Belle River	beach	core	222	Qubit	medium	74	medium	5	1.2	3	6508.075594	3.81345259
WE_2017-07-26_BR_cDNA_3b	CXR27	MST_goose	23.871	1.569	3.612586605	4098.138249	2017-07-26	Belle River	beach	core	85.4	Qubit	very low	85.4	medium	5	1.2	1	983.5531798	2.99279785
WE_2017-07-26_BR_cDNA_2b	CXR27	MST_goose	24.279	0.417	3.494803695	3124.666672	2017-07-26	Belle River	beach	core	240	Qubit	medium	80	medium	5	1.2	3	2249.760004	3.35213619
WE_2017-07-26_BR_cDNA_3a	CXR27	MST_seagull	20.749	1.148	4.411042425	25765.72844	2017-07-26	Belle River	beach	core	79.5	Qubit	very low	79.5	medium	5	1.2	1	6183.774827	3.79125367
WE_2017-07-26_BR_cDNA_2a	CXR27	MST_seagull	23.336	0.312	3.680808423	4795.218741	2017-07-26	Belle River	beach	core	137	Qubit	low	65.76	medium	5	1.2	2.08333	2397.609371	3.79777843
WE_2017-07-26_BR_cDNA_1b	CXR27	MST_seagull	23.5	0.075	3.634516047	4310.384845	2017-07-26	Belle River	beach	core	204	Qubit	low	97.92	medium	5	1.2	2.08333	2155.192422	3.3348605
WE_2017-07-26_BR_cDNA_1a	CXR27	MST_seagull	24.203	0.497	3.436079826	2729.479433	2017-07-26	Belle River	beach	core	222	Qubit	medium	74	medium	5	1.2	3	1965.225191	3.29341232
WE_2017-07-26_BR_cDNA_3b	CXR27	MST_seagull	24.214	1.986	3.43297485	2710.034687	2017-07-26	Belle River	beach	core	85.4	Qubit	very low	85.4	medium	5	1.2	1	650.4083249	2.81318609
WE_2017-07-26_BR_cDNA_2b	CXR27	MST_seagull	24.621	0.017	3.318090722	2080.13117	2017-07-26	Belle River	beach	core	240	Qubit	medium	80	medium	5	1.2	3	1497.694442	3.17542322
WE_2017-06-01_HD_cDNA_2b	CXR27	FIB_Ecoli_23S	29.612	0.16	2.735822728	544.2804414	2017-06-01	Holiday	beach	core	56.7	Qubit	very low	56.7	medium	5	1.2	1	130.6273059	2.11603397
WE_2017-06-01_HD_cDNA_2a	CXR27	FIB_Ecoli_23S	30.159	4.757	2.583165885	382.9709969	2017-06-01	Holiday	beach	core	46.8	Qubit	very low	46.8	medium	5	1.2	1	91.91303925	1.96337713
WE_2017-06-01_HD_cDNA_2a	CXR27	FIB_Enterococcus_23S	26.855	0.396	3.415193746	2601.319795	2017-06-01	Holiday	beach	core	46.8	Qubit	very low	46.8	medium	5	1.2	1	624.3167508	2.79540499
WE_2017-06-01_HD_cDNA_2b	CXR27	FIB_Enterococcus_23S	27.431	0.953	3.252039429	1786.649775	2017-06-01	Holiday	beach	core	56.7	Qubit	very low	56.7	medium	5	1.2	1	428.795946	2.63225067
WE_2017-06-01_HD_cDNA_2a	CXR27	MST_Bacteroides_16S	20.293	1.251	5.221223936	166427.0581	2017-06-01	Holiday	beach	core	46.8	Qubit	very low	46.8	medium	5	1.2	1	39942.49394	4.60143518
WE_2017-06-01_HD_cDNA_2b	CXR27	MST_Bacteroides_16S	20.831	0.312	5.069220772	117279.1398	2017-06-01	Holiday	beach	core	56.7	Qubit	very low	56.7	medium	5	1.2	1	28146.99355	4.44943201
WE_2017-06-01_HD_cDNA_2a	CXR27	MST_goose	25.306	0.169	3.198325635	1578.79461	2017-06-01	Holiday	beach	core	46.8	Qubit	very low	46.8	medium	5	1.2	1	378.9107065	2.57853688
WE_2017-06-01_HD_cDNA_2b	CXR27	MST_goose	26.016	0.283	2.993360277	984.8277493	2017-06-01	Holiday	beach	core	56.7	Qubit	very low	56.7	medium	5	1.2	1	236.3586598	2.37357152
WE_2017-06-01_HD_cDNA_2a	CXR27	MST_seagull	27.01	0.34	2.643746295	440.2975767	2017-06-01	Holiday	beach	core	46.8	Qubit	very low	46.8	medium	5	1.2	1	105.6714184	2.02395754
WE_2017-06-01_HD_cDNA_2b	CXR27	MST_seagull	29.047	0.768	2.068761114	117.1550772	2017-06-01	Holiday	beach	core	56.7	Qubit	very low	56.7	medium	5	1.2	1	28.11721852	1.44897236
WE_2017-07-26_HD_cDNA_3b	CXR27	FIB_Ecoli_23S	32.359	1.069	1.969189551	93.15143535	2017-07-26	Holiday	beach	core	60.3	Qubit	very low	60.3	medium	5	1.2	1	22.35634448	1.34940079
WE_2017-07-26_HD_cDNA_3b	CXR27	FIB_Enterococcus_23S	25.353	0.073	3.840641287	6928.532957	2017-07-26	Holiday	beach	core	60.3	Qubit	very low	60.3	medium	5	1.2	1	1662.84791	3.22085253
WE_2017-07-26_HD_cDNA_3b	CXR27	MST_Bacteroides_16S	17.481	0.746	6.015708877	1036833.157	2017-07-26	Holiday	beach	core	60.3	Qubit	very low	60.3	medium	5	1.2	1	248839.9577	5.39592012
WE_2017-07-26_HD_cDNA_3b	CXR27	MST_goose	26.068	0.973	2.97834873	951.3684169	2017-07-26	Holiday	beach	core	60.3	Qubit	very low	60.3	medium	5	1.2	1	228.32842	2.35855997
WE_2017-07-26_HD_cDNA_3b	CXR27	MST_seagull	32.607	2.18	1.063877833	11.58451439	2017-07-26	Holiday	beach	core	60.3	Qubit	very low	60.3	medium	5	1.2	1	2.780283453	0.44408908
WE_2017-06-01_KV_cDNA_1a	CXR27	FIB_Ecoli_23S	26.159	0.589	3.699486493	5005.949827	2017-06-01	Kingsville	beach	core	69.3	Qubit	very low	69.3	medium	5	1.2	1	1201.427959	3.07969773
WE_2017-06-01_KV_cDNA_1b	CXR27	FIB_Ecoli_23S	26.913	0.161	3.489060058	3083.61435	2017-06-01	Kingsville	beach	core	46.8	Qubit	very low	46.8	medium	5	1.2	1	740.067444	2.8692713
WE_2017-06-01_KV_cDNA_4b	CXR27	FIB_Ecoli_23S	29.065	1.229	2.888479571	773.5342918	2017-06-01	Kingsville	beach	core	10.7	Qubit	very low	10.7	low	5	1.2	1	185.64823	2.26869081
WE_2017-06-01_KV_cDNA_1a	CXR27	FIB_Enterococcus_23S	22.125	0.507	4.754985271	56883.36384	2017-06-01	Kingsville	beach	core	69.3	Qubit	very low	69.3	medium	5	1.2	1	13652.00732	4.13519651

WE_2017-06-01_KV_cDNA_1b	CXR27	FIB_Enterococcus_23S	23.399	0.554	4.394119646	24781.04672	2017-06-01	Kingsville	beach	core	46.8	Qubit	very low	46.8	medium	5	1.2	1	5947.451213	3.77433089
WE_2017-06-01_KV_cDNA_4b	CXR27	FIB_Enterococcus_23S	26.056	0.341	3.641513709	4380.399387	2017-06-01	Kingsville	beach	core	10.7	Qubit	very low	10.7	low	5	1.2	1	1051.295853	3.02172495
WE_2017-06-01_KV_cDNA_1a	CXR27	MST_Bacteroides_16S	17.851	0.32	5.911171385	815025.853	2017-06-01	Kingsville	beach	core	69.3	Qubit	very low	69.3	medium	5	1.2	1	195606.2047	5.29138263
WE_2017-06-01_KV_cDNA_1b	CXR27	MST_Bacteroides_16S	18.41	0.472	5.753235012	566545.7834	2017-06-01	Kingsville	beach	core	46.8	Qubit	very low	46.8	medium	5	1.2	1	135970.988	5.13344625
WE_2017-06-01_KV_cDNA_4b	CXR27	MST_Bacteroides_16S	19.365	0.721	5.483415268	304379.4081	2017-06-01	Kingsville	beach	core	10.7	Qubit	very low	10.7	low	5	1.2	1	73051.05794	4.86362651
WE_2017-06-01_KV_cDNA_1a	CXR27	MST_dog	25.706	0.407	2.870210416	741.6694937	2017-06-01	Kingsville	beach	core	69.3	Qubit	very low	69.3	medium	5	1.2	1	178.0006785	2.25042166
WE_2017-06-01_KV_cDNA_1b	CXR27	MST_dog	26.969	0.201	2.512531506	325.4853949	2017-06-01	Kingsville	beach	core	46.8	Qubit	very low	46.8	medium	5	1.2	1	78.11649477	1.89274275
WE_2017-06-01_KV_cDNA_1a	CXR27	MST_goose	21.014	0.725	4.437355658	27375.09646	2017-06-01	Kingsville	beach	core	69.3	Qubit	very low	69.3	medium	5	1.2	1	6570.023151	3.8175669
WE_2017-06-01_KV_cDNA_1b	CXR27	MST_goose	21.852	0.253	4.195438799	15683.34872	2017-06-01	Kingsville	beach	core	46.8	Qubit	very low	46.8	medium	5	1.2	1	3764.003692	3.57565004
WE_2017-06-01_KV_cDNA_4b	CXR27	MST_goose	23.252	0.014	3.791281755	6184.174778	2017-06-01	Kingsville	beach	core	10.7	Qubit	very low	10.7	low	5	1.2	1	1484.201947	3.171493
WE_2017-06-01_KV_cDNA_1a	CXR27	MST_seagull	27.759	0.822	2.432325627	270.5986511	2017-06-01	Kingsville	beach	core	69.3	Qubit	very low	69.3	medium	5	1.2	1	64.94367626	1.81253687
WE_2017-06-01_KV_cDNA_1b	CXR27	MST_seagull	32.021	2.94	1.229288396	16.95463309	2017-06-01	Kingsville	beach	core	46.8	Qubit	very low	46.8	medium	5	1.2	1	4.069111942	0.60949964
WE_2017-07-26_KV_cDNA_1b	CXR27	FIB_Ecoli_23S	20.936	0.494	5.157122125	143589.3156	2017-07-26	Kingsville	beach	core	114	Qubit	low	54.72	medium	5	1.2	2.08333	71794.6578	4.85609213
WE_2017-07-26_KV_cDNA_1a	CXR27	FIB_Ecoli_23S	24.337	0.59	4.207970529	16142.49012	2017-07-26	Kingsville	beach	core	117	Qubit	low	56.16	medium	5	1.2	2.08333	8071.245058	3.90694053
WE_2017-07-26_KV_cDNA_3a	CXR27	FIB_Ecoli_23S	25.821	0.649	3.793815584	6220.360915	2017-07-26	Kingsville	beach	core	24.6	Qubit	very low	24.6	medium	5	1.2	1	1492.88662	3.17402683
WE_2017-07-26_KV_cDNA_3b	CXR27	FIB_Ecoli_23S	26.855	0.815	3.505246707	3200.712802	2017-07-26	Kingsville	beach	core	17.2	Qubit	very low	17.2	low	5	1.2	1	768.1710724	2.88545795
WE_2017-07-26_KV_cDNA_2a	CXR27	FIB_Ecoli_23S	26.983	0.817	3.469524447	2947.97942	2017-07-26	Kingsville	beach	core	88.9	Qubit	very low	88.9	medium	5	1.2	1	707.5150609	2.84973569
WE_2017-07-26_KV_cDNA_2b	CXR27	FIB_Ecoli_23S	33.327	1.709	1.699039964	50.00805508	2017-07-26	Kingsville	beach	core	56.7	Qubit	very low	56.7	medium	5	1.2	1	12.00193322	1.07925121
WE_2017-07-26_KV_cDNA_1b	CXR27	FIB_Enterococcus_23S	22.939	0.355	4.524416497	33451.56932	2017-07-26	Kingsville	beach	core	114	Qubit	low	54.72	medium	5	1.2	2.08333	16725.78466	4.2233865
WE_2017-07-26_KV_cDNA_1a	CXR27	FIB_Enterococcus_23S	23.133	0.568	4.469465216	29475.77389	2017-07-26	Kingsville	beach	core	117	Qubit	low	56.16	medium	5	1.2	2.08333	14737.88695	4.16843522
WE_2017-07-26_KV_cDNA_2a	CXR27	FIB_Enterococcus_23S	24.199	0.554	4.167516429	14706.74048	2017-07-26	Kingsville	beach	core	88.9	Qubit	very low	88.9	medium	5	1.2	1	3529.617715	3.54772767
WE_2017-07-26_KV_cDNA_3a	CXR27	FIB_Enterococcus_23S	24.645	0.241	4.041185135	10994.74433	2017-07-26	Kingsville	beach	core	24.6	Qubit	very low	24.6	medium	5	1.2	1	2638.738639	3.42139638
WE_2017-07-26_KV_cDNA_3b	CXR27	FIB_Enterococcus_23S	24.795	0.088	3.998697031	9970.043002	2017-07-26	Kingsville	beach	core	17.2	Qubit	very low	17.2	low	5	1.2	1	2392.810321	3.37890827
WE_2017-07-26_KV_cDNA_2b	CXR27	FIB_Enterococcus_23S	26.73	0.092	3.450600499	2822.282602	2017-07-26	Kingsville	beach	core	56.7	Qubit	very low	56.7	medium	5	1.2	1	677.3478244	2.83081174
WE_2017-07-26_KV_cDNA_2b	CXR27	MST_Bacteroides_16S	17.223	0.581	6.088602588	1226316.546	2017-07-26	Kingsville	beach	core	56.7	Qubit	very low	56.7	medium	5	1.2	1	294315.9711	5.46881383
WE_2017-07-26_KV_cDNA_1a	CXR27	MST_Bacteroides_16S	17.301	0.145	6.065649555	1165641.375	2017-07-26	Kingsville	beach	core	88.9	Qubit	very low	88.9	medium	5	1.2	1	279753.93	5.4467762
WE_2017-07-26_KV_cDNA_3a	CXR27	MST_Bacteroides_16S	18.08	0.841	5.846471153	702216.6996	2017-07-26	Kingsville	beach	core	24.6	Qubit	very low	24.6	medium	5	1.2	1	168532.0079	5.2266824
WE_2017-07-26_KV_cDNA_1a	CXR27	MST_Bacteroides_16S	18.102	0.95	5.840255411	692237.9595	2017-07-26	Kingsville	beach	core	117	Qubit	low	56.16	medium	5	1.2	2.08333	346118.9797	5.53922542
WE_2017-07-26_KV_cDNA_1b	CXR27	MST_Bacteroides_16S	18.633	0.157	5.690229982	490038.2525	2017-07-26	Kingsville	beach	core	114	Qubit	low	54.72	medium	5	1.2	2.08333	245019.1263	5.38919999
WE_2017-07-26_KV_cDNA_3b	CXR27	MST_Bacteroides_16S	18.993	0.307	5.588517828	387719.6642	2017-07-26	Kingsville	beach	core	17.2	Qubit	very low	17.2	low	5	1.2	1	93052.7194	4.96872907
WE_2017-07-26_KV_cDNA_3b	CXR27	MST_dog	26.569	0.665	2.625810654	422.484377	2017-07-26	Kingsville	beach	core	17.2	Qubit	very low	17.2	low	5	1.2	1	101.3962505	2.0060219
WE_2017-07-26_KV_cDNA_1b	CXR27	MST_goose	20.998	1.084	4.441974596	27667.79797	2017-07-26	Kingsville	beach	core	114	Qubit	low	54.72	medium	5	1.2	2.08333	13833.89899	4.1409446
WE_2017-07-26_KV_cDNA_1a	CXR27	MST_goose	21.589	0.584	4.271362587	18679.38557	2017-07-26	Kingsville	beach	core	117	Qubit	low	56.16	medium	5	1.2	2.08333	9339.692784	3.97033259
WE_2017-07-26_KV_cDNA_2a	CXR27	MST_goose	21.968	0.205	4.161951501	14519.49465	2017-07-26	Kingsville	beach	core	88.9	Qubit	very low	88.9	medium	5	1.2	1	3484.678717	3.54216274
WE_2017-07-26_KV_cDNA_3a	CXR27	MST_goose	22.005	0.197	4.151270208	14166.74928	2017-07-26	Kingsville	beach	core	24.6	Qubit	very low	24.6	medium	5	1.2	1	3400.019827	3.53148145
WE_2017-07-26_KV_cDNA_3b	CXR27	MST_goose	22.388	0.423	4.040704388	10982.58032	2017-07-26	Kingsville	beach	core	17.2	Qubit	very low	17.2	low	5	1.2	1	2635.819276	3.42091563
WE_2017-07-26_KV_cDNA_2b	CXR27	MST_goose	23.325	0.593	3.770207852	5891.255418	2017-07-26	Kingsville	beach	core	56.7	Qubit	very low	56.7	medium	5	1.2	1	1413.9013	3.15041909
WE_2017-07-26_KV_cDNA_1b	CXR27	MST_seagull	23.255	0.58	3.70367234	5054.431793	2017-07-26	Kingsville	beach	core	114	Qubit	low	54.72	medium	5	1.2	2.08333	2527.215896	3.40264235
WE_2017-07-26_KV_cDNA_1a	CXR27	MST_seagull	27.015	0.518	2.642334942	438.8690376	2017-07-26	Kingsville	beach	core	117	Qubit	low	56.16	medium	5	1.2	2.08333	219.4345188	2.34130495
WE_2017-07-26_KV_cDNA_3b	CXR27	MST_seagull	28.613	0.088	2.191266548	155.3340079	2017-07-26	Kingsville	beach	core	17.2	Qubit	very low	17.2	low	5	1.2	1	37.28016191	1.57147779
WE_2017-07-26_KV_cDNA_3a	CXR27	MST_seagull	29.044	1.176	2.069607926	117.3837356	2017-07-26	Kingsville	beach	core	24.6	Qubit	very low	24.6	medium	5	1.2	1	28.17209653	1.44981917
WE_2017-07-26_KV_cDNA_2a	CXR27	MST_seagull	29.707	2.566	1.882462529	76.28910652	2017-07-26	Kingsville	beach	core	88.9	Qubit	very low	88.9	medium	5	1.2	1	18.30938557	1.26267377
WE_2017-06-01_LE_cDNA_1a	CXR27	FIB_Ecoli_23S	27.103	0.633	3.436034829	2729.196648	2017-06-01	Leamington	beach	core	72	Bioanalyzer	very low	72	medium	5	1.2	1	655.0071955	2.81624607
WE_2017-06-01_LE_cDNA_1b	CXR27	FIB_Ecoli_23S	27.778	0.112	3.247655727	1768.706316	2017-06-01	Leamington	beach	core	35.5	Qubit	very low	35.5	medium	5	1.2	1	424.4895159	2.62786697
WE_2017-06-01_LE_cDNA_4a	CXR27	FIB_Ecoli_23S	28.259	0.935	3.113418174	1298.428901	2017-06-01	Leamington	beach	core	13	Qubit	very low	13	low	5	1.2	1	311.6229363	2.49362942
WE_2017-06-01_LE_cDNA_4a	CXR27	FIB_Enterococcus_23S	25.202	0.583	3.883412644	7645.618863	2017-06-01	Leamington	beach	core	13	Qubit	very low	13	low	5	1.2	1	1834.948527	3.26362389
WE_2017-06-01_LE_cDNA_1a	CXR27	FIB_Enterococcus_23S	26.238	0.136	3.589961477	3890.106377	2017-06-01	Leamington	beach	core	72	Bioanalyzer	very low	72	medium	5	1.2	1	933.6255304	2.97017272
WE_2017-06-01_LE_cDNA_1b	CXR27	FIB_Enterococcus_23S	26.582	0.705	3.429522094	3108.294027	2017-06-01	Leamington	beach	core	35.5	Qubit	very low	35.5	medium	5	1.2	1	745.9905664	2.87273334
WE_2017-06-01_LE_cDNA_1a	CXR27	MST_Bacteroides_16S	20.34	0.325	5.207944849	161415.3564	2017-06-01	Leamington	beach	core	72	Bioanalyzer	very low	72	medium	5	1.2	1	38739.68554	4.58815609
WE_2017-06-01_LE_cDNA_1b	CXR27	MST_Bacteroides_16S	20.508	1.041	5.160479177	144703.5472	2017-06-01	Leamington	beach	core	35.5	Qubit	very low	35.5	medium	5	1.2	1	34728.85132	4.54069042
WE_2017-06-01_LE_cDNA_4a	CXR27	MST_Bacteroides_16S	21.34	0.674	4.925411087	84219.19513	2017-06-01	Leamington	beach	core	13	Qubit	very low	13	low	5	1.2	1	20212.60683	4.30562233
WE_2017-06-01_LE_cDNA_1a	CXR27	MST_goose	26.055	0.279	2.982101617	959.6251392	2017-06-01	Leamington	beach	core	72	Bioanalyzer	very low	72	medium	5	1.2	1	230.3100334	2.36231286
WE_2017-06-01_LE_cDNA_1b	CXR27	MST_goose	26.441	0.01	2.870669746	742.4543327	2017-06-01	Leamington	beach	core	35.5	Qubit	very low	35.5	medium	5	1.2	1	178.1890398	2.25088099
WE_2017-06-01_LE_cDNA_4a	CXR27	MST_goose	27.658	0.247	2.519341801	330.6296531	2017-06-01	Leamington	beach	core	13	Qubit	very low	13	low	5	1.2	1	79.35111673	1.89955304
WE_2017-06-01_LE_cDNA_1a	CXR27	MST_seagull	24.161	0.177	3.447935191	2805.015017	2017-06-01	Leamington	beach	core	72	Bioanalyzer	very low	72	medium	5	1.2	1	673.2036041	2.

WE_2017-06-01_LE_cDNA_4a	CXR27	MST_seagull	24.546	0.31	3.339261016	2184.04215	2017-06-01	Leamington	beach	core	13	Qubit	very low	13	low	5	1.2	1	524.170116	2.71947226
WE_2017-06-01_LE_cDNA_1b	CXR27	MST_seagull	25.259	0.235	3.138002089	1374.048584	2017-06-01	Leamington	beach	core	35.5	Qubit	very low	35.5	medium	5	1.2	1	329.7716601	2.51821333
WE_2017-07-26_LE_cDNA_3a	CXR27	FIB_Ecoli_23S	23.237	0.711	4.514958696	32730.95644	2017-07-26	Leamington	beach	core	50.1	Qubit	very low	50.1	medium	5	1.2	1	7855.429546	3.89516994
WE_2017-07-26_LE_cDNA_1b	CXR27	FIB_Ecoli_23S	27.3	1.001	3.381056039	2404.673068	2017-07-26	Leamington	beach	core	30.7	Qubit	very low	30.7	medium	5	1.2	1	577.1215362	2.76126728
WE_2017-07-26_LE_cDNA_1a	CXR27	FIB_Ecoli_23S	28.709	1.616	2.987832105	972.3712405	2017-07-26	Leamington	beach	core	19.7	Qubit	very low	19.7	low	5	1.2	1	233.3690977	2.36804335
WE_2017-07-26_LE_cDNA_2b	CXR27	FIB_Ecoli_23S	29.184	1.017	2.855269033	716.5871784	2017-07-26	Leamington	beach	core	34.4	Qubit	very low	34.4	medium	5	1.2	1	171.9809228	2.23548028
WE_2017-07-26_LE_cDNA_3b	CXR27	FIB_Ecoli_23S	30.873	4.931	2.383902657	242.0486456	2017-07-26	Leamington	beach	core	61.8	Qubit	very low	61.8	medium	5	1.2	1	58.09167494	1.7641139
WE_2017-07-26_LE_cDNA_3b	CXR27	FIB_Enterococcus_23S	24.681	0.107	4.03098799	10739.59713	2017-07-26	Leamington	beach	core	61.8	Qubit	very low	61.8	medium	5	1.2	1	2577.50331	3.41119923
WE_2017-07-26_LE_cDNA_3a	CXR27	FIB_Enterococcus_23S	24.936	0.481	3.958758214	9094.068358	2017-07-26	Leamington	beach	core	50.1	Qubit	very low	50.1	medium	5	1.2	1	2182.576406	3.38969646
WE_2017-07-26_LE_cDNA_2b	CXR27	FIB_Enterococcus_23S	27.081	0.019	3.351178337	2244.803531	2017-07-26	Leamington	beach	core	34.4	Qubit	very low	34.4	medium	5	1.2	1	538.7528473	2.73138958
WE_2017-07-26_LE_cDNA_1b	CXR27	FIB_Enterococcus_23S	27.153	0.445	3.330784047	2141.825314	2017-07-26	Leamington	beach	core	30.7	Qubit	very low	30.7	medium	5	1.2	1	514.0380754	2.71099529
WE_2017-07-26_LE_cDNA_1a	CXR27	FIB_Enterococcus_23S	27.701	0.111	3.175560843	1498.169126	2017-07-26	Leamington	beach	core	19.7	Qubit	very low	19.7	low	5	1.2	1	359.5605902	2.55577209
WE_2017-07-26_LE_cDNA_2a	CXR27	FIB_Enterococcus_23S	34.359	1.411	1.289655563	19.482988	2017-07-26	Leamington	beach	core	5.3	Qubit	very low	5.3	low	5	1.2	1	4.675917121	0.66986681
WE_2017-07-26_LE_cDNA_3b	CXR27	MST_Bacteroides_16S	17.1	1.042	6.123354241	1328477.615	2017-07-26	Leamington	beach	core	61.8	Qubit	very low	61.8	medium	5	1.2	1	318834.6276	5.50356548
WE_2017-07-26_LE_cDNA_3a	CXR27	MST_Bacteroides_16S	18.284	0.095	5.788834266	614942.1553	2017-07-26	Leamington	beach	core	50.1	Qubit	very low	50.1	medium	5	1.2	1	147586.1173	5.16904551
WE_2017-07-26_LE_cDNA_2b	CXR27	MST_Bacteroides_16S	22.607	1.173	4.674440809	36935.23012	2017-07-26	Leamington	beach	core	34.4	Qubit	very low	34.4	medium	5	1.2	1	8864.455229	3.94765205
WE_2017-07-26_LE_cDNA_1b	CXR27	MST_Bacteroides_16S	23.184	0.812	4.404418828	25375.74655	2017-07-26	Leamington	beach	core	30.7	Qubit	very low	30.7	medium	5	1.2	1	6090.179173	3.78463007
WE_2017-07-26_LE_cDNA_1a	CXR27	MST_Bacteroides_16S	23.365	0.704	4.353280217	22556.9417	2017-07-26	Leamington	beach	core	19.7	Qubit	very low	19.7	low	5	1.2	1	5413.666007	3.7349146
WE_2017-07-26_LE_cDNA_2a	CXR27	MST_Bacteroides_16S	24.666	0.827	3.985703792	9676.176723	2017-07-26	Leamington	beach	core	5.3	Qubit	very low	5.3	low	5	1.2	1	2322.282414	3.36591503
WE_2017-07-26_LE_cDNA_2b	CXR27	MST_dog	27.427	1.453	2.382826881	241.4498173	2017-07-26	Leamington	beach	core	34.4	Qubit	very low	34.4	medium	5	1.2	1	57.94795616	1.76303812
WE_2017-07-26_LE_cDNA_3a	CXR27	MST_goose	22.102	0.341	4.123267898	13282.13525	2017-07-26	Leamington	beach	core	50.1	Qubit	very low	50.1	medium	5	1.2	1	3187.712461	3.50347914
WE_2017-07-26_LE_cDNA_3b	CXR27	MST_goose	24.375	1.148	3.467090069	2931.501153	2017-07-26	Leamington	beach	core	61.8	Qubit	very low	61.8	medium	5	1.2	1	703.5602766	2.84730131
WE_2017-07-26_LE_cDNA_2b	CXR27	MST_goose	24.495	0.074	4.324448037	2706.749324	2017-07-26	Leamington	beach	core	34.4	Qubit	very low	34.4	medium	5	1.2	1	649.6198377	2.81265928
WE_2017-07-26_LE_cDNA_1a	CXR27	MST_goose	26.826	0.141	2.759526559	574.8129699	2017-07-26	Leamington	beach	core	19.7	Qubit	very low	19.7	low	5	1.2	1	137.9551128	2.1397378
WE_2017-07-26_LE_cDNA_1b	CXR27	MST_goose	27.645	0.61	2.523094688	333.4991169	2017-07-26	Leamington	beach	core	30.7	Qubit	very low	30.7	medium	5	1.2	1	80.03978805	1.90330593
WE_2017-07-26_LE_cDNA_2a	CXR27	MST_goose	28.824	1.024	2.182736721	152.3129117	2017-07-26	Leamington	beach	core	5.3	Qubit	very low	5.3	low	5	1.2	1	36.55509882	1.56294796
WE_2017-07-26_LE_cDNA_3a	CXR27	MST_seagull	23.44	3.366	3.651452282	4481.798038	2017-07-26	Leamington	beach	core	50.1	Qubit	very low	50.1	medium	5	1.2	1	1075.631529	3.03166352
WE_2017-07-26_LE_cDNA_2b	CXR27	MST_seagull	25.88	0.467	2.962712056	917.723929	2017-07-26	Leamington	beach	core	34.4	Qubit	very low	34.4	medium	5	1.2	1	220.253743	2.3429233
WE_2017-07-26_LE_cDNA_1b	CXR27	MST_seagull	26.14	0.994	2.889321704	775.0356932	2017-07-26	Leamington	beach	core	30.7	Qubit	very low	30.7	medium	5	1.2	1	186.0085664	2.26953295
WE_2017-07-26_LE_cDNA_3b	CXR27	MST_seagull	26.441	1.96	2.804358258	637.3210424	2017-07-26	Leamington	beach	core	61.8	Qubit	very low	61.8	medium	5	1.2	1	152.9570502	2.1845695
WE_2017-07-26_LE_cDNA_1a	CXR27	MST_seagull	27.959	0.109	2.37587151	237.6137183	2017-07-26	Leamington	beach	core	19.7	Qubit	very low	19.7	low	5	1.2	1	57.02729239	1.75608275
WE_2017-06-01_PP_cDNA_4b	CXR27	FIB_Ecoli_23S	27.851	0.048	3.227282876	1687.651912	2017-06-01	Point Pelee	beach	core	26.2	Qubit	very low	26.2	medium	5	1.2	1	405.0364588	2.60749412
WE_2017-06-01_PP_cDNA_4a	CXR27	FIB_Ecoli_23S	28.135	0.65	3.148024113	1406.125592	2017-06-01	Point Pelee	beach	core	28.2	Qubit	very low	28.2	medium	5	1.2	1	337.470142	2.52823535
WE_2017-06-01_PP_cDNA_1a	CXR27	FIB_Ecoli_23S	29.337	0.057	2.81256977	649.4859641	2017-06-01	Point Pelee	beach	core	90	Bioanalyzer	very low	90	medium	5	1.2	1	155.8766314	2.19278101
WE_2017-06-01_PP_cDNA_1b	CXR27	FIB_Ecoli_23S	29.62	1.112	2.733590087	541.4895591	2017-06-01	Point Pelee	beach	core	46.9	Qubit	very low	46.9	medium	5	1.2	1	129.9574942	2.11380133
WE_2017-06-01_PP_cDNA_2a	CXR27	FIB_Ecoli_23S	31.417	0.858	2.232083054	170.6408691	2017-06-01	Point Pelee	beach	core	72.3	Qubit	very low	72.3	medium	5	1.2	1	40.95380857	1.6122943
WE_2017-06-01_PP_cDNA_2b	CXR27	FIB_Ecoli_23S	31.699	0.872	2.153382451	142.358188	2017-06-01	Point Pelee	beach	core	17.7	Qubit	very low	17.7	low	5	1.2	1	34.16596512	1.53359369
WE_2017-06-01_PP_cDNA_4a	CXR27	FIB_Enterococcus_23S	23.662	0.279	4.319623839	20874.87284	2017-06-01	Point Pelee	beach	core	28.2	Qubit	very low	28.2	medium	5	1.2	1	5009.969482	3.69983508
WE_2017-06-01_PP_cDNA_1b	CXR27	FIB_Enterococcus_23S	24.42	0.478	4.10491729	12732.60569	2017-06-01	Point Pelee	beach	core	46.9	Qubit	very low	46.9	medium	5	1.2	1	3055.825366	3.48512853
WE_2017-06-01_PP_cDNA_1a	CXR27	FIB_Enterococcus_23S	24.964	0.412	3.950827102	8929.49918	2017-06-01	Point Pelee	beach	core	90	Bioanalyzer	very low	90	medium	5	1.2	1	2143.079803	3.33103834
WE_2017-06-01_PP_cDNA_4b	CXR27	FIB_Enterococcus_23S	25.281	0.417	3.861035577	7261.654413	2017-06-01	Point Pelee	beach	core	26.2	Qubit	very low	26.2	medium	5	1.2	1	1742.797059	3.24124682
WE_2017-06-01_PP_cDNA_2a	CXR27	FIB_Enterococcus_23S	27.264	0.963	3.299342851	1992.245482	2017-06-01	Point Pelee	beach	core	72.3	Qubit	very low	72.3	medium	5	1.2	1	478.1389157	2.67955409
WE_2017-06-01_PP_cDNA_2b	CXR27	FIB_Enterococcus_23S	27.892	0.633	3.121459325	1322.693821	2017-06-01	Point Pelee	beach	core	17.7	Qubit	very low	17.7	low	5	1.2	1	317.446517	2.50167057
WE_2017-06-01_PP_cDNA_1b	CXR27	MST_Bacteroides_16S	20.029	0.721	5.29581285	197611.7889	2017-06-01	Point Pelee	beach	core	46.9	Qubit	very low	46.9	medium	5	1.2	1	47426.82933	4.67602409
WE_2017-06-01_PP_cDNA_4b	CXR27	MST_Bacteroides_16S	20.472	0.419	5.170650393	148132.5138	2017-06-01	Point Pelee	beach	core	26.2	Qubit	very low	26.2	medium	5	1.2	1	35551.8033	4.55086163
WE_2017-06-01_PP_cDNA_4a	CXR27	MST_Bacteroides_16S	20.608	1.096	5.132225801	135589.4194	2017-06-01	Point Pelee	beach	core	28.2	Qubit	very low	28.2	medium	5	1.2	1	32541.46065	4.51243704
WE_2017-06-01_PP_cDNA_1a	CXR27	MST_Bacteroides_16S	20.729	1.353	5.908039216	125325.4336	2017-06-01	Point Pelee	beach	core	90	Bioanalyzer	very low	90	medium	5	1.2	1	30078.10405	4.47825046
WE_2017-06-01_PP_cDNA_2b	CXR27	MST_Bacteroides_16S	20.86	0.77	5.061027293	115087.2712	2017-06-01	Point Pelee	beach	core	17.7	Qubit	very low	17.7	low	5	1.2	1	27620.94509	4.44123853
WE_2017-06-01_PP_cDNA_2a	CXR27	MST_Bacteroides_16S	21.247	0.745	4.951686727	89471.91371	2017-06-01	Point Pelee	beach	core	72.3	Qubit	very low	72.3	medium	5	1.2	1	21473.25929	4.33189797
WE_2017-06-01_PP_cDNA_4b	CXR27	MST_goose	24.437	0.285	3.449191686	2813.142202	2017-06-01	Point Pelee	beach	core	26.2	Qubit	very low	26.2	medium	5	1.2	1	675.1541284	2.82940293
WE_2017-06-01_PP_cDNA_4a	CXR27	MST_goose	25.557	0.4	3.125866051	1336.183335	2017-06-01	Point Pelee	beach	core	28.2	Qubit	very low	28.2	medium	5	1.2	1	320.6840003	2.50607729
WE_2017-06-01_PP_cDNA_1b	CXR27	MST_goose	26.701	0.372	2.795612009	624.6144243	2017-06-01	Point Pelee	beach	core	46.9	Qubit	very low	46.9	medium	5	1.2	1	149.9074618	2.17582325
WE_2017-06-01_PP_cDNA_1a	CXR27	MST_goose	26.746	0.954	2.782621247	606.207419	2017-06-01	Point Pelee	beach	core	90	Bioanalyzer	very low	90	medium	5	1.2	1	145.4897806	2.16283249
WE_2017-06-01_PP_cDNA_2b	CXR27	MST_goose	26.846	0.18	2.753752887	567.2217649	2017-06-01	Point Pelee	beach	core	17.7	Qubit	very low	17.7	low	5	1.2	1	136.1332236	2.13396413
WE_2017-06-01_PP_cDNA_2a	CXR27	MST_goose	27.585	1.374	2.540415704	347.068904	2017-06-01	Point Pelee	beach	core	72.3	Qubit	very low	72.3	medium	5	1.2	1	83.29653697	1.92062695

WE_2017-06-01_PP_cDNA_4b	CXR27	MST_seagull	25.226	0.473	3.147317018	1403.838078	2017-06-01	Point Pelee	beach	core	26.2	Qubit	very low	26.2	medium	5	1.2	1	336.9211387	2.52752826
WE_2017-06-01_PP_cDNA_4a	CXR27	MST_seagull	27.523	0.417	2.498941485	315.4579562	2017-06-01	Point Pelee	beach	core	28.2	Qubit	very low	28.2	medium	5	1.2	1	75.70990949	1.87915273
WE_2017-06-01_PP_cDNA_1a	CXR27	MST_seagull	27.79	0.026	2.423575239	265.20105	2017-06-01	Point Pelee	beach	core	90	Bioanalyzer	very low	90	medium	5	1.2	1	63.648252	1.80378648
WE_2017-06-01_PP_cDNA_2b	CXR27	MST_seagull	29.698	1.864	1.885002964	76.73667262	2017-06-01	Point Pelee	beach	core	17.7	Qubit	very low	17.7	low	5	1.2	1	18.41680143	1.26521421
WE_2017-06-01_PP_cDNA_1b	CXR27	MST_seagull	31.944	1.574	1.251023231	17.82474111	2017-06-01	Point Pelee	beach	core	46.9	Qubit	very low	46.9	medium	5	1.2	1	4.277937867	0.63123447
WE_2017-07-26_PP_cDNA_2a	CXR27	FIB_Enterococcus_23S	29.479	0.315	2.671935191	469.8239929	2017-07-26	Point Pelee	beach	core	9.5	Qubit	very low	9.5	low	5	1.2	1	112.7577583	2.05214643
WE_2017-07-26_PP_cDNA_3a	CXR27	FIB_Enterococcus_23S	31.971	1.637	1.966066168	92.48390696	2017-07-26	Point Pelee	beach	core	8.3	Qubit	very low	8.3	low	5	1.2	1	22.19613767	1.34627741
WE_2017-07-26_PP_cDNA_2a	CXR27	MST_Bacteroides_16S	23.399	0.81	4.343674069	22063.48283	2017-07-26	Point Pelee	beach	core	9.5	Qubit	very low	9.5	low	5	1.2	1	5295.235879	3.72388531
WE_2017-07-26_PP_cDNA_3a	CXR27	MST_Bacteroides_16S	24.527	0.673	4.024975985	10591.95153	2017-07-26	Point Pelee	beach	core	8.3	Qubit	very low	8.3	low	5	1.2	1	2542.068367	3.40518723
WE_2017-07-26_PP_cDNA_2b	CXR27	MST_Bacteroides_16S	26.494	0.342	3.469232073	2945.99546	2017-07-26	Point Pelee	beach	core	6.2	Qubit	very low	6.2	low	5	1.2	1	707.0389104	2.84944332
WE_2017-07-26_PP_cDNA_1b	CXR27	MST_Bacteroides_16S	29.887	0.997	2.510595016	324.0373084	2017-07-26	Point Pelee	beach	core	0	Qubit	very low	1	low	5	1.2	1	77.76895402	1.89080626
WE_2017-07-26_PP_cDNA_3a	CXR27	MST_seagull	31.7	0.523	1.319897254	20.88801898	2017-07-26	Point Pelee	beach	core	8.3	Qubit	very low	8.3	low	5	1.2	1	5.013124556	0.7001085
WE_2017-07-26_PP_cDNA_2b	CXR27	MST_seagull	36.442	2.326	-0.018629859	0.958010218	2017-07-26	Point Pelee	beach	core	6.2	Qubit	very low	6.2	low	5	1.2	1	0.229922452	-0.63841862
WE_2017-06-01_SP_cDNA_2b	CXR27	FIB_Ecoli_23S	29.538	0.371	2.75647466	570.7877705	2017-06-01	Sandpoint	beach	core	80.8	Qubit	very low	80.8	medium	5	1.2	1	136.9890649	2.1366859
WE_2017-06-01_SP_cDNA_1a	CXR27	FIB_Ecoli_23S	32.223	0.406	2.907144452	101.6586766	2017-06-01	Sandpoint	beach	core	60.7	Qubit	very low	60.7	medium	5	1.2	1	24.39808239	1.38735569
WE_2017-06-01_SP_cDNA_1b	CXR27	FIB_Ecoli_23S	33.708	1.223	1.592710426	39.14807633	2017-06-01	Sandpoint	beach	core	41.4	Qubit	very low	41.4	medium	5	1.2	1	9.395538319	0.97292167
WE_2017-06-01_SP_cDNA_1b	CXR27	FIB_Enterococcus_23S	28.249	0.756	3.020337639	1047.942946	2017-06-01	Sandpoint	beach	core	41.4	Qubit	very low	41.4	medium	5	1.2	1	251.5063071	2.40054888
WE_2017-06-01_SP_cDNA_1a	CXR27	FIB_Enterococcus_23S	28.622	1.396	2.914683889	821.644379	2017-06-01	Sandpoint	beach	core	114	Qubit	low	54.72	medium	5	1.2	2.08333	410.8221895	2.61365389
WE_2017-06-01_SP_cDNA_2b	CXR27	FIB_Enterococcus_23S	29.398	0.821	2.694878767	495.3119059	2017-06-01	Sandpoint	beach	core	80.8	Qubit	very low	80.8	medium	5	1.2	1	118.8748574	2.07509001
WE_2017-06-01_SP_cDNA_2a	CXR27	FIB_Enterococcus_23S	30.759	0.317	2.309370043	203.8778491	2017-06-01	Sandpoint	beach	core	60.7	Qubit	very low	60.7	medium	5	1.2	1	48.93068377	1.68958129
WE_2017-06-01_SP_cDNA_2a	CXR27	MST_Bacteroides_16S	21.965	0.156	4.748827485	56082.51548	2017-06-01	Sandpoint	beach	core	60.7	Qubit	very low	60.7	medium	5	1.2	1	13459.80372	4.12903873
WE_2017-06-01_SP_cDNA_1a	CXR27	MST_Bacteroides_16S	22.587	1.059	4.573091484	37418.94032	2017-06-01	Sandpoint	beach	core	114	Qubit	low	54.72	medium	5	1.2	2.08333	18709.47016	4.27206149
WE_2017-06-01_SP_cDNA_2b	CXR27	MST_Bacteroides_16S	22.631	0.776	4.560659999	36363.02453	2017-06-01	Sandpoint	beach	core	80.8	Qubit	very low	80.8	medium	5	1.2	1	8727.125886	3.94087124
WE_2017-06-01_SP_cDNA_1b	CXR27	MST_Bacteroides_16S	23.127	1.008	4.420523253	26334.38937	2017-06-01	Sandpoint	beach	core	41.4	Qubit	very low	41.4	medium	5	1.2	1	6320.253448	3.80073449
WE_2017-06-01_SP_cDNA_2a	CXR27	MST_goose	26.863	0.032	2.748845266	506.8481163	2017-06-01	Sandpoint	beach	core	60.7	Qubit	very low	60.7	medium	5	1.2	1	134.6035479	2.12905651
WE_2017-06-01_SP_cDNA_2b	CXR27	MST_goose	27.177	0.509	2.658198614	455.1961858	2017-06-01	Sandpoint	beach	core	80.8	Qubit	very low	80.8	medium	5	1.2	1	109.2470846	2.03840986
WE_2017-06-01_SP_cDNA_1a	CXR27	MST_goose	29.114	0.498	2.099018476	125.6083399	2017-06-01	Sandpoint	beach	core	114	Qubit	low	54.72	medium	5	1.2	2.08333	62.80416994	1.79798848
WE_2017-06-01_SP_cDNA_1b	CXR27	MST_goose	32.439	0.105	1.139145497	13.77670936	2017-06-01	Sandpoint	beach	core	41.4	Qubit	very low	41.4	medium	5	1.2	1	3.306410247	0.51935674
WE_2017-06-01_SP_cDNA_1a	CXR27	MST_seagull	30.371	0.657	1.69503486	49.54899617	2017-06-01	Sandpoint	beach	core	114	Qubit	low	54.72	medium	5	1.2	2.08333	24.77449809	1.39400487
WE_2017-07-26_SP_cDNA_1a	CXR27	FIB_Ecoli_23S	28.51	0.157	3.043369056	1105.017245	2017-07-26	Sandpoint	beach	core	104	Qubit	low	49.92	medium	5	1.2	2.08333	552.5086223	2.74233906
WE_2017-07-26_SP_cDNA_1b	CXR27	FIB_Enterococcus_23S	28.105	0.721	3.061126218	1151.134892	2017-07-26	Sandpoint	beach	core	117	Qubit	low	56.16	medium	5	1.2	2.08333	575.567446	2.76009622
WE_2017-07-26_SP_cDNA_1a	CXR27	FIB_Enterococcus_23S	28.456	0.222	2.961704056	915.5963574	2017-07-26	Sandpoint	beach	core	104	Qubit	low	49.92	medium	5	1.2	2.08333	457.7981787	2.66067406
WE_2017-07-26_SP_cDNA_1b	CXR27	MST_Bacteroides_16S	21.802	0.574	4.794880488	62356.3216	2017-07-26	Sandpoint	beach	core	117	Qubit	low	56.16	medium	5	1.2	2.08333	31178.1608	4.49385049
WE_2017-07-26_SP_cDNA_1a	CXR27	MST_Bacteroides_16S	23.101	0.825	4.42786913	26783.6111	2017-07-26	Sandpoint	beach	core	104	Qubit	low	49.92	medium	5	1.2	2.08333	13391.80555	4.12683914
WE_2017-07-26_SP_cDNA_1b	CXR27	MST_goose	28.291	0.37	2.336605081	217.0726364	2017-07-26	Sandpoint	beach	core	117	Qubit	low	56.16	medium	5	1.2	2.08333	108.5363182	2.03557509
WE_2017-07-26_SP_cDNA_1a	CXR27	MST_goose	29.299	0.282	2.045612009	111.073897	2017-07-26	Sandpoint	beach	core	104	Qubit	low	49.92	medium	5	1.2	2.08333	55.5369485	1.74458201
WE_2017-07-26_SP_cDNA_1a	CXR27	MST_seagull	28.671	0.175	2.174894854	149.5873451	2017-07-26	Sandpoint	beach	core	104	Qubit	low	49.92	medium	5	1.2	2.08333	74.79367253	1.87386486
WE_2017-07-26_SP_cDNA_1b	CXR27	MST_seagull	28.775	0.169	2.145538713	139.8101538	2017-07-26	Sandpoint	beach	core	117	Qubit	low	56.16	medium	5	1.2	2.08333	69.90507689	1.84450872
WE_2017-06-01_BR_cDNA_4b	CXR28	FIB_Ecoli_23S	19.602	0.048	5.529415048	338388.0736	2017-06-01	Belle River	beach	core	90.1	Qubit	low	43.248	medium	5	1.2	2.08333	169194.0368	5.22838505
WE_2017-06-01_BR_cDNA_4a	CXR28	FIB_Ecoli_23S	20.892	0.667	5.169401652	147707.1954	2017-06-01	Belle River	beach	core	107	Qubit	low	51.36	medium	5	1.2	2.08333	73853.59772	4.86837166
WE_2017-06-01_BR_cDNA_4b	CXR28	FIB_Enterococcus_23S	19.499	0.02	5.498810333	315362.7057	2017-06-01	Belle River	beach	core	90.1	Qubit	low	43.248	medium	5	1.2	2.08333	157681.3529	5.19778034
WE_2017-06-01_BR_cDNA_4a	CXR28	FIB_Enterococcus_23S	19.987	0.349	5.36058237	229394.1669	2017-06-01	Belle River	beach	core	107	Qubit	low	51.36	medium	5	1.2	2.08333	114697.0834	5.05955238
WE_2017-06-01_BR_cDNA_4a	CXR28	MST_Bacteroides_16S	17.323	0.099	6.060349212	1149077.211	2017-06-01	Belle River	beach	core	107	Qubit	low	51.36	medium	5	1.2	2.08333	574538.6057	5.75931922
WE_2017-06-01_BR_cDNA_4b	CXR28	MST_Bacteroides_16S	17.81	0.015	5.922755269	837057.4561	2017-06-01	Belle River	beach	core	90.1	Qubit	low	43.248	medium	5	1.2	2.08333	418528.7281	5.62172527
WE_2017-06-01_BR_cDNA_4b	CXR28	MST_goose	24.327	0.327	3.480946882	3026.543234	2017-06-01	Belle River	beach	core	90.1	Qubit	low	43.248	medium	5	1.2	2.08333	1513.271617	3.17991689
WE_2017-06-01_BR_cDNA_4a	CXR28	MST_goose	25.028	0.615	3.278579677	1899.239249	2017-06-01	Belle River	beach	core	107	Qubit	low	51.36	medium	5	1.2	2.08333	949.6196245	2.97754968
WE_2017-06-01_BR_cDNA_4b	CXR28	MST_seagull	18.443	0.131	5.061958393	115334.2759	2017-06-01	Belle River	beach	core	90.1	Qubit	low	43.248	medium	5	1.2	2.08333	57667.13795	4.7609284
WE_2017-06-01_BR_cDNA_4a	CXR28	MST_seagull	18.573	0.195	5.025263217	105989.5913	2017-06-01	Belle River	beach	core	107	Qubit	low	51.36	medium	5	1.2	2.08333	52994.79563	4.72423322
WE_2017-07-13_BR_cDNA_1b	CXR28	FIB_Ecoli_23S	23.123	0.462	4.546773833	35218.74154	2017-07-13	Belle River	beach	core	127	Qubit	low	60.96	medium	5	1.2	2.08333	17609.37077	4.24574384
WE_2017-07-13_BR_cDNA_1a	CXR28	FIB_Ecoli_23S	24.232	0.001	4.237273945	17269.26863	2017-07-13	Belle River	beach	core	116	Qubit	low	55.68	medium	5	1.2	2.08333	8634.634313	3.93624395
WE_2017-07-13_BR_cDNA_2a	CXR28	FIB_Ecoli_23S	24.425	0.299	4.183411476	15254.97414	2017-07-13	Belle River	beach	core	183	Qubit	low	87.84	medium	5	1.2	2.08333	7627.48707	3.88238148
WE_2017-07-13_BR_cDNA_2b	CXR28	FIB_Ecoli_23S	27.168	0.69	3.417894619	2617.547789	2017-07-13	Belle River	beach	core	65.6	Qubit	very low	65.6	medium	5	1.2	1	628.2114693	2.79810586
WE_2017-07-13_BR_cDNA_4b	CXR28	FIB_Ecoli_23S	29.818	1.068	2.678332217	476.7955759	2017-07-13	Belle River	beach	core	89.2	Qubit	very low	89.2	medium	5	1.2	1	114.4309382	2.05854346
WE_2017-07-13_BR_cDNA_4a	CXR28	FIB_Ecoli_23S	29.96	1.812	2.638702835	435.2139781	2017-07-13	Belle River	beach	core	67.8	Qubit	very low	67.8	medium	5	1.2	1	104.4513547	2.01891408
WE_2017-07-13_BR_cDNA_4b	CXR28	FIB_Enterococcus_23S	23.53	0.241	4.35701337	22751.6747	2017-07-13	Belle River	beach	core	89.2									

WE_2017-07-13_BR_cDNA_1b	CKR28	FIB_Enterococcus_23S	24.076	0.393	4.202356673	15935.16899	2017-07-13	Belle River	beach	core	127	Qubit	low	60.96	medium	5	1.2	2.08333	7967.584495	3.90132668
WE_2017-07-13_BR_cDNA_4a	CKR28	FIB_Enterococcus_23S	24.475	0.579	4.089338319	12283.95788	2017-07-13	Belle River	beach	core	67.8	Qubit	very low	67.8	medium	5	1.2	1	2948.149891	3.46954956
WE_2017-07-13_BR_cDNA_2a	CKR28	FIB_Enterococcus_23S	24.602	0.122	4.053365058	11307.45994	2017-07-13	Belle River	beach	core	183	Qubit	low	87.84	medium	5	1.2	2.08333	5653.72997	3.75233506
WE_2017-07-13_BR_cDNA_1a	CKR28	FIB_Enterococcus_23S	24.643	1.273	4.041751643	11009.0956	2017-07-13	Belle River	beach	core	116	Qubit	low	55.68	medium	5	1.2	2.08333	5504.547798	3.74072165
WE_2017-07-13_BR_cDNA_2b	CKR28	FIB_Enterococcus_23S	25.383	0.553	3.832143666	6794.283532	2017-07-13	Belle River	beach	core	65.6	Qubit	very low	65.6	medium	5	1.2	1	1630.628048	3.21235491
WE_2017-07-13_BR_cDNA_2b	CKR28	MST_Bacteroides_16S	17.282	0.369	6.071933096	1180138.819	2017-07-13	Belle River	beach	core	65.6	Qubit	very low	65.6	medium	5	1.2	1	283233.3165	5.45214434
WE_2017-07-13_BR_cDNA_1a	CKR28	MST_Bacteroides_16S	19.345	0.669	5.489065943	308365.6138	2017-07-13	Belle River	beach	core	116	Qubit	low	55.68	medium	5	1.2	2.08333	154182.8069	5.18803595
WE_2017-07-13_BR_cDNA_4b	CKR28	MST_Bacteroides_16S	19.481	0.68	5.450641352	282254.81	2017-07-13	Belle River	beach	core	89.2	Qubit	very low	89.2	medium	5	1.2	1	67741.1544	4.83085259
WE_2017-07-13_BR_cDNA_4a	CKR28	MST_Bacteroides_16S	19.489	0.944	5.448381082	280789.641	2017-07-13	Belle River	beach	core	67.8	Qubit	very low	67.8	medium	5	1.2	1	67389.51383	4.82859232
WE_2017-07-13_BR_cDNA_2a	CKR28	MST_Bacteroides_16S	19.595	0.231	5.418432503	262079.1688	2017-07-13	Belle River	beach	core	183	Qubit	low	87.84	medium	5	1.2	2.08333	131039.5844	5.11740251
WE_2017-07-13_BR_cDNA_1b	CKR28	MST_Bacteroides_16S	20.19	0.369	5.250324914	177961.0313	2017-07-13	Belle River	beach	core	127	Qubit	low	60.96	medium	5	1.2	2.08333	88980.51564	4.94929492
WE_2017-07-13_BR_cDNA_4b	CKR28	MST_goose	24.99	0.409	3.289549654	1947.823735	2017-07-13	Belle River	beach	core	89.2	Qubit	very low	89.2	medium	5	1.2	1	467.4776964	2.6697609
WE_2017-07-13_BR_cDNA_1b	CKR28	MST_goose	25.73	0.156	3.075923788	1191.03298	2017-07-13	Belle River	beach	core	127	Qubit	low	60.96	medium	5	1.2	2.08333	595.5164902	2.77489379
WE_2017-07-13_BR_cDNA_2a	CKR28	MST_goose	25.764	0.089	3.066108545	1164.417021	2017-07-13	Belle River	beach	core	183	Qubit	low	87.84	medium	5	1.2	2.08333	582.2085103	2.76507855
WE_2017-07-13_BR_cDNA_1a	CKR28	MST_goose	25.938	0.88	3.015877598	1037.236039	2017-07-13	Belle River	beach	core	116	Qubit	low	55.68	medium	5	1.2	2.08333	518.6180197	2.7148476
WE_2017-07-13_BR_cDNA_2b	CKR28	MST_goose	26.035	0.665	2.987875289	972.4679313	2017-07-13	Belle River	beach	core	65.6	Qubit	very low	65.6	medium	5	1.2	1	233.3923035	2.36808653
WE_2017-07-13_BR_cDNA_4a	CKR28	MST_goose	26.464	0.42	2.864030023	731.1896294	2017-07-13	Belle River	beach	core	67.8	Qubit	very low	67.8	medium	5	1.2	1	175.4855111	2.24424127
WE_2017-07-13_BR_cDNA_4b	CKR28	MST_seagull	24.026	0.27	3.48604172	3062.257589	2017-07-13	Belle River	beach	core	89.2	Qubit	very low	89.2	medium	5	1.2	1	734.9418213	2.86625296
WE_2017-07-13_BR_cDNA_2a	CKR28	MST_seagull	24.076	0.138	3.47192819	2964.341202	2017-07-13	Belle River	beach	core	183	Qubit	low	87.84	medium	5	1.2	2.08333	1482.170601	3.1708982
WE_2017-07-13_BR_cDNA_1a	CKR28	MST_seagull	24.29	0.35	3.411522285	2579.421321	2017-07-13	Belle River	beach	core	116	Qubit	low	55.68	medium	5	1.2	2.08333	1289.71066	3.11049229
WE_2017-07-13_BR_cDNA_1b	CKR28	MST_seagull	24.64	0.116	3.312727581	2054.601405	2017-07-13	Belle River	beach	core	127	Qubit	low	60.96	medium	5	1.2	2.08333	1027.300702	3.01169759
WE_2017-07-13_BR_cDNA_2b	CKR28	MST_seagull	26.654	4.598	2.744234623	554.925425	2017-07-13	Belle River	beach	core	65.6	Qubit	very low	65.6	medium	5	1.2	1	133.182102	2.12444587
WE_2017-07-13_BR_cDNA_4a	CKR28	MST_seagull	28.003	0.484	2.363451605	230.9147126	2017-07-13	Belle River	beach	core	67.8	Qubit	very low	67.8	medium	5	1.2	1	55.41953103	1.74366285
WE_2017-07-13_HD_cDNA_4b	CKR28	FIB_Ecoli_23S	31.119	2.383	2.315248939	206.656438	2017-07-13	Holiday	beach	core	33.4	Qubit	very low	33.4	medium	5	1.2	1	49.59754512	1.69546018
WE_2017-07-13_HD_cDNA_4a	CKR28	FIB_Ecoli_23S	33.999	4.001	1.511498102	32.47118233	2017-07-13	Holiday	beach	core	17	Qubit	very low	17	low	5	1.2	1	7.793083758	0.89170934
WE_2017-07-13_HD_cDNA_4b	CKR28	FIB_Enterococcus_23S	25.966	0.264	3.667006571	4645.223041	2017-07-13	Holiday	beach	core	33.4	Qubit	very low	33.4	medium	5	1.2	1	1114.85353	3.04721781
WE_2017-07-13_HD_cDNA_4a	CKR28	FIB_Enterococcus_23S	27.672	0.937	3.18377521	1526.775596	2017-07-13	Holiday	beach	core	17	Qubit	very low	17	low	5	1.2	1	366.4261431	2.56398645
WE_2017-07-13_HD_cDNA_2a	CKR28	FIB_Enterococcus_23S	29.284	0.8	2.727169726	533.5433678	2017-07-13	Holiday	beach	core	11.6	Qubit	very low	11.6	low	5	1.2	1	128.0504083	2.10738097
WE_2017-07-13_HD_cDNA_4a	CKR28	MST_Bacteroides_16S	17.034	0.289	6.142001469	1386760.52	2017-07-13	Holiday	beach	core	17	Qubit	very low	17	low	5	1.2	1	332822.5248	5.52221271
WE_2017-07-13_HD_cDNA_4b	CKR28	MST_Bacteroides_16S	17.088	0.521	6.126744646	1338889.223	2017-07-13	Holiday	beach	core	33.4	Qubit	very low	33.4	medium	5	1.2	1	321333.4136	5.50695589
WE_2017-07-13_HD_cDNA_2b	CKR28	MST_Bacteroides_16S	18.695	0.263	5.672712889	470666.0676	2017-07-13	Holiday	beach	core	13.1	Qubit	very low	13.1	low	5	1.2	1	112959.8562	5.05292413
WE_2017-07-13_HD_cDNA_2a	CKR28	MST_Bacteroides_16S	19.277	0.64	5.508278239	322313.3093	2017-07-13	Holiday	beach	core	11.6	Qubit	very low	11.6	low	5	1.2	1	77355.19424	4.88848948
WE_2017-07-13_HD_cDNA_1a	CKR28	MST_Bacteroides_16S	22.646	0.212	4.556421992	36009.90639	2017-07-13	Holiday	beach	core	0	Qubit	very low	1	low	5	1.2	1	8642.377534	3.93663323
WE_2017-07-13_HD_cDNA_1b	CKR28	MST_Bacteroides_16S	27.163	0.284	3.280216986	1906.412978	2017-07-13	Holiday	beach	core	0	Qubit	very low	1	low	5	1.2	1	457.5391148	2.66042823
WE_2017-07-13_HD_cDNA_4b	CKR28	MST_goose	25.819	0.025	3.050230947	1122.615274	2017-07-13	Holiday	beach	core	33.4	Qubit	very low	33.4	medium	5	1.2	1	269.4276658	2.43044219
WE_2017-07-13_HD_cDNA_4a	CKR28	MST_goose	26.887	0.854	2.741916859	551.9717603	2017-07-13	Holiday	beach	core	17	Qubit	very low	17	low	5	1.2	1	132.4732225	2.1221281
WE_2017-07-13_HD_cDNA_2a	CKR28	MST_goose	28.36	0.309	2.316685912	207.3413454	2017-07-13	Holiday	beach	core	11.6	Qubit	very low	11.6	low	5	1.2	1	49.76192289	1.69689715
WE_2017-07-13_HD_cDNA_2b	CKR28	MST_goose	31.403	1.107	1.438221709	27.42974113	2017-07-13	Holiday	beach	core	13.1	Qubit	very low	13.1	low	5	1.2	1	6.583137872	0.81843295
WE_2017-07-13_HD_cDNA_4b	CKR28	MST_seagull	32.332	1.668	1.141502244	13.85167343	2017-07-13	Holiday	beach	core	33.4	Qubit	very low	33.4	medium	5	1.2	1	3.324401624	0.52171349
WE_2017-07-26_HD_cDNA_2b	CKR28	FIB_Ecoli_23S	27.174	0.573	3.416220138	2607.474911	2017-07-26	Holiday	beach	core	45.2	Qubit	very low	45.2	medium	5	1.2	1	625.7939787	2.79643138
WE_2017-07-26_HD_cDNA_2a	CKR28	FIB_Ecoli_23S	27.713	0.403	3.265795937	1844.148699	2017-07-26	Holiday	beach	core	64.2	Qubit	very low	64.2	medium	5	1.2	1	442.5956878	2.64600718
WE_2017-07-26_HD_cDNA_1a	CKR28	FIB_Ecoli_23S	28.709	0.366	2.987832105	972.3712405	2017-07-26	Holiday	beach	core	44.2	Qubit	very low	44.2	medium	5	1.2	1	233.3690977	2.36804335
WE_2017-07-26_HD_cDNA_3a	CKR28	FIB_Ecoli_23S	29.074	0.229	2.88596785	769.0735051	2017-07-26	Holiday	beach	core	58	Qubit	very low	58	medium	5	1.2	1	184.5776412	2.26617909
WE_2017-07-26_HD_cDNA_2a	CKR28	FIB_Enterococcus_23S	20.346	0.585	5.258894176	181507.3333	2017-07-26	Holiday	beach	core	64.2	Qubit	very low	64.2	medium	5	1.2	1	43561.76	4.63910542
WE_2017-07-26_HD_cDNA_3a	CKR28	FIB_Enterococcus_23S	23.686	0.63	4.312825742	20550.65849	2017-07-26	Holiday	beach	core	58	Qubit	very low	58	medium	5	1.2	1	4932.158037	3.69303698
WE_2017-07-26_HD_cDNA_2b	CKR28	FIB_Enterococcus_23S	25.983	0.295	3.662191253	4594.002774	2017-07-26	Holiday	beach	core	45.2	Qubit	very low	45.2	medium	5	1.2	1	1102.560666	3.0424025
WE_2017-07-26_HD_cDNA_1a	CKR28	FIB_Enterococcus_23S	27.288	0.657	3.292544754	1961.303278	2017-07-26	Holiday	beach	core	44.2	Qubit	very low	44.2	medium	5	1.2	1	470.7127867	2.672756
WE_2017-07-26_HD_cDNA_3a	CKR28	MST_Bacteroides_16S	14.723	0.769	6.794936995	6236443.541	2017-07-26	Holiday	beach	core	58	Qubit	very low	58	medium	5	1.2	1	1496746.45	6.17514824
WE_2017-07-26_HD_cDNA_2b	CKR28	MST_Bacteroides_16S	16.897	1.131	6.180708595	1516032.79	2017-07-26	Holiday	beach	core	45.2	Qubit	very low	45.2	medium	5	1.2	1	363847.8696	5.56091984
WE_2017-07-26_HD_cDNA_2a	CKR28	MST_Bacteroides_16S	17.396	0.007	6.039724247	1095782.214	2017-07-26	Holiday	beach	core	64.2	Qubit	very low	64.2	medium	5	1.2	1	262987.7314	5.41993549
WE_2017-07-26_HD_cDNA_1a	CKR28	MST_Bacteroides_16S	18.41	0.605	5.753235012	566545.7834	2017-07-26	Holiday	beach	core	44.2	Qubit	very low	44.2	medium	5	1.2	1	135970.988	5.13344625
WE_2017-07-26_HD_cDNA_1b	CKR28	MST_Bacteroides_16S	28.646	0.278	2.861219416	726.4728958	2017-07-26	Holiday	beach	core	0	Qubit	very low	1	low	5	1.2	1	174.353495	2.24143066
WE_2017-07-26_HD_cDNA_2b	CKR28	MST_dog	22.709	4.119	3.718954433	5235.455029	2017-07-26	Holiday	beach	core	45.2	Qubit	very low	45.2	medium	5	1.2	1	1256.509207	3.09916568
WE_2017-07-26_HD_cDNA_3a	CKR28	MST_goose	23.662	0.059	3.672921478	4708.921798	2017-07-26	Holiday	beach	core	58	Qubit	very low	58	medium	5	1.2	1	1130.141231	3.05313272
WE_2017-07-26_HD_cDNA_2b	CKR28	MST_goose	24.944	0.348	3.302829099	2008.302363	2017-07-26	Holiday	beach	core	45.2	Qubit	very low	45.2	medium	5	1.2	1	481.9925672	2.683

WE_2017-07-26_HD_cDNA_2a	CKR28	MST_goose	25.836	0.163	3.045323326	1110.000886	2017-07-26	Holiday	beach	core	64.2	Qubit	very low	64.2	medium	5	1.2	1	266.4002128	2.42553457
WE_2017-07-26_HD_cDNA_1a	CKR28	MST_goose	30.564	2.55	1.680427252	47.91011924	2017-07-26	Holiday	beach	core	44.2	Qubit	very low	44.2	medium	5	1.2	1	11.49842862	1.06063849
WE_2017-07-26_HD_cDNA_2b	CKR28	MST_seagull	29.318	0.228	1.992265786	98.23489516	2017-07-26	Holiday	beach	core	45.2	Qubit	very low	45.2	medium	5	1.2	1	23.57637484	1.37247703
WE_2017-07-26_HD_cDNA_2a	CKR28	MST_seagull	30.677	1.397	1.608660062	40.61253153	2017-07-26	Holiday	beach	core	64.2	Qubit	very low	64.2	medium	5	1.2	1	9.747007567	0.9888713
WE_2017-07-26_HD_cDNA_3a	CKR28	MST_seagull	31.718	0.103	1.314816383	20.6450711	2017-07-26	Holiday	beach	core	58	Qubit	very low	58	medium	5	1.2	1	4.954817065	0.69502763
WE_2017-07-26_HD_cDNA_1a	CKR28	MST_seagull	35.305	0.093	0.302311796	2.005911629	2017-07-26	Holiday	beach	core	44.2	Qubit	very low	44.2	medium	5	1.2	1	0.481418791	-0.31747696
WE_2017-06-01_KV_cDNA_2b	CKR28	FIB_Ecoli_23S	23.497	0.259	4.442397857	27694.77599	2017-06-01	Kingsville	beach	core	449	Qubit	medium	163.2727273	high	5	1.2	2.75	18278.55215	4.26194179
WE_2017-06-01_KV_cDNA_2a	CKR28	FIB_Ecoli_23S	25.208	0.212	3.964891717	9223.414301	2017-06-01	Kingsville	beach	core	510	Qubit	medium	185.4545455	high	5	1.2	2.75	6087.453439	3.78443565
WE_2017-06-01_KV_cDNA_2b	CKR28	FIB_Enterococcus_23S	20.125	0.065	5.321493315	209649.251	2017-06-01	Kingsville	beach	core	449	Qubit	medium	163.2727273	high	5	1.2	2.75	138368.5057	5.14103725
WE_2017-06-01_KV_cDNA_2a	CKR28	FIB_Enterococcus_23S	21.077	0.383	5.051835486	112677.0546	2017-06-01	Kingsville	beach	core	510	Qubit	medium	185.4545455	high	5	1.2	2.75	74366.85606	4.87137942
WE_2017-06-01_KV_cDNA_2b	CKR28	MST_Bacteroides_16S	16.738	0.213	6.225631463	1681246.77	2017-06-01	Kingsville	beach	core	449	Qubit	medium	163.2727273	high	5	1.2	2.75	1109622.868	6.0451754
WE_2017-06-01_KV_cDNA_2a	CKR28	MST_Bacteroides_16S	17.005	0.048	6.150194948	1413171.754	2017-06-01	Kingsville	beach	core	510	Qubit	medium	185.4545455	high	5	1.2	2.75	932693.3576	5.96973888
WE_2017-06-01_KV_cDNA_2b	CKR28	MST_dog	23.776	0.456	3.416782306	2610.852312	2017-06-01	Kingsville	beach	core	449	Qubit	medium	163.2727273	high	5	1.2	2.75	1723.162526	3.23632624
WE_2017-06-01_KV_cDNA_2a	CKR28	MST_dog	25.419	0.146	2.951488205	894.3102426	2017-06-01	Kingsville	beach	core	510	Qubit	medium	185.4545455	high	5	1.2	2.75	590.2447601	2.77103214
WE_2017-06-01_KV_cDNA_2a	CKR28	MST_goose	21.71	0.073	4.236431871	17235.81685	2017-06-01	Kingsville	beach	core	510	Qubit	medium	185.4545455	high	5	1.2	2.75	11375.63912	4.05597581
WE_2017-06-01_KV_cDNA_2b	CKR28	MST_goose	21.975	0.357	4.159930716	14452.09195	2017-06-01	Kingsville	beach	core	449	Qubit	medium	163.2727273	high	5	1.2	2.75	9538.380684	3.97947465
WE_2017-06-01_KV_cDNA_2a	CKR28	MST_seagull	28.196	0.229	2.308973382	203.691723	2017-06-01	Kingsville	beach	core	510	Qubit	medium	185.4545455	high	5	1.2	2.75	134.4365372	2.12851732
WE_2017-06-01_KV_cDNA_2b	CKR28	MST_seagull	28.365	0.652	2.261269653	182.5028509	2017-06-01	Kingsville	beach	core	449	Qubit	medium	163.2727273	high	5	1.2	2.75	120.4518816	2.08081359
WE_2017-07-13_KV_cDNA_2b	CKR28	FIB_Ecoli_23S	23.769	0.241	4.366488055	23253.4853	2017-07-13	Kingsville	beach	core	97.6	Qubit	low	46.848	medium	5	1.2	2.08333	11626.74265	4.06545806
WE_2017-07-13_KV_cDNA_1a	CKR28	FIB_Ecoli_23S	25.35	0.083	3.925262335	8419.035395	2017-07-13	Kingsville	beach	core	74.5	Qubit	very low	74.5	medium	5	1.2	1	2020.568495	3.30547358
WE_2017-07-13_KV_cDNA_4b	CKR28	FIB_Ecoli_23S	25.46	0.24	3.894563519	7844.468414	2017-07-13	Kingsville	beach	core	86.8	Qubit	very low	86.8	medium	5	1.2	1	1882.672419	3.27477476
WE_2017-07-13_KV_cDNA_1b	CKR28	FIB_Ecoli_23S	26.309	0.622	3.65762447	4545.948064	2017-07-13	Kingsville	beach	core	89.6	Qubit	very low	89.6	medium	5	1.2	1	1091.027535	3.03783571
WE_2017-07-13_KV_cDNA_4a	CKR28	FIB_Ecoli_23S	26.684	0.04	3.552969413	3572.476765	2017-07-13	Kingsville	beach	core	84.8	Qubit	very low	84.8	medium	5	1.2	1	857.3944235	2.93318066
WE_2017-07-13_KV_cDNA_2a	CKR28	FIB_Ecoli_23S	26.753	0.082	3.533712882	3417.534302	2017-07-13	Kingsville	beach	core	81.2	Qubit	very low	81.2	medium	5	1.2	1	820.2082326	2.91392412
WE_2017-07-13_KV_cDNA_1b	CKR28	FIB_Enterococcus_23S	21.389	0.364	4.963460231	91930.6289	2017-07-13	Kingsville	beach	core	89.6	Qubit	very low	89.6	medium	5	1.2	1	22063.35094	4.34367147
WE_2017-07-13_KV_cDNA_4b	CKR28	FIB_Enterococcus_23S	21.73	0.4	4.86687061	73598.77902	2017-07-13	Kingsville	beach	core	86.8	Qubit	very low	86.8	medium	5	1.2	1	17663.70696	4.24708185
WE_2017-07-13_KV_cDNA_1a	CKR28	FIB_Enterococcus_23S	21.8	0.181	4.847042828	70314.16569	2017-07-13	Kingsville	beach	core	74.5	Qubit	very low	74.5	medium	5	1.2	1	16875.39976	4.22725407
WE_2017-07-13_KV_cDNA_2b	CKR28	FIB_Enterococcus_23S	22.206	0.043	4.732041695	53956.24214	2017-07-13	Kingsville	beach	core	97.6	Qubit	low	46.848	medium	5	1.2	2.08333	26978.12107	4.4310117
WE_2017-07-13_KV_cDNA_4a	CKR28	FIB_Enterococcus_23S	22.368	0.51	4.686154543	48546.12205	2017-07-13	Kingsville	beach	core	84.8	Qubit	very low	84.8	medium	5	1.2	1	11651.06929	4.06636579
WE_2017-07-13_KV_cDNA_2a	CKR28	FIB_Enterococcus_23S	23.449	0.23	4.379956945	23985.95118	2017-07-13	Kingsville	beach	core	81.2	Qubit	very low	81.2	medium	5	1.2	1	5756.628283	3.76016819
WE_2017-07-13_KV_cDNA_2b	CKR28	MST_Bacteroides_16S	12.756	0.052	7.350680906	22422338.59	2017-07-13	Kingsville	beach	core	97.6	Qubit	low	46.848	medium	5	1.2	2.08333	11211169.29	7.04965091
WE_2017-07-13_KV_cDNA_2a	CKR28	MST_Bacteroides_16S	16.116	0.344	6.401367463	2519808.075	2017-07-13	Kingsville	beach	core	81.2	Qubit	very low	81.2	medium	5	1.2	1	604753.9381	5.78157871
WE_2017-07-13_KV_cDNA_4b	CKR28	MST_Bacteroides_16S	17.427	0.138	6.0309657	1073904.594	2017-07-13	Kingsville	beach	core	86.8	Qubit	very low	86.8	medium	5	1.2	1	257737.1027	5.41117694
WE_2017-07-13_KV_cDNA_4a	CKR28	MST_Bacteroides_16S	17.63	0.522	5.973611347	941407.0694	2017-07-13	Kingsville	beach	core	84.8	Qubit	very low	84.8	medium	5	1.2	1	225851.2967	5.35382259
WE_2017-07-13_KV_cDNA_1b	CKR28	MST_Bacteroides_16S	17.736	0.001	5.943662768	878340.2155	2017-07-13	Kingsville	beach	core	89.6	Qubit	very low	89.6	medium	5	1.2	1	210801.6517	5.32387401
WE_2017-07-13_KV_cDNA_1a	CKR28	MST_Bacteroides_16S	18.286	0.704	5.788269198	614142.5645	2017-07-13	Kingsville	beach	core	74.5	Qubit	very low	74.5	medium	5	1.2	1	147394.2155	5.16848044
WE_2017-07-13_KV_cDNA_2b	CKR28	MST_dog	25.531	0.328	2.919770043	831.3234731	2017-07-13	Kingsville	beach	core	97.6	Qubit	low	46.848	medium	5	1.2	2.08333	415.6617365	2.61874005
WE_2017-07-13_KV_cDNA_1a	CKR28	MST_dog	30.096	0.238	1.626971765	42.36154246	2017-07-13	Kingsville	beach	core	74.5	Qubit	very low	74.5	medium	5	1.2	1	10.16677019	1.00718301
WE_2017-07-13_KV_cDNA_4a	CKR28	MST_dog	32.715	0.334	0.885276543	7.678502725	2017-07-13	Kingsville	beach	core	84.8	Qubit	very low	84.8	medium	5	1.2	1	1.842840654	0.26548778
WE_2017-07-13_KV_cDNA_4b	CKR28	MST_dog	33.501	1.631	0.662683017	4.599207635	2017-07-13	Kingsville	beach	core	86.8	Qubit	very low	86.8	medium	5	1.2	1	1.103809832	0.04289426
WE_2017-07-13_KV_cDNA_1a	CKR28	MST_goose	20.369	0.407	4.623556582	42029.72825	2017-07-13	Kingsville	beach	core	74.5	Qubit	very low	74.5	medium	5	1.2	1	10087.13478	4.00376782
WE_2017-07-13_KV_cDNA_1b	CKR28	MST_goose	20.798	0.058	4.499711316	31601.76334	2017-07-13	Kingsville	beach	core	89.6	Qubit	very low	89.6	medium	5	1.2	1	7584.423202	3.87992256
WE_2017-07-13_KV_cDNA_4b	CKR28	MST_goose	20.851	0.065	4.484411085	30507.81369	2017-07-13	Kingsville	beach	core	86.8	Qubit	very low	86.8	medium	5	1.2	1	7321.875285	3.86462233
WE_2017-07-13_KV_cDNA_2b	CKR28	MST_goose	21.732	0.074	4.230080831	16985.59761	2017-07-13	Kingsville	beach	core	97.6	Qubit	low	46.848	medium	5	1.2	2.08333	8492.798805	3.92905084
WE_2017-07-13_KV_cDNA_2a	CKR28	MST_goose	21.987	0.348	4.156466513	14337.27161	2017-07-13	Kingsville	beach	core	81.2	Qubit	very low	81.2	medium	5	1.2	1	3440.945186	3.53667775
WE_2017-07-13_KV_cDNA_4a	CKR28	MST_goose	21.994	0.048	4.154445727	14270.71482	2017-07-13	Kingsville	beach	core	84.8	Qubit	very low	84.8	medium	5	1.2	1	3424.971557	3.53465697
WE_2017-07-13_KV_cDNA_2b	CKR28	MST_seagull	27.203	0.832	2.589268072	388.3900294	2017-07-13	Kingsville	beach	core	97.6	Qubit	low	46.848	medium	5	1.2	2.08333	194.1950147	2.28823808
WE_2017-07-13_KV_cDNA_4b	CKR28	MST_seagull	29.325	0.682	1.990289892	97.78897453	2017-07-13	Kingsville	beach	core	86.8	Qubit	very low	86.8	medium	5	1.2	1	23.46935389	1.37050113
WE_2017-07-13_KV_cDNA_1b	CKR28	MST_seagull	30.732	0.303	1.593135179	39.18638305	2017-07-13	Kingsville	beach	core	89.6	Qubit	very low	89.6	medium	5	1.2	1	9.404731931	0.97334642
WE_2017-07-13_KV_cDNA_4a	CKR28	MST_seagull	31.156	0.243	1.473452452	29.74763551	2017-07-13	Kingsville	beach	core	84.8	Qubit	very low	84.8	medium	5	1.2	1	7.139432522	0.85366369
WE_2017-07-13_KV_cDNA_2a	CKR28	MST_seagull	32.119	0.311	1.201625879	15.90837715	2017-07-13	Kingsville	beach	core	81.2	Qubit	very low	81.2	medium	5	1.2	1	3.818010516	0.58183712
WE_2017-07-13_KV_cDNA_1a	CKR28	MST_seagull	33.229	2.365	0.88830553	7.732243634	2017-07-13	Kingsville	beach	core	74.5	Qubit	very low	74.5	medium	5	1.2	1	1.855738472	0.26851677
WE_2017-06-01_LE_cDNA_2a	CKR28	FIB_Ecoli_23S	30.744	1.695	2.419903996	262.9686619	2017-06-01	Leamington	beach	core	37.8	Qubit	very low	37.8	medium	5	1.2	1	63.11247885	1.80011524
WE_2017-06-01_LE_cDNA_2a	CKR28	FIB_Enterococcus_23S	25.495	0.458	3.800419216	6315.666893	2017-06-01	Leamington	beach	core	37.8	Qubit	very low	37.8	medium	5	1.2	1	1515.760054	3.18063046
WE_2017-06-01_LE_cDNA_2a	CKR28	MST_Bacteroides_16S	20.5	0.428	5.1															

WE_2017-06-01_LE_cDNA_2b	CXR28	MST_Bacteroides_16S	23.263	0.139	4.382098661	24104.52961	2017-06-01	Leamington	beach	core	0	Qubit	very low	1	low	5	1.2	1	5785.087106	3.7623099
WE_2017-06-01_LE_cDNA_2a	CXR28	MST_goose	26.964	0.438	2.719688222	524.4308383	2017-06-01	Leamington	beach	core	37.8	Qubit	very low	37.8	medium	5	1.2	1	125.8634012	2.09898946
WE_2017-06-01_LE_cDNA_2b	CXR28	MST_goose	29.761	1.005	1.912240185	81.70341037	2017-06-01	Leamington	beach	core	0	Qubit	very low	1	low	5	1.2	1	19.60881849	1.29245143
WE_2017-06-01_LE_cDNA_2a	CXR28	MST_seagull	28.22	3.63	2.302198888	200.5390198	2017-06-01	Leamington	beach	core	37.8	Qubit	very low	37.8	medium	5	1.2	1	48.12936475	1.68241013
WE_2017-06-01_LE_cDNA_2b	CXR28	MST_seagull	31.638	4.586	1.33739803	21.74693367	2017-06-01	Leamington	beach	core	0	Qubit	very low	1	low	5	1.2	1	5.21926408	0.71760927
WE_2017-07-13_LE_cDNA_4b	CXR28	FIB_Ecoli_23S	27.426	0.241	3.34589194	2217.644564	2017-07-13	Leamington	beach	core	14.6	Qubit	very low	14.6	low	5	1.2	1	532.2346953	2.72610318
WE_2017-07-13_LE_cDNA_4a	CXR28	FIB_Ecoli_23S	27.667	0.994	3.278633624	1899.475182	2017-07-13	Leamington	beach	core	12.3	Qubit	very low	12.3	low	5	1.2	1	455.8740437	2.65884487
WE_2017-07-13_LE_cDNA_2a	CXR28	FIB_Ecoli_23S	28.339	0.229	3.091091762	1233.365402	2017-07-13	Leamington	beach	core	10.7	Qubit	very low	10.7	low	5	1.2	1	296.0076965	2.471303
WE_2017-07-13_LE_cDNA_2b	CXR28	FIB_Ecoli_23S	29.632	0.624	2.730241125	537.3300453	2017-07-13	Leamington	beach	core	0	Qubit	very low	1	low	5	1.2	1	128.9592109	2.11045237
WE_2017-07-13_LE_cDNA_1a	CXR28	FIB_Ecoli_23S	30.462	2.199	2.498604599	315.2133476	2017-07-13	Leamington	beach	core	0	Qubit	very low	1	low	5	1.2	1	75.65120342	1.87881584
WE_2017-07-13_LE_cDNA_1b	CXR28	FIB_Ecoli_23S	31.769	2.067	2.133846841	136.0964637	2017-07-13	Leamington	beach	core	0	Qubit	very low	1	low	5	1.2	1	32.66315129	1.51405808
WE_2017-07-13_LE_cDNA_4b	CXR28	FIB_Enterococcus_23S	26.256	0.326	3.584862905	3844.70396	2017-07-13	Leamington	beach	core	14.6	Qubit	very low	14.6	low	5	1.2	1	922.7289505	2.96507415
WE_2017-07-13_LE_cDNA_4a	CXR28	FIB_Enterococcus_23S	26.793	0.023	3.432755495	2708.666242	2017-07-13	Leamington	beach	core	12.3	Qubit	very low	12.3	low	5	1.2	1	650.079898	2.81296674
WE_2017-07-13_LE_cDNA_2a	CXR28	FIB_Enterococcus_23S	29.361	1.695	2.705359166	507.4101683	2017-07-13	Leamington	beach	core	10.7	Qubit	very low	10.7	low	5	1.2	1	121.7784404	2.08557041
WE_2017-07-13_LE_cDNA_2b	CXR28	FIB_Enterococcus_23S	32.609	2.52	1.785350102	61.00284672	2017-07-13	Leamington	beach	core	0	Qubit	very low	1	low	5	1.2	1	16.10468321	1.16556134
WE_2017-07-13_LE_cDNA_1a	CXR28	FIB_Enterococcus_23S	33.951	2.008	1.405223204	25.42278965	2017-07-13	Leamington	beach	core	0	Qubit	very low	1	low	5	1.2	1	6.101469517	0.78543445
WE_2017-07-13_LE_cDNA_4a	CXR28	MST_Bacteroides_16S	21.188	0.458	4.968356219	92972.86595	2017-07-13	Leamington	beach	core	12.3	Qubit	very low	12.3	low	5	1.2	1	22313.48783	4.34856746
WE_2017-07-13_LE_cDNA_2a	CXR28	MST_Bacteroides_16S	21.334	0.347	4.927106289	84548.5744	2017-07-13	Leamington	beach	core	10.7	Qubit	very low	10.7	low	5	1.2	1	20291.65786	4.30731753
WE_2017-07-13_LE_cDNA_4b	CXR28	MST_Bacteroides_16S	21.845	0.045	4.782731536	60636.13852	2017-07-13	Leamington	beach	core	14.6	Qubit	very low	14.6	low	5	1.2	1	14552.67325	4.16294278
WE_2017-07-13_LE_cDNA_2b	CXR28	MST_Bacteroides_16S	24.518	0.049	4.027518788	10654.14955	2017-07-13	Leamington	beach	core	0	Qubit	very low	1	low	5	1.2	1	2556.995891	3.40773003
WE_2017-07-13_LE_cDNA_1a	CXR28	MST_Bacteroides_16S	25.319	0.267	3.801209245	6327.166229	2017-07-13	Leamington	beach	core	0	Qubit	very low	1	low	5	1.2	1	1518.519895	3.18142049
WE_2017-07-13_LE_cDNA_1b	CXR28	MST_Bacteroides_16S	27.265	0.362	3.251398542	1784.015166	2017-07-13	Leamington	beach	core	0	Qubit	very low	1	low	5	1.2	1	428.1636399	2.63160978
WE_2017-07-13_LE_cDNA_2a	CXR28	MST_goose	25.547	0.277	3.128752887	1345.094779	2017-07-13	Leamington	beach	core	10.7	Qubit	very low	10.7	low	5	1.2	1	322.8227469	2.50896413
WE_2017-07-13_LE_cDNA_4a	CXR28	MST_goose	26.928	0.619	2.730080831	537.1317587	2017-07-13	Leamington	beach	core	12.3	Qubit	very low	12.3	low	5	1.2	1	128.9116221	2.11029207
WE_2017-07-13_LE_cDNA_4b	CXR28	MST_goose	27.158	0.063	2.663683603	460.9816126	2017-07-13	Leamington	beach	core	14.6	Qubit	very low	14.6	low	5	1.2	1	110.635587	2.04389484
WE_2017-07-13_LE_cDNA_2b	CXR28	MST_goose	30.581	0.981	1.67551963	47.37177201	2017-07-13	Leamington	beach	core	0	Qubit	very low	1	low	5	1.2	1	11.36922528	1.05573087
WE_2017-07-13_LE_cDNA_4a	CXR28	MST_seagull	25.841	0.167	2.973720609	941.2838526	2017-07-13	Leamington	beach	core	12.3	Qubit	very low	12.3	low	5	1.2	1	225.9081246	2.35393185
WE_2017-07-13_LE_cDNA_2a	CXR28	MST_seagull	26.62	0.101	2.753831823	567.3248712	2017-07-13	Leamington	beach	core	10.7	Qubit	very low	10.7	low	5	1.2	1	136.1579691	2.13404307
WE_2017-07-13_LE_cDNA_4b	CXR28	MST_seagull	28.319	1.796	2.2742541	188.0416702	2017-07-13	Leamington	beach	core	14.6	Qubit	very low	14.6	low	5	1.2	1	45.13000851	1.65446534
WE_2017-07-13_LE_cDNA_1a	CXR28	MST_seagull	28.862	0.51	2.120981173	132.1238355	2017-07-13	Leamington	beach	core	0	Qubit	very low	1	low	5	1.2	1	31.70972052	1.50119241
WE_2017-07-13_LE_cDNA_2b	CXR28	MST_seagull	31.72	5.241	1.314251842	20.61825193	2017-07-13	Leamington	beach	core	0	Qubit	very low	1	low	5	1.2	1	4.948380463	0.69446308
WE_2017-07-13_LE_cDNA_1b	CXR28	MST_seagull	31.982	0.316	1.240296949	17.38989456	2017-07-13	Leamington	beach	core	0	Qubit	very low	1	low	5	1.2	1	4.173574693	0.62050819
WE_2017-07-13_PP_cDNA_1a	CXR28	FIB_Ecoli_23S	31.909	1.417	2.09477562	124.3871793	2017-07-13	Point Pelee	beach	core	0	Qubit	very low	1	low	5	1.2	1	29.85292303	1.47498686
WE_2017-07-13_PP_cDNA_4a	CXR28	FIB_Ecoli_23S	32.499	2.21	1.93011833	85.1369975	2017-07-13	Point Pelee	beach	core	12	Qubit	very low	12	low	5	1.2	1	20.4328794	1.31032957
WE_2017-07-13_PP_cDNA_2a	CXR28	FIB_Ecoli_23S	32.991	1.265	1.792810895	62.05987483	2017-07-13	Point Pelee	beach	core	0	Qubit	very low	1	low	5	1.2	1	14.89436996	1.17302214
WE_2017-07-13_PP_cDNA_2b	CXR28	FIB_Ecoli_23S	33.259	1.672	1.718017415	52.24171368	2017-07-13	Point Pelee	beach	core	5.8	Qubit	very low	5.8	low	5	1.2	1	12.53801128	1.09822866
WE_2017-07-13_PP_cDNA_4a	CXR28	FIB_Enterococcus_23S	26.789	0.045	3.433888511	2715.742015	2017-07-13	Point Pelee	beach	core	12	Qubit	very low	12	low	5	1.2	1	651.7780835	2.81409975
WE_2017-07-13_PP_cDNA_4b	CXR28	FIB_Enterococcus_23S	27.851	0.992	3.13307274	1358.540968	2017-07-13	Point Pelee	beach	core	6.5	Qubit	very low	6.5	low	5	1.2	1	326.0498324	2.51328398
WE_2017-07-13_PP_cDNA_1a	CXR28	FIB_Enterococcus_23S	29.605	1.674	2.636245185	432.7580794	2017-07-13	Point Pelee	beach	core	0	Qubit	very low	1	low	5	1.2	1	103.861939	2.01645643
WE_2017-07-13_PP_cDNA_2b	CXR28	FIB_Enterococcus_23S	33.205	0.094	1.616530705	41.35525516	2017-07-13	Point Pelee	beach	core	5.8	Qubit	very low	5.8	low	5	1.2	1	9.925261238	0.99674195
WE_2017-07-13_PP_cDNA_4a	CXR28	MST_Bacteroides_16S	23.637	0.204	4.276431034	18898.66094	2017-07-13	Point Pelee	beach	core	12	Qubit	very low	12	low	5	1.2	1	4535.678626	3.65664228
WE_2017-07-13_PP_cDNA_2b	CXR28	MST_Bacteroides_16S	24.429	0.492	4.052664293	11289.22928	2017-07-13	Point Pelee	beach	core	5.8	Qubit	very low	5.8	low	5	1.2	1	2709.415027	3.43287554
WE_2017-07-13_PP_cDNA_1a	CXR28	MST_Bacteroides_16S	24.85	0.803	3.933717579	8584.550885	2017-07-13	Point Pelee	beach	core	0	Qubit	very low	1	low	5	1.2	1	2060.292212	3.31392882
WE_2017-07-13_PP_cDNA_2a	CXR28	MST_Bacteroides_16S	25.169	0.244	3.843589309	6975.724319	2017-07-13	Point Pelee	beach	core	0	Qubit	very low	1	low	5	1.2	1	1674.173837	3.22380055
WE_2017-07-13_PP_cDNA_4b	CXR28	MST_Bacteroides_16S	25.21	0.526	3.832005425	6792.121164	2017-07-13	Point Pelee	beach	core	6.5	Qubit	very low	6.5	low	5	1.2	1	1630.109079	3.21221667
WE_2017-07-13_PP_cDNA_1b	CXR28	MST_Bacteroides_16S	29.619	0.389	2.586314065	385.7572211	2017-07-13	Point Pelee	beach	core	0	Qubit	very low	1	low	5	1.2	1	92.58173307	1.96652531
WE_2017-07-13_PP_cDNA_4a	CXR28	MST_goose	30.344	0.906	1.743937644	55.4546086	2017-07-13	Point Pelee	beach	core	12	Qubit	very low	12	low	5	1.2	1	13.30910606	1.12414889
WE_2017-07-13_PP_cDNA_4b	CXR28	MST_goose	30.861	0.73	1.594688222	39.32676488	2017-07-13	Point Pelee	beach	core	6.5	Qubit	very low	6.5	low	5	1.2	1	9.438423571	0.97489946
WE_2017-07-13_PP_cDNA_4a	CXR28	MST_seagull	27.264	0.8	2.572049567	373.2927599	2017-07-13	Point Pelee	beach	core	12	Qubit	very low	12	low	5	1.2	1	89.59026237	1.95226081
WE_2017-07-13_PP_cDNA_4b	CXR28	MST_seagull	28.618	0.332	2.189855195	154.830029	2017-07-13	Point Pelee	beach	core	6.5	Qubit	very low	6.5	low	5	1.2	1	37.15920696	1.57006644
WE_2017-07-13_PP_cDNA_1a	CXR28	MST_seagull	30.531	0.234	1.649871567	44.65515148	2017-07-13	Point Pelee	beach	core	0	Qubit	very low	1	low	5	1.2	1	10.71723635	1.03008281
WE_2017-07-13_PP_cDNA_2b	CXR28	MST_seagull	31.037	2.079	1.507042651	32.13976161	2017-07-13	Point Pelee	beach	core	5.8	Qubit	very low	5.8	low	5	1.2	1	7.713542785	0.88725389
WE_2017-07-13_PP_cDNA_2a	CXR28	MST_seagull	31.803	0.46	1.290823383	19.53544836	2017-07-13	Point Pelee	beach	core	0	Qubit	very low	1	low	5	1.2	1	4.688507607	0.67103463
WE_2017-06-01_PP_cDNA_4a	CXR28	FIB_Ecoli_23S	28.185	1.314	3.134070105	1361.664468	2017-06-01	Sandpoint	beach	core	101	Qubit	low	48.48	medium	5	1.2	2.08333	680.8322341	2.83304011
WE_2017-06-01_SP_cDNA_4b	CXR28	FIB_Ecoli_23S	35.747	1.656	1.023665997	10.56005054	2017-06-01	Sandpoint	beach	core	37.1	Qubit	very low	37.1	medium	5	1.2	1	2.534412131	0.40387724

WE_2017-06-01_SP_cDNA_4b	CXR28	FIB_Enterococcus_23S	23.66	0.021	4.320190347	20902.12048	2017-06-01	Sandpoint	beach	core	37.1	Qubit	very low	37.1	medium	5	1.2	1	5016.508915	3.70040159
WE_2017-06-01_SP_cDNA_4a	CXR28	FIB_Enterococcus_23S	24.823	0.005	3.990765919	9789.621907	2017-06-01	Sandpoint	beach	core	101	Qubit	low	48.48	medium	5	1.2	2.08333	4894.810953	3.68973592
WE_2017-06-01_SP_cDNA_4b	CXR28	MST_Bacteroides_16S	19.817	0.21	5.355710007	226834.9695	2017-06-01	Sandpoint	beach	core	37.1	Qubit	very low	37.1	medium	5	1.2	1	54440.39267	4.73592125
WE_2017-06-01_SP_cDNA_4a	CXR28	MST_Bacteroides_16S	20.67	0.223	5.114708708	130229.3005	2017-06-01	Sandpoint	beach	core	101	Qubit	low	48.48	medium	5	1.2	2.08333	65114.65023	4.81367871
WE_2017-06-01_SP_cDNA_4a	CXR28	MST_goose	25.103	0.48	3.256928406	1806.876238	2017-06-01	Sandpoint	beach	core	101	Qubit	low	48.48	medium	5	1.2	2.08333	903.4381188	2.95589841
WE_2017-06-01_SP_cDNA_4b	CXR28	MST_goose	26.714	0.018	2.791859122	619.2401717	2017-06-01	Sandpoint	beach	core	101	Qubit	very low	37.1	medium	5	1.2	1	148.6176412	2.17207036
WE_2017-06-01_SP_cDNA_4a	CXR28	MST_seagull	28.942	0.631	2.098399526	125.4294523	2017-06-01	Sandpoint	beach	core	101	Qubit	low	48.48	medium	5	1.2	2.08333	62.71472614	1.79736953
WE_2017-07-13_SP_cDNA_2b	CXR28	FIB_Ecoli_23S	26.529	0.975	3.596226836	3946.633849	2017-07-13	Sandpoint	beach	core	94.7	Qubit	low	45.456	medium	5	1.2	2.08333	1973.316924	3.29519684
WE_2017-07-13_SP_cDNA_4a	CXR28	FIB_Ecoli_23S	26.771	1.328	3.52868944	3378.231753	2017-07-13	Sandpoint	beach	core	145	Qubit	low	69.6	medium	5	1.2	2.08333	1689.115876	3.22765944
WE_2017-07-13_SP_cDNA_2a	CXR28	FIB_Ecoli_23S	27.565	0.164	3.307099799	2028.148726	2017-07-13	Sandpoint	beach	core	110	Qubit	low	52.8	medium	5	1.2	2.08333	1014.074363	3.0060698
WE_2017-07-13_SP_cDNA_1a	CXR28	FIB_Ecoli_23S	30.249	0.064	2.558048672	361.4503683	2017-07-13	Sandpoint	beach	core	164	Qubit	low	78.72	medium	5	1.2	2.08333	180.7251841	2.25701868
WE_2017-07-13_SP_cDNA_1b	CXR28	FIB_Ecoli_23S	33.22	5.539	1.728901541	53.56752001	2017-07-13	Sandpoint	beach	core	183	Qubit	low	87.84	medium	5	1.2	2.08333	26.78376001	1.42787155
WE_2017-07-13_SP_cDNA_4a	CXR28	FIB_Enterococcus_23S	27.974	0.76	3.098232495	1253.81221	2017-07-13	Sandpoint	beach	core	145	Qubit	low	69.6	medium	5	1.2	2.08333	626.9061051	2.7972025
WE_2017-07-13_SP_cDNA_2a	CXR28	FIB_Enterococcus_23S	28.997	0.461	2.80846363	643.3741836	2017-07-13	Sandpoint	beach	core	110	Qubit	low	52.8	medium	5	1.2	2.08333	321.6870918	2.50743364
WE_2017-07-13_SP_cDNA_2b	CXR28	FIB_Enterococcus_23S	29.124	0.267	2.772490369	592.2299538	2017-07-13	Sandpoint	beach	core	94.7	Qubit	low	45.456	medium	5	1.2	2.08333	296.1149769	2.47146037
WE_2017-07-13_SP_cDNA_1b	CXR28	FIB_Enterococcus_23S	31.993	0.319	1.95983458	91.16635257	2017-07-13	Sandpoint	beach	core	183	Qubit	low	87.84	medium	5	1.2	2.08333	45.98317628	1.65880458
WE_2017-07-13_SP_cDNA_1a	CXR28	FIB_Enterococcus_23S	32.476	0.135	1.823022887	66.53082164	2017-07-13	Sandpoint	beach	core	164	Qubit	low	78.72	medium	5	1.2	2.08333	33.26541082	1.52199289
WE_2017-07-13_SP_cDNA_1a	CXR28	MST_Bacteroides_16S	21.22	0.004	4.959315138	91057.37748	2017-07-13	Sandpoint	beach	core	164	Qubit	low	78.72	medium	5	1.2	2.08333	45528.68874	4.65828514
WE_2017-07-13_SP_cDNA_1b	CXR28	MST_Bacteroides_16S	21.807	0.288	4.793467819	62153.8191	2017-07-13	Sandpoint	beach	core	183	Qubit	low	87.84	medium	5	1.2	2.08333	31076.90955	4.49243782
WE_2017-07-13_SP_cDNA_2a	CXR28	MST_Bacteroides_16S	22.26	0.991	4.665480025	46289.23728	2017-07-13	Sandpoint	beach	core	110	Qubit	low	52.8	medium	5	1.2	2.08333	23144.61864	4.36445003
WE_2017-07-13_SP_cDNA_2b	CXR28	MST_Bacteroides_16S	22.285	0.562	4.658416681	45542.48047	2017-07-13	Sandpoint	beach	core	94.7	Qubit	low	45.456	medium	5	1.2	2.08333	22771.24024	4.35738669
WE_2017-07-13_SP_cDNA_4a	CXR28	MST_Bacteroides_16S	24.315	0.29	4.084873142	12158.30804	2017-07-13	Sandpoint	beach	core	145	Qubit	low	69.6	medium	5	1.2	2.08333	6079.15402	3.78384313
WE_2017-07-13_SP_cDNA_1b	CXR28	MST_goose	28.446	0.338	2.291859122	195.8209361	2017-07-13	Sandpoint	beach	core	145	Qubit	low	69.6	medium	5	1.2	2.08333	97.91046807	1.99082913
WE_2017-07-13_SP_cDNA_2b	CXR28	MST_goose	28.997	1.556	2.132794457	135.7670737	2017-07-13	Sandpoint	beach	core	94.7	Qubit	low	45.456	medium	5	1.2	2.08333	67.88353683	1.83176446
WE_2017-07-13_SP_cDNA_2a	CXR28	MST_goose	29.602	1	1.958140878	90.81150592	2017-07-13	Sandpoint	beach	core	110	Qubit	low	52.8	medium	5	1.2	2.08333	45.40575296	1.65711088
WE_2017-07-13_SP_cDNA_1a	CXR28	MST_goose	30.211	0.629	1.782332564	60.58045956	2017-07-13	Sandpoint	beach	core	164	Qubit	low	78.72	medium	5	1.2	2.08333	30.29022978	1.48130257
WE_2017-07-13_SP_cDNA_1b	CXR28	MST_goose	32.027	2.155	1.258083141	18.11686887	2017-07-13	Sandpoint	beach	core	183	Qubit	low	87.84	medium	5	1.2	2.08333	9.058434434	0.95705315
WE_2017-07-13_SP_cDNA_4a	CXR28	MST_seagull	29.601	2.459	1.912383211	81.73032211	2017-07-13	Sandpoint	beach	core	145	Qubit	low	69.6	medium	5	1.2	2.08333	40.86516106	1.61135322
WE_2017-08-31_BR_cDNA_3b	CXR30	FIB_Ecoli_23S	21.005	0.541	5.137865595	137361.6804	2017-08-31	Belle River	beach	core	126	Qubit	low	60.48	medium	5	1.2	2.08333	68680.84019	4.8368356
WE_2017-08-31_BR_cDNA_1b	CXR30	FIB_Ecoli_23S	22.029	0.521	4.85208752	71135.68527	2017-08-31	Belle River	beach	core	113	Qubit	low	54.24	medium	5	1.2	2.08333	35567.84263	4.55105752
WE_2017-08-31_BR_cDNA_1a	CXR30	FIB_Ecoli_23S	22.375	0.607	4.755525787	56954.20407	2017-08-31	Belle River	beach	core	122	Qubit	low	58.56	medium	5	1.2	2.08333	28477.10203	4.45449579
WE_2017-08-31_BR_cDNA_2b	CXR30	FIB_Ecoli_23S	23.023	0.545	4.574681849	37556.21777	2017-08-31	Belle River	beach	core	142	Qubit	low	68.16	medium	5	1.2	2.08333	18778.10888	4.27365185
WE_2017-08-31_BR_cDNA_3a	CXR30	FIB_Ecoli_23S	24.996	2.442	4.024056709	10569.55515	2017-08-31	Belle River	beach	core	36.4	Qubit	very low	36.4	medium	5	1.2	1	2536.693236	3.40426795
WE_2017-08-31_BR_cDNA_2a	CXR30	FIB_Ecoli_23S	25.723	1.528	3.821165439	6624.688143	2017-08-31	Belle River	beach	core	128	Qubit	low	61.44	medium	5	1.2	2.08333	3312.344072	3.52013544
WE_2017-08-31_BR_cDNA_3b	CXR30	FIB_Enterococcus_23S	20.719	0.706	5.153240426	142311.6408	2017-08-31	Belle River	beach	core	126	Qubit	low	60.48	medium	5	1.2	2.08333	71155.82041	4.85221043
WE_2017-08-31_BR_cDNA_3a	CXR30	FIB_Enterococcus_23S	22.6	0.934	4.62043961	41729.1569	2017-08-31	Belle River	beach	core	36.4	Qubit	very low	36.4	medium	5	1.2	1	10014.99766	4.00065085
WE_2017-08-31_BR_cDNA_1b	CXR30	FIB_Enterococcus_23S	22.718	0.152	4.587015636	38638.08874	2017-08-31	Belle River	beach	core	113	Qubit	low	54.24	medium	5	1.2	2.08333	19319.04437	4.28598564
WE_2017-08-31_BR_cDNA_1a	CXR30	FIB_Enterococcus_23S	23.356	0.277	4.406299569	25485.87622	2017-08-31	Belle River	beach	core	122	Qubit	low	58.56	medium	5	1.2	2.08333	12742.93811	4.10526957
WE_2017-08-31_BR_cDNA_2b	CXR30	FIB_Enterococcus_23S	23.649	0.256	4.323306141	21052.61949	2017-08-31	Belle River	beach	core	142	Qubit	low	68.16	medium	5	1.2	2.08333	10526.30974	4.02227615
WE_2017-08-31_BR_cDNA_2a	CXR30	FIB_Enterococcus_23S	23.864	0.035	4.262406526	18298.12231	2017-08-31	Belle River	beach	core	128	Qubit	low	61.44	medium	5	1.2	2.08333	9149.061154	3.96137653
WE_2017-08-31_BR_cDNA_3a	CXR30	MST_Bacteroides_16S	16.53	0.388	6.284398486	1924857.066	2017-08-31	Belle River	beach	core	36.4	Qubit	very low	36.4	medium	5	1.2	1	461965.6958	5.66460973
WE_2017-08-31_BR_cDNA_1b	CXR30	MST_Bacteroides_16S	18.823	0.703	5.636548568	433060.4946	2017-08-31	Belle River	beach	core	126	Qubit	low	60.48	medium	5	1.2	2.08333	216530.2473	5.33551857
WE_2017-08-31_BR_cDNA_2a	CXR30	MST_Bacteroides_16S	18.875	0.13	5.621856812	418655.5105	2017-08-31	Belle River	beach	core	128	Qubit	low	61.44	medium	5	1.2	2.08333	209327.7552	5.32082682
WE_2017-08-31_BR_cDNA_2b	CXR30	MST_Bacteroides_16S	19.526	0.423	5.437927332	274111.548	2017-08-31	Belle River	beach	core	142	Qubit	low	68.16	medium	5	1.2	2.08333	137055.774	5.13689734
WE_2017-08-31_BR_cDNA_1b	CXR30	MST_Bacteroides_16S	19.597	0.779	5.417867435	261738.3951	2017-08-31	Belle River	beach	core	113	Qubit	low	54.24	medium	5	1.2	2.08333	130869.1976	5.11683744
WE_2017-08-31_BR_cDNA_1a	CXR30	MST_Bacteroides_16S	19.945	1.136	5.319545686	208711.1667	2017-08-31	Belle River	beach	core	122	Qubit	low	58.56	medium	5	1.2	2.08333	104355.5833	5.01851569
WE_2017-08-31_BR_cDNA_3b	CXR30	MST_goose	21.637	0.034	4.257505774	18092.79963	2017-08-31	Belle River	beach	core	126	Qubit	low	60.48	medium	5	1.2	2.08333	9046.399817	3.95647578
WE_2017-08-31_BR_cDNA_3a	CXR30	MST_goose	23.952	0.262	3.589203233	3883.320481	2017-08-31	Belle River	beach	core	36.4	Qubit	very low	36.4	medium	5	1.2	1	931.9969154	2.96941448
WE_2017-08-31_BR_cDNA_1b	CXR30	MST_goose	24.341	0.045	3.476905312	2998.50869	2017-08-31	Belle River	beach	core	113	Qubit	low	54.24	medium	5	1.2	2.08333	1499.254345	3.17587532
WE_2017-08-31_BR_cDNA_2a	CXR30	MST_goose	25.011	0.737	3.283487298	1920.822781	2017-08-31	Belle River	beach	core	128	Qubit	low	61.44	medium	5	1.2	2.08333	960.4113907	2.9824573
WE_2017-08-31_BR_cDNA_2b	CXR30	MST_goose	25.016	0.184	3.28204388	1914.449346	2017-08-31	Belle River	beach	core	142	Qubit	low	68.16	medium	5	1.2	2.08333	957.2246729	2.98101388
WE_2017-08-31_BR_cDNA_1a	CXR30	MST_goose	25.431	0.249	3.162240185	1452.914924	2017-08-31	Belle River	beach	core	122	Qubit	low	58.56	medium	5	1.2	2.08333	726.457462	2.86121019
WE_2017-08-31_BR_cDNA_3b	CXR30	MST_seagull	19.739	0.184	4.696135716	49674.75293	2017-08-31	Belle River	beach	core	126	Qubit	low	60.48	medium	5	1.2	2.08333	24837.37646	4.39510572
WE_2017-08-31_BR_cDNA_1b	CXR30	MST_seagull	22.154	0.453	4.014452254	10338.37435	2017-08-31	Belle River	beach	core	113	Qubit	low	54.24	medium	5	1.2	2.08333	5169.187176	3.71342226
WE_2017-08-31_BR_cDNA_2a	CXR30																			

WE_2017-08-31_BR_cDNA_1a	CXR30	MST_seagull	22.742	0.208	3.84847715	7054.677259	2017-08-31	Belle River	beach	core	122	Qubit	low	58.56	medium	5	1.2	2.08333	3527.338629	3.54744716
WE_2017-08-31_BR_cDNA_2b	CXR30	MST_seagull	23.108	0.114	3.745166116	5561.169295	2017-08-31	Belle River	beach	core	142	Qubit	low	68.16	medium	5	1.2	2.08333	2780.584648	3.44413612
WE_2017-09-13_BR_cDNA_2a	CXR30	FIB_Ecoli_235	24.787	0.404	4.082384461	12088.8353	2017-09-13	Belle River	beach	core	101	Qubit	low	48.48	medium	5	1.2	2.08333	6044.417651	3.78135447
WE_2017-09-13_BR_cDNA_2b	CXR30	FIB_Ecoli_235	25.126	0.547	3.987776289	9722.462783	2017-09-13	Belle River	beach	core	238	Qubit	medium	79.33333333	medium	5	1.2	3	7000.173203	3.84510879
WE_2017-09-13_BR_cDNA_1a	CXR30	FIB_Ecoli_235	25.131	0.801	3.986380889	9691.274359	2017-09-13	Belle River	beach	core	127	Qubit	low	60.96	medium	5	1.2	2.08333	4845.63718	3.68535089
WE_2017-09-13_BR_cDNA_1b	CXR30	FIB_Ecoli_235	25.242	0.768	3.955402992	9024.081143	2017-09-13	Belle River	beach	core	132	Qubit	low	63.36	medium	5	1.2	2.08333	4512.040571	3.654373
WE_2017-09-13_BR_cDNA_3a	CXR30	FIB_Ecoli_235	26.105	0.994	3.714556821	5182.708953	2017-09-13	Belle River	beach	core	116	Qubit	low	55.68	medium	5	1.2	2.08333	2591.354477	3.41352683
WE_2017-09-13_BR_cDNA_3b	CXR30	FIB_Ecoli_235	26.87	0.246	3.501060505	3170.009068	2017-09-13	Belle River	beach	core	85.8	Qubit	very low	85.8	medium	5	1.2	1	760.8021764	2.88127175
WE_2017-09-13_BR_cDNA_2b	CXR30	FIB_Enterococcus_235	24.038	0.351	4.213120326	16335.04467	2017-09-13	Belle River	beach	core	238	Qubit	medium	79.33333333	medium	5	1.2	3	11761.23216	4.07045282
WE_2017-09-13_BR_cDNA_1b	CXR30	FIB_Enterococcus_235	24.433	0.467	4.101234988	12625.10467	2017-09-13	Belle River	beach	core	132	Qubit	low	63.36	medium	5	1.2	2.08333	6312.552337	3.80020499
WE_2017-09-13_BR_cDNA_1a	CXR30	FIB_Enterococcus_235	24.663	0.222	4.036086562	10866.42189	2017-09-13	Belle River	beach	core	127	Qubit	low	60.96	medium	5	1.2	2.08333	5433.210943	3.73505657
WE_2017-09-13_BR_cDNA_2a	CXR30	FIB_Enterococcus_235	25.722	0.374	3.736120553	5446.538187	2017-09-13	Belle River	beach	core	101	Qubit	low	48.48	medium	5	1.2	2.08333	2723.269093	3.43509056
WE_2017-09-13_BR_cDNA_3a	CXR30	FIB_Enterococcus_235	26.192	0.491	3.602991162	4008.585604	2017-09-13	Belle River	beach	core	116	Qubit	low	55.68	medium	5	1.2	2.08333	2004.292802	3.30196117
WE_2017-09-13_BR_cDNA_3b	CXR30	FIB_Enterococcus_235	27.644	1.127	3.191706322	1554.913815	2017-09-13	Belle River	beach	core	85.8	Qubit	very low	85.8	medium	5	1.2	1	373.1793157	2.57191756
WE_2017-09-13_BR_cDNA_2a	CXR30	MST_Bacteroides_16S	18.641	0.9	5.67969712	487494.4911	2017-09-13	Belle River	beach	core	101	Qubit	low	48.48	medium	5	1.2	2.08333	243747.2456	5.38693972
WE_2017-09-13_BR_cDNA_1b	CXR30	MST_Bacteroides_16S	18.895	0.925	5.616206137	413243.6003	2017-09-13	Belle River	beach	core	132	Qubit	low	63.36	medium	5	1.2	2.08333	206621.8002	5.31517614
WE_2017-09-13_BR_cDNA_2b	CXR30	MST_Bacteroides_16S	19.133	1.071	5.548963101	353967.2657	2017-09-13	Belle River	beach	core	238	Qubit	medium	79.33333333	medium	5	1.2	3	254856.4313	5.40629556
WE_2017-09-13_BR_cDNA_3b	CXR30	MST_Bacteroides_16S	19.573	0.734	5.424648245	265857.0892	2017-09-13	Belle River	beach	core	85.8	Qubit	very low	85.8	medium	5	1.2	1	63805.70141	4.80485949
WE_2017-09-13_BR_cDNA_1a	CXR30	MST_Bacteroides_16S	19.59	1.493	5.419845171	262933.0453	2017-09-13	Belle River	beach	core	127	Qubit	low	60.96	medium	5	1.2	2.08333	131466.5227	5.11881518
WE_2017-09-13_BR_cDNA_3a	CXR30	MST_Bacteroides_16S	21.039	1.304	5.010453749	102436.2684	2017-09-13	Belle River	beach	core	116	Qubit	low	55.68	medium	5	1.2	2.08333	51218.13418	4.70942375
WE_2017-09-13_BR_cDNA_2a	CXR30	MST_goose	24.415	0.205	3.455542725	2854.583329	2017-09-13	Belle River	beach	core	101	Qubit	low	48.48	medium	5	1.2	2.08333	1427.291665	3.15451273
WE_2017-09-13_BR_cDNA_1b	CXR30	MST_goose	24.571	0.384	3.410508083	2573.40466	2017-09-13	Belle River	beach	core	238	Qubit	medium	79.33333333	medium	5	1.2	3	1852.851356	3.26784058
WE_2017-09-13_BR_cDNA_1b	CXR30	MST_goose	25.029	0.325	3.278290993	1897.977209	2017-09-13	Belle River	beach	core	132	Qubit	low	63.36	medium	5	1.2	2.08333	948.9886045	2.977261
WE_2017-09-13_BR_cDNA_3a	CXR30	MST_goose	25.862	0.127	3.037817552	1090.981916	2017-09-13	Belle River	beach	core	116	Qubit	low	55.68	medium	5	1.2	2.08333	545.4909582	2.73678756
WE_2017-09-13_BR_cDNA_1a	CXR30	MST_goose	25.878	0.197	3.033198614	1079.440266	2017-09-13	Belle River	beach	core	127	Qubit	low	60.96	medium	5	1.2	2.08333	539.7201329	2.73216862
WE_2017-09-13_BR_cDNA_1a	CXR30	MST_goose	26.58	0.282	2.830542725	676.9283847	2017-09-13	Belle River	beach	core	85.8	Qubit	very low	85.8	medium	5	1.2	1	162.4628123	2.21075397
WE_2017-09-13_BR_cDNA_2b	CXR30	MST_seagull	23.003	0.766	3.774804528	5953.941012	2017-09-13	Belle River	beach	core	238	Qubit	medium	79.33333333	medium	5	1.2	3	4286.837529	3.63213702
WE_2017-09-13_BR_cDNA_2a	CXR30	MST_seagull	23.432	0.241	3.653710447	4505.162358	2017-09-13	Belle River	beach	core	101	Qubit	low	48.48	medium	5	1.2	2.08333	2252.581179	3.35268045
WE_2017-09-13_BR_cDNA_1b	CXR30	MST_seagull	23.532	0.409	3.625483388	4221.66131	2017-09-13	Belle River	beach	core	132	Qubit	low	63.36	medium	5	1.2	2.08333	2110.830655	3.32445339
WE_2017-09-13_BR_cDNA_1a	CXR30	MST_seagull	23.703	0.467	3.577215118	3777.592595	2017-09-13	Belle River	beach	core	127	Qubit	low	60.96	medium	5	1.2	2.08333	1888.796297	3.27618512
WE_2017-09-13_BR_cDNA_3b	CXR30	MST_seagull	24.655	0.265	3.308493522	2034.667846	2017-09-13	Belle River	beach	core	85.8	Qubit	very low	85.8	medium	5	1.2	1	488.320283	2.68870476
WE_2017-09-13_BR_cDNA_3a	CXR30	MST_seagull	25.086	1.116	3.1868349	1537.570011	2017-09-13	Belle River	beach	core	116	Qubit	low	55.68	medium	5	1.2	2.08333	768.7850056	2.8858049
WE_2017-09-13_HD_cDNA_3a	CXR30	FIB_Ecoli_235	29.788	0.062	2.686704622	486.0764961	2017-09-13	Holiday	beach	core	57.5	Qubit	very low	57.5	medium	5	1.2	1	116.6583591	2.06691586
WE_2017-09-13_HD_cDNA_3b	CXR30	FIB_Ecoli_235	30.261	1.415	2.55469971	358.6738461	2017-09-13	Holiday	beach	core	60.8	Qubit	very low	60.8	medium	5	1.2	1	86.08172306	1.93491095
WE_2017-09-13_HD_cDNA_3a	CXR30	FIB_Enterococcus_235	25.521	0.305	3.793054611	6209.471118	2017-09-13	Holiday	beach	core	57.5	Qubit	very low	57.5	medium	5	1.2	1	1490.273068	3.17326585
WE_2017-09-13_HD_cDNA_3b	CXR30	FIB_Enterococcus_235	25.837	0.199	3.70354634	5052.965585	2017-09-13	Holiday	beach	core	60.8	Qubit	very low	60.8	medium	5	1.2	1	1212.71174	3.08375758
WE_2017-09-13_HD_cDNA_1b	CXR30	FIB_Enterococcus_235	29.253	1.598	2.7359506	544.4407211	2017-09-13	Holiday	beach	core	19.5	Qubit	very low	19.5	low	5	1.2	1	130.6657731	2.11616184
WE_2017-09-13_HD_cDNA_2b	CXR30	FIB_Enterococcus_235	29.623	0.959	2.631146612	427.7072503	2017-09-13	Holiday	beach	core	29.4	Qubit	very low	29.4	medium	5	1.2	1	102.6497401	2.01135785
WE_2017-09-13_HD_cDNA_2b	CXR30	MST_Bacteroides_16S	19.027	0.868	5.57891168	379237.8536	2017-09-13	Holiday	beach	core	29.4	Qubit	very low	29.4	medium	5	1.2	1	91017.08487	4.95912292
WE_2017-09-13_HD_cDNA_3b	CXR30	MST_Bacteroides_16S	19.123	0.43	5.551788439	356277.5349	2017-09-13	Holiday	beach	core	60.8	Qubit	very low	60.8	medium	5	1.2	1	85506.60837	4.93199968
WE_2017-09-13_HD_cDNA_3a	CXR30	MST_Bacteroides_16S	19.329	0.702	5.493586484	311592.1326	2017-09-13	Holiday	beach	core	57.5	Qubit	very low	57.5	medium	5	1.2	1	74782.11182	4.87379773
WE_2017-09-13_HD_cDNA_1b	CXR30	MST_Bacteroides_16S	21.191	0.492	4.967508617	92791.59017	2017-09-13	Holiday	beach	core	19.5	Qubit	very low	19.5	low	5	1.2	1	22269.98164	4.34771986
WE_2017-09-13_HD_cDNA_2a	CXR30	MST_Bacteroides_16S	23.379	0.655	4.349324744	22352.43004	2017-09-13	Holiday	beach	core	10.8	Qubit	very low	10.8	low	5	1.2	1	5364.58321	3.72953599
WE_2017-09-13_HD_cDNA_3a	CXR30	MST_goose	24.053	0.248	3.560046189	3631.16672	2017-09-13	Holiday	beach	core	57.5	Qubit	very low	57.5	medium	5	1.2	1	871.4800127	2.94025743
WE_2017-09-13_HD_cDNA_3b	CXR30	MST_goose	26.004	0.901	2.99682448	992.7147628	2017-09-13	Holiday	beach	core	60.8	Qubit	very low	60.8	medium	5	1.2	1	238.2515431	2.37703572
WE_2017-09-13_HD_cDNA_2b	CXR30	MST_goose	29.023	0.89	2.125288684	133.4408143	2017-09-13	Holiday	beach	core	29.4	Qubit	very low	29.4	medium	5	1.2	1	32.02579544	1.50549993
WE_2017-09-13_HD_cDNA_1b	CXR30	MST_goose	30.046	0.566	1.829965358	67.6029049	2017-09-13	Holiday	beach	core	19.5	Qubit	very low	19.5	low	5	1.2	1	16.22469717	1.2101766
WE_2017-09-13_HD_cDNA_3b	CXR30	MST_seagull	26.182	0.315	2.877466339	754.1649407	2017-09-13	Holiday	beach	core	60.8	Qubit	very low	60.8	medium	5	1.2	1	180.9995858	2.25767758
WE_2017-09-13_HD_cDNA_1b	CXR30	MST_seagull	28.793	0.684	2.140457843	138.1840264	2017-09-13	Holiday	beach	core	19.5	Qubit	very low	19.5	low	5	1.2	1	33.16416633	1.52066909
WE_2017-09-13_HD_cDNA_2a	CXR30	MST_seagull	31.39	1.569	1.407401135	25.55060186	2017-09-13	Holiday	beach	core	10.8	Qubit	very low	10.8	low	5	1.2	1	6.132144447	0.78761238
WE_2017-09-13_KV_cDNA_1a	CXR30	FIB_Ecoli_235	24.91	0.413	4.048057602	11170.11391	2017-09-13	Kingsville	beach	core	255	Qubit	medium	85	medium	5	1.2	3	8042.482019	3.9053901
WE_2017-09-13_KV_cDNA_2b	CXR30	FIB_Ecoli_235	26.48	0.554	3.609901764	4072.881399	2017-09-13	Kingsville	beach	core	133	Qubit	low	63.84	medium	5	1.2	2.08333	2036.4407	3.30887177
WE_2017-09-13_KV_cDNA_2a	CXR30	FIB_Ecoli_235	26.775	0.557	3.527573119	3369.559418	2017-09-13	Kingsville	beach	core	103	Qubit	low	49.44	medium	5	1.2	2.08333	1684.779709	3.22654312
WE_2017-09-13_KV_cDNA_1b	CXR30	FIB_Ecoli_235	26.85	0.147	3.506642108	3211.013324	2017-09-13	Kingsville	beach	core	234	Qubit	medium	78	medium	5	1.2	3	2311.929593	3.3639746
WE_2017-09-13_KV_cDNA_3a	CXR30	FIB_Ecoli_235	26.915	0.135	3.488501898	3079.653799	2017-09-13	Kingsville	beach	core	76.5									

WE_2017-09-13_KV_cDNA_3b	CXR30	FIB_Ecoli_23S	27.838	0.517	3.230910918	1701.809398	2017-09-13	Kingsville	beach	core	82.8	Qubit	very low	82.8	medium	5	1.2	1	408.4342555	2.61112216
WE_2017-09-13_KV_cDNA_1b	CXR30	FIB_Enterococcus_23S	23.499	0.328	4.365794244	23216.36614	2017-09-13	Kingsville	beach	core	234	Qubit	medium	78	medium	5	1.2	3	16715.78362	4.22312674
WE_2017-09-13_KV_cDNA_1a	CXR30	FIB_Enterococcus_23S	23.879	0.364	4.258157716	18119.98008	2017-09-13	Kingsville	beach	core	255	Qubit	medium	85	medium	5	1.2	3	13046.38566	4.11549021
WE_2017-09-13_KV_cDNA_3a	CXR30	FIB_Enterococcus_23S	23.922	0.46	4.245977793	17618.85952	2017-09-13	Kingsville	beach	core	76.5	Qubit	very low	76.5	medium	5	1.2	1	4228.526285	3.62618904
WE_2017-09-13_KV_cDNA_3b	CXR30	FIB_Enterococcus_23S	23.943	0.246	4.240029458	17379.18709	2017-09-13	Kingsville	beach	core	82.8	Qubit	very low	82.8	medium	5	1.2	1	4171.004901	3.6202407
WE_2017-09-13_KV_cDNA_2a	CXR30	FIB_Enterococcus_23S	24.265	0.63	4.148821663	14087.10213	2017-09-13	Kingsville	beach	core	133	Qubit	low	63.84	medium	5	1.2	2.08333	7043.551066	3.84779167
WE_2017-09-13_KV_cDNA_3b	CXR30	FIB_Enterococcus_23S	25.845	0.496	3.701280308	5026.669229	2017-09-13	Kingsville	beach	core	103	Qubit	low	49.44	medium	5	1.2	2.08333	2513.334614	3.40025031
WE_2017-09-13_KV_cDNA_3a	CXR30	MST_Bacteroides_16S	16.503	1.149	6.292026897	159865.995	2017-09-13	Kingsville	beach	core	76.5	Qubit	very low	76.5	medium	5	1.2	1	470151.8387	5.67223814
WE_2017-09-13_KV_cDNA_3b	CXR30	MST_Bacteroides_16S	16.79	0.748	6.210939707	1625323.098	2017-09-13	Kingsville	beach	core	82.8	Qubit	very low	82.8	medium	5	1.2	1	390077.5435	5.59115095
WE_2017-09-13_KV_cDNA_1a	CXR30	MST_Bacteroides_16S	18.803	0.787	5.642199243	438731.9302	2017-09-13	Kingsville	beach	core	255	Qubit	medium	85	medium	5	1.2	3	315886.9897	5.49953174
WE_2017-09-13_KV_cDNA_1b	CXR30	MST_Bacteroides_16S	19.074	0.488	5.565632593	367817.6735	2017-09-13	Kingsville	beach	core	234	Qubit	medium	78	medium	5	1.2	3	264828.7249	5.42296509
WE_2017-09-13_KV_cDNA_2a	CXR30	MST_Bacteroides_16S	20.199	0.901	5.24778211	176922.1099	2017-09-13	Kingsville	beach	core	103	Qubit	low	49.44	medium	5	1.2	2.08333	88461.05495	4.94675211
WE_2017-09-13_KV_cDNA_2b	CXR30	MST_Bacteroides_16S	20.332	1.039	5.21020512	162257.6268	2017-09-13	Kingsville	beach	core	133	Qubit	low	63.84	medium	5	1.2	2.08333	81128.81338	4.90917512
WE_2017-09-13_KV_cDNA_3b	CXR30	MST_dog	27.909	0.032	2.246325508	176.3297158	2017-09-13	Kingsville	beach	core	82.8	Qubit	very low	82.8	medium	5	1.2	1	42.3191318	1.62653675
WE_2017-09-13_KV_cDNA_3a	CXR30	MST_dog	28.194	0.631	2.165614115	146.424623	2017-09-13	Kingsville	beach	core	76.5	Qubit	very low	76.5	medium	5	1.2	1	35.14190952	1.54582536
WE_2017-09-13_KV_cDNA_3b	CXR30	MST_goose	21.435	0.377	4.315819861	20692.82865	2017-09-13	Kingsville	beach	core	76.5	Qubit	very low	76.5	medium	5	1.2	1	4966.278875	3.6960311
WE_2017-09-13_KV_cDNA_3b	CXR30	MST_goose	21.967	0.451	4.162240185	14529.14924	2017-09-13	Kingsville	beach	core	82.8	Qubit	very low	82.8	medium	5	1.2	1	3486.995818	3.54245143
WE_2017-09-13_KV_cDNA_1b	CXR30	MST_goose	23.041	0.98	3.852193995	7115.312772	2017-09-13	Kingsville	beach	core	234	Qubit	medium	78	medium	5	1.2	3	5123.025196	3.70952649
WE_2017-09-13_KV_cDNA_2a	CXR30	MST_goose	23.533	1.109	3.710161663	5130.523283	2017-09-13	Kingsville	beach	core	103	Qubit	low	49.44	medium	5	1.2	2.08333	2565.261641	3.40913167
WE_2017-09-13_KV_cDNA_1a	CXR30	MST_goose	23.708	0.001	3.659642032	4567.115894	2017-09-13	Kingsville	beach	core	255	Qubit	medium	85	medium	5	1.2	3	3288.323444	3.51697453
WE_2017-09-13_KV_cDNA_2b	CXR30	MST_goose	23.759	0.234	3.644919169	4414.882694	2017-09-13	Kingsville	beach	core	133	Qubit	low	63.84	medium	5	1.2	2.08333	2207.441347	3.34388917
WE_2017-09-13_KV_cDNA_3b	CXR30	MST_seagull	26.435	0.924	2.806051881	639.8112635	2017-09-13	Kingsville	beach	core	76.5	Qubit	very low	76.5	medium	5	1.2	1	153.5547032	2.18626312
WE_2017-09-13_KV_cDNA_3b	CXR30	MST_seagull	26.665	0.566	2.741129647	50.9721497	2017-09-13	Kingsville	beach	core	82.8	Qubit	very low	82.8	medium	5	1.2	1	132.2333159	2.12134089
WE_2017-09-13_KV_cDNA_2b	CXR30	MST_seagull	26.794	0.463	2.704716741	506.6601431	2017-09-13	Kingsville	beach	core	133	Qubit	low	63.84	medium	5	1.2	2.08333	253.3300716	2.40368675
WE_2017-09-13_KV_cDNA_1b	CXR30	MST_seagull	26.918	0.596	2.669715189	467.4285004	2017-09-13	Kingsville	beach	core	234	Qubit	medium	78	medium	5	1.2	3	336.5485203	2.52704769
WE_2017-09-13_KV_cDNA_2a	CXR30	MST_seagull	27.199	0.291	2.590397155	389.4010827	2017-09-13	Kingsville	beach	core	103	Qubit	low	49.44	medium	5	1.2	2.08333	194.7005414	2.28936716
WE_2017-09-13_KV_cDNA_1a	CXR30	MST_seagull	27.645	1.232	2.464504474	291.4100155	2017-09-13	Kingsville	beach	core	255	Qubit	medium	85	medium	5	1.2	3	209.815212	2.32183697
WE_2017-08-31_LE_cDNA_3b	CXR30	FIB_Ecoli_23S	29.667	0.452	2.72047332	525.3797384	2017-08-31	Leamington	beach	core	24.9	Qubit	very low	24.9	medium	5	1.2	1	126.0911372	2.10068456
WE_2017-08-31_LE_cDNA_3b	CXR30	FIB_Enterococcus_23S	27.019	0.304	3.368740086	2337.437924	2017-08-31	Leamington	beach	core	24.9	Qubit	very low	24.9	medium	5	1.2	1	560.9851019	2.74895133
WE_2017-08-31_LE_cDNA_3b	CXR30	MST_Bacteroides_16S	22.83	0.408	4.50443578	31947.41918	2017-08-31	Leamington	beach	core	24.9	Qubit	very low	24.9	medium	5	1.2	1	7667.380602	3.88464702
WE_2017-08-31_LE_cDNA_3b	CXR30	MST_seagull	28.924	1.397	2.103480396	126.9054859	2017-08-31	Leamington	beach	core	24.9	Qubit	very low	24.9	medium	5	1.2	1	30.45731662	1.48369164
WE_2017-09-13_LE_cDNA_3a	CXR30	FIB_Ecoli_23S	25.817	0.758	3.794931904	6236.370441	2017-09-13	Leamington	beach	core	50.3	Qubit	very low	50.3	medium	5	1.2	1	1496.728906	3.17514315
WE_2017-09-13_LE_cDNA_2a	CXR30	FIB_Ecoli_23S	26.057	0.7	3.727952668	5345.061026	2017-09-13	Leamington	beach	core	52.7	Qubit	very low	52.7	medium	5	1.2	1	1282.814646	3.10816391
WE_2017-09-13_LE_cDNA_2b	CXR30	FIB_Ecoli_23S	28.65	1.452	3.004297834	1009.945258	2017-09-13	Leamington	beach	core	49	Qubit	very low	49	medium	5	1.2	1	242.3868619	2.38450908
WE_2017-09-13_LE_cDNA_3a	CXR30	FIB_Enterococcus_23S	25.633	0.141	3.761330161	5772.051015	2017-09-13	Leamington	beach	core	50.3	Qubit	very low	50.3	medium	5	1.2	1	1385.292244	3.1415414
WE_2017-09-13_LE_cDNA_2b	CXR30	FIB_Enterococcus_23S	27.697	0.565	3.176693859	1502.082751	2017-09-13	Leamington	beach	core	49	Qubit	very low	49	medium	5	1.2	1	360.4998603	2.5569051
WE_2017-09-13_LE_cDNA_2a	CXR30	FIB_Enterococcus_23S	27.729	0.078	3.16762973	1471.057777	2017-09-13	Leamington	beach	core	52.7	Qubit	very low	52.7	medium	5	1.2	1	353.0538665	2.54784097
WE_2017-09-13_LE_cDNA_3b	CXR30	FIB_Enterococcus_23S	28.901	0.05	2.835656016	684.9454993	2017-09-13	Leamington	beach	core	31.1	Qubit	very low	31.1	medium	5	1.2	1	164.3869198	2.21586726
WE_2017-09-13_LE_cDNA_1b	CXR30	FIB_Enterococcus_23S	30.295	0.626	2.440799909	275.930628	2017-09-13	Leamington	beach	core	25.7	Qubit	very low	25.7	medium	5	1.2	1	66.22335072	1.82101115
WE_2017-09-13_LE_cDNA_2b	CXR30	MST_Bacteroides_16S	21.144	0.995	4.980787704	95672.62811	2017-09-13	Leamington	beach	core	52.7	Qubit	very low	52.7	medium	5	1.2	1	22961.43075	4.36099895
WE_2017-09-13_LE_cDNA_3a	CXR30	MST_Bacteroides_16S	21.295	0.689	4.938125106	86721.16549	2017-09-13	Leamington	beach	core	50.3	Qubit	very low	50.3	medium	5	1.2	1	20813.07972	4.31833635
WE_2017-09-13_LE_cDNA_2b	CXR30	MST_Bacteroides_16S	21.675	1.21	4.830762276	67727.0682	2017-09-13	Leamington	beach	core	49	Qubit	very low	49	medium	5	1.2	1	16254.49637	4.21097352
WE_2017-09-13_LE_cDNA_3b	CXR30	MST_Bacteroides_16S	21.953	0.299	4.75221789	56522.04807	2017-09-13	Leamington	beach	core	31.1	Qubit	very low	31.1	medium	5	1.2	1	13565.29154	4.13242913
WE_2017-09-13_LE_cDNA_1b	CXR30	MST_Bacteroides_16S	23.643	0.772	4.274735831	18825.03667	2017-09-13	Leamington	beach	core	25.7	Qubit	very low	25.7	medium	5	1.2	1	4518.008802	3.65494707
WE_2017-09-13_LE_cDNA_1a	CXR30	MST_Bacteroides_16S	30.197	1.511	2.42300955	264.8558377	2017-09-13	Leamington	beach	core	7.7	Qubit	very low	7.7	low	5	1.2	1	63.56540104	1.80322079
WE_2017-09-13_LE_cDNA_3a	CXR30	MST_dog	27.228	0.384	2.439183257	274.9053915	2017-09-13	Leamington	beach	core	50.3	Qubit	very low	50.3	medium	5	1.2	1	65.97729395	1.8193945
WE_2017-09-13_LE_cDNA_2b	CXR30	MST_dog	28.529	0.069	2.070742828	117.6908848	2017-09-13	Leamington	beach	core	49	Qubit	very low	49	medium	5	1.2	1	28.24581236	1.45095407
WE_2017-09-13_LE_cDNA_3b	CXR30	MST_goose	24.707	0.155	3.371247113	2350.97014	2017-09-13	Leamington	beach	core	50.3	Qubit	very low	50.3	medium	5	1.2	1	564.232837	2.75145836
WE_2017-09-13_LE_cDNA_2b	CXR30	MST_goose	26.45	0.198	2.868071594	738.0258838	2017-09-13	Leamington	beach	core	49	Qubit	very low	49	medium	5	1.2	1	177.1262121	2.24828284
WE_2017-09-13_LE_cDNA_2a	CXR30	MST_goose	26.702	0.156	2.795323326	624.1993695	2017-09-13	Leamington	beach	core	52.7	Qubit	very low	52.7	medium	5	1.2	1	149.8078487	2.17553457
WE_2017-09-13_LE_cDNA_1b	CXR30	MST_goose	30.385	0.211	1.732101617	53.96368725	2017-09-13	Leamington	beach	core	25.7	Qubit	very low	25.7	medium	5	1.2	1	12.95128494	1.11231286
WE_2017-09-13_LE_cDNA_2b	CXR30	MST_human_mito	28.115	0.635	2.836193537	685.7937728	2017-09-13	Leamington	beach	core	49	Qubit	very low	49	medium	5	1.2	1	164.5905055	2.21640478
WE_2017-09-13_LE_cDNA_3a	CXR30	MST_seagull	22.511	0.904	3.913681655	8197.504339	2017-09-13	Leamington	beach	core	50.3	Qubit	very low	50.3	medium	5	1.2	1	1967.401041	3.2938929
WE_2017-09-13_LE_cDNA_2b	CXR30	MST_seagull	23.689	0.455	3.581166907	3812.123015	2017-09-13	Leamington	beach	core	49	Qubit	very low	49	medium	5	1.2	1	914.8095235	2.96137815
WE_2017-09-13_LE_cDNA_2a	CXR30	MST_seagull	25.392	0.028	3.100460101	1260.259852	2017-09-13	Leamington	beach	core	52.7	Qubit	very low	52.7	medium	5	1.2	1	302.4623644	2.48067134

WE_2017-09-13_LE_cDNA_3b	CXR30	MST_seagull	29.084	2.56	2.058317103	114.3713119	2017-09-13	Leamington	beach	core	31.1	Qubit	very low	31.1	medium	5	1.2	1	27.44911486	1.43852834
WE_2017-09-13_LE_cDNA_1b	CXR30	MST_seagull	32.471	0.177	1.102266633	12.65513064	2017-09-13	Leamington	beach	core	25.7	Qubit	very low	25.7	medium	5	1.2	1	3.037231354	0.48247788
WE_2017-08-31_PP_cDNA_3a	CXR30	FIB_Ecoli_235	33.638	2.514	1.612246037	40.94925803	2017-08-31	Point Pelee	beach	core	0	Qubit	very low	1	low	5	1.2	1	9.827821927	0.99245728
WE_2017-08-31_PP_cDNA_2b	CXR30	MST_Bacteroides_16S	22.797	0.08	4.513759394	32640.69477	2017-08-31	Point Pelee	beach	core	16.1	Qubit	very low	16.1	low	5	1.2	1	7833.766744	3.89397064
WE_2017-08-31_PP_cDNA_3a	CXR30	MST_Bacteroides_16S	27.387	0.792	3.216929423	1647.894571	2017-08-31	Point Pelee	beach	core	0	Qubit	very low	1	low	5	1.2	1	395.4946971	2.59714067
WE_2017-08-31_PP_cDNA_3b	CXR30	MST_Bacteroides_16S	29.22	0.621	2.699045036	500.0863907	2017-08-31	Point Pelee	beach	core	0	Qubit	very low	1	low	5	1.2	1	120.0207338	2.07925628
WE_2017-08-31_PP_cDNA_1b	CXR30	MST_Bacteroides_16S	29.471	0.804	2.628129061	424.745769	2017-08-31	Point Pelee	beach	core	0	Qubit	very low	1	low	5	1.2	1	101.9389846	2.0083403
WE_2017-08-31_PP_cDNA_2b	CXR30	MST_seagull	30.738	0.206	1.591441556	39.03386501	2017-08-31	Point Pelee	beach	core	16.1	Qubit	very low	16.1	low	5	1.2	1	9.368127602	0.9716528
WE_2017-08-31_SP_cDNA_1a	CXR30	FIB_Ecoli_235	26.929	0.218	3.484594776	3052.072007	2017-08-31	Sandpoint	beach	core	119	Qubit	low	57.12	medium	5	1.2	2.08333	1526.036003	3.18356478
WE_2017-08-31_SP_cDNA_2b	CXR30	FIB_Ecoli_235	28.383	0.049	3.078812235	1198.980817	2017-08-31	Sandpoint	beach	core	139	Qubit	low	66.72	medium	5	1.2	2.08333	599.4904087	2.77778224
WE_2017-08-31_SP_cDNA_3a	CXR30	FIB_Ecoli_235	29.418	0.424	2.789964278	616.5442868	2017-08-31	Sandpoint	beach	core	83.1	Qubit	very low	83.1	medium	5	1.2	1	147.9706288	2.17017552
WE_2017-08-31_SP_cDNA_3b	CXR30	FIB_Ecoli_235	29.553	1.67	2.752288457	565.3123291	2017-08-31	Sandpoint	beach	core	107	Qubit	low	51.36	medium	5	1.2	2.08333	282.6561645	2.45125846
WE_2017-08-31_SP_cDNA_2a	CXR30	FIB_Ecoli_235	31.168	2.548	2.301574012	200.2506858	2017-08-31	Sandpoint	beach	core	135	Qubit	low	64.8	medium	5	1.2	2.08333	100.1253429	2.00054402
WE_2017-08-31_SP_cDNA_2b	CXR30	FIB_Enterococcus_235	27.098	0.541	3.346363018	2220.051342	2017-08-31	Sandpoint	beach	core	119	Qubit	low	57.12	medium	5	1.2	2.08333	1110.025671	3.04533302
WE_2017-08-31_SP_cDNA_1a	CXR30	FIB_Enterococcus_235	28.434	0.717	2.967935645	928.8287394	2017-08-31	Sandpoint	beach	core	83.1	Qubit	very low	83.1	medium	5	1.2	1	222.9188975	2.34814689
WE_2017-08-31_SP_cDNA_2b	CXR30	FIB_Enterococcus_235	29.576	1.07	2.644459551	441.021286	2017-08-31	Sandpoint	beach	core	139	Qubit	low	66.72	medium	5	1.2	2.08333	220.510643	2.34342956
WE_2017-08-31_SP_cDNA_2a	CXR30	FIB_Enterococcus_235	31.345	2.009	2.143383186	139.1179553	2017-08-31	Sandpoint	beach	core	135	Qubit	low	64.8	medium	5	1.2	2.08333	69.55897766	1.84235319
WE_2017-08-31_SP_cDNA_3b	CXR30	FIB_Enterococcus_235	31.567	1.006	2.080500793	120.3651588	2017-08-31	Sandpoint	beach	core	107	Qubit	low	51.36	medium	5	1.2	2.08333	60.1825794	1.7794708
WE_2017-08-31_SP_cDNA_3a	CXR30	MST_Bacteroides_16S	23.566	0.587	4.296490931	19792.05689	2017-08-31	Sandpoint	beach	core	83.1	Qubit	very low	83.1	medium	5	1.2	1	4750.093654	3.67670217
WE_2017-08-31_SP_cDNA_1a	CXR30	MST_Bacteroides_16S	24.379	0.536	4.066790982	11662.48187	2017-08-31	Sandpoint	beach	core	119	Qubit	low	57.12	medium	5	1.2	2.08333	5831.240934	3.76576099
WE_2017-08-31_SP_cDNA_2b	CXR30	MST_Bacteroides_16S	24.891	0.864	3.922133695	8358.602933	2017-08-31	Sandpoint	beach	core	139	Qubit	low	66.72	medium	5	1.2	2.08333	4179.301466	3.6211037
WE_2017-08-31_SP_cDNA_2a	CXR30	MST_Bacteroides_16S	25.291	1.011	3.80912019	6443.475623	2017-08-31	Sandpoint	beach	core	135	Qubit	low	64.8	medium	5	1.2	2.08333	3221.737812	3.50809019
WE_2017-08-31_SP_cDNA_3b	CXR30	MST_Bacteroides_16S	26.126	0.506	3.573204498	3742.867887	2017-08-31	Sandpoint	beach	core	107	Qubit	low	51.36	medium	5	1.2	2.08333	1871.433943	3.2721745
WE_2017-08-31_SP_cDNA_1a	CXR30	MST_goose	28.304	0.281	2.332852194	215.204919	2017-08-31	Sandpoint	beach	core	119	Qubit	low	57.12	medium	5	1.2	2.08333	107.6024595	2.0318222
WE_2017-08-31_SP_cDNA_3b	CXR30	MST_goose	29.737	0.238	1.919168591	83.01729745	2017-08-31	Sandpoint	beach	core	107	Qubit	low	51.36	medium	5	1.2	2.08333	41.50864872	1.6181386
WE_2017-08-31_SP_cDNA_3a	CXR30	MST_goose	30.237	0.58	1.77482679	59.54246223	2017-08-31	Sandpoint	beach	core	83.1	Qubit	very low	83.1	medium	5	1.2	1	14.29019093	1.15503803
WE_2017-08-31_SP_cDNA_2b	CXR30	MST_goose	31.115	0.828	1.521362587	33.21716675	2017-08-31	Sandpoint	beach	core	139	Qubit	low	66.72	medium	5	1.2	2.08333	16.60858337	1.2203259
WE_2017-08-31_SP_cDNA_2a	CXR30	MST_goose	31.412	2.045	1.435623557	27.26613349	2017-08-31	Sandpoint	beach	core	135	Qubit	low	64.8	medium	5	1.2	2.08333	13.6306674	1.13459356
WE_2017-08-31_SP_cDNA_3a	CXR30	MST_seagull	32.179	0.392	1.184689643	15.29993703	2017-08-31	Sandpoint	beach	core	83.1	Qubit	very low	83.1	medium	5	1.2	1	3.671984888	0.56490089
WE_2017-09-13_SP_cDNA_1b	CXR30	FIB_Ecoli_235	26.619	0.912	3.571109623	3724.857156	2017-09-13	Sandpoint	beach	core	132	Qubit	low	63.36	medium	5	1.2	2.08333	1862.428578	3.27007963
WE_2017-09-13_SP_cDNA_2a	CXR30	FIB_Ecoli_235	30.964	0.123	2.358506363	228.3002374	2017-09-13	Sandpoint	beach	core	172	Qubit	low	82.56	medium	5	1.2	2.08333	114.1501187	2.05747637
WE_2017-09-13_SP_cDNA_2a	CXR30	FIB_Enterococcus_235	27.502	0.661	3.231928393	1705.801113	2017-09-13	Sandpoint	beach	core	172	Qubit	low	82.56	medium	5	1.2	2.08333	852.9005564	2.9308984
WE_2017-09-13_SP_cDNA_1b	CXR30	FIB_Enterococcus_235	27.883	0.209	3.124008611	1330.480798	2017-09-13	Sandpoint	beach	core	132	Qubit	low	63.36	medium	5	1.2	2.08333	665.2403988	8.82297862
WE_2017-09-13_SP_cDNA_2b	CXR30	FIB_Enterococcus_235	28.925	0.123	2.82885792	674.3073907	2017-09-13	Sandpoint	beach	core	107	Qubit	low	51.36	medium	5	1.2	2.08333	337.1536954	2.52782792
WE_2017-09-13_SP_cDNA_1a	CXR30	FIB_Enterococcus_235	29.133	0.226	2.769941083	588.7637776	2017-09-13	Sandpoint	beach	core	186	Qubit	low	89.28	medium	5	1.2	2.08333	294.3818888	2.46891109
WE_2017-09-13_SP_cDNA_3a	CXR30	FIB_Enterococcus_235	32.684	1.4	1.76410605	58.09062516	2017-09-13	Sandpoint	beach	core	106	Qubit	low	50.88	medium	5	1.2	2.08333	29.04531258	1.46307606
WE_2017-09-13_SP_cDNA_2b	CXR30	MST_Bacteroides_16S	23.077	1.04	4.434649941	27205.07582	2017-09-13	Sandpoint	beach	core	107	Qubit	low	51.36	medium	5	1.2	2.08333	13602.53791	4.13361995
WE_2017-09-13_SP_cDNA_1b	CXR30	MST_Bacteroides_16S	23.174	0.837	4.407244166	25541.36866	2017-09-13	Sandpoint	beach	core	132	Qubit	low	63.36	medium	5	1.2	2.08333	12770.68433	4.10621417
WE_2017-09-13_SP_cDNA_2a	CXR30	MST_Bacteroides_16S	23.645	0.828	4.274170763	18800.55904	2017-09-13	Sandpoint	beach	core	172	Qubit	low	82.56	medium	5	1.2	2.08333	9400.279522	3.97314077
WE_2017-09-13_SP_cDNA_3a	CXR30	MST_Bacteroides_16S	24.448	0.958	4.047296152	11150.54647	2017-09-13	Sandpoint	beach	core	106	Qubit	low	50.88	medium	5	1.2	2.08333	5575.273234	3.74626616
WE_2017-09-13_SP_cDNA_1a	CXR30	MST_Bacteroides_16S	25.365	1.401	3.788212691	6140.626626	2017-09-13	Sandpoint	beach	core	186	Qubit	low	89.28	medium	5	1.2	2.08333	3070.313313	3.4871827
WE_2017-09-13_SP_cDNA_1b	CXR30	MST_goose	26.966	0.125	2.719110855	523.7341037	2017-09-13	Sandpoint	beach	core	132	Qubit	low	63.36	medium	5	1.2	2.08333	261.8670518	2.41808086
WE_2017-09-13_SP_cDNA_2b	CXR30	MST_goose	26.984	0.51	2.71391455	517.5049994	2017-09-13	Sandpoint	beach	core	107	Qubit	low	51.36	medium	5	1.2	2.08333	258.7524997	2.41288455
WE_2017-09-13_SP_cDNA_2a	CXR30	MST_goose	28.242	0.492	2.350750577	224.2593595	2017-09-13	Sandpoint	beach	core	172	Qubit	low	82.56	medium	5	1.2	2.08333	112.1296797	2.04972058
WE_2017-09-13_SP_cDNA_1a	CXR30	MST_goose	29.471	0.084	1.99595843	99.07371075	2017-09-13	Sandpoint	beach	core	186	Qubit	low	89.28	medium	5	1.2	2.08333	49.53685538	1.69492843
WE_2017-09-13_SP_cDNA_3a	CXR30	MST_goose	29.838	1.227	1.890011547	77.62677563	2017-09-13	Sandpoint	beach	core	106	Qubit	low	50.88	medium	5	1.2	2.08333	38.81338782	1.58898155
WE_2017-09-13_SP_cDNA_1b	CXR30	MST_seagull	30.381	0.575	1.692212155	49.22799577	2017-09-13	Sandpoint	beach	core	132	Qubit	low	63.36	medium	5	1.2	2.08333	24.61399788	1.39118216
WE_2017-08-31_HD_cDNA_2b	CXR33	FIB_Ecoli_235	33.222	0.85	1.72834338	53.49871863	2017-08-31	Holiday	beach	core	12.2	Qubit	very low	12.2	low	5	1.2	1	12.83969247	1.10855462
WE_2017-08-31_HD_cDNA_3b	CXR33	FIB_Ecoli_235	34.997	0.758	1.232976111	17.09921255	2017-08-31	Holiday	beach	core	11	Qubit	very low	11	low	5	1.2	1	4.103811011	0.61318735
WE_2017-08-31_HD_cDNA_2b	CXR33	FIB_Enterococcus_235	29.947	1.405	2.539372309	346.2360696	2017-08-31	Holiday	beach	core	12.2	Qubit	very low	12.2	low	5	1.2	1	83.0966567	1.91958355
WE_2017-08-31_HD_cDNA_2b	CXR33	MST_Bacteroides_16S	21.36	0.199	4.919760411	83130.50359	2017-08-31	Holiday	beach	core	12.2	Qubit	very low	12.2	low	5	1.2	1	19951.32086	4.29997165
WE_2017-08-31_HD_cDNA_1b	CXR33	MST_Bacteroides_16S	23.512	0.192	4.311747754	20499.71172	2017-08-31	Holiday	beach	core	9	Qubit	very low	9	low	5	1.2	1	4919.930814	3.691959
WE_2017-08-31_HD_cDNA_3b	CXR33	MST_Bacteroides_16S	23.529	0.17	4.30694468	20274.24451	2017-08-31	Holiday	beach	core	11	Qubit	very low	11	low	5	1.2	1	4865.818683	3.68715592
WE_2017-08-31_HD_cDNA_2a	CXR33	MST_Bacteroides_16S	23.801	0.018	4.230095496	16986.17118	2017-08-31	Holiday	beach	core	7.4	Qubit	very low	7.4	low	5	1.2	1	4076.681083	3.61030674
WE_2017-08-31_HD_cDNA_1a	CXR33	MST_Bacteroides_16S	29.595	0.522	2.593094875	391.8274654	2017-08-31	Holiday												

WE_2017-08-31_HD_cDNA_3a	CXR33	MST_Bacteroides_16S	30.165	0.001	2.43205063	270.427361	2017-08-31	Holiday	beach	core	0	Qubit	very low	1	low	5	1.2	1	64.90256664	1.81226187
WE_2017-08-31_HD_cDNA_2b	CXR33	MST_goose	28.09	0.785	2.394630485	248.1021255	2017-08-31	Holiday	beach	core	12.2	Qubit	very low	12.2	low	5	1.2	1	59.54451013	1.77484173
WE_2017-08-31_HD_cDNA_3b	CXR33	MST_goose	29.576	0.648	1.965646651	92.39461311	2017-08-31	Holiday	beach	core	11	Qubit	very low	11	low	5	1.2	1	22.17470715	1.34585789
WE_2017-08-31_HD_cDNA_2a	CXR33	MST_goose	31.526	2.457	1.402713626	25.27630725	2017-08-31	Holiday	beach	core	7.4	Qubit	very low	7.4	low	5	1.2	1	6.06631374	0.78292487
WE_2017-08-31_KV_cDNA_2b	CXR33	FIB_Ecoli_23S	25.091	0.407	3.997544095	9943.61028	2017-08-31	Kingsville	beach	core	115	Qubit	low		55.2 medium	5	1.2	2.08333	4971.80514	3.6965141
WE_2017-08-31_KV_cDNA_2a	CXR33	FIB_Ecoli_23S	25.383	0.476	3.91605269	8242.381088	2017-08-31	Kingsville	beach	core	191	Qubit	low		91.68 medium	5	1.2	2.08333	4121.190544	3.6150227
WE_2017-08-31_KV_cDNA_1b	CXR33	FIB_Ecoli_23S	26.44	0.562	3.62106497	4178.928782	2017-08-31	Kingsville	beach	core	249	Qubit	medium		83 medium	5	1.2	3	3008.828723	3.47839747
WE_2017-08-31_KV_cDNA_1a	CXR33	FIB_Ecoli_23S	26.668	0.515	3.557434695	3609.397351	2017-08-31	Kingsville	beach	core	239	Qubit	medium	79.66666667	medium	5	1.2	3	2598.766093	3.41476719
WE_2017-08-31_KV_cDNA_3b	CXR33	FIB_Ecoli_23S	27.108	0.101	3.434639428	2720.441732	2017-08-31	Kingsville	beach	core	118	Qubit	low		56.64 medium	5	1.2	2.08333	1360.220866	3.13360943
WE_2017-08-31_KV_cDNA_3a	CXR33	FIB_Ecoli_23S	27.889	0.765	3.21667783	1646.940198	2017-08-31	Kingsville	beach	core	70.7	Qubit	very low		70.7 medium	5	1.2	1	395.2656476	2.59688907
WE_2017-08-31_KV_cDNA_2a	CXR33	FIB_Enterococcus_23S	22.925	0.228	4.528382053	33758.41541	2017-08-31	Kingsville	beach	core	191	Qubit	low		91.68 medium	5	1.2	2.08333	16879.2077	4.22735206
WE_2017-08-31_KV_cDNA_1b	CXR33	FIB_Enterococcus_23S	23.078	0.028	4.485044188	30552.31954	2017-08-31	Kingsville	beach	core	249	Qubit	medium		83 medium	5	1.2	3	21997.67007	4.34237668
WE_2017-08-31_KV_cDNA_1a	CXR33	FIB_Enterococcus_23S	23.958	0.323	4.235780648	17209.99119	2017-08-31	Kingsville	beach	core	239	Qubit	medium	79.66666667	medium	5	1.2	3	12391.19366	4.09311315
WE_2017-08-31_KV_cDNA_3b	CXR33	FIB_Enterococcus_23S	24.153	0.263	4.180546114	15154.65709	2017-08-31	Kingsville	beach	core	118	Qubit	low		56.64 medium	5	1.2	2.08333	7577.328543	3.87951612
WE_2017-08-31_KV_cDNA_2b	CXR33	FIB_Enterococcus_23S	24.28	0.197	4.144572853	13949.95649	2017-08-31	Kingsville	beach	core	115	Qubit	low		55.2 medium	5	1.2	2.08333	6974.978243	3.84354286
WE_2017-08-31_KV_cDNA_2a	CXR33	FIB_Enterococcus_23S	24.438	0.248	4.099818717	12584.00023	2017-08-31	Kingsville	beach	core	70.7	Qubit	very low		70.7 medium	5	1.2	1	3020.160054	3.48002996
WE_2017-08-31_KV_cDNA_3a	CXR33	MST_Bacteroides_16S	18.196	0.158	5.813697237	651174.2775	2017-08-31	Kingsville	beach	core	70.7	Qubit	very low		70.7 medium	5	1.2	1	156281.8266	5.19390848
WE_2017-08-31_KV_cDNA_3b	CXR33	MST_Bacteroides_16S	18.64	0.362	5.688252246	487811.7378	2017-08-31	Kingsville	beach	core	118	Qubit	low		56.64 medium	5	1.2	2.08333	243905.8689	5.38722225
WE_2017-08-31_KV_cDNA_2a	CXR33	MST_Bacteroides_16S	19.191	0.228	5.532576143	340860.081	2017-08-31	Kingsville	beach	core	191	Qubit	low		91.68 medium	5	1.2	2.08333	170430.0405	5.23154615
WE_2017-08-31_KV_cDNA_2b	CXR33	MST_Bacteroides_16S	19.605	0.152	5.415607165	260379.7256	2017-08-31	Kingsville	beach	core	115	Qubit	low		55.2 medium	5	1.2	2.08333	130189.8628	5.11457717
WE_2017-08-31_KV_cDNA_1b	CXR33	MST_Bacteroides_16S	20.125	0.42	5.268689608	185647.7151	2017-08-31	Kingsville	beach	core	249	Qubit	medium		83 medium	5	1.2	3	133666.3549	5.12602211
WE_2017-08-31_KV_cDNA_1a	CXR33	MST_Bacteroides_16S	20.391	0.018	5.193535628	156147.7129	2017-08-31	Kingsville	beach	core	239	Qubit	medium	79.66666667	medium	5	1.2	3	112426.3533	5.05086812
WE_2017-08-31_KV_cDNA_3a	CXR33	MST_goose	19.054	0.345	5.00317552	100733.8701	2017-08-31	Kingsville	beach	core	70.7	Qubit	very low		70.7 medium	5	1.2	1	24176.12883	4.38338676
WE_2017-08-31_KV_cDNA_1b	CXR33	MST_goose	19.429	4.92	4.894919169	78508.94992	2017-08-31	Kingsville	beach	core	249	Qubit	medium		83 medium	5	1.2	3	56526.44394	4.75225167
WE_2017-08-31_KV_cDNA_2a	CXR33	MST_goose	20.239	0.701	4.66108545	45823.20381	2017-08-31	Kingsville	beach	core	191	Qubit	low		91.68 medium	5	1.2	2.08333	22911.6019	4.36005546
WE_2017-08-31_KV_cDNA_3b	CXR33	MST_goose	20.492	0.188	4.588048499	38730.08935	2017-08-31	Kingsville	beach	core	118	Qubit	low		56.64 medium	5	1.2	2.08333	19365.04467	4.2870185
WE_2017-08-31_KV_cDNA_2b	CXR33	MST_goose	20.772	0.063	4.50721709	32152.67347	2017-08-31	Kingsville	beach	core	115	Qubit	low		55.2 medium	5	1.2	2.08333	16076.33674	4.20618709
WE_2017-08-31_KV_cDNA_1a	CXR33	MST_goose	22.572	1.036	3.987586605	9718.217286	2017-08-31	Kingsville	beach	core	239	Qubit	medium	79.66666667	medium	5	1.2	3	6997.116446	3.8449191
WE_2017-08-31_KV_cDNA_3a	CXR33	MST_seagull	26.644	0.393	2.747057329	558.5439206	2017-08-31	Kingsville	beach	core	70.7	Qubit	very low		70.7 medium	5	1.2	1	134.0505409	2.12726857
WE_2017-08-31_KV_cDNA_1b	CXR33	MST_seagull	27.184	0.527	2.594631213	393.2160294	2017-08-31	Kingsville	beach	core	249	Qubit	medium		83 medium	5	1.2	3	283.1155412	2.45196371
WE_2017-08-31_KV_cDNA_1a	CXR33	MST_seagull	27.196	1.067	2.591243966	390.1610995	2017-08-31	Kingsville	beach	core	239	Qubit	medium	79.66666667	medium	5	1.2	3	280.9159916	2.44857646
WE_2017-08-31_KV_cDNA_3b	CXR33	MST_seagull	27.229	1.376	2.581929037	381.881867	2017-08-31	Kingsville	beach	core	118	Qubit	low		56.64 medium	5	1.2	2.08333	190.9409335	2.28089904
WE_2017-08-31_KV_cDNA_2a	CXR33	MST_seagull	27.333	0.221	2.552572896	356.9216536	2017-08-31	Kingsville	beach	core	191	Qubit	low		91.68 medium	5	1.2	2.08333	178.4608268	2.2515429
WE_2017-08-31_KV_cDNA_2b	CXR33	MST_seagull	29.031	0.202	2.073277444	118.3797569	2017-08-31	Kingsville	beach	core	115	Qubit	low		55.2 medium	5	1.2	2.08333	59.18987845	1.77224745
WE_2017-08-31_LE_cDNA_1b	CXR33	FIB_Ecoli_23S	24.466	0.026	4.17196919	14858.30228	2017-08-31	Leamington	beach	core	78.8	Qubit	very low		78.8 medium	5	1.2	1	3565.992548	3.55218043
WE_2017-08-31_LE_cDNA_1a	CXR33	FIB_Ecoli_23S	24.518	0.403	4.157457022	14370.00839	2017-08-31	Leamington	beach	core	51.5	Qubit	very low		51.5 medium	5	1.2	1	3448.802013	3.53766826
WE_2017-08-31_LE_cDNA_2b	CXR33	FIB_Ecoli_23S	24.55	0.08	4.148526457	14077.52985	2017-08-31	Leamington	beach	core	68.8	Qubit	very low		68.8 medium	5	1.2	1	3378.607163	3.5287377
WE_2017-08-31_LE_cDNA_2a	CXR33	FIB_Ecoli_23S	24.929	0.419	4.042755079	11034.56149	2017-08-31	Leamington	beach	core	45.2	Qubit	very low		45.2 medium	5	1.2	1	2648.294758	3.42296632
WE_2017-08-31_LE_cDNA_3a	CXR33	FIB_Ecoli_23S	25.455	0.614	3.895958919	7869.713453	2017-08-31	Leamington	beach	core	22.5	Qubit	very low		22.5 medium	5	1.2	1	1888.731229	3.27617016
WE_2017-08-31_LE_cDNA_2b	CXR33	FIB_Enterococcus_23S	24.911	0.105	3.965839565	9243.566393	2017-08-31	Leamington	beach	core	68.8	Qubit	very low		68.8 medium	5	1.2	1	2218.455934	3.34605081
WE_2017-08-31_LE_cDNA_1b	CXR33	FIB_Enterococcus_23S	25.069	0.326	3.921085429	8338.451929	2017-08-31	Leamington	beach	core	78.8	Qubit	very low		78.8 medium	5	1.2	1	2001.228463	3.30129667
WE_2017-08-31_LE_cDNA_1a	CXR33	FIB_Enterococcus_23S	25.48	0.348	3.804668026	6377.757855	2017-08-31	Leamington	beach	core	22.5	Qubit	very low		22.5 medium	5	1.2	1	1530.661885	3.18487927
WE_2017-08-31_LE_cDNA_2a	CXR33	FIB_Enterococcus_23S	25.686	0.236	3.746317698	5575.934939	2017-08-31	Leamington	beach	core	45.2	Qubit	very low		45.2 medium	5	1.2	1	1338.224385	3.12652894
WE_2017-08-31_LE_cDNA_1a	CXR33	FIB_Enterococcus_23S	26.095	0.538	3.630466803	4270.382755	2017-08-31	Leamington	beach	core	51.5	Qubit	very low		51.5 medium	5	1.2	1	1024.891861	3.01067804
WE_2017-08-31_LE_cDNA_2b	CXR33	MST_Bacteroides_16S	19.684	0.19	5.393286998	247335.8091	2017-08-31	Leamington	beach	core	68.8	Qubit	very low		68.8 medium	5	1.2	1	59360.59419	4.77349824
WE_2017-08-31_LE_cDNA_1b	CXR33	MST_Bacteroides_16S	19.813	0.022	5.356840142	227426.0154	2017-08-31	Leamington	beach	core	78.8	Qubit	very low		78.8 medium	5	1.2	1	45482.2437	4.73705138
WE_2017-08-31_LE_cDNA_1a	CXR33	MST_Bacteroides_16S	20.543	0.325	5.150590496	141445.9431	2017-08-31	Leamington	beach	core	51.5	Qubit	very low		51.5 medium	5	1.2	1	33947.02633	4.53080174
WE_2017-08-31_LE_cDNA_2a	CXR33	MST_Bacteroides_16S	21.053	0.809	5.006498277	101507.5338	2017-08-31	Leamington	beach	core	45.2	Qubit	very low		45.2 medium	5	1.2	1	24361.80812	4.38670952
WE_2017-08-31_LE_cDNA_3a	CXR33	MST_Bacteroides_16S	21.915	0.159	4.762954173	57936.7558	2017-08-31	Leamington	beach	core	22.5	Qubit	very low		22.5 medium	5	1.2	1	13904.82139	4.14316542
WE_2017-08-31_LE_cDNA_1b	CXR33	MST_dog	25.754	0.797	2.856616918	718.8146474	2017-08-31	Leamington	beach	core	78.8	Qubit	very low		78.8 medium	5	1.2	1	172.515154	2.23682816
WE_2017-08-31_LE_cDNA_2b	CXR33	MST_dog	27.785	0.716	2.281442044	191.1798179	2017-08-31	Leamington	beach	core	68.8	Qubit	very low		68.8 medium	5	1.2	1	45.88315629	1.66165329
WE_2017-08-31_LE_cDNA_1a	CXR33	MST_dog	27.919	0.715	2.243493529	175.1836331	2017-08-31	Leamington	beach	core	51.5	Qubit	very low		51.5 medium	5	1.2	1	42.04407195	1.62370477
WE_2017-08-31_LE_cDNA_3a	CXR33	MST_dog	30.397	0.469	1.541729206	34.81201854	2017-08-31	Leamington	beach	core	22.5	Qubit	very low		22.5 medium	5	1.2	1	8.354884451	0.92194045
WE_2017-08-31_LE_cDNA_1b	CXR33	MST_goose	24.627	0.161	3.394341801	2479.372623	2017-08-31	Leamington	beach	core	78.8	Qubit	very low		78.8 medium	5	1.2	1	595.049294	2.77455304
WE_2017-08-31_LE_cDNA_2b	CXR33	MST_goose	24.694	1.249	3.375	2371.373706	2017-08-31	Leamington	beach	core	68.8	Qubit	very low		68.8 medium	5	1.2	1	569.1296894	2.75521124

WE_2017-08-31_LE_cDNA_1a	CXR33	MST_goose	25.215	0.005	3.224595843	1677.24244	2017-08-31	Leamington	beach	core	51.5	Qubit	very low	51.5	medium	5	1.2	1	402.5381855	2.60480709
WE_2017-08-31_LE_cDNA_2a	CXR33	MST_goose	26.135	0.45	2.959006928	909.9277888	2017-08-31	Leamington	beach	core	45.2	Qubit	very low	45.2	medium	5	1.2	1	218.3826693	2.33921817
WE_2017-08-31_LE_cDNA_3a	CXR33	MST_goose	27.381	0.14	2.599307159	397.4725667	2017-08-31	Leamington	beach	core	22.5	Qubit	very low	22.5	medium	5	1.2	1	95.39341602	1.9795184
WE_2017-08-31_LE_cDNA_1a	CXR33	MST_seagull	22.922	0.139	3.797668445	6275.790609	2017-08-31	Leamington	beach	core	51.5	Qubit	very low	51.5	medium	5	1.2	1	1506.189746	3.17787969
WE_2017-08-31_LE_cDNA_1b	CXR33	MST_seagull	22.936	0.175	3.793716657	6218.944153	2017-08-31	Leamington	beach	core	78.8	Qubit	very low	78.8	medium	5	1.2	1	1492.546597	3.1739279
WE_2017-08-31_LE_cDNA_2b	CXR33	MST_seagull	22.98	0.035	3.781296751	6043.614452	2017-08-31	Leamington	beach	core	68.8	Qubit	very low	68.8	medium	5	1.2	1	1450.467469	3.16150799
WE_2017-08-31_LE_cDNA_2a	CXR33	MST_seagull	23.647	0.217	3.593022271	3917.619666	2017-08-31	Leamington	beach	core	45.2	Qubit	very low	45.2	medium	5	1.2	1	940.2287199	2.97323351
WE_2017-08-31_LE_cDNA_3a	CXR33	MST_seagull	24.336	0.922	3.398537838	2503.443754	2017-08-31	Leamington	beach	core	22.5	Qubit	very low	22.5	medium	5	1.2	1	600.826501	2.77874908
WE_2017-09-13_PP_cDNA_3a	CXR33	FIB_Ecoli_23S	20.569	0.181	5.259544541	181779.3479	2017-09-13	Point Pelee	beach	core	35.7	Qubit	very low	35.7	medium	5	1.2	1	43627.0435	4.63975578
WE_2017-09-13_PP_cDNA_3b	CXR33	FIB_Ecoli_23S	22.955	0.214	4.593659299	39233.70289	2017-09-13	Point Pelee	beach	core	22.7	Qubit	very low	22.7	medium	5	1.2	1	9416.088694	3.97387054
WE_2017-09-13_PP_cDNA_2b	CXR33	FIB_Ecoli_23S	31.154	0.477	2.305481134	202.0603655	2017-09-13	Point Pelee	beach	core	6.6	Qubit	very low	6.6	low	5	1.2	1	48.49448771	1.68569238
WE_2017-09-13_PP_cDNA_1b	CXR33	FIB_Ecoli_23S	31.836	0.585	2.115148471	130.3612363	2017-09-13	Point Pelee	beach	core	8.6	Qubit	very low	8.6	low	5	1.2	1	31.28669672	1.49535971
WE_2017-09-13_PP_cDNA_3a	CXR33	FIB_Enterococcus_23S	25.62	0.727	3.765012463	5821.199229	2017-09-13	Point Pelee	beach	core	35.7	Qubit	very low	35.7	medium	5	1.2	1	1397.087815	3.14522371
WE_2017-09-13_PP_cDNA_3b	CXR33	FIB_Enterococcus_23S	26.682	0.129	3.464196692	2912.035678	2017-09-13	Point Pelee	beach	core	22.7	Qubit	very low	22.7	medium	5	1.2	1	698.8885627	2.84440793
WE_2017-09-13_PP_cDNA_3a	CXR33	MST_Bacteroides_16S	23.976	0.84	4.180652088	15158.35549	2017-09-13	Point Pelee	beach	core	35.7	Qubit	very low	35.7	medium	5	1.2	1	3638.005319	3.56086333
WE_2017-09-13_PP_cDNA_3b	CXR33	MST_Bacteroides_16S	24.053	0.317	4.158896988	14417.73332	2017-09-13	Point Pelee	beach	core	22.7	Qubit	very low	22.7	medium	5	1.2	1	3460.255996	3.53910823
WE_2017-09-13_PP_cDNA_1b	CXR33	MST_Bacteroides_16S	26.963	0.392	3.336723738	2171.319529	2017-09-13	Point Pelee	beach	core	8.6	Qubit	very low	8.6	low	5	1.2	1	521.116687	2.71693498
WE_2017-09-13_PP_cDNA_3a	CXR33	MST_goose	28.788	0.502	2.19312933	156.0016997	2017-09-13	Point Pelee	beach	core	35.7	Qubit	very low	35.7	medium	5	1.2	1	37.44040793	1.57334057
WE_2017-09-13_PP_cDNA_3b	CXR33	MST_goose	28.943	0.371	2.148383372	140.7289255	2017-09-13	Point Pelee	beach	core	22.7	Qubit	very low	22.7	medium	5	1.2	1	33.77494213	1.52859461
WE_2017-09-13_PP_cDNA_3a	CXR33	MST_seagull	22.9	0.003	3.803878398	6366.172435	2017-09-13	Point Pelee	beach	core	35.7	Qubit	very low	35.7	medium	5	1.2	1	1527.881385	3.18408964
WE_2017-09-13_PP_cDNA_3b	CXR33	MST_seagull	24.099	0.081	3.465435967	2920.357146	2017-09-13	Point Pelee	beach	core	22.7	Qubit	very low	22.7	medium	5	1.2	1	700.8857151	2.84564721
WE_2017-07-26_SP_cDNA_2a	CXR33	FIB_Ecoli_23S	28.192	1.052	3.132116544	1355.553129	2017-07-26	Sandpoint	beach	core	131	Qubit	low	62.88	medium	5	1.2	2.08333	677.7765646	2.83108655
WE_2017-07-26_SP_cDNA_3a	CXR33	FIB_Ecoli_23S	28.526	0.42	3.038903773	1093.714005	2017-07-26	Sandpoint	beach	core	75.3	Qubit	very low	75.3	medium	5	1.2	1	262.4913611	2.41911502
WE_2017-07-26_SP_cDNA_3b	CXR33	FIB_Ecoli_23S	29.321	0.834	2.817035052	656.1982268	2017-07-26	Sandpoint	beach	core	70	Qubit	very low	70	medium	5	1.2	1	157.4875744	2.19724629
WE_2017-07-26_SP_cDNA_2b	CXR33	FIB_Ecoli_23S	29.561	0.544	2.750055816	562.4136026	2017-07-26	Sandpoint	beach	core	314	Qubit	medium	104.6666667	high	5	1.2	3	404.9377939	2.60738831
WE_2017-07-26_SP_cDNA_3a	CXR33	FIB_Enterococcus_23S	26.845	0.379	3.418026286	2618.34148	2017-07-26	Sandpoint	beach	core	75.3	Qubit	very low	75.3	medium	5	1.2	1	628.4019553	2.79823753
WE_2017-07-26_SP_cDNA_3b	CXR33	FIB_Enterococcus_23S	27.476	0.55	3.239292998	1734.974108	2017-07-26	Sandpoint	beach	core	70	Qubit	very low	70	medium	5	1.2	1	416.3937859	2.61950424
WE_2017-07-26_SP_cDNA_2a	CXR33	FIB_Enterococcus_23S	29.144	0.211	2.766825289	584.5548779	2017-07-26	Sandpoint	beach	core	131	Qubit	low	62.88	medium	5	1.2	2.08333	292.277439	2.46579529
WE_2017-07-26_SP_cDNA_2b	CXR33	FIB_Enterococcus_23S	29.542	2.291	2.654090188	450.9103334	2017-07-26	Sandpoint	beach	core	314	Qubit	medium	104.6666667	high	5	1.2	3	324.6554401	2.51142269
WE_2017-07-26_SP_cDNA_2a	CXR33	MST_Bacteroides_16S	20.97	0.378	5.029948579	107139.2443	2017-07-26	Sandpoint	beach	core	131	Qubit	low	62.88	medium	5	1.2	2.08333	53569.62216	4.72891858
WE_2017-07-26_SP_cDNA_3a	CXR33	MST_Bacteroides_16S	23.164	0.148	4.410069503	25708.07175	2017-07-26	Sandpoint	beach	core	75.3	Qubit	very low	75.3	medium	5	1.2	1	6169.93722	3.79028075
WE_2017-07-26_SP_cDNA_3b	CXR33	MST_Bacteroides_16S	23.396	0.798	4.34452167	22106.58561	2017-07-26	Sandpoint	beach	core	70	Qubit	very low	70	medium	5	1.2	1	5305.580545	3.72473291
WE_2017-07-26_SP_cDNA_2b	CXR33	MST_Bacteroides_16S	24.465	0.398	4.042493078	11027.90657	2017-07-26	Sandpoint	beach	core	314	Qubit	medium	104.6666667	high	5	1.2	3	7940.092728	3.89982557
WE_2017-07-26_SP_cDNA_3a	CXR33	MST_goose	27.975	0.069	2.427829099	267.8114244	2017-07-26	Sandpoint	beach	core	75.3	Qubit	very low	75.3	medium	5	1.2	1	64.27474185	1.80804034
WE_2017-07-26_SP_cDNA_2a	CXR33	MST_goose	28.306	0.546	2.332274827	214.9190077	2017-07-26	Sandpoint	beach	core	131	Qubit	low	62.88	medium	5	1.2	2.08333	107.4595039	2.03124483
WE_2017-07-26_SP_cDNA_3b	CXR33	MST_goose	28.72	0.493	2.212759815	163.2149045	2017-07-26	Sandpoint	beach	core	70	Qubit	very low	70	medium	5	1.2	1	39.17157708	1.59297106
WE_2017-07-26_SP_cDNA_3a	CXR33	MST_seagull	28.72	0.975	2.161063596	144.8984019	2017-07-26	Sandpoint	beach	core	75.3	Qubit	very low	75.3	medium	5	1.2	1	34.77561645	1.54127484
WE_2017-07-26_SP_cDNA_2a	CXR33	MST_seagull	29.906	0.025	1.826290682	67.03331271	2017-07-26	Sandpoint	beach	core	131	Qubit	low	62.88	medium	5	1.2	2.08333	33.51665635	1.52526069
WE_2017-09-13_SP_cDNA_3b	CXR33	FIB_Enterococcus_23S	32.029	1.543	1.949637435	89.05071993	2017-09-13	Sandpoint	beach	core	145	Qubit	low	69.6	medium	5	1.2	2.08333	44.52535996	1.64860744
WE_2017-09-13_SP_cDNA_3b	CXR33	MST_Bacteroides_16S	26.541	0.914	3.455952986	2857.281218	2017-09-13	Sandpoint	beach	core	145	Qubit	low	69.6	medium	5	1.2	2.08333	1428.640609	3.15492299

Table D-3: Plasmid serial dilutions used for assays of known concentrations for generating standard curves. Values represent plasmid concentration (i.e., number of copies/ μ L).

Dilution	Plasmid1 ¹	Plasmid2 ²
Initial	2,480,000	2,580,000
1	248,000	258,000
2	24,800	25,800
3	2,480	2,580
4	248	258
5	24.8	25.8
6	2.48	2.58

¹ included synthetic genes MST_human, FIB_Enterococcus, FIB_Ecoli, and MST_genBac

² included synthetic genes MST_dog, MST_goose, and MST_seagull

Note: 1 μ L of plasmid used for each assay

Table D-4: Limit of detection (LOD) and quantification (LOQ) for each gene of interest (GOI) identified in the sediment samples. Copy number determined from serial dilutions and qPCR assays performed for generating standard curves. P1= Plasmid 1; P2 = Plasmid 2.

GOI		LOD		LOQ	
		Copies	Log copies	Copies	Log copies
P1	FIB <i>Enterococcus</i>	2	0.39	248	2.39
	FIB <i>E. coli</i>	2	0.39	248	2.39
	MST general <i>Bacteroides</i>	2	0.39	248	2.39
	MST human	2	0.39	25	1.39
P2	MST dog	3	0.41	2580	3.41
	MST goose	3	0.41	26	1.41
	MST seagull	3	0.41	2580	3.41

Table D-5: ANOVA and subsequent Tukey's post-hoc results. Sample size (n) given directly below target name (bed, suspended sediment). ANOVA values F and p represent the ratio of two mean squares and the significance value, respectively. Cells corresponding to treatment effect on GOI target represent the mean value (log copies/g) for that group with standard deviation in brackets. Red text indicates significant effect ($p < 0.05$). Lower case letters indicate where the differences are attributed, based on Tukey's post-hoc test. SS; suspended sediment.

		FIB_Enteroto	FIB_Ecoli	MST_genBac	MST_dog	MST_goose	MST_seagull	ALL		
Factor	Treatment	140, 15	130, 11	109, 28	18, 1	134, 26	102, 6	634, 87		
Chip ID	Bed + SS	ANOVA (F, p)	0.127 0.973	5.394 4.62e-04 ***	14.78 5.28e-10 ***	1.743 0.197	11.73 2.38e-08 ***	1.995 0.101	27.1 <2e-16 ***	
		CXR25	3.29 (0.872)	4.01 (0.766) a	5.31 (0.931) a	2.68 (NA)	3.93 (0.946) a	2.83 (1.01)	4.18 (1.23) a	
		CXR27	3.13 (0.739)	2.72 (0.992) b	4.18 (0.666) b	2.36 (0.875)	2.70 (0.805) b	2.28 (0.709)	2.96 (0.992) b	
		CXR28	3.16 (1.11)	2.64 (0.985) b	3.82 (0.851) b	2.55 (0.895)	2.48 (0.943) b	2.06 (1.02)	2.81 (1.12) b	
		CXR30	3.10 (0.853)	3.10 (0.872) b	3.90 (0.883) b	1.61 (0.157)	2.52 (0.835) b	2.61 (0.928)	3.00 (0.996) b	
		CXR33	3.15 (0.739)	3.01 (0.887) b	3.91 (0.920) b	1.61 (0.538)	2.67 (1.25) b	2.51 (0.591)	3.04 (1.05) b	
		Season	Bed	ANOVA (F, p)	0.19 0.663	3.59 0.0604	9.896 0.00214 **	1.846 0.193	0.525 0.47	0.285 0.594
spring	3.20 (0.841)			2.52 (0.852)	4.43 (0.292) a	2.54 (0.589)	2.47 (0.748)	2.25 (0.933)	2.95 (1.07)	
summer	3.12 (0.890)			2.91 (0.967)	3.84 (0.881) b	1.95 (0.800)	2.62 (0.961)	2.37 (0.845)	2.94 (1.03)	
SS	ANOVA (F, p)		11.24 0.00178 **	24.74 7.65e-04 ***	2.68 0.0882	NA	4.019 0.0318 *	71.23 0.00296 **	9.268 2.31e-04 ***	
	spring		3.73 (0.260) a	4.69 (0.385) a	5.75 (0.764)	--	4.50 (0.838) a	3.29 (0.129) b	4.78 (1.04) a	
	summer		3.68 (0.780) a	--	5.04 (1.27)	--	3.39 (1.12) b	4.40 (NA) a	4.08 (1.27) ab	
	fall		2.16 (0.361) b	3.44 (0.441) b	4.92 (0.459)	2.68 (NA)	3.75 (0.460) ab	2.00 (0.209) c	3.58 (1.11) b	
Collection Date ^d	Bed		ANOVA (F, p)	1.537 0.195	2.973 0.0219 *	2.658 0.0369 *	2.209 0.125	1.055 0.382	2.775 0.0313 *	3.354 0.00991 **
			2017-06-01	3.20 (0.841)	2.52 (0.852) a	4.43 (0.292) a	2.54 (0.589)	2.47 (0.748)	2.25 (0.933) ab	2.95 (1.07) ab
		2017-07-13	2.89 (1.05)	2.51 (0.955) a	3.77 (0.813) a	1.81 (1.14)	2.39 (0.958)	1.91 (0.752) b	2.68 (1.08) b	
		2017-07-26	3.28 (0.811)	2.99 (1.02) a	3.77 (0.891) a	2.69 (0.990)	2.82 (0.878)	2.30 (0.846) ab	3.00 (0.980) ab	
		2017-08-31	3.38 (0.866)	3.16 (0.965) a	3.82 (1.03) a	1.61 (0.538)	2.73 (1.18)	2.77 (0.870) a	3.15 (1.09) a	
		2017-09-13	2.97 (0.760)	3.06 (0.815) a	3.98 (0.777) a	1.61 (0.157)	2.51 (0.797)	2.51 (0.741) ab	2.94 (0.940) ab	
		Lake	Bed	ANOVA (F, p)	0.064 0.801	8.637 0.00391 **	11.67 8.98e-04 ***	7.989 0.0122 *	2.558 0.112	20.77 1.47e-05 ***
St. Clair	3.11 (0.906)			3.14 (0.970) a	4.30 (0.570) a	3.89 (NA) a	2.43 (0.760)	2.81 (0.950) a	3.13 (1.03) a	
Erie	3.15 (0.863)			2.65 (0.901) b	3.76 (0.896) b	1.97 (0.660) b	2.69 (1.00)	2.08 (0.677) b	2.83 (1.03) b	
SS	ANOVA (F, p)		0.142 0.712	1.114 0.319	2.339 0.138	NA	1.347 0.257	1.07 0.359	0.612 0.436	
	St. Clair		3.12 (1.03)	3.61 (0.555)	4.96 (0.420)	--	3.61 (0.407)	1.88 (NA)	4.02 (0.982)	
	Erie		3.33 (0.875)	4.15 (0.811)	5.51 (1.08)	2.68 (NA)	4.07 (1.09)	3.02 (0.999)	4.25 (1.32)	
	Location ^e		Bed	ANOVA (F, p)	26.8 <2e-16 ***	16.38 2.19e-12 ***	12.24 2.55e-09 ***	5.568 0.00997 **	47.54 <2e-16 ***	15.61 3.22e-11 ***
Belle River		3.77 (0.647) a		3.64 (0.850) a	4.89 (0.279) a	3.89 (NA) a	2.90 (0.644) b	3.14 (0.796) a	3.52 (0.898) a	
Sandpoint		2.43 (0.575) b		2.44 (0.646) c	4.02 (0.446) b	--	1.86 (0.419) c	1.62 (0.195) c	2.66 (0.987) b	
Holiday		2.85 (0.712) b		1.93 (0.585) c	3.46 (0.968) bc	3.10 (NA) ab	1.97 (0.718) c	1.49 (0.522) c	2.42 (0.980) b	
Kingsville		3.94 (0.502) a		3.23 (0.688) ab	5.03 (0.0979) a	2.11 (0.690) ab	3.80 (0.382) a	2.03 (0.563) bc	3.29 (0.989) a	
Leamington		2.71 (0.665) b		2.68 (0.653) bc	3.98 (0.667) b	1.64 (0.399) b	2.21 (0.580) c	2.43 (0.612) b	2.77 (0.913) b	
Point Pelee		2.62 (0.791) b		2.03 (1.05) c	3.39 (0.886) c	--	1.89 (0.590) c	1.81 (0.776) bc	2.52 (1.06) b	
Site ^f	SS	ANOVA (F, p)	0.242 0.631	1.001 0.343	0.001 0.98	NA	3.391 0.0779	0.247 0.645	2.223 0.14	
		lake	3.17 (0.668)	3.75 (0.344)	5.31 (1.05)	2.68 (NA)	3.60 (0.861)	2.67 (0.731)	3.99 (1.26)	
		tributary	3.40 (1.05)	4.22 (0.981)	5.30 (0.833)	--	4.25 (0.945)	3.14 (1.78)	4.38 (1.18)	
		Bed vs. SS		ANOVA (F, p)	0.423 0.516	15.66 1.2e-04 ***	55.99 8.39e-12 ***	0.564 0.463	45.83 2.39e-10 ***	1.76 0.188
bed	3.14 (0.878)			2.83 (0.955) b	3.96 (0.828) b	2.08 (0.784)	2.59 (0.920) b	2.34 (0.860)	2.94 (1.04) b	
suspended	3.29 (0.872)			4.01 (0.766) a	5.31 (0.931) a	2.68 (NA)	3.93 (0.946) a	2.83 (1.01)	4.18 (1.23) a	

Significance values: * $0.05 > p > 0.01$; ** $0.01 > p > 0.001$; *** $p < 0.001$

Note: MST_human was omitted as its own representative for these statistical tests because it only had one observance (bed sediment); however, it was included in the combined category (ALL).

^e Collection Date values for SS data not recorded as they exactly correspond to Season results

^f Location values for SS data not recorded as they exactly correspond to Lake results

^g Site values for bed sediment data not applicable as only one sampling site existed (i.e., nearshore beach)

NA, not available

Table D-6: Pearson's correlation (r) summary of FIB and MST targets detected in bed and suspended sediment samples.

Correlation Pairing	Bed Sediment		Suspended Sediment	
	<i>r</i>	Correlation ^b	<i>r</i>	Correlation ^b
<i>E. coli</i> vs. general <i>Bacteroides</i>	0.1099	Little (if any)	-0.0014	Little (if any)
<i>E. coli</i> vs. MST (combined host-specific) ^a	0.4742	Low	0.5621	Moderate
<i>E. coli</i> vs. <i>Enterococcus</i>	0.5580	Moderate	-0.0580	Little (if any)
<i>Enterococcus</i> vs. general <i>Bacteroides</i>	0.0123	Little (if any)	0.8661	High
<i>Enterococcus</i> vs. MST (combined host-specific) ^a	0.5169	Moderate	0.1226	Little (if any)

^a *MST (combined host-specific)* is sum of all MST targets (goose, gull, dog, and human) except MST_genBac target

^b Describes linear correlation only

VITA AUCTORIS

NAME	Danielle Gleason (nee VanMensel)
PLACE OF BIRTH	Sarnia, ON
YEAR OF BIRTH	1988
EDUCATION	2006 – 2010: B.Sc. Biochemistry/Biotechnology (Biology minor) Department of Chemistry Wilfrid Laurier University 2013 – 2016: M.Sc. Environmental Science Great Lakes Institute for Environmental Research University of Windsor 2016 – 2022: Ph.D. Environmental Science Great Lakes Institute for Environmental Science University of Windsor